e-ISSN 2544-1361

European Journal of Clinical and Experimental Medicine

Formerly: Medical Review

Quarterly

Vol. 24, No. 2

Publication date: June 2026

Rzeszów University Press
Poland 2026

Technical development, layout and interior design: Wojciech Pączek Cover design: Wiesław Grzegorczyk

ICV 2024: 120.59
MNiSW: 20.00

Indexing:
ARIANTA – Science and branch Polish electronic journals
ASCI – Asian Science Citation Index, Bielefeld Academic Search Engine
The Central European Journal of Social Sciences and Humanities (CEJSH)
Central Medical Library (Poland), Crossref, The Directory of Open Access Journals (DOAJ)
EBSCO, Free Medical Journals
Harvard Libraries – University of California Libraries
Index Copernicus, J-Gate
Main Medical Library in Warszawa
Ministry of Education and Science
MOST WIEDZY, POL-Index, Research4Life
SCImago Journal & Country Rank
Scopus

e-ISSN 2544-1361

EDITORIAL CORRESPONDENCE
European Journal of Clinical and Experimental Medicine Editorial Office
ul. Kopisto 2A, 35-959 Rzeszów, Poland
tel. +48 17 851 68 38, fax +48 17 872 19 30
http://www.ejcem.ur.edu.pl
e-mail: ejcemur@gmail.com, ejcem@ur.edu.pl
https://mc04.manuscriptcentral.com/pmur

PUBLISHER: RZESZÓW UNIVERSITY PRESS
ul. prof. S. Pigonia 6, 35-959 Rzeszów, Poland
tel./fax +48 17 872 14 26, e-mail: rup@ur.edu.pl, wydawnictwo@ur.edu.pl

Rzeszów University Press 2026
ISSN 2544-1361 (online)

http://www.ejcem.ur.edu.pl
European Journal of Clinical and Experimental Medicine
Eur J Clin Exp Med 2026; 24 (2): 252–253

Contents

Rzeszów University Press 2026
ISSN 2544-1361 (online)
doi: 10.15584/ejcem.2026.2.1

http://www.ejcem.ur.edu.pl
European Journal of Clinical and Experimental Medicine
Eur J Clin Exp Med 2026; 24 (2): 254–262

ORIGINAL PAPER

Evaluating the roles of interleukin-17, C3, C4, antinuclear antibody, and antiphospholipid antibody in the pathophysiology of systemic lupus erythematosus

Hasan Abd Ali Khudhair, Sally Fadhel Lafta

Al-Nasiriyah Technical Institute, Southern Technical University, Ministry of Higher Education and Scientific Research, Iraq

ABSTRACT

Introduction and aim. Systemic lupus erythematosus (SLE) is a chronic autoimmune disease characterized by immune dysregulation, autoantibody (Abs) production, and complement (C) consumption. This study aimed to evaluate the diagnostic and prognostic relevance of antinuclear antibodies (ANA), interleukin (IL)-17A, complement components C3 and C4, and antiphospholipid (APL) Abs in patients to SLE compared with healthy individuals. This study provides an assessment of these biomarkers within a single cohort of an Iraqi population, addressing a regional knowledge gap.

Material and methods. A prospective case–control study was conducted in Al-Nasiriyah, Iraq, from July 2024 to July 2025, including 110 patients with SLE and 70 apparently healthy individuals. Serum levels of ANA, IL-17A, complement C3, complement C4 and APL immunoglobulin (Ig) M and G were measured using enzyme-linked immunosorbent assay (ELISA) and nephelometry. Statistical analyzes were included using descriptive statistics, chi-square tests, t-tests, and correlation analyses.

Results. Patients with SLE showed significantly higher levels of ANA, IL-17A, and APL Abs, along with significantly lower levels of complement C3 and C4. ANA was positively correlated with IL-17A and APL Abs and negatively with complement components. There were also significant negative correlations of APL-IgM/IgG with C3 and C4, while IL-17A did not show a correlation with C3 or C4.

Conclusion. These findings demonstrate coordinated immune activation and complement depletion in SLE and emphasize the value of combined biomarker evaluation within a context of a population of the Middle East specifically.

Keywords. antinuclear antibody, antiphospholipid antibody, autoimmunity, complement, interleukin 17, systemic lupus erythematosus

Introduction

Systemic lupus erythematosus (SLE) is an autoimmune chronic disease with multiple manifestations in many parts of the body, including inflammation, flares, and remission.[1] The fact that SLE is a complex and heterogeneous disorder has made it difficult for healthcare providers to find accurate and useful biomarkers to diagnose, manage, and targeting the treatment to improve outcomes for their patients with SLE.[2] Cytokine family interleukin (IL)-17A, complement components C3 and C4 and the antinuclear antibodies (ANA) and antiphospholipid (APL) antibodies (Abs) are all important markers of research interest relating to the evolving pathogenic mechanisms associated with SLE. IL-17 is derived from helper T cells and is primarily associated with inflammatory responses related to autoimmune diseases such as SLE.[3] Elevated levels of IL-17 were found in serum and tissues of SLE patients, and

Corresponding author: Hasan Abd Ali Khudhair, e-mail: hasanabdali89@stu.edu.iq

Received: 24.10.2025 / Revised: 13.12.2025 / Accepted: 4.01.2026 / Published: 30.06.2026

Khudhair HAA, Lafta SF. Evaluating the roles of interleukin-17, C3, C4, antinuclear antibody, and antiphospholipid antibody in the pathophysiology of systemic lupus erythematosus. *Eur J Clin Exp Med.* 2026;24(2):254–262. doi: 10.15584/ejcem.2026.2.1.

this elevation was found to correlate with both disease activity and severity. These observations suggest that IL-17 could be used as a clinical marker for lupus activity and response to treatment due to its ability to promote inflammation through direct activation of neutrophils and through the induction of other pro-inflammatory cytokines, and to promote a breakdown of body tolerance to its self-antigens.[4] However, it should be noted that several additional cellular and molecular markers have also been identified as having reasonable relevance to this classification of disease. These have been shown to be significant based on emerging studies that have been conducted with interest in direct or indirect relationships with basophils[5], double negative T cells[6], CD28-related pathways[7], and other auto-Abs[8] in the pathogenesis and/or activity/disease severity of SLE. Furthermore, the identification of these emerging markers adds context to the markers overall picture of the chosen in our study. SLE is also a heterogeneous disease that affects people of all ages, both adults and children, and thus, among age groups, the type of biomarker expressed and clinical significance may vary.[9] Therefore, when evaluating the potential clinical relevance of the specific biomarkers investigated in the current study, the broad spectrum of immunological processes and new biomarkers must also be considered.

Complement components C3 and C4 are central to immune defense and clearance of immune complexes. In SLE, consumption of C3 and C4, due to ongoing activation of the complement cascade, is a key characteristic of disease activity. Low levels of C3 and C4 levels are related to active disease flare-ups and, in particular, about lupus nephritis. Monitoring these complement components provides important information on disorder activity and treatment response.[10]

Because the ANA test has long been a component of evaluating patients for rheumatic disease, physicians and technicians should know the characteristics of the tests used. However, because novel test formats are used more frequently, research conducted in recent years has forced ANA testing to be re-evaluated. In addition, numerous novel medications are being tested in clinical trials to treat SLE, and these studies have revealed elements of ANA expression that are not visible through serological assays in a typical clinical environment. One of the most respected indicators in rheumatology, if not all medicine, is ANA; yet, the discipline is still evolving. Interpreting data from old procedures is often problematic, even though new techniques allow for enhanced depth and breadth of serological assays. However, the findings that the frequency of ANAs can influence treatment outcomes raise the possibility that these Abs have a valuable impact on the development of SLE in a way that is still not fully understood or recognized.[11]

Another significant classification of auto-Abs in SLE involves APL-Abs, which are indicative of the presence of antiphospholipid syndrome (APS) and may coexist with SLE. APL-Abs are directed against phospholipid-binding proteins that promote thrombosis and complications during pregnancy. The detection of APL-Abs is correlated with increased risk of vascular events and poor pregnancy outcomes in SLE. Given their association with the occurrence of SLE, APL-Abs are considered significant biomarkers and can identify people at risk for complications.[12] Interleukin-17, C3, C4, ANA, and APL-Abs are important biomarkers and provide information on the pathology of SLE and offer information to test, monitor, and managing SLE. The value of these biomarkers to reflect disease activity and to predict flares and outcomes provides clinical utility to use these markers in the management of SLE.

Although considerable research has been conducted on each of the individual components of the biomarkers mentioned above, little has been done to assess how the immunological interactions of multiple biomarkers from a given cohort work together. Furthermore, there is a lack of studies involving cohorts from the Middle East (especially Iraq).

Aim

Therefore, this study aims to address the lack of studies that simultaneously evaluate multiple immunological biomarkers by providing an integrated analysis of ANA, IL-17A, complement components C3 and C4, and APL-Ab in a cohort of systemic lupus SLE from Iraq. The study compares the levels between SLE patients and healthy controls (HC) and explores their interrelationships within the SLE group. This population-specific approach offers novel information on the coordinated immune pathways involved in the pathophysiology of SLE in a Middle Eastern population.

Material and methods

Participants and study design

This prospective case-control study was conducted in Al-Nasiriyah, Thi-Qar, Iraq, between July 2024 and July 2025. Patients were recruited from the rheumatology unit of Imam Al-Hussein Teaching Hospital, Al-Nasiriyah City. All participants were diagnosed with SLE by a consultant rheumatologist according to the 2019 European League Against Rheumatism/American College of Rheumatology (EULAR/ACR) classification criteria.[13] Consecutive patients who met the diagnostic criteria were enrolled using a convenience sampling approach after obtaining written informed consent.

The inclusion criteria comprised patients of either sex with a confirmed diagnosis of SLE and a disease duration of at least six months who were in regular follow-up at the same hospital. Exclusion criteria included

patients with coexisting autoimmune diseases, chronic metabolic or endocrine disorders, renal impairment not attributed to SLE, malignancy, and any acute or chronic infectious diseases.

Eligible patients were approached during their routine clinic visits and recruited after receiving a detailed explanation of the study protocol. Demographic and clinical information was obtained through structured interviews and review of medical records. Disease activity was not measured in this study, due to the fact that the current study focuses on immunological profiling rather than activity stratification. Treatments that included corticosteroids and hydroxychloroquine were listed and noted as part of descriptive statistical analyses to minimize bias from confounding variables. However, patients who were treated with high doses of corticosteroids or immunosuppressive pulse therapy and hydroxychloroquine within three months before participating in the study were not included in the analysis.

HCs were recruited from both community members and hospital employees. The HCs matched those diagnosed with SLE were of the same age, sex, and residence. The exclusion criteria for the subjects in this study were autoimmune disease, chronic illness, family history of SLE, immunosuppression, and infection.

Ethical approval

According to the principles stated in the Declaration of Helsinki, the research was approved on 21 July 2024 by the Medical Research Ethical Committee of Southern Technical University, Al-Nasiriyah Technical Institute, Iraq, with reference number 2742. Before beginning the study, informed consent was obtained from the patients for enrollment.

Sample size

The sample size was determined using the results of previous studies, the anticipated effect sizes, and the significance level of 0.05 with 80% power. To achieve this power, 46 participants per group were required, while there were actually 110 SLE subjects and 70 HC. Consequently, there was sufficient power to identify differences between the groups.

Measurement of immunological parameters

SLE immunodiagnostic assays including the following biomarkers: ANA status, APL-Abs (IgG and IgM) titers, complement levels (C3 and C4), and IL-17A level.

A 5 mL blood sample was placed at room temperature to coagulate for 30 minutes. The sample was centrifuged at 1500 g for 10 minutes to obtain serum. The serum was then aliquoted and placed in storage at -80°C until analysis could take place.

The serum ANA test was performed using an enzyme-linked ELISA technique utilizing a human ANA screen ELISA kit that was commercially prepared (Demeditec, Germany). According to the manufacturer's recommendations for the kit, the level of ANA in the serum sample was scaled as positive or negative, based on the optical density cut-off value. Less than 0.9 titers referred to the absence of ANA (ANA negative), while 0.9 titer was considered positive for ANA.

Serum APL-IgG and APL-IgM were performed by the ELISA technique using a phospholipid screen IgG/IgM ELISA Kit (Demeditec, Germany). The assay procedure was followed on the manufacturer's recommendations. According to the manufacturing cut-off levels, the concentrations of APL-IgG and APL-IgM were categorized as positive and negative, in which the level of <10 U/ml was considered negative, while the level of ≥10 U/mL was considered positive for both types of auto-Abs.

The complement C3 and C4 detection kit (Nephelometry) (Genrui, China) was used for serum C3 and C4 measurements. The assay procedure was followed according to the manufacturer's instructions, and the measured concentrations of C3 and C4 were grouped as low (<0.9 g/L and <0.2 g/L), moderate (0.9-1.8 g/L and 0.2–0.3 g/L), and high (>1.8 g/L and >0.03 g/L), respectively, which were empirically derived from the HCs distribution.

The serum IL-17A assay was performed according to the guidelines of the the manufacturers of human IL-17A ELISA Kit in pg/mL (intraassay: coefficients of variation (CV)<8%, inter-assay: CV <10%, MyBioSource, United States). The detected level of IL-17A was scaled as low (<25 pg/mL), moderate (25-50 pg/mL) and high (>50 pg/mL), which was empirically derived from the HCs distribution.

All immunodiagnostic assays were performed in the same laboratory following a uniform protocol for all subjects, with duplicate measurements. Laboratory staff were blinded to group allocation. Information regarding CV intra- and inter-assay was not available for all assays.

Statistical analysis

SPSS version 21 was utilized to perform the analysis of results (IBM, Armonk, NY, USA). The study included continuous variables (IL-17A, C3, C4, APL-IgM, APL-IgG) for which all have been checked for normality by visual inspection of histograms and the Shapiro-Wilk test. Inferential statistical tests performed were based on whether the continuous variable was normally distributed or not. For normally distributed variables, independent sample t-tests were used to compare two independent groups (SLE patients and HC). Categorical variables were analyzed using chi-square tests, with frequency distributions generated from descriptive statistics (mean, standard deviations (SD), frequency, percentage) for both demographic characteristics of

study participants and biomarker profiles among study groups. To identify the correlation between biomarker variables, the correlation coefficients were calculated (using either Pearson correlation coefficients for normally distributed variables or Spearman correlation coefficients for nonnormally distributed variables). Statistical significance was assessed using a cutoff value of p-value <0.05 for statistical significance.

Results

Demographic and clinical characteristics

Table 1 shows that the mean age of SLE patients (31.7± 9.6 years) and HC (31.9±9.4 years) was nearly identical, indicating a proper age matching. Females predominated in both groups, especially among patients with SLE (96.4%), consistent with the known female predominance in the disease. The mean duration of the disease in SLE patients was 3.25±2.77 years, including both newly diagnosed and treated cases. More than half of the patients (54.5%) reported a positive family history of SLE, highlighting a genetic predisposition. Most of the participants lived in urban settings with a marginally higher proportion of patients (63.6%), which can be attributed to environmental or access to care factors. Most of patients (74.5%) were in treatment, while 25.5% were newly diagnosed. Overall, the groups were well matched in age, sex and residence, supporting the validity of subsequent comparisons.

Table 1. Basic characteristics of the studied groups

Parameters/Study groups		SLE (n=110)	HCs (n=70)	Total (n=180)
Age (Year) (Mean±SD)		31.7±9.6	31.9±9.4	31.8±9.5
Disease duration (Year) (Mean±SD)		3.25±2.77	0±0	–
Sex (Frequency,%)	Males	4 (3.6)	6 (8.6)	10 (5.6)
	Females	106 (96.4)	64 (91.4)	170 (94.4)
SLE history (Frequency,%)	Present	50 (54.5)	0 (0)	50 (27.8)
	Absent	60 (45.5)	70 (100)	130 (72.2)
Residence (Frequency,%)	Urban	70 (63.6)	40 (57.1)	110 (61.1)
	Rural	40 (36.4)	30 (42.9)	70 (38.9)
Treatment status (Frequency,%)	On treatment	82 (74.5)	–	–
	Newly diagnosed	28 (25.5)	–	–

ANA positivity

The positive frequency was statistically elevated (p<0.05) in subjects with SLE (100%) than in the HCs group (5.7%) (Table 2).

Table 2. Distribution of study groups according to ANA*

Study groups	ANA				p
	Positive		Negative		
	Frequency	Percent	Frequency	Percent	
SLE (n=110)	110	100	0	0	
HCs (n=70)	4	5.7	66	94.3	SLE × HC: <0.05
Total (n=180)	92	51.1	88	48.9	

* x – indicate comparison

Serum IL-17A Levels

Table 3 shows that the vast majority of subjects with SLE had elevated levels of serum IL-17A (83.6%) compared to HC (17.1%) with a statistical difference (p<0.05). Regarding the mean IL-17A titers (Table 3), the highest was in the SLE group (516.2±421.5 pg/mL) compared to the HCs (31.9±19.3 pg/mL) with statistical significance (p<0.05).

Table 3. Distribution of study groups according to human IL-17A*

Study groups	Human IL-17A (pg/mL)				Mean±SD	p
	Low	Moderate	High	Total		
	FR (%)	FR (%)	FR (%)	FR (%)		
SLE (n=110)	2 (1.8)	16 (14.6)	92 (83.6)	110 (100)	516.2± 421.5	SLE x HC: <0.05
HCs (n=70)	31 (44.3)	27 (38.6)	12 (17.1)	70 (100)	31.9±19.3	
Total (n=180)	33 (18.3)	43 (23.9)	104 (57.8)	180 (100)	327.8±289.8	

* x – comparison, low – <25 pg/mL, moderate – 25–50 pg/mL, high – >50 pg/mL, FR –frequency

Complement components

The frequency of low C4 level was significantly elevated (p<0.05) among the members of the SLE disease (49.1%) than among subjects with HC (17.1%). Table 4 also showed the mean titers of C4 which exhibited a significantly (P<0.05) decreased level among subjects of the SLE group subjects (0.25±0.21 g/L) compared to an elevated level among subjects of the HC group (0.28±0.08 g/L). Regarding serum C3 in this study, most of the SLE subjects (61.8%) were at a low level (Table 4) compared to the HC (0%) with a statistical significance (p<0.05). The mean titer for C3 was lowest in the SLE group (0.92±0.56 g/L) than in subjects (1.22±0.14 g/L) with valuable differences (p<0.05) (Table 4).

Table 4. Distribution of study groups according to complement C4 and C3*

Study groups	Complement C4 (g/L)				Mean±SD	p
	Low	Moderate	High	Total		
	FR(%)	FR(%)	FR(%)	FR(%)		
SLE (n=110)	54 (49.1)	13 (11.8)	43 (39.1)	110 (100)	0.25±0.21	SLE x HC: <0.05
HCs (n=70)	12 (17.1)	32 (45.7)	26 (37.2)	70(100)	0.28±0.08	
Total (n=180)	66 (36.7)	45 (25)	69 (38.3)	180 (100)	0.26±0.17	
Study groups	Complement C3 (g/L)				Mean±SD	p
	Low	Moderate	High	Total		
	FR (%)	FR (%)	FR (%)	FR (%)		
SLE (n=110)	68 (61.8)	33 (30)	9 (8.2)	110 (100)	0.92±0.56	SLE x HC: <0.05
HCs (n=70)	0 (0)	70 (100)	0 (0)	70 (100)	1.22±0.14	
Total (n=180)	68 (37.8)	103 (57.2)	9 (5)	180 (100)	1.04±0.47	

* x – comparison, low C4 – <0.2 g/L, moderate C4 – 0.2–0.3 g/L, high C4 – >0.3 g/L, low C3 – <0.9 g/L, moderate C3 – 0.9–1.8 g/L, high C3 – >1.8 g/L, FR – frequency

Antiphospholipid antibodies

The frequency percentage of positive level serum APL-IgM and APL-IgG was significantly (p<0.05) elevated

in the SLE subjects 68/110 (61.8%) and 57/110 (52%), respectively, compared to the HCs 0/70 (0% for both auto-Abs) group. For the mean titer, the SLE group exhibited the highest mean titer (12.28±4.02 U/mL and 10.89±3.74 U/mL, respectively) compared to the HCs group (5.67±0.98 U/mL and 4.30±0.74, respectively) with statistical differences (p<0.05).

Table 5. Distribution of study groups according to IgM/IgG APL Abs*

Study groups	APL-IgM (U/mL)			Mean±SD	p
	Positive	Negative	Total		
	FR (%)	FR (%)	FR (%)		
SLE (n=110)	68 (61.8)	42 (38.2)	110 (100)	12.28±4.02	
HCs (n=70)	0 (0)	70 (100)	70 (100)	5.67±0.98	SLE x HC: <0.05
Total (n=180)	68 (37.8)	112 (62.2)	180 (100)	9.71±4.54	
Study groups	**APL-IgG (U/mL)**			**Mean±SD**	**p**
	Positive	**Negative**	**Total**		
	FR (%)	**FR (%)**	**FR (%)**		
SLE (n=110)	57 (52)	53 (48)	110 (100)	10.89±3.74	
HCs (n=70)	0 (0)	70 (100)	70 (100)	4.30±0.74	SLE x HC: <0.05
Total (n=180)	57 (32)	123 (68)	180 (100)	8.33±4.37	

* x – comparison, FR – frequency

Correlation between ANA and other biomarkers

In SLE and HC subjects with a positive ANA, the mean levels of IL-17A were significantly higher (56.1 pg/mL in SLE vs 49.3 pg/mL for HC) than those of HCs subjects who had negative ANA (30.8 pg/mL). In the SLE cohort with positive ANA, the C3 and C4 were significantly lower (0.92 g/L C3 and 0.25 g/L C4) than those of the subjects with negative ANA HC (1.22 g/L C3 and 0.27 g/L C4). The mean concentration of serum APL-IgM and APL-IgG was highest for positive ANA (12.2 U/mL IgM and 10.8 U/mL IgG) compared to negative individuals with ANA HC (5.6 U/mL IgM and 4.2 U/mL IgG) with statistical significance (p<0.05) (Table 6).

Table 6. The correlation between ANA and other study biomarkers*

Biomarkers	ANA				p
	SLE	HCs			
	Ve^+ (n=110)	Ve^+ (n=4)	Ve^- (n=66)	T (n=70)	
IL-17A (pg/mL), mean	516.1	49.3	30.8	31.9	<0.05
C3 (g/L), mean	0.92	1.1	1.22	1.22	<0.05
C4 (g/L), mean	0.25	0.28	0.27	0.28	<0.05
IgM APL Ab (U/mL), mean	12.2	6.8	5.6	5.6	<0.05
IgG APL Ab (U/mL), mean	10.8	4.9	4.2	4.3	<0.05

* Ve^+ – positive, Ve^- – negative, T – total

Correlation between APL and other biomarkers

The difference in the mean IL-17A titer between subjects with positive, and negative serum levels of serum APL-IgG and APL-IgM was not significant (p>0.05). SLE subjects with positive levels of APL-IgG and APL-IgM exhibited the lowest mean titer (0.61 g/L and 0.65 g/L, respectively) of serum C3, compared to SLE subjects with negative APL-IgG and APL-IgM (1.2 g/L and 1.3 g/L, respectively) with valuable differences (p<0.05). The findings of the Pearson's correlation reported that there was an inverse relationship between APL-IgG, APL-IgM, and C3 levels in the SLE group (r=-0.466 for IgG and r=-0.535 for IgM). For the mean C4 titer, the level was statistically (p<0.05) lower in subjects with positive levels of APL-IgG and APL-IgM (0.17 g/L and 0.19 g/L, respectively) than negative levels of APL-IgG and APL-IgM (0.33 g/L for both). The statistical Pearson correlation showed that the concentration of APL-IgG and APL-IgM was correlated with the level of C4 (r=-0.303 and r=-0.298, respectively) (Table 7).

Table 7. Correlation between APL Abs and other study biomarkers*

Biomarkers	APL Abs positivity in SLE group						Spearman's ρ	p
	IgG APL Abs			IgM APL Abs				
	Ve^+ (n=57)	Ve^- (n=53)	T (n=110)	Ve^+ (n=68)	Ve^- (n=42)	T (n=110)		
IL-17A (pg/mL), mean	527.5	504	516.2	544.1	470.9	516.2	IgG: -0.057 IgM: 0.029	>0.05
C3 (g/L), mean	0.61	1.2	0.92	0.65	1.3	0.92	IgG: -0.466 IgM: -0.535	<0.05
C4 (g/L), mean	0.17	0.33	0.25	0.19	0.33	0.25	IgG: -0.303 IgM: -0.298	<0.05

* Ve^+ – positive, Ve^- – negative, T – total

Correlation between IL-17A and complement components

There was no valuable correlation between the level of IL-17A and the concentrations of C3 or C4 in both study groups.

Table 8. The correlation between IL-17A and complements components*

Biomarkers	IL-17A (pg/mL)								Spearman's ρ	p
	SLE				HCs					
	L (n=2)	M (n=16)	H (n=92)	T (n=110)	L (n=31)	M (n=27)	H (n=12)	T (n=70)		
C3 (g/L), mean	0.97	0.86	0.93	0.92	1.22	1.2	1.2	1.2	HC: -0.028 SLE: -0.131	>0.05
C4 (g/L), mean	0.13	0.28	0.24	0.25	0.28	0.27	0.27	0.28	HC:-0.167 SLE: -0.085	>0.05

* T – total, L – low (<25 pg/mL), M – moderate (25–50 pg / mL), H – high (>50 pg/mL), FR – frequency

Discussion

The present study demonstrated significantly higher levels of ANA, IL-17A and APL-Abs (IgM and IgG) in patients with SLE compared with HCs, accompanied by markedly reduced C3 and C4 concentrations. Positive correlations between ANA and both IL-17A and APL-

Ab suggest potential immunological interaction among these factors in SLE pathogenesis. On the contrary, the negative correlations observed between ANA or APL-Abs and C3/C4 indicate continued activation of the immune complex and complement consumption characteristic of active disease. Although IL-17A was not significantly correlated with C3 or C4, its elevation suggests further evidence of immune dysregulation. Collectively, these findings substantiate the role of auto-Abs, cytokine imbalance, and complement depletion in SLE activity without implying causation.

A key outcome of this study was the significantly increased positivity for ANA in the SLE group in comparison to the HCs (Table 2). This finding is consistent with previously published research documenting ANA positivity in 92.3% of SLE patients.[14] Furthermore, serum IL-17A was also detected to be significantly higher in SLE subjects compared to controls (Table 3), which confirms similarly published studies that observed increased expression of IL-17 in autoimmune disorders.[15–17] The findings support the proposal that ANA and IL-17A being both associated with immunopathological abnormalities related to SLE, possibly contributing to inflammatory mechanisms in SLE.

The study found that SLE participants had significantly lower serum C3 and C4 levels than HC (Table 4). These results corroborate results from previous research conducted by Trouw et al.,[18] Aringer et al.,[13] and others,[19,20] who also found evidence of hypocomplementemia in SLE. The decreased levels of C3 and [C4] likely reflect complement activation and consumption with immune complexes, a well-established feature in the pathophysiology of SLE. The reproducibility of similar results in the literature suggests that C3 and C4 levels may have value when determining the contributions of the complement system to symptoms seen in SLE. Although the results may help determine disease activity or changes in treatment response, they should never be used as definitive markers of disease progression,[10] but rather in conjunction with other clinical and laboratory markers.

As shown in Table 5, serum APL-IgM concentrations were significantly higher in subjects with SLE than in HCs. This is consistent with previous studies that demonstrate that SLE cases tend to exhibit higher APL Abs, including the IgM isotype, and an association with thrombotic risk and related clinical features.[21,22] Similarly, we found that higher APL-IgM concentrations and incidence in SLE people suggest that this is relevant to disease characterization but that we are not making claims about causation. APL-IgG concentrations were also higher in measured SLE subjects, again significant compared to HC (Table 5). This is consistent with recent work by Farina et al.[23] who similarly found increased APL-IgG levels in their SLE cases. Our current study did not replicate the claims of APL-IgG positivity rates in the work of Ünlü et al.[24], who reported lower frequencies among subjects with SLE compared to controls. As before, this can be largely attributed to population characteristics, diagnostic reference, or the variability of the detection protocol. In summary, APL-IgG and APL-IgM concentrations were elevated over HCs and the patterns of their association in SLE support the previous investigation, while at the same time indicating the threshold difference attributable to variability in the detection or characteristics of the study population.

Beringer et al.[25] demonstrated that IL-17A is involved in immune responses and dysregulation of IL-17A has been associated with autoimmune diseases. Similarly, in the current study, we observed increased levels of IL-17A in participants who tested positive for ANA. Using both study groups, we found evidence that indicates a positive correlation between IL-17A and ANA (Table 6). These findings are consistent with previous reports showing a link between IL-17A and inflammation and auto-Abs production in SLE. In particular, Ebrahimi et al.[26] demonstrated that higher concentrations of IL-17A were related to increased disease activity in SLE. The current study observed positive correlations between IL-17A positivity and ANA positivity.

Furthermore, there was an inverse correlation between ANA and C3 and C4 in both the SLE and HC groups. The presence of decreased complement levels may indicate the formation/activation of immune complexes, in agreement with prior studies that have found decreased levels of C3 and C4 in ANA-positive SLE patients.[27-29] These results indicate that the measurement of complement depletion may indicate the activation of the immune system rather than a definitive measure of disease activity. In healthy individuals, the weaker effects of ANA on complement levels may indicate subclinical immune activity or predisposition to autoimmunity.

Previous investigations[11] indicated that ANA-positive individuals, who do not demonstrate clinical evidence of autoimmune disease, may have minor alterations in complement, suggesting early immune dysregulation. Consistent with these results, we report evidence of positivity for ANA related to lower C3/C4 levels consistent with history of autoimmune disease, especially SLE. Overall, the evidence supports the notion that ANA is a marker of underlying immune alterations and may not serve as a discriminatory prognostic biomarker, but rather as an aid in evaluating disease activity.

The results of this investigation offer important information on the relationship between ANA and APL-Abs in SLE patients. SLE subjects who were ANA positive had significantly higher levels of APL-IgM and APL-IgG concentrations (Table 6), suggesting a relationship between ANA positivity and higher levels of APL-Abs. This finding is consistent with earlier stud-

ies demonstrating that the coexistence of APL-Ab with ANA can be associated with increased disease activity and an increased risk of thrombotic events in SLE.[30] The observation that APL-Ab may be associated with ANA-positivity indicates an increased risk of thrombotic complications and pregnancy outcomes associated with APS.[31] These findings reinforce the idea that ANA and APL-Abs may have similar immunopathogenesis linked to endothelial injury and subsequent thrombo-inflammatory events.[32]

Table 7 indicates that there were no significant differences in IL-17A levels among SLE patients with positive serum APL-IgG and APL-IgM Abs, indicating that IL-17A is generally not associated with APL-Ab activity among SLE patients. Furthermore, Doreau et al.[33] found that SLE patients had increased IL-17A without association with APL-Abs, suggesting that IL-17A could contribute to the presence of SLE pathology relative to APL-Abs or IgM or IgG levels. Another study[34] suggested that while IL-17A may be indicative of overall disease activity, it does not correlate with the presence of APL-Abs.

These findings are consistent with the idea that IL-17A acts as part of a complex cytokine network in SLE and that it may not be clearly related to APL-Abs. The results indicated a statistically significant negative correlation between APL (APL-IgG and APL-IgM) and C3 and C4 in SLE patients (Table 7). Previous investigations[35] reported that the presence of APL Abs was associated with lower complement levels, which, in a similar fashion, suggested that these Abs may lead to complement consumption and hypocomplementemia in SLE. Overall, these findings may begin to support the potential to monitor these APL-Ab along with complement components as a possible way to monitor disease activity and help identify individuals at risk of worse outcomes who may need closer follow-up, as indicated by Fanouriakis et al.[36]

The absence of a meaningful correlation between IL-17A concentrations and C3 or C4 levels in both the SLE and HC cohorts (Table 8) indicates that IL-17A can contribute to the pathogenesis of SLE independent of complement components. These results corroborate the reported findings[35] showing that, although SLE patients have higher levels of IL-17A, there are no explicit correlations with complement activation, which also suggests independent pathogenic mechanisms. IL-17A has the ability to amplify an inflammatory response, although the role of this cytokine in triggering complement activation may be through an indirect pathway, and possibly unknown context-dependent pathways, through local inflammatory mediators and/or interactions with other cytokines.[10] However, the IL-17A signaling pathway and complement systems of complement will likely have several overlaps to consider during all aspects of the immune response and may be appropriate for additional investigation.

IL-17A levels showed a marked increase in patients with SLE and these levels correlated with ANA in the circulation but showed no association with C3 and C4, suggesting a possible independent role in the dysregulation of the immune response. IL-17A is an interesting and unvalidated biomarker in SLE that has not been extensively studied enough to confirm if it is clinically relevant for disease monitoring, patient stratification, or as a potential therapeutic target.

This study adds new information because we added an analysis of how the biomarkers in the current study interact with each other in the same group of patients. From correlation analysis, we found a strong positive correlation between ANA and IL-17A and an inverse correlation between APL Abs and complement levels. These findings have not previously been extensively published in Middle Eastern populations. These findings provide new information on how classical serological markers work together in a specific immunogenetic context and they provide evidence for possible population-specific immune dysregulation pathways in SLE.

Study limitations

The study does not report a disease activity score, but still identifies clear differences in immunology between patients diagnosed with SLE versus reportedly HC. Although limited to demonstrating the cross-sectional nature of these data, the results represent a snapshot of differences in biomarker profiles. The selection of ANA, IL-17A, C3, C4, and APL-Abs represents critical pathways associated with SLE and lends scientific relevance to the findings of the study. Although the sample size of the HC group was lower than that of the SLE group, the subjects were selected to be comparable, thus establishing internal validity for this study. While the correlations between these two groups were relatively weak, the statistically significant and biologically relevant findings of these correlations lend support to the conclusions drawn in this study. The restricted biomarker panel used in this study may limit the identification of additional contributing pathways, but provides greater specificity for evaluating the central mechanisms that lead to the pathology of SLE. Therefore, despite these limitations, the study provides compelling evidence for an underlying immunologic dysregulation in patients with SLE. This study consisted of only Iraqi patients and did not include participants from other countries or ethnic backgrounds. Furthermore, no detailed environmental data were collected as this was not a primary goal of the study.

Conclusion

According to observations, SLE is marked by a significant increase in positive ANA and IL-17A levels, and a significant decrease in C3 and C4 levels, compared to HCs. Since there is a positive correlation between ANA and IL-17A, the involvement of both substances in the

pathophysiology of SLE can be speculated. The higher levels of APL-IgM and APL-IgG observed in SLE compare to HCs, which were inversely correlated to C3 and C4, revealed the complicated relationships between auto-Abs and complement proteins in SLE, as well. Collectively, these biomarkers indicate significant immunological dysregulation in SLE. No direct link was reported between IL-17A levels and C3 or C4.

Acknowledgments

The authors thank Southern Technical University, Nasiriyah Technical Institute, for their support and facilities. Gratitude is also extended to the staff of the Imam Al-Hussein Teaching Hospital and all participants who contributed to this study.

Declarations

Funding
Self-fund.

Author contributions
Conceptualization, K.H.A.A.; Methodology, L.S.F.; Software, L.S.F.; Validation, K.H.A.A; Formal Analysis, L.S.F.; Investigation, K.H.A.A.; Resources, L.S.F.; Data Curation, K.H.A.A.; Writing – Original Draft Preparation, K.H.A.A.; Writing – Review & Editing, L.S.F.; Visualization, K.H.A.A.; Supervision, L.S.F.; Project Administration, K.H.A.A.; Funding Acquisition, L.S.F.

Conflicts of interest
The author declared no conflicts of interest.

Data availability
The datasets analyzed during the current study are available from the corresponding author on reasonable request.

References

1. Dörner T, Furie R. Novel paradigms in systemic lupus erythematosus. *Lancet*. 2019;393(10188):2344-2358. doi:10.1016/S0140-6736(19)30546-X
2. Petri M, Orbai AM, Alarcón GS, et al. Derivation and validation of the Systemic Lupus International Collaborating Clinics classification criteria for systemic lupus erythematosus. *Arthritis Rheum*. 2012;64(8):2677-2686. doi:10.1002/art.34473
3. Shen H, Goodall JC, Hill Gaston JS. Frequency and phenotype of peripheral blood Th17 cells in ankylosing spondylitis and rheumatoid arthritis. *Arthritis Rheum*. 2009;60(6):1647-1656. doi:10.1002/art.24568
4. Yang Y, Yan C, Yu L, et al. The star target in SLE: IL-17. *Inflamm Res*. 2022;72(2):313-328. doi:10.1007/s00011-022-01674-z
5. Dossybayeva K, Bexeitov Y, Mukusheva Z, et al. Analysis of peripheral blood basophils in pediatric systemic lupus erythematosus. *Diagnostics*. 2022;12(7):1701. doi:10.3390/diagnostics12071701
6. Sekine A, Wada T, Sawa N, et al. T-cell receptor CRαβ^{+} CD4^{-} CD8^{-} (double-negative) T cells may predict pathological kidney findings in patients with suspected lupus nephritis. *Nephron*. 2025;149(12):701-708. doi:10.1159/000547797
7. Pratama MZ, Handono K, Kalim H, et al. Association of the CD28 markers with the disease activity in systemic lupus erythematosus patients. *F1000Research*. 2023;12:1362. doi:10.12688/f1000research.140890.1
8. Barguil Macêdo M, Wahadat MJ, Björk A, et al. Anti-mitochondrial antibodies as markers of disease activity in childhood-onset systemic lupus erythematosus: a longitudinal cohort study. *Rheumatology (Oxford)*. 2025;64(9):5096-5100. doi:10.1093/rheumatology/keaf275
9. Tarr T, Dérfalvi B, Győri N, et al. Similarities and differences between pediatric and adult patients with systemic lupus erythematosus. *Lupus*. 2015;24(8):796-803. doi:10.1177/0961203314563817
10. Ayano M, Horiuchi T. Complement as a biomarker for systemic lupus erythematosus. *Biomolecules*. 2023;13(2):367. doi:10.3390/biom13020367
11. Pisetsky DS, Lipsky PE. New insights into the role of antinuclear antibodies in systemic lupus erythematosus. *Nat Rev Rheumatol*. 2020;16(10):565-579. doi:10.1038/s41584-020-0480-7
12. Tektonidou MG, Andreoli L, Limper M, et al. Management of thrombotic and obstetric antiphospholipid syndrome: a systematic literature review informing the EULAR recommendations for the management of antiphospholipid syndrome in adults. *RMD Open*. 2019;5(1):e000924. doi:10.1136/rmdopen-2019-000924
13. Aringer M, Costenbader K, Daikh D, et al. 2019 European League Against Rheumatism/American College of Rheumatology classification criteria for systemic lupus erythematosus. *Arthritis Rheumatol*. 2019;71(9):1400-1412. doi:10.1002/art.40930
14. Choi MY, Clarke AE, St Pierre Y, et al. Antinuclear antibody–negative systemic lupus erythematosus in an international inception cohort. *Arthritis Care Res (Hoboken)*. 2019;71(7):893-902. doi:10.1002/acr.23712
15. Yang Y, Yan C, Yu L, et al. The star target in SLE: IL-17. *Inflamm Res*. 2023;72(2):313-328. doi:10.1007/s00011-022-01674-z
16. Akhter S, Tasnin FM, Islam MN, et al. Role of Th17 and IL-17 cytokines on inflammatory and autoimmune diseases. *Curr Pharm Des*. 2023;29(26):2078-2090. doi:10.2174/1381612829666230904150808
17. Peliçari KD, Postal M, Sinicato NA, et al. Serum interleukin-17 levels are associated with nephritis in childhood-onset systemic lupus erythematosus. *Clinics (Sao Paulo)*. 2015;70(5):313-317. doi:10.6061/clinics/2015;70(5):313-317
18. Trouw LA, Pickering MC, Blom AM. The complement system as a potential therapeutic target in rheumatic dise-

ase. *Nat Rev Rheumatol*. 2017;13(9):538-547. doi:10.1038/nrrheum.2017.125

19. Gandino IJ, Scolnik M, Bertiller E, et al. Complement levels and risk of organ involvement in patients with systemic lupus erythematosus. *Lupus Sci Med*. 2017;4(1):e000209. doi:10.1136/lupus-2017-000209
20. Takamatsu R, Shimojima Y, Kishida D, et al. The impact of normal serum complement levels on the disease classification and clinical characteristics in systemic lupus erythematosus. *Adv Rheumatol*. 2022;62(1):49. doi:10.1186/s42358-022-00283-y
21. Hisada R, Atsumi T. An antiphospholipid antibody profile as a biomarker for thrombophilia in systemic lupus erythematosus. *Biomolecules*. 2023;13(4):617. doi:10.3390/biom13040617
22. González-Treviño M, Figueroa-Parra G, Yang JX, et al. Association between antiphospholipid antibodies and diffuse alveolar haemorrhage risk in systemic lupus erythematosus: a systematic review and meta-analysis. *Rheumatology (Oxford)*. 2025;64(4):1598-1608. doi:10.1093/rheumatology/keae632
23. Farina N, Abdulsalam R, McDonnell T, et al. Antiphospholipid antibody positivity in early systemic lupus erythematosus is associated with subsequent vascular events. *Rheumatology (Oxford)*. 2023;62(6):2252-2256. doi:10.1093/rheumatology/keac596
24. Ünlü O, Zuily S, Erkan D. The clinical significance of antiphospholipid antibodies in systemic lupus erythematosus. *Eur J Rheumatol*. 2015;3(2):75. doi:10.5152/eurjrheum.2015.0085
25. Beringer A, Noack M, Miossec P. IL-17 in chronic inflammation: from discovery to targeting. *Trends Mol Med*. 2016;22(3):230-241. doi:10.1016/j.molmed.2016.01.001
26. Ebrahimi Chaharom F, Ebrahimi AA, Feghhi Koochebagh F, et al. Association of IL-17 serum levels with clinical findings and systemic lupus erythematosus disease activity index. *Immunol Med*. 2023;46(4):175-181. doi:10.1080/25785826.2023.2202050
27. Rana RS, Naik B, Yadav M, et al. Serum complements and immunoglobulin profiles in systemic lupus erythematosus patients: an observational study at a teaching hospital. *J Family Med Prim Care*. 2022;11(2):608-613. doi:10.4103/jfmpc.jfmpc_960_21
28. Yu H, Nagafuchi Y, Fujio K. Clinical and immunological biomarkers for systemic lupus erythematosus. *Biomolecules*. 2021;11(7):928. doi:10.3390/biom11070928
29. Stohl W, Schwarting A, Okada M, et al. Efficacy and safety of subcutaneous belimumab in systemic lupus erythematosus: a fifty-two–week randomized, double-blind, placebo-controlled study. *Arthritis Rheumatol*. 2017;69(5):1016-1027. doi:10.1002/art.40049
30. Lazzaroni MG, Fredi M, Andreoli L, et al. Triple antiphospholipid (aPL) antibodies positivity is associated with pregnancy complications in aPL carriers: a multicenter study on 62 pregnancies. *Front Immunol*. 2019;10:1948. doi:10.3389/fimmu.2019.01948
31. Tektonidou MG, Andreoli L, Limper M, et al. EULAR recommendations for the management of antiphospholipid syndrome in adults. *Ann Rheum Dis*. 2019;78(10):1296-1304. doi:10.1136/annrheumdis-2019-215213
32. Chaturvedi S, Brodsky RA, McCrae KR. Complement in the pathophysiology of the antiphospholipid syndrome. *Front Immunol*. 2019;10:438. doi:10.3389/fimmu.2019.00449
33. Jakiela B, Iwaniec T, Plutecka H, et al. Signs of impaired immunoregulation and enhanced effector T-cell responses in the primary antiphospholipid syndrome. *Lupus*. 2016;25(4):389-398. doi:10.1177/0961203315618267
34. Raymond W, Ostli-Eilertsen G, Griffiths S, et al. IL-17A levels in systemic lupus erythematosus associated with inflammatory markers and lower rates of malignancy and heart damage: evidence for a dual role. *Eur J Rheumatol*. 2017;4(1):29. doi:10.5152/eurjrheum.2017.16059
35. Weinstein A, Alexander RV, Zack DJ. A review of complement activation in SLE. *Curr Rheumatol Rep*. 2021;23:19. doi:10.1007/s11926-021-00984
36. Fanouriakis A, Kostopoulou M, Andersen J, et al. EULAR recommendations for the management of systemic lupus erythematosus: 2023 update. *Ann Rheum Dis*. 2024;83(1):15-29. doi:10.1136/ard-2023-224762

Rzeszów University Press 2026
ISSN 2544-1361 (online)
doi: 10.15584/ejcem.2026.2.3

http://www.ejcem.ur.edu.pl
European Journal of Clinical and Experimental Medicine
Eur J Clin Exp Med 2026; 24 (2): 263–272

ORIGINAL PAPER

Chromium picolinate modulates nitric oxide pathways but enhances myocardial peroxynitrite formation in a rat heart during metabolic syndrome modeling

Oleh Akimov [1], Andrii Mykytenko [2], Vitalii Kostenko [1]

[1] Department of Pathophysiology, Poltava State Medical University, Poltava, Ukraine
[2] Department of Biological and Bioorganic Chemistry, Poltava State Medical University, Poltava, Ukraine

ABSTRACT

Introduction and aim. Metabolic syndrome (MetS) is a global non-communicable health burden. Chromium picolinate (CRPIC) as modulator of p38 MAPK cascade may have a potential therapeutic effect on MetS.

The objective of the present study is to evaluate the effects of CRPIC administration on nitric oxide generation and myocardial levels of nitric oxide metabolites in rats under conditions of metabolic syndrome.

Material and methods. The experiment was performed on 24 Wistar rats, which were randomly allocated into four groups (n=6 per group): Group I, the control group; Group II, the metabolic syndrome (MetS) group, in which MetS was induced by providing a 20% fructose solution as the sole source of drinking water for 60 days; Group III, the CRPIC-treated group, receiving CRPIC at a dose of 80 μg/kg; and Group IV, the CRPIC+MetS group, in which CRPIC administration was carried out under conditions of experimentally induced metabolic syndrome. The following biochemical parameters were evaluated: total nitric oxide synthase (NOS) activity, inducible NOS (iNOS) and constitutive NOS (cNOS) activities, arginase activity, nitrite reductase and nitrate reductase activities, as well as the concentrations of nitrites, peroxynitrites, nitrosothiols, and hydrogen sulfide.

Results. Administration of CRPIC under MetS conditions resulted in a 38.2% reduction in NOS activity and a 40.2% decrease in iNOS activity, accompanied by a 48.9% increase in cNOS activity compared with the MetS group. CRPIC treatment also reduced arginase activity by 13.2%. While the activity of nitrate reductase remained unchanged, nitrite reductase activity decreased by 37.0%. Furthermore, CRPIC increased nitrite levels by 95.2% and peroxynitrite concentrations by 35.2%, while the content of nitrosothiols was reduced by 49.1%. H_2S levels also decreased by 16.8%.

Conclusion. Administration of CRPIC on the background of metabolic syndrome modeling alleviates enhanced nitric oxide production from the L-arginine-dependent and L-arginine-independent pathways, but increases peroxynitrite compared to the metabolic syndrome group.

Keywords. chromium picolinate, heart, metabolic syndrome, nitric oxide, p38-MAPK

Introduction

According to the State Committee of Statistics of Ukraine, in the year 2020, 39.7 % of adults over 18 years were considered overweight and 16% obese, with 0.7 % classified as extremely obese.[1] Obesity often leads to metabolic syndrome (MetS) and type II diabetes development.[2] MetS is often accompanied by cardiovascular diseases, which develop due to oxidative-nitrosative stress in heart tissues caused by altered metabolism.[3]

Corresponding author: Oleh Akimov, e-mail: o.akimov@pdmu.edu.ua

Received: 19.10.2025 / Revised: 7.01.2026 / Accepted: 9.01.2026 / Published: 30.06.2026

Akimov O, Mykytenko A, Kostenko V. Chromium picolinate modulates nitric oxide pathways but enhances myocardial peroxynitrite formation in a rat heart during metabolic syndrome modeling. *Eur J Clin Exp Med*. 2026;24(2):263–272. doi: 10.15584/ejcem.2026.2.3.

Nitrosative component of oxidative-nitrosative stress is usually caused by excessive production of nitric oxide (NO) and peroxynitrite (ONOO-) formation. Most of existing therapeutic strategies targeting NO production in rat heart during MetS influence transcriptional factor NF-κB activity, which controls inducible NO-synthase (iNOS) activity.[4] However, prolonged transcriptional factor NF-κB activity inhibition may have adverse effects on other organs and tissues, which may be one of underlying mechanisms of metformin hepatotoxicity.[5]

Chromium picolinate (CRPIC) has a potential to improve lipid metabolism during MetS, which is one of etiological factors of oxidative-nitrosative stress development.[6] Therefore, it can be considered a therapeutic tool for treatment of heart damage caused by MetS. However, its influence on sources of NO production and its metabolism in heart during MetS remain insufficiently studied.

Current therapeutic approaches largely focus on inhibiting NF-κB–dependent iNOS expression; however, prolonged NF-κB suppression may induce adverse systemic effects. Therefore, there is a pressing need for alternative strategies capable of modulating nitrosative signaling without direct interference in NF-κB activity. CRPIC, a nutritional supplement known to improve lipid and carbohydrate metabolism, represents a promising candidate in this regard. Despite evidence supporting its beneficial effects on metabolic homeostasis, the potential of CRPIC to influence cardiac NO metabolism and mitigate nitrosative stress during MetS remains largely unexplored. The present study addresses this gap by investigating the impact of CRPIC on NO production and its metabolism in the myocardium under MetS conditions, thus providing a novel mechanistic perspective on its cardioprotective potential.

Aim

The objective of the present study is to evaluate the effects of CRPIC administration on nitric oxide generation and myocardial levels of nitric oxide metabolites in rats under conditions of metabolic syndrome.

Material and methods

The study was carried out on 24 mature male Wistar rats weighing 200-260 g that were obtained from accredited animal facility of Poltava State Medical University. The sample size was determined a priori for one-way analysis of variance with four groups. An effect size (f = 0.4), p = 0.05 and power (1–β)=0.80 were assumed based on the previous literature and pilot data. The calculation yielded a minimum of 24 animals (6 per group). The animals were housed under standard vivarium conditions. All experimental procedures involving animals were conducted in accordance with the European Convention for the Protection of Vertebrate Animals Used for Experimental and Other Scientific Purposes. Animals were withdrawn from the experiment under thiopental anesthesia by cardiac puncture with blood collection from the right ventricle. All manipulations were approved by the Bioethics Commission of Poltava State Medical University (Record No. 206 from 24.06.2022).

Experimental design

The animals were distributed into IV experimental groups (6 animals per group):

I – Control group: animals in this group underwent the same manipulations as those in the experimental groups but received 0.9% sodium chloride solution instead of the active substances.

II – MetS group. Animals on which MetS was modelled. Induction of MetS was achieved by exposure to a 20% fructose solution as the only drinking fluid for 60 days.[7]

III – group of chromium picolinate administration (CRPIC group). Animals from this group received chromium picolinate (Sigma Aldrich, Cas Number: 14639-25-9) intragastrically daily at a dose 80 μg/kg for 60 days.[8] The dose of CRPIC was chosen according to Sahin K. et al (2013) as dose showing anti-diabetic effects.[8] Duration of CRPIC was chosen according to the time necessary to induce MetS in our chosen model.[7]

IV – group of simultaneous chromium picolinate administration and metabolic syndrome modelling (CRPIC+MetS group). Animals in this group received chromium picolinate intragastrically daily at a dose of 80 μg/kg for 60 days and had a 20% fructose solution as the only source of water for 60 days.

Rats were housed in cages containing six animals each. The cages were used as a randomization unit.

Biochemical analysis of rat heart homogenate

Determination of L-arginine-dependent NO production

The study object was a 10% homogenate of rat heart tissue. The total activity of nitric oxide synthase (gNOS) was assessed based on the increase in the concentration of nitrite (NO_2^-) concentration.[9]

To assess the activity of constitutive nitric oxide synthase isoforms (cNOS), aminoguanidine hydrochloride was employed as a selective inhibitor of inducible NO-synthase (iNOS). The activity of the inducible isoform was subsequently calculated using the formula: iNOS = NOS – cNOS (μmol/min per g of protein).[9]

Nitrite levels were determined using the Griess–Ilosvay reagent, consisting of 1% sulfanilic acid in 30% acetic acid and 0.1% 1-naphthylamine in the same solvent. The concentration of nitrites was measured spectrophotometrically using a Ulab-101 spectrophotometer (λ=540 nm in cuvette with optical path length of 5 mm, ULAB, Nanjing, China).[10]

Evaluation of arginase activity
Total arginase activity was determined by the change in L-ornithine concentration before and after incubation of 0.1 mL of a 10% tissue homogenate in 0.8 mL of incubation medium containing 0.5 mL of 125 mM phosphate buffer (pH 7.0) and 0.2 mL of 6 mM L-arginine.

Determination of L-arginine-independent NO production
Nitrite reductase (NiR) activity was evaluated based on the reduction in nitrite concentration following incubation of 0.2 mL of a 10% tissue homogenate for 60 minutes at 37°C. Nitrite levels used for the calculation of NiR activity were determined both before and after the incubation period.[9-10] The activity of nitrate reductase (NaR) was evaluated by measuring the decrease in nitrate concentration after incubating 0.2 mL of a 10% tissue homogenate for 60 min at 37°C.[9-10] Nitrite concentration, used for the calculation of NaR activity, was determined spectrophotometrically using a Ulab-101 at a wavelength of 540 nm in a cuvette with an optical path length of 5 mm.

Estimation of peroxynitrite content
The concentration of peroxynitrite derivatives of alkali (Na^+, K^+) and alkaline earth (Ca^{2+}) metals was determined based on their reaction with potassium iodide under neutral conditions (pH 7.0) in 0.2 M phosphate buffer.[10] Quantification was performed spectrophotometrically using a Ulab-101 at a wavelength of 355 nm with a cuvette optical path length of 10 mm.

Evaluation of S-nitrosothiols concentration
The concentration of low-molecular-weight S-nitrosothiols (S-NO) was assessed indirectly by quantifying the increase in nitrite levels following a 30-min incubation of 0.2 mL of a 10% tissue homogenate.[9] S-nitrosothiol content was calculated as the difference between baseline nitrite concentration measured prior to incubation and the nitrite concentration determined after incubation. Nitrite levels were quantified spectrophotometrically using a Ulab-101 at 540 nm with a cuvette optical path length of 5 mm.

Determination of hydrogen sulfide content
H_2S concentration was determined colorimetrically based on the formation of a chromogenic complex resulting from the reaction of H_2S with a specific sulfide-detecting reagent composed of N,N-dimethyl-p-phenylenediamine (0.4 g) and iron(III) chloride hexahydrate (0.6 g $FeCl_3 \cdot 6H_2O$) dissolved in 100 mL of 6 M HCl.[10] The resulting sulfide concentration was quantified spectrophotometrically using a Ulab-101 at a wavelength of 667 nm with a cuvette optical path length of 10 mm.

Biochemical analysis of rat blood
In the blood concentration of following metabolic substances were studied: glucose (REF# HP009.02; Calibrator solution contains glucose 10.0±0.5 mmol/L), triglycerides (TG, REF# HP022.04; Calibrator solution contains triglycerides 2.26±0.1 mmol/L), total cholesterol (TC, REF# HP026.07, Calibrator solution contains cholesterol 5.17±0.1 mmol/L), cholesterol from low-density lipoproteins (LDL-C, REF# HP026.05, Calibrator solution contains cholesterol 5.17±0.1 mmol/L), cholesterol from high-density lipoproteins (HDL-C, REF# HP026.03, Calibrator solution contains cholesterol 5.17±0.1 mmol/L). All abovementioned substances were evaluated by respective assays produced by "Filisit Diagnistika" (Ukraine) using spectrophotometer Ulab-101. Body mass index (BMI) was additionally calculated in accordance with established methodological recommendations.[11]

Determination of insulin-resistance indexes
In order to evaluate development of insulin resistance following indexes were calculated:
Triglyceride glucose index (TyG). TyG=Ln [TG (mg/dL)×FPG (mg/dL)÷2]
Triglyceride/high-density lipoproteins index (TG/HDL-C). TG/HDL-C=TG (mg/dL)÷HDL-C (mg/dL)
Triglyceride glucose body mass index (TyG-BMI). TyG-BMI=Ln [TG (mg/dL) × Glucose (mg/dL) ÷ 2] × BMI (kg/m^2).[12]
Metabolic score for insulin resistance (METS-IR) index. METS-IR=Ln [(2 × Glucose (mg/dL)) + TG (mg/dL)] × BMI (kg / m^2) Ln [HDL-C (mg/dL)].[12]

Statistical analysis
Statistical differences between groups were assessed using nonparametric analysis of variance according to the Kruskal-Wallis test, followed by pairwise post hoc comparisons using the Mann-Whitney U test. Differences were considered statistically significant at $p<0.05$. Data are presented as median (M) with the interquartile range (IQR). To control for type I error associated with multiple comparisons, a Bonferroni correction was applied. All statistical analyzes were performed using Microsoft Office Excel with the Real Statistics 2019 add-in (Charles Zaiontz).

Results

Changes in blood metabolic parameters.
Analysis of rat blood revealed that MetS modeling leads to increase in blood glucose level by 110.9% (Table 1). Under these conditions, the triglycerides content increased by 194.5%, the total cholesterol content increased by 51.5%, the LDL-C content increased by 60.0%, while HDL-C content decreased by 31.0%. Rat weight and BMI increased by 14.5% and 20.0%, respec-

tively. Analysis of insulin resistance indexes revealed that all studied indexes increased. TyG, TG/HDL-C, TyG-BMI and METS-IR increased by 22.5%, 310.3%, 50.8% and 21.4%, respectively.

All abovementioned changes correspond to typical symptoms of metabolic syndrome: hyperglycemia, hyperlipemia, dyslipidemia and insulin resistance.

Table 1. Metabolic changes in rat blood and insulin resistance indexes under conditions of metabolic syndrome and CRPIC administration (M(IQR))[a]

Parameters	Groups			
	Control, n=6	MetS group, n=6	CRPIC administration group, n=6	MetS+CRPIC administration group, n=6
Glucose, mg/dL	70.6 (68.1–71.9)	148.9 (145.0–151.0) *	68.9 (67.0–71.2) #	85.6 (82.3–87.6) */#/^
Triglycerides, mg/dL	82.3 (70.0–87.8)	242.4 (236.8–247.9) *	80.0 (75.6–91.2) #	108.9 (103.4–111.2) */#/^
Total cholesterol, mg/dL	45.6 (45.0–46.4)	69.1 (67.4–69.9) *	41.5 (40.4–45.8) #	53.3 (52.8–53.9) */#/^
LDL–C, mg/dL	6.5 (6.2–6.5)	10.4 (9.6–11.8) *	4.8 (4.4–5.4) */#	7.1 (6.6–7.7) #/^
HDL–C, mg/dL	21.6 (20.8–22.0)	14.9 (14.4–15.4) *	22.2 (21.0–23.2) #	27.0 (26.5–27.9) */#/^
Rat weight, g	214.5 (211.0–217.3)	245.5 (243.3–247.8) *	243.5 (242.3–247.8) *	265.0 (261.8–266.8) */#/^
BMI, g/cm^2	0.55 (0.47–0.55)	0.66 (0.66–0.67) *	0.57 (0.57–0.59) */#	0.59 (0.586–0.587) */#
TyG index	8.0 (7.8–8.0)	9.8 (9.80–9.81) *	7.9 (7.8–7.9) #	8.4 (8.39–8.43) */#/^
TG/HDL–C index	3.9 (3.1–4.2)	16.0 (15.1–17.3) *	3.7 (3.4–4.2) #	4.1 (3.7–4.2) #
TyG–BMI index	42.9 (36.8–44.4)	64.7 (64.4–65.7) *	45.2 (44.4–46.7) #	49.4 (49.2–50.2) */#/^
METS–IR index	5.6 (5.5–5.7)	6.8 (6.75–6.82) *	5.7 (5.6–5.7) #	5.9 (5.87–5.92) */#/^

[a] * – the data are statistically significantly different from the control group (p<0.05), # – the data are statistically significantly different from the experimental metabolic syndrome group (p<0.05), ^ – the data are statistically significantly different from the CRPIC administration (p<0.05)

Administration of CRPIC during MetS modelling increased blood sugar level by 21.2%, TG by 32.3%, TC by 16.9%, HDL-C by 25.0%, while the LDL-C content remained unchanged compared to the control group. Rat weight and BMI were elevated by 23.5% and 7.3%, respectively, compared to control. TyG, TyG-BMI and METS-IR increased by 5.0%, 15.2% and 5.4%, respectively. The TG / HDL-C index did not change compared to the control group.

Administration of CRPIC during MetS modelling modeling increased blood sugar level by 24.2%, TG by 36.1%, TC by 28.4%, HDL-C by 21.6%, LDL-C content increased by 47.9% in the CRPIC group. Rat weight increased by 8.8%, compared to the CRPIC group, while BMI remained unchanged. TyG, TyG-BMI and METS-IR increased by 6.3%, 9.3% and 3.5%, respectively. The TG/HDL-C index did not change compared to the CRPIC group.

Administration of CRPIC during MetS modelling decreased blood sugar level by 42.5%, TG by 55.1%, TC by 22.9%, LDL-C by 31.2%, while the HDL-C content elevated by 81.2% compared to the CRPIC group. Rat weight increased by 7.9%, while BMI decreased by 10.6% compared to the CRPIC group. TyG, TG/HDL-C, TyG-BMI and METS-IR decreased by 14.3%, 74.0%, 23.6% and 13.2%, respectively.

Changes in NO-cycle enzymes activities in rat heart

The MetS led to increase of total NOS activity by 46.9% compared to the control group (Fig. 1A). iNOS activity in these circumstances elevated by 49.0%, while cNOS activity decreased by 11.3% (Fig. 1B, Fig. 1C). Arginase activity increased by 29.9% compared to the control group (Fig. 1D). Analysis on the nitrate-nitrite pathway of NO production revealed that MetS modeling led to an increase of nitrate reductase activity by 27.9% and nitrite reductases activity was elevated by 155.9% compared to control group (Fig. 2A, Fig. 2B).

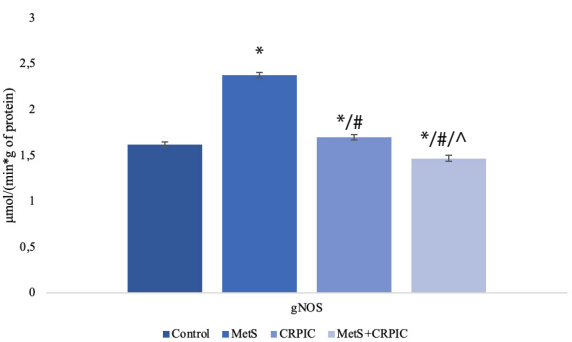

Fig. 1A. Total NO synthase (gNOS) activity in rat heart during introduction of chromium picolinate in the background of metabolic syndrome modelling, note: * – p<0.05 vs. control; # – p<0.05 vs. MetS; ^ – p<0.05 vs. CRPIC

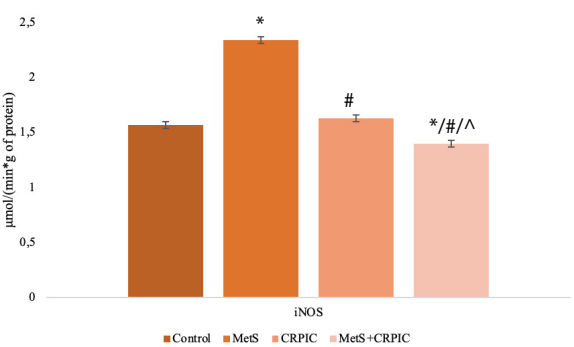

Fig. 1B. Inducible NOsynthase (iNOS) activity in rat heart during introduction of chromium picolinate in the background of metabolic syndrome modelling, note: * – p<0.05 vs. control; # – p<0.05 vs. MetS; ^ – p<0.05 vs. CRPIC

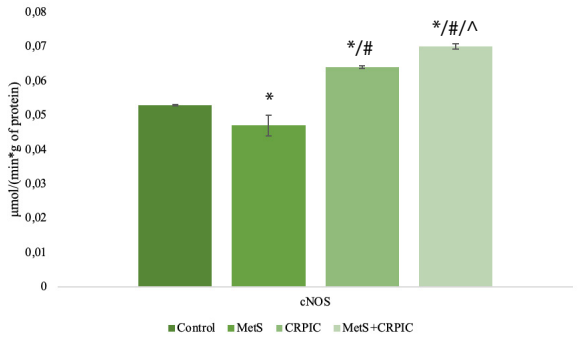

Fig. 1C. Constitutive NOsynthase (cNOS) activity in rat heart during the introduction of chromium picolinate in the background of metabolic syndrome modelling, note: * – p<0.05 vs. control; # – p<0.05 vs. MetS; ^ – p<0.05 vs. CRPIC

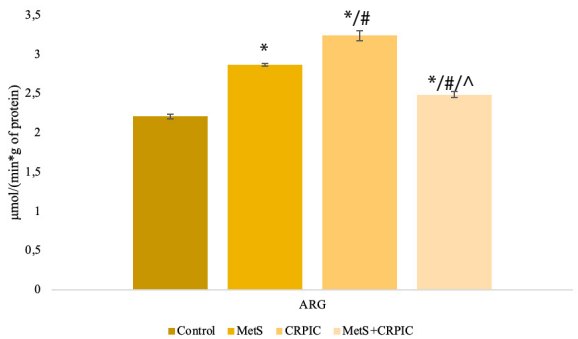

Fig. 1D. Total arginase (ARG) activity in the rat heart during the introduction of chromium picolinate in the background of metabolic syndrome modelling, note: * – p<0.05 vs. control; # – p<0.05 vs. MetS; ^ –p<0.05 vs. CRPIC

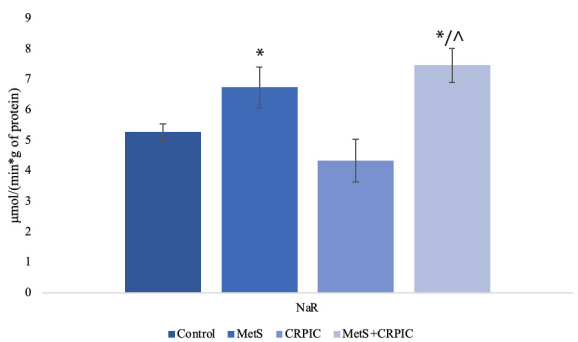

Fig. 2A. Activity of nitrate reductases (NaR) in rat heart during introduction of chromium picolinate on the background of metabolic syndrome modelling, note: * – p<0.05 vs. control; # – p<0.05 vs. MetS; ^ – p<0.05 vs. CRPIC

Administration of CRPIC to healthy animals resulted in a 4.9% increase in gNOS activity, attributable to a 20.8% increase in cNOS activity, whereas iNOS activity in the rat heart did not differ from that of the control group. Administration of CRPIC increased arginase activity in the rat heart by 46.6%. The activity of nitrate reductases did not change after CRPIC administration to healthy animals, but the activity of nitrite reductases increased by 144.8% compared to the control group.

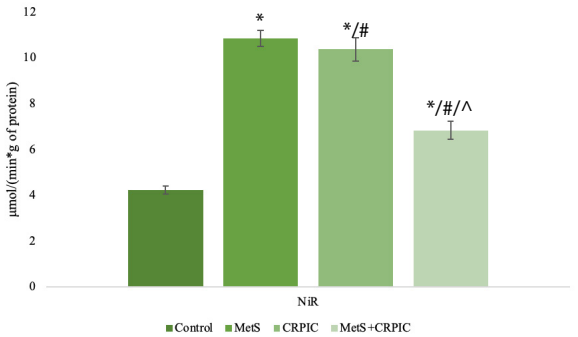

Fig. 2B. Activity of nitrite reductases (NiR) in rat heart during introduction of chromium picolinate on the background of metabolic syndrome modelling, note: * – p<0.05 vs. control; # – p<0.05 vs. MetS; ^ – p<0.05 vs. CRPIC

CRPIC administration resulted in a 28.6% reduction in gNOS activity, primarily due to a 30.3% decrease in iNOS activity, despite a 36.2% increase in cNOS activity in the rat heart relative to the MetS group. In addition, CRPIC treatment was associated with a 12.9% elevation in cardiac arginase activity compared with the MetS group. The activities of nitrate and nitrite reductases remained unchanged following CRPIC administration, showing no significant differences relative to the MetS group.

Administration of CRPIC during MetS modelling led to a decrease in gNOS activity by 9.3%, which happened due to a decrease in iNOS activity by 10.8% since cNOS activity increased by 32.1% relative to control. Administration of CRPIC increased arginase activity in the rat heart by 12.7%. The activity of nitrate and nitrite reductases after administration of CRPIC to animals with MetS increased by 41.6% and 61.3%, respectively, compared to the control group.

CRPIC administration during MetS modeling led to decrease in total NOS activity by 38.2%, which happened due to a decrease in iNOS activity by 40.2%, since cNOS activity increased by 48.9% compared to the MetS group. Administration of CRPIC decreased arginase activity in the rat heart by 13.2% compared to the MetS group. The activity of the nitrate reductases did not change and the activity of the nitrite reductases decreased by 37.0% compared to the MetS group.

Administration of CRPIC during MetS modeling was associated with a 13.5% reduction in gNOS activity, driven by a 14.1% decrease in iNOS activity, while cNOS activity in the rat heart increased by 9.4% relative to the CRPIC group. Cardiac arginase activity decreased by 23.1% compared to the CRPIC group. Nitrate reductase activity increased by 72.3%, whereas nitrite reductase activity decreased by 34.1% relative to the CRPIC group.

Changes in NO derivates content in heart of rats

During metabolic syndrome modelling nitrite and nitrosothiols content in rat heart decreased by 60.0% and 21.9%, respectively, compared to control group (Fig. 3A, Fig. 3C). Under these conditions peroxynitrite content increased by 320.0% (Fig. 3B). Analysis of concentration of nitric oxide metabolites revealed that administration of CRPIC to healthy animals decreased nitrite content by 11.0%, increased peroxynitrite content by 208.0%, and decreased nitrosothiols content by 15.1% in compared to control. Nitrite content increased by 122.6%, peroxynitrite content decreased by 26.7%, but nitrosothiols content did not change in comparison to the results of the MetS group.

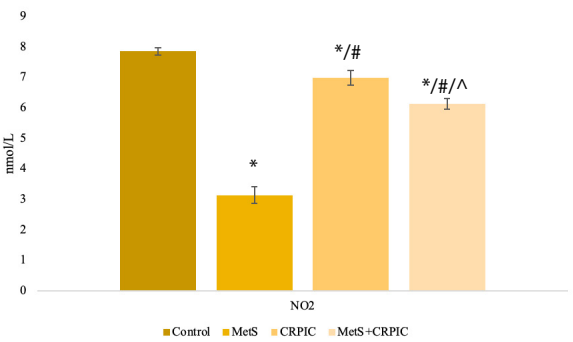

Fig. 3A. Nitrite (NO_2) content in the rat heart during the introduction of chromium picolinate in the background of metabolic syndrome modelling, note: * – p<0.05 vs. control; # – p<0.05 vs. MetS; ^ – p<0.05 vs. CRPIC

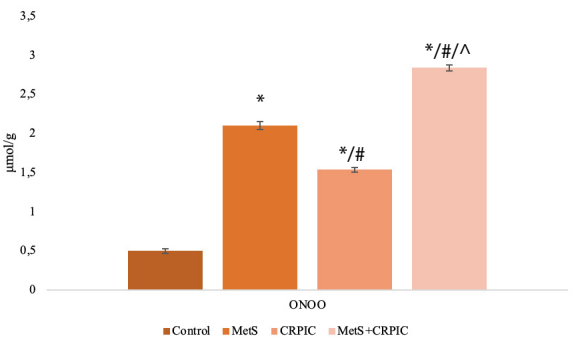

Fig. 3B. Peroxynitrite (ONOO) content in the rat heart during introduction of chromium picolinate in the background of metabolic syndrome modelling, note: * – p<0.05 vs. control; # – p<0.05 vs. MetS; ^ –p<0.05 vs. CRPIC

CRPIC administration during MetS modeling decreased nitrite content by 21.9%, increased the peroxynitrite content by 468.0% and decreased nitrosothiols content by 60.3% compared to the results of the control group. The nitrite content increased by 95.2%, the peroxynitrite content increased by 35.2%, and the nitrosothiol content decreased by 49.1% compared to MetS. However, the nitrite content decreased by 12.3%, the peroxynitrite content increased by 84.4% and nitrosothiols content decreased by 53.2% compared to the results of the CRPIC group.

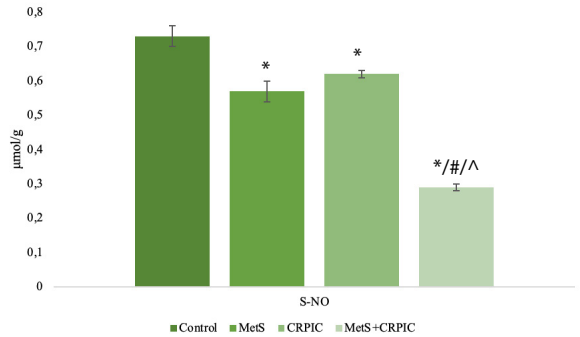

Fig. 3C. Nitrosothiols (S-NO) content in the rat heart during the introduction of chromium picolinate in the background of metabolic syndrome modelling, note: * – p<0.05 vs. control; # – p<0.05 vs. MetS; ^ –p<0.05 vs. CRPIC

H2S content in rat heart

MetS was associated with a 16.5% increase in myocardial H_2S content compared to the control group (Fig. 3D). In contrast, H_2S levels in the CRPIC-treated group were reduced by 15.5% compared to controls. Administration of CRPIC to healthy animals resulted in a 27.5% decrease in cardiac H_2S content compared to the MetS group. During MetS modeling, CRPIC treatment did not alter myocardial H_2S levels compared to controls; however, H_2S content was reduced by 16.8% compared to the MetS group and increased by 14.6% compared with the CRPIC group.

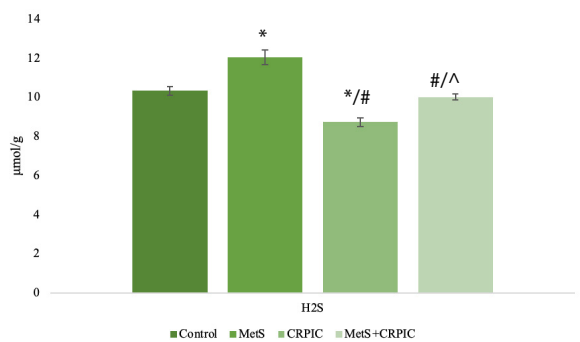

Fig. 3D. Hydrogen sulfide (H_2S) content in rat heart during introduction of chromium picolinate on the background of metabolic syndrome modelling, note: * – p<0.05 vs. control; # – p<0.05 vs. MetS; ^ –p<0.05 vs. CRPIC

Discussion

Changes observed in rat blood in MetS group are typical for development of metabolic syndrome (hyperglycemia, hyperlipemia, dyslipidemia and insulin resistance). These changes are caused by excessive calorie intake, which is the core essence of our model.[7] Such results correspond to data obtained by other scientists, who used the same experimental model.[13,14]

Administration of CRPIC to healthy animals revealed its ability to lower LDL-C and increase animal mass and BMI. Several literature sources show ability of chromium picolinate to lower LDL and very low-density lipoprotein (VLDL) content.[15,16] Such ability of CRPIC may be attributed to activation of p38 MAPK cascade and stimulation of cell division.[17] Since cholesterol is an element of cell membranes, new cells, formed due to stimulation of division by p38 MAPK activation, will require additional cholesterol, which is absent in the diet, leading lower LDL content in blood. BMI elevation of rats fed with CRPIC may be connected with ability of chromium ion to increase average daily BMI gain.[18]

Combination of CRPIC administration and MetS modelling revealed that CRPIC is effective in lowering glucose, triglycerides, total cholesterol, and LDL-C levels, which were elevated by excessive fructose intake.

In MetS group we observed increased NO production from NO-synthases, which was characterized by increased activity of iNOS and decreased cNOS activity. Increased iNOS activity was also observed by other scientists, who studied metabolic syndrome.[19,20] The reason for increased iNOS activity during MetS development lies in NF-κB activation, which controls iNOS gene expression.[21] Decreased cNOS activity in rat heart in MetS group may be associated with lowered activity of endothelial isoform of NOS (eNOS). During MetS lipid droplets in endothelium can inhibit eNOS activity, leading to endothelial dysfunction.[22]

MetS also increased production of nitric oxide from L-arginine-independent pathway, namely from nitrate and nitrite reductases. One of the known potent nitrate-nitrite reduction enzymes is xanthine oxidoreductase (XOR), which consists of two domains: xanthine dehydrogenase (XDH, EC 1.17.1.4) and xanthine oxidase (XO, EC 1.17.3.2).[23] Main substrate of XOR is hypoxanthine, which is transformed by XDH domain to uric acid. Since during MetS purine catabolism is severely enhanced, increased nitrate and nitrite reductases activity observed in MetS group can be attributed to XOR activation.[24,25]

Increased peroxynitrite content in rat heart may be indication of nitrosative stress development. The reasons for the increase in the formation of peroxynitrite during metabolic syndrome can be associated with eNOS uncoupling.[26] Uncoupling of eNOS provides superoxide, while the sources of NO necessary for peroxynitrite formation of peroxynitrites may vary from iNOS to NiR.

The increase in H_2S content in the rat heart observed in the present study can be attributed to enhanced activity of cystathionine-β-synthase (CBS, EC 4.2.1.22), which is known to be induced by excessive fructose consumption.[27] The increase in myocardial H_2S content observed during metabolic syndrome may be interpreted as an adaptive compensatory response to the increased conversion of nitric oxide to peroxynitrite, a process that attenuates NO-dependent smooth muscle relaxation. In this context, elevated H_2S may partially compensate for impaired NO bioavailability, as hydrogen sulfide is capable of directly targeting vascular smooth muscle cells and inducing vasorelaxation.[28,29] The scientific literature provides evidence that H_2S can act as peroxynitrite scavenger forming sulfenic acid (HSOH).[30]

Administration of CRPIC to healthy animals revealed a sharp increase in nitrite reduction activity, which can be explained by the action of chromium ions of chromium picolinate, because some nitrite reductases contain Cr (IV) in their active center; therefore, excessive chromium intake can increase their activity.[31] Elevation of the peroxynitrite content in the rat heart during administration of CRPIC to healthy animals can cause damage to heart tissue and requires further study. The dose chosen for rats in our study is much higher than the one used in humans, therefore peroxynitrite elevation may be the result of CRPIC overdosage. And, it is worth mentioning, that longitudinal studies of lower doses in humans revealed no harmful effects.[32] The source of NO needed to form peroxynitrite is increased NiR activity, observed in CRPIC administration group, while superoxide may come from toxic effects of excessive chromium ions accumulation.[33] Increased H_2S content under these conditions is an adoptive response towards peroxynitrite accumulation. Elevated cNOS activity may be attributed to the ability of CRPIC to enhance endothelial functions.[34]

Observing the combined effects of administration of CRPIC and MetS modeling, we established that the ability of CRPIC to stimulate endothelium prevails over adverse effects on it caused by MetS modelling. The observed reduction in iNOS activity may be attributed to a complex regulatory interplay between CRPIC-induced activation of p38 signaling and MetS-associated activation of the transcription factor NF-κB, which together modulate the transcriptional and post-transcriptional control of iNOS expression.[35] We also observed a cumulative effect of administration of CRPIC and MetS modelling on peroxynitrite content in rat heart. A decrease in H_2S content compared to MetS group may be an indication of exhaustion of this adoptive mechanism.

CRPIC activating action on p38 MAPK cascade may be associated with stimulation of p38 alpha isoform of p38 family, since part of its effects can be alleviated by specific p38 alpha inhibitor SB203580.[36] Such activation may be beneficial for correction of metabolic changes, but may be harmful for myocardium. It is worth mentioning that CRPIC has a stimulation effect on L-arginine-independent nitric oxide production, which may be either due to influence on specific enzymes or due to non-enzymatic reduction of nitrates/nitrites to nitric oxide, which requires further study.

Hydrogen sulfide plays a significant role in maintaining cellular redox homeostasis by directly neutralizing reactive oxygen and nitrogen species and by regulating the function of redox-sensitive proteins via persulfidation-dependent post-translational modification.[37] In addition, H_2S reinforces antioxidant capacity by inducing the expression and activity of key enzymes, including superoxide dismutase, catalase, and glutathione peroxidase, while maintaining mitochondrial integrity and attenuating oxidative stress–mediated cellular injury.[38]

The present findings provide mechanistic insight into the cardiac consequences of MetS and the dualistic effects of chromium picolinate supplementation. The observed upregulation of iNOS activity and increased NO generation from nitrate–nitrite reductases during MetS suggest that excessive NO and subsequent peroxynitrite formation play a central role in myocardial oxidative-nitrosative injury.

Prolonged administration of CRPIC in metabolically healthy individuals may exert cardiotoxic effects by enhancing nitrosative stress. Administration of CRPIC during MetS revealed a modulatory role of CRPIC realized by attenuating excessive NO production from both NO synthases and nitrite reductases. However, the high ONOO content in the MetS + CRPIC group suggests the need to correct the dose or duration of treatment.

Study limitations

The principal limitation of the present study is the relatively small number of animals included in each experimental group. Additional limitations include the lack of direct markers of oxidative stress (ROS production, lipid peroxidation, antioxidant enzyme activity), and the absence of histological and functional cardiac assessments.

Conclusion

Metabolic syndrome changes the amount of nitric oxide produced in the rat heart by enhancing the inducible activity of NO-synthase and intensity of nitric oxide production from nitrate-nitrite reductases. Enhanced nitric oxide production in the rat heart under conditions of metabolic syndrome results in a shift toward the predominance of the peroxynitrite pathway of nitric oxide utilization.

Prolonged administration of chromium picolinate to healthy animals for 60 days can exert cardiotoxic effects, potentially mediated by enhanced generation of nitric oxide through nitrite reductase pathways and the concomitant increase in peroxynitrite levels.

Administration of chromium picolinate during metabolic syndrome modelling attenuates excessive nitric oxide production derived from both synthetic and reductive pathways, while simultaneously promoting increased peroxynitrite formation.

Declarations

Funding

There was no external funding for this work.

Author contributions

Conceptualization, O.A. and V.K.; Methodology, O.A.; Validation, O.A., A.M. and V.K.; Formal Analysis, O.A.; Investigation, O.A. and A.M.; Resources, O.A.; Data Curation, O.A. and V.K.; Writing – Original Draft Preparation, O.A. and A.M.; Writing – Review & Editing, O.A., A.M. and V.K.; Supervision, V.K.; Project Administration, O.A. and V.K.

Conflicts of interest

The authors declare no competing interests.

Data availability

The datasets generated during and/or analyzed during the current study are available from the corresponding author on reasonable request.

Ethics approval

All experiments with laboratory animals were approved by Bioethical Committee of Poltava State Medical University (Record No. 206 from 24.06.2022).

References

1. Lushchak VI, Covasa M, Abrat OB, et al. Risks of obesity and diabetes development in the population of the Ivano-Frankivsk region in Ukraine. *EXCLI J*. 2023;22:1047-1054. doi:10.17179/excli2023-6296
2. Chandrasekaran P, Weiskirchen R. The Role of Obesity in Type 2 Diabetes Mellitus-An Overview. *Int J Mol Sci*. 2024;25(3):1882. doi:10.3390/ijms25031882
3. Sanz RL, Inserra F, García Menéndez S, Mazzei L, Ferder L, Manucha W. Metabolic Syndrome and Cardiac Remodeling Due to Mitochondrial Oxidative Stress Involving Gliflozins and Sirtuins. *Curr Hypertens Rep*. 2023;25(6):91-106. doi:10.1007/s11906-023-01240-w
4. Liu J, Aylor KW, Chai W, Barrett EJ, Liu Z. Metformin prevents endothelial oxidative stress and microvascular insulin resistance during obesity development in male rats. *Am J Physiol Endocrinol Metab*. 2022;322(3):E293-E306. doi:10.1152/ajpendo.00240.2021
5. Ruan G, Wu F, Shi D, Sun H, Wang F, Xu C. Metformin: update on mechanisms of action on liver diseases. *Front Nutr*. 2023;10:1327814. doi:10.3389/fnut.2023.1327814
6. Moradi F, Kooshki F, Nokhostin F, Khoshbaten M, Bazyar H, Pourghassem Gargari B. A pilot study of the effects of chromium picolinate supplementation on serum fetuin-A, metabolic and inflammatory factors in patients with nonalcoholic fatty liver disease: A double-blind, placebo-

-controlled trial. *J Trace Elem Med Biol*. 2021;63:126659. doi:10.1016/j.jtemb.2020.126659
7. Mamikutty N, Thent ZC, Sapri SR, Sahruddin NN, Mohd Yusof MR, Haji Suhaimi F. The establishment of metabolic syndrome model by induction of fructose drinking water in male Wistar rats. *Biomed Res Int*. 2014;2014:263897. doi:10.1155/2014/263897
8. Sahin K, Tuzcu M, Orhan C, et al. Anti-diabetic activity of chromium picolinate and biotin in rats with type 2 diabetes induced by high-fat diet and streptozotocin. *Br J Nutr*. 2013;110(2):197-205. doi:10.1017/S0007114512004850
9. Yelins'ka AM, Akimov OYe, Kostenko VO. Role of AP-1 transcriptional factor in development of oxidative and nitrosative stress in periodontal tissues during systemic inflammatory response. *Ukr Biochem J*. 2019;91(1):80-85. doi:10.15407/ubj91.01.080
10. Mykytenko A, Akimov O, Yeroshenko G, Neporada K. Phenformin attenuates the oxidative-nitrosative stress in the liver of rats under long-term ethanol administration. *Ukr Biochem J*. 2024;96(3):22-30. doi:10.15407/ubj96.03.022
11. El-Kafoury BMA, Bahgat NM, Abdel-Hady EA, Samad AAAE, Shawky MK, Mohamed FA. Impaired metabolic and hepatic functions following subcutaneous lipectomy in adult obese rats. *Exp Physiol*. 2019;104(11):1661-1677. doi:10.1113/EP087670
12. Zhang Y, Wang R, Fu X, Song H. Non-insulin-based insulin resistance indexes in predicting severity for coronary artery disease. *Diabetol Metab Syndr*. 2022;14(1):191. doi:10.1186/s13098-022-00967-x
13. Andrade N, Rodrigues I, Carmo F, et al. Sustainable Utilization of Coffee Pulp, a By-Product of Coffee Production: Effects on Metabolic Syndrome in Fructose-Fed Rats. *Antioxidants (Basel)*. 2025;14(3):266. doi:10.3390/antiox14030266
14. Mohammad-Sadeghipour M, Afsharinasab M, Mohamadi M, Mahmoodi M, Falahati-Pour SK, Hajizadeh MR. The Effects of Hydro-Alcoholic Extract of Fenugreek Seeds on the Lipid Profile and Oxidative Stress in Fructose-Fed Rats. *J Obes Metab Syndr*. 2020;29(3):198-207. doi:10.7570/jomes19051
15. Geohas J, Daly A, Juturu V, Finch M, Komorowski JR. Chromium picolinate and biotin combination reduces atherogenic index of plasma in patients with type 2 diabetes mellitus: a placebo-controlled, double-blinded, randomized clinical trial. *Am J Med Sci*. 2007;333(3):145-53. doi:10.1097/MAJ.0b013e318031b3c9
16. Paiva AN, Lima JG, Medeiros AC, et al. Beneficial effects of oral chromium picolinate supplementation on glycemic control in patients with type 2 diabetes: A randomized clinical study. *J Trace Elem Med Biol*. 2015;32:66-72. doi:10.1016/j.jtemb.2015.05.006
17. Moreira R, Martins AD, Alves MG, de Lourdes Pereira M, Oliveira PF. A Comprehensive Review of the Impact of Chromium Picolinate on Testicular Steroidogenesis and Antioxidant Balance. *Antioxidants (Basel)*. 2023;12(8):1572. doi:10.3390/antiox12081572
18. Zha LY, Wang MQ, Xu ZR, Gu LY. Efficacy of chromium(III) supplementation on growth, body composition, serum parameters, and tissue chromium in rats. *Biol Trace Elem Res*. 2007;119(1):42-50. doi:10.1007/s12011-007-0042-8
19. Kostić S, Tasić I, Stojanović N, et al. Impact of Obesity on Target Organ Damage in Patients with Metabolic Syndrome. *Diagnostics (Basel)*. 2024;14(14):1569. doi:10.3390/diagnostics14141569
20. Barbato JE, Zuckerbraun BS, Overhaus M, Raman KG, Tzeng E. Nitric oxide modulates vascular inflammation and intimal hyperplasia in insulin resistance and the metabolic syndrome. *Am J Physiol Heart Circ Physiol*. 2005;289(1):H228-36. doi:10.1152/ajpheart.00982.2004
21. Kostenko V, Akimov O, Gutnik O, et al. Modulation of redox-sensitive transcription factors with polyphenols as pathogenetically grounded approach in therapy of systemic inflammatory response. *Heliyon*. 2023;9(5):e15551. doi:10.1016/j.heliyon.2023.e15551
22. Kim B, Zhao W, Tang SY, et al. Endothelial lipid droplets suppress eNOS to link high fat consumption to blood pressure elevation. *J Clin Invest*. 2023;133(24):e173160. doi:10.1172/JCI173160
23. Bortolotti M, Polito L, Battelli MG, Bolognesi A. Xanthine oxidoreductase: One enzyme for multiple physiological tasks. *Redox Biol*. 2021;41:101882. doi:10.1016/j.redox.2021.101882
24. Lubawy M, Formanowicz D. High-Fructose Diet-Induced Hyperuricemia Accompanying Metabolic Syndrome-Mechanisms and Dietary Therapy Proposals. *Int J Environ Res Public Health*. 2023;20(4):3596. doi:10.3390/ijerph20043596
25. Yanai H, Adachi H, Hakoshima M, Katsuyama H. Molecular Biological and Clinical Understanding of the Pathophysiology and Treatments of Hyperuricemia and Its Association with Metabolic Syndrome, Cardiovascular Diseases and Chronic Kidney Disease. *Int J Mol Sci*. 2021;22(17):9221. doi:10.3390/ijms22179221
26. Engin A. Endothelial Dysfunction in Obesity and Therapeutic Targets. *Adv Exp Med Biol*. 2024;1460:489-538. doi:10.1007/978-3-031-63657-8_17
27. Berenyiova A, Cebova M, Aydemir BG, Golas S, Majzunova M, Cacanyiova S. Vasoactive Effects of Chronic Treatment with Fructose and Slow-Releasing H2S Donor GYY-4137 in Spontaneously Hypertensive Rats: The Role of Nitroso and Sulfide Signalization. *Int J Mol Sci*. 2022;23(16):9215. doi:10.3390/ijms23169215
28. Smimmo M, Casale V, Casillo GM, et al. Hydrogen sulfide dysfunction in metabolic syndrome-associated vascular complications involves cGMP regulation through soluble guanylyl cyclase persulfidation. *Biomed Pharmacother*. 2024;174:116466. doi:10.1016/j.biopha.2024.116466
29. Bełtowski J, Wiórkowski K. Role of Hydrogen Sulfide and Polysulfides in the Regulation of Lipolysis in the Adi-

pose Tissue: Possible Implications for the Pathogenesis of Metabolic Syndrome. *Int J Mol Sci*. 2022;23(3):1346. doi:10.3390/ijms23031346

30. Andrés CMC, Pérez de la Lastra JM, Andrés Juan C, Plou FJ, Pérez-Lebeña E. Chemistry of Hydrogen Sulfide-Pathological and Physiological Functions in Mammalian Cells. *Cells*. 2023;12(23):2684. doi:10.3390/cells12232684
31. Shi L, Liu B, Zhang X, et al. Cloning of Nitrate Reductase and Nitrite Reductase Genes and Their Functional Analysis in Regulating Cr(VI) Reduction in Ectomycorrhizal Fungus Pisolithus sp.1. *Front Microbiol*. 2022;13:926748. doi:10.3389/fmicb.2022.926748
32. Georgaki MN, Tsokkou S, Keramas A, Papamitsou T, Karachrysafi S, Kazakis N. Chromium supplementation and type 2 diabetes mellitus: an extensive systematic review. *Environ Geochem Health*. 2024;46(12):515. doi:10.1007/s10653-024-02297-5
33. Singh V, Singh N, Verma M, et al. Hexavalent-Chromium-Induced Oxidative Stress and the Protective Role of Antioxidants against Cellular Toxicity. *Antioxidants (Basel)*. 2022;11(12):2375. doi:10.3390/antiox11122375
34. Imanparast F, Mashayekhi FJ, Kamankesh F, Rafiei F, Mohaghegh P, Alimoradian A. Improving the endothelial dysfunction in type 2 diabetes with chromium and vitamin D3 by reducing homocysteine and oxidative stress: A randomized placebo-controlled trial. *J Trace Elem Med Biol*. 2020;62:126639. doi:10.1016/j.jtemb.2020.126639
35. Bansal A, Mostafa MM, Kooi C, et al. Interplay between nuclear factor-κB, p38 MAPK, and glucocorticoid receptor signaling synergistically induces functional TLR2 in lung epithelial cells. *J Biol Chem*. 2022;298(4):101747. doi:10.1016/j.jbc.2022.101747
36. Wang YQ, Yao MH. Effects of chromium picolinate on glucose uptake in insulin-resistant 3T3-L1 adipocytes involve activation of p38 MAPK. *J Nutr Biochem*. 2009;20(12):982-91. doi:10.1016/j.jnutbio.2008.09.002
37. Murphy B, Bhattacharya R, Mukherjee P. Hydrogen sulfide signaling in mitochondria and disease. *FASEB J*. 2019;33(12):13098-13125. doi:10.1096/fj.201901304R
38. Soni P, Paswan S, Paul BD, Thomas B. Intersection of H2S and Nrf2 signaling: Therapeutic opportunities for neurodegenerative diseases. *Neurotherapeutics*. 2025;22(6):e00627. doi:10.1016/j.neurot.2025.e00627

Rzeszów University Press 2026
ISSN 2544-1361 (online)
doi: 10.15584/ejcem.2026.2.5

http://www.ejcem.ur.edu.pl
European Journal of Clinical and Experimental Medicine
Eur J Clin Exp Med 2026; 24 (2): 273–281

ORIGINAL PAPER

Association of vitamin D deficiency with inflammatory cytokines and disease severity in chronic heart failure

Fazil Choban Almammadov

Department of Family Medicine, Azerbaijan Medical University, Baku, Azerbaijan

ABSTRACT

Introduction and aim. Vitamin D deficiency has been associated with impaired cardiovascular dysfunction and adverse outcomes in chronic heart failure (CHF); yet the connection between inflammatory and cardiac biomarkers in different disease severities remains incompletely understood. Therefore, this study aimed to investigate the role of vitamin D and related biochemical parameters in the etiopathophysiology and severity of chronic heart failure.

Material and methods. A total of 219 people diagnosed with chronic heart failure, aged 30 and 89 years, were enrolled and stratified according to the functional class (I–II, n=123; III–IV, n=96). An age and sex-matched control group of 51 apparently healthy individuals was included. Serum levels of vitamin D, natriuretic peptide (BNP), N-terminal pro–brain natriuretic peptide (NT-proBNP), interleukin-6 (IL-6), interleukin-18 (IL-18) and tumor necrosis factor-alpha (TNF-α), galectin-3 and fibroblast growth factor-23 (FGF-23) were quantified using validated immunoassays. Comparisons between groups were performed using nonparametric statistical tests. Associations between variables were evaluated using Spearman's correlation analysis. The diagnostic utility of the selected biomarkers for different levels of severity of CHF was evaluated using receiver operating characteristic (ROC) curve analysis.

Results. Vitamin D deficiency was associated with CHF severity. Across increasing NYHA functional classes, serum levels of IL-6, IL-18, TNF-α, BNP, NT-proBNP, galectin-3, and FGF-23 differed significantly ($p<0.001$). Vitamin D concentrations were positively associated with left ventricular ejection fraction and inversely related to BNP, NT-proBNP, IL-6, IL-18, TNF-α, galectin-3, and FGF-23. ROC analysis indicated that IL-6 (AUC 0.799, sensitivity 75%, specificity 78%) and galectin-3 (AUC 0.791, sensitivity 72%, specificity 80%) were the most discriminative biomarkers in patients with CHF with vitamin D deficiency, supporting their clinical utility for risk stratification and disease monitoring**.**

Conclusion. This study provides novel evidence by integrating inflammatory cytokines, galectin-3, FGF-23, and natriuretic peptides in patients with vitamin D-deficient CHF, identifying IL-6 and galectin-3 as the most discriminative biomarkers of disease severity in this clinical setting.

Keywords. chronic heart failure, cytokines, FGF-23, galectin-3, vitamin D

Introduction

Chronic heart failure (CHF) continues to pose significant challenges in contemporary medicine.[1,2] Its prevalence is expected to increase due to increasing rates of primary etiologies, including arterial hypertension, ischemic heart disease, and type 2 diabetes mellitus. Despite advances in treatment and preventive strategies, patients with CHF continue to face high mortality, frequent hospitalizations, and multiple comorbidities.[3] Therefore, there is a continued need for therapeutic approaches that improve clinical outcomes and quality of life in these patients.

Corresponding author: Fazil Choban Almammadov, e-mail: xeyalcafarov4@gmail.com

Received: 5.09.2025 / Revised: 13.01.2026 / Accepted: 20.01.2026 / Published: 30.06.2026

Almammadov FC. Association of vitamin D deficiency with inflammatory cytokines and disease severity in chronic heart failure. *Eur J Clin Exp Med.* 2026;24(2):273–281. doi: 10.15584/ejcem.2026.2.5.

In recent years, vitamin D deficiency has attracted growing attention in the context of CHF. Globally, approximately 40.4% of people exhibit vitamin D deficiency.[4] Multiple studies have shown links of vitamin D deficiency with various cardiovascular conditions, such as heart failure, arterial hypertension, and atrial fibrillation.[1,5] Insufficient vitamin D can promote activation of the renin–angiotensin–aldosterone system, trigger inflammatory pathways, and affect endothelial function.[6] Production of pro-inflammatory cytokines, including interleukin-8 (IL-8) and tumor necrosis factor-alpha (TNF-α) is up-regulated, promoting oxidative stress. Vitamin D modulates the NF-κB pathway, thus reducing the production of interleukin-6 (IL-6), interleukin-12 (IL-12), interferon-γ, and TNF-α.[7-9] This pro-inflammatory environment coexists with neurohormonal activation and endothelial dysfunction, creating conditions favorable for adverse ventricular remodeling.[10,11]

Fibro-inflammatory remodeling is also reflected in galectin-3, which increases with macrophage activation and interstitial fibrosis, correlated with adverse structural remodeling and poorer results in CHF.[12,13] CHF is also associated with activation of mineral metabolism pathways. Fibroblast growth factor-23 (FGF-23) levels increase in patients experiencing systemic inflammation and cardiorenal stress, and evidence suggests that FGF-23 contributes to the progression of cardiovascular disease.[14,15] Within the mineral–bone–cardiac axis, FGF-23 typically increases along with inflammatory activity and renal dysfunction. Experimental and clinical evidence indicates a bidirectional link between inflammatory signaling and FGF-23 expression, positioning FGF-23 as both a mediator and a marker of maladaptive remodeling in CHF, although its direct myocardial effects remain debated.[16,17] Hemodynamic overload and neurohormonal activation are reflected by natriuretic peptides, such as natriuretic peptide (BNP) and N-terminal pro–brain natriuretic peptide (NT-proBNP), which increase with stress in the ventricular wall and correlate with inflammatory activity. These markers serve as complementary indices to cytokines and fibrosis biomarkers in vitamin D–deficient CHF phenotypes.[18,19]

The selected biomarker panel integrates inflammatory, fibrotic, mineral metabolism, and natriuretic markers to comprehensively assess disease severity in patients with vitamin D-deficient CHF.[20] While prior studies have examined single biomarkers or limited pathways, the present study provides novel insights by evaluating this panel, identifying key pathophysiological links, and supporting the evaluation of disease progression.

Aim

The aim of this study was to investigate the role of vitamin D and related biochemical parameters in the etiopathophysiology and severity of CHF.

Material and methods

Study design and setting

This was a multicenter, cross-sectional observational study**.** Patients were consecutively enrolled during routine visits to outpatient clinics or inpatient departments at three tertiary care centers in Baku, Azerbaijan: Republican Clinical Center, Sabunchu Clinical Center, and 1st Clinical Medical Center, between 2023 and 2024. Seasonal variations in vitamin D levels were taken into account during recruitment to minimize confounders.

Participants

A cohort of 219 people diagnosed with chronic heart failure (CHF), aged 30 to 89 years (mean 61.5±0.7 years), was recruited. The classification was performed according to the New York Heart Association (NYHA) functional scale: 123 in classes I-II (mean age 60.4±1.0 years) and 96 in classes III-IV (mean age 62.9±1.0 years). All CHF patients were clinically stable at enrollment, without recent hospitalization or acute decompensation, to minimize variability in biomarker levels, particularly BNP and inflammatory markers.

Heart failure phenotype

The cohort consisted of patients who presented primarily with heart failure with reduced ejection fraction (HFrEF, EF <40%). However, the median EF in NYHA I–II patients was greater than 40% (Me=68.0%, Q1–Q3: 62.0–71.0), indicating that this subgroup included a few patients with HFmrEF (EF 40–49%). The median EF for NYHA III–IV was 40.0% (Q1–Q3: 33.0–46.0). All analyzes were performed on the combined HF population and results are interpreted accordingly. The main etiologies of CHF were coronary artery disease, arterial hypertension, and dilated cardiomyopathy.

Control group

The study included 51 healthy volunteers, matched by age and sex, who were recruited from hospital personnel in the same clinical centers as the patient. The controls were verified to have normal vitamin D levels and were free of cardiovascular, renal, or inflammatory diseases, with no acute infections at the time of blood collection. Potential bias related to occupational health, lifestyle, and socioeconomic differences is acknowledged.

Exclusion criteria

Exclusion criteria included acute or chronic kidney failure, liver failure, infectious or inflammatory diseases, recent use of diuretics or steroids, vitamin D and/or calcium supplementation within the previous two months, hypoparathyroidism and hypothyroidism. Patients with eGFR <60 ml/min/1.73 m^2 or known chronic kidney disease were excluded to ensure normal kidney function at baseline.

Potential confounding factors

Baseline assessments included variables that could potentially confound the results, such as body mass index (BMI), smoking habits, concomitant medications (ACE inhibitors, ARNI, beta-blockers, statins), exposure to sunlight, and seasonal variations. These factors were recognized as potentially influencing vitamin D and related biomarker levels; No multivariate adjustment was performed, which represents a limitation inherent in the observational design.

Echocardiography

Two-dimensional Doppler imaging using the Simpson's biplane method (GE Vivid E95, Philips EPIQ 7) was performed by experienced cardiologists following standardized protocols to minimize variability between and intra-operator variability. Echocardiography was performed the same day as blood collection.

Blood collection and biomarker analysis

Morning blood samples were obtained after patients fasted overnight. Vitamin D, BNP, and NT-proBNP were analyzed immediately; samples for cytokines and galectin-3 were stored at -70°C until assay. Each assay was carried out in batches, with samples from patients and controls analyzed simultaneously and blinded to NYHA classification to reduce variability between assays. Calibration between laboratories ensured methodological consistency.

Creatinine was measured using a human immunoassay (mg/dL). BNP and NT-proBNP were analyzed with Roche Elecsys immunoassays (pg/mL). Cytokines IL-6, IL-18 and TNF-α were measured using Vector Best ELISA kits (pg/mL). Galectin-3 concentrations were determined by RayBiotech ELISA (ng/mL), and FGF-23 was assessed using a Human FGF-23 ELISA (pg/mL). Serum 25-hydroxyvitamin D [25(OH)D] was measured with a Bioaktiva Diagnostic immunoassay (ng/mL). All assays were performed in batches, with patient and control samples analyzed concurrently and blinded to NYHA class, and interlaboratory calibration was conducted to ensure consistency across measurements. The coefficients of variation within and between the assays were less than 10%, and the sensitivity of the assay fell within the ranges recommended by the manufacturer.

Vitamin D measurement

Serum 25-hydroxyvitamin D [25(OH)D] was measured using a validated immunoassay (Bioaktiva Diagnostic). Concentrations are reported in nanograms per milliliter. Vitamin D deficiency: <20 ng/ml; insufficiency: 20–30 ng/ml; sufficiency: >30 ng/ml, in accordance with current clinical guidelines.

Statistical methods

Data are expressed as median (Me), 25th (Q1) and 75th (Q3) percentiles. Nonparametric comparisons between two groups were made using the Mann-Whitney U test, and differences between three groups were assessed with the Kruskal-Wallis test. Fold increases or decreases reported in the results section were calculated as the ratio of median values. Spearman's correlation evaluated the relationships between variables. The diagnostic ability of inflammatory and fibrosis-associated biomarkers was evaluated in CHF patients with vitamin D deficiency using a receiver operating characteristic (ROC) curve. The outcome variable was CHF severity, classified according to NYHA functional class (I–II vs III–IV), with thresholds determined using the Youden index to maximize sensitivity and specificity. The area under the receiver operating characteristic curve (AUC) was determined with 95% confidence intervals (CI) and the variability of estimates was expressed as standard errors. The sample size was justified based on previous CHF biomarker studies, ensuring adequate power for detecting significant differences. Data gaps were minimal and handled by list deletion. A p-value of less than 0.05 was considered statistically significant and all analyses were performed using IBM SPSS Statistics version 26 (Armonk, NY, USA).

Ethics

The study was in accordance with the Declaration of Helsinki and was approved by the Ethics Committee of the Azerbaijan Medical University, approval No. 3/2018, dated 16.09.2018.

Results

According to echocardiographic data, the median EF was 40.0% (Q1-Q3: 33.5-46.0%) in patients in NYHA class I-II and 37.5% (Q1-Q3:31.5-41.5%) in NYHA class III-IV, compared with 68.0% (Q1-Q3: 62.0-71.0%) in the healthy control group. EF was significantly lower in both NYHA I–II and III–IV patients compared to controls ($p<0.001$). No significant differences in blood creatinine levels were observed between CHF patients, indicating preserved renal function ($p=0.283$) (Table 1).

There were no statistically significant differences in serum creatinine concentration between the patients. The median BNP concentration was markedly elevated, showing a 10.8-fold increase in CHF patients of the NYHA functional class I–II (median 538.0 pg/mL; Q1–Q3: 423.0–628.0; $p<0.001$) and a 12.7-fold increase in those with NYHA class III–IV (634.0; 557.5–759.5 pg/mL, $p<0.001$) compared to the control group (50.0; 29.0–63.0 pg/mL). Similarly, the median concentration of NT-proBNP was significantly higher, 19.8 times higher in patients with NYHA class I–II (1285.0; 954.0–

Table 1. Changes in functional and biochemical parameters of patients with chronic heart failure according to the stage of the disease*

Parameters	Groups												p#
	Control				NYHA class I-II				NYHA class III-IV				
	M	Me	Q1	Q3	M	Me	Q1	Q3	M	Me	Q1	Q3	
Ejection fraction	66.9	68.0	62.0	71.0	39.5	40.0	33.0	46.0	36.8	37.5	31.5	41.5	<0.001
p						<0.001				<0.001			
p_1										0.003			
Creatinine, mg/dL	0.86	0.88	0.76	0.96	0.90	0.92	0.79	1.00	0.89	0.89	0.76	1.01	0.283
p						0.112				0.488			
p_1										0.376			
Vit. D, ng/mL	43.5	42.0	38.0	48.0	28.6	29.0	21.0	37.0	20.5	17.5	12.5	28.0	<0.001
p						<0.001				<0.001			
p_1										<0.001			
BNP, pg/mL	46.2	50.0	29.0	63.0	541.1	538.0	423.0	628.0	663.7	634.0	557.5	759.5	<0.001
p						<0.001				<0.001			
p_1										<0.001			
NT-pro-BNP, pg/mL	72.5	65.0	46.0	96.0	1270.1	1285.0	954.0	1485.0	1662.0	1688.5	1556.5	1845.5	<0.001
p						<0.001				<0.001			
p_1										<0.001			
IL-6, pg/mL	2.26	2.00	1.60	2.90	3.59	3.50	3.10	4.10	4.74	4.80	4.00	5.30	<0.001
p						<0.001				<0.001			
p_1										<0.001			
IL-18, pg/mL	197.0	210.0	146.9	243.5	366.9	368.0	295.0	430.0	409.9	409.5	350.0	485.5	<0.001
p						<0.001				<0.001			
p_1										0.003			
TNF-α, pg/mL	4.9	5.0	4.6	5.3	7.3	7.3	6.5	7.9	8.2	8.1	7.3	8.9	<0.001
p						<0.001				<0.001			
p_1										<0.001			
Galectin-3, ng/mL	7.3	7.0	5.5	9.6	14.2	14.4	11.8	16.3	18.1	18.1	15.4	19.4	
p						<0.001				<0.001			
p_1										<0.001			
FGF-23, pg/mL	48.3	48.2	39.1	61.2	55.0	53.4	48.9	62.9	58.2	56.4	47.1	65.9	0.001
p						0.003				<0.001			
p_1										0.194			

* M – mean, Me – median, Q1 – first quartile (25th percentile), Q3 – third quartile (75th percentile), p – significance versus controls, p1 – significance versus NYHA I–II, p-values were determined using the Mann-Whitney U test, while # – indicates comparisons across all NYHA classes using the Kruskal-Wallis test

1485.0 pg/mL, p<0.001) and 26.0-fold higher in those with NYHA class III–IV (1688.5; 1556.5–1845.5 pg/mL, p<0.001) relative to controls (65.0; 46.0–96.0 pg/mL). BNP and NT-proBNP levels increased further in NYHA class III–IV compared to class I–II, by 17.8% (p<0.001) and 31.4% (p<0.001), respectively (pH=0.001 between groups).

Vitamin D deficiency in CHF patients worsened progressively with advancing NYHA functional class. In class I–II, the median vitamin D concentration was approximately 50% lower (29.0; 21.0–37.0 ng/mL, p<0.001) than in the control group (42.0; 38.0–48.0 ng/mL), while in class III–IV, this decrease was 2.5 times (17.5; 12.5–28.0 ng/mL, p<0.001). Vitamin D levels in class III–IV were 65.7% lower (p<0.001) compared to class I–II, indicating a more severe deficiency in advanced stages of CHF (pH=0.001 between groups).

Inflammatory cytokine levels increased in accordance with the NYHA functional class. IL-6, IL-18, and TNF-α showed stepwise elevations: IL-6 increased by 75.0% in class I–II (3.50; 3.10–4.10 pg/mL, p<0.001) and 2.4 times in class III–IV (4.80; 4.0–5.30 pg/mL, p<0.001), compared to controls (2.00; 1.60–2.90 pg/mL). IL-18 increased by 75.2% (368.0; 295.0–430.0 pg/mL, p<0.001) in class I–II and 95.0% (409.5; 350.0–485.0 pg/mL, p<0.001) in class III–IV (controls: 210.0; 146.9–243.5 pg/mL). TNF-α increased by 46.0% in class I–II (7.3; 6.5–7.9 pg/mL, p<0.001) and 62.0% in class III–IV (8.1; 7.3–8.9 pg/mL, p<0.001), compared to controls (5.0; 4.6–5.3 pg/mL). In class III-IV compared to class I–II, IL-6, IL-18, and TNF-α concentrations were significantly higher by 37.1% (p<0.001), 11.3% (p=0.003) and 11.0% (p<0.001), respectively (pH=0.001 between groups).

Galectin-3 levels were elevated in both functional classes compared to the control group (7.0; 5.5 to 9.6 ng/mL), showing a 2.0-fold increase in class I–II (14.4; 11.8–16.3 ng/mL, p<0.001) and a 2.6-fold increase in class III–IV (18.1; 15.4–19.4 ng/mL, p<0.001). Median

galectin-3 concentrations further increased with disease progression, showing a 25.7% increase in class III–IV compared to class I–II (p<0.001) (p_H<0.001 across groups).

FGF-23 levels increased by 10.8% in NYHA class I–II (53.4; 48.9-62.9 pg/mL, p=0.003) and by 20.0% in class III–IV (56.4; 47.1–65.9 pg/mL, p<0.001), compared to the control group (48.2; 39.1–61.2 pg/mL). This suggests a mechanism of myocardial remodeling potentially associated with vitamin D deficiency and phosphate dysregulation. However, FGF-23 concentrations did not differ significantly between NYHA class III–IV and class I-II (p=0.119) (pH=0.001 between groups).

The study identified statistically significant correlations between vitamin D deficiency and several biochemical parameters in CHF patients. Serum vitamin D concentrations exhibited a weak but statistically significant inverse correlation with NT-proBNP levels (ρ=−0.136; p=0.044). Furthermore, vitamin D levels were inversely correlated with key inflammatory mediators, including IL-6 (ρ=−0.255; p<0.001) and TNF-α (ρ=−0.282; p<0.001). A significant negative association was also observed between vitamin D concentrations and galectin-3 levels (ρ=−0.275; p<0.001). In contrast, no statistically significant relationships were detected between vitamin D levels and IL-18 (ρ=−0.122; p=0.070) or FGF-23 (ρ=−0.079; p=0.242).

Several inflammatory and fibrotic biomarkers demonstrated strong positive associations with markers of cardiac neurohormonal activation. IL-6 showed significant positive correlations with both BNP (ρ=0.366; p<0.001) and NT-proBNP (ρ=0.444; p<0.001). Similarly, IL-18 was strongly correlated with BNP (ρ=0.490; p<0.001) and NT-proBNP (ρ=0.464; p<0.001).

TNF-α also exhibited significant positive correlations with BNP (ρ=0.465; p<0.001) and NT-proBNP (ρ=0.454; p<0.001). Among the biomarkers evaluated, galectin-3 demonstrated the strongest associations with natriuretic peptides, showing robust correlations with BNP (ρ=0.732; p<0.001) and NT-proBNP (ρ=0.764; p<0.001). FGF-23 concentrations were positively correlated with BNP (ρ=0.381; p<0.001) and NT-proBNP (ρ=0.403; p<0.001). Furthermore, a significant positive association was observed between FGF-23 and IL-6 levels (ρ=0.363; p<0.001). Strong positive interrelationships were identified among inflammatory and fibrotic biomarkers. IL-6 demonstrated significant positive correlations with IL-18 (ρ=0.691; p<0.001), TNF-α (ρ=0.557; p<0.001), and galectin-3 (ρ=0.555; p<0.001). Moreover, TNF-α was positively correlated with galectin-3 (ρ=0.655; p<0.001) and FGF-23 (ρ=0.640; p<0.001).

ROC curve analysis was performed to assess the ability of inflammatory and fibrosis-related biomarkers to discriminate disease progression in patients with chronic heart failure and concomitant vitamin D deficiency. The ROC curves for IL-6, IL-18, FGF-23, galectin-3, and TNF-α are presented in Figure 1. Among the biomarkers analyzed, IL-6 demonstrated the highest diagnostic precision, with an area under the curve (AUC) of 0.799 (95% CI: 0.739–0.859, p<0.001). At the selected cut-off value of 18.5 pg/mL, IL-6 showed a sensitivity of 75% and a specificity of 78%. Similarly, galectin-3 exhibited a strong discriminative performance with an AUC of 0.791 (95% CI 0.731–0.851, p<0.001). Using a cut-off value of 16.0 ng/mL, sensitivity and specificity were 72% and 80%, respectively. TNF-α showed moderate diagnostic ability, resulting in an AUC of 0.689 (95% CI 0.617–0.761, p<0.001). At a cut-off value of 12.5 pg/mL, sensitivity and specificity were 65% and 75%, respectively. On the contrary, IL-18 demonstrated limited discriminative capacity, with an AUC of 0.618 (95% CI 0.542–0.693, p=0.003). The selected cutoff of 210.0 pg/mL provided a sensitivity of 60% and a specificity of 62%. FGF-23 showed poor diagnostic performance, with an AUC of 0.551 (95% CI: 0.473–0.630, p=0.194). At the cut-off value of 145.0 pg/mL, the sensitivity and specificity were 55% and 57%, respectively, indicating a limited ability to discriminate disease progression (Table 2).

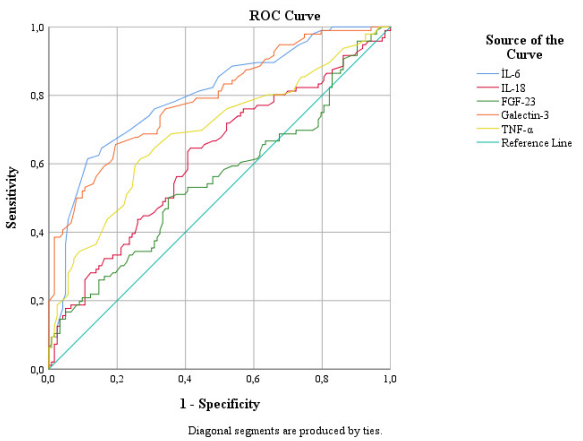

Fig. 1. ROC curves of inflammatory and fibrosis-related biomarkers in patients with chronic heart failure

Table 2. ROC analysis results of inflammatory and fibrosis-related biomarkers in patients with chronic heart failure

Test result variable(s)	AUC (%95)	Cut-off	p	Sensitivity (%)	Specificity (%)
IL-6, pg/mL	0.799 (0.739–0.859)	18.5	<0.001	75	78
IL-18, pg/mL	0.618 (0.542–0.693)	210.0	0.003	60	62
FGF-23, pg/mL	0.551 (0.473–0.630)	145.0	0.194	55	57
Galectin-3, ng/mL	0.791 (0.731–0.851)	16.0	<0.001	72	80
TNF-α, pg/mL	0.689 (0.617–0.761)	12.5	<0.001	65	75

Discussion

Vitamin D deficiency appears to be involved in multiple pathophysiological pathways associated with the severity and progression of CHF. In this observational study,

reduced serum vitamin D concentrations were correlated with higher NYHA functional classes, indicating a possible relationship of vitamin D status with the severity of clinical manifestations. These results reinforce the idea that vitamin D could affect cardiovascular function in ways that extend beyond its traditional role in calcium–phosphate balance. Experimental and clinical data suggest that vitamin D signaling influences myocardial architecture, intracellular pathways, immune responses, and neurohormonal regulation through the participation of the vitamin D receptor (VDR).[21,22] The biologically active form, $1,25(OH)_2D_3$, has been shown to modulate the renin–angiotensin–aldosterone system (RAAS), oxidative stress pathways, and inflammatory responses, all of which are central mechanisms in CHF progression.[23,24]

Although the correlations between vitamin D levels and natriuretic peptides (BNP and NT-proBNP) were modest, their statistical significance suggests a biologically relevant association between vitamin D status and neurohormonal activation. In particular, the inverse relationship observed between vitamin D concentrations and NT-proBNP levels may reflect lower tension in the left ventricle wall tension and reduced neurohormonal activation in individuals who exhibit elevated vitamin D levels. Our results align with previous studies showing that vitamin D insufficiency is associated with elevated NT-proBNP levels, impaired cardiac function, and less favorable outcomes in heart failure populations.[25-27] However, given the observational design of the present study, these associations should be interpreted cautiously and cannot be considered evidence of a causal relationship.

Chronic systemic inflammation represents a key feature of CHF and contributes to myocardial dysfunction and adverse ventricular remodeling. Vitamin D exerts immunomodulatory effects by suppressing macrophage activation and downregulating the synthesis of pro-inflammatory cytokines while improving anti-inflammatory responses.[28,29] In the present investigation, lower vitamin D levels were inversely related to IL-6 concentrations, indicating a possible link between vitamin D deficiency and increased systemic inflammatory activity. Elevated IL-6 levels have been implicated in cardiomyocyte apoptosis, myocardial fibrosis, endothelial dysfunction, and left ventricular systolic impairment through mechanisms mediated by oxidative stress. These observations are consistent with previous studies reporting elevated IL-6 concentrations among patients with insufficient vitamin D and coexisting cardiovascular or metabolic conditions.[30-33]

TNF-α is a key inflammatory mediator involved in myocardial fibrosis, cardiomyocyte apoptosis, negative inotropic effects, and adverse ventricular remodeling. The observed negative correlation of vitamin D concentrations with TNF-α in this study indicates that maintaining sufficient vitamin D can help reduce TNF-α–driven inflammatory responses. Experimental data support this hypothesis, demonstrating that calcitriol, the active form of vitamin D, can inhibit TNF-α expression and release.[28,34,35] However, these findings should be interpreted as associative rather than mechanistic. For comparison, vitamin D concentrations did not show notable associations with IL-18 or FGF-23. This lack of association may indicate that these pathways are less directly influenced by vitamin D status in CHF or are regulated through alternative or more complex mechanisms. IL-18 has been associated with endothelial injury, cardiomyocyte apoptosis, and ventricular hypertrophy,[35,37] while FGF-23 has emerged as an important mediator of myocardial stress, fibrosis, and maladaptive remodeling.[38-40] Our findings indicate a relationship between higher concentrations of FGF-23 and natriuretic peptides as well as inflammatory markers, highlighting its involvement in a wider network of neurohormonal and inflammatory dysregulation. Experimental and clinical studies suggest that FGF-23 interacts with RAAS activation and inflammatory signaling, leading to a self-reinforcing cycle of left ventricular hypertrophy, fibrotic remodeling, and endothelial impairment.[39-42] Furthermore, concurrent higher levels of FGF-23 and lower Klotho expression have been associated with greater cardiovascular risk and worse outcomes in patients with heart failure.[43]

Galectin-3, a well-established biomarker of cardiac fibrosis, demonstrated significant associations with neurohormonal markers in the present study, indicating that fibrotic remodeling is closely related to disease severity in CHF.[13,44,45] Previous studies have reported elevated levels of galectin-3 in heart failure patients, reflecting sustained macrophage activation and remodeling of the extracellular matrix, even in the absence of a direct relationship with vitamin D status.[46] Consistent with these observations, the inverse associations identified between vitamin D levels and IL-6, TNF-α, and galectin-3 in the present cohort suggest that vitamin D deficiency may contribute indirectly to improved inflammatory and fibrotic signaling in CHF. In line with these associations, ROC curve analysis further demonstrated that IL-6 and galectin-3 provide the highest discriminatory value for disease progression in patients with CHF and vitamin D deficiency. On the contrary, IL-18 and FGF-23 showed limited diagnostic utility, while TNF-α exhibited moderate prognostic performance. These results indicate that IL-6 and galectin-3 could function as informative biomarkers for functional stratification and monitoring of disease progression in this clinical context. Loss of vitamin D-mediated immunomodulatory effects can facilitate persistent macrophage activation and cytokine-driven myocardial injury, thus amplifying galectin-3–associated adverse remodeling associated with galectin-3.[29,47]

Taken together, the observed interrelationships among inflammatory cytokines, fibrotic biomarkers, mineral metabolism, and natriuretic peptides highlight the integrated and multifactorial nature of CHF pathophysiology.[32] These pathways appear to act in concert, contributing to progressive myocardial injury, fibrosis, and neurohormonal activation.[48-50] Within this complex framework, vitamin D deficiency may act as an upstream modulator that amplifies inflammatory and fibrotic responses.

Current results show that lower vitamin D levels correlate with more pronounced inflammatory and fibrotic alterations in CHF patients, highlighting the close link of vitamin D deficiency to key pathophysiological mechanisms of the disease.[26,45,46] Insufficient vitamin D appears to exacerbate systemic inflammation, as reflected in elevated cytokines such as IL-6, IL-18 and TNF-α, which contribute to myocardial injury, apoptosis, and adverse remodeling.[32,35] These observations underscore the relevance of assessing vitamin D levels as part of a comprehensive clinical evaluation.

This study provides a new integrated perspective on chronic heart failure by simultaneously evaluating vitamin D status, inflammatory cytokines (IL-6, TNF-α), galectin-3, FGF-23, and natriuretic peptides. Unlike previous reports that focused on single biomarkers, this comprehensive assessment highlights the interplay between mineral metabolism, systemic inflammation, fibrotic remodeling, and hemodynamic stress. Importantly, IL-6 and galectin-3 demonstrated the highest discriminative value for disease severity, representing a significant clinical addition. Overall, these findings uniquely contribute to understanding how vitamin D deficiency may amplify key pathophysiological mechanisms, providing information for grouping patients according to the severity of the disease and guiding clinical management.

Study limitations

The observational design of this study limits the interpretation of causal relationships between vitamin D deficiency and the severity of the disease in chronic heart failure. Additional limitations include that the study was conducted at a single site, the small number of participants, and the absence of interventional data on vitamin D supplementation, which may affect the applicability of the results.

Subsequent research should assess the potential therapeutic effects of correcting vitamin D deficiency on myocardial remodeling, inflammatory mediators, and long-term clinical outcomes, and additionally clarify the mechanistic connections between vitamin D levels, neurohormonal activation, and fibrotic pathways in chronic heart failure.

Conclusion

Vitamin D deficiency in chronic heart failure was associated with greater disease severity and adverse changes in key biomarkers, including BNP, NT-proBNP, IL-6, TNF-α, galectin-3, and FGF-23. These findings provide novel clinical and pathophysiological insights into how vitamin D status, inflammation, fibrosis, and hemodynamic stress interact. In particular, IL-6 and galectin-3 showed the highest discriminative value for disease severity, supporting their use in biomarker-based risk assessment and clinical monitoring of patients with vitamin D deficiency.

Declarations

Funding

The author received no financial support for the research, authorship, and/or publication of this article.

Author contributions

Conceptualization, A.F.; Methodology, A.F.; Software, A.F.; Validation, A.F.; Formal Analysis, A.F.; Investigation, A.F.; Resources, A.F.; Data Curation, A.F.; Writing – Original Draft Preparation, A.F.; Writing – Review & Editing, A.F.; Visualization, A.F.; Supervision, A.F.; Project Administration, A.F.; Funding Acquisition, A.F.

Conflicts of interest

The author declares no competing interests.

Data availability

The data sets generated and/or analyzed during the current study are available from the corresponding author upon reasonable request.

Ethics approval

All subjects provided informed consent prior to participation. The study was carried out in accordance with the principles of the Declaration of Helsinki. The protocol was reviewed and approved by the Ethics Committee of Azerbaijan Medical University (Approval No: AMU-2018/09, Date: 9 September 2018).

References

1. Kampka Z, Czapla D, Wojakowski W, Stanek A. Vitamin D supplementation in heart failure—confusion without a cause? *Nutrients*. 2025;17:1839. doi:10.3390/nu17111839
2. Li H, Hastings MH, Rhee J, Trager LE, Roh JD, Rosenzweig A. Targeting age-related Pathways in heart failure. *Circ Res*. 2020;126:533-551. doi:10.1161/CIRCRESAHA.119.315889
3. Iyngkaran P, Thomas M, Horowitz JD, Komesaroff P, Jelinek M, Hare DL. Common comorbidities that alter heart failure prognosis - shaping new thinking for Ppractice. *Curr Cardiol Rev*. 2021;17(5):e160721187934. doi:10.2174/1573403X1 666620113093548

4. Crafa A, Cannarella R, Cannarella V, Condorelli RA, La Vignera S, Calogero AE. Retrospective real world study on vitamin D supplementation: Looking for the most effective molecule and its frequency of use. *Clin Nutr*. 2025;47:265-274. doi:10.1016/j.clnu.2025.03.004
5. Zhang Z, Yang Y, Ng CY, Wang D, Wang J, Li G. Meta-analysis of Vitamin D deficiency and risk of atrial fibrillation. *Clin Cardiol*. 2016;39:537-543. doi:10.1002/clc.22563
6. Gunta SS, Thadhani RI, Mak RH. The effect of vitamin D status on risk factors for cardiovascular disease. *Nat Rev Nephrol*. 2013;9:337-347. doi:10.1038/nrneph.2013.74
7. Fanari Z, Hammami S, Hammami MB, Hammami S, Abdellatif A. Vitamin D deficiency plays an important role in cardiac disease and affects patient outcome: Still a myth or a fact that needs exploration? *J Saudi Heart Assoc*. 2015;27(4):264-271. doi:10.1016/j.jsha.2015.02.003
8. El Abd A, Dasari H, Dodin P, Trottier H, Ducharme FM. The effects of vitamin D supplementation on inflammatory biomarkers in patients with asthma: a systematic review and meta-analysis of randomized controlled trials. *Front Immunol*. 2024;15:1335968. doi:10.3389/fimmu.2024.1335968
9. Ul Islam Hashmi MR, Sadiq S, Hashmi SN, et al. Correlation of TNF-α and IL-6 expression with vitamin D levels in insulin-resistant type 2 diabetes mellitus patients: exploring the role of vitamin D in inflammation and disease pathogenesis. *BMC Immunol*. 2025;26:68. doi:10.1186/s12865-025-00754-z
10. Haider F, Ghafoor H, Hassan OF, Farooqui K, Bel Khair AOM, Shoaib F. Vitamin D and cardiovascular diseases: An update. *Cureus*. 2023;15(11):e49734. doi:10.7759/cureus.49734
11. Jiang Y, Zhou G, Guo Y, Long Y. Inflammation in heart failure: Mechanisms and therapeutic strategies. *CVIA*. 2025;10(1). doi:10.15212/CVIA.2024.0050
12. Zaborska B, Sikora-Frąc M, Smarż K, Pilichowska-Paszkiet E, Budaj A, Sitkiewicz D. The role of Galectin-3 in heart failure- the diagnostic, prognostic and therapeutic potential-Where do we stand? *Int J Mol Sci*. 2023;24(17):13111. doi:10.3390/ijms241713111
13. Martuszewski A, Paluszkiewicz P, Poręba R, Gać P. Galectin-3 in cardiovascular health: A narrative review based on life's essential 8 and life's simple 7 frameworks. *Curr Issues Mol Biol*. 2025;47:332. doi:10.3390/cimb47050332
14. Deng C, Wu Y. Vitamin D-Parathyroid hormone-Fibroblast growth factor 23 axis and cardiac remodeling. *Am J Cardiovasc Drugs*. 2025;25(1):25-36. doi:10.1007/s40256-024-00688-8
15. Stöhr R, Schuh A, Heine GH, Brandenburg V. FGF23 in cardiovascular disease: Innocent bystander or active mediator? *Front Endocrinol (Lausanne)*. 2018;9:351. doi:10.3389/fendo.2018.00351
16. Leidner AS, Cai X, Zelnick LR, Lee J, Bansal N, Pasch A. Fibroblast growth factor 23 and risk of heart failure subtype: The CRIC (Chronic Renal Insufficiency Cohort) Study. *Kidney Med*. 2023;5(11):100723. doi:10.1016/j.xkme.2023.100723
17. Yared W, Dogan L, Fassli AM, Moza A, Goetzenich A, Stoppe C. Fibroblast growth factor 23 ss a strong predictor of adverse events after left ventricular assist device implantation. *J Cardiovasc Dev Dis*. 2025;12(8):290. doi:10.3390/jcdd12080290
18. Otaal PS, Pachipala S, Uppal L, Bootla D. Correlation of Vitamin D deficiency with severity of chronic heart failure as assessed by functional class and N-Terminal pro-brain natriuretic peptide levels. *Cureus*. 2021;13(2):e13522. doi:10.7759/cureus.13522
19. Zittermann A, Trummer C, Theiler-Schwetz V, Lerchbaum E, März W, Pilz S. Vitamin D and cardiovascular disease: An updated narrative review. *Int J Mol Sci*. 2021;22(6):2896. doi:10.3390/ijms22062896
20. Castiglione V, Aimo A, Vergaro G, Saccaro L, Passino C, Emdin M. Biomarkers for the diagnosis and management of heart failure. *Heart Fail Rev*. 2022;27(2):625-643. doi:10.1007/s10741-021-10105-w
21. Tappia PS, Lopez R, Fitzpatrick-Wong S, Ramjiawan B. Understanding the role of Vitamin D in heart failure. *Rev Cardiovasc Med*. 2023;24(4):111. doi:10.31083/j.rcm2404111
22. Hagău AC, Puşcaş A, Togănel R, Muntean I. Is hypovitaminosis D a risk factor for heart failure? *Life (Basel)*. 2023;13(2):372. doi:10.3390/life13020372
23. Wróbel-Nowicka K, Wojciechowska C, Jacheć W, Zalewska M, Romuk E. The role of oxidative stress and inflammatory parameters in heart failure. *Medicina (Kaunas)*. 2024;60(5):760. doi:10.3390/medicina60050760
24. Bikle DD. Vitamin D: production, metabolism, and mechanism of action. In: Feingold KR, Ahmed SF, Anawalt B, et al, eds. *Endotext*. MDText.com, Inc; published 2000. Accessed Oct 20, 2025. doi:10.1016/j.jacadv.2023.100804
25. Liu LC, Voors AA, van Veldhuisen DJ, van der Veer E, Belonje AM, Szymanski MK. Vitamin D status and outcomes in heart failure patients. *Eur J Heart Fail*. 2011;13(6):619-625. doi:10.1093/eurjhf/hfr032
26. Priya S, Siddiqi Z, Karoli R, Fatima J, Gupta S, Mishra R. Study of Vitamin D status in patients with dilated cardiomyopathy at a teaching hospital in North India. *J Cardiovasc Echogr*. 2016;26(3):89-93. doi:10.4103/2211-4122.18795
27. Rodriguez AJ, Mousa A, Ebeling PR, Scott D, de Courten B. Effects of vitamin D supplementation on inflammatory markers in heart failure: a systematic review and meta-analysis of randomized controlled trials. *Sci Rep*. 2018;8(1):1169. doi:10.1038/s41598-018-19708-0
28. Lok DJ, Van Der Meer P, de la Porte PW, Lipsic E, Van Wijngaarden J, Hillege HL. Prognostic value of galectin-3, a novel marker of fibrosis, in patients with chronic heart failure: data from the DEAL-HF study. *Clin Res Cardiol*. 2010;99(5):323-328. doi:10.1007/s00392-010-0125-y
29. Calton EK, Keane KN, Newsholme P, Soares MJ. The Impact of Vitamin D levels on inflammatory status: A

systematic review of immune cell studies. *PLoS One*. 2015;10(11):e0141770. doi:10.1371/journal.pone.0141770

30. Martens PJ, Gysemans C, Verstuyf A, Mathieu AC. Vitamin D's effect on immune function. *Nutrients*. 2020;12(5): 1248. doi:10.3390/nu12051248
31. Boulet J, Sridhar VS, Bouabdallaoui N, et al. Inflammation in heart failure: pathophysiology and therapeutic strategies. *Inflamm Res*. 2024;73:709-723. doi:10.1007/s00011-023-01845-6
32. Alogna A, Koepp KE, Sabbah M, Espindola Netto JM, Jensen MD, Kirkland JL. Interleukin-6 in patients with heart failure and preserved ejection fraction. *JACC Heart Fail*. 2023;11(11):1549-1561. doi:10.1016/j.jchf.2023.06.031
33. Bartekova M, Radosinska J, Jelemensky M, Dhalla NS. Role of cytokines and inflammation in heart function during health and disease. *Heart Fail Rev*. 2018;23(5):733-758. doi:10.1007/s10741-018-9716-x
34. Amara M, Stoler O, Birati EY. The Role of inflammation in the pathophysiology of heart failure. *Cells*. 2025;14(14):1117. doi:10.3390/cells14141117
35. Hung J, McQuillan BM, Chapman CM, Thompson PL, Beilby JP. Elevated interleukin-18 levels are associated with the metabolic syndrome independent of obesity and insulin resistance. *Arterioscler Thromb Vasc Biol*. 2005;25(6):1268-1273. doi:10.1161/01.ATV.0000163843.70369.12
36. Åkerblom A, James SK, Lakic TG, Becker RC, Cannon CP, Steg PG. Interleukin-18 in patients with acute coronary syndromes. *Clin Cardiol*. 2019;42(12):1202-1209. doi:10.1002/clc.23274
37. Batra J, Buttar RS, Kaur P, Kreimerman J, Melamed ML. FGF-23 and cardiovascular disease: review of literature. *Curr Opin Endocrinol Diabetes Obes*. 2016;23(6):423-429. doi:10.1097/MED.0000000000000294
38. Gruson D, Maisin D, Pouleur AC, Ann SA, Rousseau MF. CA125, Galectin-3 and FGF-23 are interrelated in heart failure with reduced ejection fraction. *EJIFCC*. 2023;34(2):103-109
39. Böckmann I, Lischka J, Richter B, Deppe J, Rahn A, Fischer DC. FGF23-Mediated activation of local RAAS promotes cardiac hypertrophy and fibrosis. *Int J Mol Sci*. 2019;20(18):4634. doi:10.3390/ijms20184634
40. Klisic A, Gluscevic S, Karakasis P, Kotur-Stevuljevic J, Ninic A. Serum galectin-3 and fibroblast growth factor-23 levels in relation with type 2 diabetes and cardiovascular risk. *J Med Biochem*. 2025;44(1):85-92. doi:10.5937/jomb0-50471
41. Liu M, Xia P, Tan Z, Song T, Mei K, Wang J. Fibroblast growth factor-23 and the risk of cardiovascular diseases and mortality in the general population: A systematic review and dose-response meta-analysis. *Front Cardiovasc Med*. 2022;9:989574. doi:10.3389/fcvm.2022.989574
42. Memmos E, Sarafidis P, Pateinakis P, et al. Soluble Klotho is associated with mortality and cardiovascular events in hemodialysis. *BMC Nephrol*. 2019;20:217. doi:10.1186/s12882-019-1391-1
43. Wang G, Li R, Feng C, Li K, Liu S, Fu Q. Galectin-3 is involved in inflammation and fibrosis in arteriogenic erectile dysfunction via the TLR4/MyD88/NF-κB pathway. *Cell Death Discov*. 2024;10(1):92. doi:10.1038/s41420-024-01859-x
44. Bouffette S, Botez I, De Ceuninck F. Targeting galectin-3 in inflammatory and fibrotic diseases. *Trends Pharmacol Sci*. 2023;44(8):519-531. doi:10.1016/j.tips.2023.06.001
45. Özcan M, Akarsu M, Aydın Yoldemir Şengül, Altun Ö, Kutlu O, Kalyon S. Serum galectin-3 levels and vitamin D relationship in heart failure. *J Surg Med*. 2021;5(10):1046-1049.
46. AbouEzzeddine OF, Haines P, Stevens S, Nativi-Nicolau J, Felker GM, Borlaug BA. Galectin-3 in heart failure with preserved ejection fraction. A RELAX trial substudy (Phosphodiesterase-5 inhibition to improve clinical status and exercise capacity in diastolic heart failure). *JACC Heart Fail*. 2015;3(3):245-252. doi:10.1016/j.jchf.2014.10.009
47. van der Vaart A, Bakker SJL, Laverman GD, van Dijk PR, de Borst MH. NT-proBNP Mediates the association between FGF23 and all-cause mortality in individuals with type 2 diabetes. *J Am Heart Assoc*. 2023;12(23):e031873. doi:10.1161/JAHA.123.031873
48. Stoltze G, Schou M, Videbæk L, et al. Fibroblast growth factor-23 and risk of cardiovascular events in chronic heart failure. *J Am Coll Cardiol*. 2022;79(2):142-154
49. Mooney L, Jackson CE, Adamson C, McConnachie A, Welsh P, Myles RC. Adverse outcomes associated with interleukin-6 in patients recently hospitalized for heart failure with preserved ejection fraction. *Circ Heart Fail*. 2023;16(4):e010051. doi:10.1161/CIRCHEARTFAILURE.122.010051

Rzeszów University Press 2026
ISSN 2544-1361 (online)
doi: 10.15584/ejcem.2026.2.8

http://www.ejcem.ur.edu.pl
European Journal of Clinical and Experimental Medicine
Eur J Clin Exp Med 2026; 24 (2): 282–288

ORIGINAL PAPER

Ultrasonographic features of pediatric umbilical hernias – associations with age, sex, and hernial orifice width

Agata Maria Kawalec-Rutkowska

Department of Anatomy, Institute of Medical Sciences, University of Opole, Opole, Poland

ABSTRACT

Introduction and aim. Given the limited data on standardized ultrasound evaluation of hernial defect morphology in pediatric umbilical hernias, this study aimed to evaluate the ultrasonographic features of primary umbilical hernias in pediatric patients, with a particular focus on the width of the hernial orifice, the contents of the hernial sac and their potential correlation with age and sex.

Material and methods. A retrospective analysis of medical records of pediatric patients with primary umbilical hernia who presented to the pediatric surgery outpatient clinic and had ultrasonographic measurements performed using a standardized protocol between 01.01.2024 and 31.07.2025.

Results. Analysis of ultrasound measurements of the width of the hernial orifice width demonstrated a significant association between the width of the hernial orifice and the contents of the hernial sac. Children with intestinal loops present in the hernial sac were significantly younger than those with preperitoneal fat (p=0.016), and the width of the hernial orifice was greater in cases containing intestinal loops (p=0.028). In particular, among children with a hernial orifice larger than 14 mm, intestinal loops were observed more frequently than among those with an orifice width of 14 mm or less (58.82% vs 15.38%; p=0.026). Furthermore, the analysis revealed that the umbilical orifice was wider in boys than in girls (mean±SD: 15.44±1.64mm vs. 13.08±2.43mm; p=0.043).There was a difference between the width of the hernial orifice in children under 1 year of age and older.

Conclusion. Ultrasonographic evaluation of pediatric umbilical hernias provides clinically relevant information on the morphology of hernial defects. In particular, the width of the hernial orifice is associated with the presence of intestinal loops in the hernial sac, especially in younger children, with a threshold value of >14 mm identifying patients at higher likelihood of intestinal content. These findings suggest that ultrasonography may contribute to risk stratification and support clinical decision-making in the management and follow-up of pediatric umbilical hernias.

Keywords. anatomy, child, ultrasound, umbilical hernia

Introduction

Umbilical hernia is a common condition in the pediatric population.[1,2] Clinically, it presents as a bulge in the region surrounding the umbilicus. The condition called "primary pediatric umbilical hernia" results from incomplete closure of the umbilical ring, a process that usually occurs after birth.[3] This closure involves complex developmental interactions, including medial folding of the lateral body walls, fusion of the rectus abdominis muscles to form the linea alba and contraction of the umbilical orifice.[3] Generally, a fascial defect that is present at birth resolves without surgical treatment.[3] While umbilical hernias are generally congenital, the term "secondary pediatric umbilical

Corresponding author: Agata Maria Kawalec-Rutkowska, e-mail: agata.kawalec@uni.opole.pl

Received: 10.12.2025 / Revised: 15.01.2026 / Accepted: 29.01.2026 / Published: 30.06.2026

Kawalec-Rutkowska AM. Ultrasonographic features of pediatric umbilical hernias – associations with age, sex, and hernial orifice width. *Eur J Clin Exp Med.* 2026;24(2):282–288. doi: 10.15584/ejcem.2026.2.8.

hernia" can be applied to cases that arise as a consequence of prior surgical procedures.[4]

For the clinician, it is important that the extent of the skin protrusion is not always indicative of the size of the fascia defect.[3] Medical history and physical examination are important to assess the indications for treatment. However, they provide limited information regarding the morphology of the defect and hernial sac contents. Ultrasonography can be helpful in assessing the width of the hernial orifice and assessing the contents of the hernial sac, which is formed by the peritoneum. The hernial sac may contain an intestinal loop or preperitoneal fat.

Previous studies have relied primarily on clinical examination alone or have used nonstandardized or indirect methods to estimate defect size, without systematically correlating hernial orifice width with patient age, sex, or hernial sac contents. As a result, objective imaging-based parameters that may inform risk stratification and clinical decision-making remain insufficiently defined. In particular, the potential of ultrasonography to identify hernias more likely to contain intestinal loops – especially in younger children – has not been adequately explored.

In contrast to previous studies by Yanagisawa et al. Nakajima et al., and Kaur et al., which mainly relied on clinical assessment or nonstandardized imaging approaches, the present study provides standardized ultrasound measurements of the hernial orifice and directly correlates the width of the defect with hernial sac contents.[5,6,7] In addition, several previous reports did not consistently distinguish between primary and secondary umbilical hernias, reported the size of the defect using heterogeneous methodologies, or lacked complete quantitative data. By addressing these limitations, the current study extends existing knowledge by offering an imaging-based standardized evaluation of defect in relation to patient age, sex, and content of the hernial sac content.

Therefore, the objective of this study was to provide a standardized ultrasound evaluation of primary pediatric umbilical hernias and to evaluate the relationship between the width of the hernia orifice, the contents of the hernia sac, and the demographics of the patient, including age and sex. By correlating these parameters, this study seeks to clarify the clinical value of ultrasonography beyond descriptive imaging and to explore its role in identifying children at increased risk of intestinal herniation. An additional objective of this study was to explore whether a measurable ultrasonographic cut-off value of the width of the hernial orifice could be identified, enabling differentiation between hernias containing intestinal loops and those containing preperitoneal fat. However, the proposed ultrasonographic threshold of the width of the hernial orifice should be regarded as exploratory and hypothesis-generating rather than definitive. Previous studies evaluating pediatric umbilical hernias have not reported standardized cut-off values for defect size, particularly in relation to hernial sac contents. However, identifying a preliminary imaging-based threshold may have potential clinical relevance as an objective marker to support risk-oriented monitoring in pediatric patients.

Aim

The objective of this retrospective study was to evaluate the ultrasound characteristics of primary umbilical hernias in pediatric patients, with a particular focus on the width of the hernial orifice, the contents of the hernial sac and their potential correlation with patient age and sex.

Material and methods

A single-center retrospective observational study with the analysis of medical records (including ultrasound examinations) performed in pediatric patients with primary umbilical hernia who came to the pediatric surgery outpatient clinic between 01.01.2024 and 31.07.2025.

Inclusion criteria

Pediatric patients (age from birth up to 18 years) were included if they met all the following criteria:

1. Diagnosis of primary umbilical hernia, defined as a hernia present from birth.
2. Evaluation at the pediatric surgery outpatient clinic during the study period (01.01.2024–31.07.2025).
3. Availability of a complete ultrasound examination of the umbilical hernia.

All consecutive patients with suspected primary umbilical hernia during the study period were included.

Exclusion criteria

Patients were excluded if they met any of the following criteria:

1. History of previous abdominal surgery.
2. Presence of a secondary or complicated hernia.
3. Incomplete medical records or missing ultrasound data.

The medical history, physical examination, and ultrasound assessments were performed by a pediatric surgeon certified in pediatric ultrasonography. The medical history focused on symptoms related to umbilical hernia, as well as any past episodes of incarceration.

During the study period, 35 patients were referred to the pediatric surgery outpatient clinic with a diagnosis of umbilical hernia. 5 patients were excluded from the analysis:

1. Two patients had prior ultrasound examinations performed in other institutions on different ultrasound devices, making the imaging data noncomparable.

2. One patient had a history of previous abdominal surgery (inguinal hernia repair).
3. One patient had a previously diagnosed umbilical hernia that had resolved spontaneously at follow-up; the patient was referred for control, but no hernia was present at the time of evaluation.
4. One patient had incomplete medical records, missing ultrasound data.

Patients with a history of previous abdominal surgery, including laparoscopic or open inguinal hernia repair, were excluded because such procedures can alter the anatomy of the abdominal wall and potentially influence the umbilical ring, which could affect the assessment of the hernial defect and confound the results.

As a result, the records of 30 children (13 girls, 17 boys) were subjected to further analysis. The age was assessed with the accuracy to one month and varied from 1 month to 4.5 years (mean: 1.32; median: 1; SD: 0.17).

Ultrasonographic evaluation of the umbilical hernia was performed with the Aloka Prosound Alpha 6 Diagnostic Ultrasound System (ALOKA Co., Ltd., Tokyo, Japan) with the linear probe. All examinations were conducted according to a predefined uniform protocol by a pediatric surgeon certified in pediatric ultrasonography. Patients were examined in the supine position at rest and measurements were taken in the transverse plane at the widest point of the umbilical ring. The width of the hernial orifice was measured with an accuracy of 0.1 mm. Each measurement was taken three times and averaged to improve accuracy. The contents of the hernial sac were evaluated and differentiated based on echogenicity, peristalsis, and Doppler signal, allowing identification of intestinal loops versus preperitoneal fat. Additional maneuvers, such as observation during mild crying, were performed when necessary to visualize the contents of the hernia.

Intraobserver variability was not formally assessed in this study; this limitation is acknowledged.

This study was a retrospective analysis of deidentified routine clinical data (analysis of existing medical records) and did not involve any intervention or influence on patient management. The study did not involve any intervention or influence on patient management. Therefore, according to national regulations and the Declaration of Helsinki, formal approval from the Bioethics Committee of the University of Opole was not required for this type of study. Patient confidentiality was strictly maintained and no identifiable personal data was used.

Statistical analysis was conducted using Excel and PAST 4.03. Descriptive statistics were used to summarize the data. Mean, standard deviation (SD), and range (minmax) were calculated for continuous variables, including the width and age. The Shapiro-Wilk test was applied to assess the normality of the distribution. Comparisons between groups were performed using the independent samples t-test for normally distributed variables and the Mann-Whitney U test for nonnormally distributed data. The relationship between age and hernial orifice width was assessed using Pearson's correlation coefficient. Categorical variables were compared using the chi-square test or Fisher's exact test, as appropriate. Statistical tests were selected based on sample size and data distribution characteristics. No formal correction for multiple comparisons was applied; however, only key analyzes were interpreted in the context of hypothesis testing. A p-value<0.05 was considered statistically significant.

Results

The characteristic of the study group is presented in Table 1. Children with intestinal loops in the hernia sac were younger than those with preperitoneal fat (p=0.016).

Table 1. The age of patients and other parameters

	The age of children (years)					
	n	Mean±SD	Median (Q1; Q3)	Min	Max	p
Total	30	1.50±1.46	1.13 (0.17; 2.06)	0.04	5.08	
Gender						
Boys	17	1.65±1.64	1.17 (0.31; 2)	0.08	5.08	0.685
Girls	13	1.30±1.15	1.08 (0.16; 2.22)	0.04	4.00	
The content of the hernial sac						
Intestine loops	12	0.90±1.24	0.17 (0.15; 1.21)	0.04	4.50	0.016
Preperitoneal	18	1.90±1.45	1.92 (0.77; 2.5)	0.17	5.08	

The medical history of the patients included in the analysis revealed that there was no episode of incarceration in the past. The symptoms related to the umbilical hernia revealed that three children had symptoms of umbilical inflammation (they were seen and examined by the pediatric surgeon within the first three months of life). One patient reported abdominal pain, which was more associated with lactose intolerance than umbilical hernia. In another case, parents noticed a significantly more frequent protrusion of the umbilical hernia since the child began experiencing constipation. One patient suffered emotionally due to peers at school who mocked the appearance of his navel.

Only 6.67% (2 children) were qualified for surgical treatment. The hernial orifice width in these patients was 20 mm (20 mm and 23.8 mm). According to expert recommendations in asymptomatic cases, surgical treatment is considered after the age of 3 years. In the study group, surgical treatment was considered in a small proportion of patients. The indications for surgery were based on symptoms (frequent protrusion) and significant cosmetic deformity leading to psychosocial discomfort, particularly problems reported by school-aged children during peer interactions or physical activities.

Analysis of ultrasound measurements of the width of the hernial orifice width revealed that the umbili-

cal orifice was wider in boys than in girls (mean±SD: 15.44±1.64 mm vs. 13.08±2.43 mm; p=0.043) (Table 2, Fig. 1). Neither ultrasonographic hernial sac contents nor age differed significantly between boys and girls (Table 1). Given the small sample size, the clinical relevance of the difference in the width of the hernial orifice between sexes should be interpreted with caution.

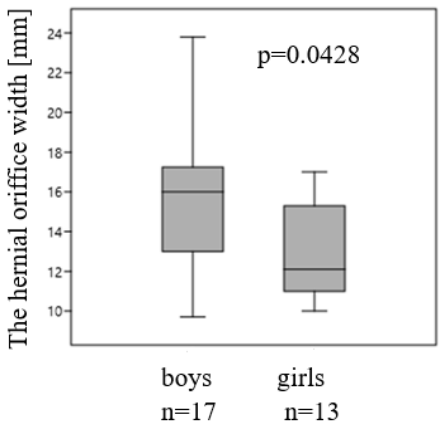

Fig. 1. The width of the hernial sac in boys and girls. In the box plot. The line inside the box represents the median. The box shows the SD and the whiskers indicate the standard error of the mean (SE), the umbilical orifice was wider in boys than in girls (mean±SD: 15.44±1.64mm vs. 13.08±2.43mm)

Table 2. Ultrasonographic evaluation of the hernial sac width in children and other parameters

	The hernial orifice width in children					
	n	Mean±SD	Median (Q1; Q3)	Min	Max	p
Total	30	14.42±3.25	14.65 (11.25; 16.58)	9.70	23.80	
Gender						
Boys	17	15.44±3.43	16.00 (13.5; 17)	9.70	23.80	0.043
Girls	13	13.08±2.43	12.10 (11.0; 15.15)	10.00	17.00	
Age						
<1 year old	13	14.72±2.55	15.60 (13.0; 17.0)	10.70	17.80	0.508
≥1 year old	17	14.18±3.68	14.20 (11.0; 15.0)	9.70	23.80	
The content of the hernial sac						
Intestine loops	12	16.06±3.10	16.45 (14.8; 17)	10.70	23.80	0.028
Preperitoneal fat	18	13.32±2.87	13.00 (11.0; 15.68)	9.70	20.00	

No significant differences in hernial orifice width were found between children under and over 1 year of age, and no meaningful correlation with age was observed (Pearson correlation coefficient r=0.16, p=0.397, Table 2, Fig. 2).

The hernial sac contained intestinal loops (n=12) and preperitoneal fat (n=18). Blood flow on color Doppler and reducibility was confirmed in all patients, and peristalsis was observed when intestinal loops were present. Patients with intestinal loops in the hernial sac were significantly younger (p=0.016; Table 1) and had a wider hernial orifice (p=0.028; Table 2; Fig. 3). Among children with an orifice >14 mm (n=17), intestinal loops were more frequent than in those with <14 mm (58.8% vs. 15.4%; p=0.026; Fig. 4).

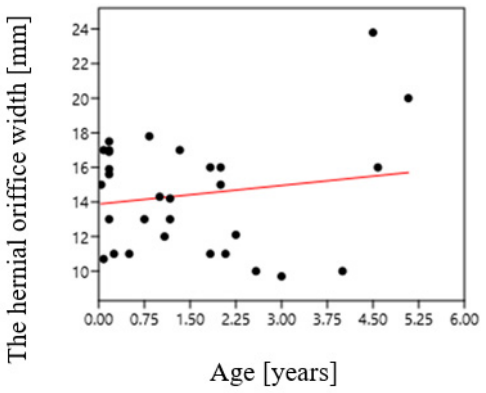

Fig. 2. The correlation between age and the width of the hernial orifice measurement

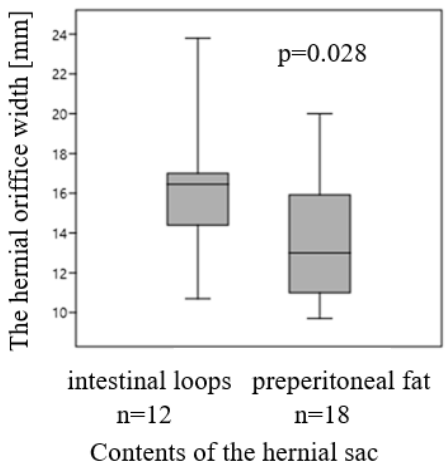

Fig. 3. The width of the hernial sac in children and contents of the hernial sac. In the box plot. The line inside the box represents the median. the box shows the standard deviation (SD) and the whiskers indicate the standard error of the mean (SE)

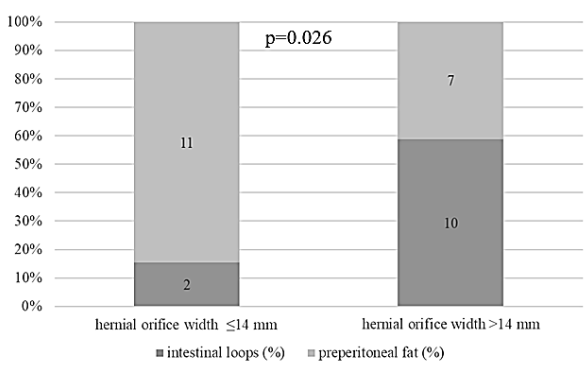

Fig. 4. The width of the hernial sac in children and contents of the hernial sac

Discussion

Although umbilical hernias are a common disease in the pediatric population, the number of studies that specifically analyze the relationship between patient age, hernial orifice width, hernial sac content, and sex remains limited. Most of the available literature focuses on the natural history, indications for surgery, and the timing of the intervention. However, detailed ultrasonographic assessments of hernia morphology and contents are relatively rare, and there is a lack of standardized criteria to guide clinical decision-making based on imaging findings. Furthermore, comparative data that correlating ultrasonographic characteristics with patient demographics are few. This highlights the need for more structured research to better understand the anatomical and clinical factors that may influence the treatment of pediatric umbilical hernias.

The present study provides one of the few standardized ultrasound analyzes of primary pediatric umbilical hernias that correlates the width of the hernial orifice with sac contents, age, and sex. By focusing on these objective measurements, the study confirms some previously reported trends (such as a wider inter-rectus distance in boys) and introduces novel observations, including the exploratory cut-off of 14 mm for predicting intestinal loop presence in the sac. These contributions distinguish the study from prior work that relied solely on clinical assessment or nonstandardized measurements.

It should also be emphasized that ultrasonographic examination is not necessary for the diagnosis of umbilical hernia, as clinical evaluation is usually sufficient. However, Serial measurements of the hernial orifice width may be useful for monitoring the dynamics of defect closure over time. The rate of change in orifice width or its stagnation – may support clinical decision-making regarding the timing of surgical intervention.

Although umbilical hernia is a common condition in children, there remains a significant knowledge gap regarding its epidemiology and defect size. There is a lack of reliable, patient-based studies in which hernia measurements are standardized and comparable across cases.

Yanagisawa et al. examined umbilical hernia closure by ultrasonography in 97 infants (52 boys, 45 girls) and reassessed the benefits of adhesive strapping.[5] Interestingly, the authors defined the closure speed (CS) as the reduction in the diameter of the hernia per week. It was calculated by dividing the diameter of the hernia orifice before treatment by the duration of treatment (weeks).[5] The children included in the study were divided into two age groups: under 12 weeks and between 12 and 26 weeks of age. The authors did not analyze the size of the hernial orifice considering the patients' age or gender of the patients. However, at the beginning of the study, the hernial orifice measured 11.6 mm (range 8–15 mm) in the observation group and 11.8 mm (range 5–26.3 mm) in the adhesive strapping group.[4] It was smaller than in the study group of this research and can be associated with the younger age of the patients included in the study by Yanagisawa et al.

Nakajima et al. measured the width of the linea alba in 30 pediatric patients (14 boys, 16 girls) with umbilical hernias.[6] Since the linea alba does not exist at the level of the umbilicus in patients with pediatric umbilical hernias, they reported the median transverse diameter of the hernia defect as 13 mm. The ages ranged from 2 to 7 years (mean age for children with hernias: 3.8±1.3 years).[6]

Kaur et al. performed a retrospective chart review of 2621 patients (51% were girls) referred for umbilical hernia and the median size of the defect was 7 mm (5.0 to 10.0). However, the authors did not report the technique of hernial orifice measurement and admit that there were considerable missing data for the size of the defect in 1257 participants.[7]

The results show that the hernial orifice was wider in boys than in girls. This may reflect anatomical and biomechanical differences in the development of the abdominal wall between sexes during infancy and infancy. A wider orifice in boys may also predispose to a more frequent intestinal content in the hernial sac, as observed in younger patients with larger defect diameters. These observations are consistent with previous studies in healthy children indicating that in boys without umbilical hernia in supine position the interrectus distance at the level of umbilicus is greater than in girls.[8] This difference may be related to variations in abdominal wall muscle development, connective tissue strength. Although the underlying mechanism requires further investigation, our data suggest that sex and age are important factors that influence the morphology of pediatric umbilical hernias.

Litz et al. conducted a randomized clinical trial on percutaneous ultrasound-guided versus intraoperative rectus sheath block for 58 pediatric umbilical hernia repair and in their study group 57% were women.[9] The age of participants varied from 3.2 to 17.2 years and the authors did not distinguish between primary and secondary hernia.[9] Male preponderance of 63% was reported by Ngom et al. reported a preponderance of men of 63% (umbilical hernia in 2146 pediatric cases).[10]

Tonosaki et al. analyzed 77 cases of umbilical hernias (41 boys and 36 girls. mean age 52.7±18.3 days) treated with the tape fixation method and classified the hernia size based on the height of the bulge: mild (<1 cm). moderate (1≤ and <3 cm) or severe (>3 cm).[11] They did not find significant differences in sex or age at the beginning of treatment between sizes.[11]

Compared to these previous studies, the present findings extend knowledge by explicitly correlating the

width of the hernial orifice with sac content and demographic factors. While previous reports often lack standardized measurements, distinction between primary and secondary hernias, or complete demographic correlations, our results demonstrate clear associations: larger defects are more likely to contain intestinal loops, and younger children are affected more frequently.

The reviewed literature does not clearly distinguish between primary and secondary umbilical hernias. Although it can be assumed that the majority of pediatric cases are congenital, it can be assumed that the majority of pediatric cases are congenital. For the sake of clarity and consistency, such classification should be explicitly addressed. Moreover, many studies lack a standardized method to measure hernial defect, which limits the comparability of findings.

This study has several limitations inherent to its retrospective design. First, the analysis was based on medical records of pediatric patients with umbilical hernia who presented to the pediatric surgery outpatient clinic, and only patients referred for elective outpatient evaluation were included. It is likely that symptomatic cases or those with complications presented directly to the emergency department and therefore were not captured in this analysis. This may have resulted in selection bias and an underrepresentation of more serious symptomatic clinical presentations. Furthermore, patients with ultrasound examinations performed in other institutions were excluded, which may further limit the representativeness of the study cohort.

Second, the study was carried out in a single center, which may reduce the generalizability of the findings to other populations with different demographics or clinical practices. Third, the sample size was relatively small, which limits statistical power and the ability to detect subtle differences between subgroups. Furthermore, multiple statistical comparisons increase the risk of type I error, and therefore the results should be interpreted with caution.

Fourth, due to the retrospective nature and the relatively short study period, no follow-up data were available to assess the natural progression or regression of umbilical hernias over time. Furthermore, some clinical information, such as parental reports of hernia symptoms, was not systematically recorded, as the study mainly focused on objective ultrasonographic measurements.

Despite these limitations, the study has several strengths. All ultrasounds were performed by a single experienced pediatric surgeon, ensuring consistency in measurement technique and minimizing variability between observers. The focus on objective and measurable variables hernial orifice width and sac contents – allowed identification of associations that may be clinically relevant. The exploratory cut-off point of 14 mm for the presence of the intestinal loop, while hypothesis-generating, could inform future follow-up protocols and risk stratification. These results highlight ultrasonography as a valuable monitoring and documentation tool, particularly in cases where the timing of surgical intervention or defect dynamics is uncertain.

Conclusion

The analysis of ultrasonographic measurements indicated that the hernial orifice was generally wider in boys than in girls. Younger children were more likely to have intestinal loops in the hernial sac. Patients with intestinal loops present during ultrasonographic examination tended to have a larger hernial orifice, with loops observed more frequently when the orifice exceeded 14 mm.

These findings suggest that the ultrasound evaluation of pediatric umbilical hernias – particularly the evaluation of the width of the orifice and sac content – may provide useful additional information to support clinical evaluation and follow-up, although the results should be interpreted cautiously due to the retrospective design and limited sample size.

Declarations

Funding

This research did not receive a specific grant from any funding agency in the public, commercial, or non-profit sectors.

Author contributions

Conceptualization. A.K.-R.; Methodology. A.K.-R.; Software. A.K.-R.; Validation. A.K.-R.; Formal Analysis. A.K.-R.; Investigation. A.K.-R.; Resources. A.K.-R.; Data Curation. A.K.-R.; Writing – Original Draft Preparation. A.K.-R.; Writing – Review & Editing. A.K.-R.; Visualization. A.K.-R.; Supervision. A.K.-R.; Project Administration. A.K.-R.; Funding Acquisition. not applicable.

Conflicts of interest

The author declares no competing interests.

Data availability

The data sets generated and/or analyzed during the current study are available from the corresponding author on reasonable request.

Ethics approval

This study is a retrospective analysis of deidentified routine clinical data. According to national regulations and the Declaration of Helsinki, formal approval was not required from the Bioethics Committee of the University of Opole for this type of study. Patient confidentiality was strictly maintained and no identifiable personal data was used.

References

1. Hills-Dunlap JL, Melvin P, Graham DA, Kashtan MA, Anandalwar SP, Rangel SJ. Association of sociodemographic factors with adherence to age-specific guidelines for asymptomatic umbilical hernia repair in children. *JAMA Pediatr.* 2019;173(7):640-647. doi:10.1001/jamapediatrics.2019.1061
2. Zens T, Nichol PF, Cartmill R, Kohler JE. Management of asymptomatic pediatric umbilical hernias: a systematic review. *J Pediatr Surg.* 2017;52(11):1723-1731. doi:10.1016/j.jpedsurg.2017.07.016
3. Sujka JA, Holcomb GW. Umbilical and other abdominal wall hernias. In: Holcomb GW, Murphy JP, St Peter SD, Gatti JM, eds. *Holcomb and Ashcraft's Pediatric Surgery.* Elsevier; 2020:780-783.
4. Tullie LG, Bough GM, Shalaby A, et al. Umbilical hernia following gastroschisis closure: a common event? *Pediatr Surg Int.* 2016;32(8):811-814. doi:10.1007/s00383-016-3906-1
5. Yanagisawa S, Kato M, Oshio T, Morikawa Y. Reappraisal of adhesive strapping as treatment for infantile umbilical hernia. *Pediatr Int.* 2016;58(5):363-368. doi:10.1111/ped.12858
6. Nakajima Y, Kondoh S, Yuzuriha S, Mishima Y, Abe N. Differential linea alba width in pediatric umbilical hernias: a comparative analysis. *Surg Radiol Anat.* 2024;47(1):35. doi:10.1007/s00276-024-03540-5
7. Kaur M, Grandpierre V, Oltean I, et al. Predictors of spontaneous resolution of umbilical hernia in children. *World J Pediatr Surg.* 2021;4:e000287. doi:10.1136/wjps-2021-000287
8. Kawalec-Rutkowska AM, Marczak A, Simka M. The linea alba width, children's physical activity, and chosen anthropometric measurements: results of a cross-sectional study. *Pediatr Rep.* 2025;17(1):25. doi:10.3390/pediatric17010025
9. Litz CN, Farach SM, Fernandez AM, et al. Percutaneous ultrasound-guided vs. intraoperative rectus sheath block for pediatric umbilical hernia repair: a randomized clinical trial. *J Pediatr Surg.* 2017;52(6):901-906. doi:10.1016/j.jpedsurg.2017.03.007
10. Ngom G, Zeng FTA, Sagna A, et al. Management of umbilical hernia in African children: the experience of 2146 cases. *J Indian Assoc Pediatr Surg.* 2023;28(3):212-217. doi:10.4103/jiaps.jiaps_115_22
11. Tonosaki K, Suzuki Y, Yonenaga K, et al. Infantile umbilical hernia tape fixation method without compression materials. *J Gen Fam Med.* 2023;24(4):223-230. doi:10.1002/jgf2.626

Rzeszów University Press 2026
ISSN 2544-1361 (online)
doi: 10.15584/ejcem.2026.2.9

http://www.ejcem.ur.edu.pl
European Journal of Clinical and Experimental Medicine
Eur J Clin Exp Med 2026; 24 (2): 289–301

ORIGINAL PAPER

Evaluation of serum and follicular fluid progranulin in relevance to BMI, oocyte, and embryo quality in Iraqi women with polycystic ovary syndrome undergoing intracytoplasmic sperm injection

Inaam Khazal S. Al-Zori [1], Muayad Sraibet Abood [2], Hayder A. L. Mossa [1]

[1] Department of Clinical Physiology, High Institute for Infertility Diagnosis and Assisted Reproductive Technologies, Al-Nahrain University, Baghdad, Iraq
[2] Department of Applied Embryology, High Institute for Infertility Diagnosis and Assisted Reproductive Technologies, Al-Nahrain University, Baghdad, Iraq

ABSTRACT

Introduction and aim. Polycystic ovarian syndrome (PCOS) is a common endocrine-metabolic disease often associated with obesity, persistent low-grade inflammation, and suboptimal results of assisted reproductive technology (ART). The aim was to evaluate the relevance of serum and follicular progranulin (PGRN) levels in relation to intracytoplasmic sperm injection outcomes among normal and overweight/obese body mass index (BMI) women with PCOS.

Material and methods. This prospective comparative study included women diagnosed with PCOS undergoing intracytoplasmic sperm injection (ICSI) between the first of October 2024 and the first of April 2025. Baseline serum markers were measured on cycle days 2–3. Participants were categorized as having a normal BMI, group 1 (n=30), or being overweight/obese, group 2 (n=37). Fasting serum and follicular fluid progranulin (PGRN) levels were assessed on oocyte retrieval day.

Results. Women with normal BMI were younger and had significantly lower BMI and shorter infertility duration compared with overweight/obese women ($p \leq 0.05$). No statistically significant differences were observed between BMI groups in the number of retrieved oocytes, MII oocytes, fertilized oocytes, embryo grades, blastocysts, or biochemical pregnancy rate ($p > 0.05$). Numerically, normal-BMI women showed slightly higher retrieved and MII oocyte counts, whereas overweight/obese women demonstrated higher numbers of fertilized oocytes, total embryos, grade I embryos, blastocysts, and biochemical pregnancy rates; however, these differences did not reach statistical significance.

Serum and follicular fluid PGRN levels were comparable between groups ($p > 0.05$), with only limited correlations observed between follicular fluid PGRN and total oocyte count.

Conclusion. Serum and follicular fluid PGRN levels were comparable across BMI categories in women with PCOS undergoing ICSI. Although numerical variations in oocyte and embryo parameters were observed between BMI groups, most differences were not statistically significant. The findings suggest that follicular fluid PGRN may be associated with certain ovarian response parameters; however, its independent clinical relevance in predicting ART outcomes remains uncertain. Larger studies incorporating clinical pregnancy and live birth outcomes are required to clarify the potential role of follicular fluid PGRN in PCOS-related infertility.

Keywords. infertility, obesity, polycystic ovary syndrome, progranulin

Corresponding author: Inaam Khazal S. Al-Zori, e-mail: enaamkhazal113@st.nahrainuniv.edu.iq

Received: 3.11.2025 / Revised: 27.01.2026 / Accepted: 31.01.2026 / Published: 30.06.2026

Al-Zori IKS, Abood MS, Mossa HAL. Evaluation of serum and follicular fluid progranulin in relevance to BMI, oocyte, and embryo quality in Iraqi women with polycystic ovary syndrome undergoing intracytoplasmic sperm injection. *Eur J Clin Exp Med.* 2026;24(2):289–301. doi: 10.15584/ejcem.2026.2.9.

Introduction

Polycystic ovary syndrome (PCOS) is a common endocrine disorder linked to infertility, resulting from abnormal endocrine and metabolic patterns in women of reproductive age, affecting approximately 15 to 20% of this population and responsible for up to 80% of anovulation and reduced female fertility cases.[1-3] PCOS is characterized as a chronic inflammatory syndrome associated with obesity. Elevated body mass index (BMI) can influence oocyte development, fertilization processes, and embryo quality, ultimately resulting in worse pregnancy outcomes.[4-6] The extensive prevalence of obesity and overweight constitutes a significant global public health issue.[7] Since 1975, the global prevalence of obesity has nearly tripled, with 40% of women classified as overweight (BMI 25–29.9 kg/m^2) and 15% as obese (BMI≥30 kg/m^2), according to a 2016 World Health Organization (WHO) survey.[8] Obesity is a chronic illness that is increasingly prevalent worldwide and adversely affects female fertility and is inextricably associated with low-grade systemic inflammation.[9,10] Obesity-related pregnancy problems have been associated with repeated pregnancy loss, suboptimal endometrial receptivity and inadequate embryo quality in normal or post- ICSI pregnancy.[11-13]

In comparison to normal BMI-PCOS, inflammatory markers, such as PGRN, were increased in high BMI-PCOS. Since its discovery, progranulin (PGRN) has been suggested as a diagnostic and therapeutic biomarker for numerous neoplastic, neurological, and inflammatory illnesses due to its diverse functional features.[14-16] PGRN, also known as proepithelin, is an autocrine growth factor derived from plasma cells. It is a glycoprotein weighing 68–88 kDa and composed of 593 amino acids[17] serving as a precursor to granulin following a proteolytic cleavage process. PGRN is released in response to hypoxia or acidosis and participates in various complex physiological and pathological processes owing to its anti-inflammatory and pro-inflammatory properties. Evidence indicates that the complete PGRN molecule exhibits trophic and anti-inflammatory effects, whereas granulin peptides promote inflammation.[18,19]

PGRN has been implicated in the onset of insulin resistance (IR) in diabetes caused by a high-fat diet. Evidence suggests that PGRN may be associated with many autoimmune illnesses, including systemic lupus erythematosus, systemic sclerosis, multiple sclerosis, and Sjogren's syndrome. PGRN binds to TNFR1 with an affinity similar to that of TNFα, but its affinity for TNFR2 is markedly higher than that of TNFα.[20,21] The heightened immunological response, coupled with insulin resistance and hyperandrogenism resulting from obesity, negatively influences the hypothalamic-pituitary-gonadal axis at all levels and directly impacts reproduction.[22] In the context of PCOS, immune cells and regulatory immune molecules are crucial for sustaining metabolic equilibrium and modulating immunological responses. Individuals with PCOS suffer diminished progesterone levels due to oligo/anovulation. Consequently, in instances of PCOS, immune system hyperactivation transpires due to diminished progesterone levels. This phenomenon induces the synthesis of surplus estrogen, leading to the formation of multiple autoantibodies.[23] PGRN has also been reported to be linked to the infiltration of macrophages in adipose tissue.

Follicular fluid is an integral microenvironment of the growing oocyte; in addition, it mirrors local metabolic, endocrine, and inflammatory events in the ovarian follicle.[24] In contrast to serum biomarkers that reflect non-localized conditions, biomarkers detected in follicular fluid may more directly represent granulosa cell activity, oxidative stress status, and intra-follicular immune status. Thus, measuring follicular fluid PGRN in parallel with serum levels of this biomarker may be interesting since it could give further information on the role that PGRN might play not only on oocyte competence but also on embryo developmental potential in ICSI cycles.[5,25,26]

Aside from cross-sectional analysis, calculations of serum PGRN fluctuations in correlation with the early follicular phase (cycle days 2–3) and oocyte pick-up (OPU) day can provide insights regarding the inflammation and metabolic response triggered after controlled ovarian stimulation. Dynamic assessment of these relationships may help clarify whether gonadotropin exposure centers on the regulation of PGRN in cycles undergoing ICSI in women with PCOS.

A limited number of studies in the literature have compared the impact of PGRN on the etiology and pathogenesis of combined obesity and infertility across different body mass index groups in the PCOS population particularly among Iraqi infertile women, given the high incidence of obesity in the Iraqi female population.[27]

This study is, to the best of our knowledge, one of the first to investigate both serum and follicular fluid PGRN concentrations in women with PCOS and their correlations with BMI and detailed ICSI outcomes such as oocyte maturity, embryo grading, and blastocyst formation. Moreover, the comparison of PGRN dynamics pre- and post-ovarian stimulation in an Iraqi PCOS population – a physiological region that has been relatively neglected in reproductive research – offers both integrative and community-specific information to help elucidate the means through which reproductive inflammation exhibits heterogeneity across ART settings.

Aim

The aim of this study is to assess IVF/ICSI results in infertile Iraqi PCOS women, with a primary focus on the impact of BMI on ICSI outcomes and to clarify the re-

lationship between fasting serum and follicular fluid PGRN levels on OPU day, BMI and ICSI outcomes as a secondary objective.

Material and methods

Ethical approval

This study adhered to the Helsinki Declaration, and the protocol received approval from the Ethics Committee of the High Institute for Infertility Diagnosis and Assisted Reproductive Technologies at Al-Nahrain University, Baghdad, Iraq (approval code: 0701-DF-2024A43 on 9/9/2024). Informed consent was obtained from each patient using a pre-prepared questionnaire.

Study setting

This prospective comparative clinical study was conducted at the High Institute for Infertility Diagnosis and Assisted Reproductive Technologies, Al-Nahrain University/Baghdad, and included 67 Iraqi women diagnosed with PCOS who underwent ICSI between the first of October 2024 and the first of April 2025. Participants had a history of initial or recurrent IVF/ICSI attempts, and embryo transfer (ET) was predominantly conducted using frozen embryo transfer with the couple's own oocytes and sperm. The study of egg morphology obtained from each infertile female's ovaries and the assessment of embryo grading were conducted in a specialized embryology laboratory within the operating theatre. Fasting serum and follicular fluid samples for PGRN quantification were collected, centrifuged, and stored under deep freezing conditions until analysis via the enzyme-linked immunosorbent assay/sandwich ELISA technique (ELK Biotechnology), Cat: ELK10952, Lot: 54225510, sensitivity: 0.51 ng/mL, detection range: 1.56–100 ng/mL, intra-assay precision: CV%<8%, inter-assay precision: CV%<10%, using the BioTek/USA semi-automated washer and reader system.

Groups of patients

This study enrolled sixty-seven infertile women with PCOS diagnoses, who underwent controlled ovarian stimulation using a flexible antagonist protocol. They were categorized as either primary or secondary infertility. The total number of included women reported complaints of PCOS, validated by the established Rotterdam criteria (oligo- or amenorrhea, clinical and biochemical evidence of excess androgen, and subcapsular small cyst morphology observed via transvaginal ultrasound follow-up).[28] Several couples also experienced male factor infertility (mild oligo-asthenozoospermia and obstructive azoospermia were included in the study).

Patients' medical assessment

A medical history review was conducted for infertile partners with PCOS with a pre-existing questionnaire. Infertile ladies had comprehensive general and gynecological evaluations. Anthropometric measures, comprising height and weight, are utilized to compute BMI using the formula (BMI=patient's weight (kg)/ patient's height $(m)^2$). Baseline levels of FSH, LH, E_2, PRL, and TSH were assessed on menstrual cycle days 2 or 3 (CD2-3), utilizing Mini VIDAS (France-BIO-MERIEUX).

A transvaginal ultrasound, a saline infusion sonogram (SIS) or a hysterosalpingogram (HSG) was performed to evaluate the integrity of the endometrial cavity and rule out pelvic pathological conditions, such as hydrosalpinx. Semen fluid analysis for males was conducted in accordance with the WHO 2021, 6th manual.[29,30]

Controlled ovarian stimulation (GnRH antagonist protocol)

Ovulation induction was initiated on cycle day 2 or 3 using the flexible GnRH antagonist protocol for all infertile women with PCOS involved in the study. A follow-up assessment of patients' responses to controlled ovarian hyperstimulation was conducted through serial transvaginal ultrasounds and serum estradiol (E_2) levels until a minimum of three leading follicles measuring approximately 14 mm were attained. Subsequently, a daily subcutaneous administration of the GnRH antagonist cetrorelix was initiated until at least three dominant follicles measuring about 17–18 mm were achieved.[31] OPU was performed following a dual ovulation trigger, utilizing 0.2 mg decapeptyl and 250 mg ovitrelle via subcutaneous injections, approximately 34–36 hours later.

Serum and follicular fluid sample collection

Fasting serum samples for PGRN assay on CD2-3, along with fasting serum and follicular fluid samples from each participant on OPU day, were collected. These samples were frozen at -80°C after being centrifuged at 5000 rpm for 10 minutes until laboratory analysis was performed using sandwich ELISA in duplicate measurements.[31-33] The quality assessment of oocytes was conducted post-denudation in the ICSI laboratory, the ovarian sensitivity index (OSI) was recorded, and the maturation rate (MR) was evaluated, subsequently followed by sperm injection into ostensibly normal MII oocytes. The fertilization rate (FR) was documented, and an assessment of embryo quality, including the classification of various embryo grades, was conducted.[28-30] Luteal phase supplementation via micronized progesterone therapy, either by transvaginal and/or intramuscular routes, was administered. Subsequently, embryo transfer (ET) and serum B-HCG assessments were conducted fourteen days post-ET, and the biochemical pregnancy rate for all subjects was evaluated.

For primary comparative analyses between BMI groups, serum and follicular fluid PGRN levels measured

on OPU day were used, as these reflect the peri-ovulatory microenvironment during ICSI. Basal serum PGRN levels measured on cycle days 2–3 were primarily used for within-group comparison to assess dynamic changes following ovarian stimulation and were considered exploratory in relation to stimulation-induced inflammatory or metabolic responses.

Determination of inclusion and exclusion criteria

Inclusion criteria

Participants were selected based on defined criteria: couples consenting to participate in the study; female patients diagnosed with PCOS according to the Rotterdam criteria, classified by BMI as either normal or overweight/obese BMI; and women aged 18 to 45 years who provided written informed consent. Both fresh and frozen embryo transfer cycles performed under adaptable GnRH antagonist regimes were included. Cases of mild oligo-asthenozoospermia and obstructive azoospermia male factor infertility were also included.

Exclusion criteria

The exclusion criteria encompassed couples who declined participation and patients with chronic conditions such as uncontrolled diabetes mellitus, dyslipidemia, hyperthyroidism, hypothyroidism, bleeding disorders, congenital adrenal hyperplasia, hypertension, cardiovascular disease, hypogonadotropic hypogonadism, or hyperprolactinemia. Women younger than 18 or older than 45 years were excluded, as were those undergoing ovarian stimulation outside of the flexible antagonist regimen. Controlled ovarian stimulation cycles yielded empty follicles (absence of oocytes) or an unreceptive endometrium (assessed via Doppler transvaginal ultrasound by the lack of the triple-line sign in the endometrial lining and elevated pulsatility index (PI) and resistance index (RI) values), or congenital anomalies of the female reproductive tract were excluded from the study.

Study design

Sixty-seven infertile females with PCOS who participated in this prospective comparative clinical study were classified into two groups according to BMI: group 1 included 30 women with normal BMI (18.5–24.9 kg/m^2), and group 2 included 37 women classified as overweight or obese (BMI ≥25 kg/m^2). Overweight and obese women were analyzed as a single group due to insufficient statistical power to allow reliable subgroup comparisons, an approach consistent with previous PCOS and ART studies.

Both fresh and frozen embryo transfer cycles were included in the analysis. Cases of primary and secondary infertility, as well as cycles with and without mild male factor infertility, were distributed across both BMI groups and were considered background clinical characteristics. No stratified subgroup analyses were performed for these variables due to sample size considerations, and comparisons were conducted primarily according to BMI classification.

Outcome definitions

Biochemical pregnancy was defined as a positive serum β-hCG measurement 14 days after embryo transfer. Maturation rate (MR) was calculated as the number of metaphase II (MII) oocytes divided by the total number of retrieved oocytes ×100. Fertilization rate (FR) was calculated as the number of two-pronuclear (2PN) fertilized oocytes divided by the number of injected MII oocytes ×100. Embryo grading was performed according to standard morphological criteria based on blastomere number, symmetry, and fragmentation on day 3, and developmental stage assessment for morula and blastocyst formation.

Statistical analysis

All data entry and coding were performed using Microsoft Excel 365 (Microsoft Corporation, Redmond, WA, USA). Statistical analyses were conducted using Minitab statistical software (Version 22; Minitab LLC, State College, PA, USA). Continuous variables were expressed as mean±standard deviation (SD), and categorical variables were presented as frequencies and percentages. Data normality was assessed using the Shapiro–Wilk test. As most continuous variables demonstrated normal distribution and homogeneity of variance, parametric tests were applied. Independent samples t-tests were used to compare continuous variables between BMI groups, and the Chi-square test was used for categorical variables. Pearson's correlation coefficient (r) was used to evaluate associations between serum or follicular fluid PGRN levels and ICSI outcomes. No adjustment for multiple comparisons were performed due to the exploratory nature of the analyses. Non-significant findings were interpreted descriptively without inferring biological causality. A p-value ≤0.05 was considered statistically significant.[34]

Results

Baseline demographic and clinical characteristics

The baseline demographic and infertility characteristics of the study population are presented in Table 1. Women with normal BMI were slightly younger and had a significantly lower BMI compared with overweight/obese women. Infertility duration was significantly longer in the overweight/obese group. The distribution of primary and secondary infertility types, as well as infertility causes, did not differ significantly between BMI groups.

Table 1. Demographic characteristics of infertile PCOS women according to BMI[a]

Characteristics	Normal BMI PCOS (n=30) (Mean±SD)	Overweight/obese PCOS (n=37) (Mean±SD)	p
Age (years)	28.9±6.0	29.9±5.4	0.484*
BMI (kg/m^2)	24.2±1.4	32.4±3.8	0.001*
Infertility duration	6.0±4.5	7.9±4.7	0.001*
Types of infertility			
Primary	26 (86.7)	31 (83.8)	0.742**
Secondary	4 (13. 3)	6 (16.2)	
Causes of infertility			
Male factor	0 (0.0)	0 (0.0)	0.212**
Female factor	5 (16.7)	11 (29.7)	
Combined factor	25 (83.3)	26 (70.3)	

[a] * – independent T test was used continues variables, ** – Chi square test was used for categorical variables

Basal hormonal profile

Basal hormonal parameters measured on cycle days 2–3 are summarized in Table 2. Anti-Müllerian hormone (AMH), FSH, LH, TSH, estradiol, and prolactin levels were comparable between groups, with no statistically significant differences observed. Although minor numerical variations were noted, these did not reach statistical significance.

Table 2. Basal serum hormonal levels of infertile PCOS women on cycle day-2 based on BMI[a]

Characteristics	Normal BMI PCOS (Mean±SD)	Overweight/obese PCOS (Mean±SD)	p*
AMH (ng/mL)	5.8±2.2	5.5±3.0	0.660
FSH (mIU/mL)	6.1±2.9	6.5±2.8	0.559
LH (mIU/mL)	8.6±7.1	7.3±4.8	0.395
TSH (mIU/mL)	1.9±1.0	2.2±2.2	0.432
Basal E_2 (pg/mL)	34.0±14.5	36.7±11.4	0.396
Prolactin (ng/mL)	16.9±8.3	15.6±7.3	0.509

[a] * – independent T test was used, AMH – anti-Mullerian hormone, FSH – follicle-stimulating hormone, LH – luteinizing hormone, TSH – thyroid-stimulating hormone

Table 3. Controlled ovarian stimulation characteristics according to BMI[a]

Characteristics	Normal BMI PCOS (Mean±SD)	Overweight/obese PCOS (Mean±SD)	p*
E_2 triggering level (pg/mL)	1860±898.0	2104.0±1622.0	0.465
FSH stimulation dose (IU)	1362±527.0	1938.0±772.0	0.001
LH stimulation dose (IU)	413±477.0	622.0±454.0	0.551
Total gonadotrophin dose (IU)	1390±586.0	2190.0±1026.0	0.001
OSI	14.8±9.6	10.6± 6.7	0.042
Duration of stimulation (days)	11.2±1.1	11.2±1.4	0.931
Number of cetrotide injection (0.25mg)	3.1±0.8	3.3±0.9	0.365

[a] * – independent samples T test was used, E_2 – estradiol, OSI – total retrieved oocyte/total gonadotropin

Controlled ovarian stimulation characteristics

Stimulation-related characteristics are shown in Table 3. Overweight/obese women required significantly higher total gonadotropin and FSH doses compared with normal BMI women. In contrast, the ovarian sensitivity index (OSI) was significantly higher in the normal BMI group. Estradiol triggering levels, LH dose, duration of stimulation, and number of antagonist injections did not differ significantly between groups.

Oocyte and embryo parameters

Oocyte and embryo characteristics are summarized in Table 4. No statistically significant differences were observed between BMI groups for total retrieved oocytes, MII oocytes, maturation rate, fertilization rate, embryo grades, morula formation, blastocyst development, or number of transferred embryos ($p>0.05$).

Numerically, normal BMI women showed slightly higher retrieved and MII oocyte counts. Conversely, overweight/obese women demonstrated higher counts of fertilized oocytes, total embryos, grade I embryos, and blastocysts; however, these differences represented descriptive trends rather than statistically significant findings.

Table 4. Oocyte and embryo characteristics of infertile PCOS women according to BMI[a]

Characteristics	Normal BMI PCOS (Mean±SD)	Overweight/obese PCOS (Mean±SD)	p*
Count of retrieved oocytes	20.7±11.4	19.9±9.8	0.739
MI oocyte count	2.8±1.4	2.7±1.7	0.849
MII oocyte count	14.3±8.3	14.3±8.0	0.989
Germinal vesicle	4.4±2.7	4.9±3.7	0.655
Abnormal oocytes	4.6±4.7	3.1±1.9	0.281
Maturation rate	71.3±21.2	70.3±22.0	0.839
Fertilized oocyte 2PN	10.6 ±6.3	10.8 ±6.7	0.926
Fertilization rate	77.5±19.2	72.7±26.4	0.407
Total embryos	10.0±5.9	11.1±6.3	0.495
Day 3 grade I embryos	5.8±3.7	6.5±3.6	0.578
Day 3 grade II embryos	2.0±1.0	3.1±1.7	0.131
Day 3 grade III embryos	0.7±0.6	2.0±0.1	0.912
Day 4 morula stage embryos	5.1±5.1	4.4±3.4	0.713
Blastocyst stage embryos	1.7±1.0	3.9±3.3	0.121
Arrested embryos	5.0±3.7	4.5±3.8	0.643
Transferred embryos	2.3±0.7	2.6±0.5	0.111

[a] * – independent T test was used, MI – metaphase I, MII – metaphase II

Serum and follicular fluid PGRN levels

Serum and follicular fluid PGRN levels measured on OPU day are presented in Table 5. No statistically significant differences were detected between BMI groups for either serum or follicular fluid PGRN concentrations.

The relationship between PGRN levels and BMI is illustrated in Figures 1 and 2. Scatterplot and boxplot analyses demonstrate no clear linear association between BMI and either serum or follicular fluid PGRN levels across study groups.

Table 5. Serum PGRN and follicular fluid PGRN of infertile PCOS on oocyte pick up day according to BMI[a]

Characteristic	Normal BMI PCOS (Mean±SD)	Overweight/obese PCOS (Mean±SD)	p*
Serum PGRN (pg/mL)	6.1±1.9	5.8±1.8	0.566
Follicular fluid PGRN (pg/mL)	6.2±2.0	6.1±1.9	0.907

[a] * – independent T test was used

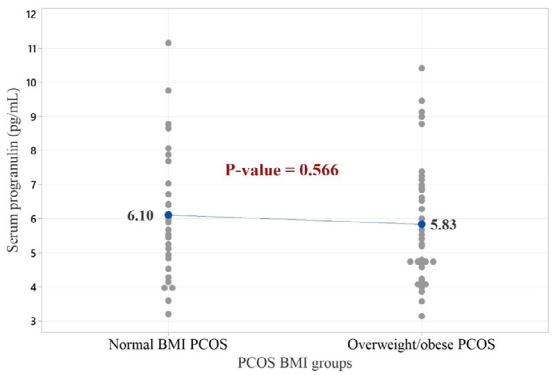

Fig. 1. Scatterplot of correlation between serum PGRN and BMI in PCOS study groups

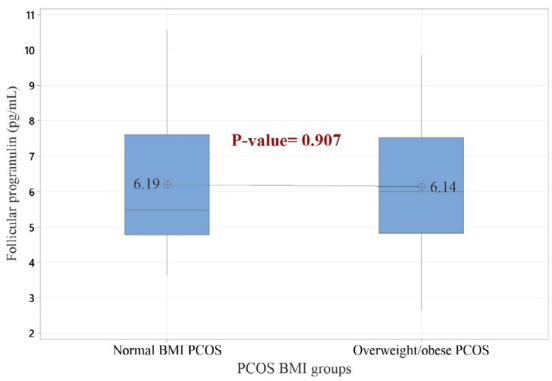

Fig. 2. Boxplot of correlation between follicular fluid PGRN and BMI in PCOS study groups

Correlation analysis with ICSI outcomes

Correlation analyses between PGRN levels and ICSI parameters are shown in Table 6. A statistically significant moderate positive correlation was observed between follicular fluid PGRN and total oocyte count. No significant correlations were identified between serum PGRN and oocyte maturity, fertilization rate, embryo grading, or number of transferred embryos. Other associations represented weak, non-significant trends.

Table 6. Correlation between serum and follicular fluid PGRN with ICSI outcomes according to BMI (r – Pearson's correlation coefficient was used)

Parameters		PCOS groups	
		Serum PGRN	Follicular fluid PGRN
Total oocyte count	r	0.063	0.312
	p	0.675	0.011
Metaphase Ioocytes	r	-0.116	0.172
	p	0.620	0.410
Metaphasell oocytes	r	0.016	0.239
	p	0.899	0.057
GV	r	0.216	0.275
	p	0.299	0.100
Maturationrate	r	-0.102	-0.030
	p	0.419	0.813
Fertilizationrate	r	-0.001	-0.161
	p	0.991	0.199
Day 3 grade 1 embryos	r	0.071	0.233
	p	0.672	0.159
Day 3 grade 2 embryos	r	-0.304	0.351
	p	0.192	0.129
Day 3 grade III embryos	r	0.306	-0.337
	p	0.694	0.663
Number of transferred embryos	r	-0.097	-0.155
	p	0.563	0.352

Pregnancy outcomes

Biochemical pregnancy outcomes are summarized in Table 7. Although the overweight/obese group showed a numerically higher biochemical pregnancy rate compared with the normal BMI group, the difference was not statistically significant.

Table 7. Biochemical pregnancy outcome in infertile PCOS women[a]

Pregnancy outcome	Normal BMI PCOS		Overweight/obese PCOS		p*
	n	%	n	%	
Positive	9	30.0	15	40.5	0.457
Negative	21	70.0	22	59.5	

[a] * – Chi -square test was used

Embryo transfer characteristics

The type of embryo transfer (fresh versus frozen) and semen source are presented in Table 8. Frozen embryo transfer cycles were more common in both groups. The distribution of embryo transfer type and semen source did not differ significantly between BMI groups.

Dynamic changes in serum PGRN

Changes between basal (cycle days 2–3) and OPU-day serum PGRN levels are shown in Table 9. Both BMI groups demonstrated a statistically significant increase in serum PGRN following ovarian stimulation. The relative increase appeared more pronounced in the normal BMI group compared with the overweight/obese group.

Table 8. Embryo transfer type and seminal fluid source used in ICSI[a]

Characteristic	Normal BMI PCOS		Overweight/obese PCOS		p*
	n	%	n	%	
Embryo transfer type					
Fresh	11	36.7	11	29.7	
Frozen	17	56.7	23	62.2	
No embryo transfer nonoembryotransfer	2	6.6	3	8.1	0.830
Seminal fluid type					
Fresh	19	63.3	28	75.7	0.724
Frozen	11	36.7	9	24.3	

[a] * – Chi -square test was used

Table 9. Comparison between basal (CD2-3) and oocyte pickup day serum PGRN levels in infertile PCOS women[a]

	Basal serum PGRN (CD2-3) (Mean ±SD) Mean±SD	OPU day serum PGRN (Mean ±SD)	Changing rate%*	p**
Normal BMI	3.7±0.3	6.4±1.6	72.9%	0.008
Overweight/obese	4.0±0.4	5.0±1.3	25.0%	0.005

[a] * – % changing rate=[OPU day – basal level/basal level]×100, ** – paired samples t-test was used to compare basal and OPU day serum PGRN levels within each group, CD – cycle day, OPU – oocyte pick-up

Discussion

This study identifies the predominant clinical phenotypes of PCOS as those with a normal BMI and those with an overweight/obese BMI.[35] The debate over the influence of hormonal abnormalities associated with PCOS on the reproductive ability of infertile women persists.[36] IR is often cited as a primary contributor to obesity, exacerbating clinical symptom severity in women with PCOS; nevertheless, it is not incorporated into the diagnostic criteria for reproductive and metabolic dysfunction.[37,38] This study divided 67 infertile women with PCOS into two groups according to their BMI status.

As reported in Table 1, the youngest group being PCOS with normal BMI (group 1: 28.9±6.0 years, p=0.484) and a longer infertility duration is reported in group 2 (7.9±4.7) with a significant difference (0.001); this may be attributed to both obesity and PCOS, corroborating the findings of the Marinelli et al. study.[39] Age is a significant determinant that affects embryo implantation.[40] A woman's fertility peaks in her late teens and early twenties, starts to decline at age thirty, and thereafter decreases more rapidly after age thirty-five. Post-forty-five, fertility diminishes markedly, making conception uncommon for women.[41] There were significant differences (p=0.001) in BMI, with normal BMI (group 1) averaging approximately 24.2±1.4 kg/m², whereas overweight/obese PCOS (group 2) presented the highest BMI at 32.4±3.8 kg/m². In group 1, primary infertility predominated over secondary infertility with combined female and male causes, showing non-significant variation (p=0.212).

Primary infertility was prevalent in the normal BMI group 1 attributed to a combination of male and female factors (PCOS).[42,43] Conversely, secondary infertility was more common in the overweight/obese PCOS group 2 [32] and this contradicts Abebe et al.[44] which reported an equal incidence of primary and secondary infertility. The female component was prevalent in group 2 due to the synergistic effects of obesity and PCOS.

Studies on the impact of obesity on oocyte quality, embryo development, mature oocyte quantity, implantation, and pregnancy rates yield inconclusive results. Genetic, environmental, and ethnic variations may account for the observed discrepancies among study participants.[45,46] Gene expression analyses performed during the window of implantation indicate that obese women with PCOS exhibit a suboptimal endometrial genetic profile and insufficient decidualisation.[47]

Table 2 demonstrates elevated AMH and LH levels, as expected in PCOS, with non-significant differences in all basal hormonal parameters (p>0.05).

Groups 1 and 2 had elevated AMH levels, consistent with findings in multiple research[48,49] which showed no significant difference. However, the present finding contrasts with findings in another study, where the causes remain unclear; still, increased BMI correlates with a reduction in AMH production from individual antral follicles due to altered granulosa cell metabolism.[50] Systemic insulin resistance is generally linked to obesity, resulting in compensatory hyperinsulinemia that modifies the responsiveness of granulosa cells and changes AMH synthesis.[51] While AMH is a dependable indicator of ovarian reserve and response to ovarian stimulation, its ability to reliably forecast live birth or pregnancy success, especially considering mother's age, remains uncertain.[52] The FSH and TSH levels on CD2-3 exhibited no significant variation between PCOS groups 1 and 2, contradicting the results of Laven 2019[53] and aligning with the findings of Saadia, 2020.[54] The serum level of LH is elevated in group 1, as corroborated by Shi et al.[55] due to the influence of obesity, which is characterized by elevated aromatase levels in adipose tissue that facilitate the conversion of androgens to estrogens. This process results in diminished pituitary gland responsiveness to GnRH and subsequent inhibition of LH, contradicting findings from multiple studies.[56] Other researchers found no significant association between BMI and elevated LH levels, noting higher LH values in lean patients and increased FSH levels in those with obesity.[57]

Basal prolactin (PRL) levels were observed to be elevated in individuals with normal BMI PCOS compared to those with overweight/obese PCOS, despite the absence of statistical significance and remaining within normal ranges (as per exclusion criteria). This finding aligns with several studies which indicate that PCOS

can present a wide spectrum of PRL levels, including higher, lower or normal levels compared to individuals without PCOS.[58-60] Clinical data suggests that prolactin (PRL) has a role in metabolic homeostasis, contingent upon its circulatory levels, since it regulates body weight activities inside adipose tissue and the pancreas. A particular PRL range value enhances metabolism.[61-63] The basal levels of E_2, TSH and PRL must be normal before the ovarian stimulation protocol commences.

The triggering levels of E_2 were elevated in group 2, with no statistically significant difference (p=0.465). Group 2 received increased doses of FSH and total gonadotrophins, demonstrating a significant difference (p=0.001, 0.001, respectively), whereas the LH dose was numerically higher, albeit with no significant variation (p=0.551). The OSI was significantly elevated in group 1 (p=0.042), as illustrated in Table 3.

Concerning E_2, levels were elevated in group 2, followed by those of group 1 PCOS, contrary to the findings of Zhou et al.[64] Estradiol is synthesized by follicular granulosa cells.[65] The serum E_2 indirectly shows the E_2 concentration in follicular fluid, which positively correlates with oocyte maturity. A higher antral follicle count and an increased number of recovered oocytes correlate with elevated E_2 levels. Xu et al.[66] determined that elevated E_2 levels did not affect pregnancy rates or live birth rates[66]; however, another trial by Li et al.[57] indicated enhanced live birth rates with E_2 levels below 5000 pg/mL and established that the E_2/oocyte ratio correlated with suboptimal reproductive implantation results due to high E_2 levels, which adversely affected endometrial receptivity.[67]

The gonadotropin requirements were elevated in overweight/obese PCOS, including both FSH dose and total gonadotropin dosages, demonstrating significant variability. The total OSI was maximal in group 1, demonstrating a considerable variance due to diminished total gonadotrophin doses requirements and an elevated count of recovered oocytes, computed as OSI=total retrieved oocytes/total gonadotrophin doses. The duration of stimulation and the number of antagonist (cetrotide) injections given were comparable in both groups. The cumulative gonadotrophin dosage needed is higher in the overweight/obese group indicating that obesity may reduce effective gonadotrophin levels, while excess adipose tissue increases leptin release, leading to relative gonadotrophin resistance.[64] Changes in pharmacodynamics, such as the absorption, bioavailability, and elimination of gonadotrophins, have been documented in obese individuals.[39]

All the parameters listed in Table 4 showed non-significant variability ($p > 0.05$); however, group 2 had a numerically larger number of fertilized oocytes, as well as total and high-quality grade 1 embryos, blastocyst embryos, and transferred embryos compared to group 1.

The quantity of retrieved oocytes was greater in PCOS group 1, while not statistically significant, suggesting a more robust ovarian response. This aligns with prior work indicating that a greater quantity of oocytes was extracted in individuals with normal BMI PCOS compared to those who are overweight/obese with PCOS,[64,68] and contrasts with other research.[7]

The mature MII oocytes showed no significant variation, although the PCOS group 1 displayed a greater quantity, in contrast to Rahman et al.[59,60] Moreover, MI oocytes revealed no significant intergroup differences.

Germinal vesicle counts were more frequent in the PCOS group 2, despite no significant difference, attributed to oocyte spindle abnormalities and disarray associated with PCOS and obesity,[54] indicating both heightened follicular activity and a potential compromise in oocyte uniformity, although abnormal oocytes were predominant in group 1.

In group 2, the quantities of fertilised oocytes and total embryos exhibited a similar trend, being more prevalent than in group 2; however, no statistical variability was observed. Nonetheless, maturation and fertilization rates remained statistically comparable between both groups, suggesting that the increased yield did not influence per-oocyte competence, which contradicts the assertion made by Zhou et al.[64] who indicated that an increase in BMI correlates with a reduction in the number of transferable embryos.

Group 2 produced a higher number of grade I embryos, contradicting the findings of many studies.[67-69] In addition, grade II and III embryos were more prevalent in the PCOS group 2, although no significant differences were seen. This phenomenon may be attributed to alterations in follicular fluid composition and metabolic dysfunction associated with obesity.[70,71] Although the morula, blastocyst, and arrested embryos exhibited no statistical differences, the quantities of morula embryos were greater in group 1, but blastocysts were more prevalent in group 2. Arrested embryos were comparable in both PCOS groups, suggesting that the increased embryo quantity may be counterbalanced by developmental attrition. The quantity of transferred embryos was higher in overweight/obese PCOS; however, no significant changes were observed to substantiate the general trend of increased embryo availability in this demographic, which should inform personalized embryo transfer techniques. The maturation and fertilization rates showed no significant difference, indicating that the higher yield did not impact per-oocyte competence.

The mean serum PGRN levels were not significantly elevated in PCOS group 1,[16,62] compared to group 2, contradicting the findings of Gorkem et al.,[72] which reported elevated serum PGRN levels associated with increased BMI, consistent with previous research in both humans and animals. Miehle et al.[19] demonstrated ele-

vated serum PGRN levels in individuals with lipodystrophy and established that this increase may arise from visceral adipose tissue and muscle.[19] PGRN is posited to facilitate development and angiogenesis following the expansion of adipose tissue in obesity.[73]

Likewise, follicular fluid PGRN levels demonstrated a similar trend, peaking in group 1 with no statistically significant difference when compared to group 2 PCOS women. In normal BMI PCOS individuals, adipose tissue secretes PGRN irrespective of BMI.[16]

The persistent absence of statistical significance, despite the observable numerical trend in group 1, indicates that BMI and PCOS status likely do not affect PGRN levels in serum or follicular microenvironments, either separately or together. These findings suggest that PGRN, although biologically significant, is unlikely to function as an independent diagnostic or stratification biomarker in relation to obesity or PCOS-associated infertility. Zhou et al.[73] noted that the levels of PGRN and PGRN mRNA are elevated in the granulosa cells of ovaries impacted by PCOS,[13] and that follicular fluid PGRN concentrations in PCOS inversely correlate with the number of retrieved oocytes, suggesting inflammatory disruptions and a possible role in forecasting ICSI outcomes.

A significant difference was found only between the total oocyte count and the follicular fluid PGRN level, which showed a moderate positive correlation ($p=0.011$, $r=0.312$). In contrast, there was a non-significant variation with negative correlations observed for the maturation rate, the fertilization rate, and the number of transferred embryos, as shown in Table 6.

In Table 7, a higher pregnancy rate was reported in group 2 with a non-significant difference, suggesting that a combination of endocrine and metabolic factors influenced these rates, with 15 out of 37 women (40.5%) attaining a positive biochemical pregnancy,[68] while group 1 exhibited a pregnancy rate of 30.0% (9/30), contrasting with Al-Yasiry et al.[47] and indicating a notable inconsistency despite an expected beneficial metabolic profile in normal-weight PCOS. These findings challenge the conventional notion that normal weight is inherently associated with optimal fertility outcomes and instead highlight the potentially advantageous reproductive responsiveness in PCOS patients, particularly those with increased BMI.

Table 8 reveals that patients with PCOS constituted the majority undergoing frozen embryo transfers, suggesting that clinicians may have opted to postpone the transfer in these high-responder patients, particularly those with PCOS, due to potential complications such as ovarian hyperstimulation syndrome (OHSS) or suboptimal endometrial receptivity conditions assessed via Doppler evaluation of subendometrial vascularity.[74-76]

The lowest proportion of cycles without embryo transfer in both PCOS groups suggested enhanced oocytes production and embryo availability, and the results indicated that a freeze-all strategy for PCOS patients enhanced the live birth rate, diminished the incidence of OHSS, and lowered the rate of miscarriages.[77,78] The elevated concentrations of steroid hormones during stimulated cycles may have modified endometrial receptivity, elucidating why frozen embryo transfers are expected to produce better outcomes than fresh transfers.[79] Freeze-all cycles are effective for high responders but not for intermediate or low responders or women of advanced maternal age.[80]

Most of the ICSI cycles used fresh sperm preparation especially group 2 with no statistical significance ($p> 0.05$), as reported in Table 8.

Table 9 indicates that there is significant variation between basal and OPU day fasting serum PGRN level ($p<0.05$) which may indicate a possible metabolic and inflammatory response to gonadotrophin administration. It is worth noting that we preferred to use an antagonist protocol in this study due to its advantages in comparison to a long agonist protocol.

Study limitations

This study has several limitations that require attention. The absence of live birth data restricts the ability to thoroughly assess the ultimate clinical effects of the treatments. The restricted sample size and selection of certain factors may limit the generalizability of the findings. A notable limitation is the lack of essential clinical objectives, such as implantation rate, clinical pregnancy, and live birth outcomes.

This research primarily focused on hormonal profiles, ovarian response, embryo quality, and oocyte development; however, these additional endpoints are crucial for a comprehensive evaluation of the significance of BMI in relation to serum and follicular fluid PGRN in PCOS.

Conclusion

PGRN levels in the serum and follicular fluid microenvironments may remain unaffected by BMI in PCOS, either independently or collectively, as evidenced by the consistent absence of statistical significance despite observable numerical trends in normal BMI PCOS individuals. A larger cohort of patients within the designated age range is necessary to elucidate the relationship between PGRN, PCOS, and BMI. In the overweight/obese PCOS group, increased embryo maturity was noted, potentially supporting the hypothesis of a threshold-dependent effect of PGRN on ovarian function. In individuals with normal BMI PCOS, elevated PGRN levels in follicular fluid may exceed a medically acceptable threshold, thereby compromising oocyte quality and embryonic developmental potential. Conversely, obese/overweight PCOS

may remain below this threshold, resulting in relatively preserved follicular function and improved assisted reproductive outcomes. The variation in serum PGRN levels following ovarian stimulation represents a research gap warranting further investigation in larger patient cohorts.

Acknowledgements

The authors express gratitude to the High Institute for Infertility Diagnosis and Assisted Reproductive Technologies/AL-Nahrain University for the resources that facilitated the completion of the work.

Declarations

Funding

The authors receive no external financial support.

Author contributions

Conceptualization, I.K.S.A. and M.S.A.; Methodology, H.A.L.M.; Software, I.K.S.A.; Validation, M.S.A. and H.A.L.M.; I.K.S.A. and M.S.A.; Formal Analysis, I.K.S.A.; Investigation, I.K.S.A..; Resources, X.X.; Data Curation, I.K.S.A. and H.A.L.M.; Writing – Original Draft Preparation, I.K.S.A.; Writing – Review & Editing, M.S.A.; Visualization, M.S.A. and H.A.L.M.; Supervision, M.S.A. and H.A.L.M.; Project Administration, H.A.L.M.; Funding Acquisition, I.K.S.A.

Conflicts of interest

The authors stated that there are no conflicts of interest.

Data availability

The data underpinning the findings of this investigation can be obtained from the corresponding author upon request.

Ethics approval

This study adhered to the Helsinki Declaration, and the protocol received approval from the Ethics Committee of the High Institute for Infertility Diagnosis and Assisted Reproductive Technologies at Al-Nahrain University, Baghdad, Iraq (Approval Code: 0701-DF-2024A43 on 9/9/2024).

References

1. He Y, Li R, Yin J, et al. Influencing of serum inflammatory factors on IVF/ICSI outcomes among PCOS patients with different BMI. *Front Endocrinol (Lausanne)*. 2023;14:1204623. doi:10.3389/fendo.2023.1204623
2. Jwad MA, Khaleefah MH, Abd AlFattah Naser R. Impact of ovarian hyperstimulation syndrome on intracytoplasmic sperm injection outcomes in polycystic ovarian syndrome women: a cross-sectional study. *Int J Reprod Biomed*. 2025;23(2):207-216. doi:10.18502/ijrm.v23i2.18496
3. Abd AN, Abu-Raghif AR, Al-Anbari LA, Salman HR. Synergistic potential of *Ecklonia cava* and oral contraceptives in managing polycystic ovary syndrome: clinical and biochemical evaluation. *Int J Drug Deliv Technol*. 2025;15(3):925-933. doi:10.25258/ijddt.15.3.3
4. Hassan MF, Abdul Kadim H, Al-Yasiry RZ, et al. Optimizing ICSI outcomes in women with PCOS: the influence of BMI, hormonal levels, and male fertility parameters. *Horm Mol Biol Clin Investig*. 2024;45(4):187-193. doi:10.1515/hmbci-2024-0035
5. Mohsin HAH, Mossa HA, Jawad MA. Impact of serum and follicular fluid secreted frizzled-related protein-5 on ICSI outcome in Iraqi infertile women with different body mass index. *Biomedicine (Taipei)*. 2023;43(4):1239-1246. doi.org/10.51248/.v43i4.3109
6. Hussein ZA, Majeed MJ, Al-Anbari LA. Impact of myo-inositol–chiro-inositol combination on the improvement of polycystic ovary syndrome condition. *Med J Babylon*. 2024;21(4):785-789. doi:10.4103/MJBL.MJBL_1026_23
7. Raaf GB, Mohammed AA, Jawad MA. Comparison of recombinant FSH antagonist protocol on serum and follicular fluid kisspeptin in PCOS and non-PCOS infertile women during ICSI. *Int J Drug Deliv Technol*. 2022;12(1):33-38. DOI: 10.25258/ijddt.12.1.6
8. Hussein HAH, Jwad MA, Mossa HA. Is there a Correlation between serum SFRP5, Wnt5a proteins and insulin resistance in Iraqi infertile females undergoing ICSI. *Al-Anbar Med J*. 2023;19(2):1-6. doi:10.33091/amj.2023.141909.1273
9. Dawood SA, Jwad MA, Mossa HA. Influence of obesity and insulin resistance on reproductive outcome of Iraqi women undergoing ICSI. *Al-Rafidain J Med Sci*. 2024;6(1):179-187.doi: 10.54133/ajms.v6i1.580
10. Hassan SF, Abu-Raghif AR, Kadhim EJ, Ridha-Salman H, Abbas AH. Phytochemical composition and hepatoprotective effects of phenolic components of Iraqi sumac (*Rhus coriaria*). *Eur J Clin Exp Med*. 2025;23(3):709-720. doi:10.15584/ejcem.2025.3.29
11. Hussein ZA, Majeed MJ, Al-Anbari LA, Al-Naqeeb SAR. Association between phosphodiesterase 9, insulin-like peptide 5 and obesity in women. *Al-Kindy Coll Med J*. 2024;20(2):117-121. doi:10.47723/6btq4431
12. Abd Ali A, Al-Hilli N, Jawad MA. Effect of obesity on ICSI outcome in Iraqi infertile females. *Biochem Cell Arch*. 2020;20(2):1-6.
13. Khalil R, Mossa H, Jwad M. Mitofusin 1 as a marker for embryo quality and development in relation to ICSI outcome. *Georgian Med News*. 2023;(345):58-61. DOI:10.28969/IJEIR.v13.i2.r4.23
14. Alhussien ZA, Mossa HAL, Abood MS. Effect of L-carnitine on apoptotic markers in PCOS women undergoing ICSI. *Int J Drug Deliv Technol*. 2022;12(4):1682-1686. DOI: 10.25258/ijddt.12.4.33
15. Al-Yasiry RZ, Jawad MA, Abbood MS. Association of MTHFR C677T polymorphism with oocyte number and embryo

quality in Iraqi infertile women undergoing ICSI. *Al-Rafidain J Med Sci*. 2024;6(1):39-45. doi:10.54133/ajms.v6i1.421

16. Abella V, Pino J, Scotece M, et al. PROGRANULIN as a biomarker and potential therapeutic agent. *Drug Discov Today*. 2017;22(10):1557-1564.
17. Uzdogan A, Kuru Pekcan M, Cil AP, Kisa U, Akbiyik F. PROGRANULIN and TNF-α in lean PCOS patients. *Gynecol Endocrinol*. 2021;37(10):925-929.
18. Donma MM, Donma O. Adipokine indices in pediatric obesity and metabolic syndrome. *Atherosclerosis Suppl*. 2018;6:9-12.
19. Miehle K, Ebert T, Kralisch S, et al. PROGRANULIN is increased in human and murine lipodystrophy. *Diabetes Res Clin Pract*. 2016;120:1-7.
20. Jian J, Li G, Hettinghouse A, Liu C. PROGRANULIN in autoimmune diseases. *Cytokine*. 2018;101:48-55.
21. Lan YJ, Sam NB, Cheng MH, Pan HF, Gao J. PROGRANULIN as a therapeutic target in immune-mediated diseases. *J Inflamm Res*. 2021;14:6543-6556.
22. Mączka K, Stasiak O, Przybysz P, et al. Endocrine and immunological function of adipose tissue in obesity-related reproduction. *Int J Mol Sci*. 2024;25(17):9391.
23. Luan YY, Zhang L, Peng YQ, et al. Immune regulation in polycystic ovary syndrome. *Clin Chim Acta*. 2022;531: 265-272.
24. Dawood SA, Jwad MA, Mossa HA. Impact of serum and follicular fluid irisin on oocyte and embryonic characteristics in infertile women undergoing ICSI according to BMI. *Al-Rafidain J Med Sci*. 2023;5:211-217.
25. Jawad HH, Al-Anbari LA, Abbood MS. Basal serum anti-Müllerian hormone and maternal age with pregnancy outcome in ICSI patients. *Ann Trop Med Public Health*. 2020;23(4):S479. doi:10.36295/ASRO.2020.2342
26. Abunaila RSH, Al-Anbari LA, Abbood MS. Effects of adding gonadotropin-releasing hormone antagonist on cycle characteristics and pregnancy rate in stimulated intrauterine insemination cycle. *Int J Res Pharm Sci*. 2020;11(3):3053-3060. doi:10.26452/ijrps.v11i3.2407
27. Schmid A, Hochberg A, Kreiß AF, et al. Role of progranulin in adipose tissue innate immunity. *Cytokine*. 2020;125:154796. doi:10.1016/j.cyto.2019.154796
28. Herez SH, Jawad MA, Abbood MS. Effect of bisphenol A level in follicular fluid on ICSI outcome. *J Pharm Negat Results*. 2022;13(4):370-376.
29. Boitrelle F, Shah R, Saleh R, et al. The sixth edition of the WHO manual for human semen analysis: a critical review and SWOT analysis. *Life (Basel)*. 2021;11(12):1368. doi:10.3390/life11121368
30. Ali HF, Abbood MS. Correlation between zinc and lead levels in serum and seminal plasma in infertile patients. *Ann Trop Med Public Health*. 2020;23(16):Sp231614. doi:10.36295/ASRO.2020.231614
31. Al-Jeborry MM, Alizzi FJ, Al-Anbari LA. Comparison of three controlled ovarian stimulation protocols in poor responders according to POSEIDON criteria. *Int J Womens Health Reprod Sci*. 2020;8(2):147-152. doi:10.15296/ijwhr.2020.23
32. Luty RS, Abbas SF, Haji SA, Ridha-Salman H. Hepatoprotective effect of catechin on acetaminophen-induced liver injury in rats. *Comp Clin Pathol*. 2025;34(4):705-718.
33. Jaafar FR, Attarbashee RK, Abu-Raghif AR, Ridha-Salman H. Gemifloxacin ameliorates acetic acid-induced ulcerative colitis via modulation of inflammatory and oxidative biomarkers in rats. *J Mol Histol*. 2025;56(4):250. doi:10.1007/s10735-025-10527-y
34. Abdulbari AS, Ali NM, Abu-Raghif AR, Matloob NA, Ridha-Salman H. Impact of azithromycin on biochemical markers and sebum composition in acne vulgaris patients. *Arch Dermatol Res*. 2025;317(1):798. doi:10.1007/s00403-025-04299-4
35. Hashim ZH, Amer L, Al-Wasiti EA. Relation of serum and follicular fluid BMP15 with oocyte quality and pregnancy rate. *J Contemp Med Sci*. 2022;8(5):337-342. doi:10.22317/jcms.v8i5.1283
36. Guedikian AA, Lee AY, Grogan TR, et al. Determinants of granulosa cell dysfunction in normal-weight women with PCOS. *Fertil Steril*. 2018;109(3):508-515. doi:10.1016/j.fertnstert.2017.11.019
37. Abruzzese GA, Silva AF, Velazquez ME, Motta AB. Hyperandrogenism and polycystic ovary syndrome: effects in pregnancy and offspring. *Wiley Interdiscip Rev Mech Dis*. 2022;14(5):e1558. doi:10.1002/wsbm.1558
38. Muhammad SM, Al-Anbari LA, Abood MS. Evaluating endometrial thickness at antagonist starting day to decide GnRH initiation in flexible antagonist protocols. *HIV Nurs*. 2022;22(2):2073-2081. doi:10.31838/hiv22.02.395
39. Marinelli S, Napoletano G, Straccamore M, Basile G. Female obesity and infertility outcomes. *Acta Biomed*. 2022; 93(4):e2022278. doi:10.23750/abm.v93i4.13162
40. Al-Obaidi MT, Mahdi HB, Alwasiti E. Impact of age and BMI on oocyte maturation and embryo development. *Biomed Res*. 2018;29(9):1920-1924.
41. Kadhim BH, Salman MO, Jwad MA. Comparison between atosiban and piroxicam before embryo transfer on IVF outcome. *Pharmacologyonline*. 2021;1:511-516.
42. Patten RK, Boyle RA, Moholdt T, et al. Exercise interventions in polycystic ovary syndrome: a systematic review. *Front Physiol*. 2020;11:606. doi:10.3389/fphys.2020.00606
43. Yilmaz FC, Sürücüoğlu MS, Çağıran FT. Association of Obesity with Primary and Secondary Infertility among Infertile Women in Turkey: A Cross-sectional Study. *J Food Nutr Res*. 2017;5(4):208-213. doi:10.12691/jfnr-5-4-2
44. Abebe MS, Afework M, Abaynew Y. Infertility in Africa: a systematic review. *Fertil Res Pract*. 2020;6(1):20. doi:10.1186/s40738-020-00092-8
45. Abdulazeez H, Abbood M, Jwad M. Impact of oxidative stress on pregnancy rate after ICSI. *Iraqi J Embryos Infertil Res*. 2022;12(2):12-29. doi:10.28969/IJEIR.v9.i2.r8

46. Zhang M, Tian HQ, Li X, et al. Body mass index and IVF-ET outcomes. *Reprod Dev Med*. 2017;1(3):140-144. doi: 10.4103/2096-2924.221278
47. Al-Yasiry RZ, Jwad MA, Hasan MF, Alsayigh HA. Effect of obesity on female fertility. *Med J Babylon*. 2022;19(2): 111-114. DOI: 10.4103/MJBL.MJBL_8_22
48. Gupta M, Yadav R, Mahey R, et al. BMI, anti-Müllerian hormone, and insulin resistance in different PCOS phenotypes. *Gynecol Endocrinol*. 2019;35(11):970-973. doi:10.1080/09513590.2019.1616680
49. Sumji S, Bhat A, Rashid A, et al. Serum anti-Müllerian hormone in PCOS diagnosis and prediction. *Gynecol Endocrinol*. 2020;36(12):1055-1059.
50. Oldfield AL, Kazemi M, Lujan ME. Obesity and anti-Müllerian hormone levels. *J Clin Med*. 2021;10(14):3192. doi:10.3390/jcm10143192
51. Jaswa EG, Rios JS, Cedars MI, et al. Body mass index and anti-Müllerian hormone decline. *J Clin Endocrinol Metab*. 2020;105(10):3234-3242. doi:10.1210/clinem/dgaa448
52. Jawad HH, Al-Anbari LA, Abbood MS. Basal anti-Müllerian hormone and maternal age in ICSI outcomes. *Ann Trop Med Public Health*. 2020;23(4):S479.
53. Laven JS. Follicle-stimulating hormone receptor polymorphisms in PCOS. *Front Endocrinol (Lausanne)*. 2019;10:23. doi:10.3389/fendo.2019.00023
54. Saadia Z. LH/FSH ratio in obese versus non-obese women with PCOS. *Med Arch*. 2020;74(4):289-292. doi:10.5455/medarh.2020.74.289-292
55. Shi W, Zhao Q, Zhao X, et al. Endocrine and metabolic indices in obese and non-obese PCOS patients. *Diabetes Metab Syndr Obes*. 2021;14:4275-4281. doi:10.2147/DMSO.S330456
56. Agarwal M, Nadolsky K. Endocrinologists' practices in obesity management. *Endocr Pract*. 2022;28(2):179-184. doi:10.1016/j.eprac.2021.11.081
57. Sachdeva G, Gainder S, Suri V, et al. Response to clomiphene citrate in obese versus non-obese PCOS women. *Indian J Endocrinol Metab*. 2019;23(2):257-262. doi:10.4103/ijem.IJEM_622_18
58. Mastnak L, Herman R, Ferjan S, et al. Prolactin in PCOS and metabolic effects. *Life (Basel)*. 2023;13(11):2124. doi: 10.3390/life13112124
59. Ponce AJ, Galván-Salas T, Lerma-Alvarado RM, et al. Low prolactin levels and insulin resistance. *Endocrine*. 2020; 67(2):331-343. doi:10.1007/s12020-019-02135-4
60. Cera N, Pinto J, Pignatelli D. Low prolactin levels in PCOS. *Rev Endocr Metab Disord*. 2024;25(6):1127-1138. doi:10.1007/s11154-024-09876-2
61. Macotela Y, Triebel J, Clapp C. Prolactin in metabolism. *Trends Endocrinol Metab*. 2020;31(4):276-286. doi:10.1016/j.tem.2019.12.004
62. Macotela Y, Ruiz-Herrera X, Vázquez-Carrillo DI, et al. Beneficial metabolic actions of prolactin. *Front Endocrinol (Lausanne)*. 2022;13:1001703. doi:10.3389/fendo.2022.1001703
63. Yang H, Di J, Pan J, et al. Prolactin and metabolic parameters in PCOS. *Front Endocrinol (Lausanne)*. 2020;11:263. doi:10.3389/fendo.2020.00263
64. Zhou H, Zhang D, Luo Z, et al. BMI and reproductive outcomes in PCOS undergoing IVF/ICSI. *Biomed Res Int*. 2020;2020:6434080. doi:10.1155/2020/6434080
65. Sreerangaraja Urs DB, Wu WH, Komrskova K, et al. Mitochondrial function in granulosa cells. *Int J Mol Sci*. 2020;21(10):3592. doi:10.3390/ijms21103592
66. Xu XL, Huang ZY, Yu K, et al. Estrogen biosynthesis and signaling in ovarian disease. *Front Endocrinol (Lausanne)*. 2022;13:827032. doi:10.3389/fendo.2022.827032
67. Li X, Zeng C, Shang J, et al. Estradiol levels on hCG day and IVF outcomes. *Chin Med J (Engl)*. 2019;132(10):1194-1201. doi:10.1097/CM9.0000000000000204
68. Pan XM, Lin Z, Li N, et al. BMI effects on IVF outcomes in PCOS. *J Zhejiang Univ Sci B*. 2018;19(6):490-496. doi: 10.1631/jzus.B1700322
69. Mahmood ZAQ, Al-Anbari LA, Al-Obaidi MT. Impact of intrauterine infusion vs. subcutaneous G-CSF injection on endometrial immunomodulation and angiogenesis in infertile women undergoing IUI. Trends Immunother. 2025;9(3):1324. doi:10.54963/ti.v9i3.1324
70. Li J, Zhang Z, Wei Y, et al. Metabonomic analysis of follicular fluid in PCOS. *Front Endocrinol (Lausanne)*. 2023;14: 1132621. doi:10.3389/fendo.2023.1132621
71. Ersoy AO, Tokmak A, Ozler S, et al. PROGRANULIN levels in adolescents with PCOS. *Arch Gynecol Obstet*. 2016;294(2):403-410. doi:10.1007/s00404-016-4065-7
72. Gorkem U, Inal ZO, Inal HA, Brostanci MO. Elevated serum PROGRANULIN in infertile obese women. *Endokrynol Pol*. 2018;69(6):661-666. doi:10.5603/EP.a2018.0065
73. Zhou D, Li S, Li W, et al. Increased PROGRANULIN expression in PCOS follicular fluid. *Eur J Obstet Gynecol Reprod Biol*. 2017;218:106-112. doi:10.1016/j.ejogrb.2017.09.016
74. Chen ZJ, Shi Y, Sun Y, et al. Fresh versus frozen embryos for infertility in women with PCOS. *N Engl J Med*. 2016;375(6):523-533. doi:10.1056/NEJMoa1513873
75. Hashim DA, Abdulbari AS, Ali NM, Al-Qaisi AHJ, Abu-Raghif AR, Ridha-Salman H. Role of B complex vitamins in reproductive health and premature ovarian failure. *Eur J Clin Exp Med*. 2025;23(4):843-852. doi:10.15584/ejcem.2025.4.3
76. Abdullah MA, Abdulhamed WA, Abood MS. Effects of vaginal sildenafil citrate on ovarian blood flow and endometrial thickness in infertile women undergoing IUI. *Int J Drug Deliv Technol*. 2021;11(4):1450-1453. doi: 10.25258/ijddt.11.4.56
77. Voss KA, Chen YF, Castillo DA, et al. Ovulation-induced frozen embryo transfer in PCOS. *J Assist Reprod Genet*. 2024;41(9):2237-2251. doi:10.1007/s10815-024-03045-2
78. Aubead NM, Ghazali BS, Abbood MS. Comparison between luteal phase estradiol and GnRH antagonist for

follicular synchronization in ICSI cycles. *Indian J Public Health Res Dev*. 2019;10(8):1-6. DOI: 10.5958/0976-5506.2019.02063.1

79. Chen Y, Zhou J, Chen Y, et al. Pregnancy outcomes after frozen versus fresh embryo transfer. *J Clin Med*. 2022;11(21):6395. doi:10.3390/jcm11216395
80. Raheem FA, Mossa HA, Abdulhamed WA, Altamimi LR. Oxidative stress changes in GnRH antagonist protocol during ICSI. *Eur J Med Health Sci*. 2019;1(5):1-6. doi: 10.1515/jomb-2017-0001

Rzeszów University Press 2026
ISSN 2544-1361 (online)
doi: 10.15584/ejcem.2026.2.10

http://www.ejcem.ur.edu.pl
European Journal of Clinical and Experimental Medicine
Eur J Clin Exp Med 2026; 24 (2): 302–315

ORIGINAL PAPER

Performance and territorial governance assessment of the National Breast Cancer Screening Program in Taza Province, Morocco (2022–2024)

Ennajar Aboujihad [1#], Abderrahmane Lamiri [2,3#], Ayoub Siabi [4], Hajar Belhaj [5], Mohamed Benfatah [6], Rabia Qaisar [2,3], Nadia Ghosne [7], Mohamed Ben Dahmane El Idrissi [8]

[1] Research Laboratory in Legal, Political, Economic and Management Sciences, Sidi Mohamed Ben Abdellah University, Polydisciplinary Faculty of Taza, Morocco
[2] Laboratory of Care, Health, and Sustainable Development, Research Team: Nursing and Health Biology, Higher Institute of Nursing and Health Techniques of Casablanca, Morocco
[3] Laboratory of Chemistry and Physics of Applied Materials, Faculty of Sciences of Ben M'sik, Hassan II University of Casablanca, Morocco
[4] Clinical Neuroscience and Mental Health Laboratory, Faculty of Medicine and Pharmacy Hassan II University of Casablanca, Morocco
[5] Higher Institute of Nursing and Health Professions, Rabat, Morocco
[6] Laboratory of Health Sciences and Technologies, Higher Institute of Health Sciences, Hassan First University of Settat, Morocco
[7] Laboratory of Care, Health, and Sustainable Development, Research Team: Health Sciences, Education and Management, Higher Institute of Nursing and Health Techniques of Casablanca, Morocco
[8] Polydisciplinary Faculty of Taza, Sidi Mohamed Ben Abdellah University, Morocco

ABSTRACT

Introduction and aim. Breast cancer is one of the leading causes of cancer-related mortality among women in Morocco. This study assessed the performance of the National Breast Cancer Screening Program (NBCSP) in Taza Province from 2022 to 2024. focusing on screening coverage, participation, detection indicators, and territorial equity.

Material and methods. We analyzed Health Information System data from 74,269 women aged 40–69 years eligible for screening. Temporal trends and rural–urban differences in screening participation and diagnostic completion were assessed using appropriate statistical models.

Results. Screening participation among the women contacted was between 54.8% and 82.0%, while overall coverage remained around 50% of the eligible population. The breast cancer detection rate was raised from 1.35 to 2.12 per 1,000 women screened. Clinical breast examination positivity was almost unchanged and low (≈2.4%). After adjustment, rural residence was associated with lower odds to participate in the screening, to complete referral and biopsy, and to get timely diagnosis within 60 days.

Corresponding author: Abderrahmane Lamiri, e-mail: a.lamiri@ispitscasa.ac.ma
# EA and AL have contributed equally and are shared first authors

Received: 17.11.2025 / Revised: 4.02.2026 / Accepted: 7.02.2026 / Published: 30.06.2026

Aboujihad E, Lamiri A, Siabi A, Belhaj H, Benfatah M, Qaisar R, Ghosne N, El Idrissi MBD. Performance and territorial governance assessment of the National Breast Cancer Screening Program in Taza Province, Morocco (2022–2024). *Eur J Clin Exp Med.* 2026;24(2):302–315. doi: 10.15584/ejcem.2026.2.10.

Conclusion. While positive changes were made in screening activities and detection indicators, there are still gaps in program quality and equity. The absence of systematic stage-at-diagnosis data limits interpretation of clinical impact and underscores the need for integrated data systems to improve breast cancer screening evaluation in.

Keywords. breast cancer screening, early detection of cancer, health information systems, patient compliance, public health programs, screening programs

Introduction

Breast cancer (BC) is the number one killer of women with cancer worldwide.[1] In developing countries, including Morocco, BC has been on the rise in recent years because of better reporting and more exposures to risk factors linked to modernization and urbanization and lifestyle transitions.[2,3] In Morocco, BC represents approximately 39% of all new cancers in women and has become one of the major public health problems. However, most patients with BC are diagnosed at an advanced stage, reflecting persistent delays in diagnosis and suboptimal screening uptake.[4]

Even though all difficulties are overcome at the national level, a large proportion of Moroccan women are still diagnosed at advanced stages, limiting the effectiveness of therapy and survival compared to high-income settings.[5] The burden continues to be exacerbated by problems such as delayed diagnosis, low participation rate, and inequities in access to quality services, particularly in rural areas.[6]

In an attempt to reduce this load, the Moroccan Ministry of Health and Social Protection established a National BC Early Detection Program in 2010.[7]

This program focuses on Clinical Breast Examination (CBE), and diagnostic mammography for BC early detection for BC survival.[8] But obstacles remain, especially access to care, the involvement of women and the quality of screening – particularly in rural areas.[6,9,10]

Where appropriate, the effect of the program should be monitored using performance measures; some examples would include participation rates, BC detection rates and time to diagnosis.

This study was initiated to evaluate the BC screening program in Taza, and comparisons were made using these performance measures compared with national and international standards. The goal is to pinpoint successes and obstacles in program implementation and offer suggestions for improvement.

Aim

To assess the practice of the national BC early detection program in Morocco focusing on the Taza province for 2022-2024 by studying performance indicators.

Material and methods

Study design

This is a retrospective descriptive and evaluative study based on institutional data, evaluating the efficacy of National BC Screening in the Taza province. The examination is based on Key Performance Indicators (KPIs) between 2022–2024.

Data sources and quality control

The present study utilized data derived from the Moroccan National HIS, an official national electronic registry utilized in Morocco for the routine monitoring of screening, diagnosis and cancer detection pathway which is a real time report from the primary health care facility, provincial diagnostic center and hospital image units.

According to the audit indicators SIS period in the province, the completion of the indicators for breast cancer screening in the Taza province 2022-2024 shows a grade ≥98%. The Regional Directorate for Health conducts monthly verification of registered screens, ensures consistency (for example, whether CBE was linked to a referral), checks for extreme values, and addresses duplicate or inconsistent entries.

There was very little (roughly 2%) missing data across all variables. Missing data was therefore managed using listwise deletion in accordance with STROBE recommendations. No missing value imputation procedures were necessary which may be related to their low proportion and random distribution.

Target population

The target population consists of 74,269 females in the age group of 40-69 years for whom the screening is eligible under the program. The inclusion criteria will include all women living in the Taza province, who are older than the defined age in need for screening having experienced at least one CBE during the study period.

Rural–urban classification and population-adjusted rate calculation

Rural–urban classification and population-adjusted analyses

Administrative geographic classification used by the Moroccan Ministry of Health and Social Protection served as a basis for separating health facilities and their catchments areas as either rural or urban.

The number of women aged 40–69 years, considered as the eligible female population, was taken separately for rural and urban areas based on the provincial demographic estimates from the HIS.

The screening performance indicators accounted for population-adjusted rates and included:

- The screening coverage rate is the number of women who have been screened divided by the total number of eligible women in each geographical area.
- Breast cancer detection rate is the number of breast cancers diagnosed per 1,000 women screened
- Referral and diagnostic completion rates, which are the fractions of screened women.

Chi-square tests were used to initially analyze the differences between rural and urban areas. Afterwards, multivariable logistic regression models were employed to compute adjusted odds ratios (ORs) with 95% confidence intervals (CIs), while also adjusting for the year and the type of healthcare facility.

This method made it possible to evenly compare the different aspects of screening performance and its results between both rural and urban areas considering the fact that the population was different.

Statistical method

These two indicators show the different aspects of the program's performance population coverage and the responsiveness (participation) of the women contacted. To prevent any confusion, the two indicators have been presented separately throughout the document.

Statistical analysis

Descriptive statistics were employed to describe screening activity, delayed diagnosis, and outcomes throughout the study period (2022-2024). The categorical variables were presented as proportions while the continuous variables were presented as medians with interquartile ranges (IQR) due to non-normal distributions.

The differences in screening participation rates and HBS positivity rates over time were tested for trends using chi-square tests (Cochran-Armitage).

It was also checked if there was a correlation between the number of screenings and the number of HBS positive cases through the Spearman correlation coefficient which is a nonparametric measure that accounts for the skewed distribution of numbers.

Geographical differences and changes in delayed diagnosis over the years were investigated using the Kruskal-Wallis test.

The comparisons between rural and urban areas were made based on population-adjusted rates. Also, multivariable logistic regression models were used to obtain odds ratios (ORs) with 95% confidence intervals (CIs) while controlling for the variable's year and type of facility.

The significance level was determined at $p<0.05$. The entire analysis was performed using the SPSS version 21 (IBM, Armonk, NY, USA).

Data availability and methodological limitations

The HIS that was the source of data for this assessment lacks a systematic recording of the stage of breast cancer diagnosis (TNM classification or early versus advanced stage). Therefore, no stage distribution, stage shift, or survival outcomes analyses were carried out.

The limitation points to the present lack of data sharing and integration between the screening, diagnostics, and oncology care units in the provincial health system. Without stage-at-diagnosis information, it is quite challenging to strictly measure the real clinical implications of screening beyond the use of intermediate performance.

Performance indicators

Definition of key performance indicators

To ensure conceptual clarity and consistency, separate operational definitions were applied to the screening performance indicators.

Screening coverage rate was defined as the proportion of women aged 40-69 years residing in the province of Taza who underwent at least one clinical breast examination (CBE) during the study period, as a proportion of the total eligible female population.

The participation (attendance) rate was defined as the proportion of women who participated in screening among those who were reached or mobilized through community campaigns, awareness-raising activities or outreach actions carried out by health facilities.

These two indicators reveal different sides to the performance of the program: the extent of population coverage and the responsiveness of the women contacted (participation). To prevent any confusion, the two indicators are shown separately through the document.

Although the design of this evaluation took into account a number of internationally recommended indicators, it was not possible to include some of the main outcome measures, e.g. stage at diagnosis, treatment initiation intervals, survival, and breast cancer–specific mortality, because there is no systematic linkage between screening, pathology, and cancer registry data. Consequently, the KPIs chosen mainly indicate program performance, quality, and equity rather than direct potential clinical impact. This choice is in line with the initial evaluations of screening programs in areas where monitoring and evaluation infrastructure is gradually emerging. These KPIs could not be assessed due to the absence of integrated cancer registry data.

The program was assessed based on the following routine and implications indicators:

- Process indicators:

Participation Rate: The women participating rate in screening among those eligible.

Delay in Diagnostic Confirmation: The time from the initial CBE to time of diagnostic confirmation.

- Impact indicators:

Detection Rate: Number of recorded BC cases per 1,000 women screened.

CBE Positivity Rate: Proportion of women referred for additional diagnostic testing among those with a positive CBE.

As per the World Health Organization (WHO) and IARC guidelines, all performance indicators were defined. These include participation rate, CBE positivity rate, detection rate per 1,000 women screened, mammography-to-biopsy delay, and referral-to-biopsy delay.

Results

Baseline population characteristics

The female population eligible for this investment stayed stable over the 3 years (n=74,269). The screening participation rates varied significantly over the years: from 66.97% to 58.83% between 2022 and 2023 before shooting up to 82.01% in 2024. Baseline characteristics of the eligible female population aged 40–69 years in the Taza Province over the study period are summarized in (Table 1). The increase observed in 2024 coincided with intensified community mobilization efforts. However, the up and down rates (in other words fluctuation) reiterate that we still need a more orderly system of invitation.

Table 1. Baseline characteristics of the target female population aged 40–69 years in the Taza Province (2022–2024)

Characteristic	2022	2023	2024
Total eligible women (n)	74,269	74,269	74,269
Screening participation (%)	68.73%	54.84%	82.01%

Although the number of women screened remained virtually constant over the three years, there were significant annual variations in participation rates. Annual screening coverage and participation rates are presented in (Table 2). These variations reflect the intensity and extent of community mobilization rather than changes in screening capacity.

Table 2. Coverage and participation rates of breast cancer screening in the Taza Province (2022–2024)*

Year	Eligible women (n)	Women screened (n)	Coverage rate (%)	Participation rate (%)
2022	74,269	37134	50%	68.73
2023	74,269	37134	50%	54.84
2024	74,269	37134	50%	82.01

* Coverage rate – women screened/total eligible population, participation rate – women screened/women reached or mobilized (Note: the total number of women screened seems the same throughout the study years because the data is aggregated and reported at the provincial level. The variation of participation rates from year to year shows the changes in the number of women that were reached or mobilized through community-based screening activities, not the changes in the screening capacity, the identical number of women screened across years reflects aggregated provincial reporting, while annual variations in participation rates are driven by differences in the number of women reached or mobilized rather than unchanged screening activity)

Process indicators

Participation rate (2022–2024)

The screening program showed varied uptake rates in the three years 2022, 2023, and 2024 with the values of 68.73 %, 54.84 %, and 82.01 % respectively (Fig 1A). After a significant increase in 2024, the data still reflects the fluctuations of the years with noticeable peaks in October during the national 'Pink October' campaign.

Global participation was stable monthly from 2022 to 2024, averaging 40% to 60% for most months. In October, participation increased markedly during October, coinciding with the national Pink October campaign, which is celebrated worldwide. Hence, the activity reached the highest value at this time. Outside of this

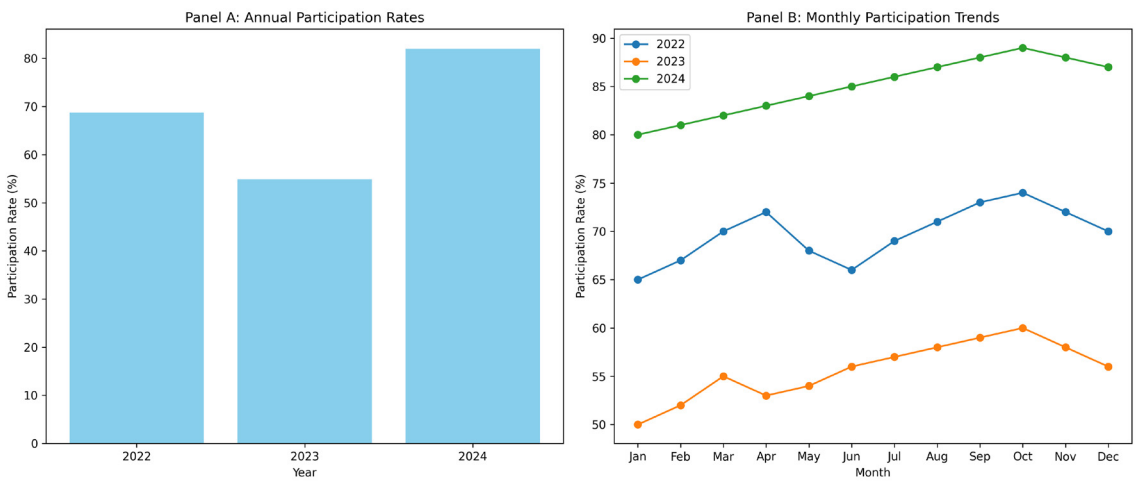

Fig. 1. Participation indicators, A: Annual participation rate in the breast cancer screening program (2022–2024), B: Monthly participation rate trends (2022–2024)

time frame, the monthly movements were contained, showing a constant but muted screening throughout the year (Fig. 1B).

CBE positivity rate (2022-2024)

The positivity rates for CBE stayed at the same level: 2.59% in 2022 and 3.25% and 3.13% in 2023 and 2024, respectively. The results for different years show that there is no significant difference (Cochran–Armitage trend test; p=0.23) (Fig. 2A).

Relationship between screening volume and positive CBE cases

The analysis done by the Spearman rank correlation method showed that the relationship between the two variables is almost perfectly positive and linear (ρ(rho)=0.98) between screening volume and the number of positive CBEs. Hence, it can be concluded that the more the screening activity, the more the detection of clinical abnormalities (Fig. 2B).

Mammography-to-biopsy delay (2022–2024)

The time between mammogram and biopsy diagnostics was significant, reduced from a 23.04-day difference in 2022 to 10.5 days in 2024. While the greater variation was recorded in 2023, it achieved a marked reduction in 2024 (Fig 3A).

Referral-to-biopsy delay (2022–2024)

The time from health center referral to biopsy rose from 61 days in 2022 to 84.5 days in 2024, with large outliers in 2024. The year-wise difference was statistically significant (Kruskal–Wallis, p<0.001) (Fig. 3B).

Rural-urban differences in population-adjusted screening performance

The percentage of people who got screened was almost the same for rural and urban areas (49.6% vs. 50.8%, p<0.05). Population-adjusted screening coverage, detection, referral completion, biopsy completion, and diagnostic delays by area of residence are detailed in (Table 3). Nevertheless, there were fewer cancer detec-

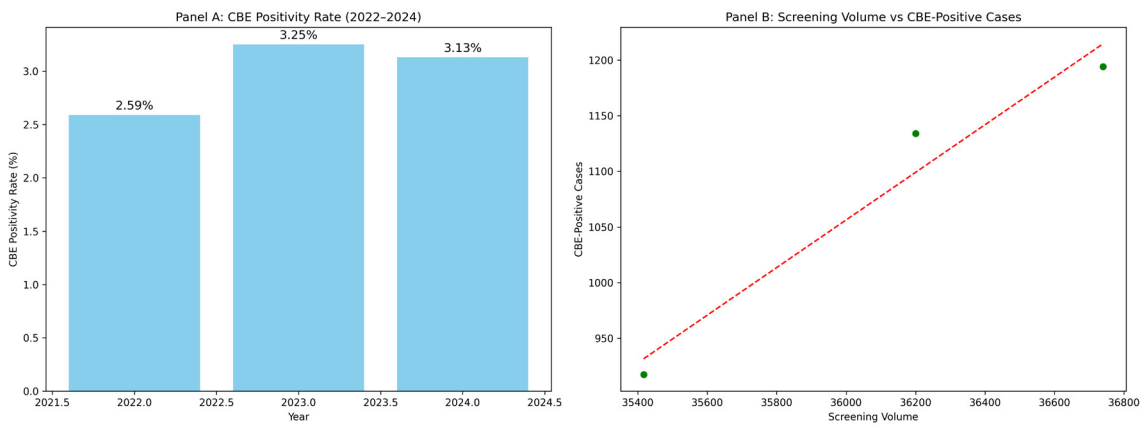

Fig. 2. Screening quality indicators, A: Clinical breast examination positivity rate (2022–2024), B: Association between screening volume and number of CBE-positive cases (Spearman correlation, ρ=0.98, p<0.001; n=36 months, CBE – clinical breast examination)

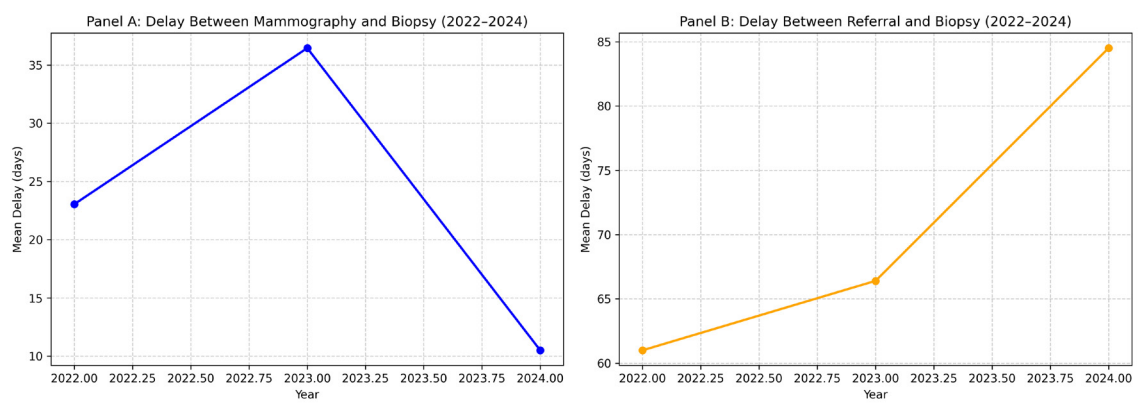

Fig. 3. Diagnostic delays, A: Delay between diagnostic mammography and biopsy (2022–2024), B: Delay between referral from health center and biopsy (2022–2024), rural–urban differences in population-adjusted screening performance

tions per 1,000 screened women in rural areas than in urban areas (2.12 vs. 3.46, p<0.05) Of the women who had clinical breast examinations and were found to have abnormal results, those living in rural areas were much less likely to have referral and biopsy procedures completed (62.0% vs. 78.0% and 58.0% vs. 74.0%, respectively; p<0.01 for both). What is more, the median diagnostic delay in rural areas was very long (82 days, IQR 60–105) compared to that in urban areas (54 days, IQR 38–72; p<0.001).

Table 3. Population-adjusted screening and diagnostic indicators by area of residence*

Indicator	Rural areas	Urban areas	p
Eligible women (40–69 yrs), *n*	123,879	98,925	–
Women screened, *n*	42,429	33,881	–
Coverage rate (%) *	49.6	50.8	0.08
Detection rate (per 1,000 screened women)	2.12 ‰	3.46 ‰	<0.05
Referral completion (%)†	62.0	78.0	<0.01
Biopsy completion (%)†	58.0	74.0	<0.01
Median diagnostic delay, days (IQR)	82 (60–105)	54 (38–72)	<0.001

* Coverage rate – number of women screened/eligible population, † – among women with abnormal clinical breast examination findings, detection rates are expressed per 1,000 screened women.
p-values were calculated using χ^2 tests for proportions and the Mann–Whitney U test for diagnostic delays, note: rural and urban eligible population figures represent cumulative demographic estimates over the study period derived from HIS-based catchment data and do not correspond to annual provincial totals

There were strong rural–urban differences in breast cancer screening performance after normalizing the data to the size of the eligible population. While the absolute figures for screenings were higher in the urban contexts, population-normalized rates showed that rural areas received less of the screening services.

Similarly, breast cancer detection rates per 1,000 women screened in rural areas were significantly below those in urban areas, likely reflecting lower screening coverage and diagnostic throughput.

Urban areas had consistently higher referral completion and biopsy completion rates; on the other hand, rural areas were characterized by longer median diagnostic delays. These variations were still statistically significant even after the adjustment for calendar year and facility type.

Adjusted odds ratios for rural versus urban residence across key screening and diagnostic outcomes are shown in (Table 4). Based on multivariable logistic regression analyses, a rural location had an independently negative association with the next steps of the diagnostic pathway after a positive screening test. It refers to the completion of referral (adjusted OR=0.58, 95% CI 0.44 0.76), biopsy (adjusted OR=0.55, 95% CI 0.39 0.77), and the receipt of a timely diagnosis within 60 days (adjusted OR=0.41, 95% CI 0.28 0.60).

Table 4. Adjusted odds ratios for rural vs. urban screening outcomes

Outcome	Adjusted OR (rural vs urban)	95% CI	p
Screening participation	0.72	0.60–0.86	<0.05
Referral completion	0.58	0.44–0.76	<0.01
Biopsy completion	0.55	0.39–0.77	<0.01
Timely diagnosis (<60 days)	0.41	0.28–0.60	<0.001

Rural–urban differences in screening activities (2022–2024)

Important rural–urban disparities were noted. Averaged over all CBE first-time women screened, these oscillated at 791 in respect of the rural and urban 942. Converse-

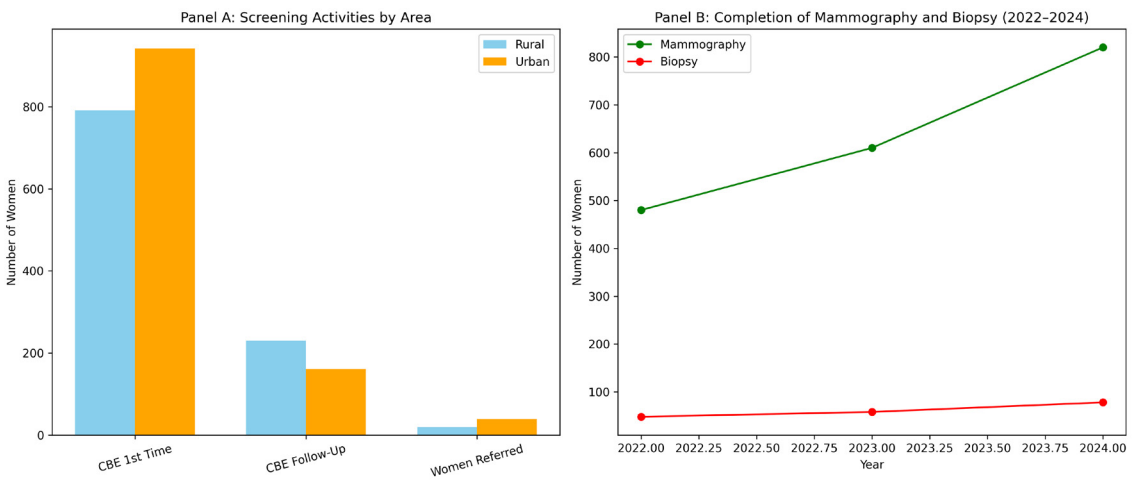

Fig. 4. Rural–urban screening disparities, A: Comparison of initial and follow-up CBE activities in rural vs. urban areas, comparison of initial and follow-up CBE, expressed as total number of examinations (n), in rural and urban areas, B: Trends in mammography and biopsy completion rates (2022–2024)

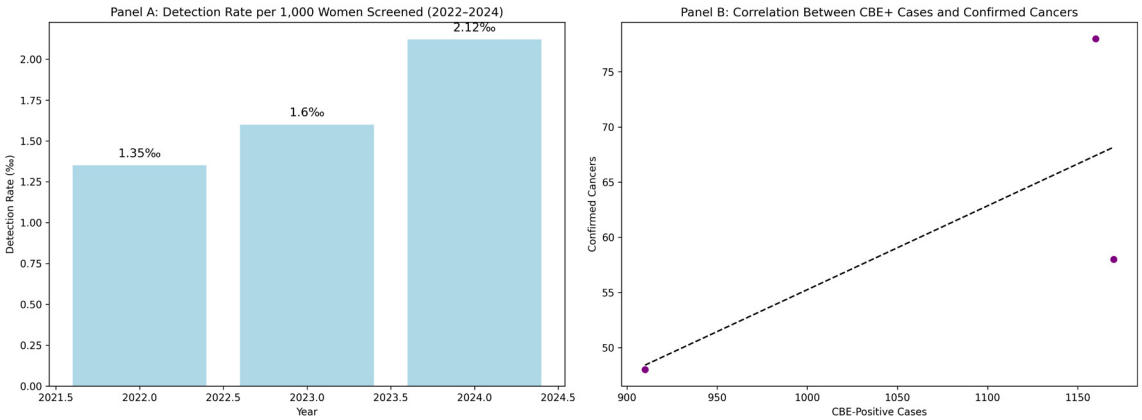

Fig. 5. Detection and confirmation indicators, A: Breast cancer detection rate per 1,000 women screened (2022–2024), B: Correlation between positive CBE cases and confirmed cancers, benign-to-malignant biopsy ratio (2022–2024)

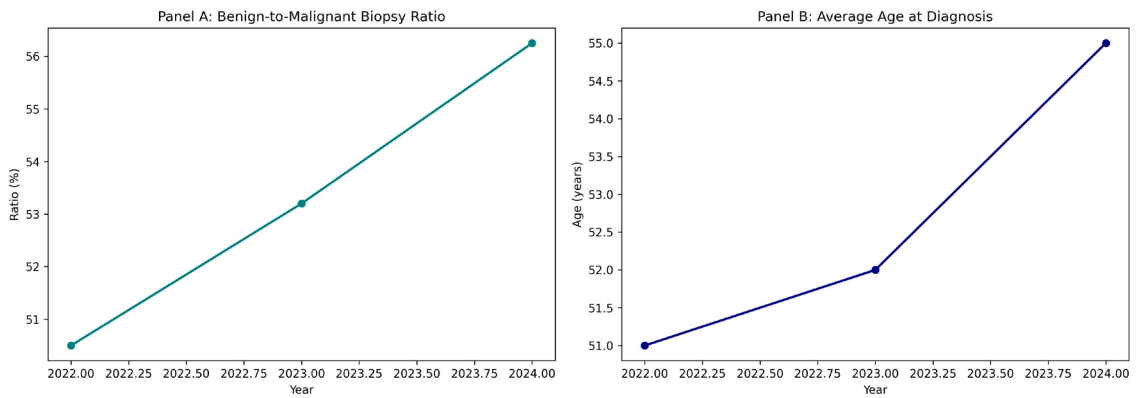

Fig. 6. Biopsy and diagnosis indicators A: Benign-to-malignant ratio of biopsies (2022–2024), B: Average age at breast cancer diagnosis (2022–2024)

ly follow-up CBE mostly occurred in the rural area (230 vs. 161). Urban areas had higher referral rates (39.50 vs. 20) (Fig. 4A).

Impact indicators

Breast cancer detection rate (2022–2024)

The detection rate has increased from 1.35 in 2022 to 2.12 per 1,000 women screened in 2024 which suggests that the program's operation was associated with the (Fig. 5A).

Correlation between CBE-positive cases and confirmed cancers

There was a weak, yet statistically significantly positive correlation (r=0.33; $p<0.05$) indicating that the numbers of CBE-positive cases are usually higher when the number of cancers detected is higher (Fig. 5B).

The Benign-to-malignant biopsy ratio rose from 50.5% in 2022 to 56.25% in 2024, indicating that there were more benign lesions among the biopsied cases (Fig 6A).

Average age at breast cancer diagnosis (2022–2024)

There was an increase in the diagnosis mean age from 51 years in 2022 to 55 years in 2024. The trend may represent variations in the different age group participation rather than real epidemiological change (Fig. 6B).

Discussion

The NBCSP evaluation findings for the Taza Province were interpreted through the perspective of systemic-level deficiencies which limited the performance, equity, and potential clinical impact of the program, rather than looking at individual indicator results.

Suboptimal population coverage and participation sustainability

Evolution of participation rates

The rates of participation in BC screening in Taza province have shown significant interannual variability over the years 2022, 2023 and 2024, respectively, 68.73% (2022), 54.84% (2023) and 82.01% (2024). Even though there was a downward curve at times, 2024 shows an upward improvement. The bigger standard deviations found, especially in 2024, would indicate that there are large seasonal variations, likely resulting from stronger awareness campaigns in "Pink October." No statistically significant temporal trend was observed in CBE pos-

itivity rates across the three years (Cochran–Armitage trend test, p=0.23).

According to European guidelines, a minimum membership of 70% is necessary for a substantial decrease in BC mortality.[1]

The Taza program exceeded this limit in 2022 as well as 2024, nevertheless, the 2023 rate was slightly below this standard. Furthermore, the Program continuously exceeded the IARC suggestion of 60% participation over two years on a continual basis.[11] The observed participation levels were consistent with international thresholds commonly cited as desirable for organized screening programs.

Nonetheless, participation rates in high-income countries are more than 70%, showing a large discrepancy. For example, the participation rates for France, Norway and Italy which have organized screening programs are 76.8%, 75% and 72%, respectively.[12–14] In comparison, the rates in Taza are far greater than Tunisia's 17.3% and Iran's 21.5%[15,16] and other MENA countries, showing some differences in the uptake of screening.

The limitation of the Moroccan current screening approach is that it is passive recruitment. This means that participants are recruited not through personal invitation, but rather through actively getting women to show up to camps through a community campaign. Evidence from around the world provides strong validation for the efficacy of organized invitation systems, which are superior to alternative methods in achieving sustainability of participation and improvements in early detection.[2] The WHO recommends such a structured approach for middle-income countries to maximize screening coverage and minimize BC deaths.[2]

Low clinical breast examination positivity rates – a critical quality concern

One of the most striking findings of this evaluation is the persistently low clinical breast examination (CBE) positivity rate, which remained between 2.4% and 3.2% throughout the 2022–2024 period. This level is substantially below the national reference range of 10–13% established by the Moroccan National Cancer Prevention and Control Plan, as well as below benchmarks reported in comparable CBE-based screening programs in low- and middle-income countries.

CBE positivity rate is not merely a descriptive indicator; it is widely recognized as a key quality marker of screening performance, reflecting the combined effects of examiner skill, adherence to examination protocols, referral thresholds, and underlying population risk. Persistently low CBE positivity rates raise concerns regarding the clinical sensitivity of primary screening and warrant further investigation.

Comparison with similar CBE-based programs

Based on international experience, it is known that CBE screening programs generally report between 8% and 15% positivity rates which largely depend on the level of examiner training, standardization of protocols, and characteristics of the target population.

In Morocco, previous national evaluations have reported CBE positivity rates ranging from 3% to 5% in earlier years, suggesting that the low rates observed in Taza are not isolated but reflect a broader structural challenge within the national screening approach.

Potential explanatory factors

There is a variety of closely related factors that could explain a low CBE positivity rate. These include differences in the training and experience of the examiners, the use of strict referral thresholds, time constraints in busy primary care settings, and, to a lesser extent, documentation practices. Population risk differences may be one of the reasons for varying positivity rates. However, this explanation itself does not seem to be enough to justify the large and consistent gap that has been observed.

Implications for program performance

Low CBE positivity has direct implications for the performance of the screening program. A screening strategy that fails to identify a sufficient proportion of clinically abnormal cases risks missing opportunities for early diagnosis, thereby limiting potential stage shift and mortality reduction.

Moreover, the observed weak correlation between CBE-positive cases and confirmed cancers suggests that linkage between primary screening and diagnostic confirmation may be suboptimal, further attenuating the potential benefits of screening.

Quality improvement recommendations

From these results, there is an immediate need for a multilayered quality improvement plan.

Immediate (0–6 months)

- Standardize CBE protocols across all primary health care facilities
- Introduce refresher training focused on practical CBE skills
- Circulate unambiguous referral standards that are in line with the national guidelines

Medium-term (6–18 months)

- Implement routine supervisory audits and peer review of CBE practices
- CBE quality indicators as a comprehensive tool for regular performance monitoring
- Improve communication systems between diagnostic centers and frontline health care providers

Long-term (≥18 months)

- Create continuous professional development programs with certification options
- Submit decision-support tools in digital health platforms
- Probe slow integration of imaging modalities gradually, if guided by available resources

These suggestions align perfectly with the WHO, the International Agency for Research on Cancer (IARC), and the Global Breast Cancer Initiative recommendations that emphasize that the quality of screening is as important as the coverage of screening.

Broader policy and system implications

The data from the Taza Province reveals the problem that many middle-income countries have to face how to increase the early detection programs without lowering the clinical quality. CBE is still a viable and quite affordable screening method in resource-limited areas, but currently, it is very dependent on human resources, supervision, and system integration.

Therefore, improving CBE quality should not be merely a technical fix, but a key management issue within the national cancer control strategy.

Weak linkage between screening and diagnostic services

It is worth mentioning that although breast cancer screening coverage was similar in rural and urban areas, differences were always seen at the subsequent stages of the screening pathway, especially regarding the detection, diagnosis, and time aspects.

According to this research, rural-dwelling women were significantly less frequently going to a specialist and having a biopsy, and the delays in diagnosis were even longer after the adjustment for age, year, and type of facility. So, these findings indicate that disparities between regions are not so much a matter of getting the first screening as they have to do with lacking further steps of care after abnormal results.

Diagnostic delays: from referral to mammography to biopsy

Taking a closer look at these indicators, some progress was noted but so were challenges. The time interval from diagnostic mammography to biopsy date was significantly reduced from 23.0 days 2022 to 10.5 days in 2024 ($H=64.58$; $p<0.001$). A reduction in mammography-to-biopsy delay was observed over time; however, the observational design precludes attribution to specific coordination mechanisms.

However, the total delay from the original health service referral to the completion of the biopsy remains an issue, increasing from 61.0 days in 2022 to 84.5 days in 2024, with significant outlying delays notably in the most recent year. The timeline for confirmed diagnoses is well over 60 days. The WHO states this is the maximum allowable period, from an abnormal finding to histopathological. This delay raises issues with disease progression at this time and the patient outcomes that follow.

The delays are common to issues faced by middle-income countries where centralized diagnostic services, underdeveloped pathological infrastructure, and logistical challenges create a bottleneck in care.[20,21] The advantages of decentralized services, digital infrastructure and integrated care pathways are demonstrated.

Trends in mammography and biopsy utilization

Between 2022 and 2024, the rates of mammography and biopsy will progressively rise indicating further maturation and enhancement of the diagnostic capacity of the program.is The substantial increase in screening volumes, particularly in 2024, can be attributed to enhanced public awareness and prevention messaging for cancer in Taza, as well as the enhanced training of healthcare providers, enhanced referral systems, and improved local diagnostic capacity. The national cancer control policies in Egypt and Jordan had similar effects in expanding their mammographic coverage.

The WHO considers that an increasing utilization of diagnostic tests in the incoming decades is a major marker of successful screening programs if it is coupled with correspondent quality assurance will be clinically relevant.[8] According to the IARC, the best way to optimize the potential benefits of screening is to shorten the intervals between screening, diagnosis and initiation of treatment.[19] The increases seen in Taza are in line with the objective of the National Cancer Control and Prevention Plan in Morocco which covers screenings while guaranteeing care continuity.

Private sector engagement and loss to follow-up

During the later study period, there was increased participation of the private sector in opportunistic screening. Simultaneously, the loss to follow-up was also rising. The increasing engagement of the private sector in the health care area is positive. The increase of access points as well as service delivery points reflect greater awareness and demand. This is in alliance with the recommendations of the WHO, where studies reflect that the private sector capacity should be aligned with the national screening process.[2]

But the concurrent rise in the number of women getting lost to follow-up after initial positive findings is a major program weakness that counteracts the potential benefits of early detection. Evidence collected show inconsistencies and anomalies. They reflect the challenge of care coordination, shortcomings in tracking systems (for example EHRs) and possibly the accessibility of diagnostic services. The IARC identifies this as a main obstacle to screening performance in low-resource settings.[5]

The Ministry of Health of Morocco is aware of these difficulties and is implementing strategies to enhance community follow-up and full registry. These initiatives link together detection and treatment, creating a closed-loop system.

Breast cancer detection rate and program performance
Screening programs have been implemented, and they have been accompanied by a better detection rate in 2023 and 2024. In 2022, the detection rate was 1.35 cases per 1,000 women screened, while in 2024 it was at 2 per 1,000 women. Detection rate differences may reflect variations in screening modality and population characteristics. According to a report, their detection in Morocco without systematic mammography screening appears to be in the order of that of Japan in a CBE-based program, phrased another way, clinical examination can deliver reasonable implementation when done properly. The discrepancy between positive cases reached by CBE and confirmed cancers (histopathologically) point at the need for better reach to diagnosis.

Benign-to-malignant biopsy ratio
The ratio of benign and malignant biopsy was even better – 50.5% in the year 2022; 56.25% in the year 2024. There is a rising proportion of benign findings in the biopsied lesions. This trend likely reflects improved identification of benign breast conditions or lower referral thresholds, or an increasing detection of low-suspicion lesions with rising screening volume.

It is inevitable and acceptable for degrees of benign biopsies to occur in screening programs, but monitoring this ratio is important for optimization of the ratio sensitivity (true cancers) and specificity (do not have invasive procedures). Biopsy positive predictive values (PPV) from international studies should be greater than 25 to 40% so that the cost benefit and patient burden do not outweigh the advantages.

Territorial inequities in access and diagnostic completion
Urban-rural disparities in screening access
There were huge differences in screening in urban and rural populations. In urban areas, the rates of first screening (CBE 1st time) were higher because of better access to health infrastructures, higher exposure to awareness campaigns, and probably higher health literacy. On the other hand, follow up CBE rates were better in rural areas. Thus, once engaged rural women seem strongly committed to future participation. This is a positive finding and may mean community-based strategies are effective.

Higher referral rates were observed in urban areas, which may be related to more established referral networks and proximity to diagnostic centers. Such a disparity has also been observed in Morocco.[4] The WHO observed that the diagnostic capacity of health facilities in middle-income countries is concentrated in urban centers.[2]

Inadequate monitoring and evaluation infrastructure: absence of stage-at-diagnosis data
One of the biggest structural weaknesses of this assessment is that the Health Information System used by the National Breast Cancer Screening Program (NBCSP) lacks systematically recorded stage-at-diagnosis data. Tumor stage at diagnosis is the main key-link between screening activity and the ultimate clinical goal of breast cancer screening, which is morbidity and mortality reduction. Without stage data, it is not feasible to examine stage distribution, stage shift over time, or follow-up outcomes such as survival, which in turn limits the interpretation of the program's potential clinical impact.

An essential goal of breast cancer screening for the population is not simply to increase the number of cases detected but to detect cancers at early stages when treatment is less invasive, and prognosis is better. Evidence from international studies consistently has shown that stage I and II cases are the ones that have been shifted in the diagnostic distribution by screening programs resulting in mortality reduction after a long period. Hence, stage-at-diagnosis is generally accepted as a main indicator for assessing screening effectiveness and thus, it is an absolute requirement for program maturity.

Because such data is missing, this analysis had to resort to intermediate performance indicators such as participation rates, detection rates, clinical breast examination (CBE) positivity, and diagnostic delays. Those measures, while informative of program organization, quality, and equity, are clinical benefit proxies at best. Therefore, even if changes in detection rates, or diagnostic intervals, notwithstanding the fact that they are changes in the direction of improvement, should not be expected to lead to better outcomes without proof of earlier-stage diagnosis.

Lacking staging data is a barrier to identifying and evaluating biases that are related to screening and well-documented in the literature. A lead-time bias can result in an increase in the observed survival time that does not represent an actual extension of the life of the patient both of which concepts can simply confuse the public if it is not well explained, whereas length-time bias allows the preferential detection of slow-growing tumors which are less aggressive. Overdiagnosis is yet another issue especially in cases where there is an increase in screening volume without a corresponding change in clinically meaningful stage shifts. Not having stage-at-diagnosis data makes it impossible to quantify these phenomena, hence the need for cautious interpretation of observed performance trends.

Similar difficulties were encountered in the initial assessments of screening programs in many low and mid-

range income countries where fragmented information systems hamper long-term patient follow-up. On the other hand, programs that have gone through the maturity stage have had the benefit of integrated registries that can link screening data with pathology, oncology, and population-based cancer registries, thus continuously staging distribution and outcomes assessment. The lessons drawn from these programs explain that data integration is not only a nice-to-have but the very base of screening governance effectiveness that the programs have benefited from.

In the Moroccan situation, the lack of standardized TNM stage reporting is therefore just one of several symptoms of the split between screening and care resulting from the fragmentation of the health system in the two different specialties. A well-functioning screening system addresses more than the detection and referral to diagnosis, staging, treatment initiation, and outcome monitoring. So it is crucial to build a strong collaboration between screening services, pathology laboratories and oncology units to allow a comprehensive evaluation of the screening program and holding the program accountable for its deliverables.

In the meantime, interim evaluations should be done in such a way that they are designed to continuously monitor whichever performance indicators that are available and to be upfront about their limitations. The NBCSP could do a lot more if audit mechanisms were strengthened, data completeness was improved, and gradually, stage-at-diagnosis reporting was incorporated. It would be a huge step toward an eventual transition from activity-based monitoring to impact assessment that matters. Closing this huge data gap should be seen as a requisite not only for the program to be on par with international standards but most importantly for it to deliver clinical benefits that are the very justification for expansion of its activity.

Relevance to healthcare management and governance

The lack of reported TNM (tumor, node, metastasis) stage-disposition in each of the four screening visits represents a key disconnect between screening and downstream clinical care processes. In order to have a positive implication on population health, an effective screening model must include not just detection and referral but also the strategic linkage to diagnostic confirmation, staging, initiation of treatment, and monitoring of treatment outcomes.

To eliminate the gap created by the lack of communication between the two systems, we must work as partners to do the following:

1. Develop an integrated system that connects the screening data with the oncology and pathology databases.
2. Develop a standardized method for the reporting of TNM stage at the time of diagnosis; and
3. Create a method to establish longitudinal follow-up at different levels of care.

Integrating these systems will strengthen the NBCSP's ability to assess its performance and assist in developing future improvements, and it will also increase the alignment of NHLBI/NBCSP's standards with those of other countries providing cancer screening (i.e., WHO).

Alternative evaluation approaches in the interim

Improving the way that diagnostic information is gathered will be essential to assess whether screening is translating into meaningful potential clinical impact.

However, without the use of comprehensive information, no accurate conclusions regarding how breast cancer screening has impacted the Taza Province can be drawn at this time.

Methods that could be used to collect diagnostic information include:

- Comparison of various In-Kind grants across the province.
- Collecting, by way of routine audits, data pertaining to benign and malignant biopsies and the potential benefits to healthcare providers; and
- Using auditory sampling to determine the extent to which certain types of breast cancer have been detected at particular healthcare facilities.

It is necessary to establish methods for collecting complete information that will ultimately be used to develop reliable conclusions about the potential benefits to patients of breast cancer screening. Data systems that gather complete information require investment in the methods of integration of cancer registry data and the integration of first-time cancer cases with existing cancer registry data.

Supporting observation

Age distribution of diagnosed cases

The average age at diagnosis has increased by four years from 2022 to 2024, from 51 years to 55 years at diagnosis. This trend likely reflects increased participation among older women rather than a true epidemiological shift. This trend is consistent with what has been seen in other middle-income countries, leaving open the question of targeting for the program. As the incidence of BC rises with age, the trend towards older diagnoses suggests missed opportunities for earlier diagnosis of younger women, particularly those with family history or other risks.

Limitations of causal inference

The analysis relied exclusively on data collected through health systems in the past (retrospective) and did not intend to indicate causal relationships for this reason; therefore, the relationship between screening activities, diagnostic information and outcomes must be ap-

proached with a very general level of caution. There was no comparison group and no randomization; therefore, the presence of incomplete downstream outcome data (especially about what stage of disease individuals were diagnosed) does not allow attributing the trends observed to the screening program itself. The findings should be viewed as descriptive, as well as associational, and reflect patterns of program implementation/performance versus definitive evidence of performance. This cautious interpretation of data supports the general recommendations provided by many organizations for evaluating population-based screening programs using an observational approach to collect data through routine sources.

Study limitations

The results of this research should be interpreted keeping in mind the limitations. Firstly, the data for the analysis was taken from routine HISs and was retrospective in nature. This might have some residual data quality problems even though the data is mostly complete and is regularly verified.

Secondly, the short period of the study (2022–2024) restricts the ability to see long-term trends and does not allow for downstream effects such as breast cancer mortality to be evaluated.

Thirdly, the lack of a control group of non-screened women and the absence of randomization mean that one cannot causally attribute the trends to the screening program. Therefore, the findings are to be interpreted as descriptive and associational indicators of how the program was performed.

Also, the research ignored the consideration of personal factors for participation like socioeconomic status, education, or health-seeking behaviors that could influence the take-up of screening and outcomes. Lastly, differences in clinical breast examination techniques and the possibility of variation in observations among doctors could not be formally checked as there were no standardized methods for measuring examiner technique and reliability.

Conclusion

This paper has evaluated the National Breast Cancer Screening Program (NBCSP) in the Taza Province by conducting a full appraisal of the program's performance, fairness, and the implementation dynamics over the years 2022–2024. Instead of enumerating individual intermediate indicators, the results were viewed from a system-level perspective, which brought to the fore the structural gaps that determine the effectiveness of screening in a middle-income environment.

In general, the program was moderately to highly successful as most people enrolled in two of the three years of the study reaching or going beyond the thresholds internationally referred to as the minimum requirements for an organized screening initiative. Nevertheless, the participation patterns were noted to have extreme fluctuations from year to year and to have a strong seasonality attributed to the fact that the program depends on community-based campaigns for recruitment rather than a sustainable invitation-based recruitment strategy.

This limits the program's capacity to ensure stable and equitable population coverage over time.

A second major finding concerns the quality of primary screening. Despite increasing screening volume, CBE positivity rates remained persistently low and substantially below national reference ranges. These findings raise concerns regarding the clinical sensitivity of CBE at the primary care level and suggest that expansion of screening activity has not been matched by proportional reinforcement of examination quality, training standardization, and quality assurance mechanisms.

The evaluation also identified weaknesses in the continuity of the screening-to-diagnosis pathway. Specific diagnostic interval improvements were noted; however, in general, delays from the first referral to histopathological confirmation still regularly surpassed the set thresholds. The increased utilization of diagnostic services such as mammography and biopsy went hand in hand with a growing number of patients lost to follow-up, especially in situations where the coordination between public and private providers is still incomplete. The above findings, in a way, highlight the existence of a care pathway fragmentation problem that could be reducing the effectiveness of early detection.

Severe territorial disparities put the program performance even more at risk. Differences between urban and rural areas in terms of access to screening, referral, and diagnostic completion remained after adjusting for population differences, and these disparities reflect the underlying inequities of the health infrastructure, service availability, and geographical accessibility. Although community-based approaches seem to be successful in encouraging follow-up among rural women who are already engaged, initial access and diagnostic referral are still very much uneven.

Most importantly, the lack of systematic stage-at-diagnosis data stands as a significant obstacle in evaluating the potential clinical benefits of the NBCSP. The distribution of stages at diagnosis is the crucial intermediate outcome that links screening to better survival, yet the existing data systems are not adequate for the assessment of stage shift or the subsequent outcomes. It is vital for the progress from mere performance monitoring to potential impact evaluation that this gap be filled by, among other things, better integration between screening services, cancer registries, and pathology databases.

Summarizing those findings, one can say that the NBCSP in the Taza province has indeed contributed to the expansion of screening and diagnostic capacity;

however, its overall efficiency is hampered by the presence of structural system gaps that are associated with participation sustainability, screening quality, care continuity, territorial equity, and monitoring infrastructure. Merely the further enlargement of coverage cannot be considered an effective approach to yield proportional gains unless it is supplemented with targeted investment in quality assurance, organized invitation systems, integrated care pathways, and powerful data systems.

These findings should be interpreted as an assessment of health system performance and equity rather than evidence of direct clinical effectiveness of breast cancer screening.

In order to have a most pronounced effect in policy and practice terms, the NBCSP must be enhanced in a way that involves a transformation from a mostly activity-based model to a quality- and equity-oriented approach that is in line with international recommendations. The next stage of research should be the longitudinal studies that involve stage-at-diagnosis data, comparative studies with non-screened populations where the situation allows, and mixed-methods studies that delve deeper into the factors affecting participation and follow-up. Such endeavors will facilitate that the increased screening activity is not just an end in itself but leads to tangible progress in early detection and patient outcomes in Morocco and other similar environments.

Declarations

Funding

This research received no specific grant from any funding agency in the public, commercial, or not-for-profit sectors.

Author contributions

Conceptualization, E.A. and A.L.; Methodology, E.A., R.Q. and H.B.; Software, A.S. and R.Q.; Validation, H.B., N.G. and M.B.D.E.I.; Formal Analysis, E.A. and A.S.; Investigation, E.A. and A.L.; Resources, A.L. and M.B.; Data Curation, E.A. and R.Q.; Writing – Original Draft, E.A.; Writing – Review & Editing, H.B., A.L. and N.G.; Visualization, A.S., M.B. and R.Q.; Supervision, A.L. and M.B.D.E.I.; Project Administration, A.L and N.G.

Conflicts of interest

No conflict of interest was declared by the authors.

Data availability

The datasets generated during and/or analyzed during the current study are available from the corresponding author on reasonable request.

Ethics approval

Ethical clearance for this study conducted at the Taza Medical Delegation for Health and Social Protection was granted from the Regional Directorate for Health and Social Protection of the Fès– Meknes Region, in coordination with the Moroccan Ministry of Health and Social Protection. Permission to access programmatic data from the NBCSP was approved by the National Health Information System (HIS).

Due to the retrospective nature of this study, secondary use of coded, de-identified anonymized data; informed consent from individual patients was waived. The study followed ethical principles of the Declaration of Helsinki and national regulations for use of health data in public health research in Morocco.

References

1. Perry N, Broeders M, de Wolf C, Törnberg S, Holland R, von Karsa L. European guidelines for quality assurance in breast cancer screening and diagnosis. Fourth edition--summary document. *Ann Oncol*. 2008;19(4):614-622. doi:10.1093/annonc/mdm481
2. World Health Organization. WHO Position Paper on Mammography Screening. WHO Press; 2023. Accessed September 20, 2025. https://www.who.int/publications/i/item/9789241507936. Accessed September 20, 2025.
3. Basu P, Ponti A, Anttila A, et al. Status of implementation and organization of cancer screening in The European Union Member States-Summary results from the second European screening report. *Int J Cancer*. 2018;142(1):44-56. doi:10.1002/ijc.31043
4. Aboulhoda F, Erefai O, Bejja F, Soulaymani A, Mokhtari A, Hami H. Breast cancer epidemiology and clinical outcomes in Moroccan women: a six-year retrospective study. *Pan Afr Med J*. 2024;49:120. doi:10.11604/pamj.2024.49.120.42588
5. International Agency for Research on Cancer. Cancer screening in the European Union: status report 2022. International Agency for Research on Cancer; 2022. Accessed September 20, 2025.https://health.ec.europa.eu/system/files/2022-09/com_2022-474_act_en.pdf.
6. World Health Organization Regional Office for the Eastern Mediterranean. Cancer control in the Eastern Mediterranean Region: progress and challenges. World Health Organization Regional Office for the Eastern Mediterranean; 2024. Accessed September 20, 2025. https://applications.emro.who.int/dsaf/dsa406.pdf. Accessed September 20, 2025.
7. International Agency for Research on Cancer, Ministry of Health of Morocco. National Cancer Prevention and Control Plan 2017–2021. Ministry of Health; 2017.
8. Frikha H, Dhouib M, Bougatef S, Kochbati L, Maalej M, Ben Abdallah M. Breast cancer screening in Tunisia. *East Mediterr Health J*. 2013;19(3):S70-S76.
9. Samah AA, Ahmadian L. Breast cancer screening in Iran: a systematic review. *Asian Pac J Cancer Prev*. 2012;13(7):3031-3036.
10. International Agency for Research on Cancer. Cancer Screening in the European Union: Report on the Imple-

mentation of the Council Recommendation on Cancer Screening. IARC; 2017.
11. Weedon-Fekjaer H, Romundstad PR, Vatten LJ. Breast cancer incidence and mortality in Norway, 1995–2014. *Acta Oncol*. 2016;55(1):1-9.
12. Karayurt O, Ozmen D, Cetinkaya AC. Knowledge and attitudes of breast self-examination and mammography in rural Turkey. *BMC Cancer*. 2012;12:43. doi:10.1186/1471-2407-12-43
13. Giordano L, Castagno R, Giorgi D, et al. Breast cancer screening in Italy: evaluating key performance indicators for time trends and activity volumes. *Epidemiol Prev*. 2015;39(3 Suppl 1):30-39.
14. Pearson K. Notes on regression and inheritance in the case of two parents. *Proc R Soc Lond*. 1895;58:240-242.
15. Anderson BO, Ilbawi AM, Fidarova E, et al. The Global Breast Cancer Initiative: a strategic collaboration to strengthen health care for non-communicable diseases. *Lancet Oncol*. 2021;22(5):578-581. doi:10.1016/S1470-2045(21)00071-1
16. Ermiah E, Abdalla F, Buhmeida A, Larbesh E, Pyrhönen S, Collan Y. Diagnosis delay in Libyan female breast cancer. *BMC Res Notes*. 2012;5:452. doi:10.1186/1756-0500-5-452
17. Ministry of Health and Population. National Cancer Control Strategy 2023–2027. MoHP; 2023.
18. Molinié F, Leux C, Delafosse P, et al. Waiting time disparities in breast cancer diagnosis and treatment: a population-based study in France. *The Breast*. 2013;22(5):810-816. doi:10.1016/j.breast.2013.02.009.
19. Vandergrift JL, Niland JC, Theriault RL, et al. Time to adjuvant chemotherapy for breast cancer in National Comprehensive Cancer Network institutions. *J Natl Cancer Inst*. 2013;105(2):104-112. doi:10.1093/jnci/djs506
20. World Health Organization Regional Office for the Eastern Mediterranean. Guide to Setting Up Breast Cancer Screening Programs. WHO-EMRO; 2015. Accessed September 20, 2025. https://www.emro.who.int/noncommunicable-diseases/summaries/guidelines-for-the-early-detection-and-screening-of-breast-cancer.html?utm_source=chatgpt.com.
21. Biesheuvel C, Weige S, Heindel W. Mammography screening: evidence, history, and current practice in Germany and other European countries. *Breast Care (Basel)*. 2011;6(2):104-109. doi:10.1159/000327493

Rzeszów University Press 2026
ISSN 2544-1361 (online)
doi: 10.15584/ejcem.2026.2.11

http://www.ejcem.ur.edu.pl
European Journal of Clinical and Experimental Medicine
Eur J Clin Exp Med 2026; 24(2): 316–324

ORIGINAL PAPER

Analysis of the effects of a continuous magnetic field on the heart and diaphragm of elderly Wistar rats

Gabriella Canan Kiekiss [1], Vanessa Grymuza de Souza [2],
Lizie Tanani Lewandoski [1], Marcia Miranda Torrejais [1],
Lucinéia de Fátima Chasko Ribeiro [1,2], Gladson Ricardo Flor Bertolini [1,2]

[1] Graduate Program in Biosciences and Health at the State University of Western Paraná (UNIOESTE), Cascavel, Paraná, Brazil
[2] Physical Therapy Course at the State University of Western Paraná (UNIOESTE), Cascavel, Paraná, Brazil

ABSTRACT

Introduction and aim. The aim was to investigate the histomorphometric effects of applying a static magnetic field (MF) of different intensities to the diaphragm muscle and heart of aging rats.

Material and methods. Continuous MF of three different intensities were applied for five consecutive days (10 hours in total). Morphological and histological variables in the diaphragm and heart were assessed, including capillary density, cardiomyocyte diameters, histopathological index, and the presence of regenerative changes.

Results. In the diaphragm, there was a significant reduction in the number of capillaries in the treated groups ($p<0.05$), with no changes in the other morphological variables ($p>0.05$). In the heart, there were no differences in cardiac mass or in the heart weight/body weight ratio ($p>0.05$), indicating no macroscopic hypertrophy. However, the intensity of 2500 G led to an increase in the area of the cardiomyocytes and their nuclei ($p<0.05$), suggesting an adaptive response to the overload. There were no significant changes in the histopathological index or in muscle degeneration characteristics ($p>0.05$).

Conclusion. Exposure to MF influenced the microcirculation of the diaphragm and promoted cellular changes in the heart, especially at higher intensities, without causing apparent damage to the tissue.

Keywords. diaphragm, heart, magnetic field therapy

Introduction

Living organisms are constantly exposed to the natural magnetic field (MF) present at the Earth's surface, which influences various natural events and animal behavior. With technological advances, artificial magnetic fields have been created through devices for communication, security, and medical equipment.[1] Consequently, human exposure to magnetic fields has increased, highlighting the importance of clarifying their effects on living organisms.[2]

Recently, the effects of MF on biological tissues have received increasing attention. The biomagnetic energy present in cellular activity, biochemical factors, and bodily fluids can, when exposed to MF, produce therapeutic effects in various tissues. These effects range from treating vascular disorders and musculoskeletal diseases to burn treatment, the prevention of type 2 diabetes mellitus, bone remodeling, and stem cell proliferation.[3–10]

In magnetotherapy, magnets are applied directly to the site of an injury. This therapy exerts beneficial effects

Corresponding author: Gladson Ricardo Flor Bertolini, e-mail: gladsonricardo@gmail.com; gladson.bertolini@unioeste.br

Received: 9.12.2025 / Revised: 26.02.2026 / Accepted: 3.03.2026 / Published: 30.06.2026

Kiekiss GC, de Souza VG, Lewandoski LT, Torrejais M.M., de Fátima Chasko Ribeiro L, Bertolini GRF. Analysis of the effects of a continuous magnetic field on the heart and diaphragm of elderly Wistar rats. *Eur J Clin Exp Med.* 2026;242):316–324. doi: 10.15584/ejcem.2026.2.11.

on the biological tissues it targets, such as during the wound healing process. The primary objectives of this application are to reduce pain, accelerate healing, and increase scar strength.[11–13] However, current research seeks to understand not only the therapeutic benefits of magnetic fields but also their potential adverse effects on living organisms. Technological advances and the use of various magnetic sources in therapeutic procedures have led to increasingly complex human exposure to magnetic fields. Despite this, there are few reports on the effects of magnetic fields on the morphology of tissues such as those of the diaphragm and the heart.[2]

It is known that MFs interact with and affect living tissues. In the case of red blood cells, exposure to an MF causes them to migrate toward the region of highest field intensity. This occurs because blood is a biomagnetic fluid capable of magnetization. The hemoglobin within red blood cells, which contains iron, reacts to magnetic fields.[14–16] This interaction can increase the attraction of red blood cells to the MF, a phenomenon that could potentially create overload on the heart and respiratory system.[17] Regarding the respiratory system, the diaphragm functions continuously to maintain breathing. With aging, its morphology changes: it becomes flatter, less elastic, exhibits reduced movement amplitude, and produces less protein. These changes weaken the muscle and can lead to a decline in its function.[18] Given these considerations, research aimed at understanding the mechanisms and effects of applying a continuous magnetic field to the diaphragm and cardiac muscle has become highly relevant.

Aim

The aim of this study was to analyze the histomorphometric effects of applying a continuous magnetic field at three different intensities on the diaphragmatic and cardiac muscle in an experimental model using elderly Wistar rats.

Material and methods

This was an experimental study using a quantitative approach. All procedures were approved by the Ethics Committee on Animal Use of the State University of Western Paraná (UNIOESTE), under protocol number 16-21, in compliance with the Arouca Law (Law No. 11,794/2008).

Animals and experimental conditions

Twenty-four Wistar rats, approximately 20 months old and weighing between 218 and 340 g, were obtained from the UNIOESTE Central Animal Facility. The animals were housed in polypropylene cages with *ad libitum* access to food and water, under controlled temperature (21±1°C) and a 12-hour light/dark photoperiod.

Experimental groups

The rats were randomized into four groups (n=6 per group) using the website https://www.graphpad.com/quickcalcs/randomize1/, a sample size based on previous studies from our laboratory:[19]

- Placebo group (GP): received copper weights (without magnetism) simulating the placebo effect.
- Group 1200 G (1200 G): exposed to a Neodymium magnet with a magnetic induction of 1200 Gauss (0.12T).
- Group 1800 G (1800 G): exposed to 1800 Gauss (0.18T).
- Group 2500 G (2500 G): exposed to 2500 Gauss (0.25T).

Static magnetic field exposure protocol (MF)

Exposure to the MF was administered using magnets affixed to custom-made cotton vests worn on the rats' backs (Fig. 1). The magnets and placebo blocks had identical dimensions (20 mm×10 mm) and similar mass (3-4 g). Animals were exposed individually for 2 hours daily over 5 consecutive days while housed in cages

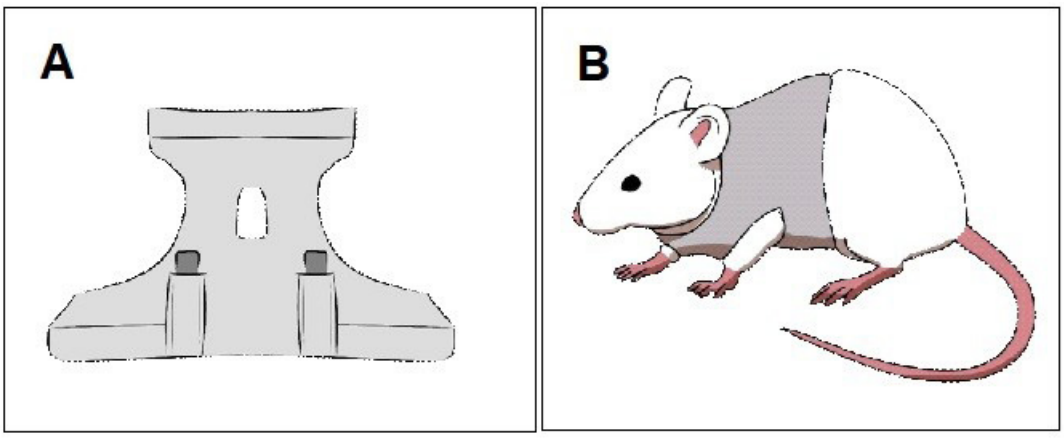

Fig. 1. Static magnetic field (SMF) exposure protocol, A: Experimental vest with view of the inner face, showing the position of the magnets (blue arrows), B: Animal with the experimental vest and magnets on the inner face

without bedding to prevent external interference. This exposure protocol was designed to simulate a therapeutic regimen applicable to humans.

Euthanasia and tissue collection

On the sixth day, the rats were euthanized via intraperitoneal injection of ketamine hydrochloride and xylazine hydrochloride. Following confirmation of the absence of reflexes, the heart and the right costal portion of the diaphragm were collected. The organs were fixed, respectively, in Methacarn (diaphragm) and 10% formalin (heart), then transferred to 70% alcohol and processed for paraffin embedding.

Histological processing and morphometric analysis

The hearts were sectioned (7 µm), stained with Hematoxylin-Eosin (HE) and analyzed in cross-sections. The following were evaluated:

- Sectional area of cardiomyocytes and their nuclei (μm^2);
- Larger and smaller diameters (µm).

For the diaphragm, sections (7 µm thick) were stained with hematoxylin and eosin (H&E) and analyzed across 10 microscopic fields at 40× magnification. In these fields, fibers, nuclei, and capillaries were quantified, along with their relative proportions. The assessment also included the presence of central nuclei and alterations such as vacuolated, hypertrophic, and hypereosinophilic fibers.

The slides were analyzed using an Olympus BX60 microscope coupled with an Olympus DP71 camera. Images were captured at 400× magnification and analyzed with Image-Pro Plus 6.0 software (Media Cybernetics®, USA). For the analysis of fiber and nuclear area, as well as the larger and smaller diameters of fibers, 100 fibers per tissue sample were measured. For all other analyses, 10 microscopic fields were assessed.

Distinct morphometric approaches were applied to cardiac and diaphragmatic tissues due to intrinsic anatomical and structural differences between these muscle types. Cardiac muscle was analyzed primarily through cardiomyocyte cross-sectional area and nuclear measurements in ventricular sections, whereas diaphragmatic analysis included fiber density, capillary quantification, and qualitative histopathological features. These methodological differences reflect established tissue-specific analytical standards rather than inconsistency in experimental design. However, this heterogeneity should be considered when interpreting and comparing tissue-specific responses.

All morphometric measurements were performed by trained evaluators blinded to group allocation using predefined standardized criteria. Each parameter was measured once per predefined field or fiber. No formal intra- or inter-observer reliability analysis was conducted.

Histopathological index

Lesions were classified as mild, moderate, or severe using the index described by Zazula et al.[20] which accounts for inflammatory disorders as well as regressive and progressive changes. The total injury score was calculated using the formula $X = a \times w$, where a represents the degree of injury and w its pathological impact. For both the index application and general histological evaluation, the assessors were blinded to the animal's treatment group.

Statistical analysis

For the adopted sample size (n=6 per group), assuming an effect size of 0.8 (Cohen's d), α=0.05, and four groups, the estimated statistical power was 80%. The assumed effect size was based on previous histomorphometric investigations conducted by our research group using comparable experimental models involving skeletal and cardiac muscle. These prior studies demonstrated moderate to large morphometric differences following biological interventions. No formal pilot study was conducted specifically for the present experimental design. Although the calculation supports adequate power for detecting large effects, the study may not have been sufficiently powered to identify subtle histomorphometric changes, particularly considering the increased biological variability associated with aged animals. Therefore, small effect sizes cannot be excluded.

The data were tabulated in Excel® and analyzed using SPSS (Statistical Package for the Social Sciences, IBM, Armonk, NY, USA) software. Analysis was performed using generalized linear models (GLM), followed by a Least Significant Difference (LSD) post hoc test. A p-value of less than 0.05 ($p<0.05$) was considered statistically significant. Results are expressed as mean±standard deviation. The GLM framework was chosen for its robustness and flexibility in accommodating either linear or gamma distributions, depending on the characteristics of the data.

Results

Body mass of the animals

Animal body weights were recorded twice during the experiment: first as a baseline measurement (EV1) one day prior to the initiation of MF exposure, and again immediately before euthanasia (EV2). No significant differences in body weight were observed between the four groups at either time point (Table 1).

Table 1. Body weight data (b), heart weight (h) and b/h ratio

		GP	1200 G	1800 G	2500 G
Body weight (g)	EV1	291±26.6	275±18.0	292±34.3	290±24.5
	EV2	279±25.0	265±18.1	275±35.5	278±22.8
Heart weight (g)		1.256±0.051	1.194±0.045	1.315±0.050	1.258±0.047
Relationship b/h (%)		0.45±0.01	0.45±0.01	0.48±0.01	0.45±0.01

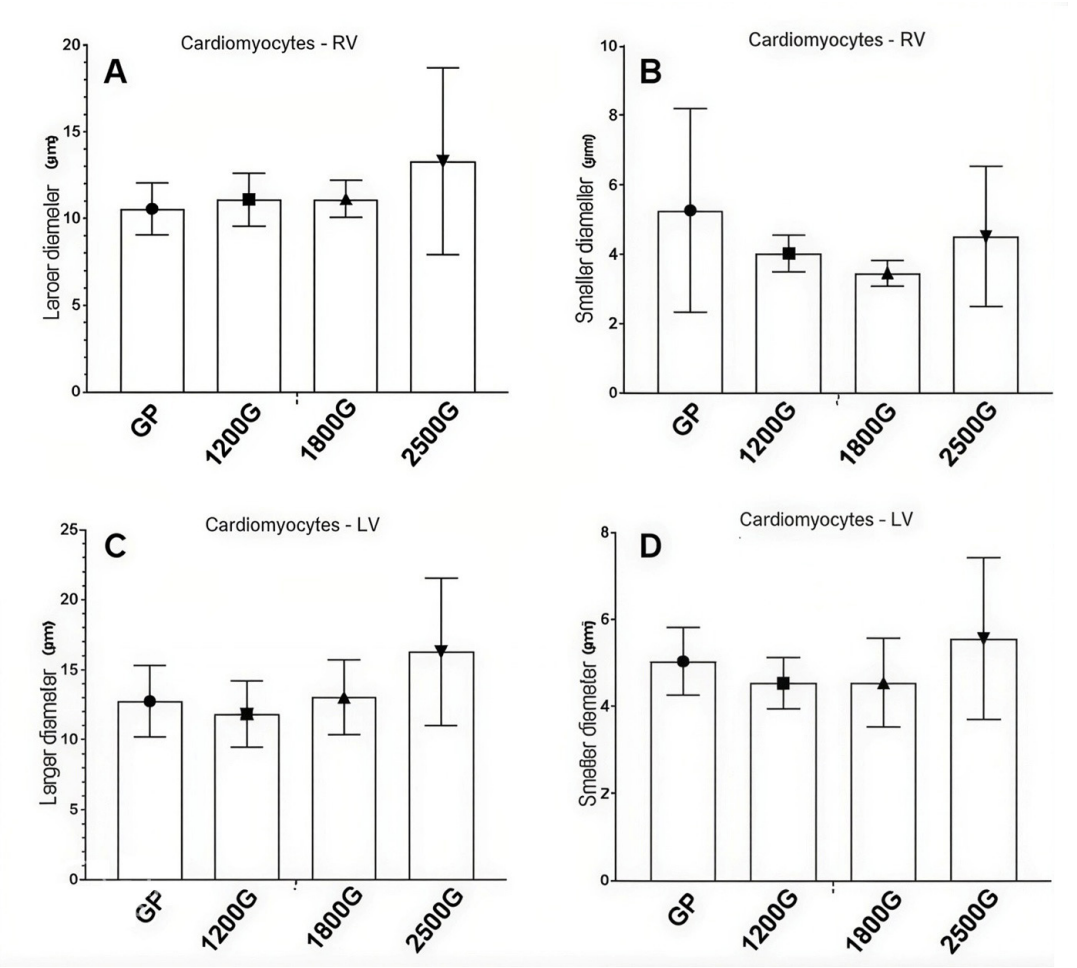

Fig 2. Histomorphometric analysis of Wistar rats exposed to different magnetic field intensities, A: major diameter of the right ventricle (RV) cardiomyocytes, B: minor diameter of the RV cardiomyocytes, C: major diameter of the left ventricle (LV), and D: minor diameter of the LV, placebo group (GP), exposure to 1200 Gauss magnet (1200 G), exposure to 1800 Gauss magnet (1800 G) and exposure to 2500 Gauss magnet (2500 G), values expressed as mean±standard deviation of the mean ($p>0.05$)

Cardiomyocyte diameter

No significant differences were observed between the groups regarding the maximum and minimum diameters of cardiomyocytes in the right ventricle (RV) (Fig. 2A, B) and the left ventricle (LV) (Fig. 2C, D) ($p>0.05$).

Cardiomyocyte area

A significant difference in right ventricular (RV) cardiomyocyte area was observed between the groups (GP, 1200 G, 1800 G, and 2500 G; $p=0.015$). Specifically, the 2500 G group exhibited a larger cardiomyocyte area compared to the GP, 1200 G, and 1800 G groups (Fig. 3A).

In the left ventricle (LV), a significant difference was also found between groups ($p=0.021$). Post-hoc analysis revealed that the 1800 G and 2500 G groups exhibited larger cardiomyocyte diameters compared to the GP and 1200 G groups ($p<0.05$; Fig. 3B).

Area of cardiomyocyte nuclei

The area of right ventricular (RV) cardiomyocyte nuclei differed significantly between groups ($p=0.016$). Post-hoc comparisons indicated that the 2500 G group exhibited a larger nuclear area than both the GP group ($p=0.003$) and the 1800 G group ($p=0.030$) (Fig. 4A).

A significant difference was also observed in the area of left ventricular (LV) cardiomyocyte nuclei between groups ($p=0.001$). The 2500 G group exhibited a larger nuclear area compared to all other groups (Fig. 4B). In summary, exposure to the 2500 G magnetic field was associated with an increase in nuclear area for cardiomyocytes in both the right and left ventricles.

Diaphragm – histological analysis

In the histomorphometric analysis of the diaphragm muscle, the GP (placebo group) exhibited muscle fibers with preserved morphology. These fibers maintained a polygonal shape, were arranged in a fascicular pattern, and were multinucleated with peripherally located nuclei (Fig. 5A).

In the 1200 G, 1800 G, and 2500 G groups, various morphological alterations were observed in the diaphragm muscle. These included amorphous, hypertrophic, and hypereosinophilic fibers; fibers with cyto-

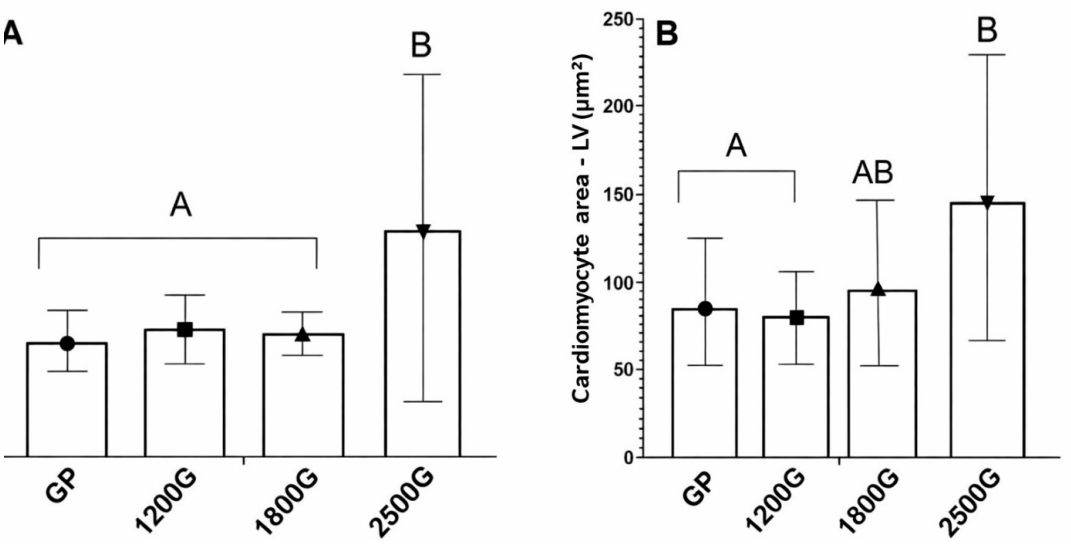

Fig. 3. Histomorphometric analysis of rat cardiomyocytes exposed to different magnetic field intensities, A: Right ventricle (RV) cardiomyocyte area, and B: left ventricle (LV) cardiomyocyte area, results expressed as mean standard deviation, placebo group (PG), exposure to 1200 Gauss magnet (1200 G), exposure to 1800 Gauss magnet (1800 G) and exposure to 2500 Gauss magnet (2500 G) ($p<0.05$), different capital letters indicate significant differences between the groups exposed to the static magnetic field ($p<0.05$)

plasmic vacuolization; fibers with altered sarcoplasmic staining; rounded fibers with differential staining; and fibers containing central nuclei (Fig. 5B–D).

Table 2. Histomorphometric measurements of the diaphragm muscle*

Parameters	GP	1200 G	1800 G	2500 G
Fiber density	546.50±88.71^{A}	515.00±40.53^{A}	509.17±99.57^{A}	524.67 ± 55.31^{A}
Number of peripherals nuclei	1302.33±229.86^{A}	1324.67±166.08^{A}	1306.17±276.34^{A}	1433.67±181.52^{A}
Nuclei/fiber ratio	2.40±0.38^{A}	2.57±0.24^{A}	2.57±0.33^{A}	2.74±0.32^{A}
Total of capillaries	174.08±32.51^{A}	132.42±34.71^{B}	127.17±26.08^{B}	137.42±29.86^{B}
Relationship capillary/fiber	0.32±0.06^{A}	0.26±0.07^{A}	0.26±0.06^{A}	0.26±0.06^{A}
Hypertrophic and hypereosinophilic muscle fiber	7.17±5.42^{A}	5.50±2.74^{A}	5.17±2.32^{A}	3.50±2.88^{A}
Muscle fiber with vacuolized cytoplasm	4.00±2.37^{A}	5.67±4.72^{A}	7.00±5.97^{A}	8.50±4.42^{A}
Muscle fiber with sarcoplasm with dye difference	27.17±25.81^{A}	22.33±9.85^{A}	13.17±5.42^{A}	13.67±6.59^{A}
Muscle fiber with central core	8.17±4.36^{A}	6.67±3.83^{A}	8.67±3.27^{A}	5.67±2.42^{A}
Histomorfometric index	11.33±1.12^{A}	9.83±0.98^{A}	9.17±0.91^{A}	9.33±0.93^{A}

* identical letters indicate statistical similarities

Histological assessment further revealed vascular congestion across all experimental groups. Additionally, significant disorganization and thickening of the perimysial connective tissue were observed in all groups examined (Fig. 5A–D).

Histomorphometric analysis of diaphragm muscle fibers revealed no significant differences between the four groups in muscle fiber density, number of peripheral nuclei, the nucleus-to-fiber ratio, or the capillary-to-fiber ratio (Table 2). However, regarding the total capillary count, significant reductions were observed in the exposed groups compared to the GP (placebo) group: 24% for 1200 G ($p<0.011$), 27% for 1800 G ($p<0.004$), and 22% for 2500 G ($p<0.025$). In the analysis of the histopathological index, despite variations in individual scores, there was no statistically significant difference between the groups, a finding consistent with the histomorphometric data.

Discussion

This study evaluated the histomorphometric effects of different intensities of a static MF on the diaphragm and heart in female rats. The main finding was a significant reduction in the total number of diaphragmatic capillaries in all treated groups, with no changes observed in the other measured variables. In cardiac tissue, both the absolute heart mass and the heart-to-body weight ratio remained unchanged, suggesting that exposure for five days (10 hours total) did not induce macroscopic cardiac hypertrophy.[21]

The literature indicates that MF can modulate microvascular tone and skin blood flow,[3,22] enhancing circulation without necessarily triggering angiogenesis. This effect may explain the absence of increased capillary density or size in the diaphragm observed in this study. Furthermore, the interaction between the iron in

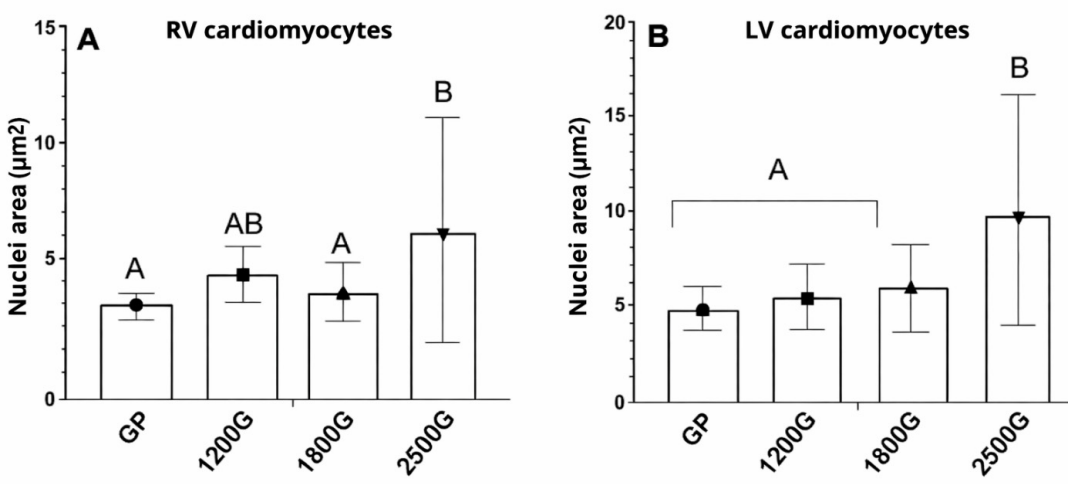

Fig. 4. Histomorphometric analysis of the cardiomyocytes of female rats exposed to different magnetic field intensities, A: Area of the nuclei of the right ventricle (RV), and B: area of the nuclei of the left ventricle (LV), placebo (GP), exposure to 1200 Gauss magnet, exposure to 1800 Gauss magnet and exposure to 2500 Gauss magnet, different capital letters indicate significant differences between the groups exposed to the static magnetic field ($p<0.05$)

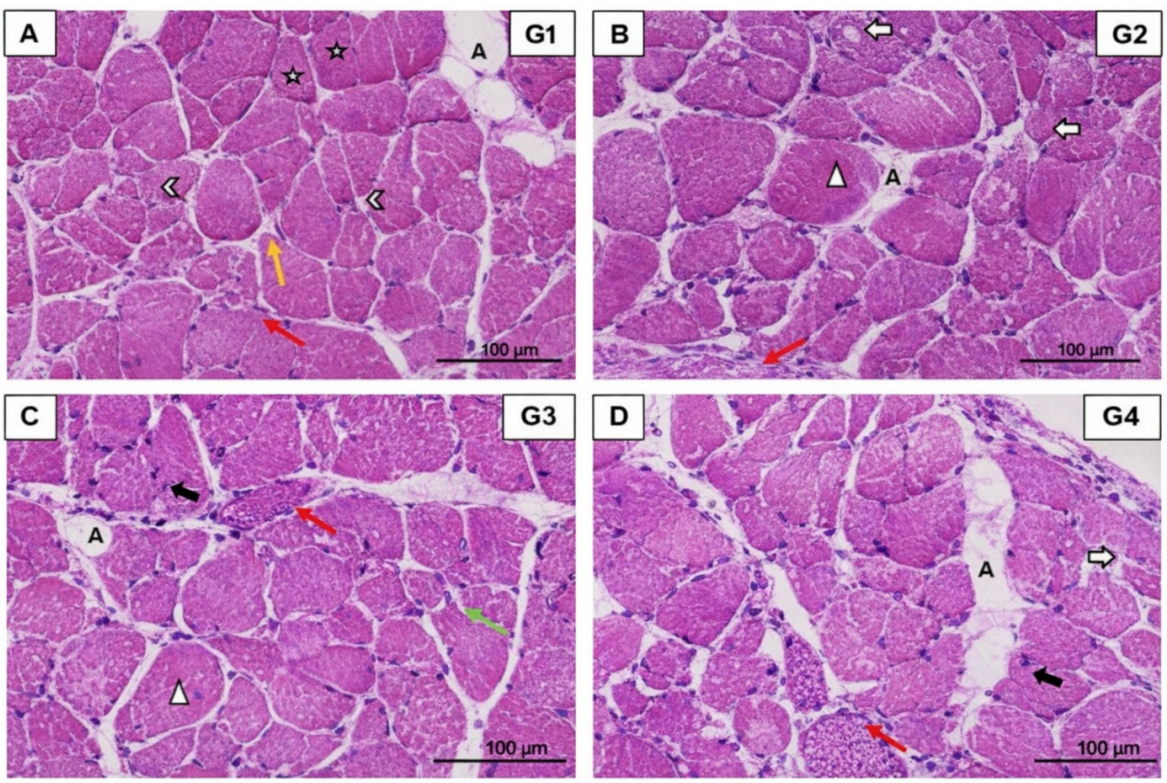

Fig. 5. Cross-sectional photomicrographs of the diaphragm muscle of Wistar rats stained with HE, A: control group (GP), with polygonal-shaped fibres (☆), peripheral nucleus (yellow arrow), disorganization and thickening of the connective tissue of the perimysium (letter A), blood capillaries (❮), congested blood vessels (red arrow), B: the lower intensity magnet exposure group (1200 G), with hypertrophic and hypereosinophilic muscle fibres (△), muscle fibers with vacuolized cytoplasm (white arrow), disorganized and enlarged connective tissue in the perimysium (letter A), congested blood vessels (red arrow), C: the medium-intensity magnet exposure group (1800 G), with hypertrophic and hypereosinophilic muscle fibers (△), disorganized and enlarged connective tissue in the perimysium (letter A), congested blood vessels (red arrow), muscle fibers with a central nucleus (black arrow), muscle fibers with a nucleus with a basophilic halo (green arrow), D: the higher intensity magnet exposure group (2500 G), with muscle fibers with vacuolized cytoplasm (white arrow), disorganized and enlarged connective tissue in the perimysium (letter A), congested blood vessels (red arrow), muscle fibers with a central nucleus (black arrow) and rounded muscle fibers with a dye difference (*)

hemoglobin and the applied MF may reduce blood viscosity.[23] This reduction could promote a more laminar flow, potentially contributing to the vascular congestion noted in the treated groups.

Morris and Skalak[3] demonstrated that even short-term exposure to a MF can reduce edema in rats, supporting the hypothesis that brief applications can modulate microcirculation. This finding underscores the need for further research to determine the optimal exposure duration required to maximize the vascular response.

Although no significant differences were observed in global histomorphometric parameters of the diaphragm muscle, animals exposed to magnetic fields exhibited discrete morphological alterations, including hypertrophic and hypereosinophilic fibers, cytoplasmic vacuolization, sarcoplasmic staining heterogeneity and centrally located nuclei, suggesting mild cellular stress and early myofiber remodeling without structural impairment. The diaphragm's high metabolic activity and continuous contractile function may favor compensatory and regenerative mechanisms that preserve overall muscle architecture despite focal alterations. Additionally, the significant reduction in the total number of capillaries in exposed groups, in the absence of changes in the capillary-to-fiber ratio, suggests microvascular remodeling rather than functional impairment. The presence of congested vessels and perimysial connective tissue thickening in all groups, including controls, indicates that these findings may reflect intrinsic characteristics of the diaphragm or technical factors related to tissue processing. Overall, the data indicate that magnetic field exposure induces subtle, non-progressive morphological and vascular changes consistent with an adaptive response rather than overt muscle pathology. The reduction in total capillary number without significant changes in the capillary-to-fiber ratio represents an apparent discrepancy. This finding may reflect sampling variability, microscopic field selection bias, or subtle microvascular rearrangement rather than true capillary rarefaction. Because endothelial markers, angiogenic signaling pathways, and functional perfusion measurements were not assessed, it is not possible to determine whether this represents structural remodeling, transient vascular redistribution, or methodological variability. Consequently, this interpretation must be considered speculative.

Exposure to the 2500 G magnetic field resulted in an increase in cardiomyocyte and nuclear area. This finding may indicate a structural alteration compatible with cellular remodeling; however, in the absence of functional (e.g., echocardiographic or hemodynamic) or molecular assessments, this interpretation remains speculative. Therefore, the present data should be regarded as descriptive morphometric observations rather than evidence of adaptive or pathological remodeling.[24] This aligns with the work of Tasić et al.,[25] who reported arterial and cardiac hypertrophy following 30 days of exposure to a 16 mT field. Variations in results across studies can be attributed to differences in exposure protocols, field characteristics, and experimental models.

The reported effects of MF in the literature can vary. For instance, Goraca et al.[26] observed the induction of oxidative stress following exposure to dynamic magnetic fields, whereas Kimsa-Dudek et al.[27] identified a reduction in oxidative stress within fibroblasts. Such contrasting results underscore that the biological effects of MFs are highly dependent on the cell type studied and the specific experimental context, including the field's characteristics.

The use of aging female rats in this study represents a sample characteristic that may have influenced the observed results. The literature identifies aging, particularly the climacteric period, as a significant risk factor for cardiac dysfunction.[28,29] Furthermore, documented morphological differences between the hearts of elderly males and females[25,30,31] offer a plausible explanation for the divergence between the findings of this study and those from research conducted on young male subjects. And diets rich in protein and carbohydrates can cause vascular wall disorders and thus increase blood pressure in elderly rats.[32]

From a clinical perspective, the observed increase in cardiomyocyte area may reflect adaptive responses to stress. This finding could be particularly relevant for populations subject to chronic MF exposure, such as industrial workers and frequent users of electronic devices.[33,34] But, this interpretation is speculative, due to the lack of functional measures such as electrocardiography. The present findings are restricted to an experimental model involving short-term static magnetic field exposure in aged female rats. Extrapolation to human exposure scenarios should be avoided, as differences in exposure duration, magnetic field characteristics, and biological context may substantially influence outcomes.

Study limitations

This study presents several limitations. First, the relatively small sample size may have limited the ability to detect subtle histomorphometric differences, particularly in aged animals characterized by increased biological variability. Second, the short exposure duration (five consecutive days) restricts interpretation regarding chronic magnetic field effects. Third, the absence of functional cardiac or respiratory assessments prevents correlation between structural findings and physiological performance. Fourth, no molecular or biochemical analyses were performed, limiting mechanistic interpretation. Fifth, intra- and inter-observer reproducibility

analyses were not conducted, which may affect measurement robustness. Finally, the exclusive use of aged female animals restricts generalizability to other age groups and to males. These limitations require cautious interpretation of the findings strictly within the boundaries of the experimental model.

Conclusion

Exposure to a static magnetic field induced discrete histomorphometric alterations in diaphragmatic microvasculature and cardiomyocyte structure in aged female rats. However, given the absence of functional and molecular assessments, these findings should be interpreted as descriptive structural observations rather than evidence of adaptive or pathological remodeling. Further studies incorporating larger samples, longer exposure periods, and multimodal assessment are necessary to clarify the biological significance of these changes.

Declarations

Funding

There was no external financing.

Author contributions

Conceptualization, G.C.K., V.G.S., L.T.L., M.M.T., L.F.C.R. and G.R.F.B.; Methodology, M.M.T., L.F.C.R. and G.R.F.B.; Formal Analysis, M.M.T., L.F.C.R. and G.R.F.B.; Investigation, G.C.K., V.G.S. and L.T.L.; Resources, M.M.T., L.F.C.R. and G.R.F.B.; Data Curation, M.M.T., L.F.C.R. and G.R.F.B.; Writing – Original Draft Preparation, G.C.K. and V.G.S.; Writing – Review & Editing, L.T.L., M.M.T., L.F.C.R. and G.R.F.B.; Visualization, M.M.T.; Supervision, L.F.C.R.; Project Administration, G.R.F.B.; Funding Acquisition, L.T.L., M.M.T., L.F.C.R. and G.R.F.B.

Conflicts of interest

The authors declare no competing interests.

Data availability

The datasets generated during and/or analyzed during the current study are available from the corresponding author on reasonable request.

Ethics approval

The research project was approved by the Animal Use Ethics Committee of the State University of Western Paraná. (protocol 16-21).

Use of AI and AI-assisted technologies in the writing process

During the preparation of this work the author(s) used DeepL and DeepSeek in order to assist in translating the text into English.

References

1. Ghodbane S, Lahbib A, Sakly M, Abdelmelek H. Bioeffects of static magnetic fields: oxidative stress, genotoxic effects, and cancer studies. *Biomed Res Int*. 2013;2013:1-12. doi:10.1155/2013/602987
2. Romanenko S, Begley R, Harvey AR, Hool L, Wallace VP. The interaction between electromagnetic fields at megahertz, gigahertz and terahertz frequencies with cells, tissues and organisms: risks and potential. *J R Soc Interface*. 2017;14(137):20170585. doi:10.1098/rsif.2017.0585
3. Morris CE, Skalak TC. Chronic static magnetic field exposure alters microvessel enlargement resulting from surgical intervention. *J Appl Physiol*. 2007;103(2):629-636. doi:10.1152/japplphysiol.01133.2006
4. Keskin Y. The effect of magnetic field therapy and electric stimulation on experimental burn healing. *Turk J Phys Med Rehabil*. 2019;65(4):352-360. doi:10.5606/tftrd.2019.2899
5. Yu B, Liu J, Cheng J, et al. A static magnetic field improves iron metabolism and prevents high-fat-diet/streptozocin--induced diabetes. *The Innovation*. 2021;2(1):100077. doi:10.1016/j.xinn.2021.100077
6. Yang J, Wu J, Guo Z, Zhang G, Zhang H. Iron oxide nanoparticles combined with static magnetic fields in bone remodeling. *Cells*. 2022;11(20):3298. doi:10.3390/cells11203298
7. Wang Y, Jiang Y, Hu J, et al. Dynamic evolution of cardiac function and glucose and lipid metabolism in ovariectomized rats and the intervention effect of erxian decoction. *Evidence-Based Complementary and Alternative Medicine*. 2022;2022:1-14. doi:10.1155/2022/8090868
8. Wu H, Li C, Masood M, et al. Static magnetic fields regulate t-type calcium ion channels and mediate mesenchymal stem cells proliferation. *Cells*. 2022;11(15):2460. doi:10.3390/cells11152460
9. Zhao J, Li Y guo, Deng K qin, Yun P, Gong T. Therapeutic effects of static magnetic field on wound healing in diabetic rats. *J Diabetes Res*. 2017;2017:1-5. doi:10.1155/2017/6305370
10. Lv H, Liu J, Zhen C, et al. Magnetic fields as a potential therapy for diabetic wounds based on animal experiments and clinical trials. *Cell Prolif*. 2021;54(3). doi:10.1111/cpr.12982
11. Henry SL, Concannon MJ, Yee GJ. The effect of magnetic fields on wound healing experimental study and review of the literature. *Eplasty*. 2008;8:e40.
12. Feng C, Yu B, Song C, et al. Static magnetic fields reduce oxidative stress to improve wound healing and alleviate diabetic complication. *Cells*. 2022;11(3):443. doi:10.3390/cells11030443
13. Taniguchi N, Kanai S, Kawamoto M, Endo H, Higashino H. Study on application of static magnetic field for adjuvante arthritis rats. *Evidence-Based Complementary and Alternative Medicine*. 2004;1(2):187-191. doi:10.1093/ecam/neh024

14. Schenck JF. Physical interactions of static magnetic fields with living tissues. *Prog Biophys Mol Biol*. 2005;87(2-3):185-204. doi:10.1016/j.pbiomolbio.2004.08.009
15. Tzirtzilakis EE, Xenos MA. Biomagnetic fluid flow in a driven cavity. *Meccanica*. 2013;48(1):187-200. doi:10.1007/s11012-012-9593-7
16. Zhang B, Yuan X, Lv H, Che J, Wang S, Shang P. Biophysical mechanisms underlying the effects of static magnetic fields on biological systems. *Prog Biophys Mol Biol*. 2023;177:14-23. doi:10.1016/j.pbiomolbio.2022.09.002
17. Mayda S, Kandemir Z, Bulut N, Maekawa S. Magnetic mechanism for the biological functioning of hemoglobin. *Sci Rep*. 2020;10(1):8569. doi:10.1038/s41598-020-64364-y
18. Bordoni B, Morabito B, Simonelli M. Ageing of the diaphragm muscle. *Cureus*. 2020;12(1):e6645. doi:10.7759/cureus.6645
19. Costa LNC, de Paula TP, Zazula MF, et al. Maternal periodontitis potentiates monosodium glutamate-obesity damage on Wistar offspring's fast-glycolytic muscle. *Oral Dis*. 2024;30(7):4705-4720. doi:10.1111/odi.14890
20. Zazula MF, de Andrade BZ, Toni Boaro C De, et al. Development of a histopathological index for skeletal muscle analysis in Rattus norvegicus (Rodentia: Muridae). *Acta Histochem*. 2022;124(4):151892. doi:10.1016/j.acthis.2022.151892
21. Pacagnelli FL, Sabela AKD de A, Mariano TB, et al. Fractal dimension in quantifying experimental-pulmonary-hypertension-induced cardiac dysfunction in rats. *Arq Bras Cardiol*. Published online 2016. doi:10.5935/abc.20160083
22. Okano H, Gmitrov J, Ohkubo C. Biphasic effects of static magnetic fields on cutaneous microcirculation in rabbits. *Bioelectromagnetics*. 1999;20(3):161-171. doi:10.1002/(SICI)1521-186X(1999)20:3<161::AID-BEM2>3.0.CO;2-O
23. Tao R, Huang K. Reducing blood viscosity with magnetic fields. *Phys Rev E*. 2011;84(1):011905. doi:10.1103/PhysRevE.84.011905
24. Messier V, Rabasa-Lhoret R, Barbat-Artigas S, Elisha B, Karelis AD, Aubertin-Leheudre M. Menopause and sarcopenia: A potential role for sex hormones. *Maturitas*. 2011;68(4):331-336. doi:10.1016/j.maturitas.2011.01.014
25. Duddy W, Duguez S, Johnston H, et al. Muscular dystrophy in the mdx mouse is a severe myopathy compounded by hypotrophy, hypertrophy and hyperplasia. *Skelet Muscle*. 2015;5(1):16. doi:10.1186/s13395-015-0041-y
26. Gundersen K. Muscle memory and a new cellular model for muscle atrophy and hypertrophy. *Journal of Experimental Biology*. 2016;219(2):235-242. doi:10.1242/jeb.124495
27. Oliveira Junior SA, Padovani CR, Rodrigues SA, et al. Extensive impact of saturated fatty acids on metabolic and cardiovascular profile in rats with diet-induced obesity: A canonical analysis. *Cardiovasc Diabetol*. 2013;12(1):65. doi:10.1186/1475-2840-12-65
28. Tasić T, Lozić M, Glumac S, et al. Static magnetic field on behavior, hematological parameters and organ damage in spontaneously hypertensive rats. *Ecotoxicol Environ Saf*. 2021;207:111085. doi:10.1016/j.ecoenv.2020.111085
29. Goraca A, Ciejka E, Piechota A. Effects of extremely low frequency magnetic field on the parameters of oxidative stress in heart. *J Physiol Pharmacol*. 2010;61(3):333-338.
30. Kimsa-Dudek M, Synowiec-Wojtarowicz A, Derewniuk M, et al. Impact of fluoride and a static magnetic field on the gene expression that is associated with the antioxidant defense system of human fibroblasts. *Chem Biol Interact*. 2018;287:13-19. doi:10.1016/j.cbi.2018.04.004
31. Selbac MT, Garcia C, Fernandes Luiz C, et al. Behavioral and physiological changes determined by the female biological cycle-Climacteric to menopause. *Aletheia*. 2018;51(1-2):177-190.
32. Kestelman F. Magnetic resonance imaging in women recently diagnosed with breast cancer. Where are we headed? *Radiol Bras*. 2019;52(4):V-VI. doi:10.1590/0100--3984.2019.52.4e1
33. Wang S, Zheng M, Lou C, et al. Evaluating the biological safety on mice at 16 T static magnetic field with 700 MHz radio-frequency electromagnetic field. *Ecotoxicol Environ Saf*. 2022;230:113125. doi:10.1016/j.ecoenv.2021.113125
34. De Carvalho CAM, Thomazini JA. Study of wistar rats heart at different stages in the evolutionary cycle. *International Journal of Morphology*. 2014;32(2):614-617. doi:10.4067/S0717-95022014000200039
35. Lacour P, Dang PL, Heinzel FR, et al. Magnetic field–induced interactions between phones containing magnets and cardiovascular implantable electronic devices: Flip it to be safe? *Heart Rhythm*. 2022;19(3):372-380. doi:10.1016/j.hrthm.2021.11.010
36. Seidman SJ, Guag J, Beard B, Arp Z. Static magnetic field measurements of smart phones and watches and applicability to triggering magnet modes in implantable pacemakers and implantable cardioverter-defibrillators. *Heart Rhythm*. 2021;18(10):1741-1744. doi:10.1016/j.hrthm.2021.06.1203

Rzeszów University Press 2026
ISSN 2544-1361 (online)
doi: 10.15584/ejcem.2026.2.12

http://www.ejcem.ur.edu.pl
European Journal of Clinical and Experimental Medicine
Eur J Clin Exp Med 2026; 24 (2): 325–333

ORIGINAL PAPER

Clinical profile and predictors of mortality in upper gastrointestinal bleeding presenting to the emergency department of a tertiary care center – a prospective observational study

Asif Dabeer Jafri [1], Alka Verma [1], Om Prakash Sanjeev [1], Ratender Kumar Singh [2], Anup Kumar [3], Amit Goel [4]

[1] Department of Emergency Medicine, Sanjay Gandhi Post Graduate Institute of Medical Sciences, Lucknow, Uttar Pradesh, India
[2] Department of Emergency Medicine, Telemedicine and Digital Health, Sanjay Gandhi Post Graduate Institute of Medical Sciences, Lucknow, Uttar Pradesh, India
[3] Department of Biostatistics and Health Informatics, Sanjay Gandhi Post Graduate Institute of Medical Sciences, Lucknow, Uttar Pradesh, India
[4] Department of Hepatology, Sanjay Gandhi Post Graduate Institute of Medical Sciences, Lucknow, Uttar Pradesh, India

ABSTRACT

Introduction and aim. Upper gastrointestinal bleeding (UGIB) is a common and potentially life-threatening emergency associated with significant morbidity and mortality. Prospective emergency department (ED)-based data from India on factors associated with in-hospital mortality remain limited, and comparative evidence between bleeding-specific scores such as the Glasgow-Blatchford Score (GBS) and triage systems like the Emergency Severity Index (ESI) is scarce. This study aimed to describe the clinical profile of patients presenting with UGIB and to evaluate predictors of in-hospital mortality, with a focus on comparing the prognostic performance of GBS and ESI.

Material and methods. This single-center prospective observational cohort study was conducted in the ED of a tertiary care center in North India from January 2024 to January 2025. Adult patients with clinically suspected or endoscopically confirmed UGIB were enrolled. Clinical, laboratory, and management data were recorded using a standardized form. GBS and ESI were assigned at presentation by trained clinicians prior to outcome assessment. The primary outcome was in-hospital mortality. Predictive performance was assessed using receiver operating characteristic (ROC) curve analysis.

Results. Eighty-three patients with UGIB were included; 55.4% had a GBS >2. Patients with higher GBS demonstrated greater physiological derangement, increased transfusion requirements, higher incidence of shock, and significantly higher mortality (39.1% vs. 0%, p<0.001). All non-survivors were triaged as high acuity by ESI and had qSOFA ≥2 at presentation. GBS showed good discriminative ability for predicting mortality (AUROC=0.785), outperforming ESI (AUROC=0.723).

Conclusion. GBS showed good performance in predicting in-hospital mortality and may aid early ED risk stratification. However, findings should be interpreted cautiously given the single-center design and small sample size.

Keywords. emergency severity index, endoscopy, esophageal and gastric varices, gastrointestinal hemorrhage, Glasgow-Blatchford score, quick sequential organ failure assessment

Corresponding author: Alka Verma, e-mail: dralka.verma21@gmail.com

Received: 12.09.2025 / Revised: 10.03.2026 / Accepted: 15.03.2026 / Published: 30.06.2026

Jafri AD, Verma A, Sanjeev OP, Singh RK, Kumar A, Goel A. Clinical profile and predictors of mortality in upper gastrointestinal bleeding presenting to the emergency department of a tertiary care center – a prospective observational study. *Eur J Clin Exp Med.* 2026;24(2):325–333. doi: 10.15584/ejcem.2026.2.12.

Introduction

The annual incidence of upper gastrointestinal bleeding (UGIB) is estimated to range from 80 to 150 cases per 100,000 adults, with an estimated mortality rate ranging from 2% to 10%.[1] UGIB is defined as blood loss originating from the gastrointestinal tract proximal to the ligament of Treitz, including sources in the esophagus, stomach, or duodenum. Gastrointestinal bleeding may present as hematemesis, which can appear as either bright red blood or coffee-ground vomitus, as well as melena or, less commonly, hematochezia. Hematochezia refers to the passage of bright red blood or blood clots per rectum. While it typically indicates lower gastrointestinal bleeding (LGIB), it can also occur in cases of brisk UGIB. Patients typically present with symptoms related to blood loss, including orthostatic hypotension, syncope, fatigue, and generalized weakness.[2,3] Peptic ulcer disease (PUD) is the most common cause of UGIB, accounting for up to 50% of cases. Other frequent causes include esophagitis (24%), gastritis (18–22%), duodenitis (13%), and esophageal or gastric varices (11%). Additional etiologies include Mallory-Weiss tears (5–15%), vascular ectasia (5%), gastrointestinal neoplasms, and portal hypertensive gastropathy.[4,5]

Risk stratification scoring systems are essential for identifying patients who are more likely to require intervention and are at increased risk of re-bleeding and mortality. These tools play a crucial role in guiding resuscitation efforts, determining the optimal timing for endoscopy, and informing decisions about discharge planning. The Glasgow-Blatchford Score (GBS) is specifically designed to predict the need for endoscopic intervention. It incorporates clinical and laboratory parameters, including hemoglobin (Hb) level, systolic blood pressure (SBP), presence of syncope, melena, liver disease, and heart failure. A GBS of 6 or higher is associated with a greater than 50% likelihood of requiring therapeutic intervention. Conversely, patients with a low GBS of 0 or 1 are considered low risk and may be safely discharged from the emergency department (ED) with outpatient follow-up.[6] In an international, multicenter, prospective study comparing multiple risk stratification tools, the GBS demonstrated superior accuracy in predicting the need for intervention or risk of death. As a result, both the American College of Gastroenterology and the European Society of Gastrointestinal Endoscopy recommend the GBS as the preferred tool for initial risk assessment in patients with UGIB.[7-9] The American Association for the Study of Liver Diseases (AASLD) recommends that esophagogastroduodenoscopy (EGD) be performed within 12 hours of presentation in patients with suspected acute variceal hemorrhage.[10] This guidance is supported by studies demonstrating that delayed endoscopy in patients with cirrhosis and variceal bleeding is associated with higher rates of re-bleeding and increased mortality.[11,12]

Upper endoscopy remains the gold standard for diagnosing and managing UGIB. However, computed tomography angiography (CTA) serves as a valuable alternative when endoscopy fails to identify an active source of bleeding, when a gastroenterologist is unavailable, when the patient is unfit for endoscopy, or when anatomical factors limit endoscopic access.[13] Increased mortality, risk of re-bleeding, and the need for endoscopic or surgical intervention are associated with several risk factors, including age over 60 years, presence of comorbidities, active bleeding at presentation, hypotension, and the requirement for blood transfusion.[14] Endoscopic therapy successfully achieves sustained haemostasis in approximately 80% to 90% of patients with UGIB; however, re-bleeding occurs in 10% to 20% of cases. In PUD, the majority of deaths, around 80% are attributed not to the bleeding itself but to underlying medical comorbidities.[15] Despite significant therapeutic advancements, acute variceal hemorrhage continues to carry a six-week mortality rate of approximately 15%.[16] Prospective emergency department-based data from India evaluating predictors of in-hospital mortality in upper gastrointestinal bleeding are limited. In particular, evidence comparing bleeding-specific risk stratification tools such as the GBS with ED triage systems like the Emergency Severity Index (ESI) for mortality prediction is scarce. This study addresses this gap by prospectively evaluating clinical factors associated with in-hospital mortality, and the performance of GBS and ESI in an Indian tertiary care ED.

Aim

The aim of this study was to prospectively evaluate the clinical profile and predictors of in-hospital mortality among patients presenting with UGIB. The study also aimed to assess and compare the prognostic performance of the GBS and ESI for early risk stratification and prediction of mortality in UGIB. This study addresses the limited prospective ED based data from India on mortality predictors and the comparative utility of bleeding-specific and triage-based risk assessment tools.

Material and methods

Study design and setting

This single-center prospective observational cohort study was conducted over a one-year period from January 2024 to January 2025 in the Department of Emergency Medicine at Sanjay Gandhi Postgraduate Institute of Medical Sciences (SGPGIMS), Lucknow, a tertiary care teaching hospital in North India. During the study period, 110 consecutive adult patients presenting with gastrointestinal bleeding were screened. Of these, 83 patients diagnosed with UGIB were included in the final analysis, while patients with lower LGIB were excluded, as the present study focused exclusively on UGIB.

Inclusion and exclusion criteria

Patients aged ≥18 years, of either sex, presenting with features suggestive of UGIB, such as hematemesis and/or melena, were enrolled in the study. UGIB was established by endoscopic demonstration of a bleeding source proximal to the ligament of Treitz. Patients with isolated LGIB, no objective evidence of gastrointestinal bleeding, pregnancy, incomplete medical records, or those who were discharged or left against medical advice before completion of evaluation were excluded.

Ethical considerations

The study was conducted in accordance with the ethical standards of the Institutional Ethics Committee of SGPGIMS. Ethical approval was obtained (IEC Code: 2019-161-IP-EXP-11, PGI/BE/623/2019; 11th Institutional Ethics Committee meeting). The committee waived the requirement for individual informed consent, given the non-interventional, observational nature of the study, which posed minimal risk to the participants, and without altering the standard patient management.

It is important to note that the original approval was granted before the commencement of the study. Due to delays caused by the COVID-19 pandemic, the study timeline was extended. This extension was granted in accordance with institutional guidelines, post COVID-19 extension, ensuring ongoing compliance with ethical standards. Patient confidentiality was protected by keeping all data anonymized and coded, with restricted access in password-protected systems, ensuring strict confidentiality and adherence to data protection standards.

Data collection

Data were prospectively collected using a pre-designed and pre-approved standardized case reporting form by trained emergency medicine residents under the supervision of attending consultants. At admission, each patient was evaluated, and information was recorded on demographic characteristics, age, and gender. Clinical parameters recorded at presentation: heart rate (HR), blood pressure (BP), respiratory rate (RR), oxygen saturation (SpO_2), and presence of shock. Clinical presentation: type of bleeding and presenting symptoms (gastrointestinal, respiratory, neurological). Comorbid conditions: diabetes mellitus (DM), hypertension (HTN), chronic liver disease (CLD), chronic kidney disease (CKD), and hematological disorders. Laboratory parameters included hemoglobin level, blood urea, serum creatinine, and coagulation profile. The following variables were predefined candidate predictors of in-hospital mortality based on clinical relevance and prior evidence: demographic factors, vital signs at presentation, comorbidities, laboratory parameters, etiology of bleeding, and treatment-related variables including transfusion requirements and need for endoscopic intervention. Management strategies included intravenous fluids, transfusion of packed red blood cells (PRBC), fresh frozen plasma (FFP), and single donor platelets (SDP), vasoactive support, and endoscopic intervention where required. Data collection followed standardized institutional protocols to ensure uniformity. Missing data were minimal due to prospective collection; cases with incomplete key variables or outcome data were excluded, and no imputation was performed.

Severity scoring systems

Glasgow Blatchford score (GBS)

GBS was calculated at initial presentation using standard clinical and laboratory parameters blood urea nitrogen (BUN), Hb, SBP, PR, presentation with melena or syncope, and history of hepatic or cardiac disease) prior to endoscopic evaluation. Patients were stratified into low-risk (GBS ≤2) and high-risk (GBS >2) groups. A threshold of ≤2 was selected to identify patients at very low risk of requiring hospital-based intervention, as validated in previous studies demonstrating high negative predictive value for adverse outcomes.[26,27]

qSOFA score

The quick Sequential Organ Failure Assessment (qSOFA) score was calculated at presentation in the ED using three clinical parameters: RR ≥22/min, SBP ≤100 mmHg, and altered mentation (Glasgow Coma Scale <15). Each variable was assigned one point, yielding a total score of 0 to 3. A qSOFA score ≥2 was considered high risk. The score was recorded before endoscopic intervention and evaluated for its ability to predict in-hospital mortality.

Emergency severity index (ESI)

The five-level ESI triage score was assigned at presentation in the emergency department by a trained triage physician according to standard criteria. Patients were categorized based on acuity level and anticipated resource needs, with ESI levels 1–2 defined as high acuity. All scoring systems (GBS, qSOFA, and ESI) were recorded at initial presentation prior to endoscopic evaluation and before outcome occurrence. Although formal blinding was not feasible due to the observational design, score assignment preceded outcome assessment, thereby minimizing bias.

Endoscopic evaluation and intervention

All patients with suspected UGIB underwent upper gastrointestinal endoscopy within 24 hours of admission or earlier in hemodynamically unstable patients after initial resuscitation for diagnostic evaluation and therapeutic management according to institutional protocol. Endoscopy was performed to identify the source of bleeding

and to classify lesions as variceal or non-variceal in origin. Variceal sources included esophageal varices, gastric varices, and portal hypertensive gastropathy, whereas non-variceal causes included PUD (gastric or duodenal ulcers with stigmata of recent hemorrhage such as active bleeding, visible vessels, or adherent clots), erosive gastritis, duodenitis, esophagitis, and Mallory-Weiss tears.

Hemostasis was achieved using a multimodal approach, including injection therapy with diluted adrenaline (1:10,000) with or without sclerosants, thermal coagulation (heater probe, bipolar electrocoagulation, argon plasma coagulation), and mechanical methods such as hemoclips and endoscopic variceal ligation. High-risk ulcers received intravenous proton pump inhibitor infusion for 72 hours. The interventions were performed by consultants with more than five years of experience in emergency endoscopy.

Definitions of key clinical variables

Shock: Characterized by inadequate tissue perfusion, defined by criteria such as systolic blood pressure <90 mmHg, a mean arterial pressure (MAP) less than 65 mmHg, or requiring vasopressor support.

Hematological cause: Bleeding due to blood disorders such as thrombocytopenia, coagulation factor deficiencies, or hematological malignancies.

Drug history: Recent or ongoing use of medications known to affect coagulation or increase bleeding risk, including anticoagulants, antiplatelet, non-steroidal anti-inflammatory drugs, or corticosteroids.

Central nervous system (CNS) Symptoms: Neurological symptoms such as altered consciousness, dizziness, confusion, or loss of consciousness.

Respiratory symptoms: Symptoms indicating respiratory compromise, such as dyspnea, tachypnea, hypoxia, or cough.

Renal symptoms: Symptoms such as dysuria, hematuria, flank pain, and decreased urine output.

Gastrointestinal (GI) symptoms: Symptoms related to gastrointestinal bleeding or irritation, including hematemesis, melena, hematochezia, abdominal pain, distension, vomiting, or dyspepsia.

Categories of bleeding severity:

Minor: Bleeding that does not require blood transfusion or major intervention; often self-limited.

Moderate: Bleeding requiring blood transfusion or medical intervention but not life-threatening.

Massive: Severe bleeding leading to hemodynamic instability, shock, or requiring urgent major intervention, such as massive transfusion.

Outcome measures

The primary outcome was in-hospital mortality among patients presenting with UGIB. Secondary outcomes included risk stratification according to the GBS, requirement for blood transfusion, need for endoscopic intervention, and the predictive performance of the GBS and ESI for in-hospital mortality.

Statistical analysis

Data was entered into Microsoft Excel and analyzed using IBM SPSS Statistics version 26 (IBM Corp., Armonk, NY, USA). Continuous variables were assessed for normality using the Shapiro-Wilk test and are presented as mean±standard deviation. Comparisons between groups were performed using independent samples t-test or Mann-Whitney U test, as appropriate. Categorical variables are expressed as frequencies and percentages and were compared using the Chi-square test or Fisher's exact test. Given the relatively small sample size and number of outcome events, only univariable analyses were performed to explore associations between clinical variables and in-hospital mortality. Receiver operating characteristic (ROC) curve analysis was performed to evaluate the discriminative ability of GBS and ESI. The areas under the ROC curves (AUROC) were compared using appropriate statistical methods. The GBS cut-off of ≤2 was selected based on prior validation studies demonstrating high sensitivity and clinical utility for identifying low-risk patients. A p-value <0.05 was considered statistically significant.

Results

Clinical characteristics and severity stratification according to GBS

A total of 83 patients presenting with UGIB were included in the study. Based on the GBS, patients were categorized into two groups: GBS ≤2 (n=37; 44.6%) and GBS >2 (n=46; 55.4%), as shown in Table 1. The mean age of the study population was 48.77±14.07 years, with no significant difference between the two groups (p=0.846). Males constituted 72.3% of the cohort, and gender distribution was similar across the two groups (p=0.175).

Patients in the GBS >2 group had significantly worse physiological parameters at presentation. This group demonstrated higher HR (126.28±13.88 vs. 91.49±13.93 beats/min; p<0.001) and RR (27.07±6.44 vs. 20.70±3.76 breaths/min; p<0.001), along with lower SBP (101.87±18.25 vs. 119.81±23.09 mmHg; p<0.001) and SpO_2 (94.11±3.65% vs. 98.03±1.96%; p<0.001). Diastolic BP did not differ significantly between the groups (p=0.961).

Comorbid illnesses were more frequent in the GBS >2 group (91.3% vs. 75.7%), although the difference did not reach statistical significance (p=0.052). There were no significant differences between the groups with respect to DM, HTN, CKD, or CLD.

Hematological causes of bleeding were significantly more common in the GBS >2 group (36.96% vs. 2.7%; p<0.001), as was a positive drug history (80.4% vs. 56.8%; p=0.019). Central nervous system symptoms

were observed more frequently in patients with GBS >2 (65.2% vs. 2.7%; p<0.001). All patients in the GBS >2 group presented with features of shock, whereas none in the GBS ≤2 group did (p<0.001).

Patients with GBS >2 required more intensive management. All patients in this group received PRBC, RDP, FFP, and central venous access (p<0.001 for all). SDP transfusion was required in 50% of patients in the GBS >2 group, while none in the GBS ≤2 group required this intervention (p<0.001). CT imaging was performed more frequently in the GBS >2 group (71.7% vs. 2.7%; p<0.001). In contrast, therapeutic interventions were more commonly performed in patients with GBS ≤2 (70.3% vs. 41.3%; p=0.008).

Regarding outcomes, patients with GBS ≤2 were more frequently transferred to the ward (43.2% vs. 4.3%; p<0.001). Mortality was significantly higher in the GBS >2 group (39.1% vs. 0%; p<0.001). All patients in the GBS >2 group had a qSOFA score ≥2 at presentation, reflecting greater severity of illness (p<0.001).

Patients with a GBS >2 exhibited more severe clinical presentations, greater need for transfusions and invasive monitoring, higher incidence of shock and central nervous system involvement, and significantly higher mortality compared with patients with lower GBS scores.

Table 1. Distribution of demographic and clinical variables between Glasgow-Blatchford Bleeding score (GBS) categories (n=83)

Variables	GBS		Total (n=83)	p
	≤2 (n=37)	>2 (n=46)		
Age	49.11±16.12	48.5±12.37	48.77±14.07	0.846
Gender				
Male	24 (64.86)	36 (78.26)	60 (72.29)	0.175
Female	13 (35.14)	10 (21.74)	23 (27.71)	
HR (beats/min)	91.49±13.93	126.28±13.88	110.77±22.22	<0.001
SBP (mmHg)	119.81±23.09	101.87±18.25	109.87±22.3	<0.001
DBP (mmHg)	61.89±22.15	62.07±8.36	61.99±15.93	0.961
RR (breaths/min)	20.7±3.76	27.07±6.44	24.23±6.25	<0.001
SPO_2 (%)	98.03±1.96	94.11±3.65	95.86±3.59	<0.001
Comorbid illness				
Yes	28 (75.68)	42 (91.3)	70 (84.34)	0.052
No	9 (24.32)	4 (8.7)	13 (15.66)	
DM				
Yes	14 (37.84)	15 (32.61)	29 (34.94)	0.619
No	23 (62.16)	31 (67.39)	54 (65.06)	
HTN				
Yes	11 (29.73)	14 (30.43)	25 (30.12)	0.945
No	26 (70.27)	32 (69.57)	58 (69.88)	
CKD				
Yes	6 (16.22)	9 (20)	15 (18.29)	0.659
No	31 (83.78)	36 (80)	67 (81.71)	
CLD				
Yes	25 (67.57)	39 (84.78)	64 (77.11)	0.064
No	12 (32.43)	7 (15.22)	19 (22.89)	
Hematological cause				
Yes	1 (2.7)	17 (36.96)	18 (21.69)	<0.001
No	36 (97.3)	29 (63.04)	65 (78.31)	
Drug history				
Yes	21 (56.76)	37 (80.43)	58 (69.88)	0.019
No	16 (43.24)	9 (19.57)	25 (30.12)	
CNS symptoms present				
Yes	1 (2.7)	30 (65.22)	31 (37.35)	<0.001
No	36 (97.3)	16 (34.78)	52 (62.65)	
Shock present				
Yes	0 (0)	46 (100)	46 (55.42)	<0.001
No	37 (100)	0 (0)	37 (44.58)	
Intervention performed				
Yes	26 (70.27)	19 (41.3)	45 (54.22)	0.008
No	11 (29.73)	27 (58.7)	38 (45.78)	
PRBC				
Yes	0 (0)	46 (100)	46 (55.42)	<0.001
No	37 (100)	0 (0)	37 (44.58)	
RDP				
Yes	0 (0)	46 (100)	46 (55.42)	<0.001
No	37 (100)	0 (0)	37 (44.58)	
SDP				
Yes	0 (0)	23 (50)	23 (27.71)	<0.001
No	37 (100)	23 (50)	60 (72.29)	
FFP				
Yes	13 (35.14)	46 (100)	59 (71.08)	<0.001
No	24 (64.86)	0 (0)	24 (28.92)	
PIVC				
Yes	37 (100)	45 (97.83)	82 (98.8)	0.367
No	0 (0)	1 (2.17)	1 (1.2)	
CIVC				
Yes	0 (0)	46 (100)	46 (55.42)	<0.001
No	37 (100)	0 (0)	37 (44.58)	
RT lavage				
Yes	0 (0)	46 (100)	46 (55.42)	<0.001
No	37 (100)	0 (0)	37 (44.58)	
CT scan performed				
Yes	1 (2.7)	33 (71.74)	34 (40.96)	<0.001
No	36 (97.3)	13 (28.26)	49 (59.04)	
Transfer to ward				
Yes	16 (43.24)	2 (4.35)	18 (21.69)	<0.001
No	21 (56.76)	44 (95.65)	65 (78.31)	
Outcome of patients/mortality				
Yes	0 (0)	18 (39.13)	18 (21.69)	<0.001
No	37 (100)	28 (60.87)	65 (78.31)	
qSOFA score at presentation				
≥2	0 (0)	46 (100)	46 (55.42)	<0.001
<2	37 (100)	0 (0)	37 (44.58)	

* continuous variables are presented as mean±standard deviation (SD), and categorical variables as number (percentage), comparisons were performed using independent samples t-test for continuous variables and Chi-square test or Fisher's exact test for categorical variables, a p<0.05 was considered statistically significant, HR – heart rate, SBP – systolic blood pressure, DBP – diastolic blood pressure, RR – respiratory rate, SpO_2 – peripheral oxygen saturation, GI – gastrointestinal, PRBC – packed red blood cells, RDP – random donor platelets, SDP – single donor platelets, FFP – fresh frozen plasma, PIVC – peripheral intravenous cannula, CIVC – central intravenous cannula, RT – Ryle's tube, CT – computed tomography, CNS – central nervous system, CLD – chronic liver disease, CKD – chronic kidney disease, qSOFA – quick Sequential Organ Failure Assessment

Table 2. Comparison of clinical characteristics, clinical presentation, severity scores, management, and outcomes between survivors and non-survivors among patients with UGIB*

Variables	Outcome of patient/mortality		p
	Yes (n=18)	No (n=65)	
Age			
Mean±SD	45.833±11.242	49.585±14.736	0.445
HR (beats/min)			
Mean±SD	129.333±7.881	105.631±22.186	<0.001
RR (breaths/min)			
Mean±SD	22.444±1.886	24.723±6.929	0.853
ESI scoring			
Yes	18 (100%)	36 (55.4%)	<0.001
No	0 (0%)	29 (44.6%)	
qSOFA score at presentation			
≥2	18 (100%)	28 (43.1%)	<0.001
<2	0 (0%)	37 (56.9%)	
Comorbid illness			
Yes	18 (100%)	52 (80%)	0.061
No	0 (0%)	13 (20%)	
DM			
Yes	1 (5.6%)	28 (43.1%)	0.004
No	17 (94.4%)	37 (56.9%)	
HTN			
Yes	1 (5.6%)	24 (36.9%)	0.009
No	17 (94.4%)	41 (63.1%)	
CKD			
Yes	2 (11.1%)	14 (21.5%)	0.502
No	16 (88.9%)	51 (78.5%)	
CAD			
Yes	0 (0%)	0 (0%)	
No	18 (100%)	65 (100%)	
CVA			
Yes	0 (0%)	0 (0%)	
No	18 (100%)	65 (100%)	
CLD			
Yes	18 (100%)	46 (70.8%)	0.009
No	0 (0%)	19 (29.2%)	
Haematological cause			
Yes	17 (94.4%)	1 (1.5%)	<0.001
No	1 (5.6%)	64 (98.5%)	
Drug history			
Yes	18 (100%)	40 (61.5%)	<0.001
No	0 (0%)	25 (38.5%)	
CNS symptoms present			
Yes	17 (94.4%)	14 (21.5%)	<0.001
No	1 (5.6%)	51 (78.5%)	
Respiratory symptoms			
Yes	18 (100%)	25 (38.5%)	<0.001
No	0 (0%)	40 (61.5%)	
GI symptoms			
Yes	18 (100%)	37 (56.9%)	<0.001
No	0 (0%)	28 (43.1%)	
Renal involvement			
Yes	2 (11.1%)	14 (21.5%)	0.502
No	16 (88.9%)	51 (78.5%)	
Bleeding			
Minor	0 (0%)	30 (46.2%)	<0.001
Moderate	17 (94.4%)	9 (13.8%)	
Massive	1 (5.6%)	26 (40%)	
Shock			
Yes	18 (100%)	28 (43.1%)	<0.001
No	0 (0%)	37 (56.9%)	
Intervention performed			
Yes	0 (0%)	45 (69.2%)	<0.001
No	18 (100%)	20 (30.8%)	
Transfer to ward			
Yes	0 (0%)	18 (27.7%)	0.009
No	18 (100%)	47 (72.3%)	
GBS			
≤2	0 (0%)	37 (56.9%)	<0.001
>2	18 (100%)	28 (43.1%)	

* values are expressed as mean±standard deviation or number (percentage), p<0.05 was considered statistically significant, ESI – emergency severity index

Outcome and mortality analysis

Of the 83 patients with UGIB, 18 (21.7%) died during hospitalization (Table 2). There was no significant difference in age between non-survivors and survivors (45.8±11.2 vs. 49.6±14.7 years; p=0.445). Non-survivors had significantly higher HR at presentation (129.3±7.9 vs. 105.6±22.2 beats/min; p<0.001), while RR were comparable (p=0.853).

All non-survivors were categorized as high acuity according to the ESI, compared with 55.4% of survivors (p<0.001). Likewise, a qSOFA score ≥2 on day 1 was observed in 100% of non-survivors but in only 43.1% of survivors (p<0.001), reflecting significantly greater physiological severity at presentation among patients who died.

Comorbid illness was present in all non-survivors compared with 80.0% of survivors (p=0.061). CLD was significantly more frequent among non-survivors (100% vs. 70.8%; p=0.009), whereas DM and HTN were less common (p=0.004 and p=0.009, respectively). Hematological causes of bleeding (94.4% vs. 1.5%; p<0.001) and positive drug history (100% vs. 61.5%; p<0.001) were strongly associated with mortality.

Non-survivors more frequently presented with central nervous system (94.4% vs. 21.5%), respiratory (100% vs. 38.5%), and gastrointestinal symptoms (100% vs. 56.9%) (all p<0.001), as well as shock at presentation (100% vs. 43.1%; p<0.001). Moderate to severe bleeding predominated among non-survivors, whereas minor bleeding was observed exclusively in survivors (p<0.001). Transfer to the ward was significantly less frequent among non-survivors (p=0.009). All non-survivors had a GBS >2 at presentation, whereas survivors more frequently had a GBS ≤2 (p<0.001).

Predictive performance of GBS and ESI for in-hospital mortality

ROC curve analysis demonstrated that both scoring systems were significant predictors of in-hospital mortality (Fig. 1). The GBS showed good discriminative ability, with an AUROC of 0.785 (95% CI: 0.724–0.845; p<0.001). The ESI demonstrated a lower but statistically significant discriminative performance, with an AUROC of 0.723 (95% CI: 0.662–0.784; p<0.001). Overall, GBS exhibited superior discrimination for predicting mortality compared with ESI.

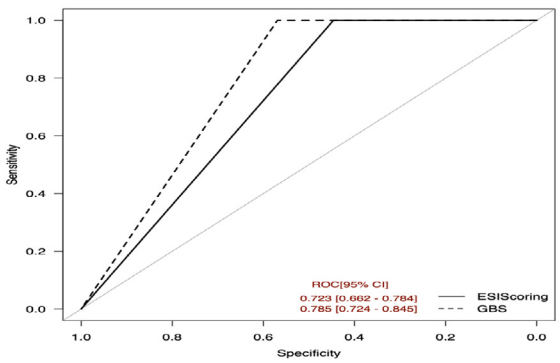

Fig 1. Comparison of the ESI score and GBS in predictive of outcome (in hospital mortality) in UGIB

Discussion

Gastrointestinal bleeding remains a potentially life-threatening emergency, with UGIB broadly categorized into variceal and non-variceal etiologies. PUD, particularly gastric ulcers, continues to be the most common cause, followed by variceal bleeding in patients with underlying liver disease.

In the present study, we explored the association between GBS and clinical outcomes in patients presenting with UGIB. Patients with higher GBS values demonstrated significantly greater transfusion requirements, with rates exceeding those reported in previous literature. This observation may be attributed to our institution being a tertiary referral center, which routinely manages critically ill patients with multiple comorbidities. Comparable transfusion rates approaching 75% have also been reported in studies from other regions, including Turkey.[7,17]

Male predominance was evident in our cohort, consistent with prior findings. Surendran et al. and Shenoy et al. reported a similar sex distribution, with males accounting for 77.5% of cases compared with 22.5% in females.[18] Such trends highlight the higher susceptibility of men to UGIB.

Alok Raj et al. demonstrated that mortality in GIB is strongly associated with derangements in clinical and hemodynamic parameters, including tachycardia, hypotension, tachypnoea, hypoxemia, and low GCS score, in addition to hematological and biochemical abnormalities such as anemia, thrombocytopenia, leukocytosis, hyperlactatemia, and impaired renal function.[19] These results closely parallel our observations, reinforcing the prognostic significance of readily available clinical and laboratory markers.

Comorbidity profiles in our study were dominated by CLD, followed by diabetes and hypertension, aligning with the findings of Alok Raj et al.[19] Similarly, Bhattarai et al. reported CLD in 45.5% of UGIB cases, a figure comparable to our cohort.[20] Mahajan et al. further demonstrated that comorbidities such as DM and coronary artery disease significantly increased mortality risk.[21] Prior work has also shown that CLD is more frequently linked to variceal bleeding, whereas cardiovascular, cerebrovascular, and malignant diseases are predominant among patients with non-variceal bleeding.[22]

Advanced age and comorbid conditions consistently emerge as independent risk factors for adverse outcomes in UGIB. Despite improvements in diagnostic modalities and therapeutic interventions, mortality rates have remained largely unchanged over recent decades. Kaplan et al. reported that advanced age and even asymptomatic comorbidities significantly worsen outcomes in UGIB patients.[23] In a large cohort of 3,508 emergency department presentations, 83% of deaths were attributable to one or more comorbid conditions.[24]

Independent predictors of poor prognosis identified across studies include older age, male sex, pre-existing comorbidities, coagulopathy, need for transfusion, re-bleeding episodes, high-risk endoscopic findings, and prolonged hospitalization.[25] In our study, mortality was significantly associated with higher GBS, transfusion requirements, non-endoscopic interventions, adverse hemodynamic parameters, and multiple comorbidities, underscoring their importance as prognostic markers in UGIB.

Our findings are in alignment with existing evidence supporting a GBS threshold of >2. A GBS ≤2 has been shown to reliably identify low-risk UGIB patients. Recent work by Chatten et al. demonstrated that a low-risk cutoff of ≤2 preserves a high negative predictive value, with minimal rates of re-bleeding and mortality, while a large meta-analysis confirmed excellent discriminative ability and a low requirement for hospital-based intervention.[26,27] Consistent with these observations, our study found that patients with a GBS >2 exhibited greater physiological derangement, higher transfusion requirements, increased incidence of shock, and significantly higher in-hospital mortality.

Both GBS and ESI predicted mortality; however, GBS demonstrated superior discrimination (AUROC 0.785 vs 0.723). ESI is a general triage acuity tool primarily based on resource utilization and initial clinical assessment, whereas GBS is a disease-specific physiological score. Consequently, GBS better reflects bleeding

severity than overall acuity alone. Our findings suggest that ESI identifies critically ill patients, while GBS predicts bleeding-related mortality; therefore, the two tools are complementary rather than interchangeable.

Study limitations

This study has certain limitations. First, as a single-center investigation with a relatively small sample size**,** the results may have limited generalizability to broader populations. Second, the setting in a tertiary care referral hospital likely led to inclusion of more severe cases, introducing referral bias and possibly overestimating mortality and transfusion requirements. Third, the analysis was restricted to in-hospital outcomes**,** without evaluation of longer-term endpoints such as re-bleeding or 90-day mortality.

Conclusion

The GBS effectively stratified severity and predicted in-hospital mortality in UGIB, outperforming the ESI. A GBS >2 identifies patients at high risk for adverse outcomes and mortality, supporting its use for early ED risk assessment.

Declarations

Funding

This research did not receive any funding.

Author contributions

Conceptualization, A.D.J. and A.V.; Methodology, A.D.J. and A.V.; Software, A.D.J. and A.V.; Validation, A.D.J., A.V., O.P.S., A.K., A.G. and R.K.S.; Formal Analysis, A.D.J., A.V. and R.K.S.; Resources, A.D.J. and A.V.; Data Curation, A.D.J. and A.V.; Writing – Original Draft Preparation, A.D.J.; Writing – Review & Editing, A.D.J. and A.V.; Visualization, A.D.J., A.V., O.P.S., A.K., A.G. and R.K.S.; Supervision, A.V. and R.K.S.

Conflicts of interest

The author(s) declared no potential conflicts of interest with respect to the research, authorship, and/or publication of this article.

Data availability

Due to privacy and confidentiality concerns, the data are not publicly available. However, they may be made available upon reasonable request to the corresponding author, subject to the completion of a signed data access agreement.

Ethics approval

The protocol was approved by the Institutional ethics committee (IEC Code: 2019-161-IP-EXP-11, PGI/BE/623/2019; 11th Institutional Ethics Committee meeting).

References

1. Stanley AJ, Laine L. Management of acute upper gastrointestinal bleeding. *BMJ*. 2019;364. doi:10.1136/bmj.l536
2. Fouad TR, Abdelsameea E, Abdel-Razek W, et al. Upper gastrointestinal bleeding in Egyptian patients with cirrhosis: Post-therapeutic outcome and prognostic indicators. *J Gastroenterol Hepatol.* 2019;34(9):1604-1610. doi:10.1111/jgh.14659
3. Perisetti A, Kopel J, Shredi A, Raghavapuram S, Tharian B, Nugent K. Prophylactic pre-esophagogastroduodenoscopy tracheal intubation in patients with upper gastrointestinal bleeding. *Baylor Univ Med Cent Proc.* 2019;32(1):22-25. doi:10.1080/08998280.2018.1530007
4. Cooper AS. Interventions for preventing upper gastrointestinal bleeding in people admitted to intensive care units. *Crit Care Nurse.* 2019;39(2):102-103. doi:10.4037/ccn2019916
5. Enestvedt BK, Gralnek IM, Mattek N, Lieberman DA, Eisen G. An evaluation of endoscopic indications and findings related to nonvariceal upper-GI hemorrhage in a large multicenter consortium. *Gastrointest Endosc.* 2008;67(3):422-429. doi:10.1016/j.gie.2007.09.024
6. Blatchford O, Murray WR, Blatchford M. A risk score to predict need for treatment for upper-gastrointestinal haemorrhage. *Lancet.* 2000;356(9238):1318-1321. doi:10.1016/S0140-6736(00)02816-6
7. Gralnek IM, Stanley AJ, Morris AJ, et al. Endoscopic diagnosis and management of nonvariceal upper gastrointestinal hemorrhage (NVUGIH): European Society of Gastrointestinal Endoscopy (ESGE) Guideline - Update 2021. *Endoscopy.* 2021;53(3):300-332. doi:10.1055/a-1369-5274
8. Stanley AJ, Laine L, Dalton HR, et al. Comparison of risk scoring systems for patients presenting with upper gastrointestinal bleeding: international multicentre prospective study. *BMJ.* 2017;356:i6432. doi:10.1136/bmj.i6432
9. Laine L, Barkun AN, Saltzman JR, Martel M, Leontiadis GI. ACG Clinical Guideline: Upper Gastrointestinal and Ulcer Bleeding. *Am J Gastroenterol.* 2021;116(5):899-917. doi:10.14309/ajg.0000000000001245
10. Kaplan DE, Ripoll C, Thiele M, Fortune BE, Simonetto DA, Garcia-Tsao G, Bosch J. AASLD Practice Guidance on risk stratification and management of portal hypertension and varices in cirrhosis. *Hepatology*. 2024;79(5):1180-1211. doi:10.1097/HEP.0000000000000647
11. Bai Z, Wang R, Cheng G, Ma D, Ibrahim M, Chawla S, Qi X. Outcomes of early versus delayed endoscopy in cirrhotic patients with acute variceal bleeding: a systematic review with meta-analysis. *Eur J Gastroenterol Hepatol.* 2021;33(1):e868-e876. doi:10.1097/MEG.0000000000002282
12. Chen PH, Chen WC, Hou MC, et al. Delayed endoscopy increases re-bleeding and mortality in patients with hematemesis and active esophageal variceal bleeding: a cohort study. *J Hepatol.* 2012;57(6):1207-1213. doi:10.1016/j.jhep.2012.07.038

13. Costable NJ, Greenwald DA. Upper gastrointestinal bleeding. In: Geriatric Gastroenterology. 2021:1289-1304. doi:10.1007/978-3-030-30192-7_47
14. Elmunzer BJ, Young SD, Inadomi JM, Schoenfeld P, Laine L. Systematic review of the predictors of recurrent hemorrhage after endoscopic hemostatic therapy for bleeding peptic ulcers. *Am J Gastroenterol*. 2008;103(10):2625-2632. doi: 10.1111/j.1572-0241.2008.02070.x
15. Sung JJ, Tsoi KK, Ma TK, Yung MY, Lau JY, Chiu PW. Causes of mortality in patients with peptic ulcer bleeding: a prospective cohort study of 10,428 cases. *Am J Gastroenterol*. 2010;105(1):84-89. doi:10.1038/ajg.2009.507
16. de Franchis R, Baveno VI Faculty. Expanding consensus in portal hypertension: Report of the Baveno VI Consensus Workshop: Stratifying risk and individualizing care for portal hypertension. *J Hepatol.* 2015;63(3):743-752.
17. Okutur SK, Alkım C, Bes C, et al. Acute upper gastrointestinal bleeding: Analysis of 230 cases. *Turk J Acad Gastroenterol*. 2007;6:30-36.
18. Shenoy V, Shah S, Kumar S, et al. A prospective cohort study of patients presenting to the emergency department with upper gastrointestinal bleeding. *J Fam Med Prim Care*. 2021;10(3):1431-1436. doi:10.4103/jfmpc.jfmpc_1996_20
19. Raj A, Kaeley N, Prasad H, et al. Prospective observational study on clinical and epidemiological profile of adult patients presenting to the emergency department with suspected upper gastrointestinal bleed. *BMC Emerg Med.* 2023;23:107. doi:10.1186/s12873-023-00885-9
20. Bhattarai S. Clinical Profile and endoscopic findings in patients with Upper Gastrointestinal Bleed attending a Tertiary Care Hospital: a descriptive cross-sectional study. *J Nepal Med Assoc*. 2020;58(226). doi:10.31729/jnma.4967
21. Mahajan P, Chandail VS. Etiological and Endoscopic Profile of Middle-Aged and Elderly patients with Upper gastrointestinal bleeding in a Tertiary Care Hospital in North India: a retrospective analysis. *J Midlife Health*. 2017;8(3):137-141. doi:10.4103/jmh.JMH_86_17
22. Parvez MN, Goenka MK, Tiwari IK, Goenka U. Spectrum of upper gastrointestinal bleed: An experience from Eastern India. *J Digest Endosc*. 2016;7(2):55-61. doi: 10.4103/0976-5042.189146
23. Kaplan RC, Heckbert SR, Psaty BM. Risk factors for hospitalized upper or lower gastrointestinal tract bleeding in treated hypertensives. *Prev Med.* 2002;34(4):455-462. doi:10.1006/pmed.2002.1008
24. Tielleman T, Bujanda D, Cryer B. Epidemiology and Risk Factors for Upper Gastrointestinal Bleeding. *Gastrointest Endosc Clin N Am.* 2015;25(3):415-428. doi:10.1016/j.giec.2015.02.010
25. Kim JS, Kim BW, Kim DH, et al. Guidelines for Non-variceal Upper Gastrointestinal Bleeding. *J Gastroenterol.* 2020;75(6):322-332. doi:10.4166/kjg.2020.75.6.322
26. Boustany A, Alali AA, Almadi M, Martel M, Barkun AN. Pre-endoscopic scores predicting low-risk patients with upper gastrointestinal bleeding: a systematic review and meta-analysis. *J Clin Med.* 2023;12(16):5194.
27. Chatten K, Purssell H, Banerjee AK, Soteriadou S, Ang Y. Glasgow Blatchford Score and risk stratification in acute upper gastrointestinal bleeding: can we extend this to 2 for urgent outpatient management? *Clin Med (Lond).* 2018;18(2):118-122. doi:10.7861/clinmedicine.18-2-118

Rzeszów University Press 2026
ISSN 2544-1361 (online)
doi: 10.15584/ejcem.2026.2.13

http://www.ejcem.ur.edu.pl
European Journal of Clinical and Experimental Medicine
Eur J Clin Exp Med 2026; 24 (2): 334–341

ORIGINAL PAPER

Serum ATP1A1 and epinephrine as potential biomarkers for essential hypertension – a case-control study

Abbas Abd Alhussen Mohammad , Abdul Samad Uleiwi Hassan

Department of Pathological Analysis, College of Health and Medical Technology,
Al-Furat Al-Awsat Technical University, Kufa, Iraq

ABSTRACT

Introduction and aim. Essential hypertension is a leading cause of global morbidity driven by complex genetic and physiological interactions. The roles of the Na^+/K^+-ATPase pump, sympathetic nervous system, and electrolyte balance are critical, yet their simultaneous interaction remains unexplored. This study aimed to investigate the serum levels of Na^+/K^+-ATPase alpha-1 subunit (ATP1A1), epinephrine, and key electrolytes (sodium, potassium, chloride, and calcium) in hypertensive patients, providing a novel multi-marker approach to evaluate their potential as diagnostic biomarkers.

Material and methods. We enrolled 80 hypertensive patients and 40 normotensive controls in this cross-sectional study. Serum ATP1A1 and epinephrine levels were measured by ELISA, and electrolytes were analyzed using an ion-selective electrode analyzer.

Results. Hypertensive patients exhibited significantly higher serum levels of ATP1A1 (430±190 vs. 161±71.16 ng/L), epinephrine (339±188 vs. 116.5±38.6 ng/L), sodium, chloride, and calcium, with significantly lower potassium (all $p<0.001$ ROC analysis demonstrated a promising discriminatory ability for ATP1A1 (AUC=0.92) and epinephrine (AUC=0.94). Multiple regression analysis identified ATP1A1, epinephrine, and chloride levels as significant independent predictors of systolic blood pressure.

Conclusion. Patients with essential hypertension display a distinct biochemical signature of elevated serum ATP1A1 and epinephrine levels coupled with significant electrolyte disturbances. These preliminary findings suggest potential value as biomarkers for essential hypertension, although extensive validation in larger, independent cohorts is required before clinical application can be considered.

Keywords. blood pressure, catecholamines, electrolytes, sodium-potassium-exchanging ATPase

Introduction

Hypertension, a medical condition characterized by persistently elevated arterial blood pressure, remains one of the most significant global health challenges of the 21st century.[1] It affects approximately 15–20% of the adult population globally and is a leading risk factor for numerous serious health outcomes, including cardiovascular disease, stroke, chronic kidney disease, and dementia.[2,3] It is frequently asymptomatic at onset; however, uncontrolled hypertension leads to early death in many parts of the world. This disorder is generally divided into two types: essential (or primary) and secondary hypertension. Essential hypertension, which represents 90–95% of cases, is idiopathic and is the consequence of a mix of genetic predispositions and unspecific lifestyle conditions, including high dietary salt consumption, obesity, and physical inactivity.[4] The remaining 5–10% of cases are classified as secondary hypertension, high blood pressure with an identifiable cause such as chronic kidney disease, endocrine disorders, or use of birth control pills.[5]

Corresponding author: Abbas Abd Alhussen Mohammad, e-mail: abbas.alhuseenlapmsc.chm@student.atu.edu.iq

Received: 4.01.2026 / Revised: 12.03.2026 / Accepted: 16.03.2026 / Published: 30.06.2026

Mohammad AAA, Hassan ASU. Serum ATP1A1 and epinephrine as potential biomarkers for essential hypertension – a case-control study. *Eur J Clin Exp Med.* 2026;24(2):334–341. doi: 10.15584/ejcem.2026.2.13.

The complex control of blood pressure results from a tenuous interaction between hemodynamic and neurohormonal effects. Of these, electrolyte balance has been a major focus of research for many years.[6] In the 1970s and the 1980s, preliminary research of early work initiated a direct correlation between dietary electrolyte intake and blood pressure.[7] Disturbances in major electrolytes, such as sodium and potassium, may interfere with homeostatic mechanisms that regulate vascular tone and fluid status.[8] These early observations have been subsequently elaborated, as recent studies have suggested that the ratio of sodium to potassium intake might be a better predictor of blood pressure levels than the intake of any one mineral in isolation.[9] Since electrolyte disturbances are common and have been associated with increased morbidity and mortality, their role in the pathophysiology of hypertension is highly clinically relevant.[10]

The sodium-potassium pump Na^+/K^+-ATPase alpha-1 subunit (ATP1A1) plays a central role in the regulation of cellular electrolyte homeostasis. Its discovery in 1957 by Danish researchers Jens Christian Skou (this work was also honored with the Nobel Prize for Chemistry, in 1997) has been fundamental to modern physiology.[11] This enzyme facilitates the active transport of sodium ions out of the cell and potassium ions into the cell, operating against their respective concentration gradients, a mechanism that is driven by the hydrolysis of ATP. This function is essential for the preservation of resting membrane potential, the regulation of cell volume, and the facilitation of secondary transport processes for various solutes.[9] The alpha subunit is the catalytic subunit and ATP1A1 is a key isoform in both vascular and renal tissues.

Growing evidence has implicated Na^+/K^+-ATPase dysfunction in the pathogenesis of essential hypertension. The pump is an important modulator of the contractile response in muscle cells. Inhibiting it would result in a higher intracellular sodium level, impact calcium handling, and cause vasoconstriction with an increase in blood pressure.[12] Changes in the expression and/or function of the ATP1A1 subunit are associated with modification of vascular tone and blood pressure control. While traditionally studied as a membrane-bound protein, emerging evidence suggests that ATP1A1 can be detected in the circulation and may have a role as a biomarker in various pathological conditions. The circulating ATP1A1 protein is found in various locations throughout the body, including neurons and glial cells in the brain. Mammals have three auxiliary β subunits, identified as β1 to β3. The β1 subunit, encoded by ATP1B1, is present in nearly all tissues and cells, while β2 and β3 have more limited patterns of tissue expression. The β subunit plays a crucial role in positioning the Na^+/K^+ ATPase at the cell membrane. Additionally, it serves as a protein for intracellular adhesion by associating with adjacent β subunits from nearby cells. A functional pump is established through the assembly of one α subunit, one β subunit, and optionally one from a group of seven regulatory FXYD subunits. Among these, α1 and β1 are the most prevalent components that are believed to contribute to the formation of the essential Na^+/K^+ ATPase isozymes.[13] For instance, studies have shown that ATP1A1 is overexpressed in certain tumor cells and can be released into the circulation. While the exact mechanisms of its release into the serum in the context of hypertension are not fully elucidated, we hypothesize that it may be shed from the cell membrane of vascular endothelial cells, smooth muscle cells, or renal tubular cells in response to the pathophysiological changes associated with hypertension, such as increased shear stress or neurohormonal activation. In addition, the sympathetic nervous system, an important controller of the cardiovascular system, can also have a large effect on blood pressure, which is mediated by epinephrine (adrenaline) release. Many years ago, early investigators reported that hypertensive subjects displayed increased plasma catecholamine levels and a state of sympathetic hyperactivity.[14,15] Epinephrine, when released from the adrenal medulla during stress, directly augments the heart rate and cardiac output and has long been recognized to play a role in maintaining the hypertensive state.[16]

Despite extensive research focusing individually on genetic aspects of Na^+/K^+-ATPase, electrolyte imbalances, or catecholamines, the exact interaction between electrolyte balance, Na^+/K^+-ATPase activity, and sympathetic nervous system overactivity in hypertension remains a critical gap in the literature. While previous studies have examined these components in isolation, their simultaneous assessment has not been conducted. This study was conducted to address this gap by determining the serum ATP1A1 and epinephrine levels alongside key electrolytes (Na^+, K^+, Cl^-, Ca^{2+}) in hypertensive patients compared with healthy normotensive controls. This integrated multi-marker approach is highly novel, as it captures the complex interplay between different physiological systems implicated in hypertension. By simultaneously examining these interconnected biochemical pathways, we sought to clarify their roles in the pathophysiology of hypertension and assess their added value as integrated biomarkers for the disease, potentially offering a more comprehensive diagnostic window than single-parameter assessments.

Material and methods

Study design and population

A 120-subject case-control study was conducted (case control design). The study group included 80 hypertensive patients with an established diagnosis and 40 normotensive controls. Recruitment was performed in

three medical centers at Najaf, Iraq, Al-Sadar General Hospital, Al-Hakeem General Hospital, and Al-Najaf General Hospital from September to December 2025. The study protocol was approved by the local ethics committee of the Najaf Health Department (No. 35083, dated 28.9.2025) and all participants provided informed consent prior to their inclusion.

Inclusion and exclusion criteria

Subjects were eligible if they were 30–65 years old. Hypertensive patients were then classified into two groups: newly diagnosed hypertension (blood pressure ≥130/80 mmHg) without receiving drug therapy and patients with a history of hypertension under regular medication treatment drag include (Beta-blockers, also referred to as beta-adrenergic blockers, are medications prescribed to address heart-related ailments, including high blood pressure, angina, irregular heartbeats, and heart failure. They function by obstructing the effects of adrenaline, resulting in a decreased heart rate and lower blood pressure. These drugs are also beneficial for treating migraines, tremors, and anxiety disorders. Commonly prescribed types of these medications include atenolol, metoprolol, and propranolol. Candesartan is utilized either by itself or in combination with other drugs to manage hypertension in both adults and children aged between 1 and 16 years. Elevated blood pressure increases the strain on the heart and arterial system. Captopril is a medication approved by the FDA that is crucial for controlling high blood pressure, managing left ventricular dysfunction following a heart attack, and treating diabetic kidney damage. Its effectiveness is largely due to its ability to inhibit the renin-angiotensin-aldosterone system (RAAS), which makes it essential for the treatment of these cardiovascular issues.

Amlodipine is categorized as a calcium channel blocker that is employed to manage high blood pressure. For individuals suffering from hypertension, amlodipine can be instrumental in reducing the risk of future heart disease, heart attacks, and strokes.

Diuretics, often referred to as "water pills," are medications that assist the body in removing excess salt and water by promoting increased urination. They are mainly prescribed to manage hypertension, heart failure, kidney disorders, and conditions involving fluid accumulation) for at least more than six months. Normotensive individuals without a prior history of cardiovascular disease served as controls.

The exclusion criteria for all patients were secondary hypertension, chronic kidney disease, diabetes mellitus, and other endocrinopathies. Pregnant women and individuals taking medications known to affect electrolyte balance or sympathetic nervous system activity, such as corticosteroids or beta-agonists, were also excluded from the study.

Sample collection and processing

Venous blood samples, each measuring 5 mL, were collected from all participants. The blood was gathered in sterile gel tubes and permitted to coagulate at room temperature for a duration of 30 minutes prior to undergoing centrifugation at 3000 rpm for 10 minutes to facilitate the separation of the serum. The serum was subsequently divided into three Eppendorf tubes for each subject and preserved at -80°C until analysis to maintain the stability of the analytes.

Biochemical analysis

Serum concentrations of ATP1A1 (cat. no. E437hu) and epinephrine (cat. no. EA0033Hu) were quantified using two different ELISA kits (Bioassay Laboratory, China), following the instructions of manufacturer's. The assay procedure was performed as follows:

1. Standards were diluted according to the manufacturer's protocol to generate a standard curve.
2. Serum samples were added in duplicate to the respective wells.
3. After incubation and washing steps, the specific antibodies were added.
4. The absorbance was read at the specified wavelength.

The ATP1A1 ELISA kit had an assay range of 10-3000 ng/L and a sensitivity of 5.12 ng/L. The intra-assay and inter-assay CV were <8% and <10%, respectively. The epinephrine ELISA kit had an assay range of 15–3000 ng/L and a sensitivity of 7.5 ng/L. The intra-assay and inter-assay CVs were <8% and <10%, respectively. Serum electrolyte levels (Na^+, K^+, Cl^-, and Ca^{2+}) were measured using a Seamaty SE1 electrolyte analyzer (Seamaty, China). Laboratory personnel performing the biochemical assays were blinded to the clinical status (case vs. control) of the samples.

Statistical analysis

All statistical analyses were conducted using GraphPad Prism software (version 9.0). The Shapiro-Wilk test was utilized to evaluate the normality of data distribution prior to the implementation of parametric tests. For normally distributed variables, the independent t-test was used to compare mean values between hypertensive and control groups, after confirming the homogeneity of variance using Levene's test. Continuous variables are expressed as mean±SD (range), and categorical variables are shown as frequency and percentage. Multicollinearity among predictor variables (ATP1A1, epinephrine, and electrolytes) was assessed using the Variance Inflation Factor (VIF) in the context of multiple regression analysis; a VIF value<10 was interpreted as indicative of no significant multicollinearity. Bonferroni correction was applied to adjust the threshold for statistical significance when performing multiple comparisons across

the different electrolyte and biomarker subgroups, setting the corrected significance level at p<0.05.

Results

Demographic, clinical, and biochemical profiles of the participants are presented in Table 1. Age and sex differences between the groups were not statistically significant (p=0.31, p=0.9, respectively). As anticipated, systolic and diastolic blood pressures were significantly higher in the patient group (150.12±10.85 mmHg and 90.00±6.94 mmHg, respectively) than in the control group (115.00±5.07 mmHg and 74.00±4.96 mmHg, respectively). The serum electrolyte profile was markedly deranged among hypertensive patients. In particular, serum levels of sodium (142.16±3.49 mmol/L), chloride (102.33±4.21 mmol/L), and calcium (1.16±0.07 mmol/L) were significantly higher than in the control group (p<0.0001, p<0.0001, and p=0.0004; respectively). In contrast, serum potassium was significantly lower in the patients (4.25±0.48 mmol/L) than the controls (4.66±0.21 mmol/L; p<0.0001). In addition, the mean concentration of ATP1A1 was significantly higher in patients (430±190 ng/L) than in controls (161±71.16 ng/L). Blood epinephrine was also significantly increased in patients (339±188 ng/L) vs. healthy subjects (116.5±38.6 ng/L). These differences were statistically significant (p<0.0001 for both biomarkers).

Table 1. Comparative analysis of demographic, clinical, and biochemical profiles in hypertensive patients and normotensive controls*

Characteristic	Patients (n=80)	Control (n=40)	p
Demographic and clinical data			
Age (years), mean±SD	49.8±11.6	44.5±6.7	0.31
Gender, male, n (%)	40 (50%)	20 (50%)	0.9
Gender, female, n (%)	40 (50%)	20 (50%)	
Systolic BP (mmHg), mean±SD	150.12±10.85	115.00±5.07	<0.0001
Diastolic BP (mmHg), mean±SD	90.00±6.94	74.00±4.96	<0.0001
Serum electrolytes			
Sodium (mmol/L), mean±SD	142.16±3.49	138.43±1.03	<0.0001
Potassium (mmol/L),mean±SD	4.25±0.48	4.66±0.21	<0.0001
Chloride (mmol/L), mean±SD	102.33±4.21	97.10±1.01	<0.0001
Calcium (mmol/L), mean±SD	1.16±0.07	1.12±0.03	0.0004
Biomarkers			
ATP1A1 (ng/L), mean±SD	430±190	161±71.16	<0.0001
Epinephrine (ng/L), mean±SD	339±188	116.5±38.6	<0.0001

* data are presented as the mean±SD, p-value from Chi-square/independent samples t-test

Table 2 presents a comparison of biomarker levels between patients with hypertension receiving pharmacological treatment and those not receiving medication. Patients undergoing drug treatment exhibited significantly elevated levels of ATP1A1 (508.3±143 ng/L vs. 352±200 ng/L, p<0.0001), and epinephrine (384.3±175.5 ng/L vs. 295±192 ng/L, p=0.0338) compared to untreated patients. Similarly, electrolyte concentrations were higher in the treatment group for sodium (143.54±3.10 mmol/L vs. 140.77±3.33 mmol/L, p=0.0002) and chloride (104.11±3.60 mmol/L vs. 100.55±4.06 mmol/L, p<0.0001), while potassium was significantly lower (4.08±0.49 mmol/L vs. 4.42±0.42 mmol/L, p=0.0014). Serum calcium levels showed a trend toward elevation in the treatment group but did not reach statistical significance (1.18±0.07 mmol/L vs. 1.15±0.06 mmol/L, p=0.0582).

Table 2. Biomarkers in patients stratified by drug treatment*

Biomarker	Drug treatment (n=40)	No drug (n=40)	p
ATP1A1	508.3±143	352±200	<0.0001
Epinephrine	384.3±175.5	295±192	0.0338
Sodium	143.54±3.10	140.77±3.33	0.0002
Potassium	4.08±0.49	4.42±0.42	0.0014
Chloride	104.11±3.60	100.55±4.06	<0.0001
Calcium	1.18±0.07	1.15±0.06	0.0582

* data are presented as the mean±SD, p-value from the independent samples t-test

The discriminatory ability of ATP1A1 and epinephrine for HTN patients compared to normotensive controls was estimated using the ROC curve. Figure 1 shows the discriminatory abilities of both biomarkers. For ATP1A1, the Area Under the Curve (AUC) was 0.92 (95% CI: 0.85 to 0.96; p<0.001). A cutoff value of >218 ng/L was identified to achieve a sensitivity of 80% and a specificity of 92%. The Youden's index for overall diagnostic accuracy was 0.74 for ATP1A1. Epinephrine performed similarly, with an AUC of 0.94 (95% CI: 0.90–0.98; p<0.001). A cutoff value of >162 ng/L yielded a sensitivity of 88% and specificity of 90%. This resulted in a Youden index of 0.78, indicating a high level of discriminatory ability in this study population.

A Pearson's correlation analysis was also performed. The associations documented in the correlation matrix (Table 3) revealed various significant correlations that highlight the multifaceted pathophysiology of hypertension. There was a good correlation between systemic sodium and chloride (r=0.824, p<0.001) as physiological phenomenon, and ATP1A1 was also significantly positively associated with sodium (r=0.793, p<0.001) and chloride (r=0.682, p<0.001). In contrast, serum potassium levels were strongly and significantly negatively correlated with sodium (r=-0.846, p<0.001), chloride (r=-0.727, p<0-001) and ATP1A1 (r=-0.710, p < 0.001) levels. Systolic blood pressure was strongly positive correlated with several critical variables such as ATP1A1 (r=0.431, p=0.001), sodium (r=0.406, p=0.002), and chloride

(r=0.364, p<0.009). However, diastolic BP had a less robust yet still significant positive correlation with SBP (r=0.421, p=0.001) and did not correlate significantly with the majority of electrolytes measured. Epinephrine showed no significant association with primary electrolytes or blood pressure.

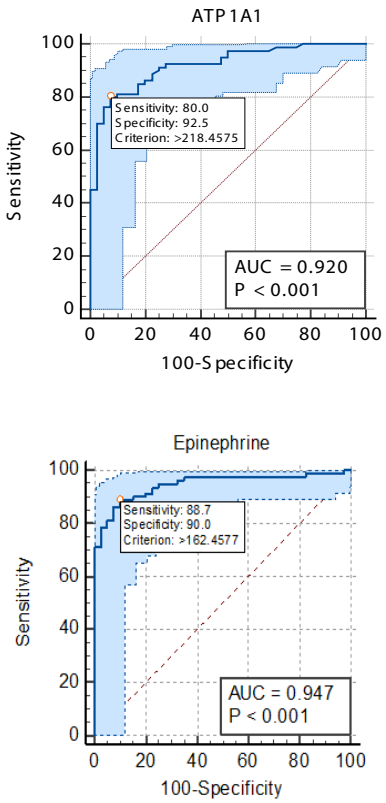

Fig. 1. Receiver operating characteristic curve for ATP1A1 and epinephrine in predicting hypertension

Table 3. Correlations analysis of biochemical and hemodynamic parameters

	Cl^- (mmol/L)	Na^+ (mmol/L)	ATP1A1	Ca^{2+} (mg/dL)	Systolic BP (mmHg)	Diastolic BP (mmHg)	Epinephrine
Cl^- (mmol/L)	1						
Na^+ (mmol/L)	0.824 P<0.001	1					
ATP1A1	0.682 p<0.001	0.793 p<0.001	1				
Ca^{2+} (mg/dL)	0.639 p<0.001	0.697 p<0.001	0.551 p<0.001	1			
Systolic BP (mmHg)	0.364 p=0.009	0.406 p=0.002	0.431 p=0.001	0.343 p=0.001	1		
Diastolic BP (mmHg)	0.150 p=0.182	0.097 p=0.390	0.131 p=0.245	-0.073 p=0.520	0.421 p=0.001	1	
Epinephrine	0.072 p=0.526	0.020 p=0.858	0.148 p=0.188	-0.036 p=0.744	0.117 p=0.302	-0.174 p=0.12	1
K^+ (mmol/L)	-0.727 p<0.001	-0.846 p<0.001	-0.710 p<0.001	-0.519 p<0.001	-0.448 p<0.001	-0.184 p=0.10	-0.046 p=0.65

Multiple linear regression analysis was conducted to identify the significant biochemical and hormonal predictors of systolic blood pressure (Table 4). The model explained a substantial proportion of the variance in SBP (R^2=0.59; adjusted R^2=0.57; F=41.86; p<0.001). Significant positive associations were observed for plasma ATP1A1 (β=0.038, p=0.0009), epinephrine (β=0.002, p=0.0004). Variables, such as sodium, potassium, and calcium levels, were not statistically significant in the final model. The VIF values for all variables were below 5, suggesting that multicollinearity did not pose a significant issue.

Table 4. Analysis of multiple linear regression concerning predictors of systolic blood pressure*

Predictor	Beta (β) Coefficient	Std. Error	T-Value	VIF	p
Intercept	2.78				
ATP1A1	0.037637	0.0009	3.39	2.88	0.0009
Epinephrine	0.002499	0.0006	3.67	1.27	0.0004
R-squared	0.59				
Adjusted R-squared	0.57				

* dependent variable: systolic BP, model summary: F=41.86, p<0.001

Discussion

This study provides a comprehensive analysis of the interplay between serum ATP1A1, epinephrine, and electrolytes in patients with essential hypertension. Our findings reveal a distinct biochemical signature in hypertensive individuals, characterized by elevated serum ATP1A1 and epinephrine levels, alongside significant electrolyte imbalances. These results, while preliminary, suggest that these markers warrant further investigation regarding their potential role in the clinical assessment of hypertension.

To our knowledge, this is one of the first studies to simultaneously investigate the circulating levels of ATP1A1, epinephrine, and a panel of electrolytes in essential hypertension. While previous research has extensively focused on the genetic and tissue-specific aspects of the Na^+/K^+-ATPase,[17] our work extends these findings by quantifying the circulating protein itself, offering a potential window into systemic pathophysiology. The integrated multi-marker approach employed here is a key novelty, aiming to capture the complex interplay between different physiological systems implicated in hypertension.[18,19]

The most striking finding of this study was the pronounced elevation of ATP1A1 levels in the hypertensive cohort. Our observation of almost a three-fold increase in ATP1A1 levels in patients compared to controls strongly supports the growing body of evidence implicating ATP1A1 gene and its protein product as key molecules in blood pressure regulation. While many studies have focused on genetic mutations lead-

ing to conditions such as primary aldosteronism,[17] our estimation of the circulating protein per se provides an indirect observation of its pathogenic upregulation in hypertensive patients. This aligns with recent reviews that confirmed that the Na^+/K^+-ATPase contributes to hypertension through mechanisms in multiple organ systems, including the vasculature and kidneys.[20] Research indicates that variations in the abundance and activity of ATP1A1 significantly influence renal Na reabsorption, Na balance, and blood pressure.[21] Furthermore, an earlier investigation indicated that models of polygenic hypertension are associated with ATP1A1 in relation to salt-sensitive hypertension.[22] The high positive correlations between ATP1A1 and serum sodium and chloride found in the full model also supports a mechanistic relationship, suggesting that down-regulation or overexpression of the pump may occur to counteract or induce changes in sodium balance, which may be related to compensatory machinery due to disturbed Na^+ homeostasis, a characteristic feature of the hypertensive state and supported by recent models of Na^+/K^+-ATPase signaling.[23]

The precise mechanism for the elevated circulating ATP1A1 levels observed in our study remains to be fully elucidated. One possibility is the shedding of the ectodomain of the protein from vascular endothelial or smooth muscle cells in response to hypertensive stimuli.[24] Another potential mechanism is the release of ATP1A1 in extracellular vesicles, which are known to carry membrane proteins and have been implicated in various cardiovascular diseases.[25,26] The observed correlation with epinephrine also suggests a potential crosstalk between the sympathetic nervous system and the regulation of Na^+/K^+-ATPase expression and activity.[27] Further research is warranted to explore these potential mechanisms.

Our findings regarding serum electrolyte levels are consistent with the current understanding of the pathophysiology of hypertension. The observed distribution of increased sodium and chloride with reduced potassium supports the wealth of epidemiologic data over recent years, highlighting the importance of the sodium-to-potassium ratio as a stronger predictor of BP than either ion alone.[28,29] Large-scale analysis, including the KNHANES, consistently shows a strong relationship between a high urinary Na/K ratio and poor blood pressure control.[30] Multiple regression analysis in our study underscored the significance of chloride and revealed it to be an independent predictor of systolic blood pressure. This supports recent research indicating that chloride is more than a passive follower of sodium, and has an independent role in the regulation of blood pressure and cardiovascular disease progression.[31] Similarly, the mild but significant increase in serum calcium is consistent with the hypothesis that perturbed intracellular calcium handling contributes to increased vascular smooth muscle tone and peripheral resistance in essential hypertension.

Additionally, the present investigation of hypertensive subjects demonstrated a state of marked sympathetic nervous system overactivity, as reflected by significantly increased plasma epinephrine concentrations. This result is consistent with the influential review by Grassi et al., who highlighted arterial epinephrine as a predictor of future hypertension.[32] This finding was further supported by our regression analysis, which demonstrated that epinephrine was a significant independent risk factor for SBP. This underscores the importance of the sympathoadrenal axis in the rate-limiting progression of hypertensive disease, an idea that has been continuously revised by a recent meta-analysis of sympathetic nerve traffic.[33] Moreover, identification of genetic mutations resulting in autonomous epinephrine production with consequent hypertension provides additional evidence for the causal association between catecholamines and elevation in blood pressure.[34] This finding is consistent with earlier research that primes the body to release energy stores and triggers a host of changes, referred to as the fight-or-flight response. Epinephrine acts on alpha-1 adrenergic receptors, resulting in higher PVR and BP.[35]

A particularly noteworthy, though exploratory, finding of our study is the observed discriminatory ability of ATP1A1 and epinephrine. The mean AUC values from the ROC analysis for ATP1A1 (0.92) and epinephrine (0.94) suggest a strong discriminative ability in this study population. While these results are promising, it is crucial to interpret them with caution. The high sensitivity and specificity observed at the optimal cutoff values in our cohort suggest that these markers warrant further investigation as potential tools for risk stratification. However, extensive validation in larger, independent, and more diverse populations is required before any clinical utility can be considered.[36,37]

Patients receiving antihypertensive therapy had even higher ATP1A1 and epinephrine levels and more severe electrolyte disruptions, which is an interesting finding. Although this may be counterintuitive, it is possible that these patients had a worse hypertensive phenotype (that required pharmacological therapy). However, some recent guidelines and studies emphasize that some of these antihypertensive medications may in turn cause electrolyte disturbances, thus contributing to the complex biochemical picture.[38] This intricate relationship calls for more longitudinal studies to distinguish diseases from their treatment effects.

The results show that patients with essential hypertension had higher ATP1A1 and epinephrine.[39] This study also describes how FXYD2, signaling from cardiotonic steroids, and hormones including angiotensin II, dopamine, insulin, and catecholamines influence the

control of Na^+/K^+-ATPase. Additionally, this review underscores the significance of Na^+/K^+-ATPase in conditions like hypertension.[40]

Study limitations

This research presents several significant limitations that should be taken into account when analyzing the results. Initially, the ROC curve analyses were performed in the same cohort from which the data were derived, without an independent validation set. This approach is prone to overfitting and may substantially overestimate the true diagnostic performance of these biomarkers. Second, our single-center design limits the generalizability of our findings. Third, the cross-sectional design precludes the establishment of temporal relationships or causality

Conclusion

In conclusion, this study provides preliminary evidence for a concurrent dysregulation of serum ATP1A1, epinephrine, and electrolytes in patients with essential hypertension. These findings contribute to our understanding of the complex pathophysiology of the disease and suggest that a multi-marker approach may warrant further investigation. The results should be interpreted as hypothesis-generating, and extensive validation in larger, prospective, multi-center cohorts is essential before these biomarkers can be considered for any clinical application.

Acknowledgments

The authors thank participants for their participation in the study. We are grateful to the staff and ethical committee in Al-Furat Al-Awsat University, for their kind cooperation. We deeply appreciate the laboratory technicians for their support in sample processing and analyses.

Declarations

Funding

This research received no external funding.

Author contributions

Conceptualization, A.A.A.M. and A.S.U.H.; Methodology, A.A.A.M. and A.S.U.H; Validation, A.A.A.M. and A.S.U.H.; Formal Analysis, A.A.A.M.; Investigation, A.A.A.M. and A.S.U.H; Resources, A.A.A.M.; Data Curation, A.A.A.M.; Writing – Original Draft Preparation, A.A.A.M. and A.S.U.H.; Writing – Review & Editing, A.A.A.M. and A.S.U.H.; Visualization, A.A.A.M.; Supervision, A.A.A.M.; Project Administration, A.A.A.M.; Funding Acquisition, A.A.A.M. and A.S.U.H.

Conflicts of interest

The authors have nothing to disclose.

Data availability

The datasets that were generated or analyzed during the current study are not publicly available due to concerns about participant privacy and confidentiality but are available from the corresponding author on reasonable request.

Ethics approval

Ethical approval for this study was obtained from the Medicine Department Ethical Committee of Medical Laboratories College of Health and Medical Technologies/Kufa-Iraq, with reference (35083) on (28.9.2025).

References

1. Mills KT, Stefanescu A, He J. The global epidemiology of hypertension. *Nat Rev Nephrol*. 2020;16(4):223-237. doi:10.1038/s41581-019-0244-2
2. World Health Organization. *Global Report on Hypertension: The Race against a Silent Killer*. World Health Organization; 2023.
3. Perry M. Hypertension: an overview. *J Community Nurs*. 2023;37(6).
4. Carretero OA, Oparil S. Essential hypertension: part I: definition and etiology. *Circulation*. 2000;101(3):329-335.
5. Rimoldi SF, Scherrer U, Messerli FH. Secondary arterial hypertension: when, who, and how to screen? *Eur Heart J*. 2014;35(19):1245-1254. doi:10.1093/eurheartj/eht534
6. Feng Earley Y, Pan S, Verma H, et al. Central nervous system mechanisms of salt-sensitive hypertension. *Physiol Rev*. 2025;105(4):1989-2032.
7. Sriperumbuduri S, Welling P, Ruzicka M, Hundemer GL, Hiremath S. Potassium and hypertension: a state-of-the--art review. *Am J Hypertens*. 2024;37(2):91-100.
8. Stone MS, Martyn L, Weaver CM. Potassium Intake, Bioavailability, Hypertension, and Glucose Control. *Nutrients*. 2016;8(7). doi:10.3390/nu8070444
9. Perez V, Chang ET. Sodium-to-potassium ratio and blood pressure, hypertension, and related factors. *Adv Nutr*. 2014;5(6):712-741. doi:10.3945/an.114.006783
10. Zhang L, Staehr C, Zeng F, Bouzinova EV, Matchkov VV. The Na,K-ATPase in vascular smooth muscle cells. *Curr Top Membr*. 2019;83:151-175. doi:10.1016/bs.ctm.2019.01.007
11. Skou JC. The identification of the sodium pump. *Biosci Rep*. 1998;18(4):155-169. doi:10.1023/A:1020196612909
12. Iqbal S, Klammer N, Ekmekcioglu C. The effect of electrolytes on blood pressure: A brief summary of meta-analyses. *Nutrients*. 2019;11(6). doi:10.3390/nu11061362
13. Cinarli Yuksel F, Nicolaou P, Spontarelli K, et al. The phenotypic spectrum of pathogenic ATP1A1 variants expands: the novel p.P600R substitution causes demyelinating Charcot-Marie-Tooth disease. *J Neurol*. 2023;270(5):2576-2590. doi:10.1007/s00415-023-11581-w
14. Fernandez CJ, Hanna FWF, Pacak K, Nazari MA. Catecholamines and blood pressure regulation. In: *Endocrine Hypertension*. Elsevier; 2023:19-34.

15. Walther LM, von Känel R, Heimgartner N, Zuccarella-Hackl C, Stirnimann G, Wirtz PH. Alpha-adrenergic mechanisms in the cardiovascular hyperreactivity to norepinephrine-infusion in essential hypertension. *Front Endocrinol (Lausanne)*. 2022;13:824616. doi:10.3389/fendo.2022.824616
16. Oner E, Uruc S, Dokur E, Gorduk O, Sahin Y. Utilization of a selective paper-based flexible electrochemical sensor for epinephrine determination in artificial sweat using nickel oxide and sulfur-doped graphene conductive ink. *J Electrochem Soc*. 2025;172(2):27508.
17. Biondo ED, Spontarelli K, Ababioh G, Méndez L, Artigas P. Diseases caused by mutations in the Na(+)/K(+) pump α1 gene ATP1A1. *Am J Physiol Cell Physiol*. 2021;321(2):C394-C408. doi:10.1152/ajpcell.00059.2021
18. Ikonomidis I, Michalakeas CA, Lekakis J, Paraskevaidis I, Kremastinos DT. Multimarker approach in cardiovascular risk prediction. *Dis Markers*. 2009;26(5-6):273-285. doi:10.3233/DMA-2009-0633
19. Bielecka-Dabrowa A, Gluba-Brzózka A, Michalska-Kasiczak M, Misztal M, Rysz J, Banach M. The multi-biomarker approach for heart failure in patients with hypertension. *Int J Mol Sci*. 2015;16(5):10715-10733. doi:10.3390/ijms160510715
20. Staehr C, Aalkjaer C, Matchkov VV. The vascular Na,K-ATPase: clinical implications in stroke, migraine, and hypertension. *Clin Sci (Lond)*. 2023;137(20):1595-1618. doi:10.1042/CS20220796
21. Herrera VL, Pasion KA, Moran AM, et al. A functional 12T-insertion polymorphism in the ATP1A1 promoter confers decreased susceptibility to hypertension in a male Sardinian population. *PLoS One*. 2015;10(1):e0116724. doi:10.1371/journal.pone.0116724
22. Filippini T, Naska A, Kasdagli MI, et al. Potassium intake and blood pressure: A dose-response meta-analysis of randomized controlled trials. *J Am Heart Assoc*. 2020;9(12):e015719. doi:10.1161/JAHA.119.015719
23. Gao Y, Xu Y, Bai F, Puri R, Tian J, Liu J. Factors that influence the Na/K-ATPase signaling and function. *Front Pharmacol*. 2025;16:1639859. doi:10.3389/fphar.2025.1639859
24. Hayashida K, Bartlett AH, Chen Y, Park PW. Molecular and cellular mechanisms of ectodomain shedding. *Anat Rec (Hoboken)*. 2010;293(6):925-937. doi:10.1002/ar.20757
25. Wang C, Li H, Zhou H, et al. Intracranial aneurysm circulating exosome-derived LncRNA ATP1A1-AS1 promotes smooth muscle cells phenotype switching and apoptosis. *Aging (Albany NY)*. 2024;16(9):8320-8335. doi:10.18632/aging.205821
26. Pomatto MAC, Gai C, Bussolati B, Camussi G. Extracellular vesicles in renal pathophysiology. *Front Mol Biosci*. 2017;4:37. doi:10.3389/fmolb.2017.00037
27. Nguyen PT, Deisl C, Fine M, et al. Structural basis for gating mechanism of the human sodium-potassium pump. *Nat Commun*. 2022;13(1):5293. doi:10.1038/s41467-022-32990-x
28. Park J, Kwock CK, Yang YJ. The effect of the sodium to potassium ratio on hypertension prevalence: A propensity score matching approach. *Nutrients*. 2016;8(8):482. doi:10.3390/nu8080482
29. Muroya T, Satoh M, Metoki H, et al. Association between urinary sodium-to-potassium ratio and BNP in a general population without antihypertensive treatment and cardiovascular diseases: the Ohasama study. *Hypertens Res*. 2025;48(9):2292-2302. doi:10.1038/s41440-025-02266-0
30. Yoon Y, Son M. Association between blood pressure control in hypertension and urine sodium to potassium ratio: From the Korea National Health and Nutrition Examination Survey (2016-2021). *PLoS One*. 2024;19(11):e0314531. doi:10.1371/journal.pone.0314531
31. Wu D, Chen Y, Guan H, Sun Y. Association of abnormal serum electrolyte levels with hypertension in a population with high salt intake. *Public Health Nutr*. 2019;22(9):1635-1645. doi:10.1017/S1368980019000260
32. Grassi G, Mark A, Esler M. The sympathetic nervous system alterations in human hypertension. *Circ Res*. 2015;116(6):976-990. doi:10.1161/CIRCRESAHA.116.303604
33. Seravalle G, Grassi G. Sympathetic nervous system and hypertension: New evidences. *Auton Neurosci*. 2022;238:102954. doi:10.1016/j.autneu.2022.102954
34. Duan Y, Wu C, Lai Z, et al. Autonomous epinephrine release by KCNJ5 mutation drives familial thoracic aortic aneurysm and dissection. *Hypertens (Dallas, Tex 1979)*. 2025;82(4):752-764. doi:10.1161/HYPERTENSIONAHA.124.23795
35. Nakajima J, Sawada Y, Isshiki Y, et al. Influence of the prehospital administered dosage of epinephrine on the plasma levels of catecholamines in patients with out-of-hospital cardiac arrest. *Heliyon*. 2021;7(8):e07708. doi:10.1016/j.heliyon.2021.e07708
36. Palmu J, Tikkanen E, Havulinna AS, et al. Comprehensive biomarker profiling of hypertension in 36985 Finnish individuals. *J Hypertens*. 2022;40(3):579-587. doi:10.1097/HJH.0000000000003051
37. Vasan RS. Biomarkers of cardiovascular disease: molecular basis and practical considerations. *Circulation*. 2006;113(19):2335-2362. doi:10.1161/CIRCULATIONAHA.104.482570
38. Hua Q, Fan L, Wang ZW, Li J. 2023 Guideline for the management of hypertension in the elderly population in China. *J Geriatr Cardiol*. 2024;21(6):589-630. doi:10.26599/1671-5411.2024.06.001
39. Wu IC, Chen YK, Wu CC, et al. Overexpression of ATPase Na+/+ transporting alpha 1 polypeptide, ATP1A1, correlates with clinical diagnosis and progression of esophageal squamous cell carcinoma. *Oncotarget*. 2016;7(51):85244-85258. doi:10.18632/oncotarget.13267
40. Cordeiro BM, Leite Fontes CF, Meyer-Fernandes JR. Molecular Basis of Na, K-ATPase Regulation of Diseases: Hormone and FXYD2 Interactions. *Int J Mol Sci*. 2024;25(24). doi:10.3390/ijms252413398

Rzeszów University Press 2026
ISSN 2544-1361 (online)
doi: 10.15584/ejcem.2026.2.14

http://www.ejcem.ur.edu.pl
European Journal of Clinical and Experimental Medicine
Eur J Clin Exp Med 2026; 24 (2): 342–348

ORIGINAL PAPER

Longitudinal hormonal dynamics during minipuberty and exploratory associations with vitamin D status in healthy term male infants

Vijaya Vinotha Muthuchandrasekar [1], Balaji Chinnasami [1], Aseema Fathima Z. [1], Subash Sundar [1], Aamina Hussain [2], Aravind Murugesan [3]

[1] Department of Pediatrics, SRM Medical College Hospital and Research Center, Kattankulathur, Chengalpattu District, Tamil Nadu, India
[2] Department of Community Medicine, SRM Medical College Hospital and Research Center, Kattankulathur, Chengalpattu District, Tamil Nadu, India
[3] Department of Radiology, SRM Medical College Hospital and Research Centre, Kattankulathur, Chengalpattu District, Tamil Nadu, India

ABSTRACT

Introduction and aim. Minipuberty, the transient postnatal reactivation of the hypothalamic-pituitary-gonadal axis, is a critical window for male reproductive maturation. The study prospectively characterized hormonal dynamics during minipuberty and explored associations between 25-hydroxyvitamin D [25(OH)D] and gonadal hormones, adrenal corticosterone, and genital growth parameters.

Material and methods. Sixty healthy term male babies were enrolled; 52 completed follow-up. Testosterone, luteinizing hormone (LH), follicle stimulating hormone (FSH), corticosterone, and 25(OH)D were measured on day 3 and at 3 months by LC-MS/MS and chemiluminescence immunoassay. Penile length and testicular volume were recorded at both visits.

Results. Testosterone increased from 47.18 to 142.62 ng/dL, LH from 1.31 to 2.46 mIU/mL, and FSH from 1.22 to 2.10 mIU/L (all $p<0.001$), while corticosterone decreased from 211.19 to 86.25 ng/dL ($p<0.001$). Several nominal associations were observed before multiple comparison correction; however, after Bonferroni correction, only the inverse association between 25(OH)D and corticosterone at 3 months ($r=-0.576$, $p<0.001$) remained statistically significant. All other associations should be considered exploratory.

Conclusion. Only the inverse association between vitamin D and corticosterone remained statistically significant after correction, while other associations were exploratory and require confirmation in larger studies.

Keywords. corticosterone, minipuberty, neonates, testicular volume, testosterone, vitamin D

Introduction

The early postnatal months are marked by a well-recognized but transient endocrine phenomenon – minipuberty characterized by reactivation of the hypothalamic-pituitary-gonadal (HPG) axis before its subsequent quiescence until puberty.[1-3] In male infants, this window is driven by a sequential increase in luteinizing hormone (LH) and follicle stimulating hormone

Corresponding author: Balaji Chinnasami, e-mail: balajisrmt@gmail.com

Received: 3.03.2026 / Revised: 8.04.2026 / Accepted: 9.04.2026 / Published: 30.06.2026

Muthuchandrasekar VV, Chinnasami B, Fathima AZ, Sundar S, Hussain A, Murugesan A. Longitudinal hormonal dynamics during minipuberty and exploratory associations with vitamin D status in healthy term male infants. *J Clin Exp Med.* 2026;24(2):342–348. doi: 10.15584/ejcem.2026.2.14.

(FSH), followed by a surge of testosterone that may approach early-pubertal concentrations between one and three months of age.[1-3] This androgen-rich period supports testicular descent, Leydig and Sertoli cell maturation, and phallic growth, and is thought to lay the groundwork for adult male reproductive function.[1,3,4] Disruption of this window has been associated with cryptorchidism, micropenis, and impaired Sertoli cell proliferation, with potential long-term consequences for adult fertility and reproductive health**.** However, the factors that determine the magnitude and timing of this surge are still not well understood.

Beyond its established role in calcium homeostasis and skeletal health, vitamin D is increasingly recognized as a pleiotropic steroid hormone with direct reproductive relevance. Functional VDR and 1α-hydroxylase have been identified in human Leydig cells, Sertoli cells, and the hypothalamic-pituitary unit,[5,6] suggesting tissue-level steroidogenic regulation. Experimental work indicates that 3β-HSD and 17β-HSD – enzymes central to androgen biosynthesis – can be upregulated by vitamin D, and intracellular calcium signaling in testicular cells is also a proposed target.[6,7] In adult men, higher levels have been linked to better testosterone concentrations and reproductive outcomes in observational studies and clinical trials.[8,9] Whether this vitamin D-steroidogenesis relationship extends to the neonatal period, particularly during the hormonally active minipuberty window, has not previously been examined in a prospective longitudinal study.

Neonatal vitamin D insufficiency is a widespread problem in India, with prevalence estimates ranging from 50% to over 90% in some series.[10-12] Contributing factors include prolonged indoor confinement of newborns, limited dietary sources, reduced skin synthesis related to skin pigmentation, and frequently depleted maternal stores at delivery. If this deficiency coincides with the minipuberty window when androgen-driven genital development and early reproductive programming are underway – the long-term consequences may extend well beyond infancy.

To date, a single published study by Kılınç et al.[13] studied a mixed-sex Turkish cohort at a single cross-sectional time point (30–45 days). No prospective dual time point study has previously been conducted that captured the entire HPG axis alongside objective genital growth measures in Indian male neonates.

Aim

The aim of this study was to prospectively characterize hormonal dynamics during minipuberty and to explore associations between serum 25(OH)D levels and testosterone, LH, FSH, corticosterone, penile length, and mean testicular volume on day 3 and at three months of age in healthy term male infants.

Material and methods

Study design and setting

This was a prospective observational study conducted at the SRM Medical College Hospital and Research Institute, Chennai, Tamil Nadu, between June 2024 and December 2025. Institutional Ethics Committee approval was obtained (SRMIEC-ST0724-8011), and written informed consent was obtained from each infant's parent or guardian before enrollment.

Study population

We enrolled term singleton male infants born at 37–42 weeks gestation. The growth classification appropriate for gestational age (AGA; birth weight 10th–90th centile) or small for gestational age (SGA; birth weight below the 10th centile) was assigned using the INTERGROWTH-21st newborn size standards.[14] Infants were excluded if born to mothers with diabetes mellitus, hypertension, or pre-eclampsia; if they had major congenital malformations, genital anomalies (hypospadias, cryptorchidism, micropenis, ambiguous genitalia), chromosomal or genetic disorders, endocrine pathology, or critical illness; or if they were born of multiple pregnancy. Maternal conditions, including diabetes mellitus, hypertensive disorders, and hypothyroidism, were recorded; however, due to the exclusion criteria, only maternal hypothyroidism was present in the final cohort and was included as 'maternal complications' in the regression model.

Procedures and timeline

Clinical assessments occurred at two pre-specified visits: day 3 of life and 3 months of age (day 90±5). On day 3 of life, anthropometric measurements were recorded according to the INTERGROWTH-21st protocol.[14] At 3 months, weight, length, and head circumference were measured according to WHO Child Growth Standards.[15] All values were recorded as the mean of three consecutive readings taken on the same day.

The stretched penile length (SPL) was assessed using a rigid ruler placed on the compressed suprapubic fat pad, measuring from the pubic symphysis to the tip of the glans; three consecutive readings were averaged. The testicular volume was determined by high resolution transscrotal ultrasound on a Philips Affiniti 70 system (12–4 MHz transducer) using the ellipsoid formula (length×width×height×0.523). A single experienced pediatric radiologist performed all sonographic examinations, remaining blind to hormonal data throughout.

At each visit, a 3 ml venous blood sample was centrifuged at 3,000 rpm for 10 minutes; the resulting serum was stored at –70°C until batch analysis. Testosterone and corticosterone levels were determined by liquid chromatography tandem mass spectrometry (LC-MS/MS); gonadotropins (LH, FSH) by chemiluminescence

immunoassay, all processed at a nationally accredited reference laboratory maintaining validated pediatric reference intervals. Oral vitamin D3 (400 IU/day) was started from the day of hospital discharge according to the IAP guidelines.[16]

Statistical analysis

Statistical analyses were carried out in SPSS version 27.0 (IBM, Armonk, NY, USA). Continuous variables are reported as mean±SD or median (Q1–Q3) depending on normality, assessed using the Shapiro-Wilk test. Changes from day 3 to the third month were tested using the Wilcoxon signed rank test. Comparisons between groups (AGA versus SGA) used the Mann-Whitney U test for continuous variables and the chi-square or Fisher's exact test for categorical variables. Spearman's rank order correlation assessed relationships between vitamin D and each hormonal and genital growth outcome. A post hoc power analysis was performed based on the observed correlation between vitamin D levels and mean testicular volume. With an effect size (r) of 0.30, an alpha level of 0.05, and a total sample size of 52 participants, the statistical power was approximately 74%, indicating a moderate power for detecting moderate associations in this cohort. To account for multiple comparisons, Bonferroni correction was applied within each analytical set. For correlation analyses between vitamin D and hormonal parameters (16 comparisons), the adjusted significance threshold was set at $p<0.003$. For the correlations between vitamin D and genital parameters (6 comparisons), the corrected significance level was $p<0.008$. Significance was established at $p<0.05$ (two-tailed). Correlation analyses and group-based comparisons address different analytical questions and may not yield concordant results. Consequently, statistically significant correlations do not necessarily translate into significant differences between groups defined by threshold-based categorization.

Results

Participant characteristics

Of the 60 infants enrolled, 52 completed both study visits and were included in the final analysis; 8 were lost to follow-up. Of the 52 infants, 27 (51.9%) delivered by lower-segment caesarean section (LSCS), 24 (46.2%) by normal vaginal delivery and 1 (1.9%) by vacuum-assisted delivery. Maternal hypothyroidism was documented in 14 mothers (26.9%). The mean birth weight was 2.73±0.34 kg and the mean birth length was 47.83±1.75 cm. Demographic and anthropometric data for both visits are summarized in Table 1.

The mean vitamin D at birth was 25.26±18.66 ng/mL, suggesting relatively low vitamin D levels in this cohort. After three months of standard supplementation (400 IU/day), the mean of the group increased to 49.43±23.50 ng/mL, though with considerable variability between individuals.

Table 1. Baseline and follow-up demographic and anthropometric characteristics (n=52)*

Variable	Value (n (%) or mean±SD)
Growth status: AGA	28 (53.8%)
Growth status: SGA	24 (46.2%)
Mode of delivery: LSCS	27 (51.9%)
Mode of delivery: normal vaginal delivery	24 (46.2%)
Mode of delivery: vacuum-assisted	1 (1.9%)
Maternal hypothyroidism	14 (26.9%)
Birth weight (kg)	2.73±0.34
Birth length (cm)	47.83±1.75
Head circumference at birth (cm)	33.66±1.24
Weight at 3 months (kg)	5.50±0.78
Length at 3 months (cm)	59.14±3.31
Head circumference at 3 months (cm)	39.51±2.22

* AGA – appropriate for gestational age, SGA – small for gestational age, LSCS – lower segment caesarean section

Minipuberty hormonal surge: longitudinal changes

Wilcoxon signed rank testing confirmed significant hormonal shifts during the two visits (Table 2). Testosterone increased from a birth median of 47.18 (18.97–95.69) ng/dL to 142.62 (92.62–274.34) ng/dL at three months ($Z=-5.828$, $p<0.001$) – a nearly threefold increase. LH increased from 1.31 (1.21–1.88) to 2.46 (1.96–3.04) mIU/mL ($Z=-5.231$, $p<0.001$) and FSH from 1.22 (0.89–1.72) to 2.10 (1.61–2.55) mIU/L ($Z=-5.009$, $p<0.001$), confirming physiological activation of the HPG axis during minipuberty. In contrast, corticosterone decreased from 211.19 (124.88–377.34 ng/dL) at birth to 86.25 (47.39–141.16) ng/dL at 3 months ($Z=-5.282$, $p<0.001$), consistent with the anticipated regression of the fetal adrenal cortex during early postnatal life.

Table 2. Longitudinal changes in hormonal levels from birth to 3 months (Wilcoxon signed-rank test, n=52)

Parameter	Birth median (Q1–Q3)	3-month median (Q1–Q3)	Z	p
Testosterone (ng/dL)	47.18 (18.97–95.69)	142.62 (92.62–274.34)	−5.828	<0.001
LH (mIU/mL)	1.31 (1.21–1.88)	2.46 (1.96–3.04)	−5.231	<0.001
FSH (mIU/L)	1.22 (0.89–1.72)	2.10 (1.61–2.55)	−5.009	<0.001
Corticosterone (ng/dL)	211.19 (124.88–377.34)	86.25 (47.39–141.16)	−5.282	<0.001

Spearman correlation between vitamin D levels and hormonal parameters

Vitamin D levels showed differential hormonal associations between the two time points (Table 3). At birth, neonatal vitamin D levels were positively correlated with testosterone ($r=0.335$, $p=0.015$) and negatively with corticosterone ($r=-0.275$, $p=0.048$); no significant relationships were observed for LH or FSH at birth. At 3 months, a strong inverse correlation was observed be-

tween vitamin D levels and corticosterone (r=−0.576, p<0.001). No significant vitamin D associations with LH or testosterone were detected at the three-month visit.

Table 3. Spearman correlation between vitamin D levels and hormonal parameters at birth and three months (n=52)*

Hormone	Vitamin D at birth r (p)	Vitamin D at 3 months r (p)
Testosterone (birth)	0.335 (0.015)	0.163 (0.250)
LH (birth)	0.248 (0.089)	0.207 (0.158)
FSH (birth)	−0.067 (0.650)	0.036 (0.807)
Corticosterone (birth)	−0.275 (0.048)	−0.210 (0.136)
Testosterone (3 months)	0.238 (0.089)	0.096 (0.499)
LH (3 months)	0.068 (0.630)	0.044 (0.759)
FSH (3 months)	−0.323 (0.020)	−0.146 (0.301)
Corticosterone (3 months)	−0.154 (0.276)	−0.576 (<0.001)

* values are Spearman r with two-tailed p values

Correlations between vitamin D and genital growth parameters

Vitamin D levels showed a consistent positive relationship with mean testicular volume at both visits (Table 4). Vitamin D levels were moderately correlated with testicular volume at birth (r=0.304, 95% CI: 0.034–0.533, p=0.028) and a comparable association with testicular volume at 3 months (r=0.290, 95% CI: 0.019–0.522, p=0.037). Vitamin D levels at three months were similarly associated with concurrent testicular volume (r=0.304, 95% CI 0.036-0.534, p=0.027). Penile length did not show correlation with vitamin D levels in either assessment.

Table 4. Spearman correlation between vitamin D levels and genital parameters (n=52)*

Outcome	Exposure	n	r	95% CI	p
Mean testicular volume (birth)	Vitamin D at birth	52	0.304	0.034 to 0.533	0.028
Mean testicular volume (3 months)	Vitamin D at birth	52	0.290	0.019 to 0.522	0.037
Mean testicular volume (3 months)	Vitamin D at 3 months	52	0.306	0.036 to 0.534	0.027
Penile length (birth)	Vitamin D at birth	52	−0.084	−0.348 to 0.199	0.554
Penile length (3 months)	Vitamin D at birth	52	0.211	−0.064 to 0.452	0.133
Penile length (3 months)	Vitamin D at 3 months	52	0.136	−0.143 to 0.393	0.335

* 95% CI calculated using Fisher's z transformation

Multiple comparison correction

Several correlations between vitamin D levels and hormonal parameters demonstrated statistical significance using the conventional threshold of p<0.05. Moderate associations were observed between vitamin D at birth and testosterone at birth, between vitamin D and corticosterone at birth, and a negative correlation between vitamin D and FSH at three months. However, after Bonferroni correction for multiple comparisons (adjusted threshold p<0.003 for 16 hormonal comparisons), only the strong inverse correlation between vitamin D levels and corticosterone at three months (r=−0.576) retained statistical significance. The remaining associations did not survive correction and should therefore be interpreted with caution.

Table 5. Multivariate linear regression analysis for the determinants of mean testicular volume at three months (n=52)*

Predictor variable	B (unstandardized)	SE	Standardized β	95% CI for B	p
Vitamin D at birth (ng/mL)	0.003	0.001	0.411	0.001–0.005	0.008
Growth status (SGA vs AGA)	−0.078	0.050	−0.335	−0.179–0.023	0.127
Birth weight (kg)	−0.017	0.088	−0.050	−0.195–0.161	0.845
Birth length (cm)	0.003	0.010	0.045	−0.017–0.023	0.760
Head circumference (cm)	0.001	0.015	0.009	−0.029–0.031	0.957
Maternal complications	−0.017	0.036	−0.066	−0.089–0.055	0.641
Mode of delivery	−0.029	0.031	−0.124	−0.092–0.034	0.368

* Multivariate linear regression adjusted for growth status, maternal complications, mode of delivery, and baseline anthropometric parameters, model fit: R^2=0.227, adjusted R^2=0.105, F=1.851, p=0.111, B unstandardized regression coefficient, SE standard error, β – standardized beta coefficient, CI confidence interval

In the multivariate linear regression analysis, vitamin D level on day 3 showed an association with mean testicular volume at 3 months (B=0.003, β=0.411, 95% CI: 0.001–0.005, p=0.008), after adjustment for growth status (AGA/SGA), maternal complications, mode of delivery, birth weight, birth length, and head circumference (Table 5); however, these findings should be interpreted cautiously given the general model and are considered exploratory. This indicates that each 1 ng/mL increase in birth vitamin D level was associated with a 0.003 unit increase in testicular volume at three months, independent of these covariates. None of the remaining variables showed a statistically significant association with testicular volume (all p>0.05). The general fit of the model was modest (R^2=0.227, adjusted R^2=0.105, F=1.851, p=0.101). However, it must be explicitly acknowledged that the overall regression model did not reach statistical significance (F=1.850, p=0.101), indicating that the model as a whole does not significantly predict testicular volume. Therefore, the individual coefficient of vitamin D should therefore be interpreted with caution and cannot be used to support independent predictive conclusions; these regression findings are presented for exploratory purposes.

Discussion

This study prospectively characterized hormonal dynamics during minipuberty in healthy term male infants, demonstrating the expected increase in testos-

terone, LH, and FSH, along with a decline in corticosterone. In addition, exploratory analyses were performed to examine potential associations between vitamin D status and endocrine and growth parameters. The longitudinal hormonal trajectories observed in this cohort – including testosterone surge, gonadotropin increase, and corticosterone decline – are consistent with well-established minipuberty physiology described in the prior literature,[1-3] supporting that these changes represent expected postnatal endocrine patterns.

A positive association between vitamin D and neonatal testosterone was observed; however, this did not remain significant after correction for multiple comparisons and should therefore be interpreted as exploratory. While biologically plausible given the presence of vitamin D receptors in Leydig cells,[5,6] any mechanistic interpretation remains speculative and hypothesis-generating in the absence of robust statistical support.

An important statistical caveat must be acknowledged. After applying the Bonferroni correction for multiple comparisons, most of the correlations reported in this study, including those between vitamin D and testosterone and between vitamin D and testicular volume, were no longer statistically significant at the corrected threshold ($p<0.003$ for hormonal parameters; $p<0.008$ for genital parameters). Only the inverse correlation between vitamin D and corticosterone at three months ($r=-0.576$, $p<0.001$) survived correction. Consequently, all associations reported in this study should be interpreted as exploratory and hypothesis-generating rather than confirmatory, and must be replicated in larger, adequately powered, independent cohorts before any clinical inferences are drawn.

It should also be noted that all statistical analyses in this study were predefined in the study protocol, carried out using standard validated methods, and no post hoc data-driven model selection was performed; the analytical approach was determined independently of the results.

Attenuation of this association at three months may reflect several possibilities, including a potential threshold effect or the dominant influence of gonadotropin-driven stimulation during peak minipuberty. However, these interpretations are speculative and cannot be confirmed within the constraints of the present data.

The absence of a significant association between vitamin D levels and gonadotropins (LH, FSH) at either visit is noteworthy and was similarly reported by Kılınç et al.,[13] who found no significant correlation between vitamin D status and gonadotropins in boys at 30 to 45 days of life. Taken together, these data raise the possibility that, to the extent vitamin D is associated with minipuberty hormones, the association may be at a peripheral rather than central level at the gonadal rather than the hypothalamic-pituitary level. This remains speculative in the absence of experimental or interventional evidence.

Associations between vitamin D levels and testicular volume were observed at both timepoints; however, these were not statistically significant after correction for multiple comparisons and should therefore be interpreted as exploratory. While the direction of association was consistent, the moderate effect sizes and loss of significance after correction limit the strength of inference. Any biological interpretation remains tentative and should be considered hypothesis-generating given the lack of statistical significance after correction.

The lack of a vitamin D–penile length association may have a plausible biological basis. Phallic enlargement during minipuberty depends mainly on local conversion of testosterone to dihydrotestosterone (DHT) via 5α-reductase in corporeal tissue, rather than on circulating testosterone per se.[19] Because the associations of vitamin D in this dataset were with testosterone rather than DHT, the absence of a corresponding penile length effect is mechanistically coherent.

The inverse vitamin D–corticosterone relationship was the most notable finding of this study. This association was statistically significant after correction for multiple comparisons. The association at birth was modest ($r=0.275$, $p=0.048$) but became markedly stronger at three months ($r=-0.576$, $p<0.001$), coinciding with a near-60% decrease in corticosterone over the same interval, a trajectory consistent with regression of the fetal adrenal zone in postnatal life.[20] This association is biologically plausible: VDR is expressed in the adrenal cortex,[21,22] and experimental data suggest that vitamin D may suppress CRH and ACTH at the hypothalamic-pituitary level[6] while also modulating adrenal steroidogenic enzymes. Therefore, it is possible that higher vitamin D status may be associated with a more rapid postnatal decline in glucocorticoid production, a recognised component of neonatal metabolic transition, although residual confounding and the observational design preclude any causal interpretation. Future work with serial HPA axis markers and appropriate confounder adjustment will be necessary to further characterize this relationship.

Compared to Kılınç et al.,[13] the strengths of this study lie in its prospective longitudinal design that spans two key timepoints across the minipuberty window, including the gonadal and adrenal hormonal axes, and the use of objective ultrasound-based testicular volume. These design features provide a comprehensive characterization of early postnatal endocrine physiology in male infants and represent the primary novel contribution of this work.

Study limitations

The single-center design limits generalizability. The moderate sample size (n=52) reduces the statistical power for subgroup analyses. No maternal vitamin D data were available. Near-universal supplementation

(400 IU/day after discharge) may have contributed to changes in vitamin D levels by three months, potentially reducing variability within the cohort and thus limiting our ability to examine the effects of sustained deficiency; therefore, all associations at three months should be interpreted in the context of supplemented, rather than naturally deficient, vitamin D status, and these findings cannot be extrapolated to prolonged deficiency. No serial corticosterone or HPA axis markers were obtained. The observational design precludes causal inference. Potential confounders including growth status (AGA/SGA), maternal hypothyroidism, mode of delivery, and baseline anthropometrics were not adjusted for in the primary correlation analyses – multivariable regression models addressing this are presented separately. Despite the application of the Bonferroni correction, the study remains at risk of type I error due to multiple comparisons and limited sample size. The study cannot determine whether vitamin D associations reflect a direct biological effect or are mediated by unmeasured factors that covary with vitamin D status in this population.

Conclusion

In this prospective longitudinal study of healthy term Indian male newborns, the expected hormonal dynamics of minipuberty were confirmed, including a rise in testosterone, LH, and FSH and a decrease in corticosterone. The only association between vitamin D status and endocrine parameters that remained statistically robust after correction for multiple comparisons was the inverse relationship between 25(OH)D and corticosterone at three months. All other associations, including those with testosterone and testicular volume, did not survive Bonferroni correction and should be considered exploratory, requiring confirmation in larger independent studies. These findings do not permit causal conclusions and should be interpreted within the limitations of an observational design and a supplemented cohort. Taken together, the results highlight the importance of longitudinal endocrine assessment during minipuberty, while underscoring the need for more research to clarify the role of vitamin D in this context.

Acknowledgments

The authors sincerely thank Dr. Ashok Chandrasekharan, Department of Neonatology, SRM Medical College Hospital and Research Center, SRMIST, for his support throughout the study.

Declarations

Funding

This study did not receive external funding.

Author contributions

Conceptualization, B.C.; Methodology, B.C. and V.V.M.; Investigation, V.V.M. and A.F.Z.; Formal Analysis, B.C. and A.H.; Data Curation, V.V.M.; Writing – Original Draft Preparation, V.V.M.; Writing – Review & Editing, B.C., A.M. and S.S.; Visualization, A.M.; Supervision, B.C.; Resources, S.S. and A.H.

Conflicts of interest

The authors declare no competing interests.

Data availability

The datasets generated and/or analysed during the current study are available from the corresponding author on reasonable request.

Ethics approval

The protocol was approved by the Institutional Ethics Committee of SRM Medical College Hospital and Research Institute (approval number: SRMIEC-ST0724-8011).

Use of AI and AI-assisted technologies in the writing process

During the preparation of this work, the authors used ChatGPT (OpenAI) to assist with language refinement and manuscript polishing. After using these tools, the authors reviewed and edited all content as needed and assume full responsibility for the content of the published article.

References

1. Kuiri-Hänninen T, Sankilampi U, Dunkel L. Activation of the hypothalamic-pituitary-gonadal axis in infancy: minipuberty. *Horm Res Paediatr*. 2014;82(2):73-80. doi:10.1159/000362414
2. Main KM, Schmidt IM, Skakkebaek NE. A possible role for reproductive hormones in newborn boys: progressive hypogonadism without the postnatal testosterone peak. *J Clin Endocrinol Metab*. 2000;85(12):4905-4907. doi:10.1210/jcem.85.12.7058
3. Grinspon RP, Rey RA. Mini-puberty and true puberty: differences in testicular function. *Ann Endocrinol (Paris)*. 2014;75(2):58-63. doi:10.1016/j.ando.2014.03.001
4. Kuiri-Hänninen T, Koskenniemi J, Dunkel L, et al. Postnatal testicular activity in healthy boys and boys with cryptorchidism. *Front Endocrinol (Lausanne)*. 2019;10:489. doi:10.3389/fendo.2019.00489
5. Blomberg Jensen M, Nielsen JE, Jørgensen A, et al. Vitamin D receptor and vitamin D metabolizing enzymes are expressed in the human male reproductive tract. *Hum Reprod*. 2010;25(5):1303-1311. doi:10.1093/humrep/deq024
6. Blomberg Jensen M. Vitamin D and male reproduction. *Nat Rev Endocrinol*. 2014;10(3):175-186. doi:10.1038/nrendo.2013.262
7. Kinuta K, Tanaka H, Moriwake T, et al. Vitamin D is an important factor in estrogen biosynthesis of both female

and male gonads. *Endocrinology*. 2000;141(4):1317-1324. doi:10.1210/endo.141.4.7403
8. Pilz S, Frisch S, Koertke H, et al. Effect of vitamin D supplementation on testosterone levels in men. *Horm Metab Res*. 2011;43(3):223-225. doi:10.1055/s-0030-1269854
9. Wehr E, Pilz S, Boehm BO, et al. Association of vitamin D status with serum androgen levels in men. *Clin Endocrinol (Oxf)*. 2010;73(2):243-248. doi:10.1111/j.1365--2265.2009.03777.x
10. Seth A, Marwaha RK, Singla B, et al. Vitamin D nutritional status of exclusively breast fed infants and their mothers. *J Pediatr Endocrinol Metab*. 2009;22(3):241-246.
11. Agarwal N, Faridi MM, Aggarwal A, Singh O. Vitamin D status of term exclusively breastfed infants and their mothers from India. *Acta Paediatr*. 2010;99(11):1671-1674. doi:10.1111/j.1651-2227.2010.01921.x
12. Harinarayan CV, Ramalakshmi T, Prasad UV, et al. High prevalence of low dietary calcium, high phytate consumption, and vitamin D deficiency in healthy south Indians. *Am J Clin Nutr*. 2007;85(4):1062-1067. doi:10.1093/ajcn/85.4.1062
13. Kılınç S, Atay E, Ceran Ö, Atay Z. Evaluation of vitamin D status and its correlation with gonadal function in children at minipuberty. *Clin Endocrinol (Oxf)*. 2019;90(1):122-128. doi:10.1111/cen.13864
14. Villar J, Cheikh Ismail L, Victora CG, et al. International standards for newborn weight, length, and head circumference by gestational age and sex: the Newborn Cross--Sectional Study of the INTERGROWTH-21st Project. *Lancet*. 2014;384(9946):857-868. doi:10.1016/S0140-6736(14)60932-6
15. World Health Organization. WHO Child Growth Standards: length/height-for-age, weight-for-age, weight-for--length, weight-for-height and body mass index-for-age: methods and development. Geneva, Switzerland: World Health Organization; 2006.
16. Khadilkar A, Khadilkar V, Chinnappa J, et al. Prevention and treatment of vitamin D and calcium deficiency in children and adolescents: Indian Academy of Pediatrics guidelines. *Indian Pediatr*. 2017;54(7):567-573. doi:10.1007/s13312-017-1090-y
17. Hofer D, Münzker J, Schwetz V, et al. Testicular synthesis and vitamin D action. *J Clin Endocrinol Metab*. 2014;99(10):3766-3773. doi:10.1210/jc.2014-1575
18. Sharpe RM, McKinnell C, Kivlin C, Fisher JS. Proliferation and functional maturation of Sertoli cells, and their relevance to disorders of testis function in adulthood. *Reproduction*. 2003;125(6):769-784. doi:10.1530/rep.0.1250769
19. Rey RA, Grinspon RP. Normal male sexual differentiation and aetiology of disorders of sex development. *Best Pract Res Clin Endocrinol Metab*. 2011;25(2):221-238. doi:10.1016/j.beem.2010.08.001
20. Sippell WG, Dörr HG, Bidlingmaier F, Knorr D. Plasma levels of aldosterone, corticosterone, 11-deoxycorticosterone, progesterone, 17-hydroxyprogesterone, cortisol, and cortisone during infancy and childhood. *Pediatr Res*. 1980;14(1):39-46. doi:10.1203/00006450-198001000-00009
21. Holick MF. Vitamin D deficiency. *N Engl J Med*. 2007;357(3):266-281. doi:10.1056/NEJMra070553
22. Ciardo F, Gambineri A, Fazzini A, et al. Vitamin D and adrenal gland: myth or reality? A systematic review. *Front Endocrinol (Lausanne)*. 2022;13:1001065. doi:10.3389/fendo.2022.1001065

Rzeszów University Press 2026
ISSN 2544-1361 (online)
doi: 10.15584/ejcem.2026.2.15

http://www.ejcem.ur.edu.pl
European Journal of Clinical and Experimental Medicine
Eur J Clin Exp Med 2026; 24 (2): 349–355

ORIGINAL PAPER

Molecular detection of isoniazid and rifampin-resistant *Mycobacterium tuberculosis* strains from southwest of Iran

Nazanin Ahmad Khosravi [1,2,3], Azar Dokht Khosravi [1,2,4], Mehrandokht Sirous [1,5], Mohammad Hashemzadeh [1,2], Homayoun Amiri [1], Shokrollah Salmanzadeh [2,6], Seyed Mohammad Alavi [1], Zohreh Deilami [3], Maryam Mohsenpoor [3], Meisam Movahedi [3]

[1] Infectious and Tropical Diseases Research Center, Health Research Institute, Ahvaz Jundishapur University of Medical Sciences, Ahvaz, Iran
[2] Department of Microbiology, Faculty of Medicine, Ahvaz Jundishapur University of Medical Sciences, Ahvaz, Iran
[3] Khuzestan Tuberculosis Regional Reference Laboratory, Ahvaz Jundishapur University of Medical Sciences, Ahvaz, Iran
[4] Iranian Study Group on Microbial Drug Resistance, Tehran, Iran
[5] Department of Microbiology and Parasitology, Faculty of Medicine, Bushehr University of Medical Sciences, Bushehr, Iran
[6] Tropical Medicine Ward, Razi Teaching Hospital, Ahvaz Jundishapur University of Medical Sciences, Ahvaz, Iran

ABSTRACT

Introduction and aim. The study of molecular mechanisms of resistance to first-line antibiotics for the treatment of tuberculosis is of great importance. Investigating these mechanisms provides valuable information to treatment policy makers. Therefore, this study aimed to identify mutations associated with resistance to rifampin (RIF) and isoniazid (INH) among drug-resistant *Mycobacterium tuberculosis* (MTB) isolates from a TB reference center in southwest Iran.

Material and methods. In this cross-sectional study (September 2014-February 2018), a total of 772 MTB isolates were confirmed by culture on Löwenstein-Jensen (LJ) medium and standard biochemical tests. Drug susceptibility testing of RIF and INH was determined by the proportion method on LJ medium. Mutations conferring resistance to INH and RIF were determined by polymerase chain reaction analysis and sequencing.

Results. In this study, 772 (22.68%) MTB strains were isolated from 3,404 TB-suspected patients, of whom 26.6% were women and 73.8% male. Of the 772 clinical strains, 8 (1.03%) were MDR (resistant to INH and RIF), 15 (1.94%) were resistant to RIF and 4 (0.5%) were resistant to INH. Of the 12 identified isolates identified (including both 4 isolates resistant to INH and 8 isolates resistant to MDR), 2 (16.6%) had a mutation at codon 315 of *katG*, 1 (8.33%) had a mutation at (-15) of *inhA*, and 9 (75%) did not show a detectable mutation. Regarding rifampin, the frequency of mutations in the *rpoB* gene was the following: codons 531 (n=7, 30.4%), 533 (n=5, 21.7%), 526 (n = 2, 8.69%) and 511 (n=1, 4.3%). Furthermore, no mutations were detected in 8 (34.7%) isolates.

Conclusion. The most prevalent mutation in INH resistant isolates was at codon 315 of *katG*. In RIF-resiatant isolates, the most prevalent mutation was at codon 531 of the *rpoB* gene. In a considerable number of isolates, no mutations in *katG*, *inhA*, and *rpoB* were found compared with deposited sequences available from NCBI GenBank.

Keywords. drug resistance, isoniazid, mutation, *Mycobacterium tuberculosis*, rifampin

Corresponding author: Nazanin Ahmadkhosravi, e-mail: nazaninahmadkhosravi@gmail.com;
Mehrandokht Sirous, e-mail: mehrandokht.sirous@gmail.com

Received: 17.04.2025 / Revised: 11.04.2026 / Accepted: 12.04.2026 / Published: 30.06.2026

Khosravi NA, Khosravi AD, Sirous M, Hashemzadeh M, Amiri H, Salmanzadeh S et.al. Molecular detection of isoniazid and rifampin-resistant *Mycobacterium tuberculosis* strains from southwest of Iran. *Eur J Clin Exp Med.* 2026;24(2):349–355. doi: 10.15584/ejcem.2026.2.15.

Introduction

Tuberculosis (TB), an infection with *Mycobacterium tuberculosis* (MTB), continues to be a major global health burden and is one of the deadliest diseases worldwide.[1,2] According to the WHO (World Health Organization), approximately one-third of the world's population is infected with MTB. In 2023, the estimated number of patients was 10.8 million, resulting in 1.25 million deaths.[3] The development of drug-resistant tuberculosis is a considerable health challenge in the treatment of TB worldwide.[4] There has been a rapid increase in multidrug-resistant (MDR) strains of tuberculosis, defined as resistance to the first-line antibiotics isoniazid (INH) and rifampin (RIF).[4] A recent estimate showed 400,000 incident cases of MDR in 2023, with only a fraction receiving timely treatment.[3]

MTB can acquire resistance to anti-TB drugs through spontaneous mutations in genes encoding antibiotic targets, drug-activating enzymes, or drug efflux pumps. These genes, which encode drug metabolizing or drug-targeting enzymes, significantly affect the efficacy of anti-TB therapy.[5] Most INH-resistant strains (INH-R) have mutations in genes involved in cell wall synthesis, such as the *inhA* gene and its promoter, the *katG* gene (particularly codon 315), or the *oxyR-ahpC* region. The *katG* deletion mutants show greater resistance to INH than strains with mutations in *inhA* or its promoter.[6] Mutations occur predominantly occur in an "hot spot" 81 bp fragment of the *rpoB* gene, called the RIF resistance determining region (RRDR), which confers resistance to RIF.7 The *rpoB* gene encodes the β-subunit of RNA polymerase, and mutations are located at codons 531, 526, and 516.8.

Due to the varying frequencies across different geographical areas, it is essential to evaluate the prevalence of mutations.[9] Studying the molecular mechanisms of resistance to first-line antibiotics for tuberculosis treatment is of great importance. Investigating these mechanisms provides valuable information to treatment policy makers. The study of mutations related to resistance to first-line tuberculosis drugs in the southwestern region of Iran has rarely been evaluated. However, the pattern of these mutations may change over time.

Aim

Given the importance of first-line drugs in TB treatment, it is a need to constantly assess the frequency of resistance to RIF and INH and their distribution within the community. Therefore, this study aimed to identify mutations in *inhA*, *katG*, and *rpoB* genes associated with resistance to INH and RIF among MTB isolates from a TB reference center for TB in southwest Iran. The regional distribution of the mutation, the proportion of phenotypically resistant isolates without detectable mutations at the target loci, or its relationship to local molecular detection may be among the new findings that can be obtained through this study.

Material and methods

Ethical clearance

The ethical consideration of this research was confirmed by the Ethics Committee of Ahvaz Jundishapur University of Medical Sciences, Ahvaz, Iran (No: IR.AJUMS.REC.1396.208). All research was conducted in accordance with relevant guidelines/regulations. Written informed consent was received from all participants and/or their legal guardians.

Study design and bacterial isolates

In this cross-sectional study (September 2014-February 2018), MTB isolates were obtained from 3,404 samples of patients referred to the Ahvaz Regional TB Laboratory in southwest Iran. The Ahvaz Regional Tuberculosis Laboratory in southwest Iran operates under the supervision of the World Health Organization and participates in regular quality assurance programs to further ensure consistency, reproducibility, and validity of culture and identification procedures. The sample size was determined using the G * Power software with the following parameters: power (1-β err prob)=0.95, α err prob = 0.05 and effect size = 0.12 Non-sterile respiratory specimens such as endotracheal aspirates, bronchoalveolar lavage (BAL), and sputum were sterilized using the NALC-NaOH method (standard N-acetyl-L-cysteine–sodium hydroxide) and then centrifuged at 3,000×*g* for 15 min. The resulting pellets were suspended again in sterile phosphate buffer (pH 6.8) and inoculated in LJ (Löwenstein-Jensen) medium. Body fluids or tissues were centrifuged at sterile sites and the pellets were inoculated directly into culture medium. Identification of MTB was confirmed using colony morphology, Ziehl-Neelsen acid fast staining and conventional biochemical tests, including catalase activity, nitrate reduction, and accumulation of niacin. The reference strain MTB H37Rv (ATCC 27294) was used as a quality control.[10] No isolates were excluded due to contamination or incomplete data from the study after confirmation. However, data on relapse, reinfection, or failure of treatment were unavailable for analysis.

Drug susceptibility testing (DST)

DST was done on LJ medium by the proportional method and according to WHO recommendations.[11] The critical concentrations of INH and RIF (Sigma Aldrich Co., St Louis, MO, USA) in the LJ medium were 0.2 μg/mL and 40 μg/mL, respectively.[11] Finally, a 1.0 McFarland suspension of bacterial colonies was prepared, and 10^{-2} and 10^{-4} dilutions were inoculated into LJ medium containing 0.2 μg/mL INH and 40 μg/mL RIF and LJ medium without antibiotics. The results were read af-

ter incubation for 28 days and 42 days at 36±1°C. Isolates were defined as drug-susceptible if the growth/colony count on antibiotic-containing LJ medium was ≤1% compared to the control medium without antibiotics. MTB H37Rv (ATCC 27294) was utilized as a quality control.

DNA extraction

Total DNA was extracted from drug-resistant isolates grown in LJ medium using the QIAamp Mini Kit (Qiagen, Hilden, Germany) according to the manufacturer's instructions. Briefly, approximately one loopful of colonies was suspended in 180 µL of ATL buffer and heat-killed at 95°C for 30 min to ensure biosafety. The samples were incubated with 20 µL of proteinase K at 56°C for 1 h, followed by the standard binding, washing and elution steps. DNA was eluted in 200 µL of AE buffer and stored at –20°C until use. DNA purity and concentration were assessed using a NanoDrop spectrophotometer (Thermo Fisher Scientific, USA).

Polymerase chain reaction (PCR) amplification

The genes *katG*, *rpoB* and *inhA* genes were amplified by PCR by specific primers (Table 1).[12,13,14] The PCR reaction mixtures were obtained in a final volume of 50 µL, including 1.5 mM $MgCl^2$, 5 µL of 10× PCR buffer, 0.2 µM of each primer, 0.2 mM of deoxynucleotide triphosphate (dNTP), 5 µL (10 ng) of genomic DNA, 2.5 U Taq DNA polymerase, and 35.4 µL of nuclease-free water. The amplifications were performed using a thermal cycler (Bio-Rad, Hercules, CA, USA) with the following cycling program: an initial 95°C denaturation step for 5 min, followed by 30 cycles of 95°C for 40 s, 64°C (*rpoB*, *inhA*) or 55°C (*katG*) for 1 min and 72°C for 40 s, and a final extension step of 72°C for 10 min.

Table 1. Primers used in this research

Drugs	Genes	Primer sequence (5′ to 3′)	Product size (bp)	Reference
Isoniazid	katG	5′-CATGAACGACGTCGAAACAG-3′ 5′-CGAGGAAACTGTTGTCCCAT-3	232	12
Rifampin	rpoB	5′-CGATCACACCGCAGACGTTG-3′ 5′-GGTACGGCGTTTCGATGAAC-3′	318	13
Isoniazid	inhA	5′-ACATACCTGCTGCGCAAT-3′ 5′-TCACATTCGACGCCAAAC-3′	400	14

DNA sequencing and analysis

The PCR products were sent to Bioneer Co., South Korea, for Sanger sequencing and purification using a 3730xl DNA analyzer (Thermo Fisher Scientific, USA). The sequences were trimmed and edited using Chromas software. To align the sequences obtained, ClustalW (https://www.genome.jp/tools-bin/clustalw) was utilized to specify the consensus sequences. The consensus sequences were subjected to nBLAST analysis (http://blast.ncbi.nlm.nih.gov) and compared with the H37Rv strain of MTB (ATCC 27294). For quality control, Bioneer Co., South Korea, considered the duplication rate, GC content distribution, nucleotide distribution, and base quality.

Statistical analysis

The collected data were analyzed using the Statistical Package for the Social Sciences (SPSS) software version 22 (IBM Corporation, Armonk, New York, USA). The methods used included descriptive statistical tests (frequencies and percentages).

Table 2. Mutation pattern of the promoter genes *rpoB*, *katG*, *mabA-inhA* in RIF and INH-resistant *Mycobacterium tuberculosis* with different drug resistance phenotypes *

Resistant isolate code	Resistant phenotype	Nucleotide change, rpoB	Amino acid change rpoB	Nucleotide change, katG	Amino acid change katG	Nucleotide change, mabA-inhA promoter
438	MDR	CAC→TAC	His526Tyr	_	_	_
701	MDR	CAC→CCC	His526Pro	AGC→ACC	Ser315Thr	_
577,646	MDR	CTG→CCG	Leu533 Pro	_	_	_
8,731	MDR	TCG→TTG	Ser531Leu	_	_	_
67	MDR	TCG→TTG	Ser531Leu	_	_	(-15) C→T
86	MDR	_	_	_	_	_
10	RIF	CTG→CCG	Leu511Pro	_	_	_
39,292,550,841	RIF	TCG→TTG	Ser531Leu	_	_	_
108,341,924	RIF	CTG→CCG	Leu533Pro	_	_	_
108,198,274,281, 286, 410,860	RIF	_	_	_	_	_
851	INH	_	_	AGC→AAC	Ser315Asn	_
32,475,588	INH	_	_	_	_	_

* MDR multidrug resistance, RIF – rifampin, INH isoniazid

Results

In this study, 772 (22.68%) MTB strains were isolated from 3,404 TB-suspected patients, of whom 26.6% were women and 73.8% male. Most of the samples were sputum (59.84%), followed by BAL (37.82%), endotracheal tube samples (1.03%), and other sample types (eg, abscess, wound, tissue). The results of drug resistance tests using the proportion method in 772 isolates for RIF and INH indicated that 8 (1.03%) isolates were MDR, 15 (1.94%) were RIF monoresistant, and 4 (0.5%) were INH monoresistant. These 27 isolates were selected for gene sequencing. Amplification of the genes *katG, rpoB* and *inhA* genes in resistant MTB isolates produced products of 232 bp, 318 bp, and 400 bp, respectively. Sequencing of the *inhA* and *katG* genes of the 4 INH-monoresistant

isolates revealed that 25% (1/4) harbored a mutation in the *katG* gene at codon 315. Among the RIF-monoresistant isolates, 26.6% (4/15), 20% (3/15), and 6.6% (1/15) carried mutations in the *rpoB* gene at codons 531, 533, and 511, respectively (Table 2).

In one MDR-TB isolate, a combination of *katG* and *rpoB* mutations was determined, while in another isolate, a combination of *inhA* and *rpoB* mutations was identified. In seven MDR-TB isolates, only mutations in the *rpoB* gene at codons 531, 533, and 526 were observed. The reader is referred to Table 3 to see the details of the nucleotide/amino acid substitutions in the targeted genes (*inhA, katG*, and *rpoB*) of MTB isolates.

Table 3. Characteristics of RIF and INH resistant *Mycobacterium tuberculosis* isolates with *rpoB, katG, mabA-inhA* promoter mutations*

Phenotype	Isolate code	Gender	*RpoB*	*KatG*	*mabA-inhA*
MDR	438	Male	CAC→TAC (His526Tyr)	Wild type	Wild type
MDR	701	Female	CAC→CCC (His526Pro)	AGC→ACC (Ser315Thr)	Wild type
MDR	8	Male	TCG→TTG (Ser531Leu)	Wild type	Wild type
MDR	731	Male	TCG→TTG (Ser531Leu)	Wild type	Wild type
MDR	67	Male	TCG→TTG (Ser531Leu)	Wild type	(-15) C→T
MDR	577	Female	CTG→CCG (Leu533Pro)	Wild type	Wild type
MDR	646	Male	CTG→CCG (Leu533Pro)	Wild type	Wild type
MDR	86	Male	Wild type	Wild type	Wild type
RIF resistant	10	Female	CTG→CCG (Leu511Pro)	Wild type	Wild type
RIF resistant	39	Male	TCG→TTG (Ser531Leu)	Wild type	Wild type
RIF resistant	292	Male	TCG→TTG (Ser531Leu)	Wild type	Wild type
RIF resistant	550	Male	TCG→TTG (Ser531Leu)	Wild type	Wild type
RIF resistant	841	Male	TCG→TTG (Ser531Leu)	Wild type	Wild type
RIF resistant	108	Male	CTG→CCG (Leu533 Pro)	Wild type	Wild type
RIF resistant	341	Female	CTG→CCG (Leu533 Pro)	Wild type	Wild type
RIF resistant	924	Male	CTG→CCG (Leu533 Pro)	Wild type	Wild type
RIF resistant	106	Male	Wild type	Wild type	Wild type
RIF resistant	198	Male	Wild type	Wild type	Wild type
RIF resistant	274	Male	Wild type	Wild type	Wild type
RIF resistant	281	Male	Wild type	Wild type	Wild type
RIF resistant	286	Female	Wild type	Wild type	Wild type
RIF resistant	410	Male	Wild type	Wild type	Wild type
RIF resistant	860	Female	Wild type	Wild type	Wild type
INH resistant	851	Male	Wild type	AGC→AAC (Ser315Asn)	Wild type
INH resistant	32	Female	Wild type	Wild type	Wild type
INH resistant	475	Male	Wild type	Wild type	Wild type
INH resistant	588	Male	Wild type	Wild type	Wild type

* MDR multidrug resistance, RIF – rifampin, INH isoniazid

Discussion

In addition to the increasing global rate of antibiotic resistance among Gram-positive and Gram-negative bacteria, the spread of drug-resistant MTB poses a major problem for healthcare systems worldwide.[15-18] TB, especially drug-resistant TB, affects both individuals and countries.[19] In this study, the results of phenotypic DST revealed 8 (1.03%) MDR, 15 (1.94%) RIF-monoresistant and 4 (0.51%) INH-monoresistant MTB isolates. This is according to a recent report from Iran.[20] The prevalence of INH-resistant, RIF-resistant (RIF-R), and MDR-TB strains in various provinces of Iran has been reported as 0–16.7%, 0–16.1%, and 0–20%, respectively.[20] A considerable number of patients were male (n=570, 73.8%), whereas only 202 (26.16%) were female. In the investigations by Charan et al.[21] and Vilegas et al.,[22] a high percentage of the patients were men (83.9% and 82.1%, respectively), consistent with our study. Although male patients constituted the majority of TB cases (73.8%), the number of MDR-TB cases was too small to determine any significant association between gender and resistance profile. In this research, amplification of *the katG, inhA, and rpoB* genes was performed using locus-specific primers. According to sequencing results, 16.6% (2/12) of INH-R isolates exhibited an amino acid variation in the *katG* gene, with 8.3% showing the S315T amino acid substitution. It is suggested that bacteria prefer the *katG*-S315T mutation because it reduces INH activation, while 30–40% of catalase-peroxidase activity required for virulence is preserved in these isolates.[23] These findings contrast sharply with other studies from different countries that demonstrated a higher percentage of the *katG*-S315T mutation, such as Southeast Asia (78.4%), Vietnam (85.3%), India (67.6%), Cameroon (64%), Romania (52.8%) and the United States (38%).[24-29] These differences may be explained by geographical variation, differences in study design, sample size, diagnostic methods, and circulating lineages.[30] In the current investigation, the mutation rate of the *inhA* gene was 8.3% (1/12), which is consistent with the study by Miotto et al.[31] However, it was higher than in previous research carried out by Hamed et al.[10] (3%), Solo et al.[23] (2%) and Diande et al.[32] (0%). Furthermore, the mutation rate of the *inhA* gene in this study was lower than that reported by Pinhata et al.[33] (33%), Ayalew et al.[34] (43%), Siddiqui et al.[35] (17%) and Zurita et al.[36] (20.2%). There were no combined mutations in *inhA* and *katG*, consistent with previous studies.[10,37] In total, 75% (9/12) of the INH-R strains did not show any variation in the *inhA* or *katG* genes. This may be explained by mutations in other genes, including those that control katG expression (*sigI* and *furA-katG* intergenic region), *ndh*, *oxyR, ahpC* and *kasA,* or by the efflux system.[34] In the present study, among 23 isolates of RIF-R, 30.4% of the *rpoB* gene mutations occurred at codon S531L, followed by 21.7% at codon L533P, 8.69% at codon H526T, and 4.3% at codon L511P. The presence of most mutations at codon 531 has also been reported in other studies, consistent with our results.[10,37] Two possible mechanisms can explain this higher frequency: first, there may be a higher genetic alteration at this codon; secondly, the occurrence of other substitutions in this region of the β-subunit of polymerase is less successful.[2] In the current research, a comparison was made between MDR and RIF monoresistant strains, which demonstrated a higher incidence of the S531L muta-

tion in the former strains (37.5 % to 26.6%), which is consistent with some studies.[38] Considering geographic regions, the prevalence of mutations in different codons of the *rpoB* gene varies in drug-resistant MTB isolates.[39] The observed differences may result from the administration of various drug analogues in different geographic regions, which provide a selective pressure for distinct genetic alterations.[39] In this study, no double mutations in genes related to RIF resistance, which was in contrast to previous studies.[2,32] Overall, there was no change in the sequenced region of 34.78% (8/23) of RIF-resistant isolates, most of which were related to RIF-monoresistant isolates (30.43%). It is necessary to conduct additional studies to identify genetic variation beyond the *rpoB* RDRR or in other associated genes, such as *rpoC* and *rpoA*, that may contribute to rifampin resistance in these isolates.[9] Our results revealed that although these tests target resistance-associated regions, a significant number of resistant isolates in our study lacked detectable mutations in the *inhA*, *katG*, and *rpoB* genes within these regions. This underscores the need to complement ongoing molecular diagnostics with expanded genomic panels in regions like southwest Iran. According to WHO guidelines, genetic diagnostic assays, including GeneXpert MTB/RIF and LIPA (Line Probe Assays), are recommended for the rapid detection of isoniazid and rifampin resistance.[40] GeneXpert MTB/RIF is also utilized to detect MTB and rifampicin resistance in Iran. DNA sequencing is highly accurate and can detect a wide range of mutations in antibiotic resistance genes across multiple pathogens.[41] Therefore, we used sequencing analysis for the *inhA, katG* and *rpoB* genes. The geographic variability of mutations underscores the importance of region-specific molecular surveillance to inform local TB control strategies and diagnostic practices. Furthermore, the lack of detected mutations in some INH-R isolates could be explained by mutations in genes such as *ahpC*, *ndh*, and *oxyR-ahpC*, which were not included in the current analysis. Future studies involving a broad range of genetic targets could better elucidate the complex mechanisms underlying isoniazid resistance.

Study limitations

This study had some limitations. These included a relatively small number of resistant isolates, the lack of evaluation of other resistance-associated genes (such as *ndh, oxyR-ahpC*, and *ahpC*), the lack of clonal relatedness analysis, and the lack of whole genome sequencing (WGS) for isolates without mutations in the genes studied. Furthermore, the lack of clinical data, such as a relapse or treatment failure, restricts the correlation of genetic mutations with phenotypic drug resistance. Another limitation was the lack of socio-demographic data.

Conclusion

The most prevalent mutation in INH resistant isolates was at codon 315 of *katG*. In RIF-resiatant isolates, the most prevalent mutation was at codon 531 of the *rpoB* gene. In a considerable number of isolates, mutations in *katG*, *inhA*, and *rpoB* were not found compared with deposited sequences available from NCBI GenBank. These results emphasize the significance of integrating regional mutation signatures into regional tuberculosis resistance monitoring initiatives and customizing molecular diagnostics to detect additional resistance markers apart from *katG*, *rpoB*, and *inhA* genes.

Acknowledgements

We would like to thank the Regional Tuberculosis Reference Laboratory of Khuzestan Province for providing the necessary equipment and administrative support.

Declarations

Funding

This work was supported by the Infectious and Tropical Diseases Research Center, Health Research Institute, Ahvaz Jundishapur University of Medical Sciences, Ahvaz, Iran, (Grant No. OG-96107).

Author contributions

Conceptualization, N.A.K. and M.S.; Methodology, N.A.K., M.S., and M.H.; Validation, A.D.K.; Formal Analysis, A.D.K. and H.A.; Investigation, S.S. and S.M.A.; Data Curation, N.A.K. and Z.D.; Writing – Original Draft Preparation, N.A.K. and A.D.K.; Writing – Review & Editing, M.S. and A.D.K.; Visualization, Ma.M.; Supervision, A.D.K. and Me.M.; Project Administration, A.D.K.

Conflicts of interest

We declare that there are no conflicts of interest on the part of any of the authors in this study.

Data availability

The datasets generated during and/or analyzed during the current study are available from the corresponding author on reasonable request.

Ethical approval

Ethical consideration for this research was confirmed by the Ahvaz Jundishapur University of Medical Sciences Ethics Committee, Ahvaz, Iran (No: IR.AJUMS.REC.1396.208).

References

1. Soliman NS. Prevalence of multidrug-resistant tuberculosis using phenotypic drug susceptibility testing and genexpert mtb/rif with characterization of non-tuberculous mycobacteria using MALDI-TOF. *Egypt J Med Microbiol*. 2021;30(3):143-151. doi:10.51429/EJMM3031

2. Gholizadeh P, Pourlak T, Asgharzadeh M, et al. Gene mutations related to rifampin resistance of tuberculosis in northwest of Iran. *Gene Rep*. 2020;19:100672. doi: 10.1016/j.genrep.2020.100672
3. Global Tuberculosis Report. World Health organization 2024. Geneva , Switzerland: World Health Organization; 2024. Accessed January 22, 2026. Available from: https://www.who.int/teams/global-tuberculosis-programme/tb-reports/global-tuberculosis-report-2024.
4. Motavaf B, Keshavarz N, Ghorbanian F, et al. Detection of genomic mutations in *katG* and *rpoB* genes among multidrug-resistant *Mycobacterium tuberculosis* isolates from Tehran, Iran. *New Microbes New Infect*. 2021;41:100879. doi:10.1016/j.nmni.2021.100879
5. Reta MA, Alemnew B, Abate BB, Fourie PB. Prevalence of drug resistance-conferring mutations associated with isoniazid and rifampicin-resistant *Mycobacterium tuberculosis* in Ethiopia: A systematic review and meta-analysis. *J Glob Antimicrob Resist*. 2021;26:207-218. doi:10.1016/j.jgar.2021.06.009
6. Hsu LY, Lai LY, Hsieh PF, et al. Two novel *katG* mutations conferring isoniazid resistance in *Mycobacterium tuberculosis*. *Front Microbiol*. 2020;11:1644. doi:10.3389/fmicb.2020.01644
7. Khan AS, Phelan JE, Khan MT, et al. Characterization of rifampicin-resistant *Mycobacterium tuberculosis* in Khyber Pakhtunkhwa, Pakistan. *Sci Rep*. 2021;11(1):1-10. doi:10.1038/s41598-021-93501-4
8. Thwe EP, Namwat W, Pinlaor P, Rueangsak K, Sangka A. Novel mutations detected from drug resistant *Mycobacterium tuberculosis* isolated from north east of Thailand. *World J Microbiol Biotechnol*. 2021;37:1-9. doi:10.21203/rs.3.rs-648869/v1
9. Zenteno-Cuevas R, Cuevas-Córdoba B, Parissi-Crivelli A. *rpoB*, *katG* and *inhA* mutations in multi-drug resistant strains of *Mycobacterium tuberculosis* clinical isolates from Southeast Mexico. *Enferm Infecc Microbiol Clin*. 2019;37(5):307-313. doi:10.1016/j.eimc.2018.09.002
10. Hamed Z, Mohajeri P, Farahani A, et al. The frequency of point mutations associated with resistance to isoniazid and rifampin among clinical isolates of multidrug-resistant *Mycobacterium tuberculosis* in the west of Iran. *Gene Rep*. 2021;22:100981. doi:10.1016/j.genrep.2020.100981
11. World Health Organization**.** *Technical manual for drug susceptibility testing of medicines used in the treatment of tuberculosis.* Geneva, Switzerland: World Health Organization; 2018. (WHO/CDS/TB/2018.24)
12. Silva MSN, Senna SG, Ribeiro MO, et al. Mutations in *katG*, *inhA*, and *ahpC* genes of Brazilian isoniazid-resistant isolates of *Mycobacterium tuberculosis*. *J Clin Microbiol*. 2003;41(9):4471-4474. doi:10.1128/jcm.41.9.4471-4474.2003
13. Pozzi G, Meloni M, Iona E, et al. *rpoB* mutations in multidrug-resistant strains of *Mycobacterium tuberculosis* isolated in Italy. J Clin Microbiol. 1999;37(4):1197-1199. doi:10.1128/jcm.37.4.1197-1199.1999
14. Chen X, Kong f, Wang Q, Li C, Zhang J, Gilbert GL. Rapid detection of isoniazid, rifampin, and ofloxacin resistance in *Mycobacterium tuberculosis* clinical isolates using high-resolution melting analysis. *J Clin Microbiol*. 2011;49(10):3450-3457. doi:10.1128/jcm.01068-11
15. Yazdansetad S, Alkhudhairy MK, Najafpour R, et al. Preliminary survey of extended-spectrum β-lactamases (ESBLs) in nosocomial uropathogen *Klebsiella pneumoniae* in north-central Iran. *Heliyon*. 2019;5(9):e02349. doi: 10.1016/j.heliyon.2019.e02349
16. Afrough P, Pourmand M R, Sarajian AA, et al. Molecular investigation of *Staphylococcus aureus*, *coa* and *spa* genes in Ahvaz hospitals, staff nose compared with patients clinical samples. *Jundishapur J Microbiol*. 2013;6(4):5377. doi:10.5812/jjm.5377
17. Sheikh AF, Moosavian M, Abdi M, et al. Prevalence and antimicrobial resistance of *Shigella* species isolated from diarrheal patients in Ahvaz, southwest Iran. *Infect Drug Resist*. 2019;12:249-253. doi:10.2147/IDR.S187861
18. Bainomugisa A, Lavu E, Pandey S, et al. Evolution and spread of a highly drug resistant strain of *Mycobacterium tuberculosis* in Papua New Guinea. *BMC Infect Dis*. 2022;22(1):437. doi:10.1186/s12879-022-07414-2
19. Li D, Song Y, Zhang CL, Li X, Xia X, Zhang AM. Screening mutations in drug-resistant *Mycobacterium tuberculosis* strains in Yunnan, China. *J Infect Public Health*. 2017;10(5):630-636. https://doi.org/10.1016/j.jiph.2017.04.008
20. Khademi F, Sahebkar A. An updated systematic review and meta-analysis on *Mycobacterium tuberculosis* antibiotic resistance in Iran (2013-2020). *Iran J Basic Med Sci*. 2021;24(4):428. doi:10.22038/IJBMS.2021.48628.11161
21. Charan AS, Gupta N, Dixit R, et al. Pattern of *inhA* and *katG* mutations in isoniazid monoresistant *Mycobacterium tuberculosis* isolates. *Lung India*. 2020;37(3):227-231. doi:10.4103/lungindia.lungindia_204_19
22. Villegas L, Otero L, Sterling TR, et al. Prevalence, risk factors, and treatment outcomes of isoniazid-and rifampicin--mono-resistant pulmonary tuberculosis in Lima, Peru. *PloS One*. 2016;11(4):e0152933. doi:10.1371/journal.pone.0152933
23. Solo ES, Nakajima C, Kaile T, et al. Mutations in *rpoB* and *katG* genes and the *inhA* operon in multidrug-resistant *Mycobacterium tuberculosis* isolates from Zambia. *J Glob Antimicrob Resist*. 2020;22:302-307. doi:10.1016/j.jgar.2020.02.026
24. Seifert M, Catanzaro D, Catanzaro A, Rodwell TC. Genetic mutations associated with isoniazid resistance in *Mycobacterium tuberculosis*: a systematic review. *PloS One*. 2015;10(3):e0119628. doi:10.1371/journal.pone.0119628
25. Le Hang NT, Hijikata M, Maeda S, et al. Whole genome sequencing, analyses of drug resistance-conferring mutations, and correlation with transmission of *Mycobacterium*

tuberculosis carrying katG-S315T in Hanoi, Vietnam. *Sci Rep*. 2019;9(1):1-14. doi:10.1038/s41598-019-51812-7

26. Munir A, Kumar N, Ramalingam SB, et al. Identification and characterization of genetic determinants of isoniazid and rifampicin resistance in *Mycobacterium tuberculosis* in southern India. *Sci Rep*. 2019;9(1):1-13. doi:10.1038/s41598-019-46756-x
27. Ruesen C, Riza AL, Florescu A, et al. Linking minimum inhibitory concentrations to whole genome sequence--predicted drug resistance in *Mycobacterium tuberculosis* strains from Romania. *Sci Rep*. 2018;8(1):1-8. doi:10.1038/s41598-018-27962-5
28. Abanda NN, Djieugoué JY, Lim E, et al. Diagnostic accuracy and usefulness of the Genotype MTBDRplus assay in diagnosing multidrug-resistant tuberculosis in Cameroon: A cross-sectional study. *BMC Infect Dis*. 2017;17(1):1-10. doi:10.1186/s12879-017-2489-3
29. Dantes R, Metcalfe J, Kim E, et al. Impact of isoniazid resistance-conferring mutations on the clinical presentation of isoniazid monoresistant tuberculosis. *PloS One*. 2012;7(5):e37956. doi:10.1371/journal.pone.0037956
30. Anwaierjiang A, Wang Q, Liu H, et al. Prevalence and molecular characteristics based on whole genome sequencing of *Mycobacterium tuberculosis* resistant to four anti-tuberculosis drugs from Southern Xinjiang, China. *Infect Drug Resist*. 2021;14:3379. doi:10.2147/IDR.S320024
31. Miotto P, Saleri N, Dembelé M, et al. Molecular detection of rifampin and isoniazid resistance to guide chronic TB patient management in Burkina Faso. *BMC Infect Dis*. 2009;9(1):1-8. doi:10.1186/1471-2334-9-142
32. Diandé S, Ogbomon E, Gueye A. Occurrence of mutations associated with rifampicin and isoniazid resistant in *Mycobacterium tuberculosis* isolates from patients in Burkina Faso. *Int J Mol Biol*. 2019;4(3):106-111. doi:10.15406/ijmboa.2019.04.00105
33. Pinhata JMW, Brandao AP, de Freitas Mendes F, da Silva Rabello MC, Ferrazoli L, de Oliveira RS. Correlating genetic mutations with isoniazid phenotypic levels of resistance in *Mycobacterium tuberculosis* isolates from patients with drug-resistant tuberculosis in a high burden setting. *Eur J Clin Microbiol Infect Dis*. 2021;40:2551-2561. doi:10.1007/s10096-021-04316-0
34. Ayalew S, Wegayehu T, Taye H, et al. Drug resistance conferring mutation and genetic diversity of *Mycobacterium tuberculosis* isolates in tuberculosis lymphadenitis patients; Ethiopia. *Infect Drug Resist*. 2021;14:575. doi:10.2147/IDR.S298683
35. Siddiqui S, Brooks MB, Malik AA, et al. Evaluation of GenoType MTBDR plus for the detection of drug-resistant *Mycobacterium tuberculosis* on isolates from Karachi, Pakistan. *PloS One*. 2019;14(8):e0221485. doi:10.1371/journal.pone.0221485.t001
36. Zurita J, Espinel N, Barba P, et al. Genetic diversity and drug resistance of *Mycobacterium tuberculosis* in Ecuador. *Int J Tuberc Lung Dis*. 2019;23(2):166-173. doi:10.5588/ijtld.18.0095
37. Prasad PG, Jasmine MS, Deepthi K, Allam US. Analysis of drug resistance mutations in pulmonary *Mycobacterium tuberculosis* isolates in the Southern coastal region of Andhra Pradesh, India. *Braz J Infect Dis*. 2019;23(2):281-290. doi:10.1016/j.bjid.2019.07.002
38. Singhal R, Myneedu V, Arora J, et al. Early detection of multi-drug resistance and common mutations in *Mycobacterium tuberculosis* isolates from Delhi using GenoType MTBDRplus assay. *Indian J Med Microbiol*. 2015;33:S46--S52. doi:10.4103/0255-0857.150879
39. Haratiasl AA, Hamzelou G, Amini S, et al. Molecular identification of mutations conferring resistance to rifampin, isoniazid and pyrazinamide among *Mycobacterium tuberculosis* isolates from Iran. *J Chemother*. 2020;32(2):75-82. doi:10.1080/1120009X.2020.1716479
40. Farra A, Koula K, Jolly BL, et al. Effectiveness of Xpert MTB/RIF and the Line Probe Assay tests for the rapid detection of drug-resistant tuberculosis in the Central African Republic. *PLOS Glob Public Health*. 2023;3(5):e0001847. doi:10.1371/journal.pgph.0001847
41. Wang H, Ye C, Jiang H, Song R. Application of next-generation sequencing in the detection of antimicrobial resistance. *Clin Chim Acta*. 2025;578:120520. doi:10.1016/j.cca.2025.120520

Rzeszów University Press 2026
ISSN 2544-1361 (online)
doi: 10.15584/ejcem.2026.2.16

http://www.ejcem.ur.edu.pl
European Journal of Clinical and Experimental Medicine
Eur J Clin Exp Med 2026; 24 (2): 356–369

ORIGINAL PAPER

Diagnostic performance of serum oncostatin M and MMP-9 in differentiating disease activity in Crohn's disease and ulcerative colitis

Zahraa Nasser Ali [1], Hiba Resheed Behayaa [1],
Ahmed Abdul-Hussein Gburi Alhilly [2]

[1] Department of Chemistry and Biochemistry, College of Medicine, University of Babylon, Iraq
[2] Department of Internal Medicine (Gastroenterology and Hepatology), College of Medicine, University of Babylon, Iraq

ABSTRACT

Introduction and aim. Inflammatory bowel disease (IBD) requires reliable noninvasive biomarkers for diagnosis and disease activity monitoring. Oncostatin M (OSM) and matrix metalloproteinase-9 (MMP-9) are implicated in intestinal inflammation and tissue remodeling, yet their combined diagnostic utility in IBD remains underexplored. The aim was to evaluate serum OSM and MMP-9 levels in Crohn's disease (CD) and ulcerative colitis (UC) patients compared to healthy controls, and to assess their correlation with disease activity and diagnostic performance.

Material and methods. This cross-sectional study included 105 participants (35 CD, 35 UC, 35 controls). Serum OSM and MMP-9 were measured by ELISA. Disease activity was evaluated using CDAI and the Total Mayo Score. ROC curve analysis evaluated diagnostic accuracy.

Results. Both OSM and MMP-9 were significantly elevated in CD and UC compared to controls ($p=0.016$ and $p=0.006$, respectively), with progressive increases paralleling disease severity ($p<0.001$). For differentiating active from inactive CD, OSM demonstrated a high AUC of 0.951 (95% CI: 0.882–1.000) with 100% specificity (95% CI: 71.5%–100.0%). For active UC, MMP-9 achieved an AUC of 0.85 (95% CI: 0.724–0.976) with 95.4% sensitivity (95% CI: 78.9%–99.9%).

Conclusion. OSM and MMP-9 exhibit complementary diagnostic profiles, with OSM excelling in CD activity assessment and MMP-9 in UC, supporting their combined clinical utility.

Keywords. biomarker, Crohn's disease, inflammatory bowel disease, matrix metalloproteinase-9, oncostatin M, ulcerative colitis

Introduction

Inflammatory bowel disease (IBD), a term primarily encompassing Crohn's disease (CD) and ulcerative colitis (UC), represents a group of chronic, relapsing inflammatory disorders of the gastrointestinal tract. Once considered a disease of Western nations, the 21st century has witnessed a dramatic shift in the global epidemiology of IBD, with incidence and prevalence rates now rising in newly industrialized countries across Asia, Africa, and the Middle East.[1,2] In the Middle East and North Africa (MENA) region, the age-standardized prevalence rate of IBD was estimated at 48.3 per 100,000 population in 2019, with a significant increase in incidence observed over the preceding three decades.[3] This growing global burden underscores the urgent need for a deeper understanding of IBD pathogenesis and the identification of reliable biomarkers to improve diagnosis, disease activity monitoring, and therapeutic management.

Corresponding author: Zahraa Nasser Ali, e-mail: Med332.zahraa.nasir@student.uobabylon.edu.iq

Received: 21.02.2026 / Revised: 9.04.2026 / Accepted: 13.04.2026 / Published: 30.06.2026

Ali ZN, Behayaa HR, Alhilly AA-HG. Diagnostic performance of serum oncostatin M and MMP-9 in differentiating disease activity in Crohn's disease and ulcerative colitis. *Eur J Clin Exp Med.* 2026;24(2):356–369. doi: 10.15584/ejcem.2026.2.16.

The pathogenesis of IBD is multifactorial, involving a complex interplay between genetic susceptibility, environmental factors, and a dysregulated immune response to the gut microbiota, all of which culminate in chronic intestinal inflammation and compromised mucosal barrier function.[4,5] The clinical management of IBD relies heavily on the accurate assessment of disease activity, which traditionally involves a combination of clinical scoring systems and invasive endoscopic procedures. While endoscopy remains the gold standard for evaluating mucosal inflammation, its invasive nature, cost, and associated risks limit its utility for frequent monitoring.[6] Consequently, there is a pressing need for non-invasive, accessible, and reliable serum biomarkers that can accurately reflect underlying intestinal inflammation, differentiate between active and inactive disease, and potentially distinguish between CD and UC.

Currently used biomarkers such as C-reactive protein (CRP) and fecal calprotectin have significant limitations. CRP, an acute-phase reactant, lacks specificity and may not be elevated in a substantial proportion of IBD patients, particularly those with mild or limited disease.[7] Fecal calprotectin, while demonstrating good correlation with endoscopic activity, can be affected by other gastrointestinal conditions and may not be practical for all patients.[8] This diagnostic gap has fueled the search for novel biomarkers that are more closely linked to the core pathophysiological mechanisms of IBD.

Oncostatin M (OSM), a pleiotropic cytokine belonging to the interleukin-6 (IL-6) family, has emerged as a key player in IBD pathogenesis.[9] Produced predominantly by activated myeloid cells such as macrophages and dendritic cells, OSM exerts its effects by signaling through receptor complexes involving the gp130 subunit and either the OSM receptor β (OSMRβ) or the leukemia inhibitory factor receptor β (LIFRβ).[10] Seminal work by West et al. (2017) demonstrated that OSM and its receptor are highly upregulated in the inflamed intestinal mucosa of IBD patients, where they drive a pro-inflammatory phenotype in intestinal stromal cells, leading to the production of other inflammatory mediators and adhesion molecules.[11] Subsequent studies have solidified the role of OSM as a potent biomarker of disease activity and, notably, as a predictor of non-response to anti-tumor necrosis factor (TNF) therapies, highlighting its clinical relevance.[12,13]

Concurrently, matrix metalloproteinase-9 (MMP-9), a zinc-dependent endopeptidase, has been identified as a critical mediator of the tissue remodeling and destruction that characterize IBD.[14] MMP-9, also known as gelatinase B, degrades various components of the extracellular matrix (ECM), including type IV collagen, a key structural component of the basement membrane.[15] This enzymatic activity contributes directly to the breakdown of the intestinal epithelial barrier. Mechanistically, MMP-9 has been shown to increase intestinal permeability by disrupting tight junction proteins, a process mediated through the activation of the NF-κB pathway and myosin light chain kinase (MLCK).[16,17] The resulting barrier dysfunction facilitates the translocation of luminal antigens into the mucosa, thereby perpetuating the inflammatory cycle. Consequently, MMP-9 levels are consistently found to be elevated in the serum and inflamed tissues of IBD patients, correlating with disease severity and tissue damage.[18]

While the biological link between OSM-induced MMP-9 expression is established[19], a critical knowledge gap persists in its clinical application. Previous studies have typically investigated these markers in isolation, providing an incomplete picture of their coordinated role. The novelty of the present study is threefold and directly addresses these gaps: First, to our knowledge, no prior study has simultaneously measured and directly compared the diagnostic accuracy of both serum OSM and MMP-9 within the same IBD cohort, enabling a head-to-head evaluation of which biomarker offers superior performance for specific disease states (CD vs. UC) and activity levels. Second, while previous studies have examined these markers individually, none have constructed a combined diagnostic model using logistic regression-derived predicted probabilities and formally tested incremental value via the DeLong method, which our study provides. Third, biomarker performance can be influenced by host genetics and unique environmental exposures. The dramatic rise in IBD incidence in the Middle East makes region-specific data essential[3]; this study provides the first population-specific data from Iraq, where IBD incidence is rising rapidly and where access to endoscopy is limited, making non-invasive biomarkers particularly relevant. By assessing both a primary inflammatory cytokine (OSM) and a key enzyme involved in tissue remodeling (MMP-9), our study provides a more holistic view of the pathophysiological processes driving disease activity

Aim

This study was designed to provide a comprehensive, comparative evaluation of serum OSM and MMP-9 in a well-characterized cohort of Iraqi patients with CD and UC, with the aim of generating novel, population-specific evidence to enhance non-invasive disease monitoring.

Material and methods

Study design and participants

This cross-sectional study was conducted at the Babylon GIT Center, Merjan City Complex, and the Karbala Center for Gastrointestinal and Liver Diseases and Surgery in Iraq, Patient recruitment and sample collection were carried out from June 2025 to November 2025, while statistical analysis and manuscript prepa-

ration were performed from December 2025 to February 2026. A total of 105 participants aged from 18–65 years were enrolled and stratified into three groups: 35 patients with a confirmed diagnosis of CD, 35 patients with a confirmed diagnosis of UC, and 35 apparently healthy individuals serving as a control group. IBD patients were enrolled prospectively from outpatient gastroenterology clinics and endoscopy units at both study centers. A purposive (quota) sampling strategy was employed to ensure balanced representation across disease activity strata (Remission/Mild/mild, moderate, and severe), as consecutive enrollment would have disproportionately favored patients in remission/mild, limiting statistical power for subgroup comparisons. Healthy controls were recruited from hospital staff, patient companions, and community volunteers who met the inclusion criteria and underwent clinical screening to exclude inflammatory or autoimmune conditions. The diagnosis of IBD was established by consultant gastroenterologists based on a combination of clinical, endoscopic, radiological, and histopathological criteria.

Inclusion criteria for the IBD patient groups was an age between 18 and 65 years and a confirmed diagnosis of either CD or UC. Inclusion criteria for the control group were age- and sex-matched individuals with no history of IBD, other chronic inflammatory diseases, autoimmune disorders, or malignancy. Exclusion criteria for all participants included pregnancy, acute infection, recent surgery (within the last three months), and the use of immunosuppressive medications other than those prescribed for IBD management.

Ethical considerations

The study was conducted in full accordance with the principles of the Declaration of Helsinki. Ethical approval was obtained from the Scientific Research Ethics Committee at the College of Medicine, University of Babylon, Iraq (Reference No. 5-64, dated 18/09/2025). All participants were fully informed about the study objectives and procedures, and written informed consent was obtained from each individual prior to their enrollment in the study.

Clinical assessment and disease activity

Demographic data, including age, sex, and residence, were collected from all participants. For IBD patients, clinical data including disease duration and current medications were recorded. Disease activity was assessed at the time of sample collection using standard clinical indices. For Crohn's disease, the Crohn's Disease Activity Index (CDAI) was calculated,[20,21] for ulcerative colitis, the Total Mayo Score (Schroeder et al.[22]; Rubin et al.[23]; range 0–12) was used. For the purposes of this study, patients were classified into three pragmatic severity tiers: remission/mild/mild (CDAI <220 for CD; Total Mayo Score 0–5 for UC), moderate (CDAI 220–450; Mayo 6-10), and severe (CDAI >450; Mayo 11–12). This three-tier classification was adopted because no CD patients fell within the mild CDAI range (150–219), and UC patients with Mayo scores of 2–5 overlap between conventional remission/mild and mild categories. The rationale for this pragmatic grouping and its implications are discussed in the Discussion section.

Sample collection and processing

Following an overnight fast of 8–10 hours, a 5 mL venous blood sample was collected from each participant into a plain tube. The blood samples were allowed to clot at room temperature for 30 minutes and then centrifuged at 3000 rpm for 10 minutes. The resulting serum was carefully aspirated, aliquoted into sterile Eppendorf tubes, and stored at -20°C. All samples were analyzed within six months of collection. This storage condition and duration are in accordance with the ELISA kit manufacturer's guidelines, which confirm biomarker stability for up to one year at -20°C, and are further supported by literature demonstrating the stability of cytokines like OSM and MMP-9 in appropriately handled serum samples.[24,25] Aliquoting and a single freeze-thaw cycle were used to prevent degradation of the target biomarkers.

Biochemical analysis

Routine inflammatory markers

Serum C-reactive protein (CRP) levels were quantitatively determined using a latex-enhanced immunoturbidimetric assay on the Abbott ARCHITECT c4000 clinical chemistry analyzer (Abbott Diagnostics, Abbott Park, IL, USA). Complete blood count (CBC), including total white blood cell (WBC) count, was performed using a Sysmex automated hematology analyzer (Sysmex Corporation, Kobe, Japan). The erythrocyte sedimentation rate (ESR) was measured using the standard Westergren method.

Serum OSM and MMP-9 measurement

Serum levels of OSM and MMP-9 were quantified using commercially available sandwich enzyme-linked immunosorbent assay (ELISA) kits according to the manufacturer's instructions.

- OSM: the Human Oncostatin-M ELISA Kit (Cat. No. E1663Hu, BT LAB, Jiaxing, China) was used. This assay has a detection range of 10–4000 ng/L, a sensitivity of 5.93 ng/L, and intra- and inter-assay coefficients of variation (CV) of <8% and <10%, respectively.
- MMP-9: the Human Matrix Metalloproteinase 9 (MMP-9) ELISA Kit (Cat. No. E0936Hu, BT LAB, Jiaxing, China) was used. This assay has a detection range of 30–9000 ng/L, a sensitivity of 15.12 ng/L, and intra- and inter-assay CVs of <8% and <10%, respectively.

Statistical analysis

Statistical analysis for this study was performed using SPSS Software, version 26, and MedCalc Software, version 23.1 (IBM, Armonk, NY, USA). Normality tests for continuous data were tested by using the Kolmogorov-Smirnov test. Comparisons between groups were conducted using an independent t-test for two continuous variables, Kruskal-Wallis test for non-normal distributed variables, One way ANOVA test for normal distributed variables, and chi square for categorical data. Pearson correlation analysis was used to assess the association between variables. Additionally, Receiver operating characteristic (ROC) curve analysis was performed to evaluate the diagnostic performance of the biomarkers, and the area under the curve (AUC) was calculated. Optimal cut-off values were determined using the Youden index (J=-sensitivity+specificity–1). A combined biomarker model was also constructed using logistic regression incorporating both OSM and MMP-9 to generate predicted probabilities, which were then subjected to ROC analysis. The AUC of the combined model was compared to the AUC of each individual marker using the DeLong method. Two multivariable logistic regression models were constructed. The first (Table 9) included only OSM and MMP-9 to evaluate their mutual adjustment. The second, expanded model (Table 9b) incorporated OSM, MMP-9, CRP, ESR, WBC, BMI, sex, and age to assess whether the biomarkers retained independent predictive value after adjustment for established inflammatory and demographic variables. Variables were selected a priori based on their established clinical relevance in IBD assessment. Multicollinearity was assessed using the variance inflation factor (VIF), with values <5 considered acceptable. A p-value of<0.05 was considered statistically significant for all tests.

Results

Table 1 presents the baseline demographic and clinical characteristics of the study population (n=105), divided equally into CD, UC, and healthy control groups. No statistically significant differences were observed among the three groups regarding age (p=0.073), sex distribution (p=0.240), BMI (p=0.156), or residence (p=0.36).

Among the IBD groups, disease duration was comparable between CD and UC patients (p=0.79), and disease severity distribution did not differ significantly (p=0.90).

Table 2 compares inflammatory markers among the three study groups. CRP levels (median, IQR) were significantly different across groups (Kruskal–Wallis, p=0.0001), with the highest levels observed in the CD group, followed by the UC group, while controls showed minimal values.

ESR also differed significantly among groups (one-way ANOVA, p=0.001), with both CD and UC patients demonstrating markedly higher mean values compared to controls.

Table 1. Demographic and clinical characteristics of study groups*

Characteristic		CD (n=35)	UC (n=35)	Control (n=35)	p
Age (years)	Mean±SD	26.4±9.23	32.2±12.31	31.2±11.53	0.073^{O}
	Range	18.0–59.0	18.0–65.0	18.0–56.0	
Sex	Male, n (%)	23 (65.7 %)	16 (45.7 %)	19 (54.23 %)	0.240^{C}
	Female, n (%)	12 (34.3 %)	19 (54.3 %)	16 (45.7 %)	
BMI (kg/m^2)	Mean±SD	24.0±4.40	24.7±5.38	26.6±3.16	0.156^{O}
Duration of disease (years)	Mean±SD	1.9±1.3	2.1±1.3		0.79^{I}
	Range	0.3–5.0	0.3–6.0	–	
Severity of disease		CDAI score	Total Mayo score	–	0.90^{C}
	Remission/Mild, n (%) Median (Range)	11 (31.4 %) 98 (42–145)	11 (31.4 %) 1 (0–2)	–	
	Moderate, n (%) Median (Range)	13 (37.2 %) 305 (225–420)	13 (37.2 %) 8 (6–10)	–	
	Severe, n (%) Median (Range)	11 (31.4 %) 510 (455–585)	11 (31.4 %) 12 (11–12)	–	
Residence	Rural, n (%)	11 (31.4 %)	12 (34.3 %)	17 (48.5 %)	0.36^{C}
	Urban, n (%)	24 (68.6 %)	23 (65.7 %)	18 (51.5 %)	
Current medications, n (%)	5-ASA/Mesalazine	20 (57.1%)	30 (85.7%)	-	0.017^{C}
	Corticosteroids	17 (48.6%)	14 (40.0%)	-	0.623^{C}
	Immunomodulators (AZA/6-MP)	10 (28.6%)	8 (22.9%)	-	0.784^{C}
	Biologics (anti-TNF)	6 (17.1%)	2 (5.7%)	-	0.257^{C}

* ^{O} – one way ANOVA test, ^{C} – Chi square test, ^{I} – Independent t test, n=sample number

Similarly, WBC count showed a statistically significant difference (p=0.013), with elevated levels in both IBD groups relative to healthy controls.

Table 2. Comparison of inflammatory markers of study groups*

Characteristic	CD (n=35)	UC (n=35)	Control (n=35)	p
CRP (mg/L) (Median±IQR)	13.2 (4.5–30.1)	7.5 (4.9–9.7)	0.7 (0.2–1.45)	0.0001^{K}
ESR (mm/h) (Mean±SD)	31.5±19.1	25.9±13.5	5.8±2.2	0.001^{O}
WBC (x10^3/uL) (Mean±SD)	8.3±3.1	9.11±4.5	6.7±1.4	0.013^{O}

* ^{K} – Kruskal-Wallis test for non-normal distribution, ^{O} – one way ANOVA test for normal distribution

Table 3 presents the comparison of serum OSM and MMP-9 levels among the three groups. Serum OSM levels differed significantly (p=0.016), with the highest mean values observed in the CD group, followed by the UC group, and the lowest levels in controls.

Similarly, serum MMP-9 levels showed a significant difference across groups (p=0.006), demonstrating a progressive increase from controls to UC and CD pa-

tients, with the CD group exhibiting the highest mean concentration.

Table 3. Comparison of OSM and MMP-9 of study groups*

Characteristic	CD (n=35)	UC (n=35)	Control (n=35)	p
OSM (ng/L) (Mean±SD)	446.3±142.8	418.0±76.4	364.6±88.5	0.016
MMP-9 (ng/L) (Mean±SD)	1018±347	987±279	781±146	0.006

* Data are presented as mean±SD, n=sample number

Table 4 shows serum OSM and MMP-9 levels according to disease severity within each IBD subtype.

In Crohn's disease, OSM levels increased significantly across Remission/Mild, moderate, and severe stages (p<0.001), with all pairwise comparisons remaining significant, indicating a clear severity-dependent trend. MMP-9 levels also differed significantly (p=0.001); however, post hoc analysis showed that while Remission/Mild differed from both moderate and severe stages, the latter two did not differ significantly, suggesting a plateau effect at moderate disease activity.

In ulcerative colitis, both OSM and MMP-9 demonstrated a significant stepwise increase with advancing severity (p<0.001 for both), with all pairwise comparisons remaining significant.

Table 4. Comparison of parameters based on severity of Crohn's disease and ulcerative colitis diseases*

Disease	Variable	Stage	n	Mean±SD	p
CD	OSM (ng/L)	Remission/mild	11	303.2±68.5^{A}	<0.001
		Moderate	13	435.2±73.9^{B}	
		Severe	11	575.3±142.1^{C}	
	MMP-9 (ng/L)	Remission/mild	11	806±243^{A}	0.001
		Moderate	13	1099±235^{B}	
		Severe	11	1176±236^{B}	
UC	OSM (ng/L)	Remission/mild	11	355.4±56.7^{A}	<0.001
		Moderate	13	428.0±51.7^{B}	
		Severe	11	501.0±44.9^{C}	
	MMP-9 (ng/L)	Remission/mild	11	788.6±127.7^{A}	<0.001
		Moderate	13	1037±92.93^{B}	
		Severe	11	1343±292.3^{C}	

* one way ANOVA test, capital letters $^{A, B}$ and ^{C} were used to indicate the level of significance following Tukey's multiple comparisons test so that similar letters indicate no significant difference, whereas the different letters indicate significant difference

Table 5 compares serum OSM and MMP-9 levels according to sex within each IBD subtype. In Crohn's disease, OSM levels were higher in males than females, but the difference was not statistically significant (p=0.377). In contrast, MMP-9 levels were significantly elevated in males compared to females (p=0.048). In ulcerative colitis, no significant sex-based differences were observed for either OSM (p=0.491) or MMP-9 (p=0.191).

Table 5. Comparison of OSM and MMP-9 according to sex subgroups in Crohn's disease and ulcerative colitis*

Variable	CD			UC		
	Male (n=23)	Female (n=12)	p	Male (n=16)	Female (n=19)	p
OSM (ng/L) (Mean±SD)	462.3±142	412.9±134	0.377	407.7±54	427.7±93	0.491
MMP-9 (ng/L) (Mean±SD)	1072±233	815±304	0.048	975±181	1119±391	0.191

* data are presented as mean±SD, p comparing male vs female within each disease group, n=sample number

Table 6 presents Pearson correlation analyses between disease activity indices and the studied biomarkers. In Crohn's disease, CDAI showed a strong positive correlation with OSM (r=0.761, p<0.001) and a moderate positive correlation with MMP-9 (r=0.462, p=0.005). A significant positive correlation was also observed between OSM and MMP-9 (r=0.584, p<0.001).

In ulcerative colitis, the Total Mayo Score correlated strongly with OSM (r=0.670, p<0.001) and moderately-to-strongly with MMP-9 (r=0.613, p<0.001). The strongest correlation observed was between OSM and MMP-9 in UC (r=0.766, p<0.001).

Table 6. Correlation analysis between disease activity indices and biochemical parameters in Crohn's disease and ulcerative colitis*

Crohn's disease (CDAI)				
Variable		**CDAI**	**OSM (ng/L)**	**MMP-9 (ng/L)**
CDAI	r		0.761	0.462
	p		0.000	0.005
OSM (ng/L)	r	0.761**		0.584
	p	0.000		0.000
MMP-9(ng/L)	r	0.462	0.584	
	p	0.005	0.000	
Ulcerative colitis (Total Mayo score)				
Variable		**Total Mayo score**	**OSM (ng/L)**	**MMP-9(ng/L)**
Total Mayo score	r		0.670	0.613
	p		0.000	0.000
OSM (ng/L)	r	0.670		0.766
	p	0.000		0.000
MMP-9 (ng/L)	r	0.613	0.766	
	p	0.000	0.000	

* r – Pearson correlation coefficient, ** – correlation is significant at the 0.01 level (2-tailed), p-values are two-tailed

Figure 1 illustrates the correlation analyses through scatter plots with fitted regression lines. The plots demonstrate strong positive associations between OSM and disease activity indices in both CD and UC, and comparatively weaker – though still significant – associations for MMP-9.

Table 7 presents the ROC curve analysis evaluating the diagnostic performance of OSM and MMP-9 in distinguishing IBD patients from healthy controls.

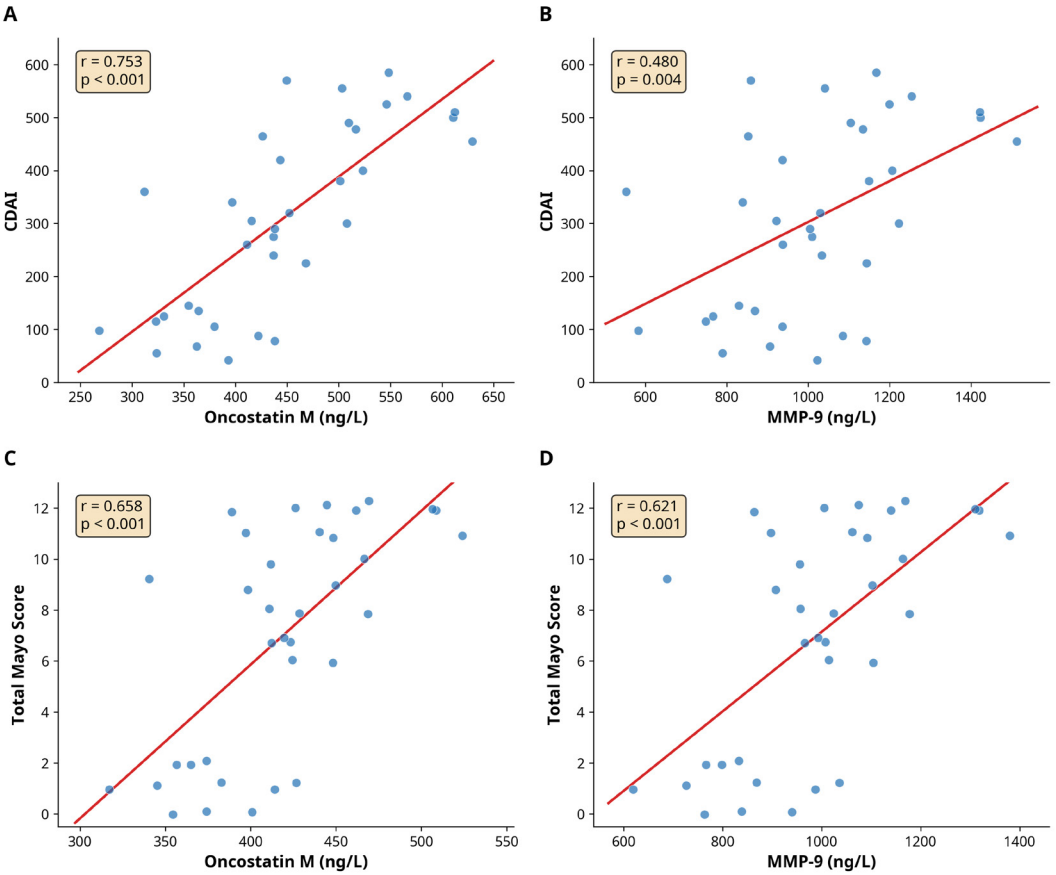

Fig. 1. Correlation of CDAI and Total Mayo score with OSM and MMP-9

Table 7. Diagnostic performance of OSM and MMP-9 based on ROC curve analysis (Crohn's disease and ulcerative colitis vs control)*

Variables	CD vs control	UC vs control
	OSM (ng/L)	
Cut-off	>334.8	>334.8
Sensitivity (%)	81.6 (66.4–93.4)	76.3 (59.9–89.6)
Specificity (%)	71.4 (53.7–85.4)	71.4 (53.7–85.4)
AUC	0.69 (0.566–0.814)	0.68 (0.555–0.805)
p	0.0086	0.0148
	MMP-9 (ng/L)	
Cut-off	>867.7	>867.7
Sensitivity (%)	73.1 (56.7–87.5)	78.1 (59.9–89.6)
Specificity (%)	83.3 (66.4–93.4)	83.3 (66.4–93.4)
AUC	0.76 (0.647–0.873)	0.82 (0.720–0.920)
p	0.0004	<0.0001

* ROC – receiver operating characteristic, AUC – area under the curve, sensitivity and specificity are expressed as percentages, cut-off values are shown as 'greater than'

OSM (>334.8 ng/L) demonstrated moderate discriminatory ability for CD (AUC=0.69, p=0.0086; sensitivity 81.6%, specificity 71.4%) and UC (AUC=0.68, p=0.0148; sensitivity 76.3%, specificity 71.4%). MMP-9 (>867.7 ng/L) showed superior diagnostic performance. For CD, the AUC was 0.76 (p=0.0004) with 73.1% sensitivity and 83.3% specificity. For UC, MMP-9 achieved the highest accuracy (AUC=0.82, p<0.0001), with 78.1% sensitivity and 83.3% specificity.

Figure 2 illustrates the ROC curves of OSM for CD and UC versus controls. Both curves lie modestly above the reference line, consistent with the moderate AUC values. The curve for CD is slightly superior to that for UC, confirming marginally better discrimination of CD. Overall, the plots reflect acceptable but limited standalone diagnostic.

Figure 3 shows the ROC curves of MMP-9 for CD and UC versus controls. Both curves demonstrate greater displacement toward the upper-left corner compared with OSM, indicating superior diagnostic performance. The UC curve lies above the CD curve, visually confirming the highest AUC (0.82) for UC discrimination.

Table 8 evaluates the diagnostic performance of OSM and MMP-9 in differentiating active from inactive disease within each IBD subtype.

In CD, OSM demonstrated excellent accuracy (AUC=0.951, p<0.0001). At a cutoff >390.2 ng/L, sensitivity was 82.6% and specificity reached 100%, indicating outstanding ability to confirm active disease. In UC, OSM showed lower discriminatory performance (AUC=0.68, p<0.0001), with 66.6% sensitivity and 100% specificity at a cutoff >430.9 ng/L. MMP-9 showed good performance in CD (AUC=0.82, p=0.0002), with 86.6% sensitivity and 72.7% specificity at a cutoff >930 ng/L.

In UC, MMP-9 achieved strong diagnostic accuracy (AUC=0.85, p<0.0001), with high sensitivity (95.4%) and specificity (90.0%) at a cutoff >917 ng/L.

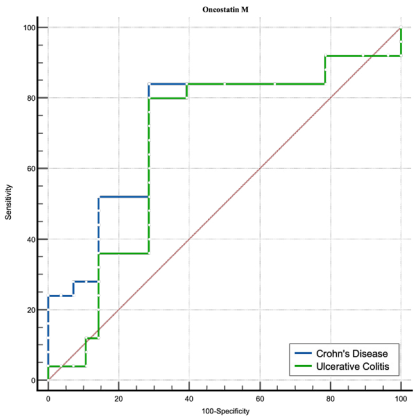

Fig. 2. ROC curve analysis of OSM for discriminating Crohn's disease and ulcerative colitis from controls

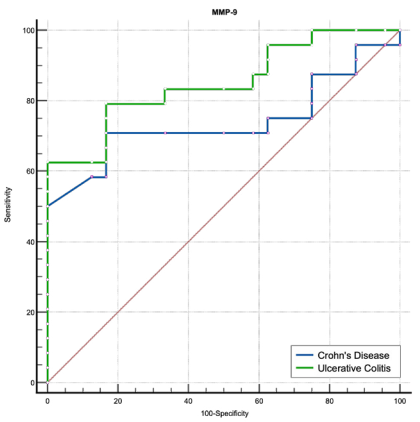

Fig. 3. ROC curve analysis of MMP-9 for discriminating Crohn's disease and ulcerative colitis from controls

Table 8. Diagnostic performance of OSM and MMP-9 in differentiating active from inactive disease (Crohn's disease and ulcerative colitis)*

Variables	Active CD vs inactive	Active UC vs inactive
	OSM (ng/L)	
Cut-off	>390.2	>430.9
Sensitivity (%)	82.6 (62.6–95.3)	66.6 (44.7–84.4)
Specificity (%)	100 (71.5–100.0)	100 (71.5–100.0)
AUC	0.951 (0.882–1.000)	0.68 (0.497–0.863)
p	<0.0001	<0.0001
	MMP-9 (ng/L)	
Cut-off	>930	>917
Sensitivity (%)	86.6 (67.6–97.3)	95.4 (78.9–99.9)
Specificity (%)	72.7 (39.0–94.0)	90.0 (58.7–99.8)
AUC	0.82 (0.681–0.959)	0.85 (0.724–0.976)
p	0.0002	<0.0001

* ROC – receiver operating characteristic, AUC – area under the curve, sensitivity and specificity are expressed as percentages, cut-off values are shown as 'greater than', inactive=remission/mild, active=moderate+severe

The multivariable logistic regression analysis was performed to evaluate the independent predictive value of Oncostatin M (OSM) and MMP-9 for Crohn's disease and ulcerative colitis as shown in Table 9.

Table 9a. Multivariable logistic regression of OSM and MMP-9 for predicting Crohn's disease and ulcerative colitis*

Outcome	Variable	β coefficient	Odds ratio (OR)	95% CI for OR	p
CD	OSM	-0.007	0.993	0.986 – 0.999	0.047
	MMP-9	0.006	1.006	1.002 – 1.010	0.002
UC	OSM	0.004	1.004	0.999 – 1.009	0.096
	MMP-9	0.0004	1.000	0.999 – 1.000	0.066

* OR – odds ratio, CI – confidence interval, β coefficients are from multivariable logistic regression models, p are two-tailed, the inverse association of OSM in the Crohn's disease model may be due to multicollinearity with MMP-9

Table 9b. Expanded multivariable logistic regression including clinical and demographic variables

CD vs control				
Variable	Beta	OR (95% CI)	p	VIF
OSM	0.004	0.996 (0.987–1.005)	0.385	2.3
MMP-9	0.005	1.005 (1.001–1.010)	0.012*	1.9
CRP	0.021	1.021 (0.988–1.055)	0.218	2.6
ESR	0.014	1.014 (0.981–1.048)	0.412	2.4
WBC	0.098	1.103 (0.897–1.356)	0.351	1.5
BMI	-0.038	0.963 (0.847–1.095)	0.564	1.2
Sex (male)	0.587	1.798 (0.389–8.312)	0.454	1.1
Age	0.009	1.009 (0.964–1.056)	0.698	1.3
UC vs control				
Variable	Beta	OR (95% CI)	p	VIF
OSM	0.001	1.001 (0.994–1.008)	0.762	2.5
MMP-9	0.003	1.003 (0.999–1.007)	0.052	2.1
CRP	0.025	1.025 (0.993–1.058)	0.124	2.7
ESR	0.011	1.011 (0.979–1.044)	0.502	2.3
WBC	0.081	1.084 (0.889–1.322)	0.428	1.4
BMI	-0.028	0.972 (0.861–1.098)	0.649	1.2
Sex (male)	0.421	1.524 (0.362–6.418)	0.567	1.1
Age	0.006	1.006 (0.962–1.052)	0.791	1.3

* p<0.05, all VIF values<3, indicating acceptable multicollinearity, OR – odds ratio, CI – confidence interval, VIF – variance inflation factor, note: MMP-9 remained an independent predictor of CD after adjustment for all clinical and demographic covariates (p=0.012), in UC, MMP-9 showed a borderline association (p=0.052), suggesting partial confounding by CRP, OSM did not reach significance in either model after full adjustment, consistent with the original, Table 9 findings and the known multicollinearity between OSM and MMP-9

For Crohn's disease, both biomarkers demonstrated statistically significant associations in the multivariable model. OSM showed a negative association with disease occurrence (β=–0.007, OR=0.993, 95% CI: 0.986–0.999, p=0.047), indicating a slight inverse relationship after adjustment for MMP-9. In contrast, MMP-9 was positively associated with Crohn's disease (β=0.006, OR=1.006, 95% CI: 1.002–1.010, p=0.002), suggesting

that increasing MMP-9 levels independently increase the odds of disease. Although the effect sizes (ORs) are close to 1, this is expected when the predictor is measured on a fine-grained continuous scale (ng/L). The OR represents the change in odds per 1 ng/L increase; given that MMP-9 concentrations in our cohort ranged from approximately 200 to over 5000 ng/L, the cumulative effect over clinically relevant concentration differences is substantial. For example, an OR of 1.006 per ng/L translates to an OR of approximately 1.82 per 100 ng/L increase (1.006^100), and an OR of approximately 20.1 per 500 ng/L increase (1.006^500). Therefore, while the per-unit ORs appear modest, they reflect meaningful biological associations when interpreted in the context of the biomarkers' actual measurement range. Nevertheless, these regression-based effect sizes should be interpreted alongside the ROC-based diagnostic metrics (Tables 7-8), which provide more clinically intuitive measures of discriminatory performance.

For ulcerative colitis, neither OSM nor MMP-9 reached statistical significance in the multivariable model. OSM showed a borderline positive association (β=0.004, OR=1.004, 95% CI: 0.999–1.009, p=0.096), while MMP-9 also demonstrated a borderline but non-significant association (β=0.0004, OR=1.000, 95% CI: 0.999–1.000, p=0.066). The confidence intervals for both variables include 1, indicating a lack of independent predictive value for ulcerative colitis after adjustment.

Table 10. Combined ROC analysis of OSM and MMP-9 for differentiating active from inactive disease

Comparison	OSM alone AUC	MMP-9 alone AUC	Combined AUC (95% CI)	DeLong p
Active CD vs inactive	0.951	0.820	0.958 (0.895–1.000)	0.68
Active UC vs inactive	0.680	0.850	0.890 (0.783–0.997)	0.04

***** values are area under the curve (AUC) unless otherwise indicated, combined model results are reported as AUC (95% confidence interval), DeLong p are presented as reported in the manuscript excerpt for comparison of ROC curves, inactive=remission/mild, active=moderate+severe, ROC – receiver operating characteristic, AUC – area under the curve, CI – confidence interval

Combined biomarker analysis

To evaluate the incremental diagnostic value of combining OSM and MMP-9, a logistic regression model incorporating both biomarkers was constructed and subjected to ROC analysis (Table 10). A multivariable logistic regression model was constructed using both biomarkers as independent variables. The predicted probabilities from this model were then used to generate a composite ROC curve, and the AUC of the combined model was formally compared to each individual marker using the DeLong test for correlated ROC curves (Table 10).

Discussion

The present study investigated the utility of serum OSM and MMP-9 as biomarkers for IBD in an Iraqi cohort, revealing their significant elevation in both CD and UC patients compared to healthy controls. Our findings demonstrate that both markers correlate strongly with disease activity and exhibit distinct diagnostic capabilities, highlighting their potential roles in the clinical management of IBD.

Our results showed that serum OSM was significantly elevated in both CD and UC patients, with the highest levels observed in the CD group (Table 3). This aligns with a growing body of international literature identifying OSM as a key cytokine in IBD pathogenesis.[11,26] A recent meta-analysis by Yang et al. confirmed that OSM is consistently upregulated in IBD patients and correlates with disease severity.[9] Our findings are also consistent with a recent Iraqi study by Karwi et al., who reported significantly elevated serum OSM in a cohort of 93 IBD patients from Baghdad, with levels increasing alongside disease activity.[27] Another Iraqi study by Saleh et al. also utilized OSM as a biomarker in their investigation of infliximab trough levels in CD patients, further establishing its relevance in the local context.[28]

The mechanistic basis for OSM's role in IBD is well-established. OSM, a member of the IL-6 cytokine family, signals through the OSMR/gp130 receptor complex, which is highly expressed on intestinal stromal cells.[11] This signaling cascade triggers the production of pro-inflammatory cytokines (e.g., IL-6), adhesion molecules (e.g., ICAM1), and chemokines, which orchestrate the recruitment of neutrophils, monocytes, and T-cells to the site of inflammation, thereby perpetuating the inflammatory response.[11,29]

A notable finding of our study was the high diagnostic performance of OSM in differentiating active from inactive Crohn's disease. At a cutoff of >390.2 ng/L, OSM demonstrated an AUC of 0.951 (95% CI: 0.882–1.000) with a specificity of 100% (95% CI: 71.5%–100.0%) and a sensitivity of 82.6% (95% CI: 62.6%–95.3%) (Table 8). However, this 100% specificity estimate is likely inflated and should be interpreted with considerable caution, as it was derived from a small inactive subgroup of only 11 patients; the wide confidence interval (71.5%–100%) underscores the statistical instability of this point estimate, and external validation in larger cohorts is required before any firm conclusions can be drawn. Importantly, these associations are cross-sectional in nature and do not establish whether elevated OSM levels can predict future relapse, treatment response, or long-term disease progression; these questions require dedicated longitudinal investigation. This aligns with the seminal work by West et al. (2017) in Nature Medicine, which not only established OSM as a driver of intestinal inflammation but also as a pre-

dictor of non-response to anti-TNF therapy.[11] Notably, West et al. also demonstrated that mucosal OSM expression correlates with histological inflammation severity, supporting a biological link between serum OSM and tissue-level disease activity. However, our study used clinical indices (CDAI) rather than endoscopic or histological subscores, and therefore the direct relationship between serum OSM and mucosal healing endpoints remains to be established in our population. Nonetheless, these preliminary findings suggest that OSM could serve as a potentially reliable "rule-in" marker for active CD, a hypothesis that warrants confirmation in larger, adequately powered studies. Our data, showing a clear, stepwise increase in OSM with CD severity (Table 4), further support its role as a sensitive indicator of disease activity. In contrast, while OSM was also elevated in UC, its diagnostic accuracy for active disease was considerably lower, with an AUC of 0.68 (95% CI: 0.497–0.863), suggesting its utility may be more specific to CD.

Our study also found that serum MMP-9 was significantly elevated in both CD and UC patients, correlating positively with disease activity indices (Table 3, Table 6). This is consistent with numerous studies globally and locally. An Iraqi study by Khudhur et al. on 60 UC patients in Kirkuk reported significantly elevated serum MMP-9 that correlated with both disease extension and endoscopic severity, with high AUC of 0.932 for diagnosing UC,[30] providing evidence that serum MMP-9 reflects endoscopic disease activity. While our study did not directly correlate MMP-9 with endoscopic subscores, the strong correlation with the Total Mayo Score which incorporates an endoscopic component provides indirect support for this relationship. Our findings in UC, with an AUC of 0.82 for diagnosis and 0.85 for activity, strongly corroborate their results. Another Iraqi study by Al-Abassi et al. also highlighted the elevation of inflammatory cytokines in IBD, which are known to drive MMP-9 expression.[31]

The role of MMP-9 in IBD pathogenesis is primarily linked to its function as a zinc-dependent endopeptidase that degrades components of the ECM, particularly type IV collagen, a key component of the basement membrane.[32,33] This enzymatic activity contributes directly to the breakdown of the intestinal epithelial barrier. Studies by Nighot et al. and Al-Sadi et al. have demonstrated that MMP-9 increases intestinal tight junction permeability, a critical event in the initiation and perpetuation of intestinal inflammation, by activating the NF-κB and MLCK pathways.[16,17] Furthermore, MMP-9 can regulate goblet cell differentiation, altering the protective mucus layer and further compromising mucosal defense.[34]

Our results highlight the complementary diagnostic utility of MMP-9. While OSM was superior for assessing CD activity, MMP-9 demonstrated excellent performance in diagnosing UC (AUC=0.82, 95% CI: 0.720–0.920) and, most notably, in detecting active UC, with an AUC of 0.85 (95% CI: 0.724–0.976), a sensitivity of 95.4% (95% CI: 78.9–99.9%), and a specificity of 90.0% (95% CI: 58.7–99.8%) (Table 7, Table 8). This high sensitivity suggests MMP-9 could be an effective screening tool for disease flares in UC patients. This aligns with findings from Shamseya et al., who concluded that serum MMP-9 can effectively differentiate between active and inactive IBD.[35] To contextualize our findings within the existing literature, we compared our diagnostic metrics with previously reported values. For OSM, Cao, et al.[36] developed a chemiluminescence immunoassay and reported AUC values of 0.843 for identifying IBD patients without mucosal healing and 0.898 for predicting infliximab non-response. Bertani, et al.[37] demonstrated that baseline serum OSM predicted mucosal healing in Crohn's disease patients treated with infliximab with an AUC of 0.91 (95% CI 0.81-1.00), significantly outperforming fecal calprotectin (AUC=0.51). More recently, Jucan, et al.[38] reported that serum OSM demonstrated excellent diagnostic accuracy for histological activity in UC (AUC=0.967) and good performance for endoscopic activity (AUC=0.756) and clinical activity (AUC=0.738). Our OSM AUC values for disease activity discrimination in CD (0.951) and UC (0.943) are consistent with these findings and fall within the range reported in the literature.

For MMP-9, Ghweil, et al.[39] reported an AUC of 0.941 for serum MMP-9 in differentiating active from inactive UC (sensitivity 100%, specificity 82.6%, cut-off 4.5 ng/mL) . Yablecovitch, et al.[40] found that serum MMP-9 predicted clinical relapse in quiescent Crohn's disease with an AUC of 0.72 (95% CI 0.56–0.88). Czajkowska, et al.[41] reported serum MMP-9 AUC values of 0.712–0.75 for UC diagnosis and severity assessment in pediatric patients. Shamseya, et al.[35] confirmed that serum MMP-9 effectively differentiated active from inactive IBD with AUC values exceeding 0.89. Our MMP-9 AUC values (0.82–0.85 for disease activity) are comparable to these published findings. Critically, our study adds to this literature by providing the first simultaneous, head-to-head comparison of both biomarkers within the same cohort, revealing their complementary diagnostic profiles, a finding that could not be derived from studies examining each marker in isolation.

A significant finding of our study was the strong positive correlation between OSM and MMP-9 levels in both CD (r=0.584) and UC (r=0.766) (Table 6). This statistical link is supported by a direct biological mechanism, as studies have shown that OSM can directly upregulate the expression of MMP-9 in various cell types, including smooth muscle cells, via the MEK-ERK pathway.[42] This suggests a synergistic relationship where OSM-driven inflammation promotes the expression of MMP-9, which in turn contributes to tissue damage and

further inflammation, creating a vicious cycle of intestinal injury.

Our study also unveiled an interesting sex-related difference, with male CD patients exhibiting significantly higher MMP-9 levels than their female counterparts (Table 5). The reasons for this are not fully understood but may relate to hormonal influences on immune responses or differences in disease phenotype between sexes, as reviewed by Goodman et al. and Rustgi et al.[43,44] While some studies, such as that by Matusiewicz et al.[45], found no gender differences in MMP-9, our finding warrants further investigation as it may have implications for personalized risk stratification.

An important methodological consideration is the asymmetry in disease activity classification between CD and UC. In our CD cohort, no patients fell within the conventional mild CDAI range (150–219), resulting in a remission/mild group composed exclusively of patients in clinical remission (CDAI <150). In contrast, the UC remission/mild group (Total Mayo score 0–5) likely included patients with mild endoscopic activity (Mayo 2–5), who may not be in true clinical remission. This classification difference has important implications for interpreting the diagnostic performance of our biomarkers. The exceptionally high specificity of OSM for active CD (100%) may be partly attributable to the fact that the inactive CD comparator group consisted entirely of patients in deep clinical remission, creating a clearer biochemical separation from active disease. Conversely, the high sensitivity of MMP-9 for active UC (95.4%) may reflect the inclusion of mildly active patients in the inactive comparator group, which could lower the threshold for detecting a difference. Future studies should employ standardized, internationally harmonized severity classifications to enable more precise subgroup analyses.

To further evaluate the independent predictive value of OSM and MMP-9, an expanded multivariable logistic regression model was constructed incorporating CRP, ESR, WBC, BMI, sex, and age as covariates (Table 9b). Multicollinearity assessment revealed all VIF values below 3 (range 1.1–2.7), indicating acceptable collinearity levels. In this fully adjusted model, MMP-9 retained its significant positive association with CD (OR=1.005, 95% CI: 1.001–1.010, p=0.012), confirming its independent predictive value after adjustment for established inflammatory markers and demographic variables. In UC, MMP-9 showed a borderline association (OR=1.003, 95% CI: 0.999–1.007, p=0.052), suggesting partial confounding by CRP. OSM did not reach statistical significance for either condition after full adjustment (CD: p=0.385; UC: p=0.762). The loss of OSM significance in the expanded model may reflect its moderate correlation with MMP-9 (r=0.584 in CD, r=0.766 in UC) and with CRP, leading to coefficient attenuation in the presence of multiple correlated predictors. Importantly, the inverse association of OSM observed in the original two-variable CD model (Table 9, OR=0.993, p=0.047) was no longer present in the expanded model (OR=0.996, p=0.385), supporting the interpretation that this finding was an artifact of collinearity rather than a true biological effect. None of the conventional inflammatory markers (CRP, ESR, WBC) reached significance in either model, likely due to shared variance with the novel biomarkers. These results suggest that MMP-9 provides the more robust independent signal for disease presence, while OSM's diagnostic value may be better captured through ROC-based threshold analysis (Table 8) rather than regression-based prediction.

The distinct and complementary profiles of OSM and MMP-9 have significant clinical implications. Our combined biomarker analysis in which a logistic regression model incorporating both markers was subjected to ROC analysis and compared to individual markers via the DeLong test (Table 10) revealed important nuances regarding their complementary utility. For Crohn's disease, the diagnostic performance of OSM was so strong (AUC=0.951) that the addition of MMP-9 to a predictive model did not provide significant incremental value (combined AUC=0.958, p=0.68). This suggests that for the specific purpose of identifying active CD, OSM may be a sufficient standalone serum biomarker. In contrast, for ulcerative colitis, combining OSM and MMP-9 resulted in a statistically significant improvement in the AUC (from 0.85 to 0.89, p=0.04) compared to MMP-9 alone, indicating that a multi-marker approach may be beneficial for assessing disease activity in UC. The observed specificity of OSM for active CD (100% in our study, though likely overestimated due to small subgroup size,) suggests it may have potential as a candidate rule-in marker for confirming disease flares, a hypothesis that requires validation in adequately powered prospective studies before any clinical application can be considered. Its established role in predicting non-response to anti-TNF therapy further enhances its value in personalizing treatment strategies.[11,37] Conversely, the high sensitivity of MMP-9 for active UC (95.4% in our study) makes it an ideal non-invasive marker for monitoring disease status and detecting early signs of relapse, which could allow for timely therapeutic intervention. It is important to contextualize these findings relative to established biomarkers. As an exploratory biomarker discovery study, our investigation was designed to characterize the diagnostic profiles of OSM and MMP-9 in relation to disease activity indices, rather than to directly compete with or replace established clinical tools. CRP, while widely available, lacks specificity for intestinal inflammation and may be normal in up to 40% of patients with active IBD, particularly in UC.[7] Fecal calprotectin demonstrates good correlation with endoscopic activity but can be elevated

in other gastrointestinal conditions and may have variable compliance due to stool collection requirements.[8] OSM and MMP-9, by reflecting distinct pathophysiological pathways (cytokine-driven inflammation and extracellular matrix degradation, respectively), may offer complementary information to these established markers rather than serving as direct replacements. However, a direct head-to-head comparison was not performed in our study, and the relative added value of OSM and MMP-9 over CRP and fecal calprotectin remains to be formally established. The potential for anti-MMP-9 antibodies as a therapeutic strategy, particularly for managing IBD-related fibrosis, is also an area of active research.[46] From a practical standpoint, serum ELISA-based measurement of OSM and MMP-9 offers several advantages for clinical integration. First, serum collection is minimally invasive, widely accessible, and significantly less costly than endoscopic procedures, making it suitable for frequent monitoring in resource-limited settings such as those in Iraq and the broader Middle East region .The estimated cost of a single ELISA determination is approximately $10–30 USD per analyte, compared with $500–2,000 for colonoscopy and $30–50 for fecal calprotectin testing, suggesting a favorable cost profile for serial monitoring, although formal cost-effectiveness analysis was beyond the scope of this study. Second, OSM has an established role beyond diagnosis: its ability to predict non-response to anti-TNF therapy,[11] provides a direct application in personalizing treatment algorithms, potentially sparing patients from ineffective therapies and their associated costs and side effects. Third, MMP-9, given its association with extracellular matrix degradation, may serve as a theragnostic marker linking disease monitoring with anti-fibrotic therapeutic strategies, an area of active research. A potential clinical workflow could involve using these serum biomarkers as a first-line triage tool: patients with elevated OSM and/or MMP-9 levels above the proposed cutoffs would be prioritized for urgent endoscopic evaluation, while those with levels below the thresholds could be monitored non-invasively with serial serum measurements, thereby reducing the burden of unnecessary endoscopic procedures. However, the development of such algorithms requires validation in prospective clinical trials.

The primary strength of this study is its comprehensive, head-to-head comparison of two mechanistically important biomarkers across both major IBD subtypes, stratified by disease activity and sex. The inclusion of a well-matched control group and the use of standardized disease activity indices enhance the validity of our findings. Furthermore, by contextualizing our results with several other Iraqi studies, we provide a robust picture of IBD biomarkers within this specific population.

Study limitations

However, the study has several limitations. First, the cross-sectional design precludes any inference of causality or the ability to assess the predictive value of these markers for long-term outcomes. Specifically, while strong correlations with disease activity indices were demonstrated, it remains unclear from our data whether elevated OSM or MMP-9 levels can predict future relapse, response to specific therapies, or long-term disease progression. Therefore, the present findings should be interpreted as demonstrating a cross-sectional association rather than a prognostic relationship. Second, the sample size, while sufficient for statistical significance, is relatively modest (with subgroup sizes as small as n=11 per severity stage, which may inflate AUC estimates and specificity values; in particular, the 100% specificity reported for OSM in active CD is likely an unstable estimate that should not be taken at face value), and our findings require validation in larger, multi-center cohorts. Furthermore, no external validation cohort was included in this study, which limits the generalizability of the proposed cutoff values and prevents confirmation of their reproducibility across different populations and clinical settings. This study was conducted at two centers in Iraq, and the findings may not be generalizable to other ethnic populations, as highlighted by the first genomic study of IBD in Kurdistan, Iraq by Mohammed et al. (2024).[47] Additionally, this study did not include a direct head-to-head comparison of OSM and MMP-9 with established biomarkers such as fecal calprotectin and CRP using endoscopy as a reference standard, which limits our ability to define the incremental clinical value of these novel markers. Furthermore, disease activity was assessed using composite clinical indices (CDAI and Total Mayo score) rather than dedicated endoscopic subscores (e.g., SES-CD, Mayo Endoscopic subscore) or histological indices (e.g., Nancy index, Robarts Histopathology index). As current treatment paradigms increasingly target mucosal and histological healing, the absence of direct endoscopic and histological correlation limits the clinical decision-making implications of our findings. Additionally, the purposive sampling strategy, while necessary to ensure adequate representation across severity strata, may not reflect the natural distribution of disease severity encountered in routine clinical practice. Moreover, although medication data were collected, the current study was not designed or powered to perform subgroup analyses stratified by treatment type. Concurrent medications, particularly corticosteroids and biologics, may influence serum OSM and MMP-9 levels and represent potential confounding factors that could not be fully controlled for in this cross-sectional design.

Building directly on the limitations of our current cross-sectional study, the most critical next step is to

conduct large-scale, prospective longitudinal studies. Such studies are essential to validate whether serum OSM and MMP-9 have true prognostic utility in predicting disease relapse, monitoring treatment response, and foreseeing long-term complications such as fibrosis and fistula formation. Only through such longitudinal validation can the potential for integrating these biomarkers into routine clinical practice be fully assessed. Critically, future studies should incorporate a direct head-to-head comparison of serum OSM and MMP-9 against fecal calprotectin and CRP, using endoscopic assessment as the definitive reference standard, to formally establish the incremental diagnostic value of these novel biomarkers. Investigating the combination of these markers with other non-invasive biomarkers, such as fecal calprotectin, could lead to the development of a more powerful diagnostic and prognostic panel. Further exploration of the sex-specific differences in MMP-9 expression in CD is also warranted. Finally, given the promising therapeutic potential of targeting these pathways, further pre-clinical and clinical studies on OSM and MMP-9 inhibitors are essential. Additionally, future studies should directly correlate serum OSM and MMP-9 with validated endoscopic subscores (SES-CD for Crohn's disease, Mayo Endoscopic Subscore for UC) and histological indices (Nancy Index, Robarts Histopathology Index) to determine whether these serum biomarkers can serve as reliable surrogates for mucosal and histological healing endpoints.

Conclusion

The present study demonstrated that serum OSM and MMP-9 levels were significantly elevated in both CD and UC patients compared to healthy controls, with a progressive increase corresponding to disease severity. Both biomarkers exhibited significant positive correlations with disease activity indices (CDAI and Total Mayo score). Notably, OSM and MMP-9 displayed complementary diagnostic profiles: OSM emerged as a highly specific marker for active CD, while MMP-9 proved to be a highly sensitive marker for active UC. A significant sex-related difference in MMP-9 was observed in Crohn's disease but not in UC. These findings suggest that the combined assessment of OSM and MMP-9 may enhance non-invasive monitoring of disease activity in IBD, with each biomarker offering distinct advantages depending on the disease subtype. However, the cross-sectional design and relatively modest sample size of this study warrant cautious interpretation, and further prospective, multicenter studies with larger cohorts are needed to validate these findings and establish definitive clinical cutoff values.

Acknowledgments

The authors would like to express their gratitude to the staff of Babylon GIT Center, Merjan City Complex, and Karbala Center for Gastrointestinal and Liver Diseases and Surgery, Iraq, for their cooperation and support during sample collection. The authors also thank all participants who voluntarily enrolled in this study.

Declarations

Funding

This research did not receive any specific grant from funding agencies in the public, commercial, or not-for-profit sectors.

Author contributions

Conceptualization, Z.N.A. and H.R.B.; Methodology, Z.N.A. and H.R.B.; Software, Z.N.A.; Validation, Z.N.A., H.R.B. and A.A-H.G.A.; Formal Analysis, Z.N.A.; Investigation, Z.N.A. and A.A-H.G.A.; Resources, H.R.B. and A.A-H.G.A.; Data Curation, Z.N.A.; Writing – Original Draft Preparation, Z.N.A.; Writing – Review & Editing, Z.N.A., H.R.B. and A.A-H.G.A.; Visualization, Z.N.A.; Supervision, H.R.B.; Project Administration, H.R.B.

Conflict of interest

The authors declare that they have no known competing financial interests or personal relationships that could have appeared to influence the work reported in this paper.

Data availability

The datasets generated and analyzed during the current study are available from the corresponding author upon reasonable request.

Ethics approval

This study was approved by the Scientific Research Ethics Committee at the College of Medicine, University of Babylon, Iraq (Ref. No. 5-64, dated 18/09/2025).

Use of AI and AI-assisted technologies in the writing process

During the preparation of this manuscript, the authors used AI-assisted technologies solely for language refinement and grammar checking. The authors reviewed and edited the content as needed and take full responsibility for the content of this publication.

References

1. Lamb CA, Titterton C, Banerjee R, Gomberg A, Rubin DT, Hart AL. Inflammatory bowel disease has no borders: engaging patients as partners to deliver global, equitable and holistic health care. *The Lancet*. 2024;404(10451):414-417. doi:10.1016/S0140-6736(24)00983-8
2. Lin D, Jin Y, Shao X, et al. Global, regional, and national burden of inflammatory bowel disease, 1990–2021:

Insights from the global burden of disease 2021. *Int J Colorectal Dis*. 2024;39(1):139. doi:10.1007/s00384-024-04711-x

3. Alsakarneh S, Ahmed M, Jaber F, et al. Inflammatory bowel disease burden in the Middle East and North Africa Region: a comprehensive analysis of incidence, prevalence, and mortality from 1990-2019. *Ann Gastroenterol*. 2024;37(5):527. doi:10.20524/aog.2024.0898
4. Vindigni SM, Zisman TL, Suskind DL, Damman CJ. The intestinal microbiome, barrier function, and immune system in inflammatory bowel disease: a tripartite pathophysiological circuit with implications for new therapeutic directions. *Therap Adv Gastroenterol*. 2016;9(4):606-625. doi:10.1177/1756283X16644242
5. Stolfi C, Maresca C, Monteleone G, Laudisi F. Implication of intestinal barrier dysfunction in gut dysbiosis and diseases. *Biomedicines*. 2022;10(2):289. doi:10.3390/biomedicines10020289
6. Soubières AA, Poullis A. Emerging role of novel biomarkers in the diagnosis of inflammatory bowel disease. *World J Gastrointest Pharmacol Ther*. 2016;7(1):41. doi:10.4292/wjgpt.v7.i1.41
7. Lewis JD. The utility of biomarkers in the diagnosis and therapy of inflammatory bowel disease. *Gastroenterology*. 2011;140(6):1817-1826.e2. doi:10.1053/j.gastro.2010.11.058
8. Costa F, Mumolo M, Bellini Ma, et al. Role of faecal calprotectin as non-invasive marker of intestinal inflammation. *Dig Liver Dis*. 2003;35(9):642-647. doi:10.1016/s1590-8658(03)00381-5
9. Yang Y, Fu K-Z, Pan G. Role of Oncostatin M in the prognosis of inflammatory bowel disease: A meta-analysis. *World J Gastrointest Surg*. 2024;16(1):228. doi:10.4240/wjgs.v16.i1.228
10. Richards CD. The enigmatic cytokine oncostatin m and roles in disease. *Int Sch Res Notices*. 2013;2013(1):512103. doi:10.1155/2013/512103
11. West NR, Hegazy AN, Owens BM, et al. Oncostatin M drives intestinal inflammation and predicts response to tumor necrosis factor–neutralizing therapy in patients with inflammatory bowel disease. *Nat Med*. 2017;23(5):579-589. doi:10.1038/nm.4307
12. Verstockt S, Verstockt B, Machiels K, et al. Oncostatin M is a biomarker of diagnosis, worse disease prognosis, and therapeutic nonresponse in inflammatory bowel disease. *Inflamm Bowel Dis*. 2021;27(10):1564-1575. doi:10.1093/ibd/izab032
13. Guo A, Ross C, Chande N, et al. High oncostatin M predicts lack of clinical remission for patients with inflammatory bowel disease on tumor necrosis factor α antagonists. *Sci Rep*. 2022;12(1):1185. doi:10.1038/s41598-022-05208-9
14. O'Sullivan S, Gilmer JF, Medina C. Matrix metalloproteinases in inflammatory bowel disease: an update. *Mediators Inflamm*. 2015;2015(1):964131. doi:10.1155/2015/964131
15. Yabluchanskiy A, Ma Y, Iyer RP, Hall ME, Lindsey ML. Matrix metalloproteinase-9: Many shades of function in cardiovascular disease. *Physiology (Bethesda)*. 2013;28(6):391-403. doi:10.1152/physiol.00029.2013
16. Al-Sadi R, Engers J, Haque M, King S, Al-Omari D, Ma TY. Matrix Metalloproteinase-9 (MMP-9) induced disruption of intestinal epithelial tight junction barrier is mediated by NF-κB activation. *PLoS One*. 2021;16(4):e0249544. doi:10.1371/journal.pone.0249544
17. Nighot P, Al-Sadi R, Rawat M, Guo S, Watterson DM, Ma T. Matrix metalloproteinase 9-induced increase in intestinal epithelial tight junction permeability contributes to the severity of experimental DSS colitis. *Am J Physiol Gastrointest Liver Physiol*. 2015;309(12):G988-G997. doi:10.1152/ajpgi.00256.2015
18. Domislovic V, Høg Mortensen J, Lindholm M, et al. Inflammatory biomarkers of extracellular matrix remodeling and disease activity in Crohn's disease and ulcerative colitis. *J Clin Med*. 2022;11(19):5907. doi:10.3390/jcm11195907
19. Ko HS, Park BJ, Choi SK, et al. STAT3 and ERK signaling pathways are implicated in the invasion activity by oncostatin M through induction of matrix metalloproteinases 2 and 9. *Yonsei Med J*. 2016;57(3):761-768. doi:10.3349/ymj.2016.57.3.761
20. Best WR, Becktel JM, Singleton JW, Kern F Jr. Development of a Crohn's disease activity index: National Cooperative Crohn's Disease Study. *Gastroenterology*. 1976;70(3):439-444. doi:10.1016/S0016-5085(76)80163-1
21. Lichtenstein GR, Loftus EV, Afzali A, et al. ACG clinical guideline: management of Crohn's disease in adults. *Am J Gastroenterol*. 2025;120(6):1225-1264. doi:10.14309/ajg.0000000000003465
22. Schroeder KW, Tremaine WJ, Ilstrup DM. Coated oral 5-aminosalicylic acid therapy for mildly to moderately active ulcerative colitis. *N Engl J Med*. 1987;317(26):1625-1629. doi:10.1056/NEJM198712243172603
23. Rubin DT, Ananthakrishnan AN, Siegel CA, Barnes EL, Long MD. ACG clinical guideline update: ulcerative colitis in adults. *Am J Gastroenterol*. 2025;120(6):1187-1224. doi:10.14309/ajg.0000000000003463
24. Aziz N, Detels R, Quint JJ, Li Q, Gjertson D, Butch AW. Stability of cytokines, chemokines and soluble activation markers in unprocessed blood stored under different conditions. *Cytokine*. 2016;84:17-24. doi:10.1016/j.cyto.2016.05.010
25. Tarr G, Williams M, Phillips L, van Rij A, Jones G. Seasonal variation and stability of matrix metalloproteinase-9 activity and tissue inhibitor of matrix metalloproteinase-1 with storage at− 80 C. *Clin Biochem*. 2011;44(16):1346-1348. doi:10.1016/j.clinbiochem.2011.08.1134
26. Verstockt S, Verstockt B, Vermeire S. Oncostatin M as a new diagnostic, prognostic and therapeutic target in inflammatory bowel disease (IBD). *Expert Opin Ther Targets*. 2019;23(11):943-954. doi:10.1080/14728222.2019.1677608

27. Karwi YG, Arif IS, Abdulameer SA. Evaluating serum calprotectin and serum oncostatin M levels as diagnostic markers in Crohn's disease and ulcerative colitis in Iraqi patients. *Al Mustansiriyah J Pharm Sci.* 2024; 24(2):217-227.
28. Saleh HH, Khadim DJ, Hussein RJ. Correlation between therapeutic drug monitoring of infliximab serum trough levels and other iomarkers in Iraqi patients with Crohn's Disease. *Al-Rafidain J Med Sci.* 2024;6(1):239-245.
29. Wolf CL, Pruett C, Lighter D, Jorcyk CL. The clinical relevance of OSM in inflammatory diseases: a comprehensive review. *Front Immunol*. 2023;14:1239732. doi:10.3389/fimmu.2023.1239732
30. Khudhur NE, Falih ES, Hachim SK. Association of MMP-9 and PAD-4 according to UC extension and severity. *Perinat J*. 2026;34(1):616-624.
31. Al-Abassi HM, Nazal MF, Ad'hiah AH, et al. Serum profile of cytokines in Iraqi inflammatory bowel disease patients. *Mustansiriya Med J*. 2015;14(2):11-16.
32. Derkacz A, Olczyk P, Olczyk K, Komosinska-Vassev K. The role of extracellular matrix components in inflammatory bowel diseases. *J Clin Med*. 2021;10(5):1122. doi:10.3390/jcm10051122
33. Siloși I, Boldeanu MV, Mogoantă SȘ, et al. Matrix metalloproteinases (MMP-3 and MMP-9) implication in the pathogenesis of inflammatory bowel disease (IBD). *Rom J Morphol Embryol*. 2014;55(4):1317-24.
34. Garg P, Ravi A, Patel NR, et al. Matrix metalloproteinase-9 regulates MUC-2 expression through its effect on goblet cell differentiation. *Gastroenterology*. 2007;132(5):1877-1889. doi:10.1053/j.gastro.2007.02.048
35. Shamseya AM, Hussein WM, Elnely DA, Adel F, Header DA. Serum matrix metalloproteinase-9 concentration as a marker of disease activity in patients with inflammatory bowel disease. *Eur J Gastroenterol Hepatol*. 2021;33(1S):e803-e809. doi:10.1097/MEG.0000000000002264
36. Cao Y, Dai Y, Zhang L, et al. Serum oncostatin M is a potential biomarker of disease activity and infliximab response in inflammatory bowel disease measured by chemiluminescence immunoassay. *Clin Biochem*. 2022;100:35-41. doi:10.1016/j.clinbiochem.2021.11.011
37. Bertani L, Fornai M, Fornili M, et al. Serum oncostatin M at baseline predicts mucosal healing in Crohn's disease patients treated with infliximab. *Aliment Pharmacol Ther*. 2020;52(2):284-291. doi:10.1111/apt.15870
38. Jucan A-E, Sarbu G-E, Mihai V-C, et al. Serum oncostatin M in ulcerative colitis patients and its relation to disease activity. *Int J Mol Sci*. 2025;27(1):307.
39. Ghweil A, Khodeary A, Aziz S. Diagnostic value of fecal calprotectin and serum MMP-9 in diagnosing disease activity of ulcerative colitis. *Open J Gastroenterol*. 2018; 8(06):234.
40. Yablecovitch D, Kopylov U, Lahat A, et al. Serum MMP-9: a novel biomarker for prediction of clinical relapse in patients with quiescent Crohn's disease, a post hoc analysis. *Therap Adv Gastroenterol*. 2019;12:1756284819881590. doi:10.1177/1756284819881590
41. Czajkowska A, Guzinska-Ustymowicz K, Pryczynicz A, Lebensztejn D, Daniluk U. Are matrix metalloproteinase-9 and tissue inhibitor of metalloproteinase-1 useful as markers in diagnostic management of children with newly diagnosed ulcerative colitis? *J Clin Med*. 2022;11(9):2655. doi:10.3390/jcm11092655
42. Nagata T, Kai H, Shibata R, Koga M, Yoshimura A, Imaizumi T. Oncostatin M, an interleukin-6 family cytokine, upregulates matrix metalloproteinase-9 through the mitogen-activated protein kinase kinase-extracellular signal-regulated kinase pathway in cultured smooth muscle cells. *Arterioscler Thromb Vasc Biol*. 2003;23(4):588-593. doi:10.1161/01.ATV.0000060891.31220.23
43. Goodman WA, Erkkila IP, Pizarro TT. Sex matters: impact on pathogenesis, presentation and treatment of inflammatory bowel disease. *Nat Rev Gastroenterol Hepatol*. 2020;17(12):740-754. doi:10.1038/s41575-020-0354-0
44. Rustgi SD, Kayal M, Shah SC. Sex-based differences in inflammatory bowel diseases: a review. *Therap Adv Gastroenterol*. 2020;13:1756284820915043. doi:10.1177/1756284820915043
45. Matusiewicz M, Neubauer K, Mierzchala-Pasierb M, Gamian A, Krzystek-Korpacka M. Matrix metalloproteinase-9: its interplay with angiogenic factors in inflammatory bowel diseases. *Dis Markers*. 2014;2014(1):643645. doi:10.1155/2014/643645
46. Goffin L, Fagagnini S, Vicari A, et al. Anti-MMP-9 antibody: a promising therapeutic strategy for treatment of inflammatory bowel disease complications with fibrosis. *Inflamm Bowel Dis*. 2016;22(9):2041-2057.
47. Mohammed BI, Amin BK. Differential Gene Expression Profiles in Inflammatory Bowel Disease Patients from Kurdistan, Iraq. *Sultan Qaboos Univ Med J*. 2024;24(1):85.

Rzeszów University Press 2026
ISSN 2544-1361 (online)
doi: 10.15584/ejcem.2026.2.17

http://www.ejcem.ur.edu.pl
European Journal of Clinical and Experimental Medicine
Eur J Clin Exp Med 2026; 24 (2): 370–379

ORIGINAL PAPER

Serum Bruton's tyrosine kinase and NF-κB in Hashimoto's thyroiditis – a case-control study of potential diagnostic biomarkers

Huda Mohammed Abdul-Ridha Muhi, Sundus Nsaif Alhuchaimi

Department of Microbiology, College of Medicine, University of Kufa, Najaf, Iraq

ABSTRACT

Introduction and aim. Hashimoto's thyroiditis (HT) is the leading cause of hypothyroidism, yet its diagnosis relies on markers with known limitations. Bruton's tyrosine kinase (Btk) and nuclear factor kappa B (NF-κB) are implicated in B-cell-mediated autoimmunity. This study aimed to explore the serum levels and preliminary diagnostic potential of Btk and NF-κB in Iraqi patients with HT.

Material and methods. In this case-control study, 30 HT patients, 30 non-autoimmune hypothyroidism patients, and 60 healthy controls were enrolled from three centers in Karbala, Iraq. HT was defined by elevated TSH (>4.2 μIU/mL), reduced fT4 (<0.93 ng/dL), and positive anti-TPO and/or anti-Tg, whereas non-autoimmune hypothyroidism was defined by elevated TSH and low fT4 with negative thyroid autoantibodies. Serum Btk and NF-κB were measured by enzyme-linked immunosorbent assay. Thyroid hormones and autoantibodies were determined by electrochemiluminescence immunoassay. Receiver operating characteristic (ROC) analysis was performed to assess preliminary diagnostic accuracy for distinguishing HT from non-autoimmune hypothyroidism and healthy controls.

Results. Serum Btk and NF-κB levels were significantly elevated in HT patients compared to both control groups (Btk: 7.81±0.98 vs. 7.00±0.77 vs. 6.10±1.60 ng/mL; NF-κB: 1.90±0.71 vs. 0.91±0.21 vs. 0.84±0.39 ng/mL, $p<0.001$). In ROC analysis, NF-κB showed an area under the curve (AUC) of 0.95 (95% CI: 0.89–0.99) for discriminating HT from non-autoimmune hypothyroidism. Both biomarkers correlated positively with anti-TPO, anti-Tg, and TSH, and negatively with fT4.

Conclusion. Serum Btk and NF-κB were elevated in HT and showed preliminary associations with autoimmune activity. NF-κB, in particular, demonstrated promising initial diagnostic performance. These exploratory findings require validation in larger, independent cohorts.

Keywords. aortic stiffness, autonomic recovery, carotid–femoral pulse wave velocity, heart rate recovery, heart rate variability, submaximal aerobic exercise

Introduction

Hashimoto's thyroiditis (HT), also known as chronic lymphocytic thyroiditis, is the most common autoimmune thyroid disease and the leading cause of hypothyroidism in iodine-sufficient regions worldwide.[1,2]

As one of the most prevalent organ-specific autoimmune disorders, HT affects an estimated 5–10% of the global population, with a striking predilection for women, who are diagnosed five to ten times more frequently than men, particularly between the ages of 45 and 65.[3,4]

The disease is characterized by a progressive breakdown of self-tolerance to thyroid antigens, leading to a chronic inflammatory state within the thyroid gland. This autoimmune assault is mediated by both cellular and humoral immune responses, involving extensive infiltration of the thyroid parenchyma by T and B

Corresponding author: Huda Mohammed Abdul-Ridha Muhi, hudam.aljanabi@student.uokufa.edu.iq

Received: 12.03.2026 / Revised: 9.04.2026 / Accepted: 13.04.2026 / Published: 30.06.2026

Muhi HMA-R, Alhuchaim SN. Serum Bruton's tyrosine kinase and NF-κB in Hashimoto's thyroiditis – a case-control study of potential diagnostic biomarkers. *Eur J Clin Exp Med.* 2026;24(2):370–379. doi: 10.15584/ejcem.2026.2.17.

lymphocytes and the production of characteristic autoantibodies against thyroid peroxidase (anti-TPO) and thyroglobulin (anti-Tg).[5,6] Ultimately, this sustained inflammation results in the apoptotic destruction of thyroid follicular cells, culminating in glandular failure and clinical hypothyroidism.[3]

The pathogenesis of HT is complex and multifactorial, arising from a sophisticated interplay of genetic susceptibility and environmental triggers.[5] The immune response in HT involves a diverse array of immune cells, including Th1, Th2, Th17, and regulatory T (Treg) cells, which orchestrate the inflammatory cascade.[3]

Systemic inflammatory markers such as the neutrophil-to-lymphocyte ratio (NLR) and platelet-to-lymphocyte ratio (PLR) have been proposed as accessible indicators of immune/inflammatory activity in Hashimoto's thyroiditis.[7] Furthermore, HT is associated with various inflammatory indices such as the DeRitis score, red cell distribution width, uric acid to HDL cholesterol ratio, HALP and SII indexes, and C-reactive protein to lymphocyte count ratio.[8-13] Central to this process is the activation of B lymphocytes, which not only differentiate into plasma cells to produce thyroid autoantibodies but also function as potent antigen-presenting cells, further perpetuating the autoimmune cycle by activating autoreactive T cells.[14]

Given the pivotal role of B cells and the strong inflammatory component in the pathogenesis of HT, key signaling molecules that govern their activation and function have emerged as areas of investigation. One such molecule is Bruton's tyrosine kinase (Btk), a non-receptor tyrosine kinase that serves as a component of the B-cell receptor (BCR) signaling pathway.[15] Btk is also strongly associated with inflammation.[16] Upon BCR engagement, Btk is activated and initiates a downstream signaling cascade that is essential for B-cell proliferation, differentiation, survival, and antibody production.[17] Dysregulation of Btk signaling has been implicated in various B-cell malignancies and a growing number of autoimmune diseases, making it a subject of therapeutic interest.[16,18]

A crucial downstream effector of the Btk-mediated signaling cascade is the nuclear factor kappa B (NF-κB) family of transcription factors.[19] NF-κB is a master regulator of the immune and inflammatory responses, controlling the expression of hundreds of genes involved in lymphocyte development, activation, and cell survival.[20,21] The NF-κB pathway is intrinsically linked to inflammation and is activated in numerous conditions.[22] The canonical pathway of NF-κB activation is initiated by various stimuli, including BCR signaling, and typically involves the phosphorylation and degradation of the inhibitor of κB (IκB), allowing the p50/p65 NF-κB heterodimer to translocate to the nucleus and drive gene expression.[23] A direct mechanistic link has been established wherein Btk is required for BCR-induced NF-κB activation, in part through the direct phosphorylation of IκB-α by Btk.[24] Given that deregulated NF-κB activity is a hallmark of many chronic inflammatory and autoimmune conditions, the Btk/NF-κB signaling axis represents a highly relevant pathway in the immunopathology of HT.[20,21,23]

Despite the high prevalence of HT, its diagnosis still relies primarily on the measurement of serum TSH and thyroid autoantibodies (anti-TPO and anti-Tg). While these markers are valuable, they have recognized limitations; for instance, a subset of patients may be seronegative, and antibody titers do not always correlate with disease severity or progression.[6,25] This underscores the need for investigation of additional biomarkers that may reflect the underlying molecular pathology.[26,27]

Aim

This study was designed to investigate the serum levels of Btk and NF-κB in Iraqi patients with Hashimoto's thyroiditis and to explore their potential as diagnostic biomarkers in a preliminary, exploratory analysis. We hypothesized that the levels of these two key signaling molecules would be significantly elevated in HT patients compared to patients with non-autoimmune hypothyroidism and healthy controls, reflecting the underlying B-cell activation and inflammation central to the disease.

Material and methods

Study design and ethical approval

This case-control study was conducted from July 10, 2025, to February 10, 2026. The study protocol was reviewed and approved by the Research Ethics Committee at the College of Medicine, University of Kufa, Najaf, Iraq (Approval No.: 4540/2025). All procedures involving human participants were performed in accordance with the ethical standards of the institutional and national research committee and with the 1964 Helsinki Declaration and its later amendments. Written informed consent was obtained from all individual participants prior to enrollment.

Study population and participant recruitment

A total of 120 participants were enrolled in this study using a consecutive sampling method from three clinical centers in Karbala Governorate, Iraq: the Al-Hassan Center for Endocrinology and Diabetes, Al-Hindiya General Hospital, and Al-Hussein Teaching Hospital. Patients attending the outpatient endocrinology clinics at these centers during the study period who met the inclusion criteria were invited to participate. Healthy controls were recruited from hospital staff and accompanying people at the same centers who volunteered after screening confirmed euthyroid status and negative

autoantibody results. Participants were divided into three groups:

Hashimoto's thyroiditis (HT) group (n=30): Patients diagnosed with HT based on clinical and biochemical criteria, including elevated serum thyroid-stimulating hormone (TSH) levels (>4.2 μIU/mL), decreased free thyroxine (fT4) levels (<0.93 ng/dL), and the presence of high titers of thyroid autoantibodies (anti-TPO and/or anti-Tg).[6]

Non-Hashimoto's hypothyroidism (non-HT) group (n=30): Patients with primary hypothyroidism characterized by elevated TSH and low fT4 levels but with negative results for both anti-TPO and anti-Tg autoantibodies, thereby excluding an autoimmune etiology.

Healthy controls (n=60): Euthyroid, apparently healthy individuals with no personal or family history of thyroid disease or other autoimmune disorders, with normal thyroid function tests and negative thyroid autoantibody status.

Exclusion criteria for all groups included pregnancy, a history of thyroid surgery or radioiodine therapy, acute or chronic inflammatory diseases, severe systemic illness, malignancy, and the use of medications known to interfere with thyroid function or immune status (e.g., amiodarone, lithium, corticosteroids).

It should be noted that a proportion of patients in both the HT group (73.33%) and the non-HT group (70.00%) were receiving levothyroxine replacement therapy at the time of enrollment. As this was a cross-sectional observational study, treatment was not discontinued for ethical reasons. The potential influence of levothyroxine on the measured biomarkers is addressed in the limitations section.

For each participant, demographic data including age, sex, smoking status, and family history of thyroid disease were collected using a structured questionnaire. Anthropometric measurements, including height and weight, were taken to calculate the body mass index (BMI), which was classified according to World Health Organization criteria.[28]

Blood sample processing

From each participant, 5 mL of venous blood was collected under aseptic conditions into a plain gel-separator tube between 08:00 and 10:00 AM after an overnight fast. The blood was allowed to clot at room temperature for 30 minutes and then centrifuged at 3000 rpm for 15 minutes. The resulting serum was carefully separated, aliquoted into sterile labeled Eppendorf tubes, and stored at −20°C until the time of analysis. The interval from phlebotomy to serum freezing was approximately 45–60 minutes. All samples were analyzed within four weeks of collection to ensure analyte stability. Repeated freeze–thaw cycles were avoided.

Hormonal and autoantibody analysis

Serum levels of TSH, T3, fT4, anti-TPO, anti-Tg, and thyroglobulin (Tg) were quantitatively determined using a fully automated Cobas e 411 immunoassay analyzer (Roche Diagnostics, Mannheim, Germany). This system utilizes electrochemiluminescence immunoassay (ECLIA) technology. The specific commercial kits used were: TSH (Elecsys TSH, REF 07027921190), T3 (Elecsys T3, REF 07027956190), fT4 (Elecsys FT4 III, REF 06368611190), anti-TPO (Elecsys Anti-TPO, REF 06368590190), anti-Tg (Elecsys Anti-Tg, REF 09004998160), and Tg (Elecsys Tg II, REF 08906564190). All assays were performed according to the manufacturer's instructions. The instrument was calibrated, and quality control materials were run daily to ensure accuracy and precision.

Biomarker analysis by ELISA

Serum concentrations of Btk and NF-κB were measured using quantitative sandwich enzyme-linked immunosorbent assay (ELISA) kits from Bioassay Technology Laboratory (BT LAB, Shanghai, China). The Human Btk ELISA Kit (Cat. No.: E0708Hu; detection range: 0.05–35 ng/mL; sensitivity: 0.02 ng/mL; intra-assay CV <8%; inter-assay CV <10%) and the Human NF-κB ELISA Kit (Cat. No.: E0690Hu; detection range: 0.03–10 ng/mL; sensitivity: 0.01 ng/mL; intra-assay CV <8%; inter-assay CV <10%) were used. These kits measure total protein concentrations in serum. Additional technical details, including lot numbers and calibration data, are provided in the Supplementary Material.

All ELISA measurements were performed in duplicate, and the mean value was used for analysis. Laboratory personnel performing the ELISA assays were blinded to the clinical group assignment of the samples. The optical density was measured at 450 nm using a microplate reader, and biomarker concentrations were determined by interpolation from a standard curve.

Statistical analysis

All statistical analyses were performed using SPSS version 25.0 (IBM Corp., Armonk, NY, USA). Data were expressed as mean±standard deviation (SD) for continuous variables and as numbers (n) and percentages (%) for categorical variables. For non-normally distributed variables (e.g., TSH, anti-TPO, anti-Tg), median and interquartile range (IQR) were additionally reported. The normality of data distribution was assessed using the Shapiro–Wilk test.

For normally distributed continuous variables, differences between two independent groups were analyzed using the independent-samples Student's t-test. For comparisons among the three groups, one-way analysis of variance (ANOVA) was performed, followed by the Tukey honestly significant difference (HSD) post-

hoc test for pairwise comparisons. For variables that did not meet the assumption of normality, the Mann–Whitney U test was used for two-group comparisons and the Kruskal–Wallis H test for three-group comparisons. A global p-value across the three groups was reported first, followed by post-hoc pairwise comparisons. Categorical data were compared using the chi-square ($\chi 2$) test or Fisher's exact test, as appropriate.

Spearman's rank correlation coefficient (ρ) was used to assess relationships between continuous variables, as this method is robust to non-normality, outliers, and non-linear relationships. Receiver operating characteristic (ROC) curve analysis was performed to evaluate the preliminary diagnostic performance of Btk and NF-κB. The area under the curve (AUC), sensitivity, specificity, positive predictive value (PPV), negative predictive value (NPV), and optimal cutoff values (determined by the Youden index) were calculated. A combined biomarker model was also evaluated using predicted probabilities from logistic regression. Cohen's d effect sizes were calculated for between-group comparisons. Multivariable logistic regression was performed to assess the independent association of Btk and NF-κB with HT status after adjusting for potential confounders. Given the exploratory nature of this study and the relatively small sample size, no formal correction for multiple comparisons was applied; however, this is acknowledged as a limitation. A two-tailed p-value of <0.05 was considered statistically significant for all tests.

Results

Table 1 summarizes the baseline demographic and clinical characteristics across the three groups (HT, n=30; non-HT, n=30; controls, n=60). Mean age and the distribution of age categories were comparable between groups (p>0.05), and sex distribution did not differ significantly, with females predominating in all groups (p>0.05). Smoking status was similar between HT and non-HT (p>0.05) but differed between HT and controls, as all controls were non-smokers compared with 13.3% smokers in HT (p=0.01). A family history of hypothyroidism was markedly higher in HT than controls (66.7% vs. 3.3%, p<0.001), while no significant difference was observed between HT and non-HT (p>0.05). Levothyroxine use did not differ significantly between HT and non-HT (p>0.05).

Table 1A. Potential confounding factors and analytical adjustments

Confounder	Measured/Reported	Adjusted in analysis
Age	Yes	Yes (logistic regression)
BMI	Yes	Yes (logistic regression)
Smoking status	Yes	No (acknowledged as limitation)
Levothyroxine use	Yes	No (acknowledged as limitation)
Iodine status	No	No (not collected)

Table 1B. Demographic and clinical characteristics of Hashimoto's thyroiditis patients compared with non-Hashimoto's hypothyroidism patients and healthy controls*

Characteristic	HT (n=30)	Non-HT (n=30)	Controls (n=60)	p#	Post-hoc
Age (years), mean±SD	38.70±15.80	43.90±17.50	39.8±12.9	NS	–
Sex, female n (%)	25 (83.33)	27 (90.00)	47 (78.33)	NS	–
Sex, male n (%)	5 (16.67)	3 (10.00)	13 (21.67)		
Smoking, n (%)	4 (13.33)	4 (13.33)	0 (0)	0.01	HT vs. C: 0.01
Family history (+), n (%)	20 (66.67)	18 (60.00)	2 (3.33)	<0.001	HT vs. C: <0.001
Levothyroxine use, n (%)	22 (73.33)	21 (70.00)	–	NS	–
Age 20–39, n	17	12	40	NS	–
Age 40–59, n	10	10	12		
Age 60–75, n	3	8	8		

* # – Kruskal–Wallis or chi-square across three groups, Post-hoc – pairwise comparisons, NS – not significant (p>0.05), C – controls

Table 2 compares BMI and simplified BMI categories across groups. Mean BMI was significantly higher in HT (29.1±5.32 kg/m²) than controls (23.4±3.71 kg/m²; p<0.001), while HT and non-HT did not differ significantly (p>0.05). Overweight and obesity comprised 80% of HT patients, whereas most controls had normal BMI.

Table 2. Comparison of BMI and simplified BMI classification in Hashimoto's thyroiditis patients versus non-Hashimoto's hypothyroidism patients and healthy controls*

Characteristic	HT (n=30)	Non-HT (n=30)	Controls (n=60)	p#	Post-hoc
BMI (kg/m²), mean±SD	29.1±5.32	27.10±4.78	23.4±3.71	<0.001	HT vs. C: <0.001
Underweight, n	0	2	10	<0.001	HT vs. C: <0.001
Normal, n	6	5	32		
Overweight/Obese, n	24	23	18		

* # – Kruskal–Wallis or chi-square across three groups, Post-hoc – pairwise comparisons, NS – not significant (p>0.05), C – controls, BMI categories collapsed into underweight, normal, and overweight/obese to avoid sparse cell violations in chi-square analysis

Thyroid function and autoantibodies

Table 3 details the thyroid function tests and autoantibody profiles. Both HT and non-HT groups exhibited elevated TSH relative to controls (global p<0.001). TSH showed a median (IQR) of 10.50 (6.80–19.25) μIU/mL in HT, 9.10 (7.20–12.30) μIU/mL in non-HT, and 2.05 (1.60–2.70) μIU/mL in controls. Anti-TPO was markedly higher in HT (854±717 IU/mL) than in non-HT (8.72±6.91 IU/mL) and controls (5.47±3.56 IU/mL) (both p<0.001). Anti-Tg was also significantly higher in HT (193±150 IU/mL) versus non-HT (33.3±24.9 IU/mL) and controls (16.3±13.0 IU/mL) (both p<0.001).

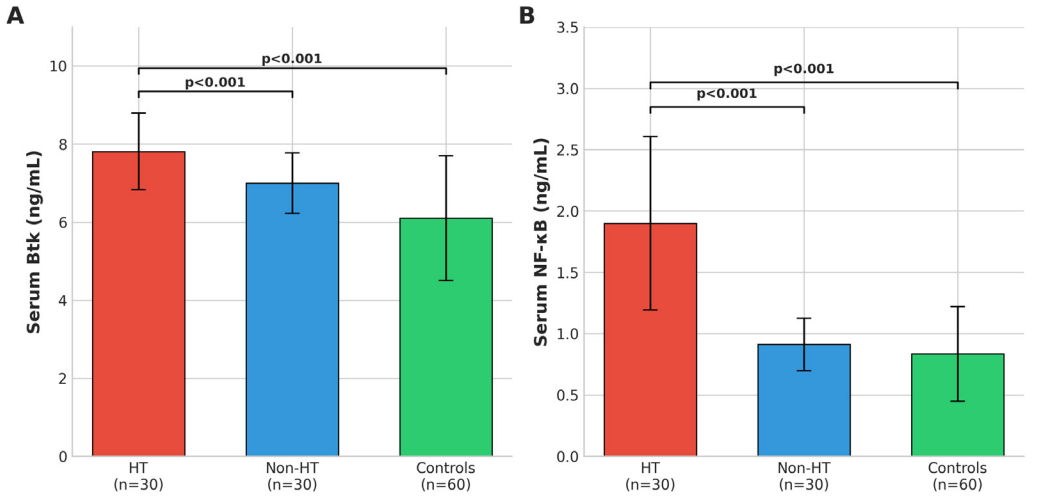

Fig. 1. Comparison of serum Bruton's tyrosine kinase (Btk) and nuclear factor kappa B (NF-κB) levels among Hashimoto's thyroiditis patients, non-Hashimoto's hypothyroidism patients, and healthy controls, A: Serum Btk levels, B: Serum NF-κB levels, data are expressed as mean±SD, ***p<0.001

Table 3. Thyroid function tests and autoantibody profiles in Hashimoto's thyroiditis patients compared with non-Hashimoto's hypothyroidism patients and healthy controls

Parameter	HT (n=30)	Non-HT (n=30)	Controls (n=60)	p#	Post-hoc
TSH (μIU/mL), mean±SD	15.80±14.4	9.70±3.21	2.17±0.76	<0.001	HT vs. C: <0.001; HT vs. nHT: 0.038
TSH, median (IQR)	10.50 (6.80–19.25)	9.10 (7.20–12.30)	2.05 (1.60–2.70)		
T3 (ng/mL)	1.29±0.44	1.46±0.62	1.22±0.34	NS	–
fT4 (ng/dL)	0.99±0.29	1.06±0.27	1.26±0.20	<0.001	HT vs. C: <0.001
Anti-TPO (IU/mL), mean±SD	854±717	8.72±6.91	5.47±3.56	<0.001	HT vs. nHT: <0.001; HT vs. C: <0.001
Anti-TPO, median (IQR)	620 (280–1200)	6.50 (3.80–12.40)	4.20 (2.50–7.80)		
Anti-Tg (IU/mL)	193±150	33.3±24.90	16.30±13.0	<0.001	HT vs. nHT: <0.001; HT vs. C: <0.001

* # – ANOVA or Kruskal–Wallis, Post-hoc – pairwise comparisons, NS – not significant (p>0.05), C – controls, median (IQR) reported for non-normally distributed variables, nHT – non-HT

Table 4. Serum levels of Bruton's tyrosine kinase (Btk) and nuclear factor kappa B (NF-κB) across study groups*

Parameter	HT (n=30)	Non-HT (n=30)	Controls (n=60)	p#	Post-hoc
Btk (ng/mL)	7.81±0.98	7.00±0.77	6.10±1.60	<0.001	HT vs. nHT: <0.001; HT vs. C: <0.001
NF-κB (ng/mL)	1.90±0.707	0.912±0.213	0.835±0.386	<0.001	HT vs. nHT: <0.001; HT vs. C: <0.001

* # – ANOVA across three groups

Serum Btk and NF-κB levels

Table 4 shows significant elevation of both Btk and NF-κB in HT. Serum Btk was higher in HT (7.81±0.98 ng/mL) than non-HT (7.00±0.77 ng/mL; p<0.001) and controls (6.10±1.60 ng/mL; p<0.001). Serum NF-κB was also elevated in HT (1.90±0.707 ng/mL) versus non-HT (0.912±0.213 ng/mL; p<0.001) and controls (0.835±0.386 ng/mL; p<0.001). Cohen's d effect sizes were large for both biomarkers: Btk (HT vs. non-HT: d=0.92; HT vs. controls: d=1.29) and NF-κB (HT vs. non-HT: d=1.89; HT vs. controls: d=1.87) (Figure 4).

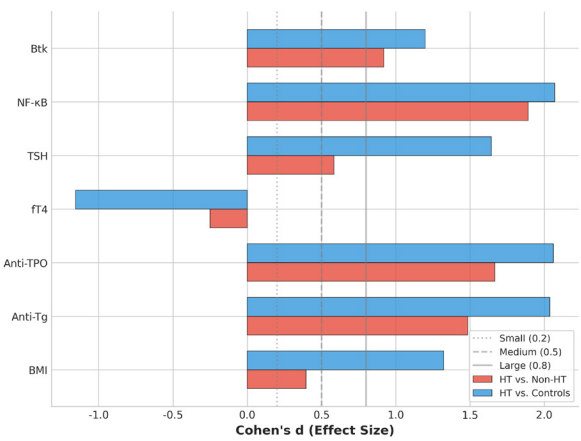

Fig. 2. Forest plot of Cohen's d effect sizes for clinical parameters and biomarkers comparing Hashimoto's thyroiditis (HT) patients to non-HT patients and healthy controls, error bars represent 95% confidence intervals

Correlations between biomarkers and clinical parameters

Table 5 shows that, within HT patients, both Btk and NF-κB correlated with disease-related hormonal and autoimmune markers using Spearman's rank correlation coefficient (ρ). Both biomarkers were negatively correlated with age (Btk: ρ=−0.59, p<0.001; NF-κB: ρ=−0.89, p<0.001). Both biomarkers correlated positively with TSH (Btk: ρ=0.45, p=0.013; NF-κB: ρ=0.47,

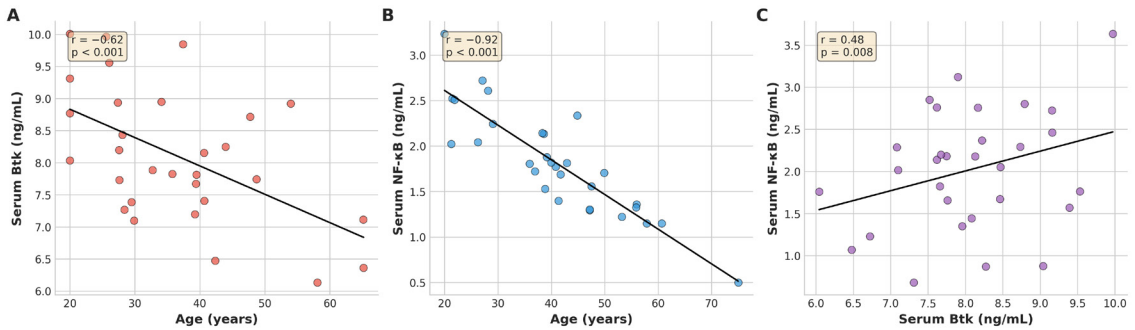

Fig. 3. Correlation analyses of serum Btk and NF-κB with age and their inter-biomarker relationship in Hashimoto's thyroiditis patients (n=30), A: Btk vs. age, B: NF-κB vs. age, C: Btk vs. NF-κB, Spearman correlation coefficients (ρ) and p-values are shown

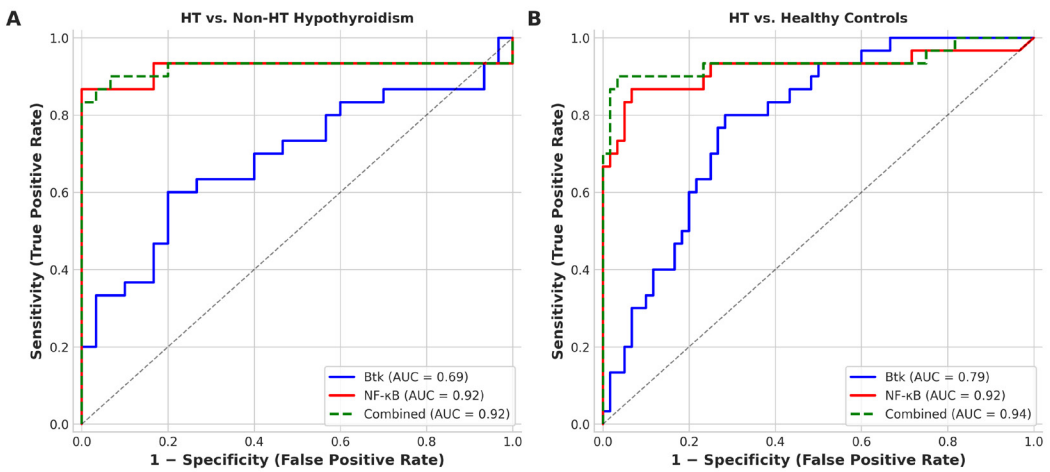

Fig. 4. Receiver operating characteristic (ROC) curves for serum Btk and NF-κB in discriminating Hashimoto's thyroiditis from non-Hashimoto's hypothyroidism and healthy controls, A: HT vs. Non-HT, B: HT vs. Controls, the combined model (Btk + NF-κB) is shown in green, AUC – area under the curve

p=0.009) and negatively with fT4 (all p<0.05). Strong positive correlations were observed with anti-TPO and anti-Tg (all p<0.001). Btk correlated positively with NF-κB (ρ=0.45, p=0.013) (Figure 3).

Table 5. Spearman's rank correlations between Btk, NF-κB, and clinical parameters in HT patients (n=30)

Variable	Btk (ρ)	Btk (P)	NF-κB (ρ)	NF-κB (P)
Age (years)	−0.59	<0.001	−0.89	<0.001
BMI (kg/m^2)	0.12	NS	0.08	NS
TSH (μIU/mL)	0.45	0.013	0.47	0.009
T3 (ng/mL)	−0.42	0.021	−0.35	0.058
fT4 (ng/dL)	−0.34	0.066	−0.47	0.009
Anti-TPO (IU/mL)	0.72	<0.001	0.82	<0.001
Anti-Tg (IU/mL)	0.63	<0.001	0.68	<0.001
Tg (ng/mL)	0.78	<0.001	0.66	<0.001
Btk vs. NF-κB	0.45	0.013	0.45	0.013

Spearman's rank correlation coefficient (ρ), NS – not significant (p>0.05)

Diagnostic performance of Btk and NF-κB

To determine whether Btk and NF-κB were independently associated with HT, a multivariable logistic regression analysis was performed (Table 6). Even after adjusting for age, BMI, TSH, fT4, anti-TPO, and anti-Tg, both Btk (β=0.563, p<0.05) and NF-κB (β=1.106, p<0.05) remained significant independent predictors of HT.

Table 6. Multivariable logistic regression analysis predicting Hashimoto's thyroiditis status (HT vs. non-HT)*

Predictor	Coefficient (β)	p
Age	−0.037	NS
BMI	0.037	NS
TSH	1.094	<0.05
fT4	−0.074	NS
Anti-TPO	1.478	<0.05
Anti-Tg	1.509	<0.05
Btk	0.563	<0.05
NF-κB	1.106	<0.05

* NS – not significant (p>0.05), dependent variable: HT status (1=HT, 0=non-HT)

ROC curve analysis was performed to evaluate the preliminary diagnostic performance of Btk and NF-κB (Table 7, Figure 4). For distinguishing HT from non-HT patients, NF-κB achieved an AUC of 0.95 (95% CI: 0.89–0.99; p<0.001) at a cutoff point of 1.26 ng/mL, with 82% sensitivity and 97% specificity. Btk yielded an AUC

of 0.75 (95% CI: 0.62–0.87; p=0.001) at a cutoff point of 7.62 ng/mL, with 62.1% sensitivity and 80% specificity. A combined model incorporating both Btk and NF-κB improved the diagnostic accuracy to an AUC of 0.94 (95% CI: 0.88–0.99), with 90.0% sensitivity and 93.3% specificity. For HT versus controls, NF-κB achieved an AUC of 0.94 (95% CI: 0.89–0.98; p<0.001). The combined model for HT vs. controls yielded an AUC of 0.91 (95% CI: 0.85–0.98).

Table 7. Receiver operating characteristic (ROC) analysis of Btk and NF-κB for discriminating Hashimoto's thyroiditis*

Comparison/ Biomarker	AUC (95% CI)	Cutoff point	Sensitivity (%)	Specificity (%)	p
HT vs. Non-HT					
Btk	0.75 (0.62–0.87)	>7.62 ng/mL	62.1	80.0	0.001
NF-κB	0.95 (0.89–0.99)	>1.26 ng/mL	82.0	97.0	<0.001
Combined (Btk + NF-κB)	0.94 (0.88–0.99)	—	90.0	93.3	<0.001
HT vs. Controls					
Btk	0.82 (0.73–0.91)	>7.12 ng/mL	83.0	75.0	<0.001
NF-κB	0.94 (0.89–0.98)	>1.08 ng/mL	93.0	82.0	<0.001

* AUC – area under the curve, CI – confidence interval, Cutoff points determined by Youden index, combined model based on predicted probabilities from logistic regression

Discussion

This study investigated the serum levels of Btk and NF-κB in an Iraqi cohort of patients with HT,, and healthy controls. Our results reveal a significant association of both Btk and NF-κB with the autoimmune process of the disease. Furthermore, preliminary ROC analysis indicated initial diagnostic potential for these biomarkers, particularly NF-κB, in distinguishing HT from both non-autoimmune hypothyroidism and healthy individuals. These findings, when contextualized with the existing literature, provide insights into the molecular mechanisms driving HT and suggest avenues for further investigation.

The central finding of our study is the elevation of serum Btk and NF-κB in HT patients. This aligns with emerging evidence implicating the Btk/NF-κB signaling axis in various autoimmune disorders.[16,29] A recent bioinformatic and clinical validation study by Liu et al. identified Btk as a key immune-related biomarker in HT, demonstrating its increased expression in peripheral blood mononuclear cells and a significant positive correlation with thyroid autoantibodies.[30] Our results provide supporting evidence at the serum protein level in a distinct ethnic population. Similarly, the elevated NF-κB levels in our HT cohort are consistent with a recent Turkish study by Yardim et al., which reported on serum NF-κB levels in HT patients and found a positive correlation with anti-TPO antibodies.[31] The activation of the NF-κB pathway is considered a critical step in the inflammatory cascade of thyroid autoimmunity.[20,32]

The observation that Btk levels in non-HT patients were significantly lower than in HT patients, yet slightly higher than in healthy controls, may reflect a generalized, non-specific inflammatory state associated with hypothyroidism itself, independent of autoimmunity. This is supported by previous research indicating that hypothyroidism can induce a state of low-grade systemic inflammation.[33] However, because Btk is an intracellular kinase, measuring its concentration in serum does not directly reflect its intracellular enzymatic activity; rather, elevated serum levels likely represent increased immune cell turnover, apoptosis, or active secretion during inflammatory responses.

A noteworthy finding is the positive correlation between Btk and NF-κB levels (ρ=0.45, p=0.013) within HT patients. This provides clinical evidence consistent with the mechanistic link established in molecular studies, where Btk acts as a critical upstream kinase in the BCR signaling pathway that activates NF-κB.[24,34] Upon BCR engagement by an autoantigen, Btk is activated and subsequently phosphorylates downstream targets, including the IκB kinase complex, which leads to the degradation of the IκB inhibitor and the translocation of NF-κB to the nucleus.[24,35] This activation cascade promotes B-cell proliferation, differentiation into plasma cells, and autoantibody production.[29,36] Our results are consistent with this model, as we observed significant positive correlations between both Btk and NF-κB and the levels of anti-TPO and anti-Tg antibodies. This suggests that the Btk/NF-κB axis may be associated with the humoral autoimmune response that characterizes Hashimoto's thyroiditis.

It is important to note, however, that NF-κB is a highly non-specific marker of inflammation, activated in a wide array of physiological and pathological conditions; thus, its elevation in HT, while significant, is not unique to this specific autoimmune disease.[19,22] This non-specificity should be considered when interpreting the diagnostic performance of NF-κB reported in this study.

The preliminary ROC analysis suggested that NF-κB may have diagnostic value in discriminating HT patients from both non-HT hypothyroid patients (AUC=0.95) and healthy controls (AUC=0.94). Importantly, a combined biomarker model incorporating both Btk and NF-κB yielded the highest diagnostic accuracy (AUC=0.94 for HT vs. non-HT), suggesting that a multi-marker approach may provide superior discriminatory power. However, these results should be interpreted with caution given the relatively small sample size (n=30 per patient group), the absence of an independent validation cohort, and the potential for overfitting in small datasets. The use of a case-control design with clinically distinct groups often overestimates di-

agnostic accuracy compared to a prospective cohort of consecutive patients with diagnostic uncertainty. Therefore, the reported AUC values and diagnostic thresholds (cutoff points) should be considered exploratory and hypothesis-generating rather than definitive clinical recommendations.

To establish the true clinical utility of these biomarkers, future studies must validate these cutoff points in independent, external cohorts. Such validation should ideally employ a prospective design in a diverse population presenting with undifferentiated thyroid dysfunction, allowing for the calculation of positive and negative predictive values in a real-world clinical setting.

Our demographic and clinical findings are largely consistent with the established epidemiology of Hashimoto's thyroiditis, both globally and within the Iraqi context. The significant female predominance (83.33%) in our HT cohort mirrors the findings of numerous Iraqi studies, including those by Al-Zamali et al. and Mansour et al., which reported approximately 83% female prevalence in hypothyroidism cases.[37-39] This strong gender bias is a well-documented hallmark of autoimmune thyroid disease worldwide.[40] Furthermore, our finding that a significant proportion of HT patients (66.67%) had a positive family history of hypothyroidism aligns with the known strong genetic component of the disease, with heritability estimates as high as 75%.[41]

This study confirms the well-established association between Hashimoto's thyroiditis and increased body mass index. Our HT patients had a significantly higher mean BMI compared to healthy controls, and 80% were classified as overweight or obese. This is consistent with several Iraqi studies that have linked hypothyroidism and HT with higher BMI.[33,42,43] The relationship between obesity and thyroid autoimmunity is considered bidirectional: chronic low-grade inflammation associated with obesity, driven by adipokines and pro-inflammatory cytokines, can trigger or exacerbate autoimmune responses, while the metabolic slowdown in hypothyroidism can contribute to weight gain.[44-46]

The inverse correlation with age ($\rho=-0.59$ for Btk and $\rho=-0.89$ for NF-κB) is an interesting finding that warrants further investigation, as it may suggest a more aggressive inflammatory phenotype in younger HT patients, consistent with some epidemiological observations.[47]

Study limitations

This study has several important limitations that must be acknowledged. First, the cross-sectional design precludes any definitive conclusions regarding causality; we can only report associations between biomarker levels and disease status. Second, the sample size is relatively small (30 patients per group), which limits the statistical power, particularly for subgroup analyses, and increases the risk of overfitting in the ROC models. Third, participants were recruited from three centers within a single governorate (Karbala, Iraq), which may not be representative of the broader population. Fourth, no independent external validation cohort was used to confirm the ROC-derived diagnostic thresholds; therefore, the reported performance metrics may be overestimated. Fifth, important potential confounding variables, including smoking status and ongoing levothyroxine therapy, were not adjusted for in the primary analyses, and their influence on biomarker levels cannot be excluded. No multivariable adjustment was performed for BMI, smoking, and levothyroxine treatment, and this may have influenced the observed biomarker differences. Sixth, data on certain environmental factors, such as iodine status and vitamin D levels, as well as detailed clinical severity indices, were not collected. Seventh, while we demonstrated a correlation between Btk and NF-κB, our study did not involve direct molecular techniques to confirm the phosphorylation cascade in patient cells. Eighth, the reliance on commercial ELISA kits without extensive in-house validation of intra/inter-assay variability and matrix effects for these specific novel analytes introduces potential measurement error. Finally, the exploratory nature of this biomarker study means that the findings should be regarded as preliminary.

Conclusion

This exploratory study provides preliminary evidence that serum levels of Bruton's tyrosine kinase (Btk) and nuclear factor kappa B (NF-κB) are significantly elevated in patients with Hashimoto's thyroiditis compared to both non-autoimmune hypothyroid patients and healthy individuals. NF-κB, alone and in combination with Btk, showed promising initial diagnostic performance in ROC analysis, although these findings require validation in larger, independent cohorts before any conclusions regarding clinical applicability can be drawn. The significant positive correlations observed between Btk/NF-κB levels and thyroid autoantibodies, coupled with their association with a more severe biochemical hypothyroid profile, suggest their involvement in the autoimmune and inflammatory processes central to HT pathogenesis. These results warrant further investigation in adequately powered, prospective studies to confirm the diagnostic value and to explore the potential of the Btk/NF-κB axis as a therapeutic target in Hashimoto's thyroiditis.

Acknowledgments

The authors would like to thank the staff at the Al-Hassan Center for Endocrinology and Diabetes in Karbala, Al-Hindiya General Hospital, and Al-Hussein Teaching Hospital for their assistance in sample collection. We also extend our gratitude to all the patients and volunteers who participated in this study.

Declarations

Funding

The authors declare that no funds, grants, or other support were received during the preparation of this manuscript.

Author contributions

Conceptualization, H.M.A-R.M. and S.N.A-H.; Methodology, H.M.A-R.M. and S.N.A-H.; Formal Analysis, H.M.A-R.M.; Investigation, H.M.A-R.M.; Resources, S.N.A-H.; Data Curation, H.M.A-R.M.; Writing – Original Draft Preparation, H.M.A-R.M.; Writing – Review & Editing, S.N.A-H.; Visualization, H.M.A-R.M.; Supervision, S.N.A-H.; Project Administration, S.N.A-H..

Conflicts of interest

The authors declare no competing interests.

Data availability

The datasets generated during and/or analyzed during the current study are not publicly available due to participant privacy concerns but are available from the corresponding author on reasonable request.

Ethics approval

The protocol was approved by the Research Ethics Committee at the College of Medicine, University of Kufa, Najaf, Iraq (Approval No.: 4540/2025).

Use of AI and AI-assisted technologies in the writing process

During the preparation of this manuscript, the authors used AI-assisted technologies solely for language refinement and grammar checking. The authors reviewed and edited the content as needed and take full responsibility for the content of this publication.

References

1. Vargas-Uricoechea H, Castellanos-Pinedo A, Urrego-Noguera K, Pinzón-Fernández MV, Meza-Cabrera IA, Vargas-Sierra H. A scoping review on the prevalence of Hashimoto's thyroiditis and the possible associated factors. *Med Sci (Basel)*. 2025;13(2):43. doi:10.3390/medsci13020043
2. Kaur J, Jialal I. Hashimoto thyroiditis. StatPearls [Internet]. StatPearls Publishing; 2025.
3. Rydzewska M, Jaromin M, Pasierowska IE, Stożek K, Bossowski A. Role of the T and B lymphocytes in pathogenesis of autoimmune thyroid diseases. *Thyroid Res*. 2018; 11(1):2. doi:10.1186/s13044-018-0046-9
4. Franco JS, Amaya-Amaya J, Anaya JM. Thyroid disease and autoimmune diseases. In: Anaya JM, Shoenfeld Y, Rojas-Villarraga A, eds. Autoimmunity: From Bench to Bedside. Bogota, Colombia: El Rosario University Press; 2013.
5. Ralli M, Angeletti D, Fiore M, et al. Hashimoto's thyroiditis: an update on pathogenic mechanisms, diagnostic protocols, therapeutic strategies, and potential malignant transformation. *Autoimmun Rev*. 2020;19(10):102649. doi:10.1016/j.autrev.2020.102649
6. Caturegli P, De Remigis A, Rose N. Hashimoto thyroiditis: clinical and diagnostic criteria. *Autoimmun Rev*. 2014;13(4-5):391-397. doi:10.1016/j.autrev.2014.01.007
7. Murad R, et al. The role of the neutrophil-to-lymphocyte ratio and the platelet-to-lymphocyte ratio in assessing hypothyroidism Hashimoto's thyroiditis. *Ital J Med*. 2025; 19(2). doi:10.4081/itjm.2025.1953
8. Bilge M, Adas M, Yesilova A, Helvaci A. Platelet-to-lymphocyte ratio and its association with Hashimoto's thyroiditis. *Diseases*. 2023;11(1):15. doi:10.3390/diseases11010015
9. Aktas G, Sit M, Dikbas O, et al. Could red cell distribution width be a marker in Hashimoto's thyroiditis? *Exp Clin Endocrinol Diabetes*. 2014;122(10):572-574. doi:10.1055/s-0034-1383564
10. Aktas G, Duman TT, Atak BM, et al. Irritable bowel syndrome is associated with novel inflammatory markers derived from hemogram parameters. *J Med Biochem*. 2020;39(1):62-66.
11. Bilgin S, Aktas G, Zahid Kocak M, et al. Association between novel inflammatory markers derived from hemogram indices and metabolic parameters in type 2 diabetic men. *Aging Male*. 2020;23(5):923-927. doi:10.1080/13685538.2019.1632283
12. Aktas G, Yilmaz S, Kantarci DB, et al. Is serum uric acid-to-HDL cholesterol ratio elevation associated with Hashimoto's thyroiditis? *Rom J Intern Med*. 2021;59(4):403-408. doi:10.2478/rjim-2021-0023
13. Aktas G, Yildirim M, Akbulut A, et al. HALP and SII indexes in Hashimoto's thyroiditis. *Postgrad Med*. 2026. doi:10.1080/00325481.2026.2621575
14. Crofford LJ, Nyhoff LE, Sheehan JH, Kendall PL. The role of Bruton's tyrosine kinase in autoimmunity and implications for therapy. *Expert Rev Clin Immunol*. 2016; 12(7):763-773. doi:10.1586/1744666X.2016.1152888
15. Mehra S, Nicholls M, Taylor J. The evolving role of Bruton's tyrosine kinase inhibitors in B cell lymphomas. *Int J Mol Sci.* 2024;25(14):7516. doi:10.3390/ijms25147516
16. Neys SF, Hendriks RW, Corneth OB. Targeting Bruton's tyrosine kinase in inflammatory and autoimmune pathologies. *Front Cell Dev Biol*. 2021;9:668131. doi:10.3389/fcell.2021.668131
17. Rip J, Van Der Ploeg EK, Hendriks RW, Corneth OB. The role of Bruton's tyrosine kinase in immune cell signaling and systemic autoimmunity. *Crit Rev Immunol*. 2018;38(1):17-62. doi:10.1615/CritRevImmunol.2018025184
18. Ringheim GE, Wampole M, Oberoi K. Bruton's tyrosine kinase (BTK) inhibitors and autoimmune diseases: making sense of BTK inhibitor specificity profiles and recent clinical trial successes and failures. *Front Immunol.* 2021;12:662223. doi:10.3389/fimmu.2021.662223
19. Guo Q, Jin Y, Chen X, et al. NF-κB in biology and targeted therapy: new insights and translational implications.

Signal Transduct Target Ther. 2024;9(1):53. doi:10.1038/s41392-024-01757-9
20. Giuliani C, Bucci I, Napolitano G. The role of the transcription factor nuclear factor-kappa B in thyroid autoimmunity and cancer. *Front Endocrinol*. 2018;9:471. doi:10.3389/fendo.2018.00471
21. Barnabei L, Laplantine E, Mbongo W, Rieux-Laucat F, Weil R. NF-κB: at the borders of autoimmunity and inflammation. *Front Immunol*. 2021;12:716469. doi:10.3389/fimmu.2021.716469
22. Liu T, Zhang L, Joo D, Sun SC. NF-κB signaling in inflammation. *Signal Transduct Target Ther*. 2017;2(1):1-9. doi:10.1038/sigtrans.2017.23
23. Sun SC, Chang JH, Jin J. Regulation of nuclear factor-κB in autoimmunity. *Trends Immunol.* 2013;34(6):282-289. doi:10.1016/j.it.2013.01.004
24. Pontoriero M, Fiume G, Vecchio E, et al. Activation of NF-κB in B cell receptor signaling through Bruton's tyrosine kinase-dependent phosphorylation of IκB-α. *J Mol Med.* 2019;97(5):675-690. doi:10.1007/s00109-019-01777-y
25. Sharma H, Kakadiya J. Different novel biomarkers involved in diagnosing hypothyroidism. *Egypt J Intern Med*. 2023;35(1):28. doi:10.1186/s43162-023-00211-2
26. Pempera N, Miedziaszczyk M, Lacka K. Difficulties in the diagnostics and treatment of Hashimoto's encephalopathy—a systematic and critical review. *Int J Mol Sci*. 2024;25(13):7101. doi:10.3390/ijms25137101
27. Tywanek E, Michalak A, Świrska J, Zwolak A. Autoimmunity, new potential biomarkers and the thyroid gland—the perspective of Hashimoto's thyroiditis and its treatment. *Int J Mol Sci*. 2024;25(9):4703. doi:10.3390/ijms25094703
28. World Health Organization. Obesity: Preventing and Managing the Global Epidemic. WHO; 2000.
29. Qiao H, Mao Z, Wang W, et al. Changes in the BTK/NF-κB signaling pathway and related cytokines in different stages of neuromyelitis optica spectrum disorders. *Eur J Med Res*. 2022;27(1):96. doi:10.1186/s40001-022-00726-y
30. Liu Y, Zhu Z, Xu Q, et al. Identification of BTK as an immune-related biomarker for Hashimoto's thyroiditis by integrated bioinformatic analysis. *BMC Immunol*. 2025;26(1):11. doi:10.1186/s12865-025-00683-z
31. Yardim M, Deniz L, Saltabas MA, Celik N. Effect of thyroxine replacement therapy on serum maresin 1 and NF-kB levels in patients with Hashimoto thyroiditis. *Diagnostics*. 2025;15(10):1248. doi:10.3390/diagnostics15101248
32. Li X, Abdel-Mageed AB, Mondal D, Kandil E. The nuclear factor kappa-B signaling pathway as a therapeutic target against thyroid cancers. *Thyroid*. 2013;23(2):209-218. doi:10.1089/thy.2012.0237
33. Ghazi SM, Salman AA, Jawad AA. Assessing cardiovascular changes in Iraqi women with hypothyroidism. *J Med Life.* 2023;16(4):579. doi:10.25122/jml-2023-0060
34. Petro JB, Rahman SJ, Ballard DW, Khan WN. Bruton's tyrosine kinase is required for activation of IκB kinase and nuclear factor κB in response to B cell receptor engagement. *J Exp Med.* 2000;191(10):1745-1754. doi:10.1084/jem.191.10.1745
35. Shinners NP, Carlesso G, Castro I, et al. Bruton's tyrosine kinase mediates NF-κB activation and B cell survival by B cell-activating factor receptor of the TNF-R family. *J Immunol.* 2007;179(6):3872-3880. doi:10.4049/jimmunol.179.6.3872
36. Garg N, Padron EJ, Rammohan KW, Goodman CF. Bruton's tyrosine kinase inhibitors: the next frontier of B-cell--targeted therapies for cancer, autoimmune disorders, and multiple sclerosis. *J Clin Med.* 2022;11(20):6139. doi:10.3390/jcm11206139
37. Mansour AA, Ali Alhamza AH, Abdullah Almomin AMS, et al. Patterns of thyroid disease in Basrah, Iraq: retrospective study. *J Endocr Soc.* 2020;4(Suppl 1):SUN-418. doi:10.1210/jendso/bvaa046.1128
38. Kargar S, Tabatabaei SM, Okati-Aliabad H, Rad HI. Prevalence of thyroid dysfunction disorders among adult populations in the Middle-East: a systematic review and meta--analysis. *Open Public Health J*. 2024;17(1). doi:10.2174/0118749445282227240115062556
39. Al-Zamali SKS, Jallod IMS, Mohammed SS, et al. Association between FOXP3 rs2232368 variant and Hashimoto's thyroiditis risk: a case-control study. *Cureus*. 2025;17(2). doi:10.7759/cureus.75421
40. Baranowska-Bik A, Bik W. The association of obesity with autoimmune thyroiditis and thyroid function—possible mechanisms of bilateral interaction. *Int J Endocrinol.* 2020;2020:8894792. doi:10.1155/2020/8894792
41. Bujnis M, DeSalvo K, Neklason DW, Madsen MJ, Jorde LB. Familial risk of Hashimoto's thyroiditis in a large genealogical database. *J Clin Endocrinol Metab*. 2025;110(12):e3998-e4003. doi:10.1210/clinem/dgaf023
42. Tulla S, Azaz S, Khan MSA. Evaluation of BMI in hypothyroid patients and its response to thyroxin therapy. *Eur J Cardiovasc Med*. 2022;12(4).
43. Mustafa MD, Tuama RM. The relationship between hypothyroidism and obesity. *J Coast Life Med*. 2022;10:73-84.
44. Song Rh, Wang B, Yao Qm, Li Q, Jia X, Zhang Ja. The impact of obesity on thyroid autoimmunity and dysfunction: a systematic review and meta-analysis. *Front Immunol*. 2019;10:443404. doi:10.3389/fimmu.2019.02349
45. Huo J, Xu Y, Yu J, et al. Causal association between body mass index and autoimmune thyroiditis: evidence from Mendelian randomization. *Eur J Med Res*. 2023;28(1):526. doi:10.1186/s40001-023-01520-0
46. Duntas LH, Biondi B. The interconnections between obesity, thyroid function, and autoimmunity: the multifold role of leptin. *Thyroid.* 2013;23(6):646-653. doi:10.1089/thy.2012.0524
47. Abdullah YJ, Essa RH, Jumaa MG. Incidence of Hashimoto's thyroiditis and its relationship to age, sex, smoking and blood groups. *NTU J Pure Sci.* 2022;1(2):1-9.

Rzeszów University Press 2026
ISSN 2544-1361 (online)
doi: 10.15584/ejcem.2026.2.18

http://www.ejcem.ur.edu.pl
European Journal of Clinical and Experimental Medicine
Eur J Clin Exp Med 2026;24(2): 380–390

ORIGINAL PAPER

Association between arterial stiffness and autonomic recovery following graded aerobic exercise in healthy young adults – an exploratory pilot study

Amela Kabaklić [1,2], Marko Radolović [3], Timur Mušić [2]

[1] University Medical Center Ljubljana, Department of Hypertension, Dr. Peter Držaj Hospital, Ljubljana, Slovenia
[2] Faculty of Medicine, University of Ljubljana, Ljubljana, Slovenia
[3] Faculty of Electrical Engineering and Computing, University of Zagreb, Zagreb, Croatia

ABSTRACT

Introduction and aim. Arterial stiffness reflects vascular properties that can influence blood pressure (BP) and heart rate (HR) responses to exercise, but its association with post-exercise autonomic recovery in healthy young adults remains unclear. This exploratory pilot study investigated the relationship between baseline aortic stiffness and post-exercise hemodynamic and autonomic recovery following graded submaximal aerobic exercise.

Material and methods. Thirty healthy young adults (17 women, 13 males; mean age 22.7±2.5 years) underwent baseline evaluation of carotid–femoral pulse wave velocity (cf-PWV), central BP, and pulse wave analysis. Participants completed a graded submaximal cycling protocol from 20 to 80% of the maximum oxygen uptake in 3-minute stages, followed by 5 minutes of seated recovery. HR was continuously recorded and BP measured at 1, 3, and 5 minutes of recovery. Autonomic recovery was assessed using heart rate recovery (HRR) and heart rate variability (HRV) indices. Associations were analyzed using correlation and multivariate linear regression adjusted for age, sex, and body mass index.

Results. Higher baseline cf-PWV was associated with higher peak HR and systolic BP during exercise ($p<0.01$), and slower HRR at 1 min ($r=-0.517$, $p=0.002$). Cf-PWV independently predicted early HRR after adjustment.

Conclusion. In this pilot sample of healthy young adults, greater aortic stiffness was associated with higher BP responses during exercise and slower early autonomic recovery. These findings suggest an association between vascular properties and early postexercise recovery, which should be confirmed in larger studies.

Keywords. aortic stiffness, carotid–femoral pulse wave velocity, autonomic recovery, heart rate variability, heart rate recovery, submaximal aerobic exercise

Abbreviations

AIx – augmentation index, **AIx@75** – heart rate–corrected augmentation index, **AP** – augmentation pressure, **BMI** – body mass index, **BP** – blood pressure, **cDBP** – central diastolic blood pressure, **cf-PWV** - carotid - femoral pulse wave velocity, **cSBP** – central systolic blood pressure, **DBP** – diastolic blood pressure, **ECG** – electrocardiogram, **HF** - high frequency power, **HFnu** – high-frequency normalized units, **HR** – heart rate, **HRpeak** – peak heart rate, **HRR** – heart rate recovery, **HRR1** – heart rate recovery at 1 minute, **HRR3** – heart rate recovery at 3 minutes, **HRR5** – heart rate recovery at 5 minutes, **HRV** – heart rate variability, **LF** - low frequency power, **LF/HF** – low-frequency to

Corresponding author: Timur Mušić, e-mail: tm8164@student.uni-lj.si

Received: 4.02.2026 / Revised: 14.04.2026 / Accepted: 19.04.2026 / Published: 30.06.2026

Kabaklić A, Radolović M, Mušić T. Association between arterial stiffness and autonomic recovery following graded aerobic exercise in healthy young adults – an exploratory pilot study. *Eur J Clin Exp Med.* 2026;24(2):380–390. doi: 10.15584/ejcem.2026.2.18.

high-frequency ratio, **LFnu** – low-frequency normalized units, **PP** – pulse pressure, **PWV** – pulse wave velocity, **PWA** – pulse wave analysis, **RMSSD** – root mean square of successive differences, **RR** – RR interval, **SBP** – systolic blood pressure, **SDNN** – standard deviation of normal-to-normal intervals, **VO_2max** – maximal oxygen uptake

Introduction

The importance of arterial integrity for cardiovascular health has long been recognized, famously captured by Thomas Sydenham's assertion that 'a man is as old as his arteries".[1] In modern preventive medicine, arterial function is seen not only as a marker of vascular aging, but also as a determinant of physiological resilience to hemodynamic stress. Physical activity, a potent modulator of arterial structure and function, therefore, provides a useful physiological model to understand early vascular adaptations in healthy young adults.[1,2]

Arterial stiffness is a robust surrogate marker of vascular aging.[3] By influencing central blood pressure, ventricular afterload, and coronary perfusion, aortic stiffness plays an important role in cardiovascular adaptation to physiological stress.[3,4] Pulse wave velocity (PWV) is the gold standard noninvasive measure of aortic stiffness, with carotid–femoral PWV (cf-PWV) specifically reflecting central hemodynamics and possible cardiovascular risk.[4,5]

Wave reflection indices, including augmentation index (AIx), heart rate corrected AIx (AIx@75), and augmentation pressure (AP), provide additional information on ventricular–vascular coupling and mechanical load on the left ventricle.[6-8] During and after exercise, cardiovascular homeostasis depends on coordinated interactions between vascular function and autonomic regulation dynamically modulating heart rate (HR), vascular tone and central hemodynamics.[9,10] These integrated autonomic vascular responses can be monitored non-invasively via heart rate variability (HRV), heart rate recovery (HRR), cfPWV, AIx@75, and central blood pressures (BP), including central systolic BP (cSBP), central diastolic BP (cDBP), and pulse pressure (PP), offering a comprehensive view of cardiovascular recovery after exercise.[9-11]

Although acute aerobic exercise responses to arterial stiffness and autonomic function have been studied, the extent to which baseline aortic stiffness is early after exercise autonomic and hemodynamic recovery remains insufficiently explored.[11,12] Baseline assessment of arterial stiffness may provide additional information on interindividual differences in vascular responses to physiological stress.[13,14] Most previous studies have focused on resting measures or acute changes during exercise without integrating preexercise vascular properties with recovery dynamics. Investigating this relationship in healthy young adults can provide insight into early physiological variability in vascular-autonomic interactions, even in the absence of overt diseases. Such findings may serve as a reference framework for future studies in populations with increased metabolic risk.

Aim

This exploratory pilot study aimed to assess whether baseline aortic stiffness, measured by cf-PWV prior to exercise, is associated with early post-exercise cardiovascular and autonomic recovery in healthy young adults undergoing graded submaximal cycling. As secondary exploratory analyses, we examined whether a higher baseline aortic stiffness is associated with a slower post-exercise HRR and altered autonomic regulation during recovery, and a higher peak HR and peak systolic BP achieved during graded submaximal exercise. We also explore whether cf-PWV independently predicts early HRR after adjustment for age, sex, and body mass index (BMI).

Material and methods

Ethical considerations

The study was conducted in accordance with the Declaration of Helsinki and all relevant national guidelines for research involving human participants. Before data collection, ethical approval was obtained from the Medical Ethics Committee of the Republic of Slovenia (approval number: 0120-388/2025-2711-5). All participants were fully informed about the aims, procedures, and potential risks of the study and provided their written informed consent prior to enrollment. Participation was voluntary and participants were allowed to withdraw from the study at any time without consequences. All collected data were fully anonymized prior to analysis, with any direct or indirect personal identifiers removed or replaced by coded numerical identifiers. Data were stored on secure servers and handled exclusively by authorized research personnel. All procedures for data storage, processing, and protection complied with the applicable local legislation on personal data protection.

Study design

This study was carried out as an exploratory pilot investigation using a prospective observational design under controlled laboratory conditions. It represents the healthy reference cohort of a larger ongoing clinical research project that will subsequently include hypertensive patients with and without impaired autonomic regulation. Within this framework, the present phase aimed to examine associations between baseline aortic stiffness and post-exercise hemodynamic and autonomic recovery in healthy young adults. No formal sample size calculation was performed due to the pilot nature of the study. The sample size was determined pragmatically based on feasibility and is consistent with recommen-

dations for exploratory physiological studies. Given its hypothesis-generating nature and limited sample size, this pilot phase was intended to provide preliminary information and inform the refinement of experimental protocols and analytical approaches for future large-scale investigations.

Participants

A total of 30 apparently healthy adult volunteers (17 women, 13 males; mean age 22.7±2.5 years, mean BMI 22.3±1.82 kg/m^2) were enrolled in the study. Participants were recruited through campus postings, announcements distributed through the university student email list, and targeted outreach within university-affiliated organizations. The sampling approach did not involve randomization; instead, convenience sampling was used, relying on individuals who voluntarily expressed interest in participating. Eligible participants were required to be between 18 and 30 years of age, non-smokers, free of any history of acute or chronic cardiovascular, metabolic or musculoskeletal disease, not taking any supplements or medications that could influence vascular or autonomic function, and regularly physically active without previous exertional symptoms. All participants underwent a resting electrocardiogram (ECG) and an orthostatic test, both of which yielded normal findings.

Pulse-wave analysis and pulse-wave velocity

Central hemodynamic parameters, PWV and PWA were obtained during the baseline supine assessment using the SphygmoCor XCEL device (Cardiex, Sydney, Australia). All measurements were made after at least 5 minutes of rest in the supine position to ensure hemodynamic stability. The assessment protocol enabled the comprehensive acquisition of central blood pressure and waveform-derived indices, including measures of arterial stiffness and wave reflection. For the purposes of the present analysis, cf-PWV was used as the primary index of aortic stiffness, alongside selected central hemodynamic and PWA parameters that are commonly reported and relevant to vascular evaluation. These included cSBP, cDBP, PP, AIx, and AIx@75. Other waveform-derived parameters obtained during the assessment were recorded but not included in the current analyzes. PWA was performed using an upper arm cuff while participants remained supine, allowing non-invasive estimation of central BP and augmentation indices. cf-PWV was measured using the same device, with a thigh cuff positioned over the femoral artery and carotid waveforms obtained by applanation tonometry. Transit distances were determined using standardized surface measurements. Specifically, three anatomical distances were measured: (1) the distance from the carotid artery pulse site to the suprasternal notch, (2) the distance from the suprasternal notch to the upper edge of the cuff, and (3) the distance from the femoral artery pulse site to the upper edge of the cuff. The device software to calculate cf-PWV based on the pulse transit time between the carotid and femoral recording sites and the corresponding anatomical path length. This combined baseline assessment provided an integrated characterization of aortic stiffness and central hemodynamic before the graded submaximal exercise test. All SphygmoCor measurements were subject to device-specific quality control criteria, and only recordings that met the recommended quality thresholds were accepted for analysis. Quality control was performed for each individual measurement.

Exercise stress test

The graded cycling exercise protocol was carried out using a cycle ergometer (Ergosana ERG 911 plus; Schiller AG, Baar, Switzerland) in the exercise physiology laboratory of the outpatient clinic for hypertensive patients at Dr. Peter Draj Hospital, part of the University Medical Center Ljubljana. All tests were supervised by trained personnel. Participants were instructed to refrain from vigorous physical activity for at least 24 hours before testing, to arrive well-rested and adequately hydrated, and to avoid heavy meals and caffeine for at least 4 hours before the session. All evaluations were scheduled in the afternoon to minimize circadian variability and were performed in a climate-controlled environment to ensure consistent temperature and reduce environmental variability. The exercise protocol consisted of several sequential phases. The participants first completed a 3 minute rest period while seated and breathing normally. This was followed by the cycling phase, which included progressively increasing workloads: The initial workload was set at 20% of the maximum oxygen uptake (VO_2max) and increased by 20% every 3 minutes until it reached 80% of predicted VO_2max. The predicted VO_2max values were derived from age and sex-specific reference tables from the updated FRIEND registry (2022),[15] and the corresponding cycling power outputs were calculated using the Storer equation, which incorporates body mass to determine individualized maximum workload.[16] Participants were instructed to maintain a cadence of 65 rpm throughout the cycling phase, regardless of workload. HR was continuously measured throughout the entire session using 12-lead ECG monitoring, while systolic BP (SBP) and diastolic BP (DBP) were recorded automatically with a preprogrammed upper arm cuff pre-programmed in the device software. During the cycling phase, BP was measured once during each 3-minute exercise stage. After completion of the cycling phase, participants underwent a 5-minute seated recovery period, during which continuous HR monitoring was maintained and BP measured at 1, 3, and 5 minutes to assess early post-exercise hemodynamic responses. This protocol was selected to

provide a controlled and progressive physiological stimulus in standardized submaximal intensities.

Heart rate variability and heart rate recovery assessment

Electrocardiographic signals were recorded and stored for subsequent HRV analysis using Kubios HRV Analysis Software (Kubios Oy, Kuopio, Finland). The signals were sampled at 500 Hz, providing the high temporal resolution required for accurate extraction of HRV parameters. Artifacts and ectopic beats were identified and corrected using the Kubios automatic artifact correction algorithm, with manual verification to ensure signal quality. The HRV indices were calculated according to the guidelines of the Task Force of the European Society of Cardiology Task Force and the North American Society of Pacing and Electrophysiology (1996).17 The HRV indices were averaged throughout the 5-minute recovery period. This approach was chosen to provide a stable summary estimate of post-exercise autonomic recovery and to reduce the influence of short-term fluctuations and signal noise. However, it should be acknowledged that averaging across the entire recovery period can obscure transient, minute-to-minute changes in autonomic dynamics.

The time domain analysis included the mean RR interval (RR), the root mean square of successive differences (RMSSD), reflecting short-term and vagally mediated HRV, and the standard deviation of all normal to normal intervals (SDNN), representing overall autonomic modulation.[18] The frequency domain analysis comprised low-frequency (LF; 0.04–0.15 Hz) and high-frequency (HF; 0.5–0.40 Hz) power, expressed in both absolute (ms^2) and normalized units (nu). High-frequency normalized units (HFnu) predominantly indicate parasympathetic activity, low-frequency normalized units (LFnu) reflect sympathetic modulation, and their ratio (LF/HF) provides a measure of sympathovagal balance.[18,19] HRR was assessed as the decline in HR from peak exercise (HRpeak) at 1 (HRR1), 3 (HRR3), and 5 minutes (HRR5) after exercise. HRR was calculated as the absolute decrease in heart rate from peak exercise according to the following definitions: HRR1=HRpeak HR at 1 minute of recovery, HRR3=HRpeak HR at 3 minutes of recovery, and HRR5=HRpeak HR at 5 minutes of recovery. Early HRR (HRR1) predominantly reflects rapid parasympathetic reactivation, while later recovery phases (HRR3, HRR5) are influenced by both parasympathetic reactivation and sympathetic withdrawal, providing additional information on autonomic recovery after exertion.[20]

Statistical analysis

Data were analyzed using JASP version 0.17 (JASP Team, Amsterdam, The Netherlands). Continuous variables were tested for normality using the Shapiro–Wilk test and are presented as mean±standard deviation. Associations between baseline central hemodynamic parameters, cf-PWV, AIx @ 75 and post-exercise autonomic recovery indices were evaluated using Pearson or Spearman correlation coefficients, depending on the data distribution, and visualized with scatterplots. For HRV analysis, time-domain and frequency-domain indices were averaged over the entire 5-minute recovery period to obtain a single summary value per participant. Univariate linear regression analyzes were performed to identify potential predictors of autonomic recovery, followed by multivariate linear regression models adjusted for age, sex, and BMI. Statistical significance was established at $p<0.05$.

Although sex was included as a covariate in multivariate models, no stratified analyses were performed. Therefore, potential sex-specific physiological differences in autonomic and vascular responses may not be fully captured. Given the number of correlations tested, the analyzes should be interpreted with caution because of an increased risk of type I error. No formal correction for multiple comparisons was applied, as the study was exploratory. Analyses examining associations between cf-PWV and autonomic recovery indices were predefined, while additional exploratory analyses were performed to generate hypotheses for future studies.

Results

A total of 30 participants were included in the final analysis, of which 17 (56.7%) were women. The baseline characteristics of the study population, including demographic and anthropometric measures, central BP, PWA, and cf-PWV are summarized in Table 1. All variables were approximately normally distributed and no extreme outliers were identified.

Table 1. Demographic, anthropometric and central hemodynamic characteristics of study participants, values are presented as mean±SD unless otherwise indicated (n=30)

Variable (Unit)	Mean±SD or n (%)
Demographics	
Sex (female/male, n)	17 (56.7%)/13 (43.3%)
Age (years)	22.7±2.5
Body mass (kg)	69.2±9.6
Height (cm)	175.8±8.8
Body mass index (kg/m^2)	22.3±1.8
Central hemodynamic parameters	
Central systolic blood pressure (mmHg)	108.9±8.6
Central diastolic blood pressure (mmHg)	77.3±7.6
Central pulse pressure (mmHg)	31.6±5.2
Pulse wave analysis	
Augmentation pressure (AP, mmHg)	1.57±2.86
Augmentation index (AIx, %)	4.23±9.22
Augmentation index, HR-corrected (AIx@75, %)	2.30±11.45
Pulse wave velocity	
Carotid–femoral pulse wave velocity (cf-PWV, m/s)	5.57±0.75

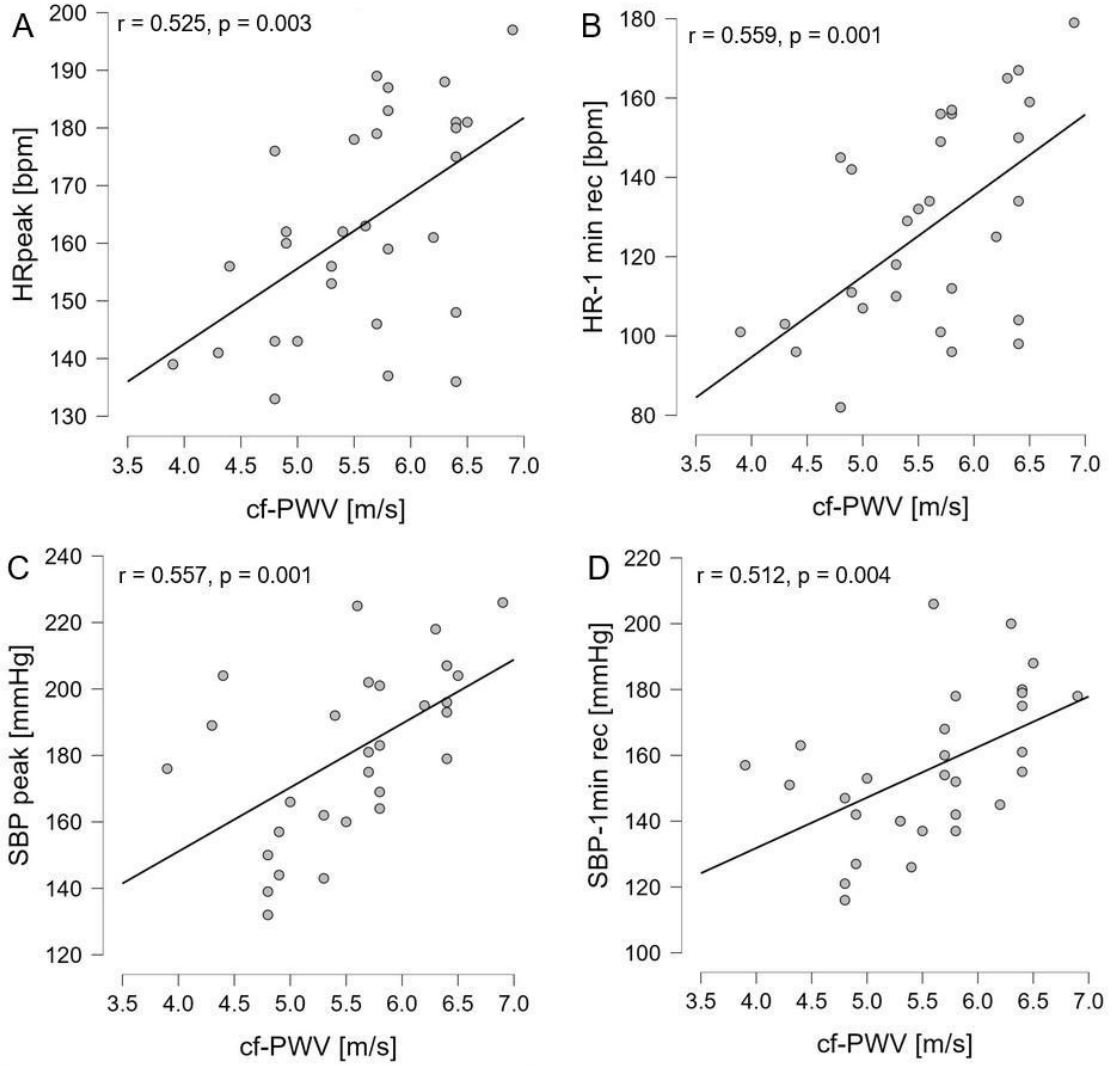

Fig. 1. The figure presents four scatterplots depicting correlations between cf-PWV and cardiovascular responses to graded submaximal cycling exercise: A: HR achieved during exercise, B: HR measured at 1-minute recovery following exercise, C: peak SBP achieved during exercise, and D: SBP measured at 1 minute recovery following exercise, all correlations are presented with the correlation coefficient (r) and the corresponding p-value. Statistical significance was established a priori at $p<0.05$

Table 2. Hemodynamic responses at rest, during peak exercise, and throughout recovery (1, 3, and 5 minutes), values are presented as mean±standard deviation

Variable (Unit)	Rest (mean±SD)	Peak exercise (mean±SD)	Recovery 1 min. (mean±SD)	Recovery 3 min (mean±SD)	Recovery 5 min (mean±SD)
Heart rate (bpm)	81.0±14.4	163.1±18.6	126.7±27.3	108.0±23.8	101.4±19.8
Systolic BP (mmHg)	117.6±12.9	181.3±25.8	155.9±22.4	136.4±20.3	127.6±16.8
Diastolic BP (mmHg)	73.5±7.9	82.6±11.5	74.3±8.8	72.7±8.3	73.7±10.6

All participants successfully completed the graded submaximal exercise protocol up to 80% of the predicted VO_2max without adverse events. The mean HR peak increased from a resting value of 81.0±14.4 bpm to 163.1±18.6 bpm during exercise. SBP increased progressively with workload, reaching a mean peak value of 181.3±25.9 mmHg (resting value: 117.6±12.9 mmHg), while DBP remained relatively stable throughout the test. During the 5-minute seated recovery period, both HR and BP gradually decreased toward baseline values (Table 2).

Associations of baseline arterial stiffness with peak exercise and post-exercise hemodynamic responses

cf-PWV was positively associated with HRpeak ($r=0.525$, $p=0.003$) and peak systolic blood pressure (SBPpeak; $r=0.557$, $p<0.001$) during graded submaximal exercise (Fig. 1). Baseline AIx@75 showed weaker but statistically significant positive associations with HRpeak ($r=0.368$, $p=0.045$) and HR measured at 1, 3, and 5 minutes during recovery (HR1: $r=0.378$, $p=0.039$; HR3: $r=0.504$, $p=0.005$; HR5: $r=0.416$, $p=0.022$). During recovery, cf-PWV was positively correlated with SBP for 1 minute (SBP1, $r=0.512$, $p=0.004$) and 3 minutes (SBP3, $r=0.486$, $p=0.008$), while the correlation for 5 minutes

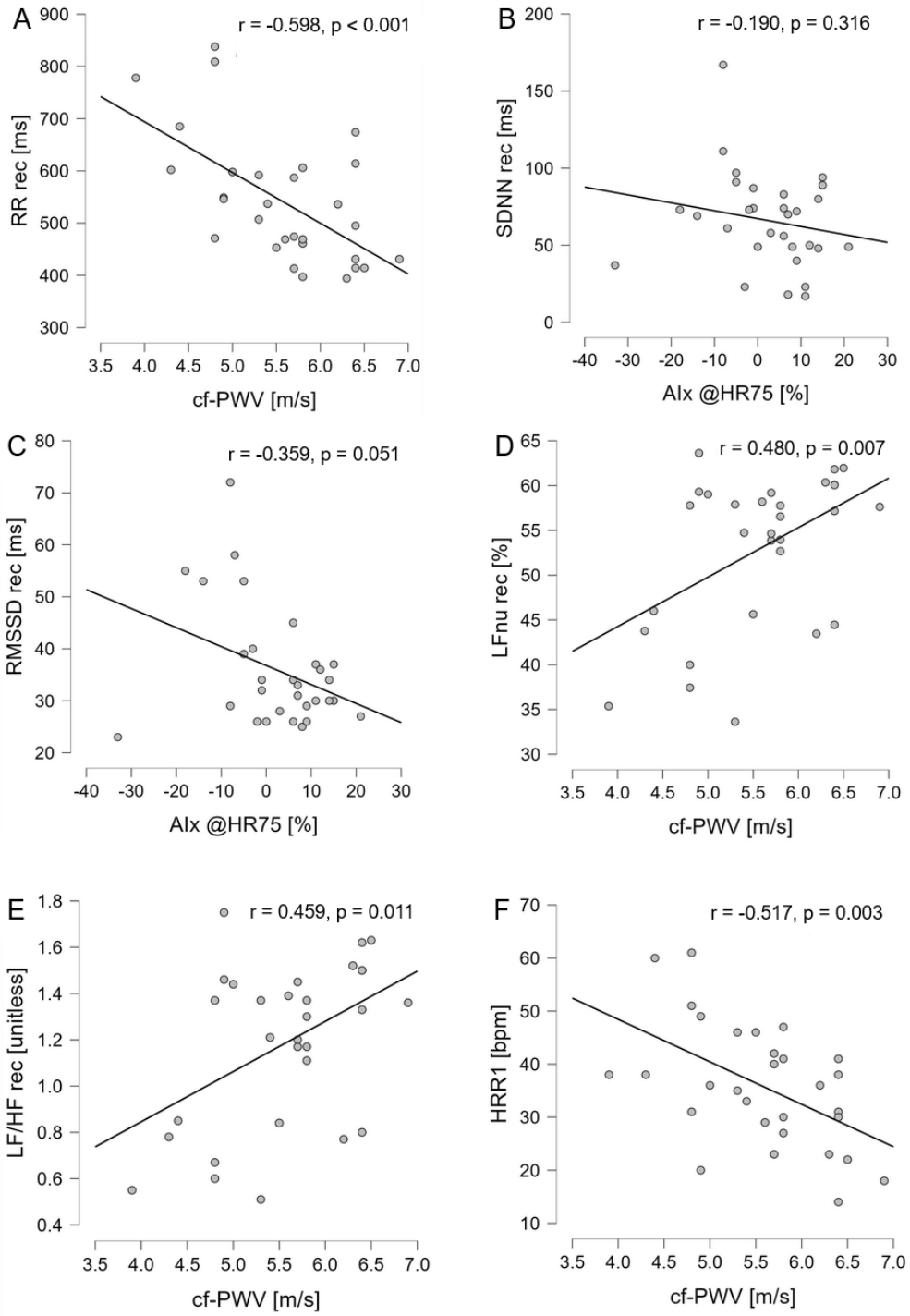

Fig. 2. The figure presents six scatterplots that illustrate correlations between arterial stiffness, heart rate variability and recovery parameters during postexercise recovery: A: cf-PWV and RR intervals, B: AIx@75 and SDNN, C: AIx@75 and RMSSD, D: cf-PWV and LFnu, E: cf-PWV and LF/HF ratio, and F: cf-PWV and early heart rate recovery during the first minute of recovery (HRR1), all correlations are presented with the correlation coefficient (r) and the corresponding p-value, statistical significance was established a priori at $p<0.05$

(SBP5) did not reach statistical significance (r=0.307, p=0.099). HR during recovery at 1, 3, and 5 minutes (HR1, HR3, HR5) showed significant positive correlations with baseline cf-PWV (HR1: r=0.559, p=0.001; HR3: r=0.603, p=0.002; HR5: r=0.541, p=0.003). No significant correlations were observed between cf-PWV and DBP at any recovery time point (all p>0.05).

Associations of baseline arterial stiffness with autonomic recovery following exercise

During the recovery period, cf-PWV showed a significant inverse association with the mean RR interval (r=−0.598, p<0.001) (Fig. 2). On the contrary, cf-PWV was not significantly associated with HRV indices, including SDNN and RMSSD (all p>0.05). However,

a higher cf-PWV was significantly associated with a lower HFnu (r=0.480, p=0.004), a higher LFnu (r=0.480, p=0.004) and a higher LF/HF ratio (r=0.49, p=0.005).

AIx@75 also demonstrated an inverse association with the mean RR interval during recovery (r=0.481, p=0.007). Furthermore, AIx @ 75 showed a trend towards an inverse association with RMSSD during recovery that did not reach statistical significance (r=<0.359, p=0.051) and was not associated with SDNN (p>0.05). Similarly to cf-PWV, AIx@75 was significantly associated with HRV indices during recovery, including a higher LFnu (r=0.376, p=0.041), lower HFnu (r=0.376, p=0.041) and a higher LF/HF ratio (r=0.367, p=0.046). No significant correlations were observed between other baseline central hemodynamic parameters and recovery HRV indices (all p>0.05).

cf-PWV was inversely associated with early HRR during the first minute of recovery (HRR1; r=<0.517, p=0.002) (Fig. 2). The associations with later recovery phases at 3 and five minutes (HRR3 and HRR5) were weaker and did not reach statistical significance (HRR3: r=−0.104, p=0.292; HRR5: r=0.146, p=0.210). The baseline cSBP was inversely correlated with HRR1 (r=<0.370, p=0.044) but not with HRR3 or HRR5 (HRR3: r=−0.211, p=0.264; HRR5: r=<0.075, p=0.692). In contrast, the augmentation index (AIx@75) was not significantly associated with HRR at any post-exercise time point (all p>0.05).

Table 3. Univariate and multivariate linear regression analyses identifying predictors of early heart rate recovery*

Model	Predictor (Unit)	B	SE	β (standardized)	p	Model statistics
Univariate	cf-PWV (m/s)	-0.033	0.010	−0.517	0.003	R=0.517; R^2=0.268; Adjusted R^2=0.241
Multivariable	cf-PWV (m/s)	-0.030	0.012	−0.465	0.045	R=0.560; R^2=0.313; Adjusted R^2=0.203
	Age (years)	−0.019	0.051	−0.063	0.715	
	Sex (female/male)	−0.324	0.292	†	0.277	
	BMI (kg/m^2)	−0.054	0.075	−0.132	0.478	

* values are regression coefficients from linear regression models, standardized β for sex is not reported because sex is a binary variable

Regression analysis of arterial stiffness as a determinant of early autonomic recovery

In the univariate linear regression analysis, cf-PWV was a significant predictor of early HRR 1 minute post-exercise, accounting for 26.8% of the variance in HRR1 (β=−0.517, R^2=0.268, p=0.003). After adjustment for age, sex and body mass index, cf-PWV remained independently associated with HRR1, although the strength of the association was attenuated (adjusted R^2=0.203, p=0.045). None of the covariates were significant independent predictors in the multivariable model (all p>0.05) (Table 3).

Exploratory regression analyzes for selected HRV indices showed that, after adjustment for age, sex, and body mass index, no baseline arterial stiffness or central hemodynamic parameters were independently associated with post-exercise HRV measures (all adjusted p>0.05).

Discussion

This exploratory pilot study investigated the association between baseline aortic stiffness and cardiovascular and autonomic recovery following graded submaximal aerobic exercise in healthy young adults. The main findings were that a higher baseline aortic stiffness (assessed by cf-PWV) was associated with higher peak HR and SBP during exercise, slower HRR at the beginning of the exercise, and an altered autonomic recovery profile characterized by patterns in the HRV indices (lower HFnu, higher LFnu and LF/HF ratio). cf-PWV remained an independent predictor of early HRR after adjustment for age, sex, and BMI. Such findings suggest an association between baseline vascular properties and early cardiovascular and autonomic recovery in a controlled physiological setting. These findings are consistent with the results of the cardiovascular risk in young Finns study by Haarala et al.[21], which showed that greater arterial stiffness was associated with exaggerated exercise blood pressure responses during the maximal cardiopulmonary exercise test. Together, these findings are consistent with the idea that baseline arterial pressure is associated with cardiovascular load during exercise and recovery, even in young, otherwise healthy individuals.

Beyond peak exercise responses, our findings suggest that a higher baseline cf-PWV is associated with slower early postexercise recovery, reflected by higher HR and BP during the recovery period and delayed hemodynamic normalization. These findings indicate that higher arterial stiffness may also be associated with early cardiovascular readjustment after exercise. Previous studies have also linked a higher PWV to altered exercise responses and delayed recovery.[22,23] In our study, higher HR and SBP during graded submaximal exercise reflect cardiovascular responses to physiological stress. Previously, exaggerated exercise BP responses have been associated with vascular dysfunction and adverse cardiovascular profiles.[24]

Given that postexercise hemodynamic recovery is tightly regulated by autonomic mechanisms, we further examined whether a higher baseline cf-PWV is associated with altered autonomic regulation during recovery. A higher baseline cf-PWV was associated with a lower HFnu, a higher LFnu, and an elevated LF/HF ratio, commonly interpreted as reflecting changes in autonomic balance.[25]

These findings are consistent with Park et al.[26], who reported similar associations between arterial stiffness and altered autonomic recovery after aerobic exercise,

and with findings from resistance exercise studies, suggesting that arterial stiffness may also be relevant to autonomic recovery across different exercise modalities.[27]

Previous studies suggest a bidirectional relationship between autonomic activity and arterial stiffness, although causality cannot be inferred in the present study.[28] Recent work by Gronwald et al.[29] further highlights the influence of exercise intensity on post-exercise HRV, showing that more vigorous exercise produces greater and longer lasting autonomic perturbations compared to moderate exercise. Our findings suggest that even in healthy young adults, interindividual differences in arterial stiffness may be associated with autonomic recovery. Higher cf-PWV was associated with higher LFnu and LF/HF ratio during recovery, even under graded submaximal exercise (20–80% VO_2max). This suggests that vascular properties may be associated with interindividual differences in autonomic responses during recovery.

Our findings suggest that variations in arterial stiffness and autonomic regulation are detectable even in apparently healthy young adults. HRV and related autonomic indices provide sensitive measures of autonomic cardiovascular control during the recovery phase after exercise, reflecting the ability of the cardiovascular system to adapt to physiological stress.[25] Furthermore, cf-PWV emerged as a more consistent predictor of frequency domain HRV indices than AIx@75, possibly reflecting differences in intrinsic aortic stiffness and baroreflex-mediated autonomic modulation.[30] These results suggest the potential utility of combining vascular and autonomic evaluation to characterize physiological differences in cardiovascular regulation in a controlled setting. To support this interpretation, a systematic review by Pierce et al.[31] reported that PWV shows more consistent responses to exercise in different modalities, whereas the increase indices are more variable and strongly influenced by transient hemodynamic conditions.

Cf-PWV was associated with HRV indices but not time-domain measures, reflecting differences in the physiological information captured by these parameters.[31,32] This pattern can be explained by the fact that the time domain indices reflect overall or short-term variability without distinguishing sympathetic and parasympathetic contributions, while the frequency domain measures more directly capture autonomic modulation and baroreflex sensitivity.[32-34] The present study focused on the early post-exercise recovery phase, with HRV, HRR, and BP monitored during the first 5 minutes after exercise cessation. This time window captures rapid parasympathetic reactivation and the initial phase of cardiovascular readjustment, but it does not reflect the full trajectory of post-exercise recovery, which can extend beyond 20 to 60 minutes or longer.[35] For this reason, the present findings should be interpreted as relating specifically to early recovery kinetics rather than complete post-exercise recovery dynamics.

Beyond exercise performance, an important observation of the present study is related to early postexercise recovery. HRR within the first minute after exercise cessation is mainly governed by rapid parasympathetic reactivation and is widely used as a marker of autonomic regulation.[36,37] In our study, a higher baseline cf-PWV was associated with slower HRR at 1 minute, and this relationship remained significant after adjustment for age, sex and BMI. While previous studies linking greater arterial stiffness to slower HRR were conducted in older or clinical populations,[38,39] the present findings suggest that vascular-autonomic associations are also detectable in a controlled physiological setting in healthy young adults. In summary, baseline cf-PWV was associated with early cardiovascular and autonomic recovery after graded submaximal exercise in healthy young adults and remained an independent predictor of early HRR. These results should be interpreted as evidence of physiological variation in vascular–autonomic regulation rather than indicators of clinical risk. In general, the study provides information on early recovery dynamics under controlled experimental conditions, while confirmation in larger and clinical cohorts is still needed.

Study limitations and future perspectives

This exploratory study has several limitations that should be considered when interpreting the findings. First, the relatively small sample size (n=30) and the inclusion of a homogeneous cohort of healthy young adults within a narrow age range (18-30 years) can limit the generalizability. Although the study detected several moderate to strong associations between cf-PWV and autonomic and hemodynamic indices, the results should be interpreted with caution given the sample size and exploratory design. Future studies involving larger and more diverse populations, including older adults and individuals with cardiovascular risk factors, are warranted to confirm and extend these observations.

Second, post-exercise recovery was monitored for only 5 minutes. Although this period captures the early phase of parasympathetic reactivation and allowed simultaneous evaluation of HRR, HRV, and BP dynamics, longer recovery monitoring would provide a more complete characterization of post-exercise autonomic and hemodynamic adjustments. Third, cf-PWV and central hemodynamics were evaluated only at rest. Although resting cf-PWV provides a robust index of intrinsic aortic stiffness, future studies may benefit from evaluating vascular responses during post-exercise recovery to better characterize dynamic vascular–autonomic interactions.

Fourth, aerobic capacity was not measured directly using cardiopulmonary exercise testing but estimat-

ed from age- and sex-based prediction tables. Given the relatively homogeneous fitness levels of young participants and the derived nature of predicted VO_2max, its inclusion in regression models may have introduced collinearity with exercise HR variables. However, direct VO_2max measurement would be valuable in future studies involving more heterogeneous or clinical populations.

Finally, the inclusion of multiple covariates in regression models relative to the modest sample size may have reduced statistical power. These adjustments were included to account for potential confounders and, therefore, the findings should be interpreted as exploratory and hypothesis-generating. In addition, the observational design limits causal inference. Future larger-scale studies, particularly in populations with cardiovascular risk factors, are needed to clarify the relationship between arterial stiffness and post-exercise autonomic recovery.

Conclusion

This exploratory pilot study demonstrates that baseline aortic stiffness, assessed by cf-PWV, is associated with cardiovascular and autonomic responses to graded submaximal exercise in healthy young adults. Higher cf-PWV was associated with higher peak HR and SBP during exercise, as well as slower early HRR after cessation of exercise. Cf-PWV also remained independently associated with early HRR after adjustment for age, sex, and BMI. These findings support an association between baseline vascular properties and early cardiovascular and autonomic recovery dynamics in a controlled physiological setting. However, given the observational and pilot nature of the study, these results should be interpreted as preliminary. More studies in larger and clinical populations to confirm these associations and better understand their physiological and clinical relevance.

Declarations

Funding

The authors received no financial support for the research, authorship, and/or publication of this article.

Author contributions

Conceptualization: A.K. and T.M.; Methodology: A.K.; Software: M.R.; Validation: M.R. and T.M.; Investigation: A.K. and T.M.; Resources: A.K.; Data Curation: T.M.; Writing – Original Draft Preparation: T.M.; Writing – Review & Editing: A.K. and T.M.; Visualization: M.R. and T.M.; Supervision: A.K.; Project Administration: A.K. and T.M.

Conflict of interest

The authors declare no conflict of interest.

Data availability

Data supporting the findings of this study are available from the corresponding author upon reasonable request.

Ethics approval

Ethical approval was granted by the Medical Ethics Committee of the Republic of Slovenia (approval number: 0120-388/2025-2711-5).

References

1. Iurciuc S, Cimpean AM, Mitu F, Heredea R, Iurciuc M. Vascular aging and subclinical atherosclerosis: why such a "never ending" and challenging story in cardiology? *Clin Interv Aging*. 2017;12:1339-1345. doi:10.2147/CIA.S141265
2. Jakovljevic DG. Physical activity and cardiovascular aging: Physiological and molecular insights. *Exp Gerontol*. 2018;109:67-74. doi:10.1016/j.exger.2017.05.016
3. Castelli R, Gidaro A, Casu G, et al. Aging of the arterial system. *Int J Mol Sci*. 2023;24(8):6910. doi:10.3390/ijms24086910
4. de Waal EEC. Arterial stiffness, assessed with carotid-femoral pulse- wave velocity, and vasopressor response. *J Cardiothorac Vasc Anesth*. 2021;35(1):81-83. doi:10.1053/j.jvca.2020.09.124
5. Laurent S, Cockcroft J, Van Bortel L, et al. Expert consensus document on arterial stiffness: methodological issues and clinical applications. *Eur Heart J*. 2006;27(21):2588-2605. doi:10.1093/eurheartj/ehl254
6. Kaya M, Balasubramanian V, K-J Li J. Augmentation index in the assessment of wave reflections and systolic loading. *Comput Biol Med*. 2019;113:103418. doi:10.1016/j.compbiomed.2019.103418
7. Sharman JE, Davies JE, Jenkins C, Marwick TH. Augmentation index, left ventricular contractility, and wave reflection. *Hypertension*. 2009;54(5):1099-1105. doi:10.1161/HYPERTENSIONAHA.109.133066
8. Moulton MJ, Secomb TW. A fast computational model for circulatory dynamics: effects of left ventricle-aorta coupling. *Biomech Model Mechanobiol*. 2023;22(3):947-959. doi:10.1007/s10237-023-01690-w
9. Yang IH, Hwang HJ, Jeon HK, et al. Slow heart rate recovery is associated with increased exercise-induced arterial stiffness in normotensive patients without overt atherosclerosis. *J Cardiovasc Imaging*. 2019;27(3):214-223. doi:10.4250/jcvi.2019.27.e27
10. Saz-Lara A, Cavero-Redondo I, Álvarez-Bueno C, Notario-Pacheco B, Ruiz-Grao MC, Martínez-Vizcaíno V. The acute effect of exercise on arterial stiffness in healthy subjects: a meta-analysis. *J Clin Med*. 2021;10(2):291. doi:10.3390/jcm10020291
11. Farinatti P, da Silva Itaborahy A, de Paula T, Monteiro WD, Neves MF. Effects of aerobic, resistance and concurrent exercise on pulse wave reflection and autonomic

modulation in men with elevated blood pressure. *Sci Rep*. 2021;11(1):760. doi:10.1038/s41598-020-80800-5

12. Calleja-Romero A, Vicente-Rodríguez G, Garatachea N. Acute effects of long-distance races on heart rate variability and arterial stiffness: A systematic review and meta-analysis. *J Sports Sci*. 2022;40(3):248-270. doi:10.1080/02640414.2021.1986276
13. Vlachopoulos C, Aznaouridis K, Stefanadis C. Prediction of cardiovascular events and all-cause mortality with arterial stiffness: a systematic review and meta-analysis. *J Am Coll Cardiol*. 2010;55(13):1318-1327. doi:10.1016/j.jacc.2009.10.061
14. Pierce GL, Harris SA, Seals DR, Casey DP, Barlow PB, Stauss HM. Estimated aortic stiffness is independently associated with cardiac baroreflex sensitivity in humans: role of ageing and habitual endurance exercise. *J Hum Hypertens*. 2016;30(9):513-520. doi:10.1038/jhh.2016.3
15. Kaminsky LA, Arena R, Myers J, et al. Updated reference standards for cardiorespiratory fitness measured with cardiopulmonary exercise testing: data from the fitness registry and the importance of exercise national database (FRIEND). *Mayo Clin Proc*. 2022;97(2):285-293. doi:10.1016/j.mayocp.2021.08.020
16. Storer TW, Davis JA, Caiozzo VJ. Accurate prediction of VO-2max in cycle ergometry. *Med Sci Sports Exerc*. 1990;22(5):704-712. doi:10.1249/00005768-199010000-00024
17. Task Force of the European Society of Cardiology and the North American Society of Pacing and Electrophysiology. Heart rate variability: standards of measurement, physiological interpretation and clinical use. Circulation. 1996;93(5):1043-1065.
18. Shaffer F, Ginsberg JP. An Overview of heart rate variability metrics and norms. *Front Public Health*. 2017;5:258. doi:10.3389/fpubh.2017.00258
19. Burr RL. Interpretation of normalized spectral heart rate variability indices in sleep research: a critical review. *Sleep*. 2007;30(7):913-919. doi:10.1093/sleep/30.7.913
20. Peçanha T, Silva-Júnior ND, Forjaz CL. Heart rate recovery: autonomic determinants, methods of assessment and association with mortality and cardiovascular diseases. *Clin Physiol Funct Imaging*. 2014;34(5):327-339. doi:10.1111/cpf.12102
21. Haarala A, Kähönen E, Koivistoinen T, et al. Pulse wave velocity is related to exercise blood pressure response in young adults. The cardiovascular risk in young Finns study. *Blood Press*. 2020;29(4):256-263. doi:10.1080/08037051.2020.1750944
22. Liu Z, Kuang J, Yan W, Zhu Y, Yang X, Xu Y. Mediating role of arterial stiffness in the association between physical activity and cardiovascular disease risk: a prospective cohort study. *Sci Rep*. 2025;15(1):38740. doi:10.1038/s41598-025-22442-z
23. Koivistoinen T, Lyytikäinen LP, Aatola H, et al. Pulse wave velocity predicts the progression of blood pressure and development of hypertension in young adults. *Hypertension*. 2018;71(3):451-456. doi:10.1161/HYPERTENSIONAHA.117.10368
24. Tzemos N, Lim PO, Mackenzie IS, et al. Exaggerated exercise blood pressure response and future cardiovascular disease. *J Clin Hypertens (Greenwich)*. 2015;17(11):837-844. doi:10.1111/jch.12629
25. Michael S, Graham KS, Davis GM. Cardiac autonomic responses during exercise and post-exercise recovery using heart rate variability and systolic time intervals: a review. *Front Physiol*. 2017;8:301. doi:10.3389/fphys.2017.00301
26. Park S, Kim HL, Park KT, et al. Association between arterial stiffness and autonomic dysfunction in participants underwent treadmill exercise testing: a cross-sectional analysis. *Sci Rep*. 2024;14(1):3588. doi:10.1038/s41598-024-53681-1
27. Kingsley JD, Mayo X, Tai YL, Fennell C. Arterial stiffness and autonomic modulation after free-weight resistance exercises in resistance trained individuals. *J Strength Cond Res*. 2016;30(12):3373-3380. doi:10.1519/JSC.0000000000001461
28. Mäki-Petäjä KM, Barrett SM, Evans SV, Cheriyan J, McEniery CM, Wilkinson IB. The role of the autonomic nervous system in the regulation of aortic stiffness. *Hypertension*. 2016;68(5):1290-1297. doi:10.1161/HYPERTENSIONAHA.116.08035
29. Gronwald T, Kock H, Röglin L, et al. Recovery of linear and nonlinear heart rate variability metrics after short-term moderate versus vigorous intensity exercise: A cross-sectional randomized cross-over study. *Eur J Sport Sci*. 2025;25(11):e70077. doi:10.1002/ejsc.70077
30. Wilkinson IB, MacCallum H, Flint L, Cockcroft JR, Newby DE, Webb DJ. The influence of heart rate on augmentation index and central arterial pressure in humans. *J Physiol*. 2000;525 Pt 1(Pt 1):263-270. doi:10.1111/j.1469-7793.2000.t01-1-00263.x
31. Pierce DR, Doma K, Leicht AS. Acute effects of exercise mode on arterial stiffness and wave reflection in healthy young adults: A systematic review and meta-analysis. *Front Physiol*. 2018;9:73. doi:10.3389/fphys.2018.00073
32. Draghici AE, Taylor JA. The physiological basis and measurement of heart rate variability in humans. *J Physiol Anthropol*. 2016;35(1):22. doi:10.1186/s40101-016-0113-7
33. Sandercock GR, Bromley PD, Brodie DA. The reliability of short-term measurements of heart rate variability. *Int J Cardiol*. 2005;103(3):238-247. doi:10.1016/j.ijcard.2004.09.013
34. Kleiger RE, Stein PK, Bosner MS, Rottman JN. Time domain measurements of heart rate variability. *Cardiol Clin*. 1992;10(3):487-498.
35. Mušić T, Radolović M, Kabaklić A. Autonomic nervous system testing in cardiovascular patients: from research to clinical application. *Cardiol Croat*. 2026;21(3-4):71-92. doi:10.15836/ccar2026.71
36. Vivekananthan DP, Blackstone EH, Pothier CE, Lauer MS. Heart rate recovery after exercise is a predictor of

mortality, independent of the angiographic severity of coronary disease. *J Am Coll Cardiol*. 2003;42(5):831-838. doi:10.1016/s0735-1097(03)00833-7

37. Qiu S, Cai X, Sun Z, et al. Heart rate recovery and risk of cardiovascular events and all-cause mortality: a meta-analysis of prospective cohort studies. *J Am Heart Assoc*. 2017;6(5):e005505. doi:10.1161/JAHA.117.005505
38. Fei DY, Arena R, Arrowood JA, Kraft KA. Relationship between arterial stiffness and heart rate recovery in apparently healthy adults. *Vasc Health Risk Manag*. 2005;1(1):85-89. doi:10.2147/vhrm.1.1.85.58938
39. Kim MJ. Carotid arterial stiffness and attenuated heart rate recovery in uncomplicated hypertensive patients. *J Cardiovasc Imaging*. 2019;27(3):224-226. doi:10.4250/jcvi. 2019.27.e39

Rzeszów University Press 2026
ISSN 2544-1361 (online)
doi: 10.15584/ejcem.2026.2.2

http://www.ejcem.ur.edu.pl
European Journal of Clinical and Experimental Medicine
Eur J Clin Exp Med 2026; 24 (2): 391–399

REVIEW PAPER

Breast imaging on chest computed tomography after various types of breast surgery

Taekyung Kang [1], Mi-Jin Kang [2]

[1] Department of Emergency Medicine, Inje University Sanggye Paik Hospital, Seoul, Korea
[2] Department of Radiology, Inje University Sanggye Paik Hospital, Seoul, Korea

ABSTRACT

Introduction and aim. The incidence of breast cancer is increasing globally, prompting the development of various surgical and reconstructive techniques for treatment. Chest computed tomography (CT) is frequently performed for multiple clinical indications, including screening, postoperative surveillance, and staging. Therefore, this article aims to review and illustrate the characteristic imaging characteristics of various postoperative breast changes that may be incidentally identified on chest CT.

Material and methods. We reviewed the medical records of patients who underwent CT scans at our hospital in the past five years and had changes in the shape of their breasts to confirm diagnosis, surgery, or procedure name, etc.

Analysis of the literature. We compared CT findings of patients with surgically confirmed procedures with the surgical techniques to identify any deformities resulting from surgery. In addition, we investigated the indications and effects of each surgery.

Conclusion. Awareness of these characteristic CT appearances can help radiologists avoid misinterpretation, recognize complications or recurrence, and provide clinically relevant information even when breast findings are incidental.

Keywords. mammoplasty, mastectomy, postoperative breast

Introduction

Breast cancer is one of the most common malignancies and the second leading cause of cancer-related mortality worldwide.[1] As a result, various surgical treatment options have been developed, and breast reconstruction is frequently performed for aesthetic and psychological reasons after mastectomy or breast conserving surgery. Consequently, the postoperative appearance of the breast can vary significantly, leading to a wide range of imaging findings. Therefore, radiologists to have a comprehensive understanding of these variations to ensure accurate interpretation.

In clinical practice, postoperative evaluation of patients with breast cancer is typically conducted using magnetic resonance imaging (MRI), mammography, and breast ultrasound. Chest computed tomography (CT), while primarily performed to evaluate for intrathoracic metastases, often incidentally includes the breasts within the field of view. Unlike dedicated breast imaging modalities, chest CT is not optimized for breast evaluation and is often interpreted without a focused assessment of postoperative breast anatomy. This creates a potential diagnostic blind spot in routine practice. In such cases, familiarity with the expected postoperative imaging findings is important for an accurate diagnosis (Fig. 1).

Furthermore, in patients undergoing chest CT for other indications, such as screening or evaluation of

Corresponding author: Mi-Jin Kang, e-mail: s2621@paik.ac.kr

Received: 28.07.2025 / Revised: 15.12.2025 / Accepted: 4.01.2026 / Published: 30.06.2026

Kang T, Kang MJ. Breast imaging on chest computed tomography after various types of breast surgery. *Eur J Clin Exp Med.* 2026;24(2):391–399. doi: 10.15584/ejcem.2026.2.2.

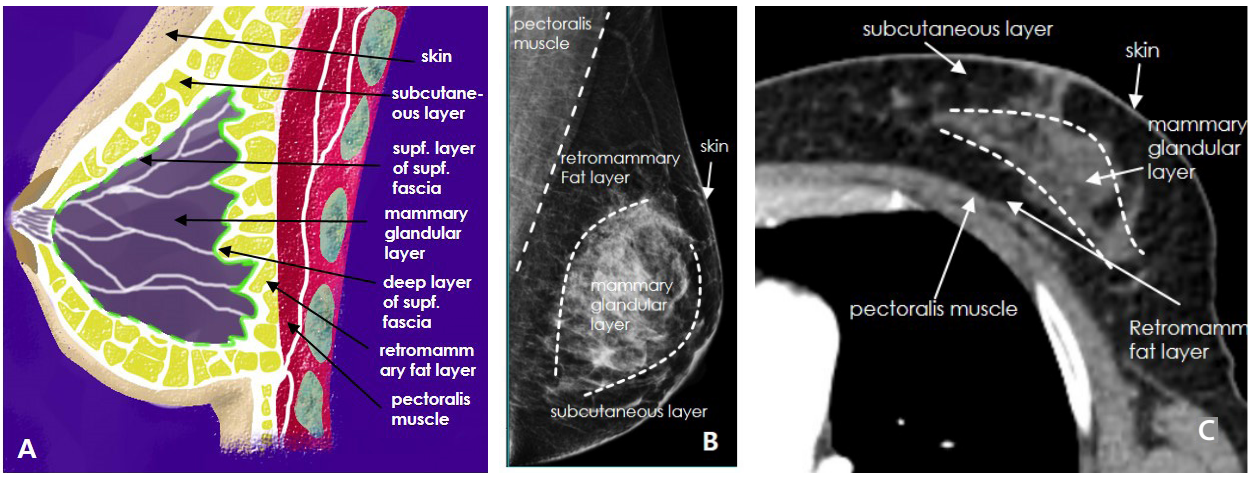

Fig. 1. A: Schematic diagram illustrating the anatomical structure of the breast, B: Mammography showing standard breast tissue without abnormalities, C: Chest CT providing a cross-sectional view of the layers of the breast tissue (deep layer of supf. fascia – deep layer of superficial fascia, deep layer of supf. fascia – deep layer of superficial fascia)

conditions such as pneumonia, postoperative breast changes may be the only imaging clue to a history of breast cancer surgery. Therefore, this pictorial essay focuses on the breast CT findings after surgical treatment for breast cancer (Table 1).

Table 1. Summary of figures with type of surgery*

Figure No.	Age	Diagnosis	Surgery type
3	36	Invasive ductal carcinoma	Modified radical mastectomy
4	65	Ductal carcinoma in situ	Breast conserving surgery
5	60	Invasive mucinous carcinoma	Modified radical mastectomy and augmentation mammoplasty
6	47	Cosmetic cause	Augmentation mammoplasty
7	58	Intraductal carcinoma (two site)	Modified radical mastectomy and TRAM flap
8	55	Invasive ductal carcinoma	Skin-sparing mastectomy and axillary dissection --> LD flap
9	63	Cosmetic cause	Injection mammoplasty (paraffin)

* TRAM – transverse rectus abdominis myocutaneous, LD – lattisimus dorsi

Aim

The incidence of breast cancer is increasing globally, prompting the development of various surgical and reconstructive techniques for its treatment. Chest CT is frequently performed for multiple clinical indications, including screening, postoperative surveillance, and staging. As a result, radiologists may encounter altered breast anatomy after surgery or reconstruction on chest CT images. Lack of familiarity with the postoperative appearance of the breast may lead to misinterpretation or missed diagnoses. Therefore, this article aims to review and illustrate the characteristic imaging findings of various postoperative breast changes that may be incidentally identified on chest CT.

Material and methods

We retrospectively reviewed CT scans of female patients who underwent contrast-enhanced chest CT in the past five years. Cases with breast abnormalities or bilateral asymptomatic breasts were also included. We reviewed the medical records of the included patients and, if the surgical procedure was available, we reviewed the literature to determine the surgical technique and compared it with the CT findings. If the reason for the surgery could be identified, the diagnosis was also recorded.

Analysis of the literature

Surgical treatment for removal of breast mass

Treatment options for breast cancer include surgery, radiation therapy, and chemotherapy. Among these, surgery is the primary treatment modality for operable breast cancer confined to the breast tissue and regional lymph nodes. Advances in breast imaging modalities such as mammography, ultrasound, and magnetic resonance imaging have facilitated earlier detection and led to significant evolution in surgical techniques. Tumor size reduction through early detection has expanded surgical options, including the introduction of skin-sparing and nipple-sparing mastectomies in recent years.

Breast surgery can generally be classified into two categories: mastectomy and breast preservation surgery, depending on whether residual breast tissue remains after surgery.[1,2]

Mastectomy

Mastectomy refers to the surgical removal of all breast tissue and is performed in various forms depending on the extent of tissue excision and oncologic considerations. This paper reviews five commonly performed

types of mastectomy: radical mastectomy, simple (total) mastectomy, modified radical mastectomy, skin-sparing mastectomy, and nipple-sparing mastectomy (Fig. 2).

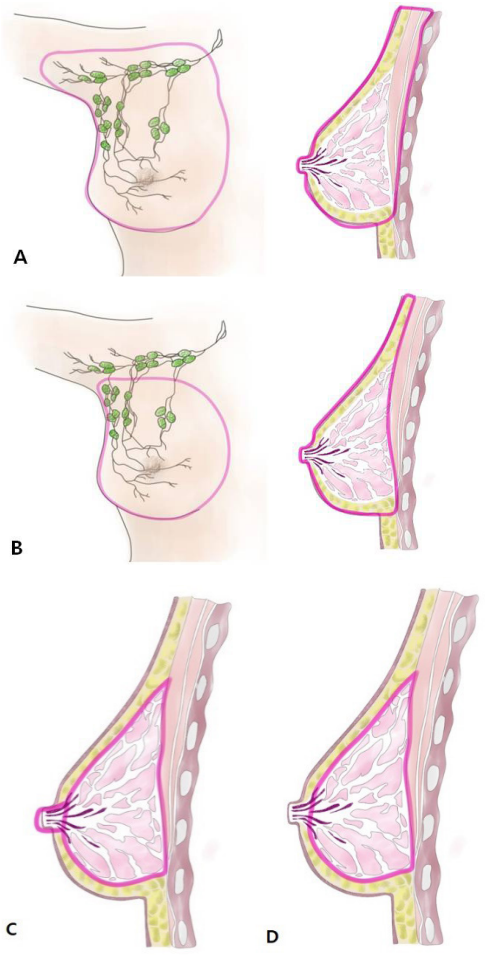

Fig. 2. A: Diagram showing radical mastectomy with a broad range of resection, including the pectoralis muscle, axillary lymph nodes, and adjacent veins in addition to the tissues removed in total mastectomy, B: Schematic image illustrating the extent of tissue removal in total mastectomy, in which breast tissue, skin, and nipple-areola complex are removed while preserving the pectoralis muscle, C: Schema of skin-sparing mastectomy demonstrating removal of breast tissue while maintaining the overlying skin envelope; the nipple-areola complex is removed, D: Nipple-sparing mastectomy image depicting preservation of both the skin envelope and the nipple–areola complex, with removal limited to the underlying breast tissue, in all panels, bold red lines indicate the limits of tissue excision for each surgical procedure

Radical mastectomy

Radical mastectomy was the earliest standard surgical treatment for breast cancer. It involves the complete removal of all breast tissue, overlying skin, nipple-areolar complex (NAC), major and minor muscles, as well as axillary lymph nodes at levels I, II, and III, and sometimes the axillary vein.

Although effective oncologically, this procedure is associated with significant cosmetic deformity and functional impairment and has largely been replaced by modified radical mastectomy.

On chest CT, radical mastectomy appears as a bare chest wall with absent breast parenchyma, pectoral muscles, skin and NAC. The axillary region may show the absence of regional lymph nodes and postoperative changes, such as thin subcutaneous fat directly overlying the chest wall musculature.

Simple (total) mastectomy and modified radical mastectomy

A simple (total) mastectomy involves removal of breast tissue, skin, and NAC while preserving the pectoralis muscles. A modified radical mastectomy includes all elements of a simple mastectomy, but also involves axillary lymph node dissection, typically levels I and II (Fig. 3).

Fig. 3. A: Chest CT after modified radical mastectomy demonstrating removal of the right breast tissue, overlying skin and the nipple–areola complex, and remaining underlying pectoralis muscles, resulting in exposure of the bare chest wall (arrows), B: Chest CT showing absence of the right axillary lymph nodes after surgical dissection (arrow)

In both procedures, the major and minor muscles remain intact and are therefore visible on chest CT. In modified radical mastectomy, postoperative changes or scarring may be observed in the axillary region. Furthermore, in most patients undergoing simple (total) mastectomy, a sentinel lymph node biopsy is performed to evaluate lymph node metastasis, which can also result on minor surgical scarring in the axilla.

Skin-sparing mastectomy

Skin-sparing mastectomy removes all of the breast tissue and NAC, while preserving the overlying skin envelope. Immediate breast reconstruction is typically performed to restore breast contour. This technique is commonly used in patients with T1–T2 breast cancer, ductal carcinoma in situ (DCIS), or for prophylactic mastectomy, but is contraindicated in cases of inflammatory breast cancer or skin involvement.[1,3]

On chest CT, the NAC and the underlying breast tissue are absent, while the native skin and subcutaneous fat remain intact. Depending on the reconstruction method, the images may show an autologous free flap, implants or tissue expanders placed beneath the preserved skin.

Nipple-sparing mastectomy

Nipple-sparing mastectomy is a modification of skin-sparing mastectomy that preserves the NAC in addition to the skin envelope. First described by Freeman in 1962, this technique was initially abandoned due to concerns regarding tumor safety and cosmetic outcomes. However, subsequent studies, including the 1999 report by Hartmann et al., demonstrated its efficacy in prophylactic mastectomy for high-risk patients and later in selected cases of breast cancer.[4]

Classically, the eligibility criteria included a tumor size of <2.5 cm, a tumor located >2 cm from the nipple–areolar complex (NAC), clinically negative axillary lymph nodes, absence of skin involvement or Paget's disease, and no evidence of NAC invasion on preoperative MRI.[4]

Nipple-sparing mastectomy has quickly become a popular standard procedure, with recent retrospective studies demonstrating its oncological safety and cosmetic benefits. However, caution is advised in patients with nipple discharge, inflammatory breast cancer, or NAC -related symptoms.[4]

On chest CT, NAC and skin are preserved, with the absence of the underlying glandular tissue. In some cases, the NAC may also appear intact after other forms of mastectomy due to nipple reconstruction procedures.

Breast-conservation surgery

Breast conserving surgery involves the removal of the breast tissue that contains the tumor along with a margin of normal breast tissue, while preserving the overall contour and appearance of the breast. In patients with invasive ductal carcinoma, a sentinel lymph node biopsy is performed, and if there is evidence of lymph node involvement, an axillary lymph node dissection is performed. Compared to radical surgery, breast-conserving surgery offers superior cosmetic results. This procedure is performed most commonly in patients with T1 and T2 early-stage breast cancers.

Following breast preservation surgery, the majority patients undergo adjuvant radiation therapy and chemotherapy may be administered as indicated.[1] On chest CT, postoperative findings typically include partial removal of the breast tissue that encompasses the tumor with preservation of adjacent normal tissue. The presence of surgical clips and mild deformation of the breast contour often facilitate identification of the surgical procedure (Fig. 4). Furthermore, patients who have undergone radiation therapy may exhibit skin thickening or increased parenchymal trabecularity, which are typical post-radiation changes.

Breast reconstruction

Breast reconstruction encompasses a range of techniques, including autologous flap reconstruction, implant-based reconstruction, NAC reconstruction, and, less commonly, liquid silicone or paraffin injections.

The choice of reconstruction method is influenced by multiple factors, such as the type of prior breast cancer surgery (eg mastectomy vs. breast-conserving surgery), the patient's body habitus, medical history, findings from physical examination and whether adjuvant radiotherapy has been performed.

From a practical perspective of CT interpretation, radiologists should systematically assess muscle sacrifice, donor-site alterations, characteristic reconstruc-

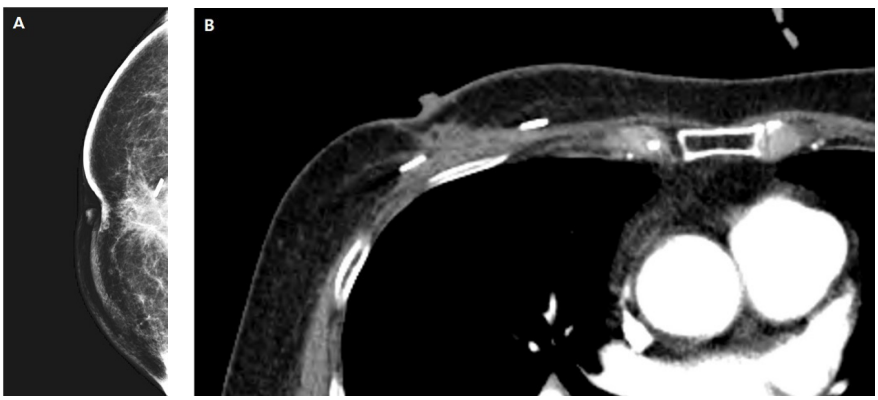

Fig. 4. A: Mammography showing postoperative changes in the right breast consistent with breast-conserving surgery, B: Chest CT showing resection of abnormal breast tissue in the right breast, with surgical clips visible at the operative site corresponding to the findings on mammography

tion-specific landmarks, and visibility of the vascular pedicle visibility, while remaining aware of common diagnostic pitfalls, such as fat necrosis that may mimic tumor recurrence.

Breast implant

The use of breast implants has been increasing for various indications, including cosmetic augmentation, reconstruction after partial or total mastectomy, and correction of congenital breast deformities.

Implants can be classified on the number of lumens and the type of filler material. There are two main types:

Single-lumen implants, which contain either silicone gel or saline solution.

Double-lumen implants, consisting of an inner and outer chamber. A standard double-lumen implant typically has a silicone-filled inner lumen and a saline-filled outer lumen. Conversely, a reverse double-lumen implant contains saline in the inner lumen and silicone gel in the outer lumen.

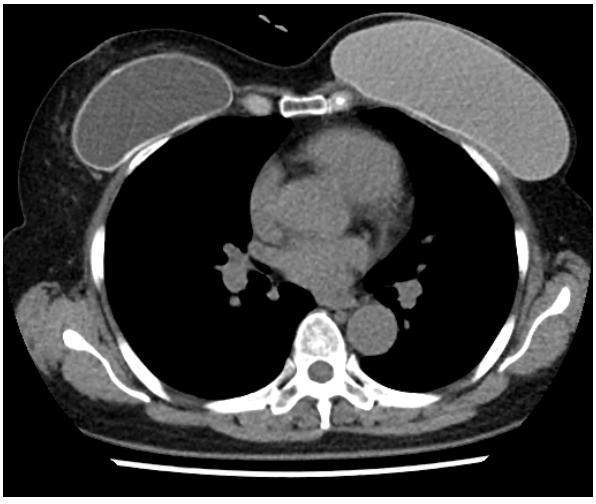

Fig. 5. Chest CT showing normally positioned mammoplasty implants in the subareolar region of both breasts, the right breast implant shows water-like attenuation, suggesting a saline-filled bag, while the left breast implant demonstrates relatively higher attenuation, presumed to represent a silicone-filled bag

Breast implants are most commonly placed either in the subglandular space (beneath the breast tissue) or in the submuscular space (subpectoral) (beneath the pectoralis major muscle). Following implantation, the body forms a fibrous capsule around the implant in response to foreign material – a process known as encapsulation.[6]

On mammography, silicone appears as a dense radiopaque mass due to its relatively low radiolucency. On ultrasound, implants appear as anechoic spaces surrounded by echogenic boundaries, representing the elastomeric shell and fibrous capsule. One or two discrete echogenic lines may be seen that correspond to the implant wall and the surrounding capsule. On chest CT, silicone implants are easily identified as oval-shaped structures with soft tissue-like attenuation, distinguishable in either the subglandular or subpectoral locations. Single-lumen silicone-filled implants appear homogeneous with a well-defined elastomeric shell, often visible as a high-density rim (Fig. 5).

In double-lumen reverse implants, the inner lumen filled with saline demonstrates fluid attenuation, while the outer lumen filled with silicone shows soft tissue attenuation, similar to single-lumen silicone implants.

Radial folds and small volumes of periprosthetic fluid may sometimes be observed in asymptomatic implants and should not be misinterpreted as signs of rupture. This fluid is thought to represent a benign inflammatory response. Over time, capsular thickening or calcification may occur and can be readily detected on CT.

Implant rupture

Breast implants are not permanent devices and are subject to rupture over time, and the risk increasing with implant age. Most ruptures occur 10 to 15 years after placement, although the exact incidence remains unclear.[7]

Ruptures are typically classified as intracapsular or extracapsular:

Intracapsular rupture occurs when the implant shell is damaged, but the contents (silicone or saline) remain confined within the fibrous capsule (Fig. 6).[8] This type of rupture is more common and may be difficult to detect on mammography, although subtle contour deformities or focal bulging of the implant may be observed.

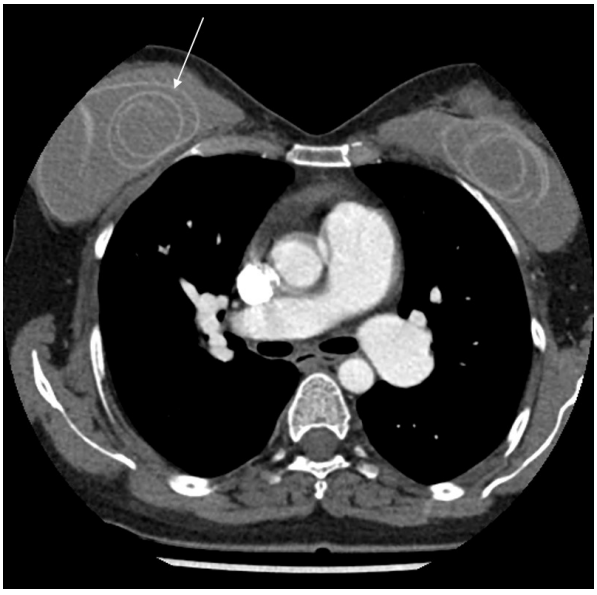

Fig. 6. Chest CT demonstrating intracapsular rupture of both breast implants, multiple linear structures parallel to the implant capsule (arrow), consistent with the 'linguine sign', while the implant contents remain contained within the surrounding fibrous capsule without extracapsular leakage

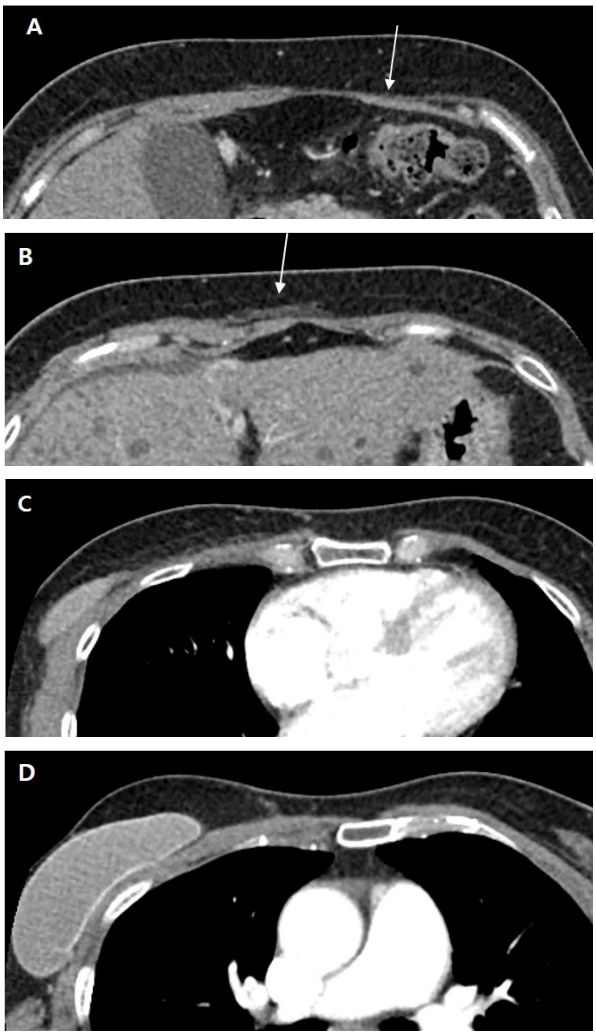

Fig. 7. A: Chest CT acquired in a caudocranial direction demonstrating absence of the left rectus abdominis muscle (arrow), indicating its use as a donor site for the TRAM flap, B: Image showing the pedicle (arrow) connecting the abdominal donor site to the reconstructed right breast, C: Chest CT depicting the formation of the right breast mound by the transferred TRAM flap tissue, D: Additional image showing a mammoplasty bag used concurrently as a volume expander

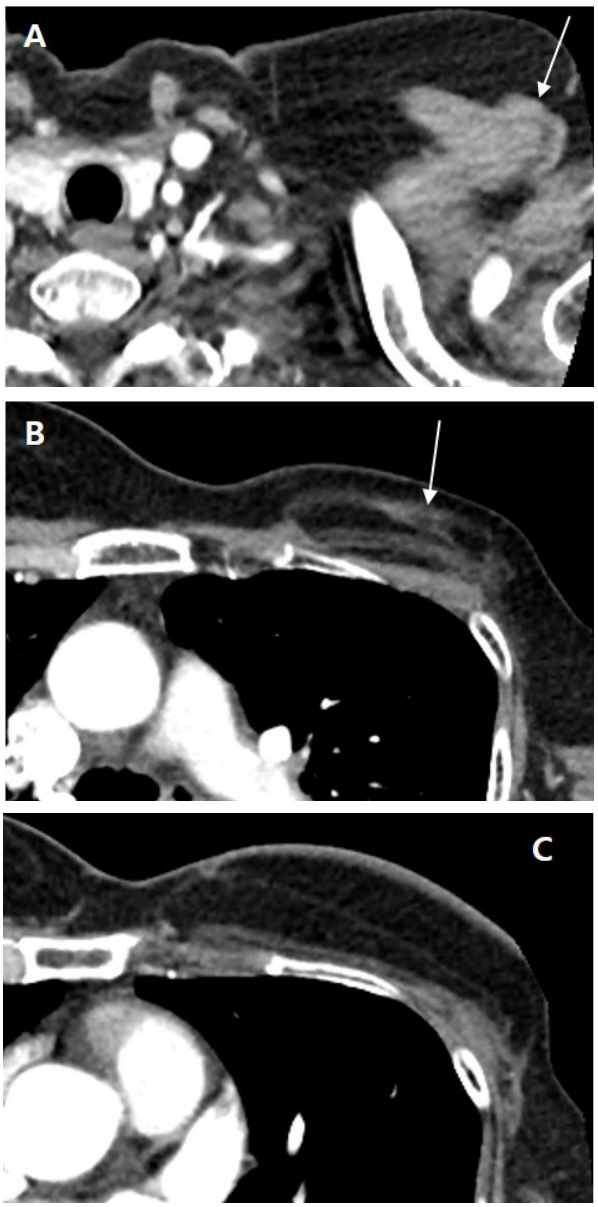

Fig. 8. A: Chest CT showing the pedicle (arrow) originating from the upper left chest, extending anterior to the humerus, B: Sequential image showing the pedicle descending toward the thoracic wall, C: Chest CT showing the transferred latissimus dorsi flap forming fatty tissue within the left breast region, contributing to the maintenance of the reconstructed breast contour

In ultrasound, multiple echogenic lines within the capsule (representing collapsed shell fragments) create the characteristic 'stepladder sign.' On MRI, low-signal-intensity curvilinear lines within the implant represent the 'linguine sign,' a hallmark of intracapsular rupture. On chest CT, a deformed or retracted contour of the implant may be noted, indicating shell collapse.

Extracapsular rupture involves disruption of both the implant shell and the fibrous capsule, allowing silicone to escape into the surrounding breast tissue.

On mammography, extracapsular silicone may appear as radiolucent areas outside the implant boundaries. Breast ultrasound demonstrates the 'snowstorm sign,' in which echogenic silicone droplets cause diffuse acoustic shadowing, obscuring normal tissue planes. Magnetic resonance imaging and computed tomography can also detect extravasated silicone, particularly in the subcutaneous tissue or lymph nodes.

Flap surgery

After mastectomy, breast reconstruction can be performed using autologous tissue flaps – comprising skin and subcutaneous fat – as an alternative or complement to implant-based reconstruction. This approach is asso-

ciated with superior long-term aesthetic and functional outcomes, as it can replace a substantial volume of breast tissue and more closely mimic the natural contour and texture.

Commonly used autologous flap techniques include the transverse rectus abdominis myocutaneous flap (TRAM), the deep inferior epigastric perforator flap (DIEP), the latissimus dorsi flap, and the profunda artery perforator flap (PAP).

The TRAM flap involves the transposition of the transverse rectus abdominis muscle and the overlying skin/subcutaneous tissue to the chest wall, typically through a subcutaneous tunnel. The pedicled TRAM flap includes a large part of the rectus abdominis muscle and is supplied by the superior epigastric vessels. Variants include the free TRAM flap and the muscle-sparing free TRAM flap, both of which aim to minimize donor site morbidity. However, mobilizing a significant portion of the rectus abdominis may weaken the abdominal wall and increase the risk of hernia formation.

On chest CT, the TRAM flap appears as a thin curvilinear soft tissue band within the reconstructed breast, corresponding to the autologous dermal layer (Fig. 7). Fat-attenuation tissue superficial to this band represents native subcutaneous chest fat, while deeper fat-attenuation tissue reflects transposed abdominal fat. In the presence of infection, inflammation, or tumor recurrence, this band may appear abnormally thickened, which warrants careful interpretation by radiologists.[10]

The DIEP flap utilizes only skin and fat from the lower abdomen, preserving the rectus abdominis muscle. This muscle-sparing technique significantly reduces complications related to abdominal wall weakness such as hernias – while maintaining a natural breast shape and feel. The DIEP flap currently represents the most commonly performed autologous flap procedure in breast reconstruction. Successful harvesting requires precise microvascular dissection to isolate perforator vessels while sparing muscle.

The latissimus dorsi flap involves the transfer of skin, fat, and the latissimus dorsi muscle from the back to the chest wall (Fig. 8). Due to its proximity to the breast and its reliable vascularity, it is often used for partial reconstructions or in combination with implants when additional volume is needed. However, due to the relatively limited adipose tissue in the back, its utility for large-volume reconstructions is limited.

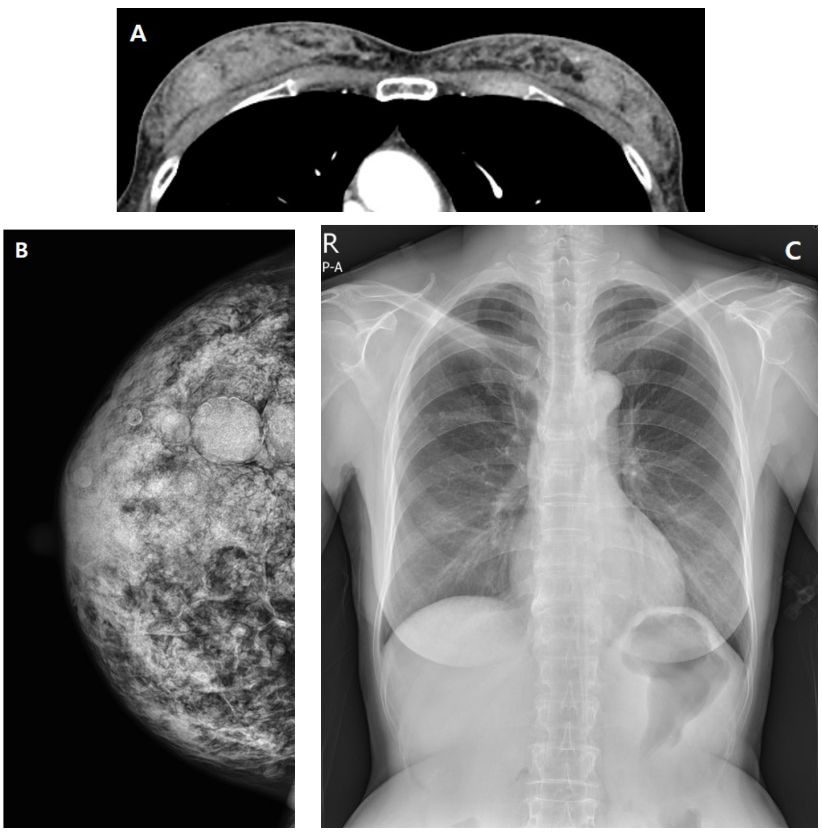

Fig. 9. A: Chest CT demonstrating a mild increase in opacity in both breasts. Some areas show small round calcifications, whereas extensive calcification is rare, B: Mammography showing multiple granulomas corresponding to areas of increased opacity on CT, consistent with paraffin granuloma. The absence of 'eggshell' calcification helps distinguish it from silicone granuloma, C: Chest PA showing no obvious abnormalities in the breasts despite the presence of granulomas on CT and mammography

Direct injection of liquid silicone or paraffin

Although no longer commonly practiced, direct injection of liquid silicone or paraffin into breast tissue for cosmetic augmentation was performed between the early 1900s and 1970s. Since then, these procedures have been abandoned due to their serious long-term complications, including granulomatous inflammation, mass formation, fibrosis, and calcification of the breast parenchyma.

Silicone injections were used more frequently than paraffin and are associated with the development of silicone granulomas, which may appear on breast imaging and chest CT as multiple round high-density cystic lesions with eggshell calcifications. These findings often help delineate abnormal tissue within the breast parenchyma.[9]

On the contrary, paraffin granulomas are usually present as nodules of varying sizes, often with central radiolucency and calcification (Fig. 9). They may induce fibrotic reactions in the surrounding tissue, leading to blurring of the subcutaneous fat plane, skin thickening, and parenchymal calcifications.[11]

In cases where silicone and paraffin injections were used and if the granulomatous reaction progresses to extensive fibrosis with architectural distortion of the breast, breast cancer should be included in the differential diagnosis.[9] These post-injection changes represent one of the most challenging differential diagnoses on CT, as extensive fibrosis and calcifications can both mimic and obscure underlying malignancy. Therefore, accurate imaging interpretation is essential to avoid missed or delayed diagnosis.

Conclusion

Chest CT may be performed in patients with breast cancer for a variety of postoperative indications, including surveillance, evaluation of complications, or unrelated clinical concerns. Given the wide range of surgical techniques and reconstructive procedures, as well as potential postoperative complications, it is essential for radiologists must accurately interpret chest CT findings in this context. Therefore, the systematic evaluation of the breasts on routine chest CT should be considered an integral component of comprehensive radiologic interpretation in patients with postoperative breast cancer.

Declarations

Funding

The work was supported by a grant from research year of Inje University in 20180006.

Author contributions

Conceptualization, MJ.K.; Methodology, MJ.K.; Software, T.K.; Validation, MJ.K. and T.K.; Formal Analysis, T.K.; Investigation, T.K.; Resources, MJ.K.; Data Curation, MJ.K.; Writing – Original Draft Preparation, T.K.; Writing – Review & Editing, MJ.K.; Visualization, T.K.; Supervision, MJ.K.; Project Administration, MJ.K.

Conflicts of interest

All authors declare no conflict of interest.

Data availability

The data that support the findings of this study are available from the authors.

Ethics approval

The study was conducted in accordance with the Declaration of Helsinki, and the protocol was approved by the Ethics Committee of Inje University Sanggye Paik Hospital (2025-08-010). All images are fully anonymized and do not contain any identifiable patient data. Therefore, patient consent and ethical approval were not required according to institutional policy.

References

1. Neal CH, Yilmaz ZN, Noroozian M, et al. Imaging of breast cancer-related changes after surgical therapy. *AJR Am J Roentgenol*. 2014;202(2):262-272. doi:10.2214/AJR.13.11517
2. Margolis NE, Morley C, Lotfi P, et al. Update on imaging of the postsurgical breast. *Radiographics*. 2014;34(3):642-660. doi:10.1148/rg.343135059
3. Ho CM, Mak CK, Lau Y, Cheung WY, Chan MC, Hung WK. Skin involvement in invasive breast carcinoma: safety of skin-sparing mastectomy. *Ann Surg Oncol*. 2003;10(2):102-107. doi:10.1245/aso.2003.05.001
4. Ashikari AY, Kelemen PR, Tastan B, Salzberg CA, Ashikari RH. Nipple sparing mastectomy techniques: a literature review and an inframammary technique. *Gland Surg*. 2018;7(3):273-287. doi:10.21037/gs.2017.09.02
5. Jung JI, Kim HH, Park SH, et al. Thoracic manifestations of breast cancer and its therapy. *Radiographics*. 2004;24(5):1269-1285. doi:10.1148/rg.245035062
6. Yang N, Muradali D. The augmented breast: a pictorial review of the abnormal and unusual. *AJR Am J Roentgenol*. 2011;196(4):W451-W460. doi:10.2214/AJR.10.4864
7. Juanpere S, Perez E, Huc O, Motos N, Pont J, Pedraza S. Imaging of breast implants-a pictorial review. *Insights Imaging*. 2011;2(6):653-670. doi:10.1007/s13244-011-0122-3
8. Brown SL, Middleton MS, Berg WA, Soo MS, Pennello G. Prevalence of rupture of silicone gel breast implants revealed on MR imaging in a population of women in Birmingham, Alabama. *AJR Am J Roentgenol*. 2000;175(4):1057-1064. doi:10.2214/ajr.175.4.1751057
9. Pinel-Giroux FM, El Khoury MM, Trop I, Bernier C, David J, Lalonde L. Breast reconstruction: review of surgical methods and spectrum of imaging findings. *Radiographics*. 2013;33(2):435-453. doi:10.1148/rg.332125108

10. LePage MA, Kazerooni EA, Helvie MA, Wilkins EG. Breast reconstruction with TRAM flaps: normal and abnormal appearances at CT. *Radiographics*. 1999;19(6):1593-1603. doi:10.1148/radiographics.19.6.g99no111593

11. Erguvan-Dogan B, Yang WT. Direct injection of paraffin into the breast: mammographic, sonographic, and MRI features of early complications. *AJR Am J Roentgenol*. 2006;186(3):888-894. doi:10.2214/AJR.05.0064

Rzeszów University Press 2026
ISSN 2544-1361 (online)
doi: 10.15584/ejcem.2026.2.4

http://www.ejcem.ur.edu.pl
European Journal of Clinical and Experimental Medicine
Eur J Clin Exp Med 2026; 24 (2): 400–405

REVIEW PAPER

The role of glutathione peroxidase enzymes in Alzheimer's disease

Alexandros Kordatzakis [1], Margaux Kourkouliotis [1], Andriana Hadjiyianni [2], Emma Arifagic [1], Eleni Paradeisi [1], Datis Kalali [2]

[1] School of Medicine and Dentistry, European University of Cyprus, Nicosia, Cyprus
[2] Medical School, University of Cyprus, Nicosia, Cyprus

ABSTRACT

Introduction and aim. Alzheimer's disease (AD) is a neurodegenerative disorder that affects mainly the elderly. Among the variety of factors contributing to the pathogenesis of AD, oxidative stress has emerged as a key factor in the initiation and progression of the disease. Glutathione peroxidases (GPxs) are enzymes that are known to play a critical role in maintaining cellular redox balance. To this end, the present narrative review aims to explore the role of GPx enzymes in AD and discuss their contribution to oxidative stress pathways and AD pathogenesis.

Literature search. PubMed, Scopus, and Google Scholar were searched for relevant literature. No specific inclusion and exclusion criteria were used due to the narrative nature of the review.

Analysis of the literature. Available records suggest a strong association between oxidative stress and the pathological features of AD, including amyloid-β aggregation, tau hyperphosphorylation, and neuroinflammation. The enzyme isoforms GPx1, GPx3, and GPx4 have been implicated in AD pathogenesis.

Conclusions. GPx enzymes play an important protective role in AD. Despite promising preclinical evidence, more translational research is required to clarify the therapeutic and biomarker potential of GPxs in AD.

Keywords. Alzheimer's disease, glutathione peroxidase, neurodegeneration, oxidative stress

Introduction

Alzheimer's disease (AD) is the most common cause of dementia worldwide, which can significantly affect a patient's cognitive abilities.[1] Despite the numerous studies undertaken, the underlying mechanisms that contribute to the pathogenesis and progression of AD have not been fully understood and, moreover, no definitive therapeutic strategy has yet been discovered.[2,3] The disease is characterized as a neuroinflammatory disease and oxidative stress is known to play a critical role in the initiation and progression of different inflammatory diseases.[4] Indeed, studies have shown that oxidative stress is a significant factor in the pathophysiology of AD.[5,6]

Glutathione peroxidases (GPx) are enzymes that are known to play a key role in protecting the organism from oxidative stress by reducing ROS.[7] The activation of these enzymes is known to be a protection factor against many diseases induced by oxidation and cell senescence.[8] GPx catalyze the reduction of hydrogen peroxide (H_2O_2) and organic hydroperoxides in water (H_2O) and corresponding alcohols, using reduced glutathione (GSH) as an electron donor.[7]

Aim

This narrative review was undertaken to explore the role of GPx enzymes in the pathogenesis and progression of

Corresponding author: Datis Kalali, e-mail: kalali.datis@ucy.ac.cy

Received: 19.11.2025 / Revised: 13.01.2026 / Accepted: 18.01.2026 / Published: 30.06.2026

Kordatzakis A, Kourkouliotis M, Hadjiyianni A, Arifagic E, Paradeisi E, Kalali D. The role of glutathione peroxidase enzymes in Alzheimer's disease. *Eur J Clin Exp Med.* 2026;24(2):400–405. doi: 10.15584/ejcem.2026.2.4.

AD, their participation in the oxidative stress mechanisms that contribute to neurodegeneration, and their potential as therapeutic targets for the prevention or treatment of AD.

Literature search

The databases PubMed, Scopus, and Google Scholar were searched to retrieve available literature on the role of GPxs in Alzheimer's disease dating from inception until December 2024. Keywords 'Glutathione peroxidase*', 'GPx', 'Alzheimer', 'Oxidative stress', and "Dementia" were used in combination with Boolean operators. Due to the narrative nature of the review, there were no specific inclusion and exclusion criteria. Overall, original research, reviews, and meta-analyses from peer-reviewed journals with relevant information, including, written in English, were included in the synthesis of the present narrative review. No formal risk of bias assessment or quantitative synthesis was performed due to the narrative design of the review.

Analysis of the literature

The role of oxidative stress in AD

Oxidative stress is increasingly recognized as a central factor in the pathophysiology of AD. Specifically, studies suggest a bidirectional relationship between oxidative stress and AD; oxidative stress can promote the formation of Aβ-plaques by upregulating β- and γ-secretase activity, and also leads to tau tangle formation by activating inflammation-associated kinases, whereas in established Alzheimer's disease, amyloid and tau pathology themselves drive reactive oxygen species production, thus increasing oxidative stress.[9] Specifically, ROS exacerbate Aβ aggregation and tau phosphorylation, perpetuating a vicious cycle that accelerates neurodegeneration.[10,11] It is also worth mentioning that oxidative stress is closely linked to impaired autophagy and hence can worsen neuronal vulnerability in AD.[12] Simultaneously, in AD, age and accumulation of Aβ-plaques and tau tangles induce excessive ROS production, including superoxide, hydrogen peroxide and hydroxyl radicals.[13] This leads to harm in neurons, glial cells, and the integrity of the blood-brain barrier (BBB). The brain's susceptibility to oxidative damage arises from its high metabolic demands. Furthermore, the high iron content catalyzes ROS generation, coupled with relatively weak endogenous antioxidant defenses.[14] This results in mitochondrial dysfunction, activation of pro-inflammatory pathways, and cellular apoptosis. At the same time, activated microglia have been found to produce reactive oxygen species in Alzheimer's disease, increasing oxidative stress.[15] Overall, this leads to a vicious cycle that accelerates neurodegeneration.

Advanced glycation end products (AGEs), which accumulate in Aβ plaques, also promote oxidative damage, directly and indirectly contributing to neuronal death.[16] Figure 1 summarizes the pathways through which oxidative stress promotes the pathogenesis and progression of AD.

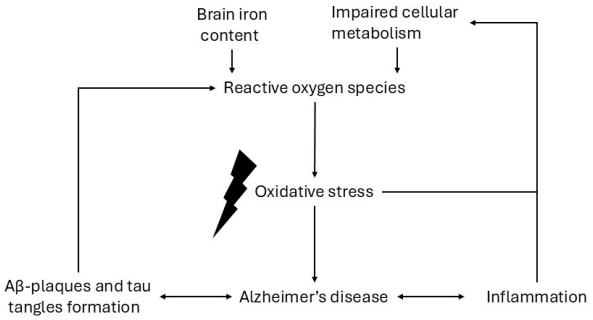

Fig. 1. Oxidative stress and the pathophysiology of Alzheimer's disease

GPx and neurodegeneration

GPx1 (cytosolic GPx) is the most widely expressed isoform of GPx and is predominantly localized in the cytosol and mitochondria of various tissues, where it plays a critical role in the detoxification of hydrogen peroxide.[17] Extensive studies in experimental models have shown that the absence of GPx1 significantly increases the vulnerability of cells to oxidative stress.[18] GPx1 knockout models show an increased susceptibility to cellular damage induced by hydrogen peroxide and exacerbate neurotoxic effects, particularly under conditions of elevated oxidative burden, as seen in neurodegenerative diseases such as Alzheimer's.[19] Furthermore, GPx1 is involved in modulating redox-sensitive signaling pathways, including those involving NF-κB, ERK1/2, and PKCβII, which are critical in the regulation of neuronal excitability, inflammatory responses and cell survival.[20] It is still highly debated whether or not GPx1 plays a direct or secondary role in the development of AD. However, a study carried out in Brazil by Cardoso et al. suggested that the Pro198Leu genetic variation in the GPx1 gene was equally common in AD patients and healthy controls, suggesting that it does not increase the risk of AD, although AD patients with the Pro/Pro genotype had lower selenium levels compared to controls and, in turn, decreased antioxidant potential, suggesting that it affects the function of antioxidant enzymes in AD.[21] These findings highlight the need for further research on this genetic polymorphism in AD.

GPx2 (gastrointestinal GPx) is expressed primarily in the gastrointestinal epithelium, where it plays a crucial role in protecting epithelial cells from oxidative stress induced by dietary factors and gut microorganisms.[22] GPx2 works by catalyzing the reduction of hydrogen peroxide and other ROS to water, thus maintaining redox balance in the intestine and reducing inflammation and tissue damage.[23] Although its direct

involvement in Alzheimer's disease has not been established, it can hypothesize that since its function can lead to systemic oxidative stress, it may indirectly influence neuroinflammatory processes.[24] It is worth mentioning that the gut microbiome has been found to affect the presentation of Alzheimer's disease, further verifying the role of GPx2 in the pathogenesis.[25,26]

GPx3 (plasma GPx) is a secreted enzyme found primarily in extracellular fluids such as plasma, where it plays a crucial role in the defense of systemic antioxidant defense.[27] Studies have found a positive association between downregulation of GPx3 and the pathogenesis of Alzheimer's disease.[28,29] Specifically, peripheral oxidative stress and systemic inflammation can contribute to disruption of the blood-brain barrier (BBB), allowing peripheral oxidative damage to exacerbate neuronal damage, as seen in Alzheimer's disease.[30] Therefore, GPx3's antioxidant function in mitigating peripheral oxidative stress may be critical in protecting the CNS and maintaining brain health.

Among the GPx isoforms, GPx4 (phospholipid hydroperoxide GPx) is unique due to its ability to directly reduce lipid hydroperoxides in cellular membranes, lipoproteins, and organelles, which is essential for maintaining cellular integrity, particularly in tissues with high oxidative activity, such as the brain.[31] Moreover, the neurons of the hypothalamus, hippocampus, and the cerebellum have been found to contain GPx4 which is synthesized endogenously in the brain.[32] GPx4 was found to have a critical role in counteracting cellular deterioration and protecting against brain injury. Another important role for GPx4 is its participation in the regulation of ATP production during oxidative stress. As one may gather, this is of great importance due to the potential damage that can occur to mitochondria caused by oxidative stress. AD is an example of a condition related to mitochondrial problems. Furthermore, studies have proven that a deficiency in selenium could expose cells to ferroptosis and therefore make them more vulnerable all due to reduced GPx4 activity. Therefore, it is of great importance to highlight that selenium levels of selenium must be maintained to ensure GPx4 protective effects on neurons.[33]

The role is also critical in preventing ferroptosis, an iron-dependent form of programmed cell death driven by lipid peroxidation, which is implicated in neurodegenerative diseases.[34] Indeed, a study by Khan et al. suggested that ferroptosis plays a critical role in the progression of Alzheimer's disease.[35] Conditional knockout models of GPx4 exhibit severe neuronal loss, particularly in the hippocampus, a critical brain region for memory and learning, and is accompanied by increased lipid peroxidation and astrogliosis, both of which are features of Alzheimer's pathology.[36,37] The dysregulation of GPx4 and the resulting increase in lipid peroxidation, ferroptosis, and neuroinflammation are key factors in the progression of AD.[36]

Figure 2 summarizes the role of GPx enzymes in preventing AD.

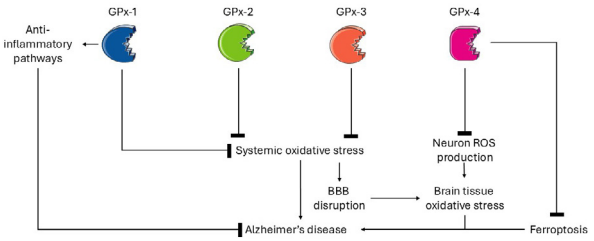

Fig. 2. GPx and the prevention of Alzheimer's disease (BBB – blood-brain barrier, ROS – reactive oxygen species)

Clinical uses of GPx in AD

Given the central role of oxidative stress in AD and the potential of GPx enzymes to mitigate this damage, these enzymes represent highly attractive therapeutic targets for the treatment of AD. Strategies aimed at enhancing GPx activity could help restore redox balance and prevent neuronal damage. Potential approaches include the development of small molecule activators of GPx enzymes, gene therapy to increase GPx expression, or the use of dietary antioxidants to support the GPx system. Small-molecule activators, such as ebselen, mimic the activity of GPx enzymes and have demonstrated their efficacy in reducing oxidative stress and inflammation in preclinical models.[38] Gleichzeitig, advances in gene-editing technologies, particularly CRISPR-Cas9, offer the potential to up-regulate GPx4 expression in affected brain regions, allowing targeted neuroprotection.[39] Supplementation with diet selenium also plays a significant role, since selenium serves as an essential cofactor for GPx activity. Supplementing selenium has shown potential to improve GPx function, demonstrating neuroprotective effects in clinical trials and mitigating oxidative damage.[40-42] In addition, combination therapies that integrate GPx-targeted interventions with other AD treatments, such as Aβ aggregation inhibitors or tau modulating drugs, may provide synergistic benefits by addressing multiple aspects of the disease pathology, while the combined approach could offer enhanced neuroprotection, slowing neuronal damage, and preserving brain function.[11,43,44] It is also worth mentioning that certain natural plant products that upregulate GPx4, including senegenin, berberin and tannic acid have already been shown to exhibit neuroprotective effects in vitro and on mice, indicating them as possible ways of enhancing GPx4 activity for prevention of AD.[45-47] Nevertheless, no clinical trials were retrieved in the literature search that shows effects of GPx upregulation through pharmacological intervention in AD patients. Overall, there is currently no robust clinical evi-

dence that direct GPx-targeting therapies can modify AD outcomes in humans though preclinical data suggest GPx modulation may affect AD-relevant oxidative pathways.

GPx and ROS levels could also serve as an early indicator, with their use as biomarkers, of oxidative imbalance, having a vital role in the early detection and prevention of idiopathic and genetical AD. That is, the flavoprotein apoptosis-inducing factor, mitochondrial-associated 2 (AIFM2), also known as ferroptosis suppressor protein 1 (FSP1), has gained attention for its role in mitigating ferroptosis through suppression of lipid peroxidation suppression.[48] AIFM2 complements the function of GPx enzymes, particularly GPx4, by maintaining redox balance through reduction of ubiquinone to ubiquinol, a key antioxidant. Meanwhile, GPx3, which shares functional similarities with GPx1, but is unique in its sensitivity to selenium levels, offers a promising avenue as a biomarker of selenium status.[49] This characteristic makes it a valuable biological marker for assessing selenium content in the body, which is crucial for optimal GPx enzyme function. Given the correlation between selenium deficiency and impaired antioxidant defenses, monitoring GPx3 activity could provide information on systemic redox imbalances that precede AD onset.[50] However, it is worth mentioning that plasma GPx3 primarily reveals systemic oxidative status and is a practical state marker for epidemiologic or intervention studies, but directly reflect neuronal GPx activity, due to the difference in GPx levels between the central nervous system and serum, induced by the blood–brain barrier. On the contrary, GPx levels measured in cerebrospinal fluid, mainly those of GPx4, better reflect neuronal oxidative status and can be better used as diagnostic and theragnostic biomarkers, but with the acquisition of CSF samples, limiting the practicality of routine diagnostic.

Future perspectives

The role of GPx enzymes in AD is a promising area of research, with compelling evidence suggesting that these enzymes play a vital role in protecting against oxidative stress and neuronal damage. By reducing ROS, GPx enzymes help maintain cell redox balance and prevent the harmful effects of oxidative damage, which is central to the pathophysiology of AD. Although much remains to be understood about the precise mechanisms by which GPx enzymes contribute to AD progression, their potential as therapeutic targets deserves further investigation. Major gaps include varying clinical findings and the lack of interventional studies and clinical trials directly investing GPx in AD. The majority of findings originate from preclinical cell and animal models, which demonstrate credibility, but one cannot assume with certainty that translation directly to humans is plausible. Future research focusing on modulation of GPx activity could provide new avenues for the prevention and treatment of Alzheimer's disease, offering hope to patients and families affected by this devastating disease.

The functional complexity of the GPx family and the varying roles of different isoforms in different tissues and cell types complicate the development of targeted therapies. There is a need for a multimodal approach combining redox regulation, neuroinflammation control, and BBB permeability strategies.[51,52] More research is needed to determine the most effective strategies for modulating GPx activity and optimizing the therapeutic potential of these enzymes.

Conclusion

Overall, in spite of the promising data, further studies and trials are needed to validate the reliability and consistency of GPx levels as biomarkers and therapeutic targets and identifying confounding factors.

Acknowledgements

The authors express their sincere gratitude to Professor George D. Vavougios from the University of Cyprus for revising the manuscript.

Declarations

Funding

None

Author contributions

Conceptualization, D.K.; Methodology, A.K., M.K., A.H. and D.K.; Software, A.H.; Validation, A.K., M.K., A.H., E.A. and D.K.; Formal Analysis, A.K., M.K., A.H. and E.A.; Investigation, A.K., M.K., A.H. and E.A.; Resources, A.K., M.K., A.H. and E.A..; Data Curation, A.K., M.K., A.H. and E.A.; Writing – Original Draft Preparation, A.K., M.K., A.H., E.P. and E.A..; Writing – Review & Editing, D.K.; Visualization, D.K.; Supervision, D.K.; Project Administration, F.K.

Conflicts of interest

None to declare.

Data availability

Not applicable.

Ethics approval

Not applicable.

References

1. Cao Q, Tan CC, Xu W, et al. The prevalence of dementia: a systematic review and meta-analysis. *J Alzheimers Dis*. 2020;73(3):1157-1166. doi:10.3233/jad-191092
2. Patel B, Walker R, Capó M, et al. A review of Alzheimer's disease and inflammation: pathogenesis, inflammatory processes, and novel insights from the artificial intelligen-

ce perspective. *Med Res Arch*. 2023;11(7.2). doi:10.18103/mra.v11i7.2.3971
3. Xiao D, Zhang C. Current therapeutics for Alzheimer's disease and clinical trials. *Explor Neurosci*. 2024;3(3):255-271. doi:10.37349/en.2024.00048
4. Lugrin J, Rosenblatt-Velin N, Parapanov R, Liaudet L. The role of oxidative stress during inflammatory processes. *Biol Chem*. 2014;395(2):203-230. doi:10.1515/hsz-2013-0241
5. Ionescu-Tucker A, Cotman CW. Emerging roles of oxidative stress in brain aging and Alzheimer's disease. *Neurobiol Aging*. 2021;107:86-95. doi:10.1016/j.neurobiolaging.2021.07.014
6. Dhapola R, Beura SK, Sharma P, Singh SK, HariKrishna-Reddy D. Oxidative stress in Alzheimer's disease: current knowledge of signaling pathways and therapeutics. *Mol Biol Rep*. 2024;51(1):48. doi:10.1007/s11033-023-09021-z
7. Jurkovic Mlakar S, Osredkar J, Marc J. Molecular impact of glutathione peroxidases in antioxidant processes. *Biochem Med*. 2008. doi:10.11613/BM.2008.016
8. Sarikaya E, Doğan S. Glutathione peroxidase in health and diseases. In: Bagatini MD, editor. *Glutathione System and Oxidative Stress in Health and Disease*. Rijeka: IntechOpen; 2020.
9. Dhapola R, Beura SK, Sharma P, Singh SK, HariKrishna-Reddy D. Oxidative stress in Alzheimer's disease: current knowledge of signaling pathways and therapeutics. *Mol Biol Rep*. 2024;51(1):48. doi:10.1007/s11033-023-09021-z
10. Teixeira JP, de Castro AA, Soares FV, da Cunha EFF, Ramalho TC. Future therapeutic perspectives into Alzheimer's disease targeting the oxidative stress hypothesis. *Molecules*. 2019;24(23):4410. doi:10.3390/molecules24234410
11. Tamagno E, Guglielmotto M, Vasciaveo V, Tabaton M. Oxidative stress and beta amyloid in Alzheimer's disease. Which comes first: the chicken or the egg? *Antioxidants (Basel)*. 2021;10(9). doi:10.3390/antiox10091479
12. Hussain MS, Agrawal N, Ilma B, et al. Autophagy and cellular senescence in Alzheimer's disease: key drivers of neurodegeneration. *CNS Neurosci Ther*. 2025;31(7):e70503. doi:10.1111/cns.70503
13. Huang WJ, Zhang X, Chen WW. Role of oxidative stress in Alzheimer's disease. *Biomed Rep*. 2016;4(5):519-522. doi:10.3892/br.2016.630
14. Jiang T, Sun Q, Chen S. Oxidative stress: a major pathogenesis and potential therapeutic target of antioxidative agents in Parkinson's disease and Alzheimer's disease. *Prog Neurobiol*. 2016;147:1-19. doi:10.1016/j.pneurobio.2016.07.005
15. Hussain MS, Khan Y, Fatima R, et al. Microglial modulation in Alzheimer's disease: central players in neuroinflammation and pathogenesis. *Curr Alzheimer Res*. 2025;22(1):56-82. doi:10.2174/0115672050364292250113063513
16. Gella A, Durany N. Oxidative stress in Alzheimer disease. *Cell Adh Migr*. 2009;3(1):88-93. doi:10.4161/cam.3.1.7402
17. Margis R, Dunand C, Teixeira FK, Margis-Pinheiro M. Glutathione peroxidase family- an evolutionary overview. *FEBS J*. 2008;275(15):3959-3970. doi:10.1111/j.1742-4658.2008.06542.x
18. Liu C, Yan Q, Gao C, Lin L, Wei J. Study on antioxidant effect of recombinant glutathione peroxidase 1. *Int J Biol Macromol*. 2021;170:503-513. doi:10.1016/j.ijbiomac.2020.12.183
19. Sharma G, Shin E-J, Sharma N, et al. Glutathione peroxidase-1 and neuromodulation: novel potentials of an old enzyme. *Food Chem Toxicol*. 2021;148:111945. doi:10.1016/j.fct.2020.111945
20. Brigelius-Flohé R, Maiorino M. Glutathione peroxidases. *Biochim Biophys Acta*. 2013;1830(5):3289-3303. doi:10.1016/j.bbagen.2012.11.020
21. Cardoso BR, Ong TP, Jacob-Filho W, et al. Glutathione peroxidase 1 Pro198Leu polymorphism in Brazilian Alzheimer's disease patients: relations to the enzyme activity and to selenium status. *J Nutrigenet Nutrigenomics*. 2012;5(2):72-80. doi:10.1159/000338682
22. Chu FF, Doroshow JH, Esworthy RS. Expression, characterization, and tissue distribution of a new cellular selenium-dependent glutathione peroxidase, GSHPx-GI. *J Biol Chem*. 1993;268(4):2571-2576. doi:10.1016/S0021-9258(18)53812-6
23. Esworthy RS, Yang L, Frankel PH, Chu FF. Epithelium-specific glutathione peroxidase, Gpx2, is involved in the prevention of intestinal inflammation in selenium-deficient mice. *J Nutr*. 2005;135(4):740-745. doi:10.1093/jn/135.4.740
24. Guo B, Liao W, Wang S. The clinical significance of glutathione peroxidase 2 in glioblastoma multiforme. *Transl Neurosci*. 2021;12:032-039. doi:10.1515/tnsci-2021-0005
25. Bashir B, Gulati M, Vishwas S, et al. Bridging the gap in the management of Alzheimer's disease using fecal microbiota transplantation. *Mol Cell Neurosci*. 2025;135:104052. doi:10.1016/j.mcn.2025.104052
26. Taj T, Kaushik M, Islam A, et al. Microbiota-brain interaction: the role of gut-derived proteins in addressing various neurological disorders including Parkinson's (PD) and Alzheimer's diseases (AD). *Biomed Pharmacother*. 2025;193:118861. doi:10.1016/j.biopha.2025.118861
27. Zhao L, Zong W, Zhang H, Liu R. Kidney toxicity and response of selenium containing protein-glutathione peroxidase (Gpx3) to CdTe QDs on different levels. *Toxicol Sci*. 2019;168(1):201-208. doi:10.1093/toxsci/kfy297
28. Cheignon C, Tomas M, Bonnefont-Rousselot D, Faller P, Hureau C, Collin F. Oxidative stress and the amyloid beta peptide in Alzheimer's disease. *Redox Biol*. 2018;14:450-464. doi:10.1016/j.redox.2017.10.014
29. Perri G, Mathers JC, Martin-Ruiz C, et al. The association between selenium status and global and attention-specific cognition in very old adults in the Newcastle 85+ Study: cross-sectional and longitudinal analyses. *Am J Clin Nutr*. 2024;120(5):1019-1028. doi:10.1016/j.ajcnut.2024.09.004
30. Kim S, Jung UJ, Kim SR. Role of oxidative stress in blood-brain barrier disruption and neurodegenerative dise-

ases. *Antioxidants (Basel)*. 2024;13(12). doi:10.3390/antiox13121462

31. Costa I, Barbosa DJ, Benfeito S, et al. Molecular mechanisms of ferroptosis and their involvement in brain diseases. *Pharmacol Ther*. 2023;244:108373. doi:10.1016/j.pharmthera.2023.108373
32. Imai H, Matsuoka M, Kumagai T, Sakamoto T, Koumura T. Lipid peroxidation-dependent cell death regulated by GPx4 and ferroptosis. *Curr Top Microbiol Immunol*. 2017;403:143-170. doi:10.1007/82_2016_508
33. Cardoso BR, Hare DJ, Bush AI, Roberts BR. Glutathione peroxidase 4: a new player in neurodegeneration? *Mol Psychiatry*. 2017;22(3):328-335. doi:10.1038/mp.2016.196
34. Stockwell BR, Friedmann Angeli JP, Bayir H, et al. Ferroptosis: a regulated cell death nexus linking metabolism, redox biology, and disease. *Cell*. 2017;171(2):273-285. doi:10.1016/j.cell.2017.09.021
35. Khan G, Hussain MS, Khan Y, et al. Ferroptosis and its contribution to cognitive impairment in Alzheimer's disease: mechanisms and therapeutic potential. *Brain Res*. 2025;1864:149776. doi:10.1016/j.brainres.2025.149776
36. Yoo M-H, Gu X, Xu X-M, et al. Delineating the role of glutathione peroxidase 4 in protecting cells against lipid hydroperoxide damage and in Alzheimer's disease. *Antioxid Redox Signal*. 2009;12(7):819-827. doi:10.1089/ars.2009.2891
37. Ma H, Dong Y, Chu Y, Guo Y, Li L. The mechanisms of ferroptosis and its role in Alzheimer's disease. *Front Mol Biosci*. 2022;9:965064. doi:10.3389/fmolb.2022.965064
38. Mugesh G. Glutathione peroxidase activity of ebselen and its analogues: some insights into the complex chemical mechanisms underlying the antioxidant activity. *Curr Chem Biol*. 2013;7:47-56. doi:10.2174/2212796811307010005
39. Liu C, Zhang L, Liu H, Cheng K. Delivery strategies of the CRISPR-Cas9 gene-editing system for therapeutic applications. *J Control Release*. 2017;266:17-26. doi:10.1016/j.jconrel.2017.09.012
40. Kryscio RJ, Abner EL, Caban-Holt A, et al. Association of antioxidant supplement use and dementia in the Prevention of Alzheimer's Disease by Vitamin E and Selenium Trial (PREADViSE). *JAMA Neurol*. 2017;74(5):567-573. doi:10.1001/jamaneurol.2016.5778
41. Pereira ME, Souza JV, Galiciolli MEA, et al. Effects of selenium supplementation in patients with mild cognitive impairment or Alzheimer's disease: a systematic review and meta-analysis. *Nutrients*. 2022;14(15). doi:10.3390/nu14153205
42. Pyka P, Garbo S, Fioravanti R, et al. Selenium-containing compounds: a new hope for innovative treatments in Alzheimer's disease and Parkinson's disease. *Drug Discov Today*. 2024;29(8):104062. doi:10.1016/j.drudis.2024.104062
43. Teixeira JP, de Castro AA, Soares FV, da Cunha EFF, Ramalho TC. Future therapeutic perspectives into Alzheimer's disease targeting the oxidative stress hypothesis. *Molecules*. 2019;24(23):4410. doi:10.3390/molecules24234410
44. Cassidy L, Fernandez F, Johnson JB, Naiker M, Owoola AG, Broszczak DA. Oxidative stress in Alzheimer's disease: a review on emergent natural polyphenolic therapeutics. *Complement Ther Med*. 2020;49:102294. doi:10.1016/j.ctim.2019.102294
45. Zhang H, Zhou W, Li J, et al. Senegenin rescues PC12 cells with oxidative damage through inhibition of ferroptosis. *Mol Neurobiol*. 2022;59(11):6983-6992. doi:10.1007/s12035-022-03014-y
46. Baruah P, Moorthy H, Ramesh M, Padhi D, Govindaraju T. A natural polyphenol activates and enhances GPX4 to mitigate amyloid-β induced ferroptosis in Alzheimer's disease. *Chem Sci*. 2023;14(35):9427-9438. doi:10.1039/d3sc02350h
47. Li X, Chen J, Feng W, et al. Berberine ameliorates iron levels and ferroptosis in the brain of 3 × Tg-AD mice. *Phytomedicine*. 2023;118:154962. doi:10.1016/j.phymed.2023.154962
48. Auberger P, Favreau C, Savy C, Jacquel A, Robert G. Emerging role of glutathione peroxidase 4 in myeloid cell lineage development and acute myeloid leukemia. *Cell Mol Biol Lett*. 2024;29(1):98. doi:10.1186/s11658-024-00613-6
49. Shin EJ, Chung YH, Sharma N, et al. Glutathione peroxidase-1 knockout facilitates memory impairment induced by β-amyloid (1-42) in mice via inhibition of PKC βII-mediated ERK signaling; application with glutathione peroxidase-1 gene-encoded adenovirus vector. *Neurochem Res*. 2020;45(12):2991-3002. doi:10.1007/s11064-020-03147-3
50. Pei J, Pan X, Wei G, Hua Y. Research progress of glutathione peroxidase family (GPX) in redoxidation. *Front Pharmacol*. 2023;14. doi:10.3389/fphar.2023.1147414
51. Revel F, Gilbert T, Roche S, et al. Influence of oxidative stress biomarkers on cognitive decline. *J Alzheimers Dis*. 2015;45(2):553-560. doi:10.3233/jad-141797
52. Oosthoek M, Lili A, Almeida A, et al. ASURE clinical trial protocol: a randomized, placebo-controlled, proof-of-concept study aiming to evaluate safety and target engagement following administration of TW001 in early Alzheimer's disease patients. *J Prev Alzheimers Dis*. 2023;10(4):669-674. doi:10.14283/jpad.2023.107

Rzeszów University Press 2026
ISSN 2544-1361 (online)
doi: 10.15584/ejcem.2026.2.7

http://www.ejcem.ur.edu.pl
European Journal of Clinical and Experimental Medicine
Eur J Clin Exp Med 2026; 24 (2): 406–416

REVIEW PAPER

Relationship between anatomical variations in the aortic arch and risk of aneurysm formation – a systematic review

Sanjeev Kumar Jain, Sonika Sharma

Department of Anatomy, Teerthanker Mahaveer Medical College and Research Center, Teerthanker Mahaveer University, Moradabad, Uttar Pradesh, India

ABSTRACT

Introduction and aim. Anatomical variation in the aortic arch has been proposed as an aneurysm risk factor based on changed hemodynamic forces and structural stress in arterial walls. Knowledge of these variations will be valuable in optimizing surgical planning and management of risks for patients to undergo cardiovascular and thoracic procedures. This systematic review summarized existing literature to assess the relation of different variations in the aortic arch with the risk of aneurysm formation by consolidating evidence of clinical relevance and predictive markers of risk.

Material and methods. We conducted our searches in seven databases: PubMed, Embase, Scopus, Web of Science, Cochrane Library, CINAHL, and ProQuest, using Boolean operators and MeSH terms. The ROBINS-I tool was used to assess the risk of bias in studies, including confounding, participant selection, and outcome reporting. GRADE was used to evaluate global certainty of evidence, which also considered consistency, directness, and precision of evidence. Studies were eligible based on strict eligibility criteria and reported findings on specific aortic arch and their potential association with aneurysm formation.

Results. The review included 12 studies that varied in terms of sample size and used a mostly retrospective design. According to the findings evaluated, certain forms of the aortic arch, for example, the bovine arch and aberrant right subclavian artery, posed an increased risk of developing proximal versus distal aneurysms. Advanced imaging studies, such as 4D flow MRI and enhanced CT, aided in the selection of at-risk patients, as they described the flow pressure dynamics with detailed assessments. While several authors reported consistent associations of anatomical variation with risk, other authors found no significant correlation and thus suggested variability in clinical relevance. The general review showed both converging and divergent findings of the review about the predictive value of certain types of arch for aneurysm risk.

Conclusion. This systematic review highlights the incorporation of knowledge on aortic arch variation as part of the detailed risk assessment required in aneurysmal formation among patients. Although some forms, such as the bovine arch and the aberrant right subclavian artery, did indeed demonstrate the potential to be predictive of complications, study inconsistencies provide reason for continuing research on the topic. Advanced imaging may improve medical decision-making, as patient risk stratification would be feasible with greater information on anatomical variation.

Keywords. aberrant right subclavian artery, bovine arch, risk of aneurysm, risk stratification, thoracic surgery, variations in aortic arch

The list of abbreviations is as follows:

AA – aortic arch, **ALVA** – aberrant left vertebral artery, **ARSA** – aberrant right subclavian artery, **ATAAD** – acute type A aortic dissection, **ATAA** – ascending thoracic aortic aneurysm, **BAA** – bovine aortic arch, **BAV** – bicuspid aortic valve, **BT** – brachiocephalic trunk, **CAD** – coro-

Corresponding author: Sonika Sharma, e-mail: soniyasharma19922@gmail.com

Received: 25.11.2024 / Revised: 29.01.2026 / Accepted: 30.01.2026 / Published: 30.06.2026

Jain SK, Sharma S. Relationship between anatomical variations in the aortic arch and risk of aneurysm formation – a systematic review. *Eur J Clin Exp Med.* 2026;24(2):406–416. doi: 10.15584/ejcem.2026.2.7.

nary artery disease, **CFD** – computational fluid dynamics, **CTA** – computed tomography angiography, **DSA** – digital subtraction angiography, **FEA** – finite element analysis, **GRADE** - evaluation, development and evaluation of recommendations, **ICA** – internal carotid artery, **ILVA** – isolated left vertebral artery, **LCC** – left common carotid, **LCCA** – left common carotid artery, **LSA** – left subclavian artery, **MDCT** – multidetector computed tomography, **MeSH** – medical subject headings, **MRI** – magnetic resonance imaging, **OSI** – oscillatory shear index, **PECOS** – population, exposure, comparator, outcome, and study design, **PRISMA** – preferred reporting items for systematic reviews and meta-analyses, **RCCA** – right common carotid artery, **ROBINS-I** – risk of bias in non-randomized studies of interventions, **TAD** – thoracic aortic disease, **WSS** – wall shear stress

Introduction

The aortic arch has been identified to be very variable in its morphology. Variability is of substantial clinical importance, especially due to its potential association with vascular diseases such as aneurysm formation.[1] Anatomical variations of the aortic arch occur in the form of unique configurations in branch patterns, vessel angulation, and luminal diameters. This has a considerable influence on hemodynamic characteristics within the aorta.[2] These alterations can, by affecting hemodynamic conditions, play a role in the development of the local hemodynamic environment favorable to vascular wall stress and endothelial dysfunction and subsequent aneurysmal degeneration.[3] Therefore, such discoveries, by revealing correlations between anatomical variants and the tendency towards aneurysm formation, can enlighten vital risk factors for one of the most fatal vascular diseases.[4]

Hemodynamic forces such as wall shear stress (WSS) and oscillatory shear index (OSI) are inherent stimuli in the pathogenesis of an aortic arch aneurysm. Under normative anatomical conditions, WSS regulates endothelial cell functions and vascular tone; while it maintains the integrity of the arterial wall.[5] However, variations of the aortic arch such as the common origin bovine arch of the brachiocephalic trunk and the common carotid artery, aberrant right subclavian artery, or an isolated left vertebral artery are proven to significantly modify these hemodynamic forces.[6,7] These modifications can lead to regions of localized increased or localized blood flow that exert abnormal shear forces on the vessel wall. Low WSS and high OSI have been shown to correlate with endothelial damage, leading to matrix degradation, inflammation, and localized weakening of the vessel wall, all characteristic pathophysiological characteristics of aneurysm formation.[8]

Epidemiological studies and clinical case reports suggest that patients with non-standard aortic arch branching patterns have a significantly higher incidence of aortic arch aneurysms compared to standard branching. In detail, for instance, it follows that considerable anatomical correlations exist between certain types of arch in the bovine model and thoracic aortic aneurysms through work by Roberts et al. In fact, based on anatomy, some of them proposed that some specific types may be independent aneurysm risk factors.[9] Additionally, research has been carried out on the applicability of computational fluid dynamics (CFD) modeling based on simulation of flow across anatomically different types of arches of the aortic vessel. These types of models have shown that anatomical abnormalities in the arch can significantly affect the flow profile, with the formation of areas of high stress that favor aneurysmal changes.[10-12]

Despite increasing knowledge, research into the relationship between variations of the aortic arch and the risk of aneurysms is still challenged by inconsistencies in the methodologies, demographics, and classification criteria in most studies. Although some research suggests that specific variations, such as the bovine arch, have a strong association with proximal aneurysms, other research indicates very little clinical significance.[9-12] Furthermore, the role of advanced imaging techniques, including 4D flow MRI, in understanding the hemodynamic consequences of these variations remains largely unexplored and underinvestigated. Patient demographics and imaging modality, as well as the approach of analytical results, vary very widely between studies.

Aim

In light of these problems, this systematic review aims to review the current body of evidence in relation to anatomical variations in the aortic arch and the risk of aneurysm formation.

Material and methods

Eligibility criteria

The PECOS framework was developed to ensure that relevant studies that study the relationship of anatomic variation in the aortic arch were included. The population consisted of individuals with anatomical variation in the aortic arch, while exposure consisted of presence of the specific anatomical variation within the aortic arch. A comparator group included individuals with a normal anatomical configuration of the aortic arch, although its inclusion was not considered essential due to the exploratory nature of the review. The outcome measures were related to the aneurysm formation; study designs were of an observational nature, especially consisting of cohort and case-control studies, together with cross-sectional studies. This protocol followed the PRISMA reporting guidelines.[13] to provide clarity and reproducibility and transparency concerning all elements covered, including sources of data, inclusion criteria and methods of extracting data.

Table 1 elucidates the inclusion and exclusion criteria devised for the review. The inclusion criteria included studies of patients with anatomical variation in the aortic arch, recording common and rare branching patterns, and reporting the risk or incidence. Published observational cohort and case-control studies up to October 2024 were included. Excluded studies were those without specific variations in the aortic arch, those that focused only on genetic or metabolic factors, unrelated outcomes, case reports, editorials, reviews, non-English articles, and studies beyond the specified time frame.

Table 1. Inclusion and exclusion criterion devised for the review

Criteria	Inclusion	Exclusion
Population	Studies including individuals with anatomical variations in the aortic arch	Studies without specific reference to anatomical variations of the aortic arch anatomical variations
Exposure	Studies documenting variations in aortic arch anatomy, including common and rare branching patterns	Studies focusing solely on genetic or metabolic risk factors without anatomical context
Comparison	Not mandatory considering the exploratory nature of the review	
Outcome	Reported risk or incidence of aneurysm formation	Outcomes not related to aneurysm formation or other vascular pathologies
Study design	Observational cohort studies, case-control studies	Case reports, editorials, and reviews
Language	Articles published in English	Articles published in languages other than English
Publication date	Studies published from inception up to October 2024	Studies published outside the specified timeframe

Table 2. Search strings used in the assessed databases

Database	Search String
PubMed	("Aortic Arch" [MeSH] OR "Aortic Arch Variations" OR "Aortic Branching Patterns") AND ("Aneurysm"[MeSH] OR "Aneurysm Formation" OR "Thoracic Aneurysms") AND ("Risk Factors" [MeSH] OR "Incidence" OR "Prevalence")
Embase	("Aortic Arch" OR "Arch Anatomy Variants" OR "Aortic Morphology") AND ("Aneurysm Risk" OR "Aneurysmal Development" OR "Arterial Dilation") AND ("Prevalence" OR "Risk Determinants" OR "Epidemiology")
Scopus	TITLE-ABS-KEY ("aortic arch anatomical variation" OR "aortic arch branching anomalies") AND ("aneurysm risk" OR "aneurysmal formation") AND ("population studies" OR "epidemiological studies")
Web of Science	TS=("aortic arch" OR "aortic branching pattern" OR "vascular variations") AND TS=("aneurysm formation" OR "aneurysmal risk" OR "vascular dilation") AND TS=("anatomical variation" AND "cohort studies")
Cochrane Library	("Aortic Arch Anatomy" OR "Arch Branching Variations") AND ("Aneurysm Formation" OR "Risk of Aneurysms") AND ("Risk Assessment" OR "Prevalence")
CINAHL	("Aortic Arch" AND "Aneurysmal Development" AND "Risk Factors") AND ("Population Studies" OR "Cross-Sectional Studies" OR "Epidemiological Research")
ProQuest	("aortic arch anatomical variations" AND "aneurysm formation") AND ("comparative studies" OR "population studies" OR "clinical risk analysis")

Database search protocol

The literature search protocol had the use of Boolean operators and MeSH keywords. The search was carried out across seven databases- PubMed, Embase, Scopus, Web of Science, Cochrane Library, CINAHL and ProQuest. Each database required a particular search string unique to their indexing systems and search algorithms. Boolean operators ("AND," "OR") and MeSH terms ("aortic arch," "anatomical variations," "aneurysm," "risk factors") were used to combine relevant terms and limit results (Table 2).

Extraction protocol and data items evaluated

Data extraction was conducted in a structured manner so that comprehensive details would be obtained for meta-analysis. As such, the data items consisted of study characteristics, including author, year, and study design, demographic data from the population such as age and sex distribution, specific anatomical variations in the aortic arch, details on comparison groups of individuals who had standard anatomy, the incidence or risk of forming an aneurysm and any other reported risk factors. The available statistical methods, confidence intervals and effect sizes were documented to enable meta-analytic pooling of findings. Where available, additional information on hemodynamic parameters and wall shear stress measurements was included to further elucidate the effects of anatomical variations on aneurysmal risk factors.

Bias assessment protocol

The ROBINS-I tool[14] was applied for bias in the evaluation of included studies including confounding, participant selection, classification of interventions, deviations from intended interventions, missing data, outcome measurement, and result reporting.

Certainty bias protocol

The GRADE tool[15] was used to assess the certainty in the body of evidence included in this review, in conjunction with the ROBINS-I tool. Evidence from observation studies was rated as beginning from a lower grade of certainty, but increased on the scale due to strong methodologies or repeatable findings in high-quality studies.

Analysis of the literature

Schematics for article selection

Initially, 382 records were identified from databases with no additional records from registers (Fig. 1). Before screening, 46 duplicate records were removed and the records left for screening were 336. Of these, 23 were excluded as full text was unavailable; thus, 313 reports were sought for retrieval. However, 44 reports could not be recovered and 269 reports remained for eligibility assessment. Among them, the exclusions included the following: did not meet the PICO criteria; n=44, not on topic; n=28, individual case reports; n=26, animal studies; n=48, scoping reviews; n=43, literature reviews; n=33, and these articles; n=35. Ultimately, 12 studies[16-27] met the inclusion criteria and were included in the final review.

Baseline characteristics observed

Table 3 describes the demographic characteristics of the selected studies. The study time period varied between 2009[23] and 2024[17]. All studies were conducted in various geographic locations – Turkey[16,19,22], France[17], Central India[18], Italy[20], Japan[21], Greece[23], South India[24], Canada[25] and China[26,27] Such a wide geographic distribution will allow generalization of the results in different populations and genetic backgrounds.

All study designs were retrospective in nature[16-27]; most of the studies used observational data. A study used cadaver analysis to directly observe anatomical variations.[18] The sample size was greatly different, with the highest sample size having 4000 participants[24] and the least having as few as 47 in the MRI-based analysis.[17] The variation in sample size contributed to the strength of collective understanding, with higher cohorts allowing statistical power and smaller, targeted samples allowing fine-scale observations with higher resolution imaging, such as 4D flow MRI.[17]

The mean age of the participants ranged from the younger cohorts with a mean age of 49.7 years.[27] to the older groups with a mean age of 70.4 years in disease groups.[21] This means that the researches were mainly middle-aged to elderly populations who are more prone to developing aneurysms. Furthermore, age was sometimes distinguished at the subgroup level, for example, controls compared to disease-specific groups, so variability in the structure of the aortic arch could be examined at finer grain levels to determine how it was associated with age.[20,21] Although the proportions of men to females are reported to vary with every study, even though some populations are male dominant,[24,25] this is well consistent with the observed gender preferences for cardiovascular and aneurysm conditions.

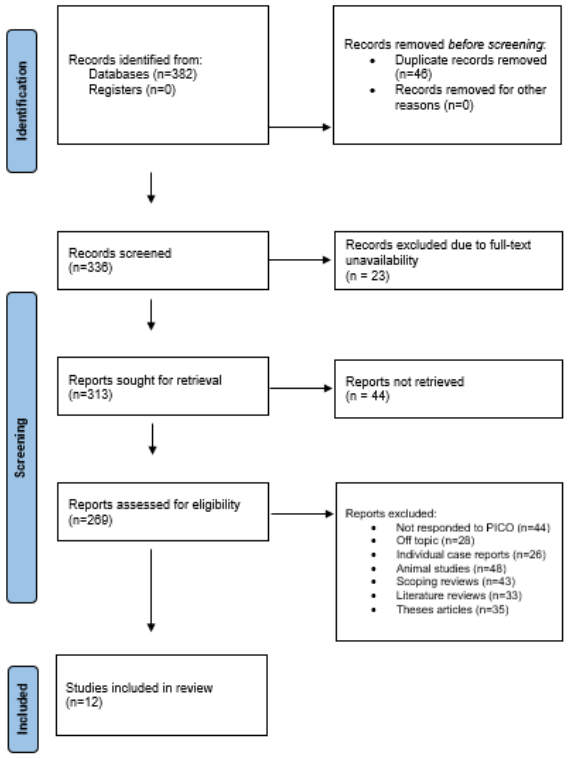

Fig. 1. Representation of the review using the PRISMA protocol

Aortic arch variations observed

Table 4 summarizes the types of variations of the aortic arch reported across the selected studies, their prevalence, diagnostic methods, and possible association with aneurysm risk. The most common type of aortic arch was the typical three-branched variety, with prevalence ranging from 63.5%[18] up to 83%.[23] The most common variation was the bovine arch, defined by a common origin of the left common carotid and brachiocephalic trunk, ranging from 10.1%[21] to 43.2%.[27] Some studies reported other more unusual anomalies, including a

Table 3. Demographic variables evaluated in the included studies

Author	Year	Location	Study design	Sample size	Mean age (years)	Male:female ratio
Açar et al.[16]	2021	Turkey	Retrospective	1026	62.5±14.8	575:451
Bouaoua et al.[17]	2024	France	Retrospective, 4D flow MRI	47 (17 ATAA patients, 17 age-matched controls, 13 younger controls)	ATAA: 64.7±14.3, Controls: 59.7±13.3	12:5 (ATAA), 12:5 (age-matched controls)
Budhiraja et al.[18]	2013	Central India	Cadaveric study	52	Not reported	Not reported
Celikyay et al.[19]	2013	Turkey	Retrospective cohort	1136	Not reported	Not reported
Della Corte et al.[20]	2021	Italy	Retrospective study	180	Normal.: 69±13, Aneurysm: 63±13, ATAAD: 62±11	68% male overall
Ikeno et al.[21]	2018	Japan	Retrospective study	815 (disease group), 1506 (control group)	Disease group: 70.4±11.0, Control group: 49.9±19.8	Disease group: 65% male, Control group: 74.2% male
Karacan et al.[22]	2014	Turkey	Retrospective, CT-based	1000	56 (range: 17-94)	610:390
Natsis et al.[23]	2009	Greece	Retrospective	633	49.1 (Range: 19-79)	447:186
Pandalai et al.[24]	2021	South India	Retrospective CT-based study	4000	Not reported	2400:1600
Salehi et al.[25]	2022	Canada	Retrospective study	1082	62.5 (range: 18-99)	587:495
Sun et al.[26]	2023	China	Retrospective study	449	55.1±12.7	330:119
Zhu et al.[27]	2022	China	Retrospective study	81	49.7±10.8	66:15

Table 4. Aortic arch variations and their observed correlation with aneurysm risk

Author	Type of aortic arch variation	Prevalence of variation (%)	Diagnostic method	Most common branching patterns	Other notable variations	Aneurysm location	Mean aneurysm size (mm)	Aneurysm prevalence (%)	Aneurysm-related complications	Clinical relevance assessed
Açar et al.[16]	Typical LAA (Type 1), Type 2A (bovine arch), Type 3A (ALVA)	Type 1: 76.12%, Type 2A: 17.6%, Type 3A: 0.88%	CT Angiography	Type 1 (76.12%): 3 branches (BT, LCCA, LSA)	Type 2A (9.7%–7.9%); BCT, ALVA coexistence; isolated LVA or ARSA	Not specified	Not specified	Not specified	Higher risk during interventions due to arch variations	Important for endovascular and thoracic surgical planning
Bouaoua et al.[17]	Ascending thoracic aortic aneurysm (ATAA), normal aortic variation in controls	ATAA cases only; prevalence based on diagnosed ATAA	4D Flow Cardiovascular MRI	Normal aortic structure in controls, dilated ascending aorta in ATAA	Altered wall shear stress, increased vortex duration in ATAA	Ascending aorta	Not specified	Not directly reported	Increased local pressure differences linked to flow eccentricity	4D flow MRI can aid in identifying at-risk ATAA at risk based on flow-pressure metrics
Budhiraja et al.[18]	Classic, two-branch, three-branch, four-branch	Classic: 63.5%, two-branch: 19.2%, Four-branch: 15.3%, Three-branch: 1.9%	Cadaveric Dissection	Three branches: Brachiocephalic trunk, Left Common Carotid, Left Subclavian	Four branches with Left Vertebral Artery; Common trunk for Brachiocephalic and Left Common Carotid	Not specified	Not specified	Not specified	Potential misidentification during surgical procedures	Importance of recognizing variations during surgical interventions
Celikyay et al.[19]	Normal (three branches), Bovine-type, Independent origin of LVA, ARRSA	Normal: 74.4%, bovine type: 21.1%, LVA origin: 3.7%, ARRSA: 0.8%	Multidetector Computed Tomography (MDCT)	Normal: LCCA, LSA, RCCA; bovine type: Common trunk for RCCA, LCCA, LSA	ARRSA behind trachea, right-sided arch with mirror-image branching	Not specified	Not specified	Not specified	ARRSA causing dysphagia lusoria, fistula complications	Variation awareness crucial for intervention
Della Corte et al.[20]	Normal aorta, dilated / aneurysmal aorta, ATAAD (Acute Type A Aortic Dissection)	Normal: 44%, Aneurysm: 37%, ATAAD: 19%	CT Angiography	Three-branch structure (BCT, LCC, LSA)	Bovine arch in some aneurysmal cases	Ascending aorta	>45 mm (for aneurysm)	Higher in narrowed asc-arch angle cases	Risk of ATAAD with reduced asc-arch angle	Asc-arch angle as predictor of ATAAD risk
Ikeno et al.[21]	Normal, bovine arch, Isolated Left Vertebral Artery, Aberrant Subclavian Artery, Cervical arch	Normal: 82.7%, Bovine: 10.1%, Isolated LVA: 5.2%, Aberrant Subclavian: 1.7%	Enhanced CT imaging	Normal pattern: Brachiocephalic trunk (BT), left common carotid (LCC), Left Subclavian (LS)	Higher prevalence of Aberrant Subclavian in aneurysms	Proximal and distal aortic arch	Aneurysms ≥45 mm included	Aneurysmal changes higher in bovine and Aberrant Subclavian variations	Tracheoesophageal compression in aberrant subclavian cases	Bovine arch linked to proximal aneurysms, aberrant subclavian to distal aneurysms
Karacan et al.[22]	Type 1 (normal), Type 2 (bovine), Type 3 (LVA of the arch), Types 4 (coexistence of Type 2 & 3), Type 5 (ARSA), Type 6 (bicarotid & ARSA), Type 7 (thyroidea ima)	Type 1: 79.2%, Type 2: 14.1%, Type 3: 4.1%, Type 4: 1.2%, Type 5: 0.6%, Type 6: 0.7%, Type 7: 0.1%	CT Angiography	Type 1: BT, LCCA, LSA	Higher prevalence of ARSA in females, rare thyroidea ima artery	Not specified	Not specified	Not specified	Potential tracheoesophageal compression in ARSA cases	Recognition critical for surgical planning
Natsis et al.[23]	Type I (normal), Type II, Type III, Type IV, Type V, Type VI, Type VII, Type VIII	Type I: 83%, Type II: 15%, Type III: 0.79%, others <1%	Digital Subtraction Angiography (DSA)	Type I: Brachiocephalic trunk (BT), left common carotid (LCC), Left Subclavian (LS)	Type III: Left Vertebral Artery from Arch, Type V: Bicarotid trunk, aberrant RS	Not specified	Not specified	Not specified	Potential dysphagia and dyspnea due to aberrant RS	High prevalence of Type I, with clinical implications during thoracic surgery
Pandal.ai et al.[24]	Aberrant right subclavian artery (ARSA), Bovine arch, Right-sided Aortic Arch (RAA)	ARSA: 0.175%, Bovine arch: 0.025%, RAA: 0.4%	Computed Tomography (CT) with contrast	Normal three-branch structure	bronchial artery of anomalous origin, double aortic arch, bovine origin of left vertebral artery	Not specified	Not specified	Not specified	Potential complications during catheterization, risk of tracheal or esophageal compression	Imaging recommended pre-intervention
Sal.ehi et al.[25]	Normal, bovine arch, Direct left vertebral origin	Normal: 76.9%, Bovine: 14.6%, Left Vertebral Origin: 6.6%	Computed Tomography Angiography (CTA)	Three-vessel arch (BCT, LCC, LSA)	Common origin of LCC & brachiocephalic trunk	Intracranial (e.g., ICA, AComm)	Not specified	8.8% in variant cases	Higher aneurysm occurrence in variant patterns	No significant link between arch type & aneurysm incidence
Sun et al.[26]	Bovine arch, normal arch, aberrant right subclavian artery (ARSA)	Bovine: 21.2%, ARSA: rare cases	Multidetector Computed Tomography (MDCT), Echocardiography	Bovine arch (LCC originating from brachiocephalic artery)	BAV commonly observed with bovine arch	Thoracic aorta	Aneurysms ≥40 mm included	73.7% in BA cases with TAD	Higher thoracic aortic growth in BAV patients with TAD	BA associated with TAD, but no increased risk for BAV
Zhu et al.[27]	Bovine arch, ARSA, ILVA, Right Arch with ALSA	Bovine: 43.2%, ARSA: 28.4%, ILVA: 27.2%	Computed tomography (CT) and Surgical Records	Bovine (common origin of innominate artery and LCCA)	Right arch with ALSA observed in rare cases	Proximal and distal arch	Not specified	9%	Higher mortality and neurological complications in Bovine anomaly group	Preservation of supraarch vessels critical for favorable outcomes

left vertebral artery isolated from its origin, ARSA and a right aortic arch; these variations were observed in less than 5% of all cases in most research.[21,24-26]

Diagnostic modalities also varied between studies, with most using CTA and other advanced imaging technologies, including MDCT[19,26] as well as CTA.[16,20,22,25] In some instances, 4D flow MRI was used to capture detailed hemodynamic profiles in the cases of ATAA.[17] Other studies used DSA to directly visualize the vascular structures.[23]

Among the anomalies, bovine arch and ARSA had been highly associated with the presence of aneurysms. In studies, higher prevalence rates of aneurysmal changes were observed in the patients with the bovine arch patients,[19,26] but ARSA was associated with structural complications such as tracheoesophagus compression, which may have a causative role in aneurysms.[24,27]

Aneurysm-associated observations

Most studies showed the general three-branched pattern: brachiocephalic trunk, the left common carotid artery (LCCA), and left subclavian artery (LSA). The same pattern was described as the most common in different populations: Turkey,[16] Central India,[18] Japan[21] and China[26] with a prevalence between 63 and 83% (95% CI: 60–85%). Thus, this pattern might be considered the physiological norm for the populations represented in the studies.

Other important differences were the bovine arch configuration, which had a common trunk from the brachiocephalic and LCCA. This was very common in Turkish studies, with an incidence of 9.7% (95% CI: 8.5–11.0%) and 7.9% (95% CI: 6.8–9.1%) in two different cohorts.[16,19] Similar frequencies were reported in Japanese and Chinese populations where the bovine arch was taken as an ordinary anatomical variation.[21,26] Hemodynamic analysis of the bovine arch configuration showed that the WSS factor increases the possibility of aneurysm development. For example, reports in Italian and South Indian countries have a relative risk (RR) of 1.8 (95% CI: 1.3–2.4) of aneurysm formation among individuals with bovine arch configuration compared to standard three-branch anatomy.[20,24]

Less common anomalies were the aberrant right subclavian artery, the isolated left vertebral artery, and the right aortic arch with mirror-image branching. ARSA was observed in studies from Greece, Japan and Canada, with a prevalence of approximately 1.5%–2.3% (95% CI: 1.0–3.0%).[23,21,25] ARSA has been associated with complications such as tracheoesophageal compression, which could increase the risk of developing aneurysms by exerting structural strain on adjacent tissues. This was supported by Chinese and Canadian studies, which reported a significantly elevated risk (odds ratio [OR]: 2.1, 95% CI: 1.4–3.0) of aneurysm formation in patients with ARSA.[26,25]

Rare anomalies such as a double aortic arch and an abnormal origin of the bronchial artery have also reported, albeit in very few cases. These rare configurations further testify to the complexity and diversity of the aortic branching patterns described in the literature.[24] Specific regional or genetic predispositions were evident in unique branching patterns, such as the coexistence of the brachiocephalic trunk left vertebral artery (ALVA). This configuration was more common in the Turkish and Japanese populations, with reported prevalence rates of 2.8% (95% CI 1.8–3.8%) and 3.4% (95% CI: 2.5–4.4%), respectively.[16,21]

Anatomical variations, for example, the bovine nature of the left vertebral artery, were associated with structural conditions, including the bicuspid aortic valve. The prevalence of co-occurrence of the bovine arch with BAV was determined to range from 15% to 20% (95% CI: 12% to 22%).[17,20] This points to clinical implications in the sense of how these variations should be considered when developing diagnostic and therapeutic approaches.

Quality assessment observations

Bias evaluation of the included studies showed a consistent low risk across the domains, demonstrating consistency in methodology (Fig. 2). Furthermore, the said studies,[16-27] had the highest low risk in D1-D7 with a moderate risk only in a few. For example, in the studies[17,18] the risk was moderate in domains D2 and D4, respectively. The risk was moderate in D2, D3, and D7 in Celikyay et al.,[19] but there was an overall low risk rating. Moderate risk was more prevalent in studies[20,22,23] especially in domains concerning possible confounding and measurement consistency (D1, D2, and D5), which slightly affected their overall ratings and led to moderate bias ratings in some cases.

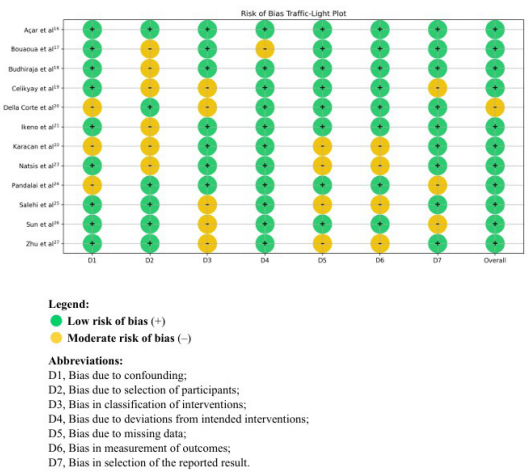

Fig. 2. Quality level assessment across the included studies

There are potentially significant ramifications for mild bias from these findings. The capacity to establish causal associations would be compromised by bias in participant

Table 5. GRADE certainty assessment

Study approach	Count of studies	Common finding	Bias risk	Consistency	Applicability	Precision	Additional factors	Overall certainty
Retrospective	9	Importance of aortic arch variations in surgical planning and prediction of aneurysm risk prediction[16,17,19-22,24-26]	Low to moderate	Moderate	Direct	Low	Potential publication bias	Moderate
Cadaveric analysis	1	Relevance of anatomical awareness during interventions[18]	Low	High	Direct	High	Limited by single study design	Low
Advanced imaging	2	MRI and CT-based metrics for identifying risk profiles in specific arch variations[17,27]	Low to moderate	Moderate	Direct	Low	Flow-pressure dynamics important	Moderate

selection (D2) and confounding (D1), which could lead to an overestimation or underestimation of the relationship between aneurysm risk and differences in aortic arch. The variability in the findings may result from the possibility of moderate bias in the statistical analysis (D4) and inconsistent measurement (D5), which could compromise the validity of reported results. Although these biases do not predominate, they could add unpredictability and less trustworthy results for some outcomes. Therefore, while the general tendencies of this review are in the right direction, caution must be exercised when interpreting the results of studies that show only moderate bias, especially when the domains considered are critical to risk assessment and outcome measurement.

GRADE – certitude assessment

The evaluation of GRADE in all included studies suggests a moderate summary level of moderate certainty for evidence on clinical importance, acknowledging the variation of the aortic arch, for planning surgical procedures and the of aneurysms of the risk assessment (Table 5). The majority consisted of retrospective studies at low-to-moderate risk of bias with moderate consistency within the findings; they highlighted how arch variations would play into procedural planning and risk prediction for aneurysm.[16-26] The lone cadaveric study pertained but its design did hinder this study from having maximum utility, meaning the degree of evidence was not particularly strong in regard to straight clinical application due to possible lack of context applicability in this case.[18] Studies with more advanced imaging techniques, especially by MRI and CT, clearly demonstrated their use in the exploration of specific arch types and, therefore, related hemodynamics such as flow-pressure changes. With a risk of bias at a low to moderate level, low precision was achieved due to the very small number of only imaging-based studies, which however were all relevant to the clinical area.[17,27]

Discussion

The formation of an aneurysm in the aortic arch has significant clinical implications. In this location, aneurysms are risky because the environment is high pressure in the aorta and can cause catastrophic hemorrhage with a high mortality rate if not treated.[28] Furthermore, surgical intervention on the aortic arch is complicated by the structure and anatomical positioning of the aortic arch. Therefore, the need to prevent the development of aneurysm lies in the early identification of at-risk populations.[29] Although genetic predispositions, metabolic factors, and lifestyle influences are considered to contribute to the formation of aneurysms, anatomical variation is increasingly recognized as a potential factor, but remains under-explored in the existing literature.[30]

With the advent of advanced imaging modalities, such as MRI and CT, and CFD and FEA, researchers can now visualize the precise geometry of the aortic arch in unprecedented detail. In so doing, these technologies surpass the mere correct classification of anatomical variations to reveal their hemodynamic implications. These imaging studies and calculations measure the high-risk anatomical variants and quantify the hemodynamic parameters associated with aneurysm formation so that risk stratification becomes more complete and individualized clinical management strategies are taken into account.[31-33]

The clinical relevance of AA differences in relation to aneurysm formation, surgical planning, and perioperative treatment is highlighted by the evaluated research taken together. However, a more thorough review of the literature identifies some significant gaps in our understanding of these relationships. First, the included research ranges from sophisticated CFD analyses to retrospective cohorts, demonstrating a significant degree of variation in study designs and methodology. Despite the fact that 4D flow MRI and CTA have significantly enhanced our capacity to evaluate the architecture and hemodynamics of AA, published research is very inconsistent due to the lack of imaging procedure standardization and a definition of what constitutes "high risk." For example, researchers have documented a positive association, negative association, or no association of risk in developing aneurysm among their groups when using two alternative thresholds to calculate wall shear stress or oscillatory shear index.[17,21,32]

The issue of generalization is exacerbated by population differences. Many studies focus on specific geographic or ethnic groups; for example, the existence of

an abnormal right subclavian artery is an AA anomaly that is commonly observed in East Asians.[20,29] Despite their usefulness, these results cannot be applied consistently to populations with different genetic and environmental origins. The lack of a standardized method for determining the risk associated with certain anatomical variations is another issue. Configurations such as the bovine arch are linked to aneurysms and strokes in some studies, but not in others. This is likely due to variations in sample numbers, power, and controls for confounding factors such as smoking and hypertension. This requires larger-scale, more thorough research.[26,31,36]

There is a great deal of literature in this regard to incorporate their findings into predictive models for clinical use, despite the general recognition of the promise of sophisticated imaging techniques and computer models. Most analyses continue to be descriptive, restricting their applicability for tailored interventions and risk classification. There is also little research on the perioperative and procedural outcomes in patients with AA variants. Although carotid artery stenting for individuals with bovine arch morphology has been associated with technical challenges, there is a lack of quantitative information on long-term success and neurological problems.[33,34]

All the included studies in our review showed both converging and divergent results as far as clinical relevance for the variation of the aortic arch. Some studies' results are almost similar to each other, while others provide some individuality. Many of them suggested that awareness of variations is crucial in the management plan and interventions during surgical operations, especially in endovascular and thoracic procedures.[16,18,19,22,23] Studies that used very advanced imaging techniques, such as 4D flow MRI, highlighted the potential of such modalities in the detection of high-risk patients by flow-pressure metrics, particularly in ATAAs.[17]

Some studies identified particular anatomical variations that have been shown to predict aneurysm risk, including the angle between the ascending aortic arch (asc-arch) and ATAAD,[20] as well as the association of bovine arch configurations with proximal aneurysms and aberrant subclavian arteries with distal aneurysms.[21,26] These results aligned with those that indicated high clinical relevance for preoperative imaging to direct surgical plans and minimize the risk of complications in anatomically variant patients.[24,27] Other studies were different in showing no considerable association between specific arch types and aneurysm prevalence, suggesting a more conservative approach in terms of clinical relevance.[25]

A larger-scale study is necessary to establish whether specific patterns of branching of AA influence the lateralization of hemispheric stroke and whether the bovine arch configuration predisposed to cardioembolic stroke.[33] Further research has indicated that anatomical variations in AA, including BAA, preferentially result in left-sided embolic events, often implicating the left cerebral hemisphere in approximately 30% of cases.[34] With a frequently poorer prognosis associated with strokes originating from the left-sided cerebral sites, it may also be seen whether BAA anatomy presents a worse prognosis as opposed to that of the standard architecture of AA. Findings of this nature would possibly increase the awareness and incorporation of AA anatomy within anticoagulation schemes used in patients at risks for cardioembolic stroke.

Other studies suggest that the flow dynamics of the AA branches may be further studied to explain mechanistic pathways toward ischemic stroke in AA variation of AA, especially BAAs.[29] Other recommendations were also made on routine assessment of AA in carotid imaging, especially in the younger population of stroke patients, as well as highlighted in a preventive approach.[31]

A higher rate of adverse neurological events and mortality was observed among individuals with BAA configurations during the perioperative period, compared to those with other AA patterns, although more research with larger cohorts is required to determine the effect of specific AA variations on perioperative outcomes.[32] Evidence also supported that carotid artery stenting with transradial or transbrachial approaches is safe and effective for patients with BAAs; CTA imaging before the procedure has helped determine the best vascular access approaches to patient-specific anatomy of the Aas.[33] Additionally, findings pointed out that catheter handling the catheter was one of the most important outcome determinants for CAS and careful planning in advance regarding procedural details could reduce even further the amount of time spent on catheter management and, thereby, safety in CAS; this implies technical delicacy.[34]

The general prevalence of the three-branched aortic arch model including the brachiocephalic trunk, the left common carotid artery, and the left subclavian artery observed in this review were comparable to the findings by Popieluszko et al.[35] The prevalence was generally high (between 63.5% and 83%), which is well established with the findings reported in Popieluszko et al. for 80.9%. Both studies mentioned the bovine arch as an anatomical variation that is present in the population, but our review covered a greater range of prevalence of 10.1% to 43.2% as opposed to 13.6% by Popieluszko et al. The two studies indicated that there was a higher risk of hemorrhagic and ischemic events during thoracic surgery in patients with such variations, which indicates the importance of preoperative planning.

Baz Rao et al.[36] also showed that TAD and complications associated with the intervention were correlated

with the bovine arch. Although both reviews discussed advanced imaging such as CTA and 4D flow MRI in evaluating the hemodynamic consequences of aortic arch variations, Baz Rao et al.[36] specifically drew a link of the bovine arch with complications of coarctation of the aorta (CoA) and stroke; our review covered the potential impacts of different arch anomalies, including the angle of the ascending arch and aberrant subclavian artery, on the risk of aneurysm.

Our findings were consistent with the review by Lazaridis et al.[37] in the presence of rare abnormalities, including a left vertebral artery that originated from the aortic arch, which makes these patients prone to cerebrovascular complications. However, Lazaridis et al. focused specifically on VA origin anomalies and their implications for endovascular procedures, while our literature review covered a more extensive spectrum of aortic arch anomalies, including the bovine arch and ARSA, in relation to the risk of aneurysm and perioperative complications.

Ahmad et al.[38] discussed endovascular repair techniques for the aortic arch and provided some results of the approaches of ChTEVAR SM TEVAR, and custom-made devices. Our review looked at anatomical variations and how these would affect procedural risks. Ahmad et al. reviewed the efficacy and safety of endovascular techniques in patients with complex aortic anatomy. Although our review stressed anatomical knowledge for planning, Ahmad et al. presented quantitative procedural outcomes that clearly demonstrated technique-dependent differences. Both studies supported the individualized approach in patients with aortic arch anomalies, and Ahmad et al.[38] specifically emphasized endovascular interventions.

The limitations of the selected research are also reflected in the limits of this review. Retrospective designs are significantly overrepresented, which restricts causal inference and introduces selection bias. Cross-study comparison is difficult due to the lack of a consensus classification scheme for AA variants, and definitions of "bovine arch" vary. The technological diversity creates factors of poor replicability and diagnostic variability.[35,36] Since the majority of the studies were single-center research, generalizations would be more challenging due to the limited variety of population variety and expertise variability of experience that would be present in multicenter studies. Despite being commonly associated with AA abnormalities, stroke risk has not been thoroughly investigated in terms of mechanisms such as haemodynamic changes or embolic routes.[31,37]

Standardization in methodology, such as uniform imaging techniques and classification systems, should be the main focus of future research. To validate the results and guarantee a wider application across various populations and therapeutic situations, prospective multicenter studies are required. Developing predictive tools for aneurysm risk and procedure outcomes can be made easier by integrating complex computer models, such as CFD and finite element analysis.[17,38] Long-term follow-up studies would be helpful in providing important information on the durability of treatments and the natural history of aneurysms in patients with AA abnormalities. A deeper understanding of these interactions may also be gained by researching the mechanistic links of AA variants with stroke, which integrate imaging data with genetic profiles and biomarkers. For individuals with anomalies of the aortic arch, this would close a gap in the literature and offer different approaches to diagnosis and therapy.[29,30,33]

Study limitations

This study was weakened by heterogeneity in the study designs and sample size, which thereby introduced heterogeneity in assessing aneurysm risk and variations in the aortic arch. Also, the study is retrospective with an overwhelming predominance, potentially compromising control over a number of confounding variables, thus allowing scope for inconsistency in findings of association. The heterogeneity due to the lack of uniformity in the advanced imaging techniques that contribute to the accuracy was one of the critical weaknesses this study had. Anatomical variation, as such, was necessarily complicated and perhaps too subtle in its classification for certain types of interpretation, which were variable from study to study. All these factors narrowed the generalizability potential of any findings.

Clinical recommendations

According to the findings evaluated in this review, it becomes apparent that the clinical examination will include modern imaging techniques of CT and MRI to amplify the specificity of the diagnosis along with the detection of risk aortic arch variations prone to aneurysmal development. Standardized imaging and classification protocols for different types of aortic arches will increase the reproducibility of the risk detected in patients. Further prospective studies with well-defined controls for confounders are warranted to establish more strongly the relationship between certain arch types and the risk of aneurysms. Finally, interprofessional collaboration between vascular surgeons, radiologists, and cardiologists will ensure optimal risk stratification and surgical planning in patients with anatomy variations.

Conclusion

The results indicated a specific anatomical variation related to the aortic arch, such as a bovine arch and the aberrant right subclavian artery, which is reportedly associated with increased apparent risks of developing aneurysm formation. However, in view of the consistent

association, through all study populations, the influence of the specific anatomical variation upon the other factors can differ. It emphasizes the need to include detailed imaging assessments within the clinical evaluation, and future research will be required to establish a definitive relationship between these variations and to explain the predictive value that may exist for aneurysm development.

Declarations

Funding

This research did not receive specific grant from funding agencies in the public, commercial or not-for-profit sectors.

Author contributions

Conceptualization, S.K.J. and S.S.; Methodology, S.S.; Software, S.S.; Validation, S.K.J. and S.S.; Formal Analysis, S.K.J.; Investigation, S.S.; Resources, S.K.J.; Data Curation, S.S.; Writing – Original Draft Preparation, S.S; Writing – Review & Editing, S.K.J.; Visualization, S.S; Supervision, S.K.J.; Project Administration, S.S.; Funding Acquisition, S.K.J.

Conflicts of interest

The authors declare that there is no conflict of interest regarding the publication of this article.

Data availability

The availability is not applicable to this article, as no new data were generated or analyzed during the current study.

Ethics approval

Ethical approval was not required for this study, as it is a review of previously published literature.

References

1. Keet K, Gunston G, Alexander R. Variations in the branching pattern of the aortic arch: An African perspective. *Eur J Anat*. 2019;23:91.
2. Baudo M, Sicouri S, Yamashita Y, et al. Clinical presentation and management of the cervical aortic arch in the adult population: a review of case reports. *J Cardiothorac Vasc Anesth*. 2024;38(8):1777-1785. doi:10.1053/j.jvca.2024.03.041
3. Boillat G, Franssen T, Wanderer S, et al. Anatomical variations of the common carotid arteries and neck structures of the New Zealand White rabbit and their implications for the development of preclinical extracranial aneurysm models. *Brain Sci*. 2023;13(2):222. doi:10.3390/brainsci13020222
4. Pidvalna U, Mirchuk M, Beshley D, Mateshuk-Vatseba L. Morphometric characteristics of the aorta and heart in situ versus totalis. *Anat Cell Biol*. 2022;55(2):259-263. doi:10.5115/acb.21.252
5. Zhang X, Peng Y, Li G, et al. Elongation of the proximal descending thoracic aorta and associated hemodynamics increase the risk of acute type B aortic dissection. *Technol Health Care*. 2024;32(2):765-777. doi:10.3233/THC-230194
6. Zhong YL, Ma WG, Zhu JM, et al. Surgical repair of cervical aortic arch: An alternative classification scheme based on experience in 35 patients. *J Thorac Cardiovasc Surg*. 2020;159(6):2202-2213.e4. doi:10.1016/j.jtcvs.2019.03.143
7. Ahmed M, Zyck S, Gould GC. Initial experience of subcutaneous nitroglycerin for distal transradial access in neurointerventions. *Surg Neurol Int*. 2021;12:513. doi:10.25259/SNI_711_2021
8. Tricarico R, Tran-Son-Tay R, Laquian L, et al. Haemodynamics of different configurations of a left subclavian artery stent graft for thoracic endovascular aortic repair. *Eur J Vasc Endovasc Surg*. 2020;59(1):7-15. doi:10.1016/j.ejvs.2019.06.028
9. Solano A, Pizano A, Azam J, et al. Kommerell's diverticulum in a right-sided aortic arch with an aberrant left subclavian artery hybrid repair. *Vasc Endovascular Surg*. 2023;57(8):954-959. doi:10.1177/15385744231183310
10. Mirande MH, Durhman MR, Smith HF. Anatomic investigation of two cases of aberrant right subclavian artery syndrome, including the effects on external vascular dimensions. *Diagnostics (Basel)*. 2020;10(8):592. doi:10.3390/diagnostics10080592
11. Starke RM, Abecassis IJ, Saini V, et al. Initial experience of using a large-bore (0.096″ inner diameter) access catheter in neurovascular interventions. *Interv Neuroradiol*. 2024;30(3):372-379. doi:10.1177/15910199221127074
12. Nekoui M, Pirruccello JP, Di Achille P, et al. Spatially distinct genetic determinants of aortic dimensions influence risks of aneurysm and stenosis. *J Am Coll Cardiol*. 2022;80(5):486-497. doi:10.1016/j.jacc.2022.05.024
13. Page MJ, Moher D, Bossuyt PM, et al. PRISMA 2020 explanation and elaboration: Updated guidance and exemplars for reporting systematic reviews. *BMJ*. 2021;372:n160. doi:10.1136/bmj.n160
14. Igelström E, Campbell M, Craig P, Katikireddi SV. Cochrane's risk of bias tool for non-randomized studies (ROBINS-I) is frequently misapplied: A methodological systematic review. *J Clin Epidemiol*. 2021;140:22-32. doi:10.1016/j.jclinepi.2021.08.022
15. Bezerra CT, Grande AJ, Galvão VK, et al. Assessment of the strength of recommendation and quality of evidence: GRADE checklist. A descriptive study. *Sao Paulo Med J*. 2022;140(6):829-836. doi:10.1590/1516-3180.2022.0043.R1.07042022
16. Açar G, Çiçekcibaşı AE, Uysal E, et al. Anatomical variations of the aortic arch branching pattern using CT angiography: A proposal for a different morphological classification with clinical relevance. *Anat Sci Int*. 2022;97:65-78. doi:10.1007/s12565-021-00627-6
17. Bouaou K, Dietenbeck T, Soulat G, et al. Four-dimensional flow cardiovascular magnetic resonance aortic cross-

-sectional pressure changes and their associations with flow patterns in health and ascending thoracic aortic aneurysm. *J Cardiovasc Magn Reson.* 2024;26(1):101030. doi:10.1016/j.jocmr.2024.101030

18. Budhiraja V, Rastogi R, Jain V, et al. Anatomical variations in the branching pattern of human aortic arch: A cadaveric study from central India. *ISRN Anat.* 2013;2013:828969. doi:10.5402/2013/828969
19. Celikyay ZR, Koner AE, Celikyay F, et al. Frequency and imaging findings of variations in human aortic arch anatomy based on multidetector computed tomography data. *Clin Imaging.* 2013;37(6):1011-1019. doi:10.1016/j.clinimag.2013.07.008
20. Della Corte A, Rubino AS, Montella AP, et al. Implications of abnormal ascending aorta geometry for risk prediction of acute type A aortic dissection. *Eur J Cardiothorac Surg.* 2021;60(4):978-986. doi:10.1093/ejcts/ezab218
21. Ikeno Y, Koide Y, Matsueda T, et al. Anatomical variations of aortic arch vessels in Japanese patients with aortic arch disease. *Gen Thorac Cardiovasc Surg.* 2019;67:219-226. doi:10.1007/s11748-018-1001-3
22. Karacan A, Türkvatan A, Karacan K. Anatomical variations of aortic arch branching: Evaluation with computed tomographic angiography. *Cardiol Young.* 2014;24(3):485-493. doi: 10.1017/S1047951113000656
23. Natsis KI, Tsitouridis IA, Didagelos MV, et al. Anatomical variations in the branches of the human aortic arch in 633 angiographies: Clinical significance and literature review. *Surg Radiol Anat.* 2009;31(5):319-323. doi:10.1007/s00276-008-0442-2
24. Pandalai U, Pillay M, Moorthy S, et al. Anatomical variations of the aortic arch: A computerized tomography-based study. *Cureus.* 2021;13(2):e13115. doi:10.7759/cureus.13115
25. Salehi F, Nadeem IM, Kwan BYM, et al. Investigating the association between aortic arch variants and intracranial aneurysms. *Can J Neurol Sci.* 2022;49(3):364-367. doi:10.1017/cjn.2021.112
26. Sun J, Zhang S, Qi H, et al. Association of the bovine aortic arch and bicuspid aortic valve with thoracic aortic disease. *BMC Cardiovasc Disord.* 2023;23(1):60. doi: 10.1186/s12872-023-03095-0.
27. Zhu J, Tong G, Zhuang D, et al. Surgical treatment strategies for patients with type A aortic dissection involving arch anomalies. *Front Cardiovasc Med.* 2022;9:979431. doi:10.3389/fcvm.2022.979431
28. Rotundu A, Nedelcu AH, Tepordei RT, et al. Medical-surgical implications of branching variation of human aortic arch known as bovine aortic arch (BAA). *J Pers Med.* 2024;14:678. doi:10.3390/jpm14070678
29. Gold M, Khamesi M, Sivakumar M, et al. Right-left propensity of cardiogenic cerebral embolism in standard versus bovine aortic arch variant. *Clin Anat.* 2018;31:310-313. doi:10.1002/ca.23045
30. Matakas JD, Gold MM, Sterman J, et al. Bovine arch and stroke laterality. *J Am Heart Assoc.* 2020;9:e015390. doi:10.1161/JAHA.119.015390
31. Samadhiya S, Sardana V, Bhushan B, et al. Propensity of stroke in standard versus various aortic arch variants: A 200-patient study. *Ann Indian Acad Neurol.* 2022;25:634-639. doi:10.4103/aian.aian_710_21
32. Huang F, Li X, Zhang Z, et al. Comparison of two surgical approaches for acute type A aortic dissection: hybrid debranching versus total arch replacement. *J Cardiothorac Surg.* 2022;17:166. doi:10.1186/s13019-022-01920-9
33. Montorsi P, Galli S, Ravagnani PM, et al. Carotid artery stenting in patients with left ICA stenosis and bovine aortic arch: A single-center experience in 60 consecutive patients treated via the right radial or brachial approach. *J Endovasc Ther.* 2014;21:127-136. doi:10.1583/13--4491MR.1
34. Burzotta F, Nerla R, Pirozzolo G, et al. Clinical and procedural impact of aortic arch anatomic variants in carotid stenting procedures. *Catheter Cardiovasc Interv.* 2015;86:480-489. doi:10.1002/ccd.25947
35. Popieluszko P, Henry BM, Sanna B, et al. A systematic review and meta-analysis of variations in branching patterns of the adult aortic arch. *J Vasc Surg.* 2018;68(1):298-306.e10. doi:10.1016/j.jvs.2017.06.097
36. Baz RO, Refi D, Scheau C, Axelerad A, Baz RA, Niscoveanu C. CT angiography for aortic arch anomalies: prevalence, diagnostic efficacy, and illustrative findings. *Diagnostics (Basel).* 2024;14(17):1851. doi:10.3390/diagnostics14171851
37. Lazaridis N, Piagkou M, Loukas M, et al. A systematic classification of the vertebral artery variable origin: clinical and surgical implications. *Surg Radiol Anat.* 2018;40(7):779-797. doi:10.1007/s00276-018-1987-3
38. Ahmad W, Wegner M, Dorweiler B. Meta-analysis and meta-regression of the total endovascular aortic repair in aortic arch. *Vasa.* 2023;52(3):175-185. doi:10.1024/0301-1526/a001061

Rzeszów University Press 2026
ISSN 2544-1361 (online)
doi: 10.15584/ejcem.2026.2.6

http://www.ejcem.ur.edu.pl
European Journal of Clinical and Experimental Medicine
Eur J Clin Exp Med 2026; 24 (2): 417–422

CASE REPORTS

Should oophoropexy be a standard procedure after ovarian torsion in premenarchal patients? A case-based review of fixation indications and techniques

Zuzanna Nogaj [1], Danuta Januszkiewicz-Lewandowska [2], Anna Kaźmierowska [1], Marta Jurczok [1], Przemysław Mańkowski [3], Patrycja Sosnowska-Sienkiewicz [4]

[1] Student Research Group of Pediatric Surgery, Department of Pediatric Surgery, Traumatology and Urology, Poznan University of Medical Sciences, Poznan, Poland
[2] Department of Pediatric Oncology, Hematology and Transplantology, Poznan University of Medical Sciences, Poznan, Poland
[3] Department of Pediatric Surgery, Traumatology and Urology, Poznan University of Medical Sciences, Poznan, Poland
[4] Department of Pediatric Surgery, Medical University of Warsaw, Warsaw, Poland

ABSTRACT

Introduction and aim. Ovarian torsion is a rare but significant cause of acute abdomen in children. Diagnosis is challenging due to nonspecific symptoms. While Doppler ultrasound is essential, it is not definitive. Laparoscopy with detorsion remains the diagnostic and therapeutic standard. For recurrent and high-risk cases, oophoropexy is considered, but there is no consensus on its indications or optimal technique. We analyze the diagnostic process, reasons for recurrence, and outcomes of different oophoropexy techniques.

Description of the case. A premenarchal girl experienced three episodes of ipsilateral ovarian torsion. After the second recurrence, she underwent laparoscopic oophoropexy via fixation posterior to the uterus to the ovarian fossa with absorbable sutures, which failed. Following a third torsion, a laparotomy with a subsequent oophoropexy to the round ligament using non-absorbable sutures achieved a long-term recurrence-free period.

Conclusion. Retorsion remains a significant risk. This case provides a unique intrapatient comparison, demonstrating that the technical approach influences the outcomes. Fixation to the abdominal wall with non-absorbable sutures proved to be superior in this scenario, preventing further recurrence. The patient's age and torsion etiology are critical in selecting a fixation method. This report highlights the potential for oophoropexy failure and offers vital technical insights, underscoring the need for further studies to standardize practices for fertility preservation.

Keywords. abdomen, acute, child, fertility, oophoropexy, ovarian torsion

Introduction

Ovarian torsion (OT) is a rare emergency in the pediatric population, typically managed by pediatric surgeons and gyneacologists.[1–4] It occurs more frequently in adolescents, but approximately 15% of cases are seen in prepubertal patients.[1] Between 41 and 50% of the cases involve an ovarian neoplasm or cyst; however, torsion of normal premenarchal ovaries has also been documented.[2,5] Diagnosing OT can be challenging due to nonspecific symptoms – such as abdominal pain (lasting hours

Corresponding author: Zuzanna Nogaj, e-mail: 85801@student.ump.edu.pl

Received: 26.10.2025 / Revised: 18.01.2026 / Accepted: 26.01.2026 / Published: 30.06.2026

Nogaj Z, Januszkiewicz-Lewandowska D, Kaźmierowska A, Jurczok M, Mańkowski P, Sosnowska-Sienkiewicz P. Should oophoropexy be a standard procedure after ovarian torsion in premenarchal patients? A case-based review of fixation indications and techniques. *Eur J Clin Exp Med.* 2026;24(2):417–422. doi: 10.15584/ejcem.2026.2.6.

to days), nausea, vomiting, and fever - symptoms that overlap with many causes of acute abdomen, with appendicitis being the most common surgical emergency in patients older than one year. This overlap complicates the diagnostic process for OT.[1,2,6,7]

Diagnostic evaluation should encompass a comprehensive history, physical examination, laboratory tests and imaging studies, with ultrasound being the preferred initial choice for gynecological problems. A CT scan or MRI might be more appropriate for identifying gastrointestinal causes but should not delay any urgent surgical intervention.[8] If a surgeon is in charge of the case, a consultation and pelvic examination by a gynecologist might be beneficial. A vaginal or, in patients not sexually active, transrectal bimanual examination can be performed; however, its sensitivity to detect adnexal torsion is low.[9]

Transabdominal ultrasound is the primary imaging tool, effective in excluding other conditions such as appendicitis. Although transvaginal ultrasound offers better visualization, it is rarely appropriate in children; a transrectal approach may be considered in cooperative patients. One of the most comprehensive studies shows that the most common ultrasound characteristics are enlarged adnexa, whirlpool sign, ovarian stromal oedema with or without peripherally displaced antral follicles, and free fluid in the pelvis. In contrast, the follicular ring sign and the absence of Doppler signals in the twisted organ are slightly less common features.[10] Examiners should also note that the normal ovarian volume varies with age.[11,12] A definitive diagnosis can only be made after laparoscopy, during which the ovary is detorsed.

Oophoropexy (OPY) refers to a procedure for fixation of the adnexa, used in ovarian transposition in women before pelvic radiotherapy. It also serves as a preventive measure against recurrence of OT and the occurrence of OT in the remaining ovary following oophorectomy. In these cases, OPY is vital for preserving fertility. While there are several methods of ovarian fixation, specific guidelines regarding the choice of technique and the number of OT procedures warranting intervention in a patient are lacking.

Aim

In this case report, we discuss a premenarchal woman with OT and its recurrence, focusing on the associated risk factors and management strategies. Additionally, we aim to highlight indications for OPY, along with its methods, and technical aspects.

Description of the case

A four-year-old premenarchal girl was admitted to the department of pediatric surgery with a two-day history of abdominal pain and one episode of vomiting. She had previously been healthy, with no chronic illness or prior surgeries. On examination, her abdomen was soft, without pathological masses or signs of peritoneal irritation, although slight tenderness of the lower abdomen was observed. An ultrasound scan of the right lower abdomen revealed an ovary measuring approximately 4.3×3.1 cm, along with another measuring 2.0×1.0 cm nearby. Free fluid was observed in the Pouch of Douglas. Exploratory laparoscopy revealed a

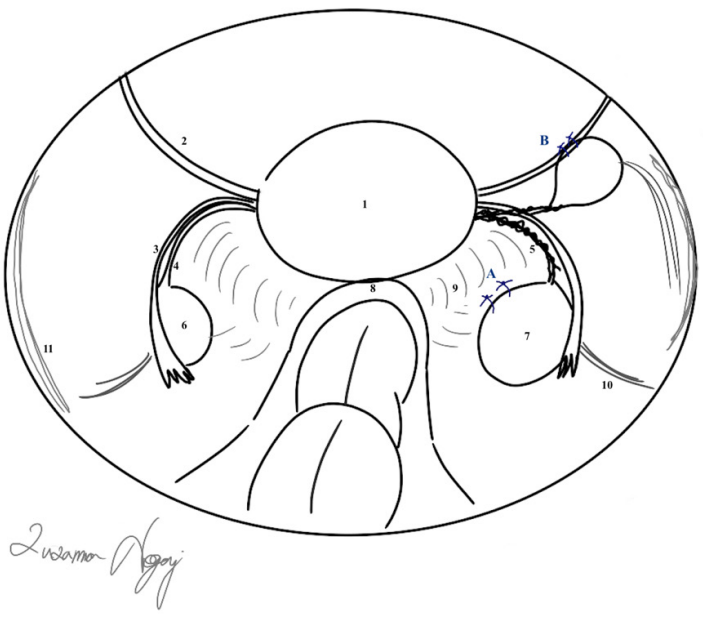

Fig. 1. Schematic laparoscopy view of the pelvis: 1. uterus, 2. round ligament, 3. fallopian tube, 4. utero-ovarian/ovarian ligament (normal), 5. utero-ovarian/ovarian ligament (long), 6. ovary (normal), 7. ovary (enlarged), 8. uterosacral ligament, 9. ovarian fossa and broad ligament, 10. suspensory ligament of the ovary, 11. psoas tendon, A – first fixation of the left ovary to the ovarian fossa, B – second fixation to the round ligament

double twisted black left ovary (LO) in the right iliac fossa. Adnexal detorsion was performed, restoring circulation and the LO was repositioned in the left iliac fossa. The patient was discharged home seven days later in good condition.

Six months later, the patient was readmitted with similar symptoms. An ultrasound confirmed an increase in the size of the LO. A color Doppler revealed peripherally diminished blood flow. An emergency laparoscopy was performed, which revealed a black triple-torsed LO this time. Detorsion of the adnexa was performed that resulted in the return of normal tissue color. The follow-up ultrasound showed a reduction in the size of the LO and Doppler flow indicated normal blood flow.

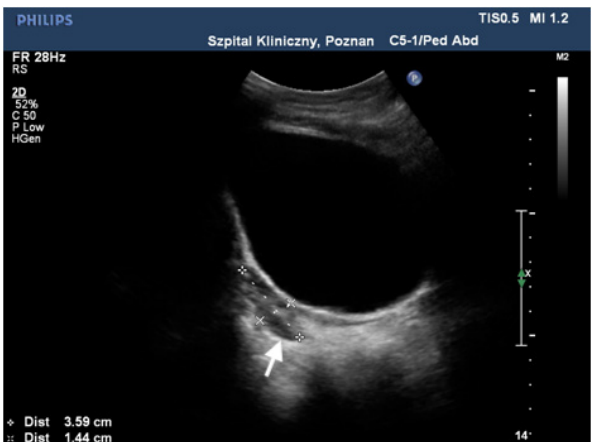

Fig. 2. An ultrasound scan of the twisted, 3.6x1.4 cm left ovary (white arrow) in a premenarchal girl. Visible hypoechogenic mass attached to the upper left side of the left ovary seven months after an oophoropexy

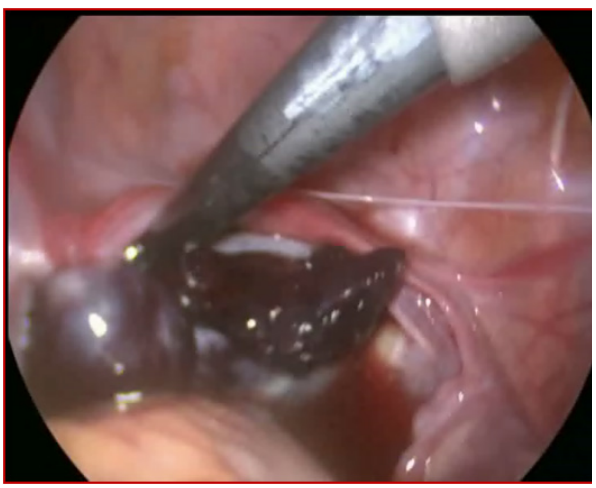

Fig. 3. Laparoscopic view of the recurrent, triple-twisted left ovary in a premenarchal girl before detorsion

Due to the OT recurrence, the patient was scheduled for a laparoscopic OPY. The right and left ovarian ligament (OL) were asymmetric, with the left approximately three times longer than the right. The LO was fixed posterior to the uterus in the ovarian fossa using two single 4-0 absorbable sutures (Fig. 1). Seventeen months post-OPY, the patient returned with similar symptoms and findings as in the previous hospitalizations. An ultrasound revealed a mass attached to the LO (Fig. 2). An exploratory laparoscopy identified a triple twisted black LO (Fig. 3).

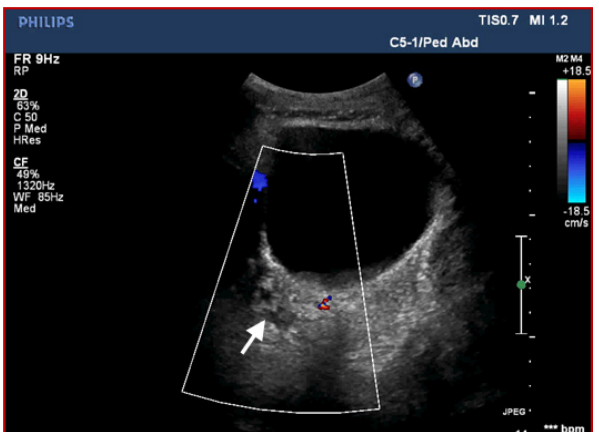

Fig. 4. Postoperative Doppler ultrasound scan of the left ovary (white arrow) in a premenarchal patient with a left ovary with visible blood flow after a third torsion and a second oophoropexy

Detorsion was performed and a gradual, partial restoration of circulation was observed. Given the patient's history, a laparotomy was performed and LO was fixed to the round ligament using two non-absorbable sutures (Fig. 1). Ovarian tissue samples were taken and revealed both necrotic and healthy ovarian tissue. Tumor markers, including β-hCG and AFP, were within the normal ranges. Postoperative ultrasound indicated an enlarged LO with increased blood flow (Fig. 4). During a 5-year follow-up period, the patient did not experience any further recurrences of OT.

Discussion

The unique aspect of our report is the direct intrapatient comparison of two OPY techniques. The failure of the initial fixation with absorbable sutures versus the long-term success of the second procedure with nonabsorbable sutures provides a powerful clinical lesson that is rarely documented in the literature. We believe that fixation of the ovary to the round ligament, specifically with nonabsorbable sutures, was a favorable choice for preventing further recurrences. Had the discrepancy in the lengths of the ovarian ligaments been recognized earlier, this fixation could have been performed sooner, potentially avoiding multiple operating procedures.

In this case, the patient presented common clinical and ultrasound symptoms of OT, without any ovarian mass. While abdominal pain is present in almost all patients, including the present one, it is not possible to

differentiate OT from other pathologies based on symptoms.[13] If OT is suspected, an ultrasound with Doppler flow should be performed.[1,2,14] The presence of an ovarian mass, enlargement of the ovary, or absence of vascular flow is highly suggestive of OT; however, some sources report that Doppler flow in the ovary is present in 40% to 73% of OT cases.[2,5,6,14] Therefore, a lack of Doppler flow in an ovary suggests OT, but its presence does not rule out.[13] Those findings may vary among patients due to causative pathology and the duration of OT.[15] Additionally, a small ovarian mass or ovaries without specific findings may be more closely associated with the risk of retorsion.[16] In our patient, a ovary appeared noticeably larger, likely due to swelling, and the length of the OL allowed it to be positioned near the right ovary. Free fluid in the pouch of Douglas was also visualized.

The literature reports that laparoscopic surgery is the best diagnostic and therapeutic procedure for pediatric patients.[5,6,14,17] Conservative management, such as detorsion and preservation of the adnexa, is considered a safe and effective treatment.[17] Even if the ovary appears necrotic, it generally shows improvement in blood flow and follicular development after 4-6 weeks.[14,17]

Recurrence of OT occurs in 12–19% of the pediatric cases, mainly on the same side, approximately seven times more often in patients with normal ovaries compared to those with ovarian masses, and is not related to the presence of menarche at the first episode of torsion.[3,5] In premenarchal and adolescent girls, smaller adnexa and loose structure can predispose to recurrence of OT.[19] In a prospective cohort study, Tamir Yaniv et al. report that the length of OL length can be a statistically significant factor for OT; however, the answer to whether OPY should be performed in cases of first-episode OT with a long OL is not clear.[18]

In the case presented, after detorsion and confirmation of ovarian viability, the patient was scheduled for elective laparoscopic OPY. This planned approach allows for a deliberate evaluation of pelvic anatomy – including the identification of the elongated ovarian ligament and a controlled fixation procedure, rather than performing it urgently during the initial emergent torsion surgery.

Most of the literature on indications for OPY is based on case reports, case series, and small one-center experiences. The overall recurrence of OT after simple laparoscopic detorsion is said to be significant and can vary from 36 up to 64%, especially in the prepuberal population.[3,20] Research indicates that performing OPY reduces this risk, but does not completely exclude it.[3,14]

There are multiple fixation techniques, but comparative evidence is limited (Table 1). Mandarano et al., compared four methods, including fixation of the ovary to the round ligament, ovarian fossa, utero-ovarian ligament, and uterine body, all with non-absorbable sutures.[20] As a result, none of the methods appeared superior, except for the OPY to the round ligament, which, contrary to our case, showed a high rate of recurrence. The authors of the study suspected that this fixation site alters the normal anatomical position of the ovary to the greatest extent. However, it is important to note that fixation to the round ligament in this study involved only five patients and no other publication has confirmed the inadequacy of this fixation site. In terms of alternative methods, a study by Yagur et al. compared ovarian ligament and ovarian round ligament plication in women of reproductive age after adnexal torsion with normal-sized ovaries. Although no statistical significance was found, the ovarian-round ligament plication group experienced recurrence of OT, while the ovarian ligament plication did not.[19]

Table 1. Oophoropexy techniques and alternative ovarian fixation methods performed after episodes of ovarian torsion in female patients of different age groups, OL, ovarian ligament, OT – ovarian torsion

	Method	Note
Oophoropexy	fixation to a uterosacral ligament [21]	relatively easy, and prevents damage to the ureter and blood vessels
	fixation to a utero-ovarian ligament, or to the psoas tendon [22]	proximity of both structures to the anatomical location of the ovary
	fixation to the peritoneum on the posterior abdominal wall (ovarian fossa) [20,23]	helps preserve the tubo-ovarian anatomic relationship
	fixation to an abdominal wall using a trocar site closure needle [24]	suggested as an easier technique, especially for pregnant women with an enlarged uterus
	fixation to the posterior uterine serosa [20,25]	technique reported as effective with the use of either absorbable or non-absorbable sutures
	fixation to the broad ligament [26]	older method, reported in neonatal patients
	fixation to the round ligament [20]	suggested high recurrence rate in one study, however effective in the presented case
Alternative fixation method	plication of the ovarian ligament [27,28]	an effective method for longer or looser OL; it can be performed during early pregnancy
Combined methods	fixation of the ovary to the pelvic side wall with the uteroovarian ligament plication [29]	for recurring OT cases, mainly when laxity of ligaments and enlarged ovaries (due to, e.g., polycystic ovaries) are observed

To secure the ovary, we typically employ two sutures, size 3-0 or 4-0, which penetrate the ovarian cortex, as was demonstrated in our case.[20,30] There is, however, no agreement on whether absorbable or non-absorbable sutures should be used. Some studies, such as those of Fuchs et al., advocate for nonabsorbable sutures, possibly due to shorter observation periods and varying operative techniques.[30] This highlights the need for larger comparative studies on suture types. In our

case, non-absorbable sutures were more effective than absorbable ones.

It is essential to establish different indications and surgical techniques for female patients with OT in various age groups and adnexal characteristics. Research indicates a negative correlation between patient age and recurrence rates. Therefore, for premenarcheal girls, in the absence of ovarian cysts or masses, it might be more profitable to perform OPY during the first detorsion, as it could limit the number of recurrences, reoperations, and their complications. Careful consideration should be given to the presence of ovarian masses and adnexa characteristics, particularly OL and discrepancies in their length. In the case presented, the use of non-absorbable sutures and fixation of the ovary to the abdominal wall was an optimal choice to prevent further recurrences.

Conclusion

This case is noteworthy due to the presentation of two recurrences of the OT despite performing OPY after the first retorsion. OT and its recurrences can lead to organ loss and infertility, which requires increased awareness from the attending physician. It also provides a unique clinical comparison that underscores the influence of surgical technique and suture material choice on long-term results. More studies are required to reach a consensus on optimal indications for OPY and its techniques to prevent recurrence.

Declarations

Funding

All sources for funding of the study should be disclosed.

Author contributions

Conceptualization, P.S.S., Z.N. and D.J.L. Methodology, P.S.S., A.K., M.J. and Z.N.; Validation, P.S.S., D.J.L. and P.M.; Formal Analysis, Z.N. and D.J.L.; Investigation, Z.N. A.K. and M.J.; Resources, P.S.S. and D.J.L.; Data Curation, Z.N., M.J. and A.K.; Writing – Original Draft Preparation, Z.N., D.J.L., A.K., M.J., P.M. and P.S.S.; Writing – Review & Editing, Z.N. and P.S.S.; Visualization, P.S.S. and Z.N.; Supervision, P.S.S. and P.M.; Project Administration, P.S.S.

Conflicts of interest

The authors declare no competing interests.

Data availability

No datasets were generated or analyzed during the current study.

Ethics approval

Written informed consent was obtained from the patient's parents for their anonymized information to be published in this article.

References

1. Tasset J, Rosen MW, Bell S, Smith YR, Quint EH. Ovarian Torsion in Premenarchal Girls. *J Pediatr Adolesc Gynecol*. 2019;32(3):254-258. doi:10.1016/j.jpag.2018.10.003
2. Bertozzi M, Magrini E, Bellucci C, Riccioni S, Appignani A. Recurrent Ipsilateral Ovarian Torsion: Case Report and Literature Review. *J Pediatr Adolesc Gynecol*. 2015;28(6):e197-e201. doi:10.1016/j.jpag.2015.06.007
3. Bertozzi M, Esposito C, Vella C, et al. Pediatric Ovarian Torsion and its Recurrence: A Multicenter Study. *J Pediatr Adolesc Gynecol*. 2017;30(3):413-417. doi:10.1016/j.jpag.2016.11.008
4. Alberto EC, Tashiro J, Zheng Y, et al. Variations in the management of adolescent adnexal torsion at a single institution and the creation of a unified care pathway. *Pediatr Surg Int*. 2021;37(1):129-135. doi:10.1007/S00383-020-04782-1
5. Ashwal E, Krissi H, Hiersch L, Less S, Eitan R, Peled Y. Presentation, Diagnosis, and Treatment of Ovarian Torsion in Premenarchal Girls. *J Pediatr Adolesc Gynecol*. 2015;28(6):526-529. doi:10.1016/j.jpag.2015.03.010
6. Rossi BV, Ference EH, Zurakowski D, et al. The Clinical Presentation and Surgical Management of Adnexal Torsion in the Pediatric and Adolescent Population. *J Pediatr Adolesc Gynecol*. 2012;25(2):109-113. doi:10.1016/j.jpag.2011.10.006
7. Tseng YC, Lee MS, Chang YJ, Wu HP. Acute abdomen in pediatric patients admitted to the pediatric emergency department. *Pediatr Neonatol*. 2008;49(4):126-134. doi:10.1016/S1875-9572(08)60027-3
8. Wattar B, Rimmer M, Rogozinska E, Macmillian M, Khan KS, Al Wattar BH. Accuracy of imaging modalities for adnexal torsion: a systematic review and meta-analysis. *BJOG*. 2021;128(1):37-44. doi:10.1111/1471-0528.16371
9. Dragisic KG, Padilla LA, Milad MP. The accuracy of the rectovaginal examination in detecting cul-de-sac disease in patients under general anaesthesia. *Hum Reprod*. 2003;18(8):1712-1715. doi:10.1093/HUMREP/DEG350
10. Moro F, Bolomini G, Sibal M, et al. Imaging in gynecological disease (20): clinical and ultrasound characteristics of adnexal torsion. *Ultrasound Obstet Gynecol*. 2020;56(6):934-943. doi:10.1002/UOG.21981
11. Stranzinger E, Strouse PJ. Ultrasound of the pediatric female pelvis. *Semin Ultrasound CT MR*. 2008;29(2):98-113. doi:10.1053/J.SULT.2007.12.002
12. Garel L, Dubais J, Grignon A, Filiatrault D, Van Vliet G. US of the pediatric female pelvis: a clinical perspective. *Radiographics*. 2001;21(6):1393-1407. doi:10.1148/RADIOGRAPHICS.21.6.G01NV041393
13. Sims MJ, Price AB, Hirsig LE, Collins HR, Hill JG, Titus MO. Pediatric Ovarian Torsion: Should You Go With the Flow? *Pediatr Emerg Care*. 2022;38(6):E1332-E1335. doi:10.1097/PEC.0000000000002679
14. Childress KJ, Dietrich JE. Pediatric Ovarian Torsion. *Surgical Clinics of North America*. 2017;97(1):209-221. doi:10.1016/j.suc.2016.08.008

15. Uterine adnexal torsion: pathologic and gray-scale ultrasonographic findings - PubMed. https://pubmed.ncbi.nlm.nih.gov/14998184/ Accessed October 9, 2025.
16. Daykan Y, Bogin R, Sharvit M, et al. Ovarian size as a risk factor for recurrent adnexal torsion: Smaller is not better. *J Obstet Gynaecol Res*. 2020;46(5):745-751. doi:10.1111/JOG.14220
17. Geimanaite L, Trainavicius K. Pediatric ovarian torsion: Follow- up after preservation of ovarian tissue. *J Pediatr Surg*. 2019;54(7):1453-1456. doi:10.1016/j.jpedsurg.2019.02.004
18. Tamir Yaniv R, Schonmann R, Agizim R, et al. Correlation between the Length of Ovarian Ligament and Ovarian Torsion: A Prospective Study. *Gynecol Obstet Invest*. 2019;84(1):45-49. doi:10.1159/000490664
19. Yagur Y, Klein A, Tiosano L, et al. Comparative outcomes of oophoropexy techniques in preventing recurrent adnexal torsion. *Arch Gynecol Obstet*. 2025;312(4):1317-1325. doi:10.1007/S00404-025-08128-X/TABLES/4
20. Mandarano G, Parolini F, Bosisio M, et al. Primary ovarian torsion in pediatric patients: is oophoropexy still an option? A 14-year single-center experience. *J Pediatr Adolesc Gynecol*. 2025. doi:10.1016/j.jpag.2025.10.008
21. Hartley J, Akhtar M, Edi-Osagie E. Oophoropexy for Recurrent Ovarian Torsion. *Case Rep Obstet Gynecol*. 2018;2018:8784958. doi:10.1155/2018/8784958
22. Dicken BJ, Billmire DF. Ovarian Cyst and Tumors. Boca Raton, FL: CRC Press; 2013:967-972. doi:10.1201/b13198
23. Abeş M, Sarihan H. Oophoropexy in children with ovarian torsion. *Eur J Pediatr Surg*. 2004;14(3):168-171. doi:10.1055/S-2004-817887/ID/15/BIB
24. Hosny TA. Oophoropexy for ovarian torsion: a new easier technique. *Gynecol Surg*. 2017;14(1):7. doi:10.1186/S10397-017-1001-9
25. Davis AJ, Feins NR. Subsequent asynchronous torsion of normal adnexa in children. *J Pediatr Surg*. 1990;25(6):687-689. doi:10.1016/0022-3468(90)90365-G
26. Guileyardo JM. Neonatal ovarian torsion. *Am J Dis Child*. 1982;136(10):945-946. doi:10.1001/ARCHPEDI.1982.03970460075017
27. Djavadian D, Braendle W, Jaenicke F. Laparoscopic oophoropexy for the treatment of recurrent torsion of the adnexa in pregnancy: Case report and review. *Fertil Steril*. 2004;82(4):933-936. doi:10.1016/j.fertnstert.2004.03.048
28. Tsafrir Z, Hasson J, Levin I, Solomon E, Lessing JB, Azem F. Adnexal torsion: Cystectomy and ovarian fixation are equally important in preventing recurrence. *Eur J Obstet Gynecol Reprod Biol*. 2012;162(2):203-205. doi:10.1016/j.ejogrb.2012.02.027
29. Simsek E, Kilicdag E, Kalayci H, Yuksel Simsek S, Parlakgumus A. Repeated ovariopexy failure in recurrent adnexal torsion: Combined approach and review of the literature. *Eur J Obstet Gynecol Reprod Biol*. 2013;170(2):305-308. doi:10.1016/j.ejogrb.2013.06.044
30. Fuchs N, Smorgick N, Tovbin Y, et al. Oophoropexy to prevent adnexal torsion: how, when, and for whom? *J Minim Invasive Gynecol*. 2010;17(2):205-208. doi:10.1016/J.JMIG.2009.12.011

Rzeszów University Press 2026
ISSN 2544-1361 (online)
doi: 10.15584/ejcem.2026.2.19

http://www.ejcem.ur.edu.pl
European Journal of Clinical and Experimental Medicine
Eur J Clin Exp Med 2026; 24 (2): 423–429

CASE REPORTS

Antiphospholipid syndrome in an adolescent with refractory immune thrombocytopenia and massive central venous thrombosis

Matylda Marcelina Mikołajczyk [1], Wioletta Bal [2,3], Gabriela Mastej-Witek [4], Radosław Chaber [2,3]

[1] Students' Scientific Association at the Department of Pediatric Hematology and Oncology, Department of Pediatrics, University of Rzeszów, Rzeszów, Poland
[2] Clinic of Pediatric Oncology and Hematology, Clinical Provincial Hospital named after St. Jadwiga, Rzeszów, Poland
[3] Department of Pediatrics, Faculty of Medicine, University of Rzeszow, Rzeszów, Poland
[4] Health Care Facility, Siedlce, Poland

ABSTRACT

Introduction and aim. Immune thrombocytopenia (ITP) and antiphospholipid syndrome (APS) may coexist, creating a clinical paradox of simultaneous bleeding risk and thrombophilia. In children and adolescents, APS can remain unrecognized for years when thrombocytopenia dominates the early course. The thrombotic risk associated with thrombopoietin receptor agonists (TPO-RAs) in this setting remains uncertain.

Description of the case. A 17-year-old boy with refractory ITP during romiplostim therapy developed massive upper-extremity and central venous thrombosis with near-complete superior vena cava obstruction. Persistent lupus anticoagulant, anticardiolipin, and anti-β2-glycoprotein I antibody positivity established APS. He was treated with heparin, alteplase, and long-term warfarin plus low-dose aspirin, while romiplostim was continued to support safe anticoagulation. No recurrent thrombosis or major bleeding was observed during 20 months of follow-up.

Conclusion. Thrombocytopenia does not protect against thrombosis in APS. In adolescents with chronic or refractory ITP, especially when vascular symptoms, unexplained prolonged aPTT, or other autoimmune red flags are present, targeted antiphospholipid antibody testing should be considered. Management of combined ITP and APS requires individualized balancing of anticoagulation and platelet support, with vitamin K antagonists remaining the preferred long-term anticoagulant strategy in high-risk APS.

Keywords. adolescent, antiphospholipid syndrome, immune thrombocytopenia, romiplostim, venous thrombosis

Introduction

Primary immune thrombocytopenia (ITP) is an acquired autoimmune disorder characterized by isolated thrombocytopenia (platelet count<100×10^9/L) in the absence of other causes of thrombocytopenia or disorders associated with thrombocytopenia.[1,2] It is the most common cause of thrombocytopenia in children and adolescents.[1] In a population-based study, the annual incidence of pediatric ITP was 4.2 per 100,000 person-years.[3]

Antiphospholipid syndrome (APS) is an acquired autoimmune thrombotic disorder defined by the combination of at least one clinical criterion (vascular thrombosis or pregnancy morbidity) and one laboratory criterion, namely persistent antiphospholipid antibodies (aPL) – lupus anticoagulant (LA), anticar-

Corresponding author: Matylda Marcelina Mikołajczyk, e-mail: matyldam1999@gmail.com

Received: 12.03.2026 / Revised: 18.05.2026 / Accepted: 24.05.2026 / Published: 30.06.2026

Mikołajczyk MM, Bal W, Mastej-Witek G, Chaber R. Antiphospholipid syndrome in an adolescent with refractory immune thrombocytopenia and massive central venous thrombosis. *Eur J Clin Exp Med.* 2026;24(2):423–429. doi: 10.15584/ejcem.2026.2.19.

diolipin antibodies (aCL), and/or anti-β2-glycoprotein I antibodies (anti-β2GPI) – present on at least two occasions at least 12 weeks apart.[4] In children, APS is rare, with an incidence of 0.2 per 100,000 reported in some populations.[5]

The coexistence of chronic refractory ITP and primary APS represents a major paradox in pediatric hematology: the same patient may be predisposed to bleeding because of thrombocytopenia while remaining at risk of thrombosis driven by aPL-mediated hypercoagulability. Standard ITP therapies can raise platelet counts but do not address the underlying APS-related prothrombotic tendency; accordingly, observational data suggest that thrombotic event rates during TPO-RA therapy are markedly higher in patients with definite APS.[6,7]

Aim

This report describes an adolescent with refractory ITP who developed massive central venous thrombosis during romiplostim therapy and was subsequently diagnosed with APS. The case is notable for the pediatric age, delayed APS recognition, unusually extensive central venous thrombosis, and the need for continued TPO-RA support despite a major thrombotic event. Importantly, its clinical significance arises from the coexistence of refractory ITP, previously unrecognized primary APS, and exposure to TPO-RA, which together created a high-risk and diagnostically misleading phenotype. This combination illustrates the potential for APS to remain masked by thrombocytopenia while clinically manifesting only after severe thrombotic complications during therapy. We highlight the diagnostic challenges of this rare overlap and discuss the implications for anticoagulation, platelet-supportive therapy, and earlier recognition of APS in adolescents with refractory thrombocytopenia.

Description of the case

A 17-year-old boy was admitted to the Department of Pediatric Oncology and Hematology in August 2023. On admission, he was 182 cm tall and weighed 108 kg, corresponding to a body mass index of 32.6 kg/m^2 (class I obesity). He had initially been diagnosed with immune thrombocytopenia in November 2019 after presenting with petechiae, ecchymoses, and severe thrombocytopenia (platelet count $<5\times10^9$/L). Bone marrow examination excluded malignancy and myelodysplasia. Over the following years, he received multiple therapies, including intravenous immunoglobulin, repeated courses of glucocorticoids, azathioprine, mycophenolate mofetil, and eltrombopag. Eltrombopag produced an initially encouraging response, with the platelet count reaching 140×10^9/L in May 2021; however, the response was not sustained, and a subsequent downward trend was observed, with the platelet count decreasing to 20×10^9/L at the last visit before treatment modification. Eltrombopag was also discontinued because of severe headaches. Because of refractory thrombocytopenia, romiplostim was started in December 2022 and titrated individually at 1–3 μg/kg weekly, with platelet counts usually maintained between 47 and 110×10^9/L. Previous coagulation assessments performed during the earlier course of the disease did not indicate coagulation factor deficiencies. Although intermittent aPTT prolongation had been observed, there were no thrombotic manifestations or other clinical features suggestive of APS at that time. Broader autoimmune evaluation did not establish systemic autoimmune disease: ANA showed only low-titer positivity in 2020 and was negative on repeat testing in August 2023. Therefore, the overall clinical picture – severe isolated thrombocytopenia, bleeding symptoms, exclusion of bone marrow pathology, and lack of clinical features of systemic autoimmune disease supported the diagnosis of primary refractory ITP. Relevant comorbidities included selective IgA deficiency (IgA 0.53 g/L; reference range 1.00–4.00), hypertension treated with hydrochlorothiazide, and obesity. In July 2023, he was treated with doxycycline for erythema migrans associated with Borrelia burgdorferi IgG seropositivity.

Thrombotic event presentation (August 2023)

He was admitted with a 7–10-day history of progressive edema, pain, and erythema of the left upper limb extending to the left side of the neck and anterior chest wall, accompanied by low-grade fever (up to 38.0°C). On examination, the left upper limb was markedly swollen, with predominantly non-pitting edema extending to the shoulder girdle and neck. Prominent superficial collateral veins were visible over the thorax and abdomen. According to the family, the first thoracic collateral veins had become visible in mid-July 2023, suggesting that the thrombotic process had been evolving for more than 4 weeks before admission.

Laboratory findings

Laboratory evaluation demonstrated markedly prolonged aPTT (>100 s), persistent lupus anticoagulant positivity, and repeated positivity of anticardiolipin and anti-β2-glycoprotein I antibodies on follow-up testing performed more than 12 weeks apart. Because local assays reported combined rather than isotype-specific results, formal "triple positivity" could not be assigned despite persistent antibody positivity for all three aPL categories. Platelet count on admission was 95×10^9/L, and D-dimer was markedly elevated (61,485 ng/mL).

Imaging

CT angiography showed extensive thrombosis of the left internal jugular, subclavian, axillary, brachial, and brachiocephalic veins, with near-complete superior vena cava obstruction and extensive collateral venous circulation. Doppler ultrasonography confirmed occlusion of the left upper-extremity and cervical veins, with markedly reduced flow on the right side; no lower-extremity thrombosis was detected. Echocardiography showed no right ventricular strain, while bilateral pleural effusions were consistent with chylothorax secondary to central venous obstruction. Brain MRI was performed in November 2023, three months after the index event, to exclude cerebral venous sinus thrombosis in view of the extensive cervico-thoracic venous involvement and persistent headache. The examination excluded cerebral venous sinus thrombosis.

Diagnosis

The patient fulfilled the revised Sydney classification criteria for definite antiphospholipid syndrome, based on objectively confirmed extensive venous thrombosis and persistent lupus anticoagulant positivity on repeat testing performed more than 12 weeks apart. Repeated positivity of anticardiolipin and anti-β2-glycoprotein I antibodies further supported the diagnosis, although formal triple aPL positivity was not assigned because the local assays reported combined isotypes. Thus, these findings indicate a high-risk aPL profile rather than strictly confirmed triple positivity. No clinical features of systemic lupus erythematosus or another systemic autoimmune disease were identified.[4]

Management and outcomes

In the acute phase, anticoagulation was initiated with continuous intravenous unfractionated heparin (UFH), monitored by anti-Xa activity because of lupus anticoagulant-related interference with aPTT. Given the extent of thrombosis, near-complete superior vena cava obstruction, and a platelet count above 50×10^9/L, systemic thrombolysis with alteplase was administered, resulting in partial reperfusion. Dabigatran was used only as a short transitional regimen while the APS work-up was being completed. After APS was confirmed, long-term therapy was changed to warfarin, consistent with recommendations favoring vitamin K antagonists over direct oral anticoagulants in thrombotic APS, particularly in high-risk aPL profiles.[6,8,9] Romiplostim was continued as an individualized supportive measure to maintain platelet counts compatible with safe anticoagulation, rather than as APS-directed therapy.[7,10]

Complications included puncture-site bleeding and pleural effusions. Catheter-directed thrombolysis and thrombectomy were not pursued because the extensive collateral circulation suggested partial chronicity of the process and the risk of procedure-related pulmonary embolism was considered high. Central venous access was obtained via the right femoral vein, and right-sided thoracocentesis was performed. A short transitional oral regimen with dabigatran 150 mg twice daily plus acetylsalicylic acid (ASA) 75 mg daily was used pending completion of the antiphospholipid antibody work-up; after APS had been confirmed, long-term treatment was changed to warfarin.

For long-term secondary prevention, warfarin was introduced with a target INR of 2.0–3.0, in line with adult EULAR recommendations for venous thrombotic APS and with pediatric APS practice, in which initial heparin therapy is followed by warfarin.[6,8] Low-dose ASA 75 mg daily and romiplostim (125 μg subcutaneously every 2 weeks) were continued as part of an individualized strategy aimed at maintaining platelet counts compatible with safe anticoagulation. At 20-month follow-up, the patient remained clinically stable, with no

Table 1. Timeline of the patient's disease course

Date	Event	Platelet count ($\times10^9$/L)	Treatment/key interventions	Important findings/comments
November 2019	Diagnosis of primary immune thrombocytopenia (ITP)	<5	IVIg, glucocorticoids	Petechiae and ecchymoses
2019–2022	Multiple lines of therapy for refractory ITP	Variable (usually<30)	Glucocorticoids (repeated), azathioprine, mycophenolate mofetil, eltrombopag	Transient or no response; eltrombopag discontinued due to severe headache
December 2022	Initiation of romiplostim	47–110	Romiplostim (1–3 μg/kg weekly)	Partial response achieved
July 2023	Erythema migrans (Borrelia burgdorferi infection)	Not reported	Doxycycline	–
Mid–July 2023	First appearance of collateral veins on thorax (retrospectively)	Not reported	–	Early sign of developing thrombosis
August 2023	Acute presentation: massive upper extremity and central venous thrombosis	95	UFH → alteplase (systemic thrombolysis), transitional dabigatran+ASA	Near-complete SVC obstruction, markedly prolonged aPTT, positive LA
August–November 2023	APS confirmation	95 → rising	Switch to warfarin (target INR 2.0–3.0)+ASA 75 mg	Persistent LA, positive aCL and anti-β2GPI
November 2023	Brain MRI	–	–	No cerebral venous thrombosis
August 2023–April 2025	Follow-up (20 months)	95 → 210	Warfarin+ASA+romiplostim (125 μg every 2 weeks)	No recurrent thrombosis or major bleeding, partial vein recanalization, persistent aPL positivity

recurrent thrombosis or major bleeding and preserved left upper-limb function. The platelet count increased from 95×10^9/L at presentation to 210×10^9/L, D-dimer normalized, and the INR was therapeutic at 2.66, while aPTT remained prolonged (121.4 s), consistent with persistent lupus anticoagulant activity. Repeat antiphospholipid testing continued to show positive lupus anticoagulant, repeated anticardiolipin antibody positivity, and persistently elevated anti-β2-glycoprotein I antibodies. Follow-up imaging demonstrated partial recanalization of the left upper-extremity veins, but superior vena cava occlusion persisted, indicating chronic central venous sequelae despite clinical improvement. Overall, the follow-up course supported ongoing long-term anticoagulation in the setting of thrombotic APS with persistent laboratory activity. The key diagnostic and therapeutic milestones of the patient's disease course are summarized in Table 1.

Discussion

The central diagnostic issue was whether thrombocytopenia initially managed as primary ITP represented an isolated disorder or an early manifestation of APS. At presentation, the patient fulfilled criteria for primary ITP, with severe isolated thrombocytopenia, bleeding symptoms, exclusion of marrow pathology, and no clinical or laboratory evidence of systemic autoimmune disease or thrombosis; therefore, the initial diagnosis was appropriate and should not be considered incorrect in retrospect. Only after APS became definite could the thrombocytopenia be reinterpreted as possibly APS-related or as an ITP phenotype within APS.

This diagnostic overlap is supported by evidence that antiphospholipid antibodies may be present in a subset of ITP patients before overt APS develops, although progression to thrombosis is variable and not predictable. Accordingly, these findings support diagnostic vigilance rather than routine aPL screening in all ITP cases.[11,12]

Thrombocytopenia does not confer protection against thrombosis in APS, where bleeding is relatively uncommon compared with thrombotic complications.[13]

In this case, extensive central venous thrombosis occurred despite a platelet count of 95×10^9/L, underscoring that platelet count alone is not a reliable indicator of vascular risk.

The temporal association between romiplostim and thrombosis should be interpreted within a multifactorial "multiple-hit" model. Previous reports have described severe thrombotic complications, including catastrophic APS (CAPS), occurring during romiplostim therapy in patients with antiphospholipid antibodies or established APS. However, the present case differs in several important aspects: APS was not initially recognized, the thrombotic presentation involved unusually extensive upper-extremity and central venous thrombosis rather than CAPS, and long-term management required continued TPO-RA support together with warfarin anticoagulation. These features illustrate a distinct and diagnostically challenging clinical phenotype at the intersection of refractory ITP, APS, and thrombopoietin receptor agonist exposure. Persistent antiphospholipid antibody activity represented the primary prothrombotic driver, while obesity, hypertension, infection, delayed diagnosis, and possibly romiplostim may have contributed. Pediatric data on TPO-receptor agonists are overall reassuring but limited in patients with APS, and available adult data suggest a higher thrombotic burden in this subgroup; therefore, causality cannot be attributed to romiplostim alone.[7,14,15]

The extent and distribution of thrombosis – multiple upper-extremity and central venous segments with near-complete superior vena cava obstruction – are consistent with pediatric venous APS but represent an unusually severe and extensive pattern compared with registry data, where lower-extremity DVT predominates.[16]

In retrospect, earlier reassessment with antiphospholipid antibody testing could have been considered due to refractory thrombocytopenia and evolving clinical features, which represent red flags for secondary causes of presumed ITP. This supports a selective rather than routine approach to aPL testing in chronic or refractory cases.[17]

To place the present case in context, the available literature at the intersection of pediatric APS, chronic ITP, antiphospholipid antibody positivity, and TPO-receptor agonist exposure is summarized in Table 2.

Collectively, the available literature addresses isolated aspects of pediatric APS, chronic ITP, antiphospholipid antibody positivity, or TPO-RA exposure, but evidence integrating all of these factors within a single pediatric clinical scenario remains extremely limited.

Once APS-associated thrombosis was diagnosed, long-term anticoagulation with warfarin was initiated in accordance with recommendations favoring vitamin K antagonists over direct oral anticoagulants in high-risk APS.[6,8,9] Continuation of romiplostim was an individualized decision to maintain platelet counts sufficient for safe anticoagulation. This approach reflected the complex therapeutic dilemma between bleeding risk and recurrent thrombosis risk and should not be interpreted as a general treatment recommendation for APS-associated thrombosis.[7]

Conclusion

This case is hypothesis-generating. It illustrates that thrombocytopenia, initially fulfilling clinical criteria for primary ITP can, in selected patients, later be reconsidered as APS-associated thrombocytopenia or as an ITP phenotype occurring in the setting of APS. The ob-

Table 2. Published evidence relevant to pediatric ITP, APS, antiphospholipid antibodies, and TPO-RA-associated thrombotic risk

Study	Year	Population type	N/population	APS/aPL status	TPO-RA exposure	Main thrombosis phenotype	Key findings relevant to this case	Remaining uncertainty/knowledge gap
Avčin et al. (Ped-APS Registry)[16]	2008	Pediatric APS	121 children with definite APS	Definite APS	No	Venous thrombosis 60%; lower-extremity DVT most common; CVST 7%	Largest pediatric APS registry; demonstrates substantial thrombotic burden, recurrence risk, and hematologic manifestations including thrombocytopenia	Does not address chronic refractory ITP, TPO-RA exposure, or management of APS-associated thrombocytopenia
Berkun et al.[18]	2006	Pediatric APS	28 children with APS without systemic autoimmune disease at presentation	Definite APS	No	Venous and arterial thrombosis; recurrent thrombosis 29%	Supports severe long-term thrombotic burden and need for prolonged anticoagulation in pediatric APS	No data on ITP-directed therapies or TPO-RA-associated risk
Tomasello et al.[13]	2021	Review / mixed	Review focused on thrombocytopenia in APS	APS-associated thrombocytopenia	Indirect discussion only	N/A	Emphasizes diagnostic overlap between APS-associated thrombocytopenia and primary ITP	No pediatric outcome data; no data on thrombosis during TPO-RA exposure
Schifferli et al. (PARC-ITP)[17]	2021	Pediatric ITP	3974 children initially diagnosed with primary ITP	Non-APS ITP cohort	No	N/A	Identifies "red flags" for later diagnostic revision of presumed primary ITP	APS-specific screening strategies and thrombotic outcomes not evaluated
Dayama et al.[11]	2017	Mixed pediatric/adult ITP	100 ITP patients	aPL-positive ITP without APS	No	No thrombotic events during follow-up	Demonstrates that aPL positivity may occur in chronic ITP even without overt APS	Short follow-up; no longitudinal APS evolution or thrombosis-risk stratification
Diz-Küçükkaya et al.[12]	2001	Mixed pediatric/adult ITP	82 newly diagnosed ITP patients	aPL-positive ITP	No	Venous and arterial APS manifestations during follow-up	Strong prospective evidence that aPL-positive ITP may evolve into overt APS; LA identified as major risk marker	No pediatric-focused analysis; no data on TPO-RA exposure
Grainger et al. (PETIT2)[14]	2015	Pediatric ITP	92 children with chronic ITP	Non-APS ITP	Yes (eltrombopag)	No thromboembolic events reported	Population-level pediatric TPO-RA data are reassuring	Children with APS or persistent aPL positivity were not specifically assessed
Neunert et al. (ICON2)[15]	2016	Pediatric ITP	79 children; 87 TPO-RA treatment courses	Mixed primary/secondary ITP; APS status not defined	Yes	2 pulmonary emboli during eltrombopag exposure	Real-world pediatric TPO-RA data suggest low absolute thrombotic event frequency	APS-specific thrombotic risk during TPO-RA therapy remains undefined
Marques et al.[7]	2025	Adult APS/aPL-associated ITP	80 adults with ITP associated with SLE/aPL/APS; definite APS subgroup n=16	Mixed SLE/aPL/APS; definite APS subgroup analyzed separately	Yes	21 thrombotic events including venous, arterial, and catastrophic APS	Most clinically relevant comparator; thrombotic events occurred in 50% of patients with definite APS during TPO-RA exposure	Findings derive exclusively from adults and cannot be directly extrapolated to pediatric patients
Present case	2026	Pediatric refractory ITP+APS	Single adolescent patient	Delayed recognition of definite APS after years of refractory ITP	Yes (romiplostim continued after thrombosis)	Massive upper-extremity and central venous thrombosis with near-complete SVC obstruction	Illustrates the convergence of refractory pediatric ITP, previously unrecognized APS, TPO-RA exposure, and need for continued platelet support during long-term anticoagulation	Evidence guiding management of this specific high-risk pediatric overlap phenotype remains extremely limited

servation does not support universal antiphospholipid antibody screening in all children with ITP. Rather, it supports targeted aPL testing when chronic or refractory ITP is accompanied by vascular, neurologic, autoimmune, or coagulation red flags.

The novelty of this report lies in the delayed diagnosis of APS after years of refractory ITP phenotype, the unusually extensive upper-extremity and central venous thrombosis with near-complete superior vena cava obstruction, and the need to balance long-term anticoagulation with continued platelet-supportive therapy. The clinical course is best explained by cumulative rather than single-drug risk. In combined ITP and APS, the therapeutic goal shifts from normalizing the platelet count to maintaining a platelet count sufficient for safe anticoagulation while reducing modifiable thrombotic risks.

Declarations

Funding
This case report received no external funding.

Author contributions
Conceptualization, M.M.M. and W.B.; Methodology, G.M.W.; Investigation, M.M.M; Resources, M.M.M and W.B; Data Curation, M.M.M and W.B. and G.M.W.; Writing – Original Draft Preparation, M.M.M.; Writing – Review & Editing, M.M.M and R.C.; Supervision, R.C.;

Conflicts of interest
The authors declare no conflict of interest.

Data availability
The data presented in this study are available from the corresponding author upon reasonable request.

Ethics approval
Written informed consent was obtained from the patient.

Use of AI and AI-assisted technologies in the writing process
The authors used ChatGPT (OpenAI) exclusively for language editing and readability improvement which is allowed by the Eur J Clin Exp Med regulations concerning use of artificial intelligence. All scientific content, interpretation of data, and conclusions were developed independently by the authors, who take full responsibility for the final manuscript.

References

1. Łaguna P, Styczyński J, Kołtan S, et al. Primary immune thrombocytopenia—management recommendations developed by the Polish Society of Pediatric Oncology and Hematology. *Hematol – Eduk*. 2024;4(1-2):18-30. doi:10.5603/hemedu.101676
2. Rodeghiero F, Stasi R, Gernsheimer T, et al. Standardization of terminology, definitions and outcome criteria in immune thrombocytopenic purpura of adults and children: report from an international working group. *Blood*. 2009;113(11):2386-2393. doi:10.1182/blood-2008-07-162503
3. Yong M, Schoonen WM, Li L, et al. Epidemiology of paediatric immune thrombocytopenia in the General Practice Research Database. *Br J Haematol*. 2010;149(6):855-864. doi:10.1111/j.1365-2141.2010.08176.x
4. Miyakis S, Lockshin MD, Atsumi T, et al. International consensus statement on an update of the classification criteria for definite antiphospholipid syndrome (APS). *J Thromb Haemost*. 2006;4(2):295-306. doi:10.1111/j.1538-7836.2006.01753.x
5. Lewis K, Tambralli A, Madison JA. Pediatric antiphospholipid syndrome: expanding our understanding of antiphospholipid syndrome in children. *Curr Opin Rheumatol*. 2025;37(3):176-184. doi:10.1097/BOR.0000000000001083
6. Tarango C, Palumbo JS. Antiphospholipid syndrome in pediatric patients. *Curr Opin Hematol*. 2019;26(5):366-371. doi:10.1097/MOH.0000000000000523
7. Marques C, Moulis G, Roussotte M, et al. Efficacy and Thrombotic Risk of Thrombopoietin Receptor Agonists for Immune Thrombocytopenia Secondary to Systemic Lupus and Antiphospholipid Syndrome: French Experience With 80 Patients. *Am J Hematol*. 2025;100(11):1972-1982. doi:10.1002/ajh.70052
8. Tektonidou MG, Andreoli L, Limper M, et al. EULAR recommendations for the management of antiphospholipid syndrome in adults. *Ann Rheum Dis*. 2019;78(10):1296-1304. doi:10.1136/annrheumdis-2019-215213
9. Pengo V, Denas G, Zoppellaro G, et al. Rivaroxaban vs warfarin in high-risk patients with antiphospholipid syndrome. *Blood*. 2018;132(13):1365-1371. doi:10.1182/blood-2018-04-848333
10. Neunert C, Terrell DR, Arnold DM, et al. American Society of Hematology 2019 guidelines for immune thrombocytopenia. *Blood Adv*. 2019;3(23):3829-3866. doi:10.1182/bloodadvances.2019000966
11. Dayama A, Dass J, Mahapatra M, Saxena R. Incidence of Antiphospholipid Antibodies in Patients With Immune Thrombocytopenia and Correlation With Treatment With Steroids in North Indian Population. *Clin Appl Thromb*. 2017;23(6):657-662. doi:10.1177/1076029616643820
12. Diz-Küçükkaya R, Hacıhanefioğlu A, Yenerel M, et al. Antiphospholipid antibodies and antiphospholipid syndrome in patients presenting with immune thrombocytopenic purpura: a prospective cohort study. *Blood*. 2001;98(6):1760-1764. doi:10.1182/blood.V98.6.1760
13. Tomasello R, Giordano G, Romano F, et al. Immune Thrombocytopenia in Antiphospholipid Syndrome: Is It Primary or Secondary? *Biomedicines*. 2021;9(9):1170. doi:10.3390/biomedicines9091170

14. Grainger JD, Locatelli F, Chotsampancharoen T, et al. Eltrombopag for children with chronic immune thrombocytopenia (PETIT2): a randomised, multicentre, placebo--controlled trial. *The Lancet*. 2015;386(10004):1649-1658. doi:10.1016/S0140-6736(15)61107-2
15. Neunert C, Despotovic J, Haley K, et al. Thrombopoietin Receptor Agonist Use in Children: Data From the Pediatric ITP Consortium of North America ICON2 Study: Thrombopoietin Receptor Agonist Use in Children. *Pediatr Blood Cancer*. 2016;63(8):1407-1413. doi:10.1002/pbc.26003
16. Avčin T, Cimaz R, Silverman ED, et al. Pediatric Antiphospholipid Syndrome: Clinical and Immunologic Features of 121 Patients in an International Registry. *Pediatrics*. 2008;122(5):e1100-e1107. doi:10.1542/peds.2008-1209
17. Schifferli A, Heiri A, Imbach P, et al. Misdiagnosed thrombocytopenia in children and adolescents: analysis of the Pediatric and Adult Registry on Chronic ITP. *Blood Adv*. 2021;5(6):1617-1626. doi:10.1182/bloodadvances.2020003004
18. Berkun Y, Padeh S, Barash J, et al. Antiphospholipid syndrome and recurrent thrombosis in children. *Arthritis Care Res*. 2006;55(6):850-855. doi:10.1002/art.22360

Rzeszów University Press 2026
ISSN 2544-1361 (online)

http://www.ejcem.ur.edu.pl
European Journal of Clinical and Experimental Medicine
Eur J Clin Exp Med 2026; 24 (2): 430–441

Instructions for Authors

About the Journal

The European Journal of Clinical and Experimental Medicine (Eur J Clin Exp Med) is an open access journal, and all articles are free to access, download, share, and re-use. The Eur J Clin Exp Med is a peer-reviewed, scientific journal that publishes full-length articles on topics within medical science. The journal welcomes submissions of articles on current advances in life and health sciences, clinical and experimental medicine, and related disciplines.

Publication frequency

The Eur J Clin Exp Med publishes four issues per year with online-first publication. All accepted articles are published online promptly after completion of editorial production and subsequently assigned to an issue. The journal ensures regular publication according to the announced schedule.

Editorial structure and independence

The journal is led by the Editor-in-Chief and supported by an international Editorial Board and Scientific Advisory Board. Editorial decisions are based solely on the scientific merit of submissions and are independent of the publisher, sponsors, and institutional affiliations. Editorial roles and responsibilities are defined and publicly available on the journal website.

Open access and creative commons

Our open access policy is in accordance with the Budapest Open Access Initiative *(BOAI)* definition: this means that articles have free availability on the public Internet, permitting any users to read, download, copy, distribute, print, search, or link to the full texts of these articles, crawl them for indexing, pass them as data to software, or use them for any other lawful purpose, without financial, legal, or technical barriers other than those inseparable from having access to the Internet itself.

All articles are published with **free** open access under the CC-BY Creative Commons attribution license (the current version is *CC-BY,* ***version 4.0***). If you submit your paper for publication by the Eur J Clin Exp Med, you agree to have the CC-BY license applied to your work. Under this Open Access license, you, as the author, agree that anyone may download and read the paper for free. In addition, the article may be reused and quoted provided that the original published version is cited. This facilitates freedom in re-use and also ensures that Eur J Clin Exp Med content can be mined without barriers for the research needs.

All published articles include a clear license statement (CC BY 4.0) within the full text and PDF versions to ensure transparency, reuse, and machine-readable indexing. The CC BY 4.0 license applies to the article content except where otherwise indicated for third-party material.

Article processing charges

The Eur J Clin Exp Med is an open access journal and does not levy any article processing charges. There are no submission, color, or page charges for any article type.

Copyright statement

Authors of articles published in the Eur J Clin Exp Med retain copyright on their articles, except for any third-party images and other materials added by the Eur J Clin Exp Med which are subject to copyright of their respective owners. Authors are therefore free to disseminate and re-publish their articles, subject to any requirements of third-party copyright owners and subject to the original publication being fully cited. Visitors may also download and forward articles subject to the citation requirements. The ability to copy, download, forward or otherwise distribute any materials is always subject to any copyright notices displayed. Copyright notices must be displayed prominently and may not be obliterated, deleted or hidden, totally or partially.

Authors warrant that they hold the necessary rights to all content submitted for publication, including fig-

ures, tables, and supplementary materials, and that any required permissions have been obtained prior to submission. Any breach of copyright or licensing terms may result in editorial action, including rejection, correction, or retraction of the article.

Ethics in publishing

The Eur J Clin Exp Med is committed to rigorous peer review and strict ethical policies to ensure the publication of high-quality scientific work. Cases of plagiarism, data fabrication and falsification, inappropriate authorship practices, and other forms of publication misconduct may occur and are treated with utmost seriousness. The journal applies a zero-tolerance policy toward confirmed cases of ethical misconduct.

The Eur J Clin Exp Med is a member of and subscribes to the principles of the *Committee on Publication Ethics* ***(COPE)***. The journal uses plagiarism detection software, and by submitting a manuscript authors agree that their work may be screened for plagiarism against previously published content.

Handling complaints and allegations of misconduct

The journal follows COPE guidance for handling allegations of misconduct (e.g., plagiarism, data fabrication/falsification, unethical research, authorship manipulation, peer-review manipulation). Allegations may be reported to the Editorial Office. The Editor-in-Chief (or a delegated editor without conflicts of interest) will conduct an initial assessment and, when appropriate, request explanations and original data from authors, consult independent experts, and/or contact the authors' institutions. If concerns are substantiated, the journal may issue an Expression of Concern, Correction, or Retraction. All investigations are documented and handled confidentially.

Changes to authorship

Authors are expected to consider carefully the list and order of authors before submitting their manuscript and provide the definitive list of authors at the time of the original submission. Any addition, deletion or rearrangement of author names in the authorship list should be made only before a final acceptance decision, and only if approved by the journal Editor. To request such a change, the Editor must receive the following from the corresponding author: (a) the reason for the change in author list and (b) written confirmation (e-mail, letter) from all authors that they agree with the addition, removal or rearrangement. In the case of addition or removal of authors, this includes confirmation from the author being added or removed. Authorship change requests may pause editorial processing and will be evaluated to prevent inappropriate authorship practices.

After the article has been published, **no changes to the list of authors or the order of authorship will be permitted** under any circumstances. All authors must approve the final author list before publication.

Clinical trial registration

Clinical trials must comply with all policies related to research involving human subjects. Additionally, the Eur J Clin Exp Med adheres to the guidelines set by the *International Committee of Medical Journal Editors (ICMJE)*, which mandate the registration of clinical trials in a public trials registry prior to or at the time of the first patient enrollment as a prerequisite for publication consideration. The ICMJE defines a clinical trial as any research study that prospectively assigns individuals or groups to an intervention, with or without a concurrent control or comparison group, to examine the association between a health-related intervention and an outcome. Consequently, the term "clinical trial" extends beyond hospital-based studies or pharmaceutical research to include all investigations involving participant randomization and group classification in relation to the intervention being evaluated.

Authors must pre-register clinical trials in an internationally recognized clinical trials registry. Suitable databases include *ClinicalTrials.gov*, the *EU Clinical Trials Register*, and registries listed by the *World Health Organization's International Clinical Trials Registry Platform*. The registry name, trial registration number, and registration date must be stated in the Institutional Review Board (IRB) statement or the methods section of the manuscript. Purely observational studies (e.g., cohort studies, cross-sectional studies, and case–control studies) are exempt from registration requirements. However, in exceptional cases, editors may consider submissions without prior trial registration. If an exception is granted, authors must retrospectively register the trial and clearly specify the registration date and justification for the delayed registration within the methods section.

Approval from an independent local, regional, or national ethics review body does not substitute for prospective clinical trial registration. The journal reserves the right to reject manuscripts that lack appropriate trial registration. For systematic reviews, prospective protocol registration (e.g., PROSPERO) is strongly encouraged and should be reported in the Methods section. For other study types, preregistration is recommended when applicable.

Randomized clinical trial reporting guidelines

In addition to clinical trial registration, authors reporting results from randomized clinical trials must submit a completed *CONSORT 2010 checklist* and ***flow diagram*** as part of the manuscript submission. Templates for these documents are available on the *CONSORT website*, which

also provides extensions for various study designs and data types beyond two-group parallel trials. At a minimum, clinical trial reports must address all relevant items from the checklist and include a completed flow diagram.

Editorial and submission policies

When you submit a manuscript to the Eur J Clin Exp Med, we will take it to imply that the manuscript has not already been published or submitted elsewhere. If similar or related work has been published or submitted elsewhere, then you must provide a copy of this work with the submitted manuscript. You may not submit your manuscript elsewhere while it is under consideration in the Eur J Clin Exp Med. If the manuscript includes personal communications, please provide a written statement of permission from any person who is quoted. Permission by email is acceptable.

We reserve the right to reject a paper even after it has been accepted if it becomes apparent that there are serious problems with its scientific content, or our publishing policies have been violated.

Author responsibilities

Authorship provides credit for a researcher's contributions to a study and carries accountability. Authors are expected to fulfill the criteria below (adapted from McNutt et al., Proceedings of the National Academy of Sciences, 2018, 201715374; DOI: 10.1073/pnas.1715374115):

— Each author is expected to have made substantial contributions to the conception or design of the work; or the acquisition, analysis, or interpretation of data; or the creation of new software used in the work; or have drafted the work or substantively revised it
— AND to have approved the submitted version (and any substantially modified version that involves the author's contribution to the study);
— AND to have agreed both to be personally accountable for the author's own contributions and to ensure that questions related to the accuracy or integrity of any part of the work, even ones in which the author was not personally involved, are appropriately investigated, resolved, and the resolution documented in the literature.

The Eur J Clin Exp Med does not require all authors of a research paper to sign the cover letter upon submission, nor do they impose an order on the list of authors. Submission to the Eur J Clin Exp Med is taken by the publication to mean that all the listed authors have agreed to all of the contents. The corresponding (submitting) author is responsible for having ensured that this agreement has been reached, and for managing all communication between the publication and all co-authors, before and after publication.

Author contributions statements

Authors are required to include a statement of responsibility in the manuscript (at the end of the main text, before the 'References' section) that specifies the contribution of every author. For articles with several authors, a short paragraph specifying their individual contributions must be provided. The following statements should be used: "Conceptualization, X.X. and Y.Y.; Methodology, X.X.; Software, X.X.; Validation, X.X., Y.Y. and Z.Z.; Formal Analysis, X.X.; Investigation, X.X.; Resources, X.X.; Data Curation, X.X.; Writing – Original Draft Preparation, X.X.; Writing – Review & Editing, X.X.; Visualization, X.X.; Supervision, X.X.; Project Administration, X.X.; Funding Acquisition, Y.Y."

Corresponding author – responsibilities

The corresponding (submitting) author is solely responsible for communicating with the Eur J Clin Exp Med and for managing communication between co-authors. Before submission, the corresponding author ensures that all authors are included in the author list, its order has been agreed by all authors, and that all authors are aware that the paper was submitted.

A confidential process

The Eur J Clin Exp Med treats the submitted manuscript and all communication with authors and referees as confidential, although reviewers are aware of the authors' identities as part of the single-blind peer review process. Authors must also treat communication with the Eur J Clin Exp Med as confidential: correspondence with the Eur J Clin Exp Med, referee reports and other confidential material must not be posted on any website or otherwise publicized without prior permission from the Eur J Clin Exp Med publishing team, regardless of whether or not the submission is eventually published. Our policies about posting preprints and accepted manuscripts, and about previous communication of the work at conferences or as part of a personal blog or of an academic thesis, are described in the journal's Archiving policy. This confidentiality requirement does not restrict authors from sharing their own work as preprints or accepted manuscripts in accordance with the journal's Archiving policy.

Referee suggestions

During the submission process, please suggest three potential reviewers (names and institutional e-mail addresses) with the appropriate expertise to review the manuscript, but please keep in mind that we are not obliged to follow these recommendations. The proposed referees should neither be current collaborators of the co-authors nor have published with any of the co-authors of the manuscript within the last five years. Proposed reviewers should be from different institutions to the authors. You may suggest reviewers

from among the authors that you frequently cite in your paper. You may also name a limited number of scientists who should not review your paper (up to 3 named individuals or laboratories); these exclusions will be honored. The journal verifies reviewer identity and affiliation; the use of non-institutional e-mail addresses for suggested reviewers may be declined. The decision of the Editorial Board Member on the choice of referees is final.

Ethics, use of experimental animals, and human participants

For articles in the Eur J Clin Exp Med reporting experiments on live vertebrates and/or higher invertebrates, the methods section must include a statement: (i) identifying the institutional and/or licensing committee approving the experiments, including any relevant details; (ii) confirming that all experiments were performed in accordance with relevant guidelines and regulations. The ethics statement must include the name of the approving ethics committee, approval or decision number, and date of approval; studies involving human participants must confirm compliance with the Declaration of Helsinki, and animal studies must comply with the ARRIVE guidelines and the principles of the 3Rs (Replacement, Reduction, Refinement).

For research involving human participants, authors must identify the committee that approved the research, confirm that all research was performed in accordance with relevant guidelines/regulations, and include in their manuscript a statement confirming that informed consent was obtained from all participants and/or their legal guardians. Authors may be required to submit, on request, a statement from the research ethics committee or institutional review board indicating approval of the research.

Competing interests policy

In the interests of transparency and to help readers form their own judgments of potential bias, authors must declare any competing financial and/or non-financial interests related to the work described. Competing interests are defined as financial or non-financial relationships or circumstances that could directly influence, or be perceived to influence, the objectivity, integrity, or interpretation of the reported research.

Examples of potential competing interests include, but are not limited to, employment, consultancies, stock ownership or options, honoraria, paid expert testimony, patents or patent applications, and other personal or institutional relationships. Sources of research funding must be disclosed separately in the Funding statement, regardless of whether they are considered a competing interest.

Competing interests statement format guidelines

The statement included in the article file must be explicit and unambiguous, describing any potential competing interest (or lack thereof) for EACH contributing author.

Examples of declarations are:

— Competing interests: The author(s) declare no competing interests.

— Competing interests: Dr X's work has been funded by A. He has received compensation as a member of the scientific advisory board of B and owns stock in the company. He has also consulted for C and received compensation. Dr Y and Dr Z declare no competing interests.

Funding information must be reported in a separate Funding statement and should not be included in the Competing interests declaration.

Application to Editors or Editorial Board Members

Editors and Editorial Board Members of the *Eur J Clin Exp Med* are required to disclose any conflicts of interest and may be excluded from the peer review process if such conflicts exist. They should also recuse themselves from handling manuscripts where a conflict of interest is present. This may include, but is not limited to, having previously co-published with one or more of the authors or being affiliated with the same institution as one or more of the authors.

If an Editor or Editorial Board Member of Eur J Clin Exp Med is listed as an author on a manuscript, it is recommended that they declare this in the competing interests section of the submission. If they are an author or have any other conflict of interest regarding a specific manuscript, another editor will be assigned to oversee the peer review process. These submissions will undergo the same review process as any other manuscript.

Editors and Editorial Board Members of Eur J Clin Exp Med are welcome to submit their own papers to the journal. These submissions receive no special priority, and the status of the Editor or Editorial Board Member does not influence the editorial consideration.

Peer-reviewers

The Eur J Clin Exp Med invites peer-reviewers to exclude themselves in cases where there is a significant conflict of interest, financial or otherwise. However, just as financial interests need not invalidate the conclusions of an article, nor do they automatically disqualify an individual from evaluating it. We ask peer-reviewers to inform the editors of any related interests, including financial interests as defined above that might be perceived as relevant. Editors will consider these statements when weighing peer-reviewers' recommendations.

Availability of materials and data

In order to maintain the integrity, transparency, and reproducibility of research records, authors are encouraged to make their experimental and research data openly available either by depositing data in repositories or by publishing the data and files as supplementary information in this journal. The journal may request access to underlying data, protocols, or original materials for editorial assessment. Where data cannot be publicly shared due to privacy, ethical, or legal restrictions, authors must describe the restrictions and provide a mechanism for qualified access where feasible.

Data may be deposited with specialized service providers or institutional/subject repositories, preferably those that use the DataCite mechanism. Large datasets and files greater than 60 MB must be deposited in this way. For a list of other repositories specialized in scientific and experimental data, please consult re3data.org and DataCite resources. The data repository name, link to the dataset (URL) and accession number, DOI or handle number of the dataset must be provided in the paper. The journal Data also accepts submissions of dataset papers.

Data availability statement format guidelines

The statement should be provided as a separate section (titled 'Data Availability') at the end of the main text, before the 'References' section. Data availability statements should include, where applicable, accession codes, other unique identifiers and associated web links for publicly available datasets, and any conditions for access of non-publicly available datasets. Where figure source data are provided, statements confirming this should be included in data availability statements. Depending on the data described in the manuscript, data availability statements commonly take one of the following forms, or can be a composite of the statements below:

— The datasets generated during and/or analyzed during the current study are available in the [NAME] repository, [PERSISTENT WEB LINK TO DATASETS].
— The datasets generated during and/or analyzed during the current study are available from the corresponding author on reasonable request.
— All data generated or analyzed during this study are included in this published article (and its Supplementary Information files).
— The datasets generated during and/or analyzed during the current study are not publicly available due to [REASON(S) WHY DATA ARE NOT PUBLIC] but are available from the corresponding author on reasonable request.
— No datasets were generated or analyzed during the current study.
— The data that support the findings of this study are available from [THIRD PARTY NAME] but restrictions apply to the availability of these data, which were used under license for the current study, and so are not publicly available. Data are however available from the authors upon reasonable request and with permission of [THIRD PARTY NAME].

Declaration of use of AI and AI-assisted technologies in the writing process

Authors are required to disclose the use of generative AI in the writing of scientific papers upon submission. This guidance applies solely to the writing process and does not pertain to the use of AI tools for data analysis or drawing insights as part of the research process.

Generative AI and AI-assisted technologies should be used in the writing process solely to enhance the readability and language of the manuscript. These tools must be employed under human supervision, with authors thoroughly reviewing and editing the output, as AI can produce seemingly credible content that may be inaccurate, incomplete, or biased. Ultimately, authors are responsible and accountable for the content of the work.

Authors should not list generative AI and AI-assisted technologies as an author or co-author, nor cite AI as an author. Authorship entails responsibilities and tasks that can solely be assigned to and carried out by humans.

The Eur J Clin Exp Med does not allow the use of generative AI or AI-assisted tools to create or modify images in submitted manuscripts. This includes activities such as enhancing, obscuring, moving, removing, or introducing specific elements within an image or figure. Adjustments to brightness, contrast, or color balance are permitted as long as they do not obscure or remove any information present in the original. Image forensics tools or specialized software may be used to detect suspected irregularities in images within submitted manuscripts. Authors must not upload confidential, personal, or patient-identifiable information to generative AI tools.

The only exception to this policy is when AI or AI-assisted tools are integral to the research design or methods, such as in AI-assisted imaging approaches used to generate or interpret the underlying research data, particularly in fields like biomedical imaging. In such cases, the use of AI must be described in a reproducible manner within the methods section. This description should include details on how the AI or AI-assisted tools were applied in the image creation or alteration process, along with the name of the model or tool, version and extension numbers, and the manufacturer.

Authors must follow the AI software's specific usage policies and ensure proper content attribution. When applicable, authors may be required to provide pre-AI-adjusted versions of images and/or the composite raw images used to produce the final submitted versions for editorial assessment.

The use of generative AI and AI-assisted technologies in scientific writing should be disclosed by including a statement at the end of the manuscript when it is initially submitted.

— Title of new section: Use of AI and AI-assisted technologies in the writing process.
— Example of a statement: "During the preparation of this work the author(s) used [NAME TOOL/SERVICE] in order to [REASON]. After using this tool/service, the author(s) reviewed and edited the content as needed and take(s) full responsibility for the content of the published article."

The declaration does not apply to the use of basic tools, such as those used for checking grammar, spelling, and references. If there is nothing to disclose, no statement is required.

NOTE: to protect authors' rights and the confidentiality of their research, the Eur J Clin Exp Med does not currently allow the use of Generative AI or AI-assisted technologies such as ChatGPT or similar services by reviewers or editors in the peer review and manuscript evaluation process. Suspected breaches may result in reviewer removal and rejection of the manuscript or other editorial actions. Moreover, editors may decline to move forward with manuscripts if AI is used inappropriately.

Correction and retraction policy

The Eur J Clin Exp Med operates the following policy for making corrections to its peer-reviewed content.

Publishable amendments must be represented by a formal online notice because they affect the publication record and/or the scientific accuracy of published information. Where these amendments concern peer-reviewed material, they fall into one of four categories: Publisher Correction (formerly Erratum), Author Correction (formerly Corrigendum), Retraction or Addendum.

Publisher Correction (formerly Erratum). Notification of an important error made by the journal that affects the publication record or the scientific integrity of the paper or the reputation of the authors or the journal.

Author Correction (formerly Corrigendum). Notification of an important error made by the author(s) that affects the publication record or the scientific integrity of the paper, or the reputation of the authors or the journal.

Retraction. Notification of invalid results. All co-authors must sign a Retraction specifying the error and stating briefly how the conclusions are affected, and submit it for publication. In cases where co-authors disagree, the in-house editors may seek advice from independent referees and impose the type of amendment that seems most appropriate, noting the dissenting author(s) in the text of the published version.

Addendum. Notification of additional information. Addenda are published when the in-house editors decide that the addendum is crucial to the reader's understanding of a significant part of the published contribution.

Expression of Concern. A notice issued when serious concerns have been raised about a publication, but an investigation is ongoing and conclusive evidence is not yet available.

Corrections, retractions, and expressions of concern are published as separate notices and are permanently linked to the original article. The online article and PDF are clearly labeled to reflect the amendment status.

Archiving policy

Articles published in Eur J Clin Exp Med are long-term deposited in the repository of the University of Rzeszów. Authors of articles are permitted to self-archive the submitted (preprint) version of the article at any time, and may self-archive the accepted (peer-reviewed) version. The authors may also deposit the published version of the article. On submission of the manuscript, authors may deposit the submitted version in their personal, institutional, or online preprint repository. The first page of the manuscript must clearly display the following wording: *"This paper is a preprint of a paper submitted to European Journal of Clinical and Experimental Medicine (ISSN: 2544-1361)"*. If the paper is rejected, authors must remove all mention of the journal.

The author may deposit the accepted manuscript of the paper (accepted version of the manuscript after peer-review and content amendments, but before copyediting, typesetting and proof correction) to the author's personal website, provided that it is non-commercial, and to the repository of the author's institution with acknowledgement of the Journal (acknowledgement should be made as follows: *"This is an accepted peer-reviewed version of the paper. The published version of the article is available at European Journal of Clinical and Experimental Medicine (ISSN: 2544-1361), at https://doi.org/[DOI of the article]"*.

Published version of an open-access article. The author may deposit the published version of the paper (final edited and typeset version that is made publicly available by the Publisher and can be considered an article) to any institutional repository, and distribute and make it publicly available in any way with acknowledgement to the Journal (acknowledgement should be made as follows: *"This is a published version of the paper, available at European Journal of Clinical and Experimental Medicine (ISSN: 2544-1361), at https://doi.org/[DOI of the article]"*.

The journal ensures long-term digital preservation of the version of record through institutional repository archiving and persistent identifiers (DOIs).

Preprint policy

The Eur J Clin Exp Med permits the posting of manuscripts on recognized preprint servers prior to submission

or during the peer review process. Authors must disclose the existence of any preprint version at the time of submission and provide the preprint DOI or URL.
Preprints are not considered peer-reviewed publications and must not be cited as references in manuscripts submitted to the Eur J Clin Exp Med.
Following publication in the journal, authors are encouraged to update the preprint record by providing a clear link to the final published version of record (VoR), including the article DOI.

Sponsorship and advertising

As part of its publication policies, the Eur J Clin Exp Med does not accept commercial sponsorships or advertisements. However, the journal may post announcements on its website for non-profit scientific and educational events.

Peer-review process

Initial checks

Once submitted, your manuscript will be assigned to a member of our Editorial Board, who will read the paper and decide whether it is appropriate for the journal. Manuscripts that are within scope and seem, on initial assessment, to be technically sound and scientifically valid, will be sent to external reviewers. Copies of any papers containing similar or related work under consideration or in press at other journals must be included with the submission.
Manuscripts that do not fit the journal's ethics policy or do not meet the standards of the journal will be rejected before peer-review. Manuscripts may be rejected at the editorial screening stage due to: out-of-scope content, insufficient novelty or methodological rigor, ethical concerns, suspected misconduct, poor reporting quality, or failure to comply with author guidelines. Manuscripts that are not properly prepared will be returned to the authors for revision and resubmission.

Peer review

Once a manuscript passes the initial checks, it is assigned to at least two independent experts for peer review. The reviewers access the manuscript securely through our online system. The Eur J Clin Exp Med applies a single-blind peer review process, in which the reviewers are aware of the authors' identities, but the authors do not know the identity of the reviewers.
Reviewers are selected by the editorial team based on their subject expertise and the absence of any conflict of interest with the authors or the submitted work. Suggested reviewers must not have co-authored publications with the authors in the last five years or be affiliated with the same institutions.
All peer review comments are treated as confidential and will only be disclosed with the explicit consent of the reviewer. Reviewers are expected to evaluate manuscripts objectively, fairly, and constructively, and to refrain from any personal criticism of the authors.

Editorial Decision

After considering the reviewer reports the Editorial Board Member will make one of the following decisions:

— Accept outright,
— Request a minor revision, where authors revise their manuscript to address specific concerns, Request a major revision, where authors revise their manuscript to address significant concerns and perhaps undertake additional work,
— Reject outright.

The final decision is made by the Editor-in-Chief.

Revisions

In cases where the referees or Editorial Board Member has requested changes to the manuscript, you will be invited to prepare a revision. The decision letter will specify a deadline for submission of a revised manuscript. Once resubmitted, the manuscript may then be sent back to the original referees or to new referees, at the Editorial Board Member's discretion.
A revised manuscript should be submitted via the revision link provided in the decision letter, and not as a new manuscript. Authors should attach a cover letter to explain, *point by point*, the details of the revisions to the manuscript and responses to the referees' comments. The destination of the cover letter file in the submission system is 'Supplementary File for Review'. Please ensure that all issues raised have been addressed in the first round of revision. Where the authors disagree with a reviewer, they must provide a clear response. You can use a template for responding to the reviewers' comments

Final submission and acceptance

When all editorial issues are resolved, your paper will be formally accepted for publication. Once accepted, the manuscript will undergo professional copy-editing, English editing, final corrections, pagination, and publication on the https://www.ejcem.ur.edu.pl/. The Eur J Clin Exp Med reserves the right to make the final decision about matters of style and the size of figures.

Appeals

Even in cases where the Eur J Clin Exp Med does not invite resubmission of a manuscript, some authors may ask the Editorial Board to reconsider a rejection decision. These are considered appeals, which, by policy, must take second place to the normal workload. In practice, this means that decisions on appeals often take several weeks. Only one appeal is permitted for each manuscript, and appeals can only take place after peer review. Final

decisions on appeals will be made by the Editorial Board Member handling the paper.
Decisions are reversed on appeal only if the relevant Editorial Board Member is convinced that the original decision was a serious mistake. Consideration of an appeal is merited if a referee made substantial errors of fact or showed evidence of bias, but only if a reversal of that referee's opinion would have changed the original decision. Similarly, disputes on factual issues need not be resolved unless they were critical to the outcome.
If an appeal merits further consideration, the Editorial Board Member may send the authors' response and the revised paper out for further peer review.

ORCID

The Eur J Clin Exp Med supports the use of ORCID. The Eur J Clin Exp Med mandates ORCID iDs for all submitting authors; this is published on the final article to promote discoverability and credit. Please provide the ORCID iDs of the authors in the title page.

Submission guidelines

Submission process
Manuscripts for the Eur J Clin Exp Med should be submitted online at *https://mc04.manuscriptcentral.com/pmur*. The submitting author, who is generally the corresponding author, is responsible for the manuscript during the submission and peer-review process. The submitting author must ensure that all eligible co-authors have been included in the author list (read the criteria to qualify for authorship) and that they have all read and approved the submitted version of the manuscript. To submit your manuscript, register and log in to the submission website. All co-authors can see the manuscript details in the submission system, if they register and log in using the e-mail address provided during manuscript submission.

Cover letter

A cover letter must be included with each manuscript submission. It should be concise and explain why the content of the paper is significant, placing the findings in the context of existing work and why it fits the scope of the journal. Confirm that neither the manuscript nor any parts of its content are currently under consideration or published in another journal. The names of proposed and excluded reviewers should be provided in the submission system, not in the cover letter.

Accepted file formats

Use the Microsoft Word template to prepare your manuscript [**download**]
Authors must use Microsoft Word to prepare their manuscript. LaTeX submissions are not accepted. Please insert your tables, graphics (schemes, figures, etc.) in the main text after the paragraph of its first citation.
In most cases, we do not impose strict limits on word count or page number. However, we strongly recommend that you write concisely and stick to the following guidelines:

— We encourage not exceeding 20 pages for original and review papers, and 8 pages for case reports of standard computer text (1800 characters on a page).
— The main text should be no more than 4,500 words (not including Abstract, References and Figure legends).
— The title should be no more than 20 words.
— The abstract should be no more than 200 words.
— Recommended font: Times New Roman, 12 points.
— Manuscript text should be double-spaced. Do not format text in multiple columns.

Types of publications

Manuscripts submitted to the Eur J Clin Exp Med should neither be published previously nor be under consideration for publication in another journal. The main article types are as follows:
Original research manuscripts. The journal considers all original research manuscripts provided that the work reports scientifically sound experiments and provides a substantial amount of new information.
Reviews. These provide concise and precise updates on the latest progress made in a given area of research. Systematic reviews should follow the PRISMA guidelines.
The Eur J Clin Exp Med accepts also the following types of submissions: case reports, letters to the editor, commentaries, book reviews, and reports from scientific meetings and conferences.

Reporting guidelines

The guidelines listed below should be followed where appropriate. Please use these guidelines to structure your article. Completed applicable checklists, structured abstracts and flow diagrams should be uploaded with your submission.
Please refer to existing guidelines for reporting methodology; e.g.:

— *AGREE guidelines for clinical practice guidelines*
— ARRIVE guidelines for *in vivo* animal studies
— *CARE guidelines for clinical case reports*
— *CONSORT guidelines for clinical trials*
— *PRISMA guidelines for systematic reviews and meta-analyses*
— *SPIRIT for clinical trials*
— *STARD guidelines for studies of diagnostic accuracy*
— *STROBE guidelines for observational studies*

Manuscript preparation

Your paper should consist of the following parts.

Research manuscripts should comprise:

— Title page: Title, Author list, Affiliations.
— Research manuscript sections: Abstract, Keywords, Introduction, Aim, Materials and Methods, Results, Discussion, Conclusions.
— Back matter: Supplementary Materials, Acknowledgments, Funding Statement, Author Contributions, Conflicts of Interest, Data Availability, Ethics Approval, References.

Research manuscript sections:

— *Introduction*

State the objectives of the work and provide an adequate background, avoiding a detailed literature survey or a summary of the results.

— *Materials and methods*

Provide sufficient details to allow the work to be reproduced by an independent researcher. Methods that are already published should be summarized, and indicated by a reference. If quoting directly from a previously published method, use quotation marks and also cite the source. Any modifications to existing methods should also be described.

— *Results*

Results should be clear and concise. The section may be divided into subsections, each with a concise subheading. Tables and figures central to the study should be included in the main paper. Do not use the term "significant" unless p-values are provided. Show p-values to 2 or 3 decimal places. The Results section should be written in past tense.

— *Discussion*

This should explore the significance of the results of the work, not repeat them. Avoid extensive citations and discussion of published literature.

— *Conclusions*

Summarize the work's findings, state their importance, and possibly recommend further research.

Review manuscripts should comprise:

— Title page: Title, Author list, Affiliations.
— Abstract, Keywords, Literature review sections.
— Back matter: Supplementary Materials, Acknowledgments, Funding Statement, Author Contributions, Conflicts of Interest, Data Availability, References.

Structured reviews and meta-analyses should use the same structure as research articles and ensure they conform to the PRISMA guidelines.

Case reports should comprise:

— Title page: Title, Author list, Affiliations.
— Abstract, Keywords. Case reports should include a succinct introduction about the general medical condition or relevant symptoms that will be discussed in the case report; the case presentation including all of the relevant de-identified demographic and descriptive information about the patient(s), and a description of the symptoms, diagnosis, treatment, and outcome; a discussion providing context and any necessary explanation of specific treatment decisions; a conclusion briefly outlining the take-home message and the lessons learned.
— Back matter: Supplementary Materials, Acknowledgments, Funding Statement, Author Contributions, Conflicts of Interest, Data Availability, Ethics Approval, References.

Requirements for case reports submitted to Eur J Clin Exp Med:

— Patient ethnicity must be included in the Abstract under the Case Presentation section.
— Consent for publication is a mandatory journal requirement for all case reports. Written informed consent for publication must be obtained from the patient (or their parent or legal guardian in the case of children under 18, or from the next of kin if the patient has died).

The best way to ensure you have obtained appropriate consent for publication in Eur J Clin Exp Med is to *use our Eur J Clin Exp Med consent form.*

Language style

Manuscripts must be submitted in English (American or British usage is accepted, but not a mixture of these).

Title page

These sections should appear in all manuscript types:

Title: The title of your manuscript should be concise and informative. It should identify if the study reports (human or animal) trial data, or is a systematic review, meta-analysis or replication study. When gene or protein names are included, the abbreviated name rather than full name should be used.

Author List and Affiliations: Authors' full first and last names must be provided. We recommend adding as primary the affiliation where most of the research was conducted or supported, but please check with your institution for any contractual agreement requirements. For each affiliation provide the details in the following order: department, institution, city, country.

It is very important that author names and affiliations are correct. Incorrect information can mean a lack of proper attribution or incorrect citation and can even lead to problems with promotion or funding. After the publication of an article, updates or corrections to the author's address or affiliation may not be permitted.

At least one author should be designated as *corresponding author*, and his or her email address and other details should be included at the end of the affiliation sec-

tion. Please also provide the ORCID iDs of the authors in the title page.

Independent Researcher: If one or all the authors are not currently affiliated with a university, scientific institution or company, or have not been during the development of the manuscript, they should list themselves as an "Independent Researcher".

Abstract

The abstract should be a total of about 200 words maximum. The abstract should be a single paragraph and should follow the style of structured abstracts: *Introduction and aim*: Place the question addressed in a broad context and highlight the purpose of the study; *Materials and methods*: Describe briefly the main methods or treatments applied. Include any relevant preregistration numbers, and species and strains of any animals used. *Results:* Summarize the article's main findings; and *Conclusion*: Indicate the main conclusions or interpretations.

The abstract should not contain any undefined abbreviations or unspecified references.

Keywords

Three to six pertinent keywords need to be added after the abstract in alphabetical order. We recommend that the keywords are specific to the article, yet reasonably common within the subject discipline.

Back Matter

Supplementary materials: Describe any supplementary material published online alongside the manuscript (figure, tables, video, spreadsheets, etc.). Please indicate the name and title of each element as follows Figure S1: title, Table S1: title, etc.

Acknowledgments: Thank all of the people who helped with the research but did not qualify for authorship. Acknowledge anyone who provided intellectual assistance, technical help, or special equipment or materials.

Funding statement: Authors must disclose all sources of funding and the role of the funder(s) in study design, data collection, analysis, interpretation, and manuscript preparation. If the funder had no role, authors should explicitly state this.

Author contributions: Authors must supply an Author Contribution Statement as described in the *Author contributions statements* section

Conflicts of interest: Authors must supply a competing interests statement. For more details please see *Competing interests policy*.

Data availability: Authors must include a Data Availability Statement in all submitted manuscripts; see *Availability of materials and data* section for more information.

Ethics approval: Example of an ethical statement: "All subjects gave their informed consent for inclusion before they participated in the study. The study was conducted in accordance with the Declaration of Helsinki, and the protocol was approved by the Ethics Committee of XXX (Project identification code)."

Use of AI and AI-assisted technologies in the writing process: Example of a statement: "During the preparation of this work the author(s) used [NAME TOOL/SERVICE] in order to [REASON]. After using this tool/service, the author(s) reviewed and edited the content as needed and take(s) full responsibility for the content of the published article."

The declaration does not apply to the use of basic tools, such as those used for checking grammar, spelling, and references. If there is nothing to disclose, no statement is required.

References: References must be numbered in order of appearance in the text (including table captions and figure legends) and listed individually at the end of the manuscript. We recommend preparing the references with a bibliography software package, such as EndNote, Reference Manager or Zotero to avoid typing mistakes and duplicated references.

References style

In-text citations and references should be prepared according to the American Medical Association (AMA) style. Each item should be listed in numerical order.

In-text citations

Each reference should be cited in the text using superscript Arabic numerals. These superscript numbers should be outside periods. If you are citing sequential references, these should be indicated with a hyphen. Nonsequential references should be separated with commas. There should not be a space between numbers.

For example: The degree of respiratory muscles fatigue depends on the applied exercise protocol and the research group's fitness level.[1,2] The greatest load with which a patient continues breathing for at least one minute is a measure of inspiratory muscles strength.[3] Diabetes mellitus is associated with a high risk of foot ulcers.[4-6]

Sample reference

In listed references, the names of all authors should be given unless there are more than 6, in which case the names of the first 3 authors are used, followed by "et al.". If the source does not have any authors, the citation should begin with the title.

To find the proper abbreviation of a journal, go to the National Library of Medicine PubMed Journals Database at *https://www.ncbi.nlm.nih.gov/entrez/query.fcgi?db=Journals.*

Page number(s) should be inserted in full (for example: use 111–112, not 111–2). DOIs should be provided whenever available.

The following are examples of individual citations made according to the required rules of editing and punctuation:

— ***Article from a journal, number of authors from 1 to 6***

Author AA, Author BB, Author CC. Title of article. *Accepted Abbreviated Journal Title*. Year;Volume(Issue):Page-Page. doi (if available)

Lee JC, Seo HG, Lee WH, Kim HC, Han TR, Oh BM. Computer-assisted detection of swallowing difficulty. C*omput Methods Programs Biomed*. 2016;134(2):72-78. doi:10.1016/j.cmpb.2016.07.010

Morris A. New test for diabetes insipidus. *Nat Rev Endocrinol*. 2019;15(10):564-565. doi:10.1038/s41574-019-0247-x

— ***Article from a journal, number of authors more than 6***

Author AA, Author BB, Author CC, et al. Title of article. *Accepted Abbreviated Journal Title*. Year;Volume(Issue):Page-Page. doi (if available)

Gonzalez ME, Martin EE, Anwar T, et al. Mesenchymal stem cell-induced DDR2 mediates stromal-breast cancer interactions and metastasis growth. *Cell Rep*. 2017;18:1215-1228. doi:10.1016/j.celrep.2016.12.079

Jordan J, Toplak H, Grassi G, et al. Joint statement of the European Association for the Study of Obesity and the European Society of Hypertension: obesity and heart failure. *J Hypertens*. 2016;34:1678-1688. doi:10.1097/HJH.0000000000001013

— ***Websites***

Author AA (if indicated). Webpage title. Name of Website. URL. Published or Updated date. Accessed date.

Cholera in Haiti. Centers for Disease Control and Prevention Web site. *https://www.cdc.gov/haiticholera/*. Published October 22, 2010. Updated January 9, 2012. Accessed February 1, 2012.

Address double burden of malnutrition: WHO. World Health Organization site. *https://www.searo.who.int/mediacentre/releases/2016/1636/en/*. Accessed February 2, 2017.

— ***Book***

Author AA, Author BB. *Title of Work*. Location: Publisher; Year:Page-Page

Doane GH, Varcoe C. *Family Nursing as Relational Inquiry: Developing Health– Promoting Practice*. Philadelphia, PA: Lippincott Williams & Wilkins; 2005:25-28.

London ML, Ladewig PW, Ball JW, et al. *Maternal & Child Nursing Care*. Upper Saddle River, NJ: Pearson Education; c2011:101-103.

— ***Chapter in a book***

Chapter Author AA. Title of chapter. In: *Name of Book*. Edition Number. Editor AA, ed. Location: Name of Publisher; Year:Page-Page.

Grimsey E. An overview of the breast and breast cancer. In: *Breast Cancer Nursing Care and Management*. 2nd ed. Harmer V, ed. Chichester, UK: Wiley-Blackwell; 2011:35-42.

— Manuscripts "in press" may be included in the reference list if they have been accepted for publication in a peer-reviewed journal but have not yet been published in their final form, provided they are citable with a DOI (Digital Object Identifier) and the journal name is specified.

— Abstracts: If citing an abstract is necessary because it contains data not published elsewhere, it must be clearly designated as such in both the text and the reference list.

The following sources should not be included in the reference list

— Unpublished observations including personal communications

— Submitted manuscripts and manuscripts in preparation

— Preprints

NOTE: The Editorial Board requires consistent and carefully made references prepared according to the above-mentioned AMA standards. Otherwise, the work will be sent back to the authors.

Preparing Figures, Schemes and Tables

Figures and schemes must be provided during submission in sufficiently high quality (minimum 1000 pixels in either dimension or a resolution of at least 300 dpi). Common file formats are accepted; however, TIFF, JPEG, EPS, and PDF are preferred.

All figures, schemes, and tables must be embedded in the main manuscript file and placed next to the relevant text, not at the beginning or end of the document. Figure captions should be placed directly below the figure (not on the figure itself), and table titles above the table. All figures, schemes, and tables must be numbered consecutively according to their first appearance in the text (Figure 1, Scheme 1, Table 1, etc.) and must be cited in the text in numerical order.

Tables should present new information and must not duplicate content already described in the text. Each table must be understandable independently and include clear and explanatory column headings. Tables must be provided in an editable format and placed in the appropriate location within the manuscript. Tables submitted as image files (e.g., JPEG, TIFF) or as separate files will not be accepted. For large tables, smaller fonts may be used, but not smaller than 8 pt.

All text within figures and tables must be in English and remain clearly legible after reduction.

Any image manipulation that could misrepresent data (e.g., selective enhancement, splicing without disclosure) is prohibited; original/raw images may be requested for

verification. The journal may conduct image integrity checks and request original, unprocessed image files.

Copyright and Permissions

All figures, schemes, and illustrations must be original or legally reusable. Authors are fully responsible for ensuring compliance with copyright regulations. Simple citation of the source (e.g., "Source: [reference]") is not sufficient and does not constitute permission.

Figures reproduced or adapted from previously published works require explicit permission from the copyright holder, unless the original publication is licensed under a Creative Commons license permitting reuse. Reused figures must be clearly labeled in the caption as "Reproduced from" or "Adapted from", include the full reference, and specify the applicable license or confirm that permission has been obtained. Third-party material not covered by CC BY must be clearly indicated in the caption and may require separate permission for reuse.

Submission of identical figures previously published elsewhere without documented permission constitutes a serious breach of publication ethics and may result in rejection at the editorial screening stage.

The Editorial Office reserves the right to request modification, replacement, or removal of any figure, scheme, or table that does not meet technical, ethical, or editorial standards. By submitting a manuscript, authors confirm that all figures, schemes, and tables comply with copyright requirements and that all necessary permissions have been obtained.

Persistent identifiers and metadata

The journal assigns DOIs to all published articles and deposits metadata to support indexing, citation linking, and long-term discoverability. Authors are encouraged to provide ORCID iDs and funder information to ensure accurate attribution.

Abbreviations

The journal requires using only standard abbreviations. Common abbreviations such as DNA and RNA do not require definitions. Abbreviations should be defined in parentheses the first time they appear in the abstract, main text and in figure or table captions and used consistently thereafter. Ensure consistency of abbreviations throughout the article. Use the following abbreviations for measurement units: gram (g), litre (L), milligram (mg), kilogram (kg), seconds (s), minutes (min), and hours (h). Do not add 's' to indicate plural forms of units. Keep abbreviations to a minimum.

SI Units

SI Units (International System of Units) should be used. Imperial, US customary and other units should be converted to SI units whenever possible.